

**State of Florida  
Department of Transportation**

**Project Number: BDZ36**

**Automated Identification and Quantification of  
Flexible and Rigid Pavement Distresses**

**Final Report**

**Submitted to:**  
**FDOT Project Manager**  
**Abdenour Nazef, PE**  
5007 Northeast 39th Avenue  
Gainesville, FL 32609

**Submitted by:**  
**Fugro Roadware**  
8613 Cross Park Drive  
Austin, TX 78754  
Phone: (512) 977-1800  
Fax: (512) 973-9565  
[www.fugroroadware.com](http://www.fugroroadware.com)

## **DISCLAIMER PAGE**

The opinions, findings, and conclusions expressed in this publication are those of the authors.

# METRIC CONVERSION CHART

SI* (MODERN METRIC) CONVERSION FACTORS				
APPROXIMATE CONVERSIONS TO SI UNITS				
Symbol	When You Know	Multiply By	To Find	Symbol
<b>LENGTH</b>				
in	inches	25.4	millimeters	mm
ft	feet	0.305	meters	m
yd	yards	0.914	meters	m
mi	miles	1.61	kilometers	km
<b>AREA</b>				
in <sup>2</sup>	square inches	645.2	square millimeters	mm <sup>2</sup>
ft <sup>2</sup>	square feet	0.093	square meters	m <sup>2</sup>
yd <sup>2</sup>	square yard	0.836	square meters	m <sup>2</sup>
ac	acres	0.405	hectares	ha
mi <sup>2</sup>	square miles	2.59	square kilometers	km <sup>2</sup>
<b>VOLUME</b>				
fl oz	fluid ounces	29.57	milliliters	mL
gal	gallons	3.785	liters	L
ft <sup>3</sup>	cubic feet	0.028	cubic meters	m <sup>3</sup>
yd <sup>3</sup>	cubic yards	0.765	cubic meters	m <sup>3</sup>
NOTE: volumes greater than 1000 L shall be shown in m <sup>3</sup>				
<b>MASS</b>				
oz	ounces	28.35	grams	g
lb	pounds	0.454	kilograms	kg
T	short tons (2000 lb)	0.907	megagrams (or "metric ton")	Mg (or "t")
<b>TEMPERATURE (exact degrees)</b>				
°F	Fahrenheit	5 (F-32)/9 or (F-32)/1.8	Celsius	°C
<b>ILLUMINATION</b>				
fc	foot-candles	10.76	lux	lx
fl	foot-Lamberts	3.426	candela/m <sup>2</sup>	cd/m <sup>2</sup>
<b>FORCE and PRESSURE or STRESS</b>				
lbf	poundforce	4.45	newtons	N
lbf/in <sup>2</sup>	poundforce per square inch	6.89	kilopascals	kPa
APPROXIMATE CONVERSIONS FROM SI UNITS				
Symbol	When You Know	Multiply By	To Find	Symbol
<b>LENGTH</b>				
mm	millimeters	0.039	inches	in
m	meters	3.28	feet	ft
m	meters	1.09	yards	yd
km	kilometers	0.621	miles	mi
<b>AREA</b>				
mm <sup>2</sup>	square millimeters	0.0016	square inches	in <sup>2</sup>
m <sup>2</sup>	square meters	10.764	square feet	ft <sup>2</sup>
m <sup>2</sup>	square meters	1.195	square yards	yd <sup>2</sup>
ha	hectares	2.47	acres	ac
km <sup>2</sup>	square kilometers	0.386	square miles	mi <sup>2</sup>
<b>VOLUME</b>				
mL	milliliters	0.034	fluid ounces	fl oz
L	liters	0.264	gallons	gal
m <sup>3</sup>	cubic meters	35.314	cubic feet	ft <sup>3</sup>
m <sup>3</sup>	cubic meters	1.307	cubic yards	yd <sup>3</sup>
<b>MASS</b>				
g	grams	0.035	ounces	oz
kg	kilograms	2.202	pounds	lb
Mg (or "t")	megagrams (or "metric ton")	1.103	short tons (2000 lb)	T
<b>TEMPERATURE (exact degrees)</b>				
°C	Celsius	1.8C+32	Fahrenheit	°F
<b>ILLUMINATION</b>				
lx	lux	0.0929	foot-candles	fc
cd/m <sup>2</sup>	candela/m <sup>2</sup>	0.2919	foot-Lamberts	fl
<b>FORCE and PRESSURE or STRESS</b>				
N	newtons	0.225	poundforce	lbf
kPa	kilopascals	0.145	poundforce per square inch	lbf/in <sup>2</sup>

\*SI is the symbol for the International System of Units. Appropriate rounding should be made to comply with Section 4 of ASTM E380.  
(Revised March 2003)

## TECHNICAL REPORT DOCUMENTATION PAGE

1. Report No.	2. Government Accession No.	3. Recipient's Catalog No.	
4. Title and Subtitle Automated Identification and Quantification of Flexible and Rigid Pavement Distresses		5. Report Date October 2019	
		6. Performing Organization Code	
7. Author(s) Nima Kargah-Ostadi, Thomas Burchett, Jerome Daleiden, and Yuxiao Zhou		8. Performing Organization Report No.	
9. Performing Organization Name and Address Fugro Roadware 8613 Cross Park Drive Austin, TX 78754		10. Work Unit No. (TRAIS)	
		11. Contract or Grant No. FDOT-BDZ36	
12. Sponsoring Agency Name and Address Florida Department of Transportation 605 Suwannee Street, MS 30 Tallahassee, FL 32399		13. Type of Report and Period Covered Final, March 2015 to March 2019	
		14. Sponsoring Agency Code	
15. Supplementary Notes The FDOT Project Manager was Abdenour Nazef, PE.			
16. Abstract This research project was conducted with the objective of evaluating the viability of using an automated computer application to detect, classify, and quantify cracks on flexible and rigid pavement surfaces from digital images, to be implemented in the annual Pavement Condition Survey (PCS). Phase I of this project was focused on identification and quantification of the rigid pavement cracks from two-dimensional (2D) images collected using the FDOT data collection vehicle. The developed FDOT Rigid Pavement Distress Application (FRPDA) was able to detect joints and assign slabs, detect, classify, and quantify longitudinal, transverse, and corner cracks with higher accuracy, repeatability, and efficiency compared to the current manual windshield method of the PCS. Phase II of this project was focused on identification and quantification of the flexible pavement cracks from three-dimensional (3D) images collected using the Fugro data collection vehicle. The developed FDOT Flexible Pavement Distress Application (FFPDA) was able to detect, classify, and quantify all crack types with higher accuracy, repeatability, and efficiency compared to the current manual windshield method of the PCS. It is recommended that the automated FRPDA and FFPDA be used on a longer length of highway pavements along with a semi-automated survey to conduct quality control of the results and to identify and quantify non-cracking distress types for the PCS.			
17. Key Words Automated Pavement Distress Identification, Automated Crack Detection, Distress Classification, Distress Rating, Automated Distress Survey		18. Distribution Statement No restrictions.	
19. Security Classif. (of this report) Unclassified	20. Security Classif. (of this page) Unclassified	21. No. of Pages 656	22. Price



## **ACKNOWLEDGEMENTS**

The authors would like to recognize the direction and support provided by the FDOT Project Manager, Mr. Abdenour (Nour) Nazef. In addition, the authors would like to appreciate the contributions of staff at FDOT State Materials Office, including Bouzid Choubane, James (Jamie) Greene, Stacy Scott, Jason Noel, Ronald (Hank) Lambert, Keith Parrish, John Schiffermuller, William (Thad) Bryant, Frank Ostanik, Guangming Wang, David Hernando, and Wayne Allick. Finally, the authors would also like to acknowledge the contributions by other Fugro staff, including Awais Shah, Thomas Burchett, Mohammad Ilias, D.J. Swan, Ben Ong, Monty Cliff, Alex Vuotto, and Yaoming Gu.

## **EXECUTIVE SUMMARY**

This research project was conducted with the objective of evaluating the viability of using an automated computer application to detect, classify, and quantify cracks on flexible and rigid pavement surfaces from digital images, to be implemented in the annual Pavement Condition Survey (PCS). Phase I of this project was focused on identification and quantification of the rigid pavement cracks from two-dimensional (2D) images collected using the FDOT data collection vehicle. The developed FDOT Rigid Pavement Distress Application (FRPDA) was able to detect joints and assign slabs, detect, classify, and quantify longitudinal, transverse, and corner cracks with higher accuracy, repeatability, and efficiency compared to the current manual windshield method of the PCS. Phase II of this project was focused on identification and quantification of the flexible pavement cracks from three-dimensional (3D) images collected using the Fugro data collection vehicle. The developed FDOT Flexible Pavement Distress Application (FFPDA) was able to detect, classify, and quantify all crack types with higher accuracy, repeatability, and efficiency compared to the current manual windshield method of the PCS. It is recommended that the automated FRPDA and FFPDA be used on a longer length of highway pavements along with a semi-automated survey to conduct quality control of the results and to identify and quantify non-cracking distress types for the PCS.

# TABLE OF CONTENTS

Disclaimer Page .....	ii
Metric Conversion Chart .....	iii
Technical Report Documentation Page .....	iv
Acknowledgements .....	v
Executive Summary .....	vi
Table of Contents .....	vii
List of Figures .....	x
List of Tables .....	xvii
Introduction .....	1
Chapter 1 – Technology State of the Practice Assessment .....	2
1.1 Introduction to the Literature Review .....	3
1.2 Automated Distress Data Collection Hardware and Data Management .....	6
1.3 Automated Image Analysis and Processing .....	23
1.4 Implementation of Automated Crack Detection .....	39
1.5 Summary and Recommendations .....	62
Chapter 2 – Rigid Pavement Application Design .....	65
2.1 Validation of the Collected Image Quality .....	65
2.2 Evaluation of Existing Distress Survey Methods .....	80
2.3 Appropriate Settings for Automated Survey .....	103
2.4 Gap Analysis and Design Considerations .....	113
2.5 Summary and Recommendations .....	120
Chapter 3 – Rigid Pavement Application Development and Validation .....	127
3.1 Rigid Pavement Application Design Solutions .....	129
3.2 Results of the Developed Rigid Pavement Distress Identification Application .....	144
3.3 Summary and Recommendations for Implementation .....	155
Chapter 4 – LRIS Feasibility on Flexible Pavements .....	158
4.1 Data Collection .....	158
4.2 Data Processing .....	160
4.3 Evaluation of the LRIS Technology for Crack Detection and Distress Identification ...	187
4.4 Conclusion and Recommendations .....	202
Chapter 5 – Flexible Pavement Application Design .....	203

5.1	Representative Test Sections .....	203
5.2	Manual Windshield Survey .....	204
5.3	Automated Distress Survey Using Vision 3.1 .....	205
5.4	Comparison of Different Survey Methods .....	218
5.5	Gap Analysis and Design Considerations .....	222
Chapter 6 – Flexible Pavement Application Development and Validation .....		229
6.1	Application Development .....	229
6.2	Validation Experiment Design .....	245
6.3	Validation Experiment Results .....	247
6.4	Summary and Recommendations for Implementation .....	259
Chapter 7 – Automated Application Implementation .....		261
7.1	Implementation Activities for FRPDA .....	261
7.2	Implementation Activates for FFPDA .....	262
7.3	Data Quality Management Program .....	264
7.4	Recommendations for Further Implementation .....	290
Chapter 8 – Technology Needs and Gaps Assessment .....		291
8.1	Remaining Gaps in the Data Collection Equipment .....	291
8.2	Remaining Gaps in the FDOT Rigid Pavement Distress Application (FRPDA) .....	297
8.3	Remaining Gaps in the FDOT Flexible Pavement Distress Application (FFPDA) .....	300
8.4	Summary of Key Remaining Gaps and Pertinent Solutions .....	304
References .....		305
Appendices .....		317
A.	Recommended Protocol for FDOT LRIS Hardware Maintenance .....	318
A.1	General Image Properties .....	318
A.2	Image Issues .....	321
A.3	Image Feature Capturing (optical distortion) .....	322
A.4	LRIS Hardware: Check Annually .....	328
A.5	Environmental Effects: no need for checks .....	330
B.	Determination of Suitable Automated Settings for Processing LRIS Images for Rigid Pavement Distress in the Existing Automated Software .....	331
C.	Results from Field Distress Workshop on Rigid Pavements .....	351
D.	Manual Windshield Survey Results on Rigid Pavements .....	360
E.	Semi-Automated Survey Results on Rigid Pavements .....	374

F.	Automated Survey Results on Rigid Pavements Using the Existing Software.....	388
G.	FDOT Rigid Pavement Distress Application (FRPDA) User's Guide.....	392
	G.1. Preliminary Adjustments.....	393
	G.2. Lane Edge Adjustments .....	395
	G.3. Automated Pre-Filtering and Crack Detection .....	401
	G.4. FDOT Rigid Pavement Distress Application: FRPDA.....	409
	G.5. Setting Up a Schema .....	426
	G.6. Using Basic Vision Functions .....	428
	G.7. Installation Instructions for Fugro Vision Platform and the FRPDA .....	436
H.	Documentation of 24 Selected Processed Images of Rigid Pavements .....	439
I.	Purchase Order Number PR10026557: LCMS Feasibility on Flexible Pavements .....	452
	I.1. Data Collection.....	453
	I.2. Data Processing.....	456
	I.3. Comparison of Automated Distress Survey Results on 2D versus 3D Images .....	475
	I.4. Advantages of the 3D Technology.....	493
	I.5. Findings and Recommendations.....	501
J.	Manual Windshield Survey Results on Flexible Pavements.....	507
K.	FDOT Flexible Pavement Distress Application (FFPDA) Test Results.....	509
L.	FDOT Flexible Pavement Distress Application (FFPDA) Reference Manual .....	513
	L.1. Vision Batch Processing Quick Start Guide .....	514
	L.2. Reference Manual .....	521
	L.3. Installation Instructions for Vision Platform and the FFPDA.....	572
	L.4. The Difference Between Crack and Distress .....	574
	L.5. Project Advanced Settings.....	575
	L.6. Segmentation .....	579
M.	Workflow for Transfer of FDOT MPSV Data to Vision Software.....	613
	M.1. Folder Instructions.....	613
	M.2. Steps to Converting the Data Format.....	614
	M.3. Steps to Transfer the Converted Data into a Vision Database .....	615
N.	Workflow for Transfer of FDOT Contractor Data to Vision Software.....	630
	N.1. Folder Instructions .....	630
	N.2. Transferring the Data into a Vision Database .....	631

## LIST OF FIGURES

Figure 1. The system concept for automated pavement data collection (McGhee 2004) .....	3
Figure 2. Fugro Roadware's ARAN equipped with area scan system.....	9
Figure 3. Road survey vehicle equipped with constant lighting .....	9
Figure 4. Fugro BRE Automated Distress Vehicle (ADV).....	10
Figure 5. Example Line-Scan Pavement Image with Vehicle-Cast Shadow in Left Wheel Path (McGhee 2004).....	11
Figure 6. LRIS system on inspection vehicle.....	12
Figure 7. Example LRIS pavement image (right) showing dark streaks that cannot be seen on the ROW image (left) .....	13
Figure 8. LCMS sensors mounted on a survey vehicle.....	14
Figure 9. LCMS image types; (a) range, (b) intensity, (c) merged 3D .....	15
Figure 10. A LiDAR survey of a highway (left), and a LiDAR antenna (right).....	16
Figure 11. Fugro's FLI-MAP400 (Fast Laser Imaging - Mapping and Profiling) system.....	17
Figure 12. General example procedure for crack detection, quantification, and classification ....	25
Figure 13. Typical pavement cross section and the identified zones for automated distress identification (AASHTO 2014b) .....	40
Figure 14. The multi-scale crack fundamental element concept (Tsai and Wang 2014).....	45
Figure 15. Framework of the proposed overall crack evaluation index (Wang, et al., 2015) .....	46
Figure 16. "Precision" and recall curve for different crack detection algorithms (Wang et al. 2011) .....	51
Figure 17. Repeatability trials of simulated real time cracking analysis using the RoadCrack <sup>®</sup> algorithm on LCMS images (2.5 mm sampling at 40 mph) (Warren et al. 2013) .....	55
Figure 18. Calibration dialog box. ....	67
Figure 19. Example LRIS pavement image (right) showing intensity streaks that cannot be seen on the ROW image (left) .....	68
Figure 20. Pavement section with optical distortion study points. ....	69
Figure 21. LRIS 2D image of FDOT target site. ....	70
Figure 22. Image measurements compared to field measurements in a) transverse, b) longitudinal, and c) diagonal directions.....	74
Figure 23. Correction factors for transversal image measurements in a) 2D LRIS and b) 3D LCMS. ....	75
Figure 24. Sample Target Images used as a Reference for Evaluating Signal to Noise Ratio ...	76
Figure 25. Schematic of LRIS image collection system (Pavemetrics). ....	78
Figure 26. Comparison of Different Methods in terms of Accuracy (100 - Absolute Bias(%)) .....	95
Figure 27. Comparison of Different Methods in terms of Precision (Standard Deviation of Normalized Error (%) Among 12 Sections) .....	96
Figure 28. Comparison of Different Methods in terms of Reliability (Standard Deviation of Normalized Error (%) Among 3 Raters/Runs) .....	97
Figure 29. Agreement Among Multiple Raters/Runs, A measure of Reproducibility/Repeatability .....	98
Figure 30. Percentage of "Outlier" Ratings, A measure of Reproducibility/Repeatability .....	98
Figure 31. Comparison of the Efficiency (Speed) of Survey Methods .....	99
Figure 32. Detection Parameter Settings for Evaluation of Existing Software .....	110

Figure 33 Group Tile Height/ Width.....	111
Figure 34. Distress Angle Definitions .....	112
Figure 35. Framework for Evaluation and Design of Automated Pavement Distress Application .....	128
Figure 36. Final Detection Parameter Settings Applied After Pre-Filtering.....	132
Figure 37. Detecting Adjacent Candidate Joint Cells (Dark Cells, each 8 by 8 pixels) .....	133
Figure 38. Narrow Window to Identify Joints from Detected Joint Cells.....	134
Figure 39. Removing False Positive Joints According to the Gap Between Joint Cells .....	135
Figure 40. Examples of Exceptional Situations with Falsely Detected Longitudinal Joints (Curb Edge on the Left Image, and Lane Edge on the Right Image).....	137
Figure 41. (left) Very Straight Longitudinal Cracks Resulting in False Longitudinal Joints in Section 5; (right) Faded Lane Stripes in the Middle of Image Resulting in False Longitudinal Joints in Section 9 .....	138
Figure 42. Example Removing Straight Lines (False Positive Cracks) in Section 4 .....	140
Figure 43. Example of Two Transverse Cracks Grouped into One Crack .....	141
Figure 44. Example Corner Cracks and Spalling .....	143
Figure 45. Accuracy of Automated Methods in Identifying the Number of Cracks (higher bars are more accurate results).....	147
Figure 46. Accuracy of Automated Methods in Identifying the Length of Cracks (higher bars are more accurate results).....	147
Figure 47. Repeatability of Automated Methods Compared to Reproducibility of Manual and Semi-Automated Methods in Identifying the Number of Cracks (Standard Deviation of Error Among Multiple Runs/Raters: lower bars are more precise results).....	148
Figure 48. Repeatability (Precision) of Automated Methods in Identifying the Length of Cracks (Standard Deviation of Error Among Multiple Runs/Raters: lower bars are more precise results) .....	149
Figure 49. Reliability of Automated Methods in Identifying the Number of Cracks (100 – Coefficient of Variation in Total Distress Amounts Among Multiple Runs/Raters: higher bars show more reliable results).....	149
Figure 50. Reliability of Automated Methods in Identifying the Length of Cracks (100 – Coefficient of Variation in Total Distress Amounts Among Multiple Runs/Raters: higher bars show more reliable results).....	150
Figure 51. Variability of Automated Methods in Identifying the Number of Cracks (Standard Deviation of Error Among Different Test Sections: lower bars mean less variable results) .....	150
Figure 52. Variability of Automated Methods in Identifying the Length of Cracks (Standard Deviation of Error Among Different Test Sections: lower bars mean less variable results) .....	151
Figure 53. Comparison of Efficiency (Speed) of Automated to Semi-Automated Methods. ....	152
Figure 54. Verification of Length of Automatically Detected Cracks Against Reference on Sample Images.....	154
Figure 55. Verification of Length of Automatically Rated Cracks Against True Positives on Sample Images.....	155
Figure 56. FDOT LRIS Equipment .....	159
Figure 57. Agreed Folder Structure.....	162
Figure 58. Folder Structure Example .....	162
Figure 59. Fugro DBGen Software Interface for Creating Blank Vision Databases .....	163

Figure 60. Fugro Vision Interface Showing the Imported Sections .....	164
Figure 61. Vision Database Basic Tables and Relations .....	165
Figure 62. Typical Error in Mile Post Data.....	166
Figure 63. Vision Distress Schema Editor Interface with One Distress Type for Both Wheel Path and Outside Wheel Path Zones (Option 1) .....	168
Figure 64. Vision Distress Schema Editor Interface with Separate Distress Types Defined for Wheel Path and Outside Wheel Path Zones (Option 2).....	169
Figure 65. Cracks Menu in the Distress Schema Editor .....	171
Figure 66. Changing the Colors of the Displayed Cracks.....	171
Figure 67. Detection and Classification Profiles in the Distress Schema Editor .....	172
Figure 68. Group Tile Height and Width .....	174
Figure 69. Comparison of Classification Control Parameter Settings: Density .....	175
Figure 70. Comparison of Classification Control Parameter Settings: Tile Height and Width ...	175
Figure 71. Comparison of Classification Control Parameter Settings: Group Tile Height and Width .....	176
Figure 72. Wheel Path Designation in FDOT Flexible Distress Handbook (2017) .....	177
Figure 73. Road Zone Settings .....	178
Figure 74. Automatically Separated Wheel Path and Non-Wheel Path Distress Rating .....	181
Figure 75. Crack Table.....	182
Figure 76. Crack Set Table.....	183
Figure 77. Demonstrating the Reason for Using 3D Images for Reference Survey: Example 1 .....	184
Figure 78. Demonstrating the Reason for Using 3D Images for Reference Survey: Example 2 .....	185
Figure 79. ROW Image of Patching Area.....	185
Figure 80. Vision Pavement Rating Module for Semi-Automated Distress Survey .....	187
Figure 81. Lane boundaries identified as cracks.....	198
Figure 82. Other Features Falsely Detected as Cracks.....	199
Figure 83. Low Contrast Between Crack and Surrounding Pixels Resulting in Missed Cracks	200
Figure 84. White Alligator Cracks on Dark Pavement .....	201
Figure 85. Selected 12 Flexible Pavement Test Sections .....	204
Figure 86. Crack Detection Success Metrics for Vision 3.1.....	210
Figure 87. Example LCMS Intensity (left), Range (center), and Detected Crack Map (right) ....	211
Figure 88. Example LCMS Intensity (left), Range (center), and Detected Crack Map (right) ....	211
Figure 89. Longitudinal Cracking Success Metrics for Vision 3.1.....	212
Figure 90. Transverse Cracking Success Metrics for Vision 3.1 .....	213
Figure 91. Alligator Cracking Success Metrics for Vision 3.1.....	214
Figure 92. Wheel Path Cracking (CW) Success Metrics for Vision 3.1 .....	215
Figure 93. Outside Wheel Path Cracking (CO) Success Metrics for Vision 3.1 .....	215
Figure 94. Severity Level 1B Rating Results for Vision 3.1 .....	217
Figure 95. Severity Level II Rating Results for Vision 3.1.....	217
Figure 96. Severity Level III Rating Results for Vision 3.1.....	218
Figure 97. Comparison of Different Methods in terms of Accuracy.....	220
Figure 98. Comparison of Different Methods in terms of Consistency .....	221



Figure 99. Comparison of the Reproducibility of Manual Windshield Survey to the Repeatability of Vision 3.1 Results .....	221
Figure 100. Example Showing Resizing, Dilation, and Skeletonizing to Create Crack Map .....	224
Figure 101. Example Showing Extraction of Alligator Cracking Areas from the Crack Map .....	225
Figure 102. Example Showing Extraction of Single and Branch Cracks from the Crack Map...	226
Figure 103. Joint Pixels and Branch Cracks .....	226
Figure 104. Example Preprocessing of 3D Range Image .....	227
Figure 105. Example Development of Enhanced Crack Map for Crack Width Determination...	228
Figure 106. Example Showing Resizing, Dilation, and Skeletonizing to Create Improved Crack Map.....	231
Figure 107. A 3x3 Square Structuring Element.....	232
Figure 108. The Pixel Arrangement in the Zhang-Suen Thinning Algorithm .....	233
Figure 109. Example Showing Extraction of Alligator Cracking Areas from the Crack Map .....	235
Figure 110. Schematic Description of Contour Hierarchy Analysis.....	236
Figure 111. Example Showing Extraction of Single and Branch Cracks from the Crack Map...	237
Figure 112. Joint Pixels and Branch Cracks .....	237
Figure 113. FDOT Defined Road Zones Across the Lane Width .....	238
Figure 114. Cropping Bounding Box into Sub-Boxes According to Road Zone.....	239
Figure 115. Grouped Bounding Box.....	240
Figure 116. Example Preprocessing of 3D Range Image .....	241
Figure 117. Example Development of Enhanced Crack Map for Crack Width Determination...	244
Figure 118. Comparison of Automatically Identified Single Cracks to Reference Survey .....	248
Figure 119. Comparison of Automatically Identified Branch Cracks to Reference Survey .....	249
Figure 120. Comparison of Automatically Identified Alligator Cracking to Reference Survey ...	249
Figure 121. Comparison of Automatically Identified Class 1B Cracks to the Manual Windshield and Reference Surveys.....	251
Figure 122. Comparison of Automatically Identified Class II Cracks to the Manual Windshield and Reference Surveys.....	251
Figure 123. Comparison of Automatically Identified Class III Cracks to the Manual Windshield and Reference Surveys.....	252
Figure 124. Comparison of Automatically Identified Wheel Path Cracking to the Manual Windshield and Reference Surveys .....	253
Figure 125. Comparison of Automatically Identified Non- Wheel Path Cracking to the Manual Windshield and Reference Surveys .....	253
Figure 126. Comparison of Different Methods in terms of Accuracy .....	254
Figure 127. Comparison of Different Methods in terms of Bias .....	255
Figure 128. Comparison of Different Methods in terms of Consistency .....	255
Figure 129. Comparison of Different Methods in terms of Repeatability/Reproducibility.....	256
Figure 130. Comparison of FFPDA to Manual Windshield Survey Crack Rating Statistics .....	257
Figure 131. Comparison of FFPDA to Manual Windshield Survey Crack Rating Averages .....	258
Figure 132. Quality Management Approach .....	266
Figure 133. Calibration dialog box.....	319
Figure 134. Example LRIS pavement image (right) showing intensity streaks that cannot be seen on the ROW image (left).....	322
Figure 135. Pavement section with optical distortion study points.....	323

Figure 136. LRIS 2D image of FDOT target site. ....	324
Figure 137. Sample Target Images used as a Reference for Evaluating Signal to Noise Ratio.....	328
Figure 138. Schematic of image collection concept. ....	329
Figure 139. Crack Detection Sample Image Number 1 .....	336
Figure 140. Crack Detection Sample Image Number 2 .....	336
Figure 141. Crack Detection Sample Image Number 3 .....	337
Figure 142. Crack Detection Sample Image Number 4 .....	337
Figure 143. Crack Detection Sample Image Number 5 .....	338
Figure 144. Crack Detection Sample Image Number 6 .....	338
Figure 145. Crack Detection Sample Image Number 7 .....	339
Figure 146. Crack Detection Sample Image Number 8 .....	339
Figure 147. Crack Detection Sample Image Number 9 .....	340
Figure 148. Crack Detection Sample Image Number 10 .....	340
Figure 149. Crack Detection Sample Image Number 11 .....	341
Figure 150. Crack Detection Sample Image Number 12 .....	341
Figure 151. Crack Detection Sample Image Number 13 .....	342
Figure 152. Crack Detection Sample Image Number 14 .....	342
Figure 153. Crack Detection Sample Image Number 15 .....	343
Figure 154. Crack Detection Sample Image Number 16 .....	343
Figure 155. Crack Detection Sample Image Number 17 .....	344
Figure 156. Crack Detection Sample Image Number 18 .....	344
Figure 157. Crack Detection Sample Image Number 19 .....	345
Figure 158. Crack Detection Sample Image Number 20 .....	345
Figure 159. Crack Detection Sample Image Number 21 .....	346
Figure 160. Crack Detection Sample Image Number 22 .....	346
Figure 161. Crack Detection Sample Image Number 23 .....	347
Figure 162. Crack Detection Sample Image Number 24 .....	347
Figure 163. Crack Detection Sample Image Number 25 .....	348
Figure 164. Crack Classification Sample Image Number 1 .....	349
Figure 165. Crack Classification Sample Image Number 2.....	349
Figure 166. Crack Classification Sample Image Number 3.....	350
Figure 167. Distance from average in standard deviation (transverse cracking).....	351
Figure 168. Transverse cracking on rigid pavements. ....	352
Figure 169. Distance from average in standard deviation (longitudinal cracking). ....	353
Figure 170. Longitudinal cracking on rigid pavement. ....	353
Figure 171. Distance from average in standard deviation (spalling). ....	354
Figure 172. Spalling on rigid pavements. ....	355
Figure 173. Distance from average in standard deviation (corner cracking). ....	356
Figure 174. Corner cracking on rigid pavement. ....	356
Figure 175. Shattered slab of rigid pavement.....	358
Figure 176. Distance from average in standard deviation (transverse cracking).....	361
Figure 177. Distance from average in standard deviation (longitudinal cracking). ....	363
Figure 178. Distance from average in standard deviation (spalling). ....	365
Figure 179. Distance from average in standard deviation (corner cracking). ....	367

Figure 180. Distance from average in standard deviation (patching). .....	369
Figure 181. Distance from average in standard deviation (shattered slab). .....	371
Figure 182. Distance from average in standard deviation (surface deterioration). .....	373
Figure 183. Distance from average in standard deviation (transverse cracking). .....	375
Figure 184. Distance from average in standard deviation (longitudinal cracking). .....	377
Figure 185. Distance from average in standard deviation (spalling). .....	379
Figure 186. Distance from average in standard deviation (corner cracking). .....	381
Figure 187. Distance from average in standard deviation (patching). .....	383
Figure 188. Distance from average in standard deviation (shattered slab). .....	385
Figure 189. Distance from average in standard deviation (surface deterioration). .....	387
Figure 190. Distance from average in standard deviation (transverse cracking count) .....	389
Figure 191. Distance from average in standard deviation (longitudinal cracking count) .....	389
Figure 192. Distance from average in standard deviation (transverse cracking length). .....	391
Figure 193. Distance from average in standard deviation (longitudinal cracking length). .....	391
Figure 194. (Left) Image Number 1 (Frame 19); (Right) Image Number 2 (Frame 20) from Section 1 .....	440
Figure 195. (Left) Image Number 3 (Frame 115); (Right) Image Number 4 (Frame 116) from Section 2 .....	441
Figure 196. (Left) Image Number 5 (Frame 29); (Right) Image Number 6 (Frame 22) from Section 3 .....	442
Figure 197. (Left) Image Number 7 (Frame 14); (Right) Image Number 8 (Frame 24) from Section 4 .....	443
Figure 198. (Left) Image Number 9 (Frame 767); (Right) Image Number 10 (Frame 768) from Section 5 .....	444
Figure 199. (Left) Image Number 11 (Frame 22); (Right) Image Number 12 (Frame 23) from Section 6 .....	445
Figure 200. (Left) Image Number 13 (Frame 62); (Right) Image Number 14 (Frame 61) from Section 7 .....	446
Figure 201. (Left) Image Number 15 (Frame 6); (Right) Image Number 16 (Frame 10) from Section 8 .....	447
Figure 202. (Left) Image Number 17 (Frame 31); (Right) Image Number 18 (Frame 38) from Section 9 .....	448
Figure 203. (Left) Image Number 19 (Frame 52); (Right) Image Number 20 (Frame 53) from Section 10 .....	449
Figure 204. (Left) Image Number 21 (Frame 44); (Right) Image Number 22 (Frame 45) from Section 11 .....	450
Figure 205. (Left) Image Number 23 (Frame 87); (Right) Image Number 24 (Frame 88) from Section 12 .....	451
Figure 206. The ARAN Data Collection System Used for the FDOT Project .....	455
Figure 207. Fugro Data Process Flow .....	456
Figure 208. Vision Software for Segmenting .....	457
Figure 209. Vision Distress Schema Editor Interface with One Distress Type for Both Wheel Path and Outside Wheel Path Zones (Option 1) .....	459
Figure 210. Vision Distress Schema Editor Interface with Separate Distress Types Defined for Wheel Path and Outside Wheel Path Zones (Option 2) .....	460

Figure 211. Cracks Menu in the Distress Schema Editor .....	462
Figure 212. Detection and Classification Profiles in the Distress Schema Editor .....	463
Figure 213. Group Tile Height and Width .....	465
Figure 214. Comparison of Classification Control Parameter Settings: Density .....	466
Figure 215. Comparison of Classification Control Parameter Settings: Tile Height and Width ..	467
Figure 216. Comparison of Classification Control Parameter Settings: Group Tile Height and Width .....	468
Figure 217. Wheel Path Designation in FDOT Flexible Distress Handbook.....	469
Figure 218. Road Zone Settings .....	469
Figure 219. Automatically Separated Wheel Path and Non-Wheel Path Distress Rating .....	473
Figure 220. Vision Pavement Rating Module for Semi-Automated Distress Survey .....	475
Figure 221. Patching Area Boundary Falsely Detected as Cracks .....	482
Figure 222. AVC Loops and WIM Devices Falsely Detected as Cracks .....	482
Figure 223. Comparison of 2D versus 3D Crack Detection Success Metrics .....	493
Figure 224. Example LCMS Intensity (left), Range (center), and Detected Crack Map (right) ..	494
Figure 225. Example LRIS Image (left) and Detected Crack Map (right) Corresponding to the LCMS Example in Figure 224 .....	495
Figure 226. Example LCMS Intensity (left), Range (center), and Detected Crack Map (right) ..	496
Figure 227. Example LRIS Image (left) and Detected Crack Map (right) Corresponding to the LCMS Example in Figure 226 .....	497
Figure 228. Comparison of 2D versus 3D Longitudinal Cracking Success Metrics .....	498
Figure 229. Comparison of 2D versus 3D Transverse Cracking Success Metrics .....	499
Figure 230. Comparison of 2D versus 3D Alligator Cracking Success Metrics.....	499
Figure 231. Comparison of 2D versus 3D Wheel Path Cracking (CW) Success Metrics .....	500
Figure 232. Comparison of 2D versus 3D Outside Wheel Path Cracking (CO) Success Metrics .....	500
Figure 233. Folder Structure for FDOT MPSV Data .....	613
Figure 234. Screen Capture of Roadware DBGen .....	616
Figure 235. Folder Structure for FDOT Data .....	630
Figure 236. Roadware DBGen Software Screen Capture .....	631
Figure 237. Database Settings in Roadware DBGen software.....	632
Figure 238. FDOT Vision Controller Blank Interface .....	633
Figure 239. FDOT Vision Controller Interface with Options Selected.....	635
Figure 240. FDOT Vision Controller Interface After Running the SQL Code .....	636

## LIST OF TABLES

Table 1. Image resolution and theoretical minimum visible crack width (Wang and Smadi 2011)	19
Table 2. Example specs for line-scan and area-scan cameras	19
Table 3. Advantages and limitations of location referencing systems	22
Table 4. Major techniques used for pre-processing pavement images	29
Table 5. Example methods for classifying crack features	31
Table 6. Summary of pavement condition data collection methods (Pierce et al. 2013)	41
Table 7. Accuracy and precision for LTPP manual ratings of AC pavements (Rada, et al., 1999)	48
Table 8. Accuracy and precision for LTPP manual ratings of PCC pavements (Rada, et al., 1999)	49
Table 9. False positives and missed cracks using three different crack detection software before and after manual human intervention (Serigos et al. 2015)	52
Table 10. Quantification errors using three different crack detection software before and after manual human intervention (Serigos et al. 2015)	53
Table 11. Alabama DOT paired t-test between manual and automated distress data (Timm and Turochy 2014)	54
Table 12. Reference points for measurements	71
Table 13. Statistics for normalized error compared to field measurement	72
Table 14. Average and standard deviation of error excluding measurements affected by stitching	72
Table 15. Example Partial Factorial Plan	87
Table 16. Final Selected 12 Test Sections	87
Table 17. Overall Agreement Among Raters in Manual Windshield Survey (See Appendix D for Details)	89
Table 18. Overall Agreement Among Raters in Semi-Automated Survey (See Appendix E for Details)	90
Table 19. Comparison of Manual Windshield Survey Rating to “Ground Truth”	94
Table 20. Comparison of Semi-Automated Rating to “Ground Truth”	94
Table 21. Comparison of Automated Rating to “Ground Truth” (Length and Count)	94
Table 22. Verification of Automatically Detected Distress on Sample Image Frames (Raw Data)	101
Table 23. Verification of Automatically Detected Distress on Sample Image Frames (Metrics)	102
Table 24. Image Pre-Processing Investigation Sample Test Results	105
Table 25. Image Pre-Processing Investigation Test Results After Fine-Tuning Detection Settings	105
Table 26. Investigation of Key Detection Parameters	109
Table 27. Example Figures in Appendix B that Describe the Impact of Changing Key Detection Parameters	110
Table 28. Classification Parameter Settings	111
Table 29. Settings used for Rating in WiseCrax	112
Table 30. Identified Gaps and Recommended Solutions	117
Table 31. Identified Gaps in Automated Software System and Recommended Solutions	129

Table 32. Preliminary Joint Detection Results.....	136
Table 33. Example Slabs Identified Using Joints.....	139
Table 34. Overall Success Metrics based on Cumulative Count Values .....	152
Table 35. Average Values for Crack Verification Metrics based on 24 Sample Images (based on length) .....	153
Table 36. Remaining Gaps at Conclusion of Task 3 .....	156
Table 37. Representative Flexible Pavement Test Sections.....	160
Table 38. Four Types of FDOT ICC Vehicle Files Used in Importing Process.....	161
Table 39. Classification Parameter Settings .....	173
Table 40. Distress Types and Corresponding Crack Classification and Severity Levels (option 1 corresponding to Figure 62 used for the reference survey).....	178
Table 41. Distress Types and Corresponding Crack Classification and Severity Levels (option 2 corresponding to Figure 63 used for automated results) .....	179
Table 42. Crack Width Range .....	180
Table 43. Batch Processor .....	182
Table 44. Relation Between the 2D Database and the 3D Reference Database .....	186
Table 45. Verification of Crack Detection on 2D images Using Fugro Machine Learning Algorithm.....	191
Table 46. Accuracy, Repeatability, and Consistency of Crack Detection based on 2D Images.....	192
Table 47. Accuracy, Repeatability, and Consistency of Longitudinal Cracks based on 2D Images .....	193
Table 48. Accuracy, Repeatability, and Consistency of Transverse Cracks based on 2D Images .....	194
Table 49. Accuracy, Repeatability, and Consistency of Alligator Cracks based on 2D Images .....	195
Table 50. Accuracy, Repeatability, and Consistency of Cracking Outside Wheel Paths (CO) Based on 2D Images .....	196
Table 51. Accuracy, Repeatability, and Consistency of Cracking Within Wheel Paths (CW) Based on 2D Images .....	197
Table 52. Selected 12 Flexible Pavement Test Sections.....	204
Table 53. Overall Agreement Among Raters in Manual Windshield Survey (See Appendix J for Details) .....	205
Table 54. Verification of Crack Detection on 3D images Using Vision 3.1 .....	210
Table 55. Summary Statistics for Vision 3.1 Results from 3D Images .....	216
Table 56. Comparison of Manual Windshield Survey Rating to the Reference Survey.....	219
Table 57. Comparison of Vision 3.1 Rating to the Reference Survey .....	220
Table 58. Identified Gaps and Recommended Solutions .....	223
Table 59. Identified Gaps and Recommended Solutions .....	230
Table 60. Definition of Quality Terms.....	264
Table 61. Contents of the Data Quality Management Program .....	266
Table 62. Recommended Protocols and Quality Standards for HPMS Data.....	268
Table 63. Recommended Protocols and Quality Standards for FDOT Pavement Management Data.....	270
Table 64. Planned Control and Verification Sites.....	274
Table 65. Available Equipment Calibration and Certification Protocols.....	275
Table 66. Quality Control Activities Conducted Before Data Collection .....	277

Table 67. Quality Control Activities Conducted During Data Collection .....	278
Table 68. Quality Control Activities Conducted After Data Collection .....	279
Table 69. Recommended Quality Acceptance Procedures and Criteria .....	282
Table 70. Example QC Log Format.....	286
Table 71. Example Acceptance Log Format.....	286
Table 72. Example QA Log Format.....	286
Table 73. Recommended Quality Team Roles and Responsibilities .....	287
Table 74. Remaining Gaps in FRPDA and Recommended Solutions .....	297
Table 75. Recommended Development Initiatives for FRPDA and the Level of Effort.....	298
Table 76. Remaining Gaps in FFPDA and Recommended Solutions .....	300
Table 77. Recommended Development Initiatives for FRPDA and the Level of Effort .....	302
Table 78. Reference points for measurements .....	325
Table 79. Recommended Range for Annual Error Estimation based on Previous Estimation of Average and Standard Deviation of Error Compared to Field Measurements .....	326
Table 80. Settings for WiseCrax pre-set detection profiles .....	331
Table 81. Settings for WiseCrax pre-set detection profiles (continued) .....	333
Table 82. Crack Detection Legend for Figure 138 through Figure 162 .....	335
Table 83. Distress Identification Legend for Figure 163 through Figure 165.....	348
Table 84. Statistics of transverse cracking at different severity level.....	351
Table 85. Statistics of longitudinal cracking at different severity level .....	352
Table 86. Statistics of spalling at different severity level.....	354
Table 87. Statistics of corner cracking at different severity level .....	355
Table 88. Statistics of patching at different severity level .....	357
Table 89. Statistics of shattered slabs .....	357
Table 90. Statistics of surface deterioration .....	358
Table 91. Statistics of pumping .....	359
Table 92. Transverse cracking (count): light, moderate, and severe .....	360
Table 93. Longitudinal cracking (count): light, moderate, and severe .....	362
Table 94. Spalling (linear feet): moderate and severe .....	364
Table 95. Corner cracking (count): light, moderate, and severe.....	366
Table 96. Patching (sq. yards): fair and poor.....	368
Table 97. Shattered slab (count): moderate and severe.....	370
Table 98. Surface deterioration (sq. feet): moderate and severe .....	372
Table 99. Transverse cracking (count): light, moderate, and severe .....	374
Table 100. Longitudinal cracking (count): light, moderate, and severe .....	376
Table 101. Spalling (linear feet): moderate and severe .....	378
Table 102. Corner cracking (count): light, moderate, and severe .....	380
Table 103. Patching (sq. yard): fair and poor .....	382
Table 104. Shattered slab (count): moderate and severe .....	384
Table 105. Surface deterioration (sq. feet): moderate and severe.....	386
Table 106. Transverse and longitudinal cracking (count) .....	388
Table 107. Transverse and longitudinal cracking (linear feet) .....	390
Table 108. List of Sample Image Frames Processed for Rigid Pavements .....	439
Table 109. 12 Representative Flexible Pavement Test Sections .....	456

Table 110. Classification Parameter Settings.....	464
Table 111. Distress Types and Corresponding Crack Classification and Severity Levels (option 1 corresponding to Figure 208 used for the reference survey) .....	470
Table 112. Distress Types and Corresponding Crack Classification and Severity Levels (option 2 corresponding to Figure 209 used for automated results).....	470
Table 113. Crack Width Range .....	472
Table 114. Vision Automated Batch Processors.....	474
Table 115. Verification of Crack Detection on 3D images Using Fugro Machine Learning Algorithm.....	481
Table 116. Verification of Crack Detection on 2D images Using Fugro Machine Learning Algorithm.....	481
Table 117. Accuracy, Repeatability, and Consistency of Crack Detection based on 3D Images .....	483
Table 118. Accuracy, Repeatability, and Consistency of Crack Detection based on 2D Images .....	484
Table 119. Accuracy, Repeatability, and Consistency of Longitudinal Cracks on 3D .....	486
Table 120. Accuracy, Repeatability, and Consistency of Longitudinal Cracks on 2D .....	486
Table 121. Accuracy, Repeatability, and Consistency of Transverse Cracks based on 3D .....	487
Table 122. Accuracy, Repeatability, and Consistency of Transverse Cracks based on 2D .....	488
Table 123. Accuracy, Repeatability, and Consistency of Alligator Cracks based on 3D Images .....	489
Table 124. Accuracy, Repeatability, and Consistency of Alligator Cracks based on 2D Images .....	489
Table 125. Accuracy, Repeatability, and Consistency of CO Based on 3D Images .....	491
Table 126. Accuracy, Repeatability, and Consistency of CO Based on 2D Images .....	491
Table 127. Accuracy, Repeatability, and Consistency of Cracking within Wheel Paths (CW) Based on 3D Images .....	492
Table 128. Accuracy, Repeatability, and Consistency of Cracking within Wheel Paths (CW) Based on 2D Images .....	492
Table 129. Summary Statistics for Automated Distress Identification Results from 2D and 3D Images .....	498
Table 130. ARAN Rutting Capabilities .....	504
Table 131. Amount of Cracking by Crack Type, Severity, and Road Zone for Each Run .....	509
Table 132. Amount of Cracking by Crack Type and Severity for Each Run .....	510
Table 133. Amount of Cracking by Road Zone and Crack Severity for Each Run .....	511



## INTRODUCTION

This research project was conducted with the objective of evaluating the viability of using an automated computer application to detect, classify, and quantify cracks on flexible and rigid pavement surfaces from digital images, to be implemented in the annual Pavement Condition Survey (PCS). Phase I of this project was focused on identification and quantification of the rigid pavement cracks from two-dimensional (2D) images collected using the FDOT data collection vehicle. The developed FDOT Rigid Pavement Distress Application (FRPDA) was able to detect joints and assign slabs, detect, classify, and quantify longitudinal, transverse, and corner cracks with higher accuracy, repeatability, and efficiency compared to the current manual windshield method of the PCS. Phase II of this project was focused on identification and quantification of the flexible pavement cracks from three-dimensional (3D) images collected using the Fugro data collection vehicle. The developed FDOT Flexible Pavement Distress Application (FFPDA) was able to detect, classify, and quantify all crack types with higher accuracy, repeatability, and efficiency compared to the current manual windshield method of the PCS. It is recommended that the automated FRPDA and FFPDA be used on a longer length of highway pavements along with a semi-automated survey to conduct quality control of the results and to identify and quantify non-cracking distress types for the PCS.

This Final Report is organized as follows:

- Chapter 1: Task 1. Technology State of the Practice Assessment
- Chapter 2: Task 2. Rigid Pavement Application Design
- Chapter 3: Task 3. Rigid Pavement Application Development and Validation
- Chapter 4: Task 4. LRIS Feasibility on Flexible Pavements
- Chapter 5: Task 5. Flexible Pavement Application Design
- Chapter 6: Task 6. Flexible Pavement Application Development and Validation
- Chapter 7: Task 7. Automated Application Implementation
- Chapter 8: Task 8. Technology Needs and Gaps Assessment

## **CHAPTER 1 – TECHNOLOGY STATE OF THE PRACTICE ASSESSMENT**

Pavement evaluation can be a complex process. Many agencies have developed procedures that they follow for conducting such evaluations. Where “manual” or human raters were (or are still) involved, it was (is) fairly common to have an annual training and “calibration” to provide relatively consistent results, but there is limited data available on how much variability may actually exist within these existing procedures.

As technology advances and traffic concerns continue to test the limits of safety, automation continues to be evaluated as a potential substitute for existing procedures. As is to be expected, questions arise regarding the “acceptability” of such automated data. Of course, this begs the question of what is “truly” acceptable. Each agency needs to establish a context-sensitive and systematic approach to evaluate the accuracy, precision, and efficiency of potential automated distress identification systems for network and project level data collection objectives.

To conduct such an evaluation in a systematic fashion, it is first reasonable to conduct a review of the literature on automated technology for aiding in pavement evaluation. In this process, the current literature review report documents the following:

1. Evolution of automated data collection hardware technology and future trends in the industry
2. Advancements in automated image analysis and processing for aiding in pavement evaluation, and future improvements
3. Implementation considerations and initiatives, including:
  - a. Metrics and analyses for conducting evaluations of accuracy and precision
  - b. Methods for calibration and verification of the technology

In subsequent tasks, the findings from this literature review will be applied to identify:

1. How best to evaluate and compare the current procedures employed by Florida DOT to automated options.

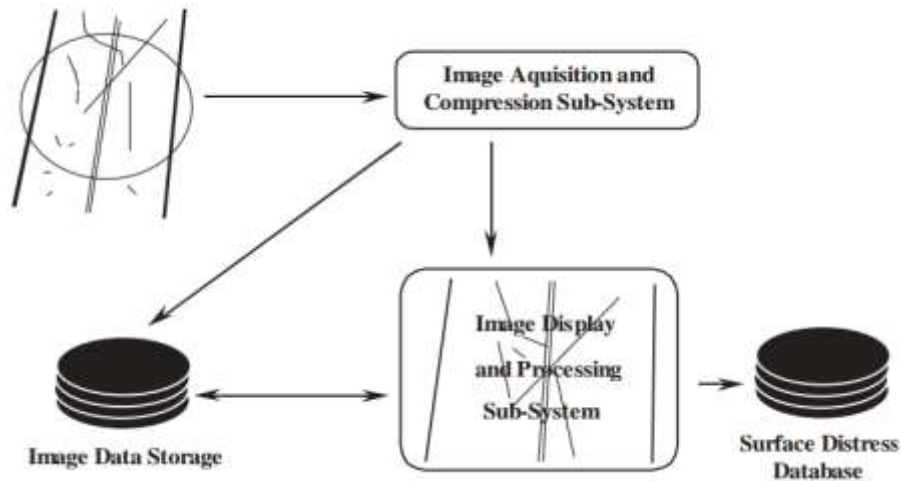
2. Recommendations for getting the optimal results from the system currently available to the DOT.
3. Finally, recommendations for future considerations in the development and/or application of technology to satisfy the needs of Florida DOT.

Every effort has been made to be as thorough as possible in the conduct of this literature review, while keeping these stated objectives (of equal importance) in mind.

## 1.1 Introduction to the Literature Review

During Task 1, the research team reviewed the available literature on the state of the practice regarding technologies for automated crack data collection and analysis for rigid and flexible pavements. The corresponding literature can be divided into three segments; the first on automated distress data collection hardware and data management, the second on automated image analysis and processing, and the third on implementation considerations and initiatives. As displayed in Figure 1, the first two components comprise the system concept for image-based pavement surface distress surveys (McGhee 2004).

The NCHRP Synthesis number 334 provided a summary of the state of the automated pavement distress data collection practice in 2004 and was a relevant document to start the literature review. In addition, the NCHRP Synthesis number 401 reviewed the quality management practices being employed by public road and highway agencies for automated, semi-automated, and manual pavement condition data collection (Flintsch and McGhee 2009).



**Figure 1. The system concept for automated pavement data collection (McGhee 2004)**

Task 1a – state of the practice regarding automated crack data collection: The existing and emerging technologies for collecting pavement surface distress images were reviewed. The current practice by various State Highway Agencies (SHA) and other roadway authorities within the United States and across the world were examined. This examination included investigation of the following parameters:

- Imaging Technology Hardware and Capabilities (scan dimensions, speed, illumination, dynamic range, resolution, crack width, limitations, etc.)
- Location Referencing Equipment
- Image Sampling, Storage, and Compression Information
- Advantages and Disadvantages to network-level condition surveys

Task 1b – state of the art and practice regarding automated crack data analysis: The existing and promising emerging tools for cracking data processing and interpretation were investigated. While the state of the art is constantly advancing, the literature review in Task 1 focused on practical techniques that show promise for implementation. This investigation included but was not limited to the following aspects of data analysis:

- Image Display Tools
- Automatic Crack Type and Severity Identification
- Crack/distress editing and review tools
- Cracking Extent Measurement and Location Referencing
- Accuracy, Precision, and Reliability
- Crack Sampling and Reporting Interval
- Advantages and Disadvantages to network-level condition surveys

To gain from the experiences of past work in this area, the research team reviewed and summarized previous efforts that have been conducted in this area. Several of these are included in the following example reference documents:

- NCHRP Project 1-27: Video Image Processing for Evaluating Pavement Surface Distress (Fundakowski 1991).
- Paredes's PAS: Automated Distress Measuring Device (Lee 1991).
- University of Texas at Austin Center for Transportation Research (CTR): Automated Pavement Cracking Rating System (Xu and Huang 2003).
- NCHRP IDEA Project 88: Automated Pavement Distress Survey through Stereovision (Wang 2004).
- NCHRP IDEA Project 111: Automated Real-Time Pavement Crack Detection and Classification (Wang and Gong 2007).
- Visual Retrieval of Concrete Crack Properties for Automated Post-Earthquake Structural Safety Evaluation (Zhu et al. 2011).
- Automatic Crack Detection and Classification Method for Subway Tunnel Safety Monitoring (Zhang et al. 2014).
- Multiscale Crack Fundamental Element Model for Real-World Pavement Crack Classification (Tsai et al. 2014).
- US DOT RITA: A Remote Sensing and GIS-Enabled Asset Management System (RS-GAMS), (Tsai and Wang 2014).

In this task, the research team was looking for ideas, concepts and approaches to facilitate the codification of the proposed protocols. These findings were highlighted to aid in subsequent tasks of this project. Known deficiencies in current automated detection practices occur when the pavement is slightly damp, when the cracks are sealed, spalled, filled with salt or sand, where there is staining in fine cracks (this makes them evident in a forward image, but not necessarily in downward pavement views) or various types of crack sealant.

The current automation practices still focus on cracking related distresses and not on other common visual distresses such as bleeding, depressions, and patching. While cracking is the focus of this project, ravelling and patching among other distresses are also a concern and are captured in the current FDOT manual windshield surveys.

This chapter is organized in five sections. Following this introduction, Section 1.2 provides a summary of the information reviewed on automated distress data collection hardware and data management. Section 1.3 summarizes the findings on image applications, analysis and processing. Section 1.4 addresses implementation considerations. This is considered of particular importance, as the actual implementation into practice has tended to present the greatest challenges in the advancement of the automation process. Section 1.5 provides the summary and recommendations based on these reviews.

## **1.2 Automated Distress Data Collection Hardware and Data Management**

This section discusses the state of the practice regarding automated distress data collection hardware for identification and documentation of pavement surface distresses and related information, as well as the associated management of this data. The following technologies are discussed:

1. The right of way cameras used for forward roadway images
2. Analog vs. digital pavement imaging
3. Area scan
4. Laser imaging
5. 3D imaging
6. Other technologies such as LiDAR, satellites, airplanes, unmanned aerial vehicles, and photogrammetry

### **1.2.1 Right of Way (ROW) Cameras**

One of the earliest methods of obtaining pavement images was simply to use a right of way camera and focus it down towards the pavement surface. This method was utilized throughout the 1980's when video cassette tapes were the main storage source for

video. The technology has advanced with time and is still used in some areas of the world with high resolution digital camera systems (PMS 2015). The advantage to this method is that it is cost effective and requires standard configurations of hardware, power, and computing power that are commercially available. The disadvantages are that it is susceptible to shadows and the image is on an angle, so some cracking will be difficult to see. The other significant disadvantage is that it does not facilitate automated processing of the images and requires manual identification of distresses. This method is still utilized today mainly as a method of collecting highway asset imagery due to it being very cost effective and the high amount of detail that can be captured with the new high-resolution cameras.

### **1.2.2 Analog versus Digital Pavement Imaging**

The move from analog to digital imaging was a big advancement in the video log industry. Digital images retained all the benefits of analog video but also provided a number of key advantages:

- Centralized storage of images – images can all be stored on a central server that everyone can access so there is no longer the need to hunt down the correct video tape.
- Increased access speed – analog video required you to find the video tape then fast forward to the correct spot using a VCR. With digital images users can access them from their own computers and jump right to the image(s) needed.
- Distribution – Digital images can be easily e-mailed or copied and sent to others (Fugro Roadware 2004).
- Quality – Digital image technologies have greatly improved the resolution and quality of images beyond the storage capacity of video cassettes.

As technology advances so do the advantages of using digital images. The cameras become faster, able to capture images more frequently, and with better quality than analog video. The evolution of digital technology in the pavement evaluation industry was largely a result of significant advancements in existing camera technologies and data storage capacity.

### **1.2.3 Area Scan**

Pavement imagery using area scan technology consists of high-resolution cameras extending from the back of the vehicle. They point straight down at the pavement and

each takes an image of the pavement surface that is flat and consistent for measurement. Early on in development, the images were recorded and displayed side by side on the office workstation. As technology advanced, area scan cameras created digital images usually in Joint Photographic Experts Group (JPEG) format that could be stitched together to create continuous pavement images.

Advantages to area scan systems are that they are cost effective and as technology improves better quality cameras can be used to increase resolution and image quality. The image resolution and quality depend both on the quality of the used cameras and the lighting system.

The disadvantage to an area scan system is that it requires a light source to reduce shadows for trees, buildings or overpasses significantly increasing the power output required by the vehicle. This additional lighting is often a large draw of electrical power for the data collection vehicles requiring additional generators or power generation.

These 2D images were designed to be used for both automated and semi-automated pavement distress identification and were easily calibrated to measure within the images to quantify crack lengths, areas, and widths. The range in quality of the cameras can show a range of surface textures, but coarse-grained pavement textures can sometimes make it difficult to identify smaller width cracks and other defects between large aggregates. Also, area scan images are very susceptible to other optical challenges in the field such as unusual lighting conditions, damp pavement, and crack spalling. These issues can cause the images to show irregularities along the crack that make the width of the cracks difficult to accurately measure. This has also impacted visual surveys where a slight dampness can cause distress to appear more severe than it actually is.

Figure 2 shows an older version of Fugro Roadware's Automatic Road Analyzer (ARAN) vehicles equipped with an area scan system.





**Figure 2. Fugro Roadware's ARAN equipped with area scan system**

### **Continuous Lighting**

To properly view the pavement surface, lighting was found to be very important in capturing conditions, as there needs to be enough lighting to adequately illuminate the surface and still show shadows within the cracks. Constant lighting was an older technology used to illuminate the pavement for imaging. As an example, the early FDOT line scan system utilized ten 150-watt lamps to illuminate the pavement surface for the camera (Gunaratne et al. 2003). The drawback to this method was that the illumination was not as bright as the strobe system and it used considerably more power. Figure 3 shows an example van with constant lighting equipment.



**Figure 3. Road survey vehicle equipped with constant lighting**

## Strobe Lights

An effective light source for area scan cameras is the use of strobe lighting. These lights are synched with the camera to fire a high intensity light as the image is captured. Since these lights are strobes they can be a lot brighter than standard lights and consume less power. This allows collection of pavement images at any time of the day from bright sunlight to nighttime collection. Figure 4 shows a Fugro BRE Automated Distress Vehicle (ADV) with strobe lights, and a sample of the pavement surface images captured with that system.



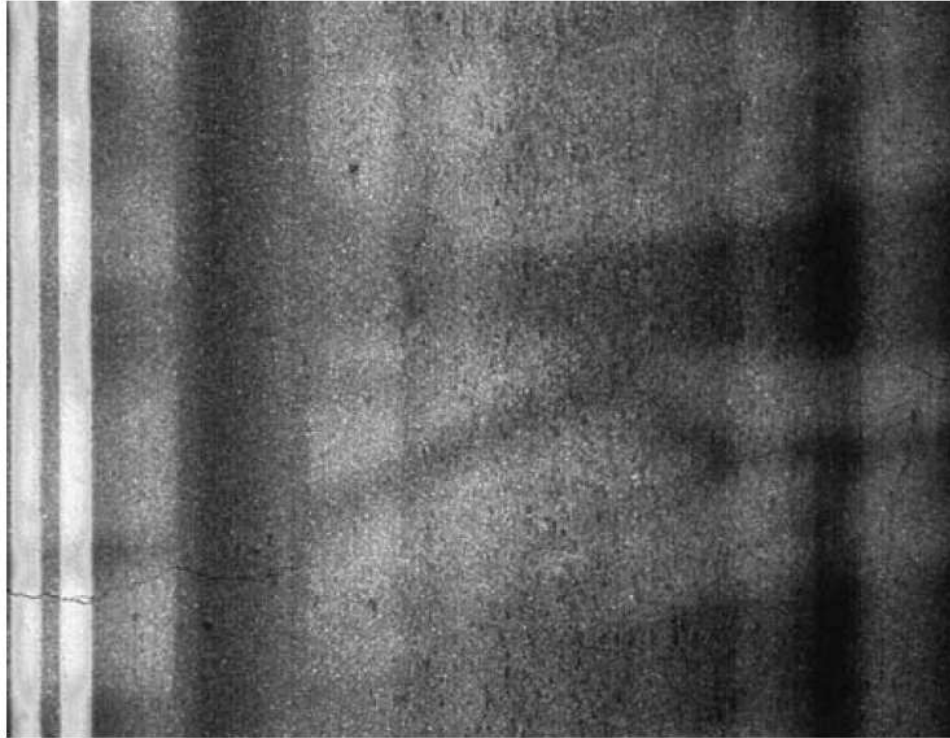
**Figure 4. Fugro BRE Automated Distress Vehicle (ADV)**

### 1.2.4 Line Scan

#### Non-Laser Line Scan

Early line-scan cameras capture single lines which are then compiled to form a 2-D image. One of the advantages the line scan camera has over area scan is that many of the production systems were higher resolution images, up to 6,000 pixels per line (Gunaratne et al. 2003). The main disadvantage to line-scan cameras is that they require a higher light intensity than area scan. Shadows on the road can be picked up by the system and mistaken for distress if the lighting is not sufficient. Many of these

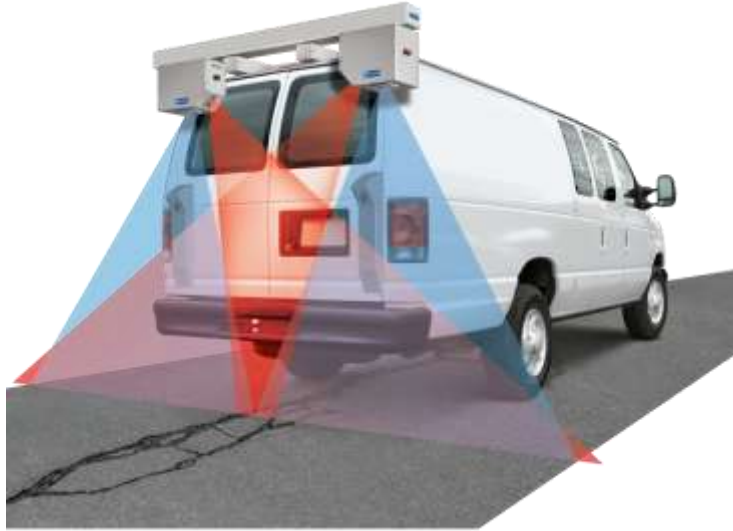
systems had long dark streaks from shadows of mounted equipment that caused complications during crack identification. Figure 5 shows an example non-laser line-scan camera image with the shadows cast on the pavement surface (McGhee 2004).



**Figure 5. Example Line-Scan Pavement Image with Vehicle-Cast Shadow in Left Wheel Path (McGhee 2004)**

### **Laser Road Imaging System (LRIS)**

Introduced in 2006 by the INO (Institut National d'Optique) of Quebec in Canada, Laser Road Imaging System (LRIS) is composed of two high resolution line-scan cameras and two illuminating lasers that are configured to capture images of full 4m transverse road sections with up to 1mm x 1mm resolution (4096 pixels/line) at speeds that can surpass 62 mph (INO 2014). This system uses two illuminating laser beams that are angled transversely onto the road and then two cameras that pick up this laser line. Because the lasers are angled, they create shadows within the cracking area and therefore the cracks become more visible in the images. Figure 6 shows a schematic of the LRIS on an inspection van. Based on the LRIS sensors produced by INO, Pavemetrics provides the hardware and software libraries to the integrators and vendors who have the responsibility to develop their own software. INO recommends JPEG or JPEG 2000 to be used for data compression (Wang and Smadi 2011).



**Figure 6. LRIS system on inspection vehicle**

The main advantage of the LRIS system over other camera-based systems is that it is not dependent on light as it can collect through shadows or at night with the same quality of image due to the intensity of the lasers. Another advantage to this system is that because it uses laser illumination it consumes less power, about 200 watts versus thousands of watts of traditional lighting systems (Wang and Smadi 2011). The LRIS is also more compact than the area scan systems. The high resolution and consistency of this equipment caused the LRIS to be a widely used system globally.

A disadvantage to the LRIS system is that because it creates images line by line any dirt or dust on the camera lens can create streaks in the image. These streaks result in black lines appearing in the images and can cause difficulty with automated crack detection software that uses the light and dark contrast to identify cracks. Figure 7 shows an example LRIS pavement image showing dark streaks that cannot be seen on the ROW image.



**Figure 7. Example LRIS pavement image (right) showing dark streaks that cannot be seen on the ROW image (left)**

### **1.2.5 3D Pavement Imaging Systems**

3D pavement systems use synchronized scanning lasers that are projected onto the pavement surface which are then captured by one or more cameras. The lasers can also measure the distance to the surface to give the image a depth. This is where the advantage to these systems lie, the depth measurement makes crack detection much easier than 2D pavement systems where pavement texture and lighting can make fine cracks hard to distinguish. Another advantage to 3D systems is that they are less sensitive to the problems of identifying cracking on damp pavements. On 2D systems dampness causes a lot of false positives and increased width results as the cracks are highlighted and have a wider dark range on the surface than they actually are to both the naked eye and imaging technology.

3D pavement systems are quickly becoming the most popular method of collecting pavement data due to the additional information available, high resolution images, and repeatable results. Many large road agencies have already or are currently transitioning to the use of a 3D laser pavement system and it looks like this trend will continue.

#### **Laser Crack Measurement System (LCMS)**

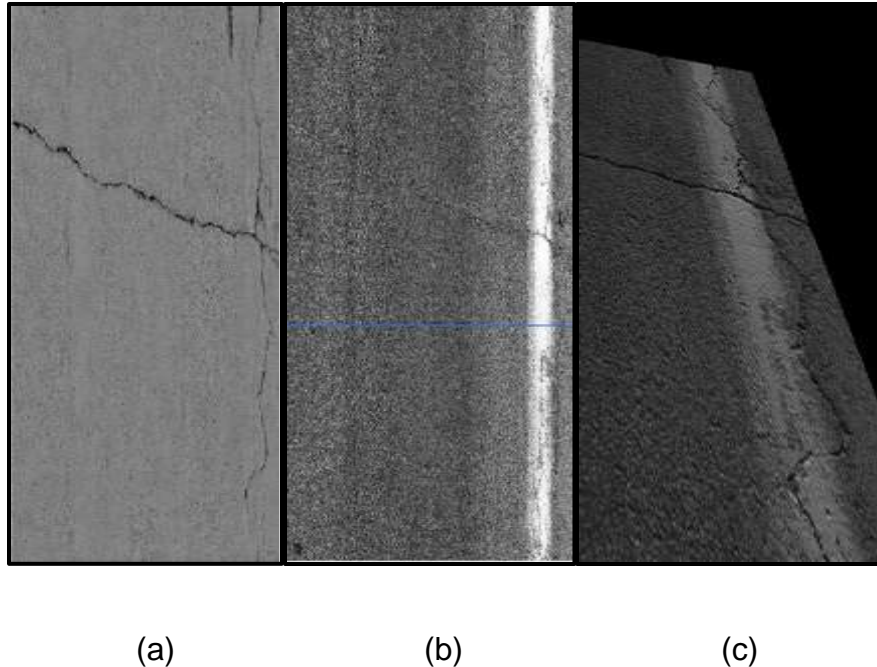
The most commonly used 3D imaging technology globally is the Laser Crack Measurement System (LCMS) developed by INO and provided by Pavemetrics Systems Inc. The LCMS consists of two high-speed cameras, custom optics and laser



line projectors to acquire both the intensity of reflected light and depth ranging information of infrastructure surfaces at speeds up to 62 mph (Habel et al. 2014). The LCMS system has a resolution of up to 4,096 points and captures 5,600 profiles per second for a transverse spacing between profiles of 5 mm (0.2 in) at 62 mph (Fugro Roadware 2012). The two lasers are projected onto the surface to be inspected and its image is captured by a camera system on a different angle (Figure 8). This allows the sensors to simultaneously triangulate both the 3D “Range” (height of each pixel) and the reflected light “Intensity” (the intensity of the reflected laser light for each pixel) of the scanned surfaces (Figure 9). This data is recorded in a proprietary and licensed file format known as a FIS file. Through post processing of these FIS files, automatic distress detection can be completed along with creation of the orthogonal images for viewing.



**Figure 8. LCMS sensors mounted on a survey vehicle**



**Figure 9. LCMS image types; (a) range, (b) intensity, (c) merged 3D**

The LCMS is often used by data collection device integrators and vendors including: APSA (Administracion de Pimientos Sociedad Anomia), Australian Road Research Board (ARRB), Dynatec, enterInfo, EuroConsult, Fugro Roadware, International Cybernetics Corporation (ICC), Mandi Communications, Rambolt, Ronda's, and Vectra. The LCMS is the most widely used pavement imaging technology for new vehicles in 2015.

#### **Others in Development**

Waylon Systems has developed the PaveVision3D which is a multi-camera system for 1mm resolution in all dimensions of pavement surface 3D imaging. This system utilizes up to 4 cameras on each side of the lane to collect the surface information on higher frequencies. Data stitching algorithms are used to assemble the measurements on each side of the lane and then both sides are stitched together into a single file with 1mm x 1mm resolution for both the intensity and range data (Wang 2011). The disadvantage to this system is that it can only get a true 1mm resolution at low speeds of around 15 mph. Another disadvantage is that it's much harder to synch multiple cameras with movement of the vehicle that often occur while testing at higher speeds during network level collection.

Waylink Systems has also been experimenting with other frequency lasers to improve the accuracy of the measurements with high frequency, short wavelengths of light. There are distinct advantages to the measurements with other frequencies. However,

the increased power also changes the health and safety class of these lasers, which may have challenges with testing on open roads.

### **1.2.6 Other Technologies**

#### **LiDAR**

Light Detection And Ranging (LiDAR) is a laser-based technology that measures distance by lighting a target with a laser beam and analyzing the reflected light. LiDAR is very useful for surveying applications like digital terrain modeling from airplanes or road geometry and assets inventory for transportation agencies. The biggest drawback for the use of current LiDAR systems for pavement imagery is the resolution and frequency of collection on current models. Currently LiDAR can get an accuracy of up to 10mm, but this would be insufficient to accurately measure pavement cracks. Many of these systems focus only on the distance measurement information in the image, which provides no information regarding changes in pavement surface color. The color intensity information is needed for detecting construction changes, repairs, and patching along the pavement surface.



**Figure 10. A LiDAR survey of a highway (left), and a LiDAR antenna (right)**

#### **Satellite**

Satellites can cover large areas very quickly but are limited by revisit times, atmospheric interferences, and spatial resolution (Schnebele et al. 2015). In the future if satellite imagery was able to improve on the resolution, they would still be affected by things like lighting and line of sight caused by overpasses, traffic, and trees.

#### **Air Based Surveys**

Air based surveys (both fixed wing and rotary wing) can get better resolutions than satellites due to the reduced elevations and can be fitted with various sensors and recording devices (Schnebele et al. 2015). Currently airplanes and helicopters are used for various remote sensing applications but when it comes to pavement imagery there are limitations. Due to the speed that airplanes travel it would be hard to achieve the required resolution to create usable pavement images due to motion blur. Aircraft are



also susceptible to wind shear and turbulence that would make getting constant imagery difficult and like satellites they would be subject to line of sight and lighting concerns. Operating aircraft is also expensive and requires properly trained personnel to operate. Airspace restrictions also are another concern as many network surveys are conducted around urban areas that could have security concerns and reduced visibility due to structures. Figure 11 shows Fugro's FLI-MAP 400 system, which provides high accuracy topographic and surveying data by integrating state of the art surveying techniques, such as LiDAR and high-resolution photo and video imagery.



**Figure 11. Fugro's FLI-MAP400 (Fast Laser Imaging - Mapping and Profiling) system**

### **Unmanned Aerial Vehicle**

Unmanned Aerial Vehicles (UAV) or Drones are a less expensive alternative to airplanes or satellites and can provide high resolution, near real-time imagery (Schnebele et al. 2015). An UAV has a few advantages over other aircraft with respect to collecting pavement images. UAV's are cheaper, can fly at lower altitudes and are quicker to deploy than most manned aircraft. With changing government regulations, these will also not have all the airspace restrictions that the larger aircraft would have and are much more maneuverable although more susceptible to wind shear. UAV's can currently be effective for collecting data on gravel roads where high-resolution distress imagery is not required. Limitations include objects blocking road surfaces like traffic, bridges, trees, and buildings. As with the other airborne methods lighting is an issue where shadows from trees, vehicles, and power lines can affect the quality of imagery.

Aircraft options for pavement imagery have possibilities but currently have not been explored thoroughly. Current technology for vehicle surveys has limitations when applied to aerial platforms such as distance, location accuracy and collection path.

## **Photogrammetry**

Photogrammetry is a stereo vision technique that involves taking multiple images of the same object from multiple angles and using these images to generate a 3D image of the object. Initial investigations show significant potential for 3D distress detection and modelling with higher spatial precision and a higher level of automation than laser-based 3D profilers (Ahmed and Haas 2010). This system could also be easily upgraded over time as new technologies and higher resolution cameras become available. The main drawback to this method is the need for real time processing which can be limited by computing power and image blurring due to camera motion. However, as technology improves, these drawbacks will have less of an impact.

### **1.2.7 Image Capturing Specifications and their Effects on Crack Identification**

The image quality plays a crucial role in gathering the most accurate and comprehensive data on distress from pavement images collected using the area scan technology. The ideal pavement image is crisp with no motion blur, evenly and well lit, and of high enough resolution to view details. The quality of digital image can be affected by the illumination, dynamic range, shutter speed, resolution, optic quality, size of pixels and the image sensor capabilities.

To capture high quality pavement images, illumination or brightness is an important element, which is proportionally dependent on the wavelength and the surface reflectance (Sokolic 2004). Image brightness is also dependent on the exposure time controlled by the shutter speed and aperture, and the sensitivity of the image sensor. Brightness resolution refers to the number of brightness levels that can be recorded in any given pixel. In an 8-bit grayscale black and white image, each pixel is black, white or one of 254 shades of gray (total 256 levels).

Dynamic range defines the ability of an imaging device to record or display the full range of optical density. Theoretically, higher dynamic range can detect greater image detail in dark shadow areas of photographic images (Wang and Smadi 2011). Dynamic range for pavement images is normally 8, 10 or 12 bits. Currently 24-bit color images are used only in right-of-way color images for asset management applications.

The shutter speed of an area scan camera is measured in two ways; number of images captured per unit time, and absolute time the camera shutter is open for one image collection. As the shutter speed increases, more images can be taken within a given timeframe, which translates to a higher operating speed with less blur. But as the shutter speed increases, there must be an adjustment since the exposure time is decreased. This means that for the image to be properly lit there must be an adjustment to either aperture or International Standards Organization's (ISO) sensitivity rating – the sensitivity of the image sensor to light. If the exposure is not adjusted, the cracks may not be well detected due to poor lighting conditions. Area scan systems typically take

one pavement image every 2 to 3 feet. Typically, ROW images are taken once every 26.4 feet, and travelling at 60 mph, a shutter speed of 3 or 4 fps is sufficient for this purpose (Fugro Roadware 2004).

One of the image quality indicators is the degree of resolution in terms of pixels per area. In general, the higher the number of pixels per area, the more likely it is that pavement surface details are picked up. It is important that the other aspects of image quality (e.g. optimum illumination) are also satisfied to ensure that the data reflected in the pixels are accurate.

For example, a line scan camera with a resolution of 4096 pixels/profile ensures areas as small as 1 mm can be detected. Typically, it is expected that two pixels are required to identify patterns such as cracks. This indicates a 1mm resolution is capable of recognizing cracks with a width as small as 1mm and more reliably 2mm. Table 1 shows the theoretical minimum visible crack widths corresponding to camera resolution using both line scan and area scan cameras. However, determining crack width from the images is subjective as representation of a crack in an image may include many levels of shades (Wang and Smadi 2011).

**Table 1. Image resolution and theoretical minimum visible crack width (Wang and Smadi 2011)**

<b>Transverse Resolution (pixel)</b>	1,300	2,048	4,096
<b>Visible Crack Width (mm)</b>	3	2	1

The specific technical details such as shutter speed, aperture, depth of field, lens quality, sensor type, dynamic range, focus range, and resolution varies with the model and build of the imaging system used, but an example of both an area-scan and line-scan camera are listed in Table 2.

**Table 2. Example specs for line-scan and area-scan cameras**

<b>Area Scan Camera</b>	Hitashi KP-F120	<b>Line Scan Camera</b>	LRIS
<b>Shutter Speed (fps)</b>	15, 30, 60, or 120	<b>Line Rate (lps)</b>	28,000
<b>Image Resolution</b>	1392 x 1040 pixels	<b>Image Resolution</b>	4096 pixels/line

### 1.2.8 Image Quality Management

Pavement surface imagery is typically collected in compliance with the American Association of State Highway and Transportation Officials (AASHTO) provisional protocol (PP) number 68 (AASHTO 2014a), which was later adopted as AASHTO

Standard R86-18 (AASHTO 2018b). This standard calls for these requirements in terms of image quality:

*“4.3.1. The images must provide sufficient difference between data point values representing distressed and non-distressed areas that subsequent distress detection techniques can delineate a minimum of 33 percent of all cracks under 3 mm (0.12 in.), 60 percent of all cracks present from 3 mm (0.12 in.) and under 5 mm (0.2 in.) wide, and 85 percent of all cracks 5 mm (0.2 in.) wide or wider regardless of orientation or type. The determination of this capability will be made utilizing a minimum of ten 0.03-km (100-ft) samples containing an average of at least five such cracks per sample.*

*4.3.2. The images should be sufficiently void of erroneous differences between data point values that a section of pavement without distress, discontinuities, or pavement markings contains less than 3 m (10 ft) total length of detected false cracking in 50 m<sup>2</sup> (540 ft<sup>2</sup>) of pavement. The determination of this capability will be made utilizing a minimum of ten 0.03-km (100-ft) samples of various types that meet the criteria.”*

There are no other standards that would recommend more comprehensive requirements for quality management measures taken for pavement images for crack identification. This is an important topic that has received little attention. There are two ways to filter through the collected images, automated or manual. One example of an image QA procedure is to run the collected images through software designed to review the range of values recorded in images. These pixel values will indicate if the images are too bright or dark to be helpful. Other information can also be verified such as metadata and camera settings stored within files. Automated checks do not reliably evaluate image quality, focus, or ability to identify features.

The following two documents are the predominant source of information regarding the state of practice in quality management of pavement data collection. While they address some aspects of pavement images, they do not provide specific guidelines to ensure pavement image quality.

- NCHRP Synthesis 401, Quality Management of Pavement Condition Data Collection (Flintsch & McGhee, 2009)
- FHWA Practical Guide for Quality Management of Pavement Condition Data Collection (Pierce et al. 2013)

Recognizing the need for a unifying image format that can facilitate data analysis, reporting, sharing, and evaluation, the Federal Highway Administration has recently issued a request for quote on Standard Data Format for 2D/3D Pavement Image Data.

Expected benefits include facilitating workable protocols for condition surveys, improving implementation of new technologies, and accelerating the development potential of analysis tools for pavement condition.

### **1.2.9 Image Storage, Compression, and Database Management**

The collected pavement images are a valuable resource due to the large amounts of data they provide, but they come with large file sizes. This raises issues with the image storage, compression, and database management. While collecting the data, there must be enough memory to store at least one run's worth of data on-board the vehicle. An example of the vehicle memory capacities of the on-board system is a computer for each camera system with removable hard drives with sizes proportional to the length of road to be tested and the resolution of the images. The estimated storage required is 1.3 GB per lane-mile for the pavement image data and 76 MB per lane-mile for high definition ROW images. Some imaging technologies are proprietary and require software license information to review contained data.

The images are often compressed to optimize the amount of data available and the storage requirements. Different file types have different balance of files size reduction and potential reduction in data quality. Traditionally, the imaging data was often saved as a JPEG file with around 75% compression at the end of the run before being sent to the workstation, but later a compression format called JPEG 2000 was found to compress the image from around 1.4 MB to 400 KB, with comparable image quality (Gunaratne et al. 2003; McGhee 2004).

To obtain greater compression ratio, the JPEG algorithm used in pavement imaging is lossy, which means some information is lost during the compression process and original raw image cannot be restored (Wang and Smadi 2011). Database tables are commonly used to store the location data, sensor data, image location and other relevant details regarding the field operation. Custom software can be made for easy and rapid access to the compressed images through the computer networks.

### 1.2.10 Location Referencing

The collected road data must be provided with location context, and there are a couple of systems that can be used in conjunction or isolation. The three most commonly used types are Global Positioning System (GPS), inertial aided GPS systems, and linear referencing systems. The advantages and limitations of each system are summarized in Table 3.

**Table 3. Advantages and limitations of location referencing systems**

System	GPS	Inertial	Linear Distance
<b>Description</b>	Uses satellites and triangulation for location and time information	Uses GPS, accelerometers and gyroscopes to calculate data on acceleration, angular rotation, vehicle orientation, grade, and road curvature	Measures linear distance and velocity travelled by the vehicle
<b>Advantages</b>	Detailed information	Highly accurate even with vehicle motion	Simple; reliable; not affected by speed
<b>Limitations</b>	Clock errors; delays or occasional data loss; noise and bias	Still requires GPS for start and end position; errors can accumulate between high quality GPS positions.	Limited data; requires external reference for start and end position; systematic error grows with distance traveled
<b>Best Uses</b>	In open locations, travelling at low speeds, good weather, and minimum of 4 visible satellites	For short-term observations	Used in conjunction with another system to provide more context

The GPS uses triangulation and satellite information to provide location and time information most commonly in terms of latitude, longitude and elevation. This system provides a high level of detail and information. But there are limitations such as loss of signal and reduced accuracy (Gunaratne et al. 2003).

The inertial measurement unit (IMU) is a self-contained unit (working in tandem with a GPS system), which measures relative displacement from a start point based on three accelerometers (one for each of the primary axes), and three gyroscopes. The combination of these six units measure acceleration in all directions to determine change in position, as well as angular rotations, vehicle orientation, grade and road curvature. The benefit for using this system while it is coupled with the GPS results is that it is self-contained and is highly accurate even with vehicle motion. This improves the accuracy of GPS and helps to fill in some gaps in satellite coverage. The addition of

vehicle roll, pitch, and yaw to vehicle position allows for the measurement of other factors such as pavement cross-slope, longitudinal grade, and measurements within ROW images (Gunaratne et al. 2003).

A linear DMI system is one which measures the linear distance that the vehicle has travelled. This particular system is simple, reliable, but like the inertial system, needs an external reference start position. As the system only provides linear measurements, it does not provide detailed enough information when used in isolation. There are two broad methods to measuring linear distance: contact and non-contact. Contact DMI's require frequent calibration but offer an increased accuracy compared to non-contact DMI's.

Most vehicles collecting pavement data are equipped with a combination of the above systems to mitigate the drawbacks to each and provide reliable location data for every point along the run. For example, the ProGPS-DMI system integrated by Ames Engineering uses GPS and a linear distance measuring instrument (DMI) to achieve a reported location measurement accuracy of 0.05%.

In summary of this section, it should be noted that significant advancements in automated distress data collection hardware have occurred over the past decade. It should be expected that similar advancements will likely be experienced in the decade ahead. With this in mind, implementation efforts should be modular and flexible in nature to take advantage of the technology evolution.

### **1.3 Automated Image Analysis and Processing**

This section discusses the results of the literature review regarding the state of the art and practice of automated crack detection software. Knowing pavement conditions and symptoms of the deterioration type is critical to maintaining road networks in a safe and cost-effective manner, and to make informed decisions, there must be reliable data on which to make such evaluations. Traditional methods of obtaining data include manual and semi-automated surveys, which involve significant human intervention and have proven time-consuming given the extensive length of road networks. In response, there has been extensive research in automating the process to establish a more efficient and repeatable distress evaluation system.

#### **1.3.1 Basic Image Processing Concepts**

As it was discussed in Section 1.2 of this document, there are a variety of mediums which can be used to collect the pavement images such as lasers, 2D or 3D imaging systems. Once the data is collected, it is often pre-processed to be fit for use for manual or automated distress detection. The focus of the current project is mainly on cracking distresses. A cracking distress is a crevice or an opening on the pavement surface as a

result of stresses caused by traffic loading or environmental conditions. Each occurrence of cracking is described by its features. To collect crack features, such as length, orientation, and width, the potential cracks must be identified in calibrated images. Once the locations of cracks are identified, width, shape, and patterns are extracted.

Due to the proprietary nature of most of the available software, the details of the crack detection algorithms are not published in the literature. Figure 12 illustrates an example of general steps for feature (crack) detection, quantification, and classification procedures, which are typically followed to conceptualize pavement crack detection algorithms. The steps illustrated in Figure 12 can be succinctly described as follows:

**(Step 1) Image Normalization:** The first step of the process is to normalize the image depending on the road surface type. If this step is not performed, then automated crack detection would not be possible across many surface types since a heavily textured road (i.e. open graded) would output many false positive cracks. This is corrected by using a depth threshold parameter which is determined automatically using the local texture information of the road surface. For roadways with rougher surface texture, the depth threshold for crack detection should be higher to avoid classifying texture anomalies (e.g. raveling) as cracks.

Appropriate transformations are applied to the input image to normalize the intensity response. This normalization is necessary to neutralize the effect of:

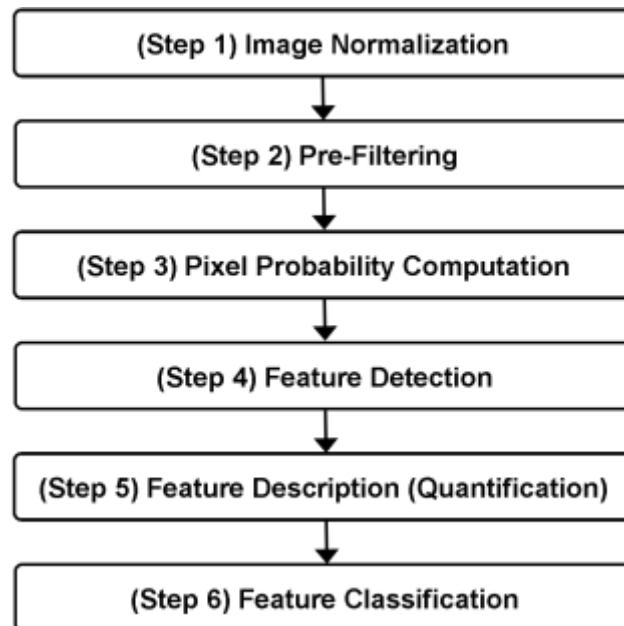
- 1) Ambient lighting
- 2) Artificial lighting
- 3) Difference in sensor impulse response
- 4) White balance of images

There are several transformations that may be employed for this purpose, and the selection of a suitable one depends on the image configuration. A few of the common transformations are:

- a) Histogram equalization
- b) Histogram matching



- c) Color transforms
- d) Shadow identification and removal
- e) Gamma correction



**Figure 12. General example procedure for crack detection, quantification, and classification**

**(Step 2) Pre-Filtering:** The pavement surface image is divided into smaller regions and each region is then subjected to a battery of tests of increasing complexity to quickly identify regions where it can be trivially concluded no feature of interest (specifically cracks) exists. This helps save processing time by limiting the computationally expensive detection operations to be limited only to regions where there is a high chance of occurrence of cracks. It also helps reduce the number of false positives. Region division may be done based on:

- a) Rectangular tiles
- b) Super pixel
- c) Texture analysis
- d) Segmentation

The common tests to identify such regions can be based on:

- a) Histogram
- b) First order and second order statistics
- c) Texture properties
- d) Local binary patterns
- e) Steerable filters
- f) Difference of Gaussian features
- g) Integral images

**(Step 3) Pixel Probability Computation:** In this step, each pixel in the identified regions (where there is a high chance of occurrence of cracks) is assigned a probability score to indicate the possibility of it belonging to a feature (specifically a crack). The higher the score, the more likely it is to belong to a feature. These scores may be computed using one of the following methodologies:

- 1) A pixel can be assigned a sum of tuned filters (e.g. Gabor filter) response.
- 2) A pixel can be assigned a weighted sum of pixel features in the neighborhood. The optimal weights can be determined using Supervised/Unsupervised Machine Learning techniques (for example Support Vector Machines, or Neural Networks) from prior example sets.
- 3) In the case of a crack, it can also be computed as the difference of pixel value from the median/mean value of pixel intensity in the neighborhood.

The computed pixel probability map can be combined with a similar map from other calibrated sensors (for example a Range Sensor, or GPR) to improve the probability estimates. The final probability map is then filtered using morphological operations, as the expected features (cracks) have a structure to them. Pixels belonging to the true feature are not significantly affected by these operations, but the pixels having high probability due to noise are suppressed.

**(Step 4) Feature Detection:** The final pixel probability map is divided into regions as in the pre-filtering step and in each region the multiple features (for example two cracks, one longitudinal and one transverse) are extracted. The extraction can be done by:

- a) Dynamic programming-based path selection
- b) Flood fill followed by boundary/skeleton detection
- c) Connected pixel tree/graph extraction based on adaptive threshold

**(Step 5) Feature Description:** For each detected feature, various properties can be computed to describe the feature. The properties can be:

- 1) Geometric properties like length, width, area, bounding box, axis of orientations
- 2) Photometric properties like texture parameters, average intensity, intensity variations
- 3) Feature specific properties like in the case of cracks it can be crack width, crack density in neighborhood, crack nodes
- 4) Longitudinal and transverse linear and spatial location referencing

**(Step 6) Feature Classification:** For each detected feature, the descriptor can be used to classify the feature. In case of cracks it may be as follows:

- 1) Axis of orientation can be used to classify Transverse and Longitudinal cracks
- 2) Crack density can be used to classify pattern cracking (such as map cracking or fatigue)
- 3) Width, density, and position of cracks can be used to classify cracks by severity
- 4) Proximity to other detected cracks or joints

### 1.3.2 2D Image Processing

The following sections will focus on the state of the practice in application of 2D pavement images for the general steps of image enhancement, identification of potential cracks, and classification of crack features.

#### **Image Enhancement: Normalization and Pre-Filtering**

To mitigate noisy data and improve crack visibility from the raw 2D pavement images, there have been a variety of research efforts in refining pre-processing methods to enhance these images. This step aims to reduce the crack detection sensitivity to lighting conditions and pavement texture to focus solely on cracks (Sy et al. 2008). Most image enhancement methods involve the initial segmentation of the pavement images to grey-scale, image equalization, or combinations including the use of morphological tools (Gavilan et al. 2011). This image processing has most commonly been applied in two locations, as the first step or after image segmentation if the process involved splitting up the pavement images (Wang and Gong 2007). There are many variations in the processes and steps taken to prepare the images for crack detection. For example, the Canny edge detector uses a Gaussian filter, where a method developed by Ayenu-Prah and Attoh-Okine (2008) called the bi-dimensional empirical mode decomposition (BEMD) uses a transformation to remove noise (Ayenu-Prah and Attoh-Okine 2008). Table 4 represents the major techniques used for pre-processing pavement images.

Often, the underlying assumptions govern exactly what the image enhancement focuses on. For example, if cracks are identified as having darker intensity than surrounding cells, a histogram equalization method can be used in conjunction with a gray-scale thresholding method to filter the images (Sy et al. 2008; Gavilan et al. 2011). But in most cases, these filtering methods need to be adapted to support the specific texture conditions, and even still will reduce effectiveness at detecting cracks in highly textured pavements (Subirats et al. 2006). A recent research study performed a texture analysis to address the issue of detecting cracks in highly textured pavements, where other methods often mistake the surface texture for cracks. By splitting the pavement image into sub-images with relatively uniform texture backdrops described by five unique parameters, an Artificial Neural Network (ANN) can identify the cracks within the sub-images (Mathavan et al. 2013).

**Table 4. Major techniques used for pre-processing pavement images**

<b>Pre-Processing Technique</b>	<b>Description</b>	<b>Advantages</b>	<b>Limitations</b>
Texture Analysis and Self Organizing Map (SOM)	Define 5 texture properties to identify different surfaces (distinguish different surfaces through overall texture), then the SOM splits the pavement image into several sub-images based on pavement normal background	Reduces noise based on pavement texture by isolating cracks into areas with relatively uniform background texture	Used in conjunction with SOM (which requires program training and sensitive to under or over fitting), precision of roughly 75%
Gradient Histogram Analysis	Define crack pixel intensity as darker than non-crack pixels based on histogram analysis of pavement images	Filters out noise and is simple	Often thresholds are empirical or must be adjusted per pavement surface variations and lighting conditions
Bi-Dimensional Empirical Mode Decomposition (BEMD)	BEMD removes noise via transform by sifting the data to validate instantaneous frequency	Allows for separation of filtering from certain crack edge detection methods	Not well researched and thus not very effective

### **Identifying Potential Cracks: Feature Detection**

Most methods for crack identification on 2D pavement images fall under one of the five general categories:

- 1) intensity-threshold-based
- 2) edge detection
- 3) transform-based
- 4) seed-based
- 5) machine-based

Generally, the intensity-threshold-based methods define cracks as having a darker intensity than surrounding non-crack area. The edge detection methods define a crack edge as the local maximum of the gradient (measured as a change in intensity), and as

such defines a crack map (Zou et al. 2012). Transform-based methods use a transformation such as Fourier transform to take the data extracted from pavement images to different domains (coordinates or states), to find the locations and sometimes the properties of cracks. The seed-based methods initiate by identifying certain cells as crack seeds, and then grow connecting paths by either percolation or calculation of normalized distance to create the crack areas. Lastly machine-based methods involve training of a machine learning network to learn a human rater's response to a series of pavement images representative of various field conditions (Gavilan et al. 2011).

The histogram-methods are the basic type of intensity-based methods, they are simple, but often produce noisy results. They are also unsuccessful in changing pavement environments, sensitive to changing light conditions, and can produce disjointed crack fragments. There has been work on improving the use of these methods through more effective filtering and using these principles in other methods (Zou et al. 2012).

Edge detection is effective but usually doesn't adhere to crack connectivity, rather identifies disjoint crack fragments and may mistake noise as crack fragments (Peng et al. 2014). Some examples of edge detectors are the Sobel edge detector, and the widely-used Canny edge detector (Ayenu-Prah and Attoh-Okine 2008).

The transform-based methods like Wavelet-transform based models were found to be reliable, but they do not perform well for cracks with high-curvature and with low continuity (Zou et al. 2012). A widely-known example of a transform-based method is the fuzzy logic approach, which uses multiple transformations to define cracks. Following transformation of the image from the difference domain to the brightness domain, an intensity-based method is applied to define pixels having brightness less than a certain threshold as crack pixels. Finally, in the crack domain, the connectivity's of crack pixels are investigated to identify cracks longer than a minimum length. This method has a similar issue with light sensitivity but addresses texture sensitivity by considering isolated dark pixels as noise (Mathavan et al. 2013). The Beamlet transform is highly effective at extracting cracks from noisy, textured and unevenly lit images, but is used for extracting linear features, therefore cannot be extended to identify non-linear defects such as potholes (Ying 2009).

The seed-based methods consider crack connectivity well but are dependent on lighting conditions as they use intensity values to determine whether a cell is a crack seed or not (Gunaratne et al. 2008). The ability of the seed-based method to successfully identify crack areas depends on the path-growing technique. There has been research on the different path-growing techniques; the most widely used being the percolation technique due to its relatively lower computational cost (Gavilan et al. 2011).

The machine-based methods are more sophisticated, but often involve a learning nature which requires a large number of samples to accurately represent the specific

conditions (Gavilan et al. 2011). Additionally, since the learning is done as local methods on sub-images, the software may not always connect cracks over image boundaries (Zou et al. 2012). Section 1.3.4 includes more detail on machine vision techniques for crack detection.

### Classifying Crack Features

Automatically retrieving the crack features like length, orientation, and width has not been as fully documented as the previous steps have been. There are a couple of general methods in order to gather properties from an original crack map; the first uses image thinning to create a crack skeleton in order to retrieve crack properties, the second uses a distance transform to create a distance field for properties. Other methods included the use of ANNs to gather crack properties (Zhu et al. 2011). Table 5 shows some example methods for classifying crack features.

**Table 5. Example methods for classifying crack features**

Type	Description	Advantages	Limitations
Crack Skeletons	Crack skeletons (segment information) gathered from maps through binary image thinning and a distance field was created from a Euclidean transform	Crack maps are common output for many methods of crack identification	Average precision for this method is roughly 60%
Graph search	Visual tool to gather crack geometry properties after manual start and end input from user	Efficient process	Requires manual input on start and end points of crack
Artificial Neural Networks	Used learning methods to identify crack properties from images	Efficient process after ANN is trained	Challenging process to form network training data
Closing & Thinning Algorithms with Hough Transform	Properties are directly determined from using algorithms and transforms on the preprocessed images	No crack map or skeleton needed	Process not well documented

In addition to crack length and width, Amarasiri et al. (2010) used the optical modeling of the image formation process and the subsequent analysis of the variation in pixel intensity profiles within digital images to evaluate crack depth. Using the variation of reflection properties at surface discontinuities, a bidirectional reflection distribution function was employed to model shallow longitudinal and transverse cracks as well as joints in concrete pavements. This preliminary study revealed a definitive relationship among the crack widths and depths and the maximum pixel intensity contrasts seen in the images of the cracks. To calibrate the models, the reflection properties were modified to match the pixel intensity contrasts across model generated images of cracks

and joints against those of identical cracks formed in concrete pavements. The model predictions of crack depths were also verified using actual crack data not used in the calibration. This preliminary study showed promising results in terms of using the generated depth information in differentiating cracks from joints on concrete pavements (Amarasiri, Gunaratne, & Sarkar, 2010).

### **1.3.3 The Use of 3D Imaging for Crack Detection**

Although there have been many methods addressing the issues inherent with the use of 2D imaging for 3D distress information, the potential for the use of 3D data is promising. If 3D data were used in conjunction with pavement images, many of these issues would be addressed (Peng et al. 2014). The most common method for collecting 3D data (which is essentially depth data collected as a line scan across the road) is using laser sensors for road profiling. By collecting both 2D and 3D data simultaneously, the comparison of data can infer whether a potential crack is truly a crack with depth. A method developed by Peng et al. used 3D laser data with 2D pavement images under a seed-based method and resulted in 92.5% precision and 90.6% true detection for the sample data used (Peng et al. 2014). Another approach developed by Wang was the use of two offset 2D images to produce a 3D stereovision set, which used imaging cameras as opposed to laser sensors. Testing for the application of crack detection has not been verified (Wang and Gong 2007).

Sponsored by the U.S. Department of Transportation (US DOT) Research Innovative Technology Administration (RITA) program, Tsai and Li (2012) evaluated the feasibility of using elevation data from 3D laser technology as opposed to 2D intensity data to detect cracks under different lighting and poor intensity contrast conditions. Cracks ranging from 1 to 5 mm wide were measured in a laboratory setting to evaluate the performance of a 3D data acquisition and crack segmentation method based on dynamic optimization. The study concluded that the 3D system could effectively detect cracks equal to or greater than 2 mm wide under controlled laboratory environment. The significance of this study was to demonstrate the consistency of the 3D detection method under various lighting conditions including night-time, daytime with shadows and daytime with no shadows. The software was capable of detecting cracks even with low intensity contrast (Tsai & Li, 2012).

### **1.3.4 Machine Vision**

The process of automated detection and the measuring of pavement cracks is one application of machine vision, which in general terms captures and analyzes visual information. Machine vision takes advantage of a subset of computational intelligence techniques called machine learning (ML) techniques. ML techniques typically involve massive networks of parallel processing nodes that become capable of recognition without definition, after proper training on a representative data set. The ML network uses a series of parameters to form a connection between the inputs and outputs. These parameters are optimized to enhance the capability of the network in recognizing



(and differentiating) the pattern (from the noise) within the data. ML algorithms have demonstrated great generalization capability and have been successfully used in pattern recognition, prediction, and control applications among others.

These similar networks of processors are trained using different learning paradigms to estimate model parameters based on observed input-output data records. While Artificial Neural Networks (ANNs) are inspired by biological neurons, Radial Basis Function (RBF) networks and Support Vector Machines (SVMs) are based on statistical learning theory. The learning paradigm for ANN is a recursive stochastic approximation used in supervised training of multi-layer perceptrons (MLP). Network parameters are randomly initialized and then adjusted recursively in a manner that the mean squared error (MSE) between predicted versus measured outputs moves in the direction of steepest slope. The RBF learning paradigm is termed hyper-surface reconstruction which is essentially smooth curve fitting using regularized interpolation. The SVM learning paradigm is an approximate implementation of the principle of structural risk minimization adopted from the statistical learning theory. The maximum degradation (distance) of an approximating hyper-plane from the observed data is minimized. To learn more about the details of these paradigms, the reader is referred to instructive published resources (Haykin 1998; Smola and Schölkopf 2004). Any superior performance of each technique compared to others has proved to be problem specific and a systematic benchmarking and comparison approach is required to determine the most appropriate technique for each specific problem at hand (Kargah-Ostadi & Stoffels, 2015).

Most related topics discussed in the literature are components of machine vision systems, the hardware capturing the information and the software providing the analysis of the data (Najarian et al. 2011). Omer used a machine vision system for monitoring the condition of a winter road surface, automating the procedure. This system included the use of a machine learning technique called a Support Vector Machine (SVM), trained through a localized model approach with images that were smoothed and normalized (Omer and Fu 2010). This application can be extended to the use of machine vision to detecting and reporting characteristics of pavement cracks.

Best used for situations where there is a large amount of data with difficult to describe variables, machine learning has found applications in many fields, such as pharmaceutical, business, as well as in the pavement engineering sector. One specific method of machine learning is the use of Artificial Neural Networks. ANNs use a learning strategy similar to the human brain in exploiting the strength and flexibility of connections between simple processing elements (Fieguth and Sinha 1999; Mathavan et al. 2013). The following sections will focus on the applications to crack detection and elsewhere, as well as the link to machine vision.

## **Artificial Neural Networks**

The learning style of ANNs fall under one of three categories, supervised (user-defined input and expected output to give the system inference of the relations), unsupervised (only input is provided and the system recognizes patterns), and reinforcement learning (trial and error based method), all of which adapt values of free parameters according to the training (Gao 2009; Mathavan et al. 2013; Lu et al. 2002).

Within supervised learning, there are two more sub-divisions: parametric and non-parametric learning. Parametric learning uses pre-defined knowledge on the data, like probability distributions, where non-parametric has classifiers that do not have the conditional probability distributions. The advantage of using parametric learning is that it requires less training data, but non-parametric does not make assumptions or need information on the distribution of the data. Oliveria and Correia performed supervised learning with both classification strategies for crack detection in pavements, three methods were parametric – based on bivariate class-conditional normal density – and three non-parametric. The best system was found to be one using a quadratic boundary with parametric learning and classification with a precision of 92.5% and true detection of 97% (Oliveira and Correia 2008).

The application to crack detection done by Mathavan et al. used unsupervised learning to remove human subjectivity from the training of the computer to identify cracks. By allowing the computer to distinguish crack regions from non-crack regions after a series of training images, the texture analysis software was able to reach a detection precision of 77% and true detection of 73% for highly textured pavements (Mathavan et al. 2013).

In a research project sponsored by FDOT, ANNs were trained using manual ratings of transverse cracks to estimate crack depth. In addition to pavement related parameters (type, age, material, functional class, and traffic) and the transverse cracking information, data on geometry of the cracks from laser sensors (installed on a manually operated push-car) were used to identify and estimate the depth of cracks at walking speed. Through supervised training and testing, the developed system found field cracks with detection rates above 90% and accurately measured crack depths with errors as low as 0.5% compared to field measured data (Lu et al. 2002).

### **1.3.5 Currently Available Software**

Mirroring the large amount of research efforts, the industry has produced many different systems aiming to automate pavement distress collection and analysis. In the following sections, ten systems were reviewed for general reported function and performance (in alphabetical order). Due to the proprietary nature of the majority of available software, the details of the crack detection algorithms are not published in the literature.

### **Automated Distress Analyzer (ADA) – Kelvin Wang, University of Arkansas**

Working with the Digital Highway Data Vehicle (DHDV) and the line-scan images, the ADA detects and calculates the lengths and widths of longitudinal, transverse, block and alligator cracking in real-time up to 40 mph as claimed by the developer (Wang and Gong 2007). Another function of the software is to analyze pavement distresses such as rutting and roughness (Gunaratne et al. 2008). The software takes advantage of multiple on-board computers with multiple CPUs each to employ a real-time database and run a parallel computing code to allegedly achieve real-time identification of pavement cracking.

### **CrackScope – International Cybernetics**

CrackScope can operate both offline and online (real-time with a vehicle operating at highway speed), operating with a crack-seed method to determine punch-outs, spalled, transverse, longitudinal, alligator and block cracking (International Cybernetics 2015). The CrackScope system uses a line-scan camera and laser illumination (Shah et al. 2010).

### **LcmsRoadInspect - Pavemetrics**

The LcmsRoadInspect software combines 2D and 3D data collected at speeds up to 62 mph, to detect and analyze cracks, and other distresses such as rutting, patches, potholes, and ravelling (Pavemetrics Inc. 2015). Basically, the LcmsRoadInspect application is built using the LCMS Data Processing Library (DLL library of C/C++ functions). Pavemetrics also supply an acquisition software called LcmsAcquisitionControl.

### **PAVUE – Ramboll**

This system uses area or line scan cameras with strobe lights that can capture pictures up to 55 mph, where the PAVUE analysis parameters must be manually selected to extract crack data (Kim 2008). The system uses transformations to produce crack boundaries, where features are then extracted for the user (Timm and McQueen 2004). After the overlay type and macro texture settings are defined for each pavement section, the automated analysis can be run (Aijo, 2005).

### **PicCrack – Hosin (David) Lee, University of Iowa**

PicCrack's main image analysis methods are edge detection, binarization (image binarization converts an image of up to 256 gray levels to a black and white image, where a threshold value is chosen to classify all pixels with values above this threshold as white and all other pixels as black), morphology (shape analysis), and the use of a Hough Transform. All of the crack detection and analysis is completed offline (Cheng and Glazier, 2007). By using an ANN, PicCrack is an adaptive machine learning system

that has been reported to have a crack detection accuracy of about 95% (Lee et al. 2004).

### **RoadCrack - ARRB**

Developed by the Australian Commonwealth Scientific and Industrial Research Organization (CSIRO) and the Australian Road Research Board (ARRB), the RoadCrack system uses line-scan cameras, lasers, and a seed-based approach to detect road cracks as small as 1 mm wide (Mathavan et al. 2013). The system can operate at night at speeds up to 65 mph with real-time crack detection and classification, allowing a report on type, severity and extent of cracks to be generated (Kim 2008).

### **uniANALYZE – Adhara Systems**

Using a seed-based method, uniANALYZE allows both manual and automatic crack identification and measurement (Adhara Systems n.d.). This system first completes image segmentation by dividing the pavement into grids; the image is then filtered for noise and run under a white line detection filter to reduce white line errors. After these three steps, a crack detection analysis is run to distinguish crack cells from non-crack cells (Aijo, 2005).

### **VCrack – Texas DOT**

Using a line-scan camera and LED linear lighting, the image analysis software VCrack classifies punch-outs, longitudinal, transverse, block, alligator and spalled cracks through a seed-based method. The system can record images up to 70 mph, and generate real-time crack maps for speeds less than 45 mph (Gunaratne et al. 2008). Using a grid-cell analysis technique, VCrack produced a repeatability score consistently over 0.95 – calculated as a correlation coefficient for the analysis of multiple runs on the same pavement section (Huang and Xu 2006).

### **WiseCrax – Fugro Roadware**

Out of the 30 highway agencies surveyed in a 2004 study (McGhee 2004), 8 reported using the WiseCrax software for an interactive crack detection process. Using data from area or line scan cameras, strobe lighting and/or infrared lighting from an Automatic Road Analyzer (ARAN) system, WiseCrax can detect cracks as small as 1 mm wide through an offline system (Gunaratne et al. 2008). The system can operate either manually or automatically, working to identify cracks by first establishing the start and end points, with user-customizable crack criteria for classification (Timm and McQueen 2004).

An initial step involves selection of representative pavement images for each project. The program uses these representative images to identify an optimum set of detection parameters according to pavement type, texture, pixel by pixel grayscale variation as related to crack contrast and brightness. Following this initial step, WiseCrax can be used in an interactive or fully automated mode. Typically, users run the software in automated mode and then use the interactive mode for modifying the results.

### **1.3.6 Challenges and Future Development**

#### **Challenges**

Most systems have focused on asphalt concrete surfaced roads, presumably because it is significantly more prevalent than any other pavement type. As a result, less experience with Portland Cement Concrete (PCC) surface roads is documented. There are several unique features of PCC that present challenges in the process of automated crack detection.

Tine texturing of PCC pavements (commonly applied during construction to provide for skid resistance) typically masks cracking in PCC pavements. While texturing follows a definite pattern, it is not uncommon for some finer (narrower) cracks to be hidden (or lost) in the tine pattern.

Similarly, jointed concrete pavements (JCP) have 'constructed cracks' (joints) built into them. While joints look (and act) like cracks, they are typically handled quite differently in pavement evaluation. Joint detection is required to establish where slabs begin and end, so that distresses associated with a slab can be quantified. However, great care is required to not include joints as cracks or vice versa. Several options are available to use pavement profile data to detect JCP joints.

Typically, the width of cracks in PCC pavements can also tend to be much narrower. While most systems today claim to detect crack widths down to 1mm, the crack widths of PCC truly challenge this claim. Many of the materials related distresses such as durability cracking and alkali silicate reactions cause very fine cracking with little or no measurable depth.

For asphalt concrete surfaced roads, this has not yet been considered as a significant concern, perhaps because there is enough other distress to focus on. For PCC surfaced roads however, any working cracking is a concern (perhaps because of the efforts taken to avoid or eliminate cracking or the expense to repair). Considering that some PCC pavements are reinforced to reduce the potential for cracking (or at least hold the cracks tightly together, if they do occur), this combination makes the detection of cracking more

challenging in JRCP and CRCP. However, the vast majority of concrete pavements in Florida are jointed plain concrete pavements (JPCP).

Finally, just the difference in color of PCC surfaced roads tends to create some unique challenges for pavement evaluation. Light tends to reflect differently off of the lighter PCC surfaced road. While this can be adjusted for, a system needs to be able to recognize such differences in pavement surface type and make the necessary adjustments accordingly.

Regarding flexible pavement distress identification, one of the challenges is detection of cracks in heavily weathered and raveled pavement sections, where the deep surface texture results in patterns that are perceived as cracks by the automated algorithms. These misleading features are often called “phantom” cracks, and this issue is also prevalent during manual distress surveys.

Another challenge on asphalt concrete pavements is the automated identification of patching areas. Several solutions have been proposed in the past, but a robust methodology is yet to be created. The most promising technique in this regard has been the application of the texture information provided by 3D images.

Regardless of pavement surface type, there are a couple of other significant challenges that remain. One of these is establishing a true reference on which the capabilities of crack detection system can be judged. Precision and bias for detection systems are not readily available because of the lack of agreement on a true reference. As a result, it is difficult (if not impossible) to establish what systems work ‘better’ and/or how much so. This challenge has significantly stymied the advancement of the evolution of automated pavement evaluation.

The other significant challenge (as previously noted in the discussion on hardware) is depth perception. Cracks that have been sealed (or filled) are treated differently in evaluation systems. This distinction is in part, because the actual width of such cracks is masked, but it is also important to record the number and length of cracks that have already been addressed.

### **Future Development**

Significant effort is under way nationally to address the issue of depth perception. With the advent of 3D systems, this concern is expected to be significantly diminished in the near future.

Efforts are underway to establish reference standards on which comparison can be made (AASHTO 2014b; UK Roads Board, 2009), but until a more universally accepted 'ground truth' is established, future development will continue to be challenging.

To address some of the challenges described above, multiple research studies have applied the learning capabilities of machine vision systems to simulate the manual ratings of the collected images by human raters. These machine learning techniques need to be further investigated to evaluate their reliability before being employed in practice.

## **1.4 Implementation of Automated Crack Detection**

This section of the literature review focuses on initiatives to implement an automated distress data collection. The discussed topics include the major previous implementation efforts, the success metrics used to evaluate the effectiveness, efficiency, and reliability of automated distress identification techniques, and finally the considerations required for integration of automated distress surveys into practice.

### **1.4.1 Previous Implementations of Automated Distress Collection**

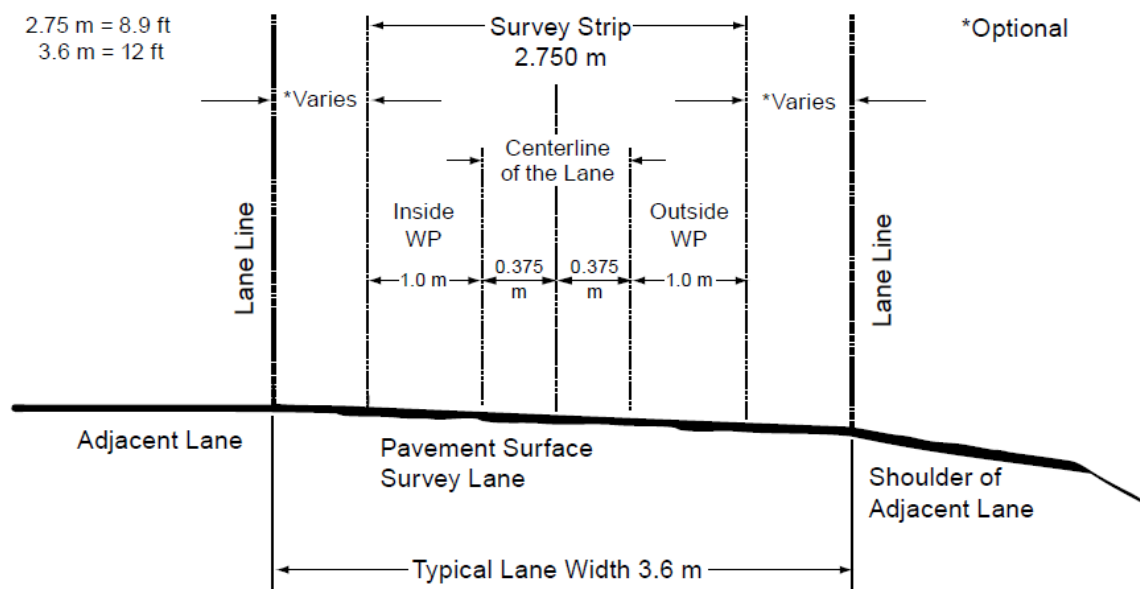
In semi-automated condition evaluations, professional raters process pavement images to identify and calculate various pavement distress quantities and severity levels. Using a point and trace manual method, the type, extent, and severity of pavement surface distresses are examined one image at a time by a rater at an office work station. This approach is very time consuming especially for long projects and network level evaluation. Currently, most State Highway Agencies (SHA) are using this semi-automated approach (Pierce et al. 2013). Similar to manual distress surveys, semi-automated distress evaluations involve significant human intervention.

The fully automated distress evaluations are conducted using image processing and pattern recognition software for distress identification and quantification. Along with quality assurance testing of the software, professional raters are used to perform quality control of the software distress ratings.

A range of national, international, and state specific standards have been created to facilitate automation, such as the AASHTO provisional protocol (PP) number 67 (AASHTO 2014b) and United Kingdom's Surface Condition Assessment of the National Network of Roads (SCANNER) specifications (UK Roads Board, 2009), but such standards are still in various stages of adoption. In the AASHTO PP 67-14 standard, the pavement surface area is divided into five zones across the lane width: two outer edge zones, two wheel-path zones, and one center zone (Figure 13). A similar approach was adopted by the SCANNER specifications, with slightly different widths for each zone (UK Roads Board, 2009).

Unlike the manual (and semi-automated) distress identification procedures, distresses are not identified according to the crack generation mechanism, but according to the geometric characteristics. For example, in lieu of identifying fatigue (or alligator) cracking, the amount and severity of “pattern” cracking is measured within each of the five identified zones. Also, instead of discrete severity levels, continuous average crack width is recorded to account for the intensity of surface distresses (McGhee 2004).

In NCHRP Synthesis Report 334 on automated pavement distress collection techniques, the researchers published the results of surveying 43 State Highway Agencies (SHA) and 10 Canadian provinces or territories (McGhee 2004). The results indicated that 30 of the surveyed agencies were collecting pavement forward, lateral, or downward images through automated means at highway speeds. However, only 14 of those agencies were using an automated procedure to identify and summarize pavement distress data from the collected images. The other agencies used semi-automated procedures, where distress data were manually obtained and reduced from the collected images. Of the 30 agencies collecting pavement imagery, only four used the AASHTO provisional protocols (AASHTO 2014a; AASHTO 2014b), five used a portion of the Long-Term Pavement Performance (LTPP) Distress Identification Manual (DIM) (Miller and Bellinger 2014) and the other 21 used an in-house distress identification protocol.



**Figure 13. Typical pavement cross section and the identified zones for automated distress identification (AASHTO 2014b)**

Studies conducted in 2004 and updated in 2008 show that among the 50 states, Puerto Rico, 11 Canadian provinces and the Eastern Federal lands, 44 out of 65 (68%) use automated pavement data collection (Pierce et al. 2013). A summary of the findings is included in Table 6, which demonstrates that most of the highway agencies while



collecting the pavement imagery are still reluctant to use a fully automated approach. A large range of methods are currently used, and many advances have been made over the years (Attoh-Okine and Adarkwa 2013). Unlike the advanced data collection technology available in the pavement industry, pattern recognition software are perceived to be in need of further enhancements to accurately detect and classify the various types of pavement surface distress (although, without a true reference, it is not possible to accurately establish the true effectiveness of such systems).

**Table 6. Summary of pavement condition data collection methods (Pierce et al. 2013)**

Process	Method	Number of Agencies		
		Agencies	Vendors	Total (Percentage)
Collection	Automated	23	21	44 (68%)
	Manual	19	2	21 (32%)
Processing	Fully-Automated	7	7	14 (32%)
	Semi-automated	16	14	30 (68%)

The data and images collected today provide an opportunity for reprocessing in future years when crack detection software are more capable and faster with the future increased computing powers. This means that collecting the data today may have additional long-term analysis potential. The same is true for monitoring the potential deterioration of other roadside assets such as signs and guiderails. More effort should be made today in developing calibration and quality standards for image collection equipment and for the captured images.

### **Use of Semi-Automated Distress Surveys**

Many SHAs in the US use a semi-automated approach (Table 6). This approach involves digital image collection and some level of manual post-processing and distress identification by professional raters.

Pennsylvania Department of Transportation (PennDOT) had implemented a semi-automated pavement distress condition surveying program based on pavement video-logging. Additionally, the automated data collection provides pavement roughness data, geometric information, and other features that are uploaded and stored in PennDOT Roadway Management System. Data collection for PennDOT is conducted with a vehicle equipped with ROW camera, area scan pavement images and other condition sensors (Pennsylvania DOT 2015a; Pennsylvania DOT 2015b). PennDOT pavement condition data and images are collected by contracted service providers. Then, images are analyzed through data reduction and each section of highway is rated. Distress severity and extent data is derived, through a combination of automated distress programs and a manual visual rating of the pavement images (Pennsylvania DOT 2015a).

Virginia Department of Transportation (VDOT) and North Carolina Department of Transportation (NCDOT) have adopted a similar semi-automated approach, evaluating pavement distress using digital images. The data collected is interpreted and processed with some level of human intervention. Pavement distress data is used to determine pavement condition index (PCI) values which in turn are used to estimate the required pavement maintenance and rehabilitation treatments. When the automated pavement distress identification is utilized, DOT requests the contracted service providers to conduct a manual visual review of the collected images on all pavement sections prior to submitting results (Virginia DOT 2012; North Carolina DOT 2011). This is different than the manual review of a sample for quality control or independent verification purposes.

Oklahoma Department of Transportation (OK DOT) also uses contractors to collect the pavement condition images and manually measure and record the pavement distresses according to ODOT protocols (Oklahoma DOT 2005).

### **Use of Fully-Automated Distress Evaluations**

There are several States that are actively moving towards using a fully automated approach. However, a rigorous quality control, acceptance testing, and independent verification is typically required. While most agencies explore the concept of full automation, many fall back to some level of human intervention out of lack of confidence in the results being obtained. Many of the agencies that use the fully-automated approach perform the data collection with in-house staff and equipment.

Vermont DOT uses a fully automated approach to identify the location and type of all distresses in their network since 2001. The cracking information is primarily divided into longitudinal, transverse, and alligator cracking. They do some manual adjustment of the results only to identify which of the cracks found have been sealed (Papagiannakis et al. 2009).

Maryland SHA uses a fully automated approach to crack detection with a sampling QC to better understand the limitations and results. As a standard part of the Maryland data collection procedure, Fugro's Wisecrux software is used to measure the length of cracking in any given portion of the pavement (Groeger et al. 2003a). The results of this analysis are a modified version of the AASHTO PP 67-14 results, including distribution of cracking length by road zone and by severity (AASHTO 2014b).

In addition to the fully automated approach, Maryland SHA staff members conduct a manual review and adjustment of a small sample of the pavement imagery to determine the impact of manual review and adjustment (Groeger et al. 2003b). Then adjustment factors are created based on the difference between the fully automated approach and the samples in which adjustments have been made. These adjustment factors are

applied to the fully automated data on pavement sections that have similar conditions to the reviewed sample sections.

## **Research Studies**

Automated Distress identification has been investigated by a range of academic and research organizations over time to get a better objective rating of pavement distress.

Oregon Department of Transportation (ODOT) completed a research study in automated data collection equipment for monitoring highway condition (Mullis et al. 2005). Some of the research objectives were the evaluation of accuracy of Oregon's current pavement condition data collection, the accuracy and consistency of available ADC technology, and the potential to combine data collection efforts using automated technology. The ADC equipment were provided by four vendors: Fugro-BRE, Infrastructure Management Services (IMS), Roadware, and Pathway Services. The vendors were required to provide pavement distress data according to ODOT protocol and using the video log images that they collected using their ADC systems.

Eight test sections (6 AC and 2 CRCP) were selected, having in total 187 segments of 0.1 mile each. These sections were selected to cover a range of pavement types and a variety of pavement conditions. Two sections were rated twice by each rater to test repeatability. Each test section was rated by three ODOT rating crews and by four ADC system vendors. A walking survey and rating was done by experienced Oregon pavement personnel to establish a baseline (ground truth) to which ODOT rating crews and vendor's equipment could be compared. They found that the ADC and manual distress were significantly correlated with the ground truth for raveling and rutting, although the ADC systems did not do as well as the rating crews, based on the evaluations of this study. The raw data analysis shows that rating crews did better at identifying the patches on AC pavement and punchouts in CRCP and the ADC systems tended to report larger totals of transverse and longitudinal cracking quantities than the ground truth showed.

A study conducted for the Texas DOT (Serigos et al. 2015) compared a range of methods including semi-automated and fully automated distress to a detailed manual survey. The initial assessment showed that the fully automated data showed a large variability around the manually established "ground truth". Also, this study showed that the accuracy improved after applying manual post-processing (visual interpretation and correction of the results produced by the vendors algorithms), and the number of false positives was reduced for most cracking types. However, the amount of reported false positives was larger for several combinations of service providers and crack types, even after the significant improvement achieved by the manual intervention. Based on insignificant correlations found between collected surface macro-texture data and distress measurement errors for all the vendors, they concluded that the cracking measurement accuracy of the service providers was not affected by surface texture.

This was because all service providers used 3D systems that are less prone to challenges faced by 2D systems in identifying cracks on rough textures.

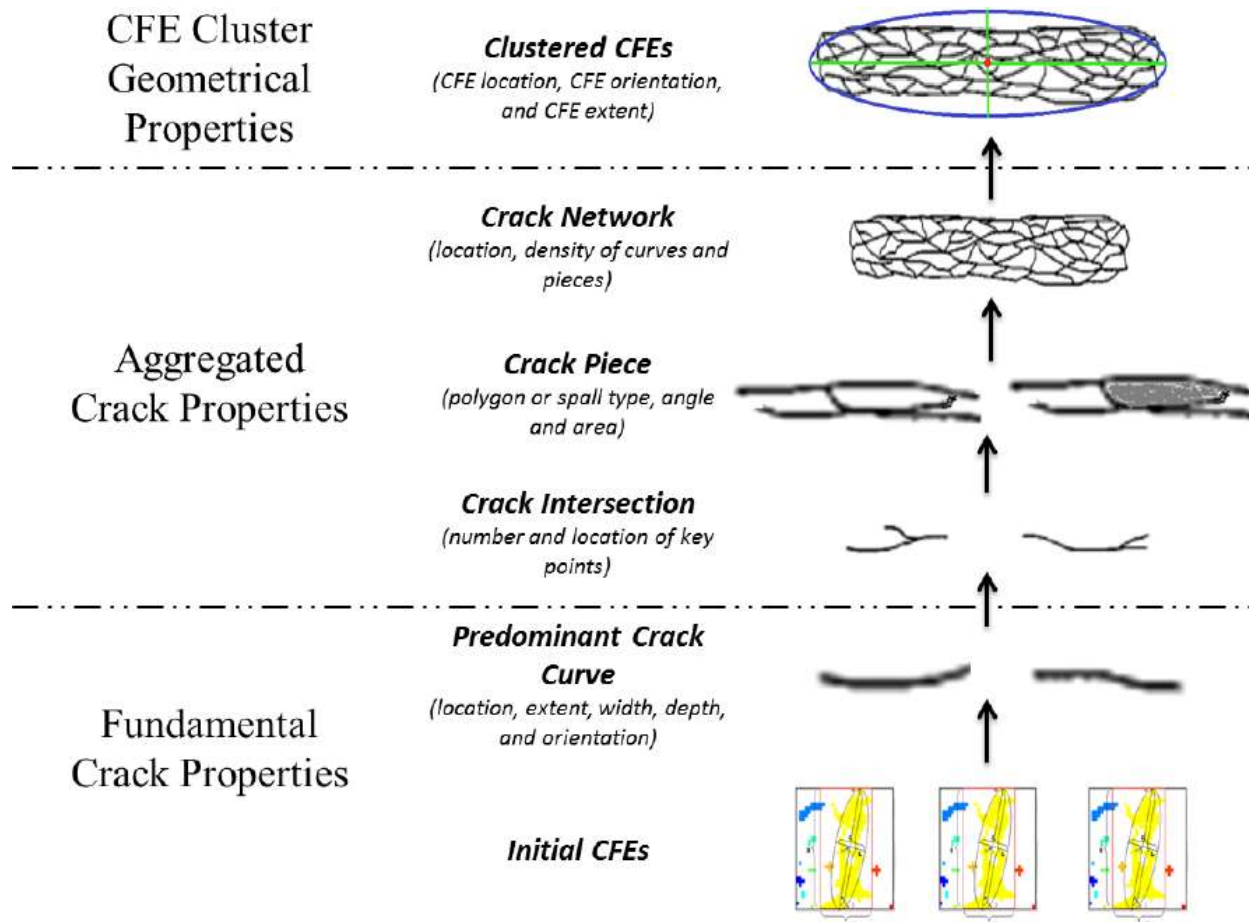
In a 2002 study, Groeger et al. compared two automated crack detection algorithms based on cumulative length of longitudinal and transverse cracking on a network of approximately 2000 data points (Groeger et al. 2003a). Three experienced evaluators classified the test section based on a five-level condition scale (very good to very poor) and established the reference values. That study found that 94 percent of the time, both examined automated procedures had matched the reference condition rating by one deviation in reported condition level. For example, if the reference overall condition was reported poor, the automated procedure had reported the overall condition to be very poor.

The Ontario Ministry of Transportation conducted a comparison study between their in-house manual distress survey results and automated and semi-automated distress surveys provided by three service providers (Tighe et al. 2008). This study used the summary quantity of the overall pavement condition called distress manifestation index (DMI). The study concluded that automated results were generally comparable with manual surveys. However, the authors emphasized that some of the distresses were difficult to identify through the automated approaches and supplemental manual surveys were suggested specifically for project-level analyses. The authors did not mention the performance of the automated and semi-automated surveys with regards to individual distresses, but the paper (Tighe et al. 2008) hints that the disintegration type of distress (e.g. ravelling, stripping, or spalling) were more difficult to identify as opposed to cracking and rutting distresses.

To develop an automated crack classification methodology, Tsai et al. (2014) proposed a multi-scale crack fundamental element (CFE) model, which provides crack topological properties at three different scales (Tsai et al. 2014):

- 1) Fundamental crack properties, which describe the physical properties of each crack including length, width, depth, etc.
- 2) Aggregated crack properties, which focus more on patterns within the CFE and represent the interaction of cracks with one another, such as intersections, polygons, crack density, etc.
- 3) Clustered CFE geometrical properties, which describe the overall properties of each CFE including element center, orientation, length, and width.

This concept is illustrated in Figure 14 (Tsai and Wang 2014), which shows crack properties at three scales defined in the CFE model.

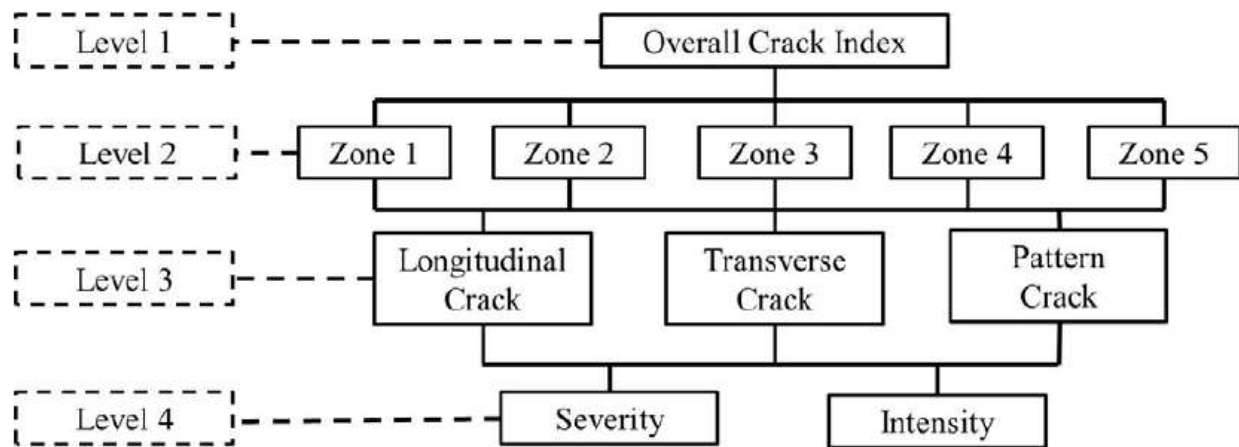


**Figure 14. The multi-scale crack fundamental element concept (Tsai and Wang 2014)**

To handle the diversity among different distress identification protocols used by various highway agencies, the authors used this model to standardize crack performance measures for different transportation agencies. The authors argue that experienced pavement engineers tend to first identify a group of cracks to be clustered together as one element (CFE), and then look at the pattern inside that element, and finally measure the length and width of individual cracks (Tsai et al. 2014). The model input is the automatically detected crack map, which can be delivered through either 2D or 3D systems. This research study, which was sponsored by the US DOT RITA program reported promising results in terms of precision and recall (the ratio of correctly classified cases to total actual cases).

In an effort to create an overall pavement condition index based on the AASHTO provisional protocol 67 (AASHTO 2014b) for flexible pavements, Wang et al. (2015)

proposed application of the analytical hierarchy process (AHP) concept to a hierarchical framework as demonstrated in Figure 15. The severity and intensity of each crack type are calculated using the Fuzzy set theory based on the average width and the total length of each crack, respectively. The classic pairwise comparison method developed in the AHP concept is employed to determine the weighing factors required for the linear combination of the various cracks in each zone and the multiple zones for each pavement section (Wang et al. 2015).



**Figure 15. Framework of the proposed overall crack evaluation index (Wang, et al., 2015)**

### 1.4.2 Success Metrics

The three principal success metrics of any process are effectiveness, efficiency, and reliability. With respect to automated condition evaluations, these three metrics could be considered for two aspects of the process, first for the detection and classification of individual surface defects (cracks), and second for the overall evaluation and quantification of the pavement condition in a distinct section.

In the context of automated distress identification, effectiveness can be expressed in terms of accuracy of the crack detection software when compared to a reference baseline. Accuracy is a qualitative term referring to whether there is agreement between a measurement made on an object and its true (target or reference) value. Bias is a quantitative term describing the difference (or error) between the average of measurements made on the same object and its true value.

Reliability of automated distress surveys is often expressed in terms of precision. Precision is also a qualitative term describing the degree of repeatability of a measurement value. Variance and standard deviation of error are quantitative estimates of precision. Accuracy and precision (or the corresponding quantitative estimates: bias

and variance) ultimately define how effective and reliable a system is as described in greater detail below.

### **Verification of Identified Cracking: “Ground Truth”, False Positives, and Missed Cracks**

Multiple research efforts in the past have introduced various methods to establish reference values or “ground truth” for pavement surface defects by using the “most appropriate” methodology available (Flintsch and McGhee 2009). The major types of reference values include:

1. Manual distress identification: In this method, professional (trained and experienced) distress raters are used to identify the surface distresses on a set of pavement sections that are deemed representative of conditions across a network.
2. Semi-automated detection: This method is similar to the manual method, but the professional raters use the images collected by monitoring vehicle to identify the distresses.
3. Artificially fabricated distress: In this method, cracks are designed and fissured into steel plates or cut into an existing asphalt surface, so the precise dimensions of the defects are known. This method is mostly used to resolve image distortion issues caused by the camera lens or the image sensor.

Each method has its own advantages and limitations. The manual method simulates the actual distress identification process that has been in use by many SHA for a long period; however, there is a low degree of agreement among different professional raters which renders the “ground truth” as a highly variable measure.

The LTPP program conducts annual accreditation workshops for the LTPP certified distress raters, during which the identification methods of various pavement distresses are clarified, maximum harmonization among different raters is sought, and the potentially required modifications to the LTPP Distress Identification Manual (Miller and Bellinger 2014) are identified. In a 1999 study (Rada, et al., 1999), the variability of the LTPP manual distress ratings was investigated based on 9 different workshops, including 119 ratings on 18 test sections (9 AC and 9 PCC), by 6 to 16 individual raters per workshop. The manual rating of the same test sections through a consensus between the instructors immediately before each workshop were used as reference values, to determine the individual rater variability in terms of accuracy and precision.

For AC pavements, Table 7 shows accuracy as the bias between the reference values and the corresponding group means, and precision as the standard deviation among various raters interpolated across various workshops. To overcome the often very small quantities of some distresses, the coefficient of variation (COV), in percentages, was estimated by plotting the standard deviation versus mean for each distress type/severity level combination and fitting the best line through these data. The slope of the best-fit line (in percentages) forced through zero is a measure of the ratio of standard deviation to mean and was taken as the COV.

It was found that combining distresses of a particular type across all severity levels resulted in significantly lower bias and precision values for the total sums than for individual severity levels. As indicated in Table 7, there was a better agreement among different raters in terms of the total length of transverse cracks (COV of 9% or 91% agreement) as opposed to the total length of longitudinal wheel path cracking (67% agreement), or the total area of fatigue cracking (62% agreement) on AC pavements.

**Table 7. Accuracy and precision for LTPP manual ratings of AC pavements (Rada, et al., 1999)**

Distress Type	Unit	Distress Severity	Pooled Reference	Group Statistics			
				Mean	Std. Dev.	COV (%)	Bias
Fatigue Cracking	Sq. meters	All Levels (Total)	14.2	16.5	6.2	38	2.3
Longitudinal Cracking WP	meters	All Levels (Total)	18.4	18.3	6.0	33	-0.2
Longitudinal Cracking NWP	meters	All Levels (Total)	75.0	70.7	14.7	21	-4.3
Transverse Cracking	number	All Levels (Total)	26.4	24.7	3.2	13	-1.7
Transverse Cracking	meters	All Levels (Total)	44.3	44.6	4.2	9	0.3

Table 8 shows similar values for PCC pavements. There seems to be much less agreement among the raters in terms of the total length of spalling of longitudinal and transverse joints (32% and 29% agreement, respectively), compared to the total length of longitudinal and transverse cracks (78% and 92% agreement, respectively) on PCC pavements.



**Table 8. Accuracy and precision for LTPP manual ratings of PCC pavements (Rada, et al., 1999)**

Distress Type	Unit	Distress Severity	Pooled Reference	Group Statistics			
				Mean	Std. Dev.	COV (%)	Bias
Corner Breaks	number	All Levels (Total)	3.9	3.7	0.5	14	-0.2
Longitudinal Cracking	meters	All Levels (Total)	7.5	7.0	1.6	22	-0.5
Transverse Cracking	number	All Levels (Total)	9.4	9.6	1.4	15	0.2
Transverse Cracking	meters	All Levels (Total)	24.8	25.0	2.1	8	0.2
Spalling of Long. Joints	meters	All Levels (Total)	6.6	7.2	4.9	68	0.5
Spalling of Trans. Joints	number	All Levels (Total)	3.7	3.4	0.9	25	-0.3
Spalling of Trans. Joints	meters	All Levels (Total)	1.7	2.0	1.4	71	0.3

Between Table 7 and Table 8, the only distress values that can be compared include longitudinal cracking (m, combining WP and NWP for AC), transverse cracking (m), and transverse cracking (number). By normalizing these results (bias divided by Pooled Reference or the mean x 100%) one finds that there is a greater relative bias between the average group ratings and the reference ratings of various AC pavements compared to PCC pavements for only one distress type (transverse cracking, number). Furthermore, the relative bias is in the same order of magnitude for both pavement types (i.e. single digit). While there seems to be more disagreement among various raters on PCC pavement distresses, the average of the rater distress values seems to be closer to the reference values on PCC pavements compared to AC pavements. On both pavement types, there is a tendency for the agreement among raters to increase (coefficient of variation to decrease) with an increase in the magnitude of the amount of distress present. The authors reported similar results in a later study on the LTPP distress variability (Rada et al. 2007).

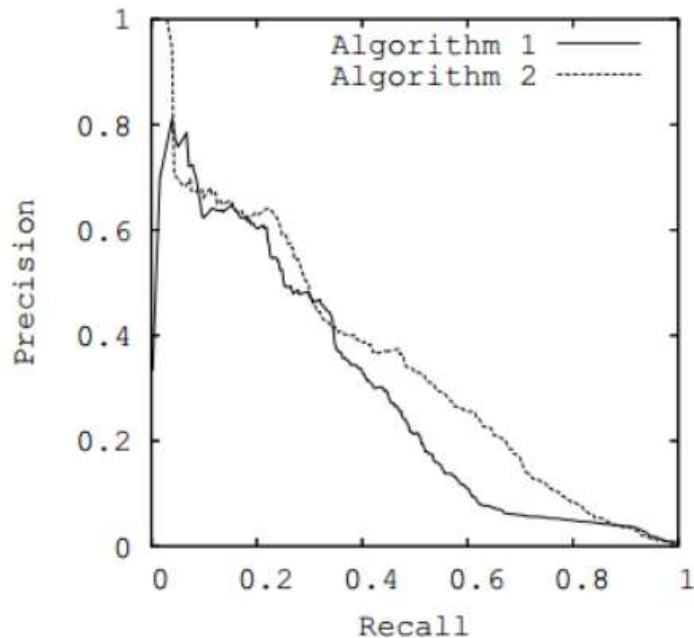
The semi-automated option might be superior to the manual method for establishing “ground truth,” because the collected images are available for multiple raters to view in an office environment with less distraction from field traffic. However, some of the low severity cracks that are at initial stages of development might not be visible from the collected images. Increasing the number of raters could result in a more reliable ground truth.

The artificially fabricated distress while precise is not always representative of pavement surface defects and the variability observed in the field. However, such fabricated boards have been frequently used as calibration targets to address dimensional systematic errors, dynamic range, and signal to noise ratio issues in the collected images.

Accuracy of the measured distress against the established reference values (“ground truth”) is evaluated to identify the systematic and random errors. The systematic error or bias could be addressed by calibration, but the random errors need to be addressed by increasing the reliability of the crack detection algorithm through various control parameters within the algorithm. Regarding the effect of error type in network-level pavement management decisions, Saliminejad and Gharaibeh (2013) suggested that systematic errors in pavement condition data have a higher impact on the PMS outputs than random errors (Saliminejad and Gharaibeh 2013).

False positives are cracks that have been reported by the automated crack detection software, while no crack has been recorded in the “ground truth” at the same location. On the other hand, missed cracks are existing cracks that have been reported in the “ground truth”, but are not detected by the software (i.e. false negatives). As with the manual rating conducted in the field, the reference values on the computer may also have a range of agreement from professional raters in terms of how to measure crack width, severity, and in some cases crack extent.

Studies have been conducted to evaluate the performance of automated crack detection algorithms in terms of detecting individual cracks (Wang et al. 2011). Wang assumed a “precision” indicator to be calculated as the ratio of the correctly detected cracks (true positives) to the total detected cracks (true positives and false positives). He also defined a recall parameter to be calculated as the ratio of the correctly detected cracks to the total actual cracks existing on the pavement surface (true positives and false negatives). As indicated in Figure 16, these two parameters have an inverse relationship for each algorithm. An algorithm with properties closer to the upper right corner (high “precision” and recall values) should be selected. It should be noted that this “precision” parameter is different than the statistical precision of the overall automated crack detection surveys, which is calculated as the standard deviation or the coefficient of variation of the error in estimating each distress type along each pavement section.



**Figure 16. “Precision” and recall curve for different crack detection algorithms (Wang et al. 2011)**

Tsai and Wang (2014) used a linear-buffered Hausdorff scoring method to quantitatively evaluate the crack segmentation performance by comparing each of the detected cracks with the manually established ground truth (Tsai and Wang 2014). Incorporating mean squared error and a modified Hausdorff distance metric, this method compares the binary crack maps produced by the automated software and the manually digitized ground truth. The buffered distance can be interpreted as the average Euclidean distance between the crack pixels in the ground truth image and the segmented images, which represents the accuracy of the software in detecting the same cracks as the ground truth reference crack maps. The authors evaluated their experimental 3D image processing system on two example test roads in Georgia. The average score of the automated software was about 86% on the flexible pavement section, and about 65% on the concrete pavement section (Tsai and Wang 2014).

In a study conducted for Texas DOT (Serigos et al. 2015), the results of automated surveys with varying levels of human intervention were compared among three different 3D image processing software tools. Two of them used the INO LCMS 3D images and the third used the PaveVision 3D image collection system. Manual distress surveys of 20 (0.1-mile-long) representative test sections according to the LTPP distress identification protocol were used as reference values. There were 7 Hot Mix Asphalt (HMA) pavements, 7 Surface Treatment (ST) sections, 1 Permeable Friction Course (PFC) surface with negative macro-texture, 2 Jointed Concrete Pavements (JCP), and 3 Continuously Reinforced Concrete Pavements (CRCP). Each test section was divided into twelve 50-foot segments to conduct the comparison analysis.

Table 9 demonstrates the number of false positives and missed cracks reported by each of the three automated survey methods before and after manual post-processing of the automated crack identification results (Serigos et al. 2015). The values in each cell indicate the number of segments out of the total 144 (12 sub-sections of 12 test sections), where false positives or missed cracks were identified. The numbers in parentheses show percentages of segments with reported issues. The third vendor (using PaveVision images) did not manually post-process their data, because they reported confidence in their automated algorithms. It was concluded that generally, the manual post-processing reduced the number of false positives and missed cracks. However, Table 9 does not fully support this conclusion.

**Table 9. False positives and missed cracks using three different crack detection software before and after manual human intervention (Serigos et al. 2015)**

Distress	Vendor	False Positives		Missed cracks	
		Before	After	Before	After
Fatigue Cracking	INO LCMS 1	23 (26%)	20 (23%)	40 (52%)	44 (57%)
	INO LCMS 2	33 (38%)	34 (39%)	36 (47%)	25 (32%)
	Pave Vision	12 (14%)	12 (14%)	36 (47%)	36 (47%)
Longitudinal cracking	INO LCMS 1	81 (74%)	45 (41%)	22 (20%)	37 (34%)
	INO LCMS 2	83 (75%)	69 (63%)	8 (7%)	7 (6%)
	Pave Vision	64 (58%)	64 (58%)	41 (37%)	41 (37%)
Transverse cracking	INO LCMS 1	90 (63%)	11 (8%)	17 (22%)	18 (24%)
	INO LCMS 2	97 (67%)	79 (55%)	4 (5%)	3 (4%)
	Pave Vision	27 (19%)	27 (19%)	11 (14%)	11 (14%)

### Effectiveness of Automated Surveys: Quantification Accuracy

In evaluating the effectiveness of a methodology, efforts are made to identify the bias or average error between methodologies (the average ratings from manual and automated distress surveys such as total length of transverse cracks, etc.) and evaluate how to reduce or minimize the bias. In the practical application of the network-level condition evaluation data for pavement management systems, it is the aggregate representative condition of an entire pavement section and not the specific localized defects that influences corresponding decisions. Most of the highway agencies that use an overall pavement condition rating (PCR) with a 100 point index (such as PCI) have typically set an acceptable limit of  $\pm 5$  PCR points on the difference between the automated results and the independent reference values (Flintsch and McGhee 2009).

To establish automated data quality management procedures for Indiana DOT (IN DOT), three quantitative measures were used to evaluate the effectiveness of automated distress data compared to benchmark manual ratings by experienced IN DOT staff (Ong, et al., 2010). The first measure was hypothesis testing on the statistical significance of the difference in PCR values. The second measure was the percentage cumulative differences between the PCR collected by the two systems over the entire range of PCR, thereby accounting for the mean-variance dependency of PCR. The third measure was Cohen's Kappa statistic for individual distresses, which estimates the strength of agreement between the automated and reference systems.

For the Texas DOT study (Serigos et al. 2015), the accuracy and precision of each of the three automated systems before and after human intervention are presented in Table 10. The average measurement error or bias between the software measured distress quantity and the reference values are the first number in each cell representing software accuracy. The second value, shown in parenthesis, is the standard deviation of the errors, which is an estimate of software precision. The last number is the median of the errors expressed as a percentage relative to the manual measurement. It was observed that generally, the manual post-processing improved the accuracy of distress quantification. However, the precision (as represented by the standard deviation of error) does not seem to improve with manual intervention.

**Table 10. Quantification errors using three different crack detection software before and after manual human intervention (Serigos et al. 2015)**

Distress	Vendor	Quantification Errors	
		Before	After
Fatigue Cracking	INO LCMS 1	-11.76 m <sup>2</sup> (9.34 m <sup>2</sup> ) - 80%	0.69 m <sup>2</sup> (16.49 m <sup>2</sup> ) 7%
	INO LCMS 2	-6.56 m <sup>2</sup> (11.31 m <sup>2</sup> ) - 56%	2.32 m <sup>2</sup> (10.92 m <sup>2</sup> ) 33%
	Pave Vision	-13.88 m <sup>2</sup> (8.62 m <sup>2</sup> ) - 92%	-13.88 m <sup>2</sup> (8.62 m <sup>2</sup> ) - 92%
Longitudinal cracking	INO LCMS 1	1.09 m (9.86 m) 13%	4.1 m (11.95 m) 17%
	INO LCMS 2	4.41 m (10.7 m) 57%	1.51 m (8.51 m) 11%
	Pave Vision	7.24 m (23.73 m) 9%	7.24 m (23.73 m) 9%
Transversal cracking	INO LCMS 1	-15.54 m (23.75 m) - 44%	-1.24 m (13.08 m) 1%
	INO LCMS 2	-8.36m (17.41 m) -30%	-3.55 m (13.39 m) -11%
	Pave Vision	-12.79 m (15.94 m) - 54%	-12.79 m (15.94 m) - 54%

Timm and Turochy (Timm and Turochy 2014) compared manual and automated data sets for Alabama DOT. They found large discrepancies and very little correlation between transverse cracking manually and automatically collected. Also, very poor

correlation was found between the two methods for wheel path cracking and non-wheel path cracking. The following table summarizes the Pearson correlation coefficient between manual and automated distress data calculated for each severity level and for three data sets.

**Table 11. Alabama DOT paired t-test between manual and automated distress data (Timm and Turochy 2014)**

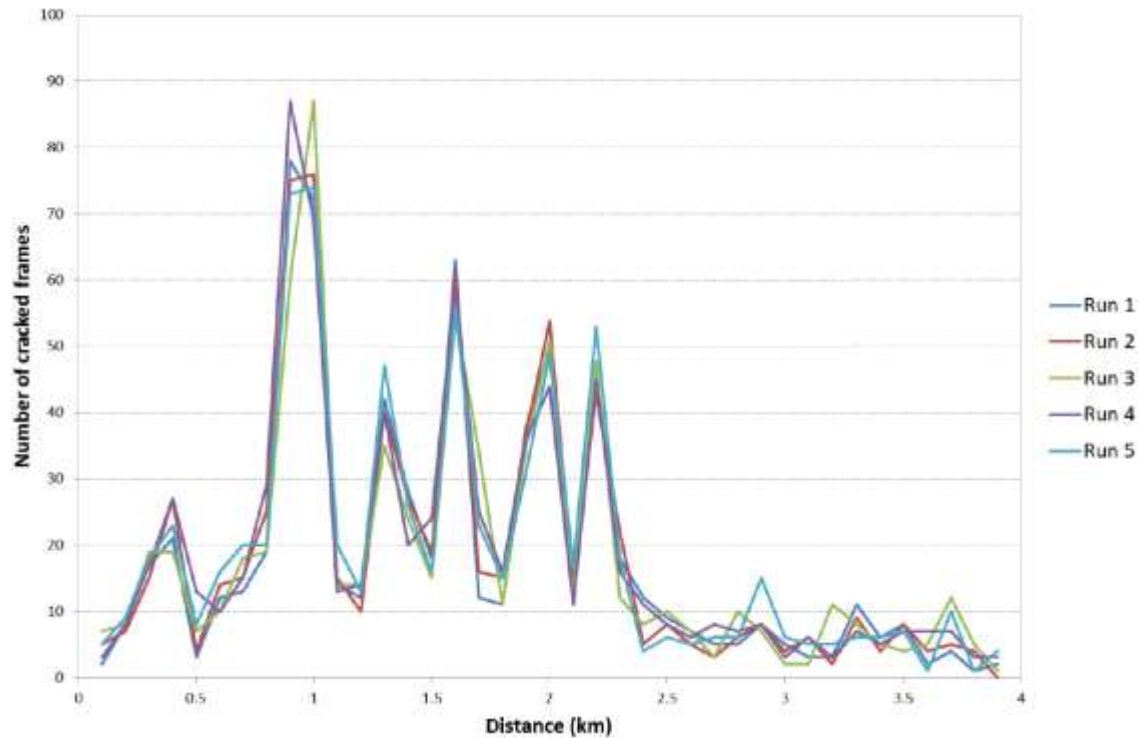
Severity level	Pearson correlation coefficient		
	Transverse cracking	Wheel path cracking	Non-wheel path cracking
Low	0.568	0.248	0.241
Medium	0.277	0.258	0.391
High	Undefined	0.102	Undefined

### **Reliability of Automated Surveys: Precision and Repeatability**

While systematic errors identified in the bias can be calibrated out, such evaluations must also address the random errors as well. The average results may be quite comparable, but individual results can deviate significantly. Efforts must also be made to control these deviations to produce results which can ultimately be classified as reliable. The values in parentheses in Table 10 represent an estimate of the precision of the three software methods used for automated crack detection in the Texas DOT research study (Serigos et al. 2015).

The ASTM E177 (ASTM 1998) includes a criterion called “difference two standard deviation (D2S)”, which states that the difference between two laboratories running the same test on the same material should not exceed D2S more than 1 time out of 20 or 5% of the time (i.e., there is a 95% confidence limit). In that relationship, S is the pooled standard deviation of all paired test results to be compared. In practice, it is possible to apply a similar approach to either process control or as an acceptance criterion in automated pavement condition data collection (McGhee 2004). This repeatability criterion could be applied to pavement condition indices; as well as to individual distresses making up the indices.

In a research study conducted by the ARRB Group (Warren et al. 2013) the repeatability of the RoadCrack crack detection algorithm with LCMS images was evaluated by conducting multiple runs (trials) on a test section (Figure 17). As noted in the work published by ARRB, many of the statistics are often simplified to show a higher level of consistency. Statistics such as number of cracked frames and total length of cracking are often used to identify the quality of crack detection rather than the severity and classification of the measured cracks.



**Figure 17. Repeatability trials of simulated real time cracking analysis using the RoadCrack® algorithm on LCMS images (2.5 mm sampling at 40 mph) (Warren et al. 2013)**

### Efficiency of Automated Surveys

Ultimately, for such a system to be truly beneficial, it must be able to generate results that are considered reliable (minimized standard deviations compared to suitable alternatives), effective (with minimal bias to the suitable reference) and efficient (when comparing the resources required compared to comparable alternatives)

The surveys typically do not require a large number of staff to process the data, but rather require additional computing power. As noted by ARRB (Warren et al. 2013), the crack identification can be completed at rates of 14 mph, plus additional classification and reporting. This was reported for 2080x2000 pixel images, which result in 0.8 GB of data per mile. Higher resolution images can reduce the processing speed.

Distress quality control for fully automated distress collection is also an important step in the process. Sampling of automated crack detection can indicate any potential quality issues and identify systematic issues. Systematic issues may be identified in different manners such as adjusting image settings or detection parameters to better address specific field conditions.

## **Benefits to Agency**

Successful development and application of crack detection software will result in the following potential advantages to the data collection and pavement management initiatives by every roadway authority:

- Increased safety of the data collection staff
- Increased efficiency and productivity of network-level evaluations using real-time automated crack detection software
- Enhanced objectivity of crack rating (identifying type and severity) using the automated applications
- Increased accuracy and precision in measuring crack extent, identifying crack location, and providing summary statistics
- Better pavement management decisions and improved rehabilitations activities

### **1.4.3 Integration into Practice**

Of equal (if not greatest) importance, is the necessity to be able to integrate any such system into practice. This requires evaluation of what if any impacts such a transition will have on decisions made utilizing the system. What if any adjustments or calibrations may be anticipated or required? What training will be required to facilitate the new system is properly understood, executed and incorporated into the existing practice? What limitations should be acknowledged (and what steps are recommended / proposed to address those limitations)? What is the plan for continuous improvement to give the new system the greatest opportunity to reach its full potential?

Each of these concerns must be fully explored to identify and address any obstacles that can be anticipated. This process will identify actions required to provide the greatest opportunity for successful integration and realization of the benefits expected from the implementation of an improved system.

## **Quality Management Procedures**

Quality by definition is “the degree to which a set of inherent characteristics fulfill requirements” (ISO 2005). According to TRB, quality management is the overarching system of policies and procedures that govern the performance of quality control and acceptance activities (TRB 2009). In order, to achieve a consistent level of quality, it is



necessary to adopt a systematic approach for the quality management practices that includes methods, techniques, tools and model problem solutions. Quality management involves the specification of data collection protocols, quality standards, responsibilities of personnel, quality control, quality acceptance, corrective action and quality management documentation (Attoh-Okine and Adarkwa 2013).

With respect to automated distress identification software, the level of quality can be quantified according to the aforementioned success metrics. One purpose of quality management is to quantify variability in the process and maintain it within the range of acceptable limits. It should be noted that the quantity being measured by the software is by itself an indicator of variability in pavement condition along the length of the highway, and therefore it will inherently exhibit variability. Due to this characteristic of the measured pavement condition, the determination of acceptable limits is a challenging task. Quality management procedures include comprehensive and systematic steps for:

1. Quality Control: to ensure that a desired level of quality is obtained for the developed product or service.
2. Quality Acceptance: to confirm that the quality of the developed product or service is indeed acceptable for application by the user
3. Quality Assurance: to increase the ability of the development process to fulfill quality requirements for the product or service being provided

In the transportation infrastructure industry, quality control by the product or service provider (contractor), and quality acceptance by the roadway authority (user) are the major areas of focus in quality management of pavement condition data collection (Flintsch & McGhee, 2009). In addition to the quality control and acceptance practices, independent validation and verification (IV&V) by a third party are recommended as external audit in quality management plans. In most pavement condition data collection projects, where IV&V are used, the main focus has been the quality acceptance.

The quality control of distress data is typically conducted in two steps. Initially pilot runs are performed, and the data collected is compared with data obtained from manual surveys to ensure the equipment is functioning. Then during data collection, random sections are chosen, and data is compared with manual survey to ensure that data is not exceeding the acceptable variability (Attoh-Okine and Adarkwa 2013). According to a recent survey, approximately 64% of state and provincial highway agencies have a form of data collection quality control plan in place (Attoh-Okine and Adarkwa 2013). An active quality control plan is also a requirement under the proposed rules for MAP-21 (FHWA 2015).

A minimum sample size needs to be adopted to ensure that the sample is representative of the observed pavement conditions to evaluate accuracy and precision of the automated distress surveys. There are a series of statistical techniques that estimate the required sample size based on the desired accuracy and the degree of risk (uncertainty). Typically, the sample size is selected by balancing accuracy and cost. In a study for the National Park Service pavement management system (PMS), Selezneva et al. (2004) proposed promising statistical sampling approaches for quality acceptance of automated pavement distress data. The interested reader is referred to that study (Selezneva et al. 2004) and the Quality Assurance Manual for the Road Inventory Program at the National Park Service (2003).

A 5 percent sample is common for most of the quality control and acceptance testing. Out of the service providers surveyed in 2009 (Flintsch and McGhee 2009), 29 percent reported reviewing 2 to 5 percent of the data, another 29 percent indicated sampling 6 to 10 percent, and the remaining 42 percent of the contractors reported reviewing 10 percent or more as part of their regular quality control practice.

Raman et al. (2004) conducted a statistical analysis on the severity and extent of transverse cracks reported by various procedures. In the situations where data was normally distributed, analysis of variance was used. In the cases where data was not normally distributed, the Kruskal-Wallis nonparametric test was conducted. Following a comparison of sampled and full-section image data, the authors concluded that a 5% sampling rate was adequate to evaluate transverse cracks with the desired precision for network-level evaluations in Kansas (Raman et al. 2004).

Using the provisional AASHTO protocol on data obtained from Arkansas highways, Wang et al. (2004) compared the results of manual versus automated cracking surveys. For each comparison section, only 5 percent of the images were investigated. The study found some differences between the manual and automated procedures but suggested that these discrepancies might have been the result of low repeatability of the manual surveys (Wang et al. 2004).

PennDOT distress condition survey quality assurance program entails field testing over 2.5% of the annual survey mileage. The goal is to assure the quality of the service and product provided by PennDOT's pavement data collection vendor (Pennsylvania DOT 2015b). Up to 5% of the vendor IRI data is allowed to exceed  $\pm 25\%$  of their own independent measurement. They allow up to 10% of the other distresses to exceed either  $\pm 20\%$  or  $\pm 30\%$  depending on the distress type (Timm and Turochy 2014).

Using standard variability control concepts with pavement data collection, Stoffels et al. (2001) proposed a process to identify acceptable ranges for comparing results from two independent sources. Based on the difference of two standard deviation (D2S) criteria applied to laboratory materials testing results (ASTM 1998), the authors established that

in 95% of the contractor processed data for the Virginia DOT network, the difference in pavement condition indices from the reference values should not exceed D2S. Average results from the individual ratings by the production contractor and quality monitoring (by VDOT staff or an independent contractor) were used to determine the bias (D). The pooled standard deviation of all ratings (S) was used to determine the acceptable limits for each pavement condition index.

One of the most important objectives in a quality management plan is to minimize the variability in the pavement condition measurements. Regarding the automated crack detection software, this objective translates into increasing the reliability (repeatability) of distress identification results. In order to accomplish this objective, the following predominant sources of variability in automated distress identification need to be considered (McNeil et al. 1991; Flintsch and McGhee 2009):

- Pavement surface condition: the optimum pavement condition for automated crack detection is a dry surface following rain that has removed all the loose debris. In conditions other than the optimum, significant variability can exist.
- Image capturing technology:
  - Additional collected data: some technologies such as the 3D imaging provide additional data that can assist in enhancing crack detection and identification, and thereby reducing variability.
  - Image resolution: detection of smaller cracks requires higher resolution equipment. Lower resolution images result in higher variability in crack detection.
  - Lighting method: optimum illumination is required for the processing software to provide robust crack identification.
  - Color contrast quality: for the crack detection software to successfully identify cracks, the contrast of color between the crack and the surrounding pavement area is an important factor.
  - Field of view: if the images do not cover the entire lane, some cracks might be missed.

- Processing algorithm: the level of sophistication of a crack detection algorithm dictates how many of the existing cracks will be detected and how many false positives will emerge.
  - Algorithm control parameters: the control parameters adjust the normalization approach and sensitivity of the software for crack detection by changing the probability of crack existence. Adjusting the image normalization can handle larger textures such as tined concrete surfaces and surface treated roads but may reduce the ability to detect smaller cracks. By increasing the sensitivity, more of the existing cracks will be detected by the algorithm, but this will come at the cost of potential false positives. The optimum control parameters need to be identified for each algorithm to produce robust results.
- Software operator training: even in fully automated crack detection, there is still some level of human intervention in determining the algorithm settings and quality control of the software results. The training and experience of the operator affects the final report.

In software terminology, validation is referred to the process of checking whether the specification captures an agency's needs, while verification is the process of checking that the software meets the specification. Calibration is necessary in the entire process of data collection to ensure accuracy, knowing that variations between different devices and operators can exist (Flintsch and McGhee 2009). Verification tests should be included in the quality management programs to verify data consistency.

The independent verification of data is usually conducted by a quality assurance auditor, who checks the databases. The verification includes the completeness of the data based on a random sample of a percent of the data collected. Virginia Department of Transportation applies an independent verification and validation of 10% of the data provided by the contractor. Determined indices are calculated in randomly selected sections of a lot, then are compared with the contractor's results. For a lot to be accepted, the differences in distress indices should be within 10 points (or the value determined from evaluation of the contract). When the previous criterion is not met the Contractor is responsible to adjust and/or reprocess the lot (Virginia DOT 2012).

### **Data Management Considerations**

There are many practical considerations that also need to be addressed when dealing with the volume of data discussed for pavement data collection and related imagery. Some of the data size information was briefly noted in Section 1.2.9.

Due to the large amount of data required for collection, there are many challenges faced by those collecting and processing pavement condition data with automated data collection. Some of these issues include:

- Backing up of raw field data from collection
- Data and image storage for processing and access to processed data
- Data and image backups during processing of altered data
- Data and image storage of processed data for distribution of results
- Data and image backups of final results.

Due to the cost of collecting pavement condition data in the field and the cost associated with processing, proper data management and backup is also required. Potential loss of data can occur due to corrupted hard drives in the field and in the office as well as potential for the loss of data if shipping of hard drives is required from the field or to additional processing centers. In some cases, up to 5 copies of the data need to be maintained during processing to prevent significant loss of data or repeat of collection or processing effort.

In many cases the raw data is collected at a much higher interval than is required for reporting. For example, longitudinal profile is often measured at a frequency of 1 in along the roadway yet reported IRI values are often summarized at intervals of 0.1 miles.

For the case of images, changes are not frequently made to the images themselves. The most common duplicate of the data encountered is the extraction of still images if data is recorded as video. In the case of 3D pavement systems, different image views are often extracted from the 3D file type to ensure they are easily viewed in other tools.

If different normalization or other image adjustments are completed, additional copies of the images may be maintained for repeatability. Other changes to files such as geotagging, adding metadata, or stamping location information on the file may also require additional copies or a backup of the final product.

Data compression, including images, has long been used to try to best use the available resources. In many cases compression can be completed on some data formats without

any loss in data quality. Examples of this include the use of data compression with zipped file formats.

For images, many of the formats available also have lossless compression available. Additional compression can be accomplished by using adjacent data to closely approximate data not stored. Image compression can save valuable hard drive space, but data lost in this compression cannot be later recovered and care must be used.

Image compression and reduced image size (i.e. thumbnails) are often used for the distribution of the final results. In many of these cases viewing the data visually can be done with a reduced impact with no noticeable impact on quality, but with considerable improvements in computer performance through reduced network bandwidth and reduced file storage or widely accessible servers.

The use of metadata incorporated into the pavement images has gotten increased use in recent years as a consistent, open sourced method to store additional information about image contents such as cracking location and levels.

In most cases, the metadata is added to the images as one of the last steps during processing. This reduces the number of changes to occur on the pavement images and the number of intermediate backups required during the data processing phase.

## **1.5 Summary and Recommendations**

From this review, it is evident that the field of pavement evaluation has experienced significant advancements over the past couple of decades, and in fact still appears to be an area of significant interest for technological advancement. Using the information identified from this review (and the objectives and constraints of this specific study, as they are understood) this summary highlights the aspects of automated pavement evaluation that are believed to be critical to the successful completion of this study as well as the recommendations for the path forward.

### **1.5.1 Image Capturing Hardware**

This study will be using the 2D system operated by Florida DOT. It is evident that advancements in 3D technology will likely provide future opportunities for improvement in the pavement evaluation process. These will be documented when identified to provide recommendation for future consideration. If there is a need to compare results from various technologies, a systematic procedure needs to be developed. Since the data processing software for 2D and 3D systems have different algorithms, each software-hardware system needs to be benchmarked on a predetermined set of representative pavement sections. Then, the comparison should be conducted

according to established reference values on each section. Increases in both data collection resolution and image quality will also improve the ability to match the capabilities of human raters and the expectations of the pavement management process.

### **1.5.2 Crack Detection**

Many different systems and/or techniques are under development and/or being investigated for improving the state of the art in image analysis and specifically crack detection. Recognizing this is a rapidly evolving field, every effort will be made to objectively consider and explore the multitude of methodologies available (within the resource constraints of this specific study). These investigations will initially focus on the needs (and challenges) specifically associated with PCC surfaced roads (as noted in Section 3.6). Where crack detection opportunities are perceived to exist that are beyond the resources available for this specific initiative, these will be documented and reported for consideration.

### **1.5.3 Implementation of Automated Crack Detection Surveys**

Only a few highway agencies have implemented a fully automated crack detection system for network-level data collection. From the existing experience, a sound and systematic quality management process seems to be the central consideration for a successful implementation. Such a quality management system requires quantitative quality investigations and corresponding acceptable (and context-sensitive) thresholds for quality control, quality acceptance, and independent verification. These components are determined through an evaluation of the automated technologies in terms of accuracy, precision or reliability, efficiency, and the benefits to the agency. In addition to assisting with the selection of an available technology and adoption of a quality management system, these success metrics also aid in identification of the potential improvements.

Recognizing the importance of producing results that can be put into practice, all aspects of these investigations will be performed with consideration for future implementation. Specifically:

1. Optimizing LRIS image capture and quality.
2. Defining (quantitatively) deviations from current pavement evaluation procedures.
  - a. Both on a distress specific basis, as well as aggregated statistics.

- b. As well as recommendations for correction (or adjustments) where warranted or deemed appropriate.
- 3. Identification of training needs (for both pavement evaluators as well as those using the results)
- 4. Recommendations for quality management procedures.
- 5. Data management recommendations.

#### **1.5.4 The Value Added by Automated Crack Detection**

The development and implementation of an automated crack detection and quantification software and supporting work processes is key for this project. To truly (and fairly) investigate the merits of the options investigated throughout this study, objective assessments of the value added must also be taken into consideration. These value assessments will be documented throughout the study to aid in both future planning as well as management and development of the pavement evaluation process going forward.



## **CHAPTER 2 – RIGID PAVEMENT APPLICATION DESIGN**

Task 2 was subdivided into three (3) subtasks. Each of these subtasks serves a vital role in ultimately defining what is needed and why: 1) Validation of the Collected Image Quality, 2) Evaluation of Existing Distress Survey Methods, and 3) Gap Analysis and Design Recommendations.

This chapter is organized in five sections. Following this introduction, Section 2 provides a report on an investigation conducted by Fugro staff to determine whether the collected pavement images are of acceptable quality for crack detection and how FDOT can potentially measure various image quality indicators in future. Section 2.2 explains the evaluation and comparison study details and includes the findings on evaluation of the existing distress survey methods. Section 2.3 describes the efforts to determine the appropriate settings for automated crack detection, classification, and rating. Section 2.4 addresses the gaps between existing automated algorithm and the required development efforts to address the gaps. This was the foundation for Task 3. Section 2.5 summarizes all the efforts and the resulting recommendations from Task 2.

### **2.1 Validation of the Collected Image Quality**

This section discusses the investigation conducted by Fugro staff to determine whether the collected pavement images are of acceptable quality for crack detection and how FDOT can potentially measure various image quality indicators in future. As a result of this study, Fugro developed a hardware calibration protocol to be used by FDOT staff in order to ensure long term image quality and consistency. This protocol is included in Appendix A. A Fugro hardware expert visited FDOT on October 2015 to examine the multi-purpose survey vehicle (MPSV) system and discuss quality assurance precautions.

Before evaluation of the available distress survey methodologies, there is a need to evaluate the pavement images collected with the Laser Road Imaging System (LRIS) and validate the optimum quality of the images and provide guidelines for routine validation in the future. To conduct such an evaluation, there is a need for a control site with established surface features. FDOT has an established imaging target site containing longitudinal and transverse stripes for evaluation of the image alignment between the two LRIS cameras, and for any potential optical distortions.

The following factors need to be considered in the image quality validation process, as they might affect the subsequent crack detection. It should be noted that while all these considerations can be evaluated, there are limitations with the available hardware system that might not allow for resolution of all of the identified issues. In addition, a number of these quality evaluations include subjective judgments by an experienced engineer or technician in practice. The INO calibration procedure for LRIS is also based

on human judgment of image quality. Many of the objective quality assessment methodologies in the image processing literature require a complete reference (distortion-free) image to calculate the errors against, and such evaluation is not feasible when dealing with miles and miles of highway pavement images. Surrogate techniques that are no-reference or reduced-reference methods are also available.

### **2.1.1 General Image Properties**

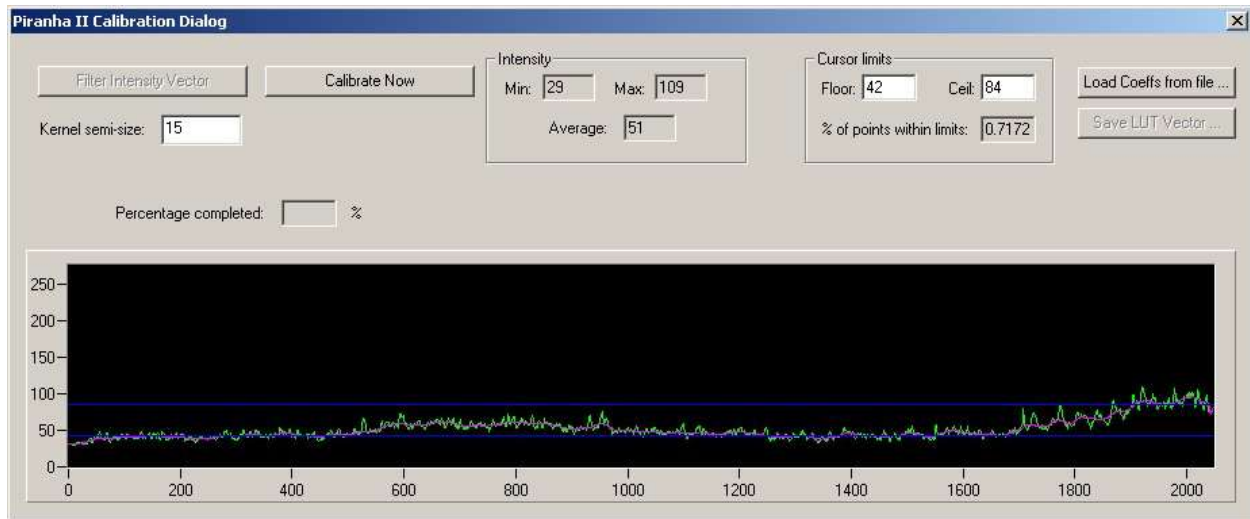
The typical state of the practice regarding these image properties is a subjective evaluation by an experienced human interpreter. Unsuitable values for these image properties could impact crack detection by increasing the potential for missed cracks, detection of false positives, or erroneous crack width measurements.

#### **Minimum Resolution**

Minimum resolution is defined as the level of detail at which you can still see distinct lines next to each other. Theoretically to be able to see 1 mm wide cracks on a pavement image that is 4 meters wide, a transversal resolution of about 4,096 pixels is required. The FDOT LRIS images have about 4,044 pixels, which is deemed as adequate. It should be noted that this theoretical minimum does not always translate into practical detection of all cracks that are 1 mm wide or larger. This is because a variety of other properties including exposure and dynamic range can impact crack detection.

#### **Appropriate Exposure**

The required lighting or illumination needs to increase with higher resolution cameras. In addition, the wide-angle lenses used for pavement imagery result in darker edges which need to be either further illuminated or post-processed. Excessive exposure can result in washed out images that hinder detection of finer cracks. Adequate level of exposure is a very subjective matter and typically it is evaluated by an experienced engineer/technician. While executing the INO calibration procedure for LRIS (the application RoadCrack.exe displayed in the below screen capture), the calibration software will try to adjust pixel coefficients based on the non-uniformity found in the reference image, and when the expert is satisfied with the image displayed in the graphical interface, they press Stop. The images used for calibration should not contain any defects like large cracks, shoulders, drop-off, marking, etc. They should also be acquired on a road section that is as uniform as possible. Finally, it is also better to use images acquired while the vehicle is moving (could be moving slow), this gives a more representative intensity profile vector (small defects and surface inconsistencies are averaged).



**Figure 18. Calibration dialog box.**

## Dynamic Range

Dynamic range determines the level of detailed information contained in the image regarding the full spectrum of color or gray scale. The higher the dynamic range, the more levels of differences exist in the digital values of image pixels. In the 8-bit dynamic range of the FDOT LRIS images (which is currently widely used in the industry), there are 256 levels on the spectrum which translates into 256 shades of gray in a black and white image. The Laser Crack Measurement System (LCMS) images typically have a 24-bit dynamic range. This indicates that representation of a crack in an image may include numerous shades of gray affecting its width along its length. Therefore, manual rating of the images is very subjective and automated crack detection and rating (severity levels) will depend on how the automated algorithm handles a combination of image resolution, exposure, and dynamic range to best identify crack width.

## White balance

It is recommended that a wide uniform standard 18% gray carpet be used for calibration of the white balance. The ICC software includes a routine for such calibration.

### 2.1.2 Image Issues

Following are the issues that could be caused by defective hardware and/or unsuitable hardware settings. These issues could impact crack detection by increasing the potential for false positives.

## Streaks

A disadvantage to the LRIS system is that because it creates images line by line any dirt or dust on the camera lens can create streaks in the image. These streaks result in black lines appearing in the images and can cause difficulty with automated crack detection software that uses the light and dark contrast to identify cracks. Based on the past experience of Fugro staff, this is a characteristic of the LRIS system (see Figure 19 below).

## Alignment of the established longitudinal/transverse control lines

There are settings parameter files that control the stitching of the left and right images. These settings are adjusted according to a visual examination of the images of the target site. Based on the currently collected LRIS images of the FDOT target site, it seems that correct settings have been implemented. It is recommended that the images of the target site be checked at least once every year that the MPSV is in service to make sure that the diamond stripes in the center of the lane (see Figure 20) are appropriately displayed in the image.



**Figure 19. Example LRIS pavement image (right) showing intensity streaks that cannot be seen on the ROW image (left)**

The precaution that FDOT can adopt is to clean the camera lenses (the exterior windows on the LRIS units) every morning before data collection and make sure that camera covers are on while the vehicle is not collecting images. In addition, FDOT staff should use reference images with a minimum number of defects and/or non-uniformity for the exposure calibration process.

When necessary, all windows should be cleaned with a soft fabric using isopropanol or methanol. Avoid scratches that could damage the optical quality of windows and affect system performances. The controller and the sensor's body should be cleaned with a soft fabric using water only. Appropriate precautions should be taken to make sure that the isopropanol or methanol is not used over the different labels that are affixed on the sensors and on the controller. It is recommended to protect the external windows with covers when the LRIS is not in use.

### **2.1.3 Image Feature Capturing (optical distortion)**

These properties are related to misrepresentation of actual pavement features due to inherent optical distortions in the camera and the wide-angle lens. These issues could impact crack detection by increasing the potential for detecting erroneous crack lengths and widths.

#### **Crack Length in Longitudinal, Transverse, and Diagonal Orientations**

FDOT has measured the ground truth horizontal, vertical, and diagonal distances among physical diamond shaped stripes at the imaging target site (see Figure 20).



**Figure 20. Pavement section with optical distortion study points.**



The same distances have been measured on LRIS 2D images and LCMS 3D images. The results of this exercise (which is according to the previous FDOT research documented in Report No. BD-544-11, chapter 2) are detailed here. The errors in these measurements are a good representation of the optical distortions in the images. In addition, these results could be used for checking the long-term consistency of the image capturing hardware. It is recommended that this exercise be conducted once annually to ensure optical distortions are not increasing with time.

The normalized error between field measurements and image measured distances on the FDOT imaging target site were evaluated in the transverse, longitudinal and diagonal directions. Figure 21 depicts the target site setup and Table 12 shows the reference measurement patches that were considered for this evaluation.

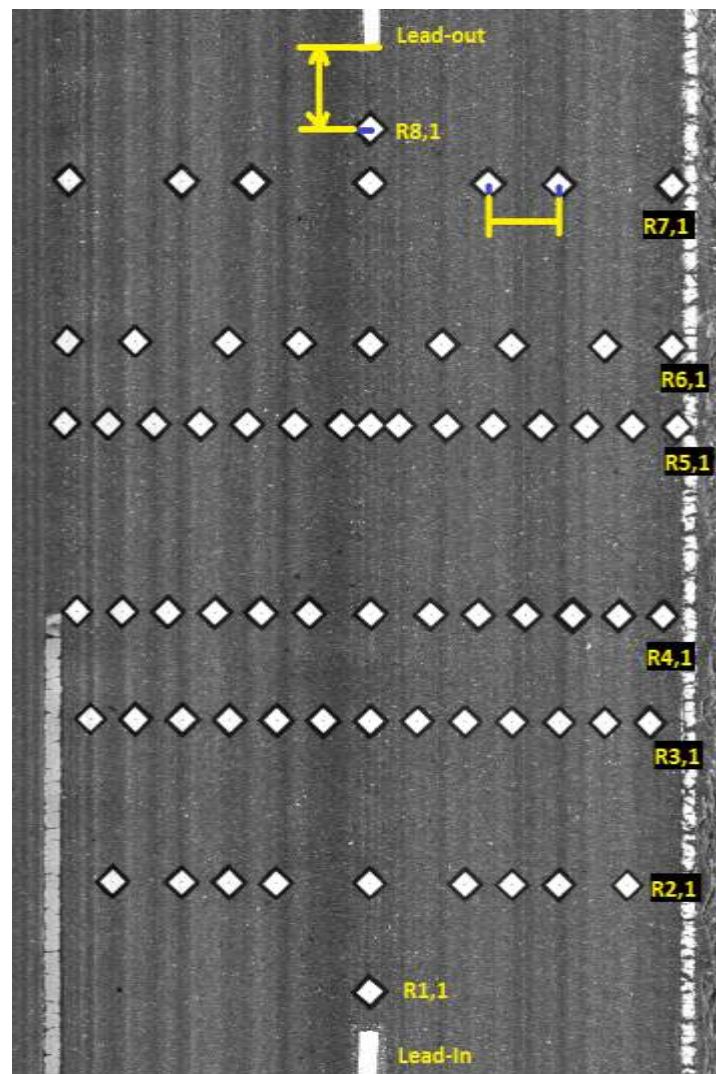


Figure 21. LRIS 2D image of FDOT target site.

**Table 12. Reference points for measurements**

TRANSVERSE												
Row	Patch Number	Row	Patch Number	Row	Patch Number	Row	Patch Number	Row	Patch Number	Row	Patch Number	
R2	1 - 2	R3	1 - 2	R4	1 - 2	R5	1 - 2	R6	1 - 2	R7	1 - 2	
	2 - 3		2 - 3		2 - 3		2 - 3		2 - 3		2 - 3	
	3 - 4		3 - 4		3 - 4		3 - 4		3 - 4		3 - 4	
	4 - 5		4 - 5		4 - 5		4 - 5		4 - 5		4 - 5	
	5 - 6		5 - 6		5 - 6		5 - 6		5 - 6		5 - 6	
	6 - 7		6 - 7		6 - 7		6 - 7		6 - 7		6 - 7	
	7 - 8		7 - 8		7 - 8		7 - 8		7 - 8			
	8 - 9		8 - 9		8 - 9		8 - 9		8 - 9			
					9 - 10		9 - 10					
					10 - 11		10 - 11					
					11 - 12		11 - 12					
					12 - 13		12 - 13					
							13 - 14					
							14 - 15					
LONGITUDINAL		DIAGONAL										
Patch Number		Patch Number										
R1,1 - R2,5		R1,1 - R3,9										
R2,5 - R3,7		R1,1 - R3,3										
R3,7 - R4,7		R6,7 - R7,4										
R4,7 - R5,8		R7,4 - R6,6										
R5,8 - R6,5		R8,1 - R6,3										
R6,5 - R7,4		R3,7 - R6,7										
R7,4 - R8,1												

In the transverse direction, all the distances between consecutive diamond stripes have been measured in each row. For the longitudinal and diagonal directions, a sample of the distances have been measured in the field. FDOT staff have conducted three measurements per patch and the average of those measurements was considered as the field reference measurement to estimate the error in image measurements due to optical distortions. The image measurements were done on FDOT provided LRIS 2D images and the Fugro collected LCMS 3D images.

The width of LRIS 2D image and LCMS 3D image are typically 4044 and 4164 pixels, respectively. This depends on the amount of overlap between the left and right camera images during stitching. Each pixel has been assumed as 1 mm (which might not always be true but is the best estimate) and based on this, the error percentage of LRIS 2D and LCMS 3D images have been calculated with respect to field measurements. The normalized error percentage (normalized to field measurements) was calculated as follows:

$$\text{normalized error (\%)} = 100 \times \left( \frac{\text{image measurement} - \text{average field measurement}}{\text{average field measurement}} \right)$$

The average, standard deviation, minimum, and maximum percentage of normalized errors for all the measurement patches in longitudinal, transverse, and diagonal directions have been summarized in Table 13. Average error percentage in transverse direction is found to be slightly higher in 3D LCMS image compared to 2D LRIS image. However, average error percentages in longitudinal and diagonal direction are lower in 3D LCMS image compared to 2D LRIS image.

**Table 13. Statistics for normalized error compared to field measurement**

Direction	Image Technology	Normalized Error (%)			
		Average	Standard Deviation	Minimum	Maximum
Transverse	2D LRIS	3.12	2.92	-3.38	7.61
	3D LCMS	3.98	3.15	-3.00	8.95
Longitudinal	2D LRIS	-2.30	0.46	-3.11	-1.90
	3D LCMS	-0.46	1.42	-1.81	1.98
Diagonal	2D LRIS	-0.92	0.81	-1.80	0.05
	3D LCMS	-0.03	0.74	-0.79	1.27

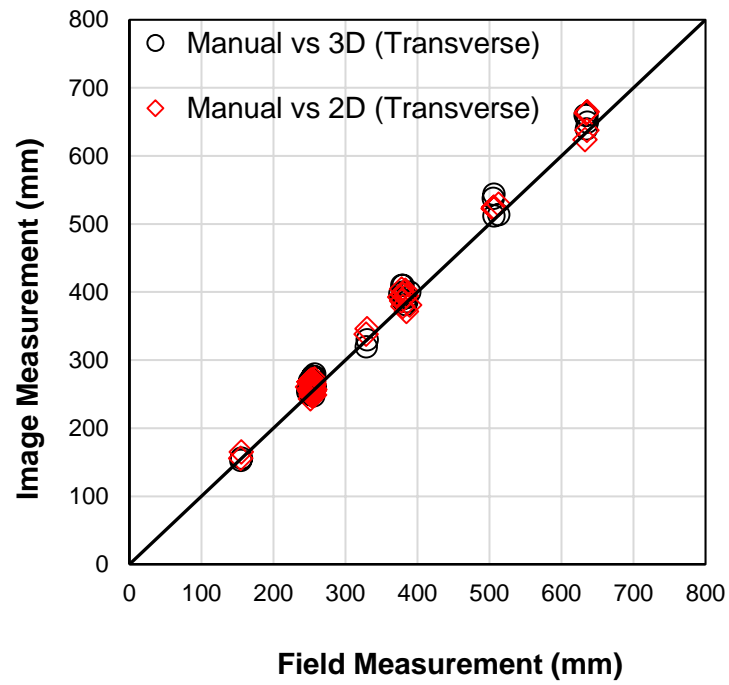
It should be noted that the overlap resulting from the stitching of the left and right camera images could affect the distance measurements from the images in the two patches in the middle of each row. Measurement patches that could be affected by image stitching have been highlighted in gray in Table 12. Table 14 shows the average percentage of errors (normalized to field measurements) in the transverse direction only for the measurements that were entirely on one image and therefore not affected by the image overlap. The exclusion of the LRIS image edge measurements resulted in lower average error but higher standard deviation of error. In contrast, the exclusion of LCMS image edge measurements resulted in higher average error and lower standard deviation of error.

**Table 14. Average and standard deviation of error excluding measurements affected by stitching**

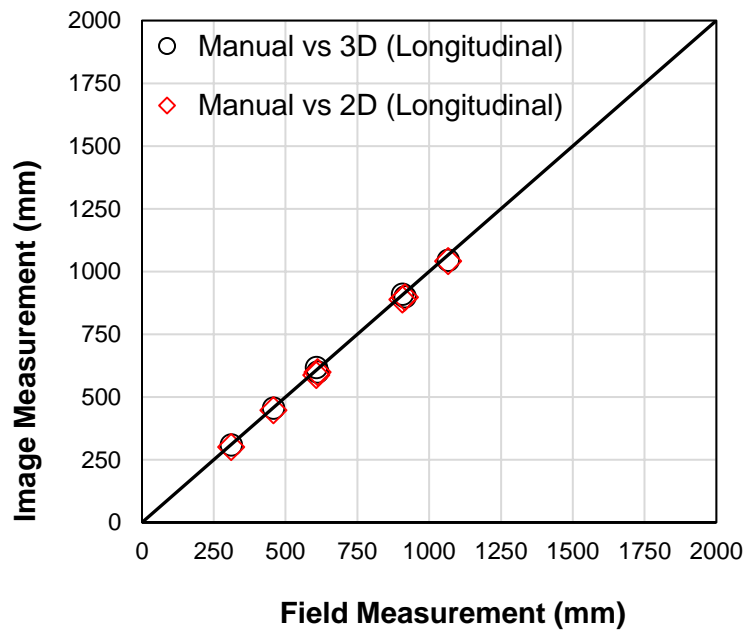
Direction	Average Error (%)		Standard Deviation of Error (%)	
	2D LRIS Image	3D LCMS Image	2D LRIS Image	3D LCMS Image
Transverse	2.95	4.92	3.16	2.68

A side-by-side comparison of the measurements (distances between diamond markers) from the field to the measurements from the images have been shown individually in Figure 22 for transverse, longitudinal, and diagonal directions.

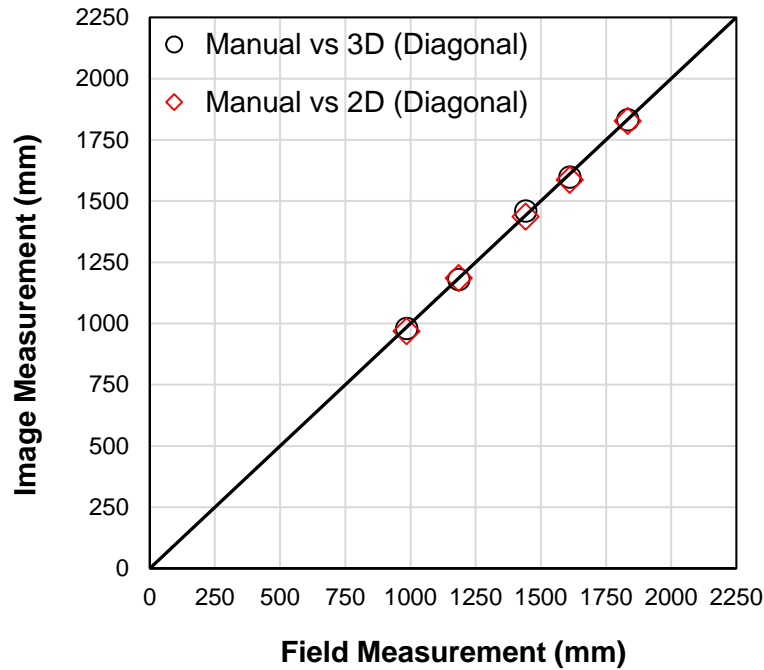




(a) Transverse Direction



(b) Longitudinal Direction



(c) Diagonal Direction

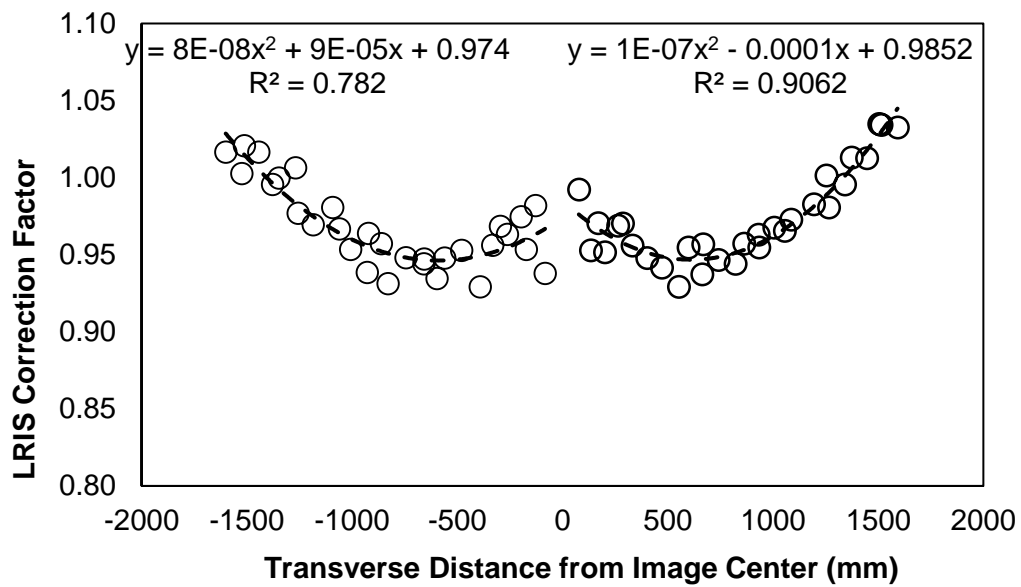
**Figure 22. Image measurements compared to field measurements in a) transverse, b) longitudinal, and c) diagonal directions.**

The ratio of the field measurements to the 2D LRIS or 3D LCMS image measurements has been estimated as a correction factor. The transversal correction factors for 2D LRIS image and 3D LCMS image have been shown in Figure 23 as a function of the distance from the center of each measurement patch to the center of the image. The distance has been measured from the center of image to center of consecutive diamond marker points shown in Figure 21. The correction factor for 3D LCMS image measurements is lower than that of the 2D LRIS image most of the time, with some exceptions towards the edge of rows. It is also evident that there is a higher variance in the correction factors for the 3D LCMS image compared to the 2D LRIS image.

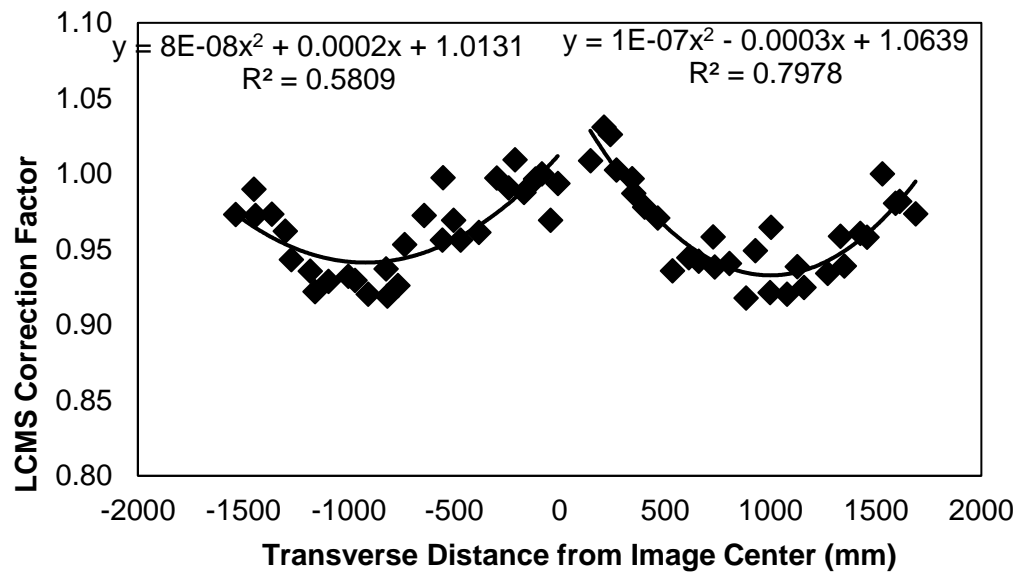
It should be noted that all the field and image measurements were done to the nearest full millimetre. However, it is not expected that anyone can accurately measure to the 'center' of these targets, in the field or off an image by conducting only one measurement. Therefore, multiple measurements (in this case 3) need to be averaged.

It is evident that the amount of these optical distortion errors and correction factors are fairly small and variable depending on the location of the measurement within an image. Therefore, it is not realistic to adjust the detected cracks according to these correction

factors. The intention is to use these errors as a check for long term consistency of the errors in image capturing hardware.



(a) Correction Factor for LRIS Image



(b) Correction Factor for LCMS Image

**Figure 23. Correction factors for transversal image measurements in a) 2D LRIS and b) 3D LCMS.**

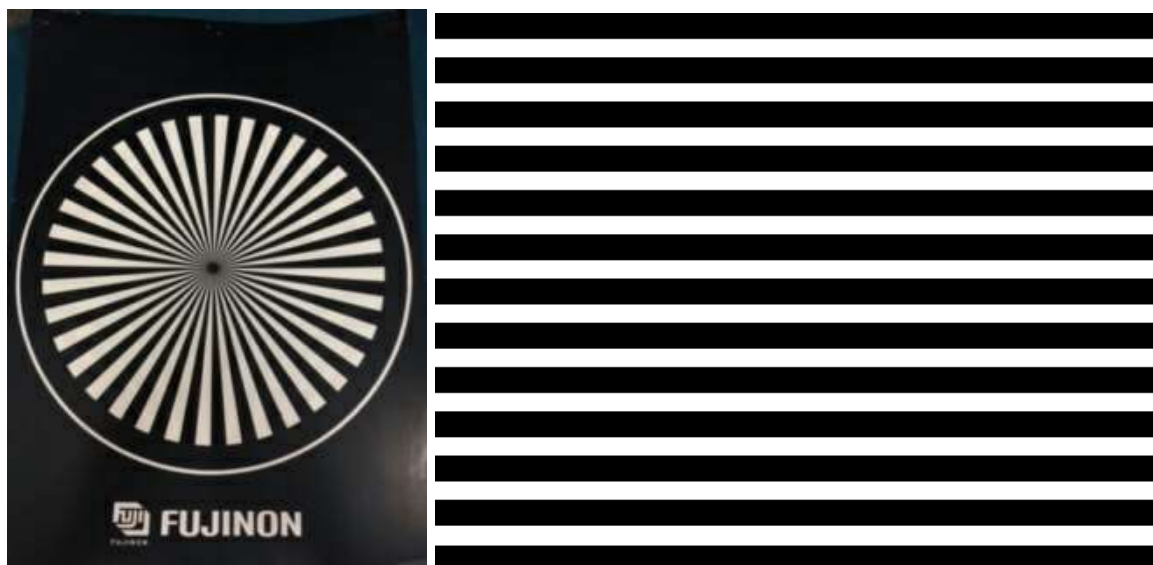
### **Crack Width in Longitudinal, Transverse, and Diagonal Orientations**

Unlike length measurements which are very objective, crack width measurements are subjective due to the gray areas in the images and subjectivity in visual field inspections. In addition, the small magnitudes of crack width make it a challenge (if not impossible) to measure the errors which are in sub millimeters, while the image resolution is at 1 mm. The smallest crack width threshold of interest for FDOT is 3.18 mm which defines the threshold between low and moderate severity cracking.

### **Signal-to-Noise Ratio**

This is a traditional quantitative measure representing the ratio of the amount of undistorted features captured in an image (signal) to the distortion errors (noise) in detecting features, expressed in decibels. Therefore, this measure and similar measures such as mean squared error (MSE) require a reference “undistorted” image. An estimate of the signal to noise ratio (SNR) can be approximated as the average value of the image pixels (0 to 255 for 8-bit images) divided by the standard deviation of the image intensity values. This approximation eliminates the need for a reference image, but an image with a high SNR value approximated through this method does not necessarily remain faithful to the reality.

A target could be synthetically manufactured to serve as the reference undistorted image. A picture of the target taken by the available camera could be used to evaluate the SNR of the captured image as compared to the reference. Figure 24 shows two sample target images used as a reference for evaluating the signal to noise ratio.



**Figure 24. Sample Target Images used as a Reference for Evaluating Signal to Noise Ratio**

Detailed investigation of SNR values was conducted in a previous FDOT study and it is documented in Report No. BD-544-11. It is recommended that a similar target image be used for annual control checks of the SNR values. In Appendix A, an exercise is recommended to be conducted annually to ensure signal to noise ratio is not increasing with time.

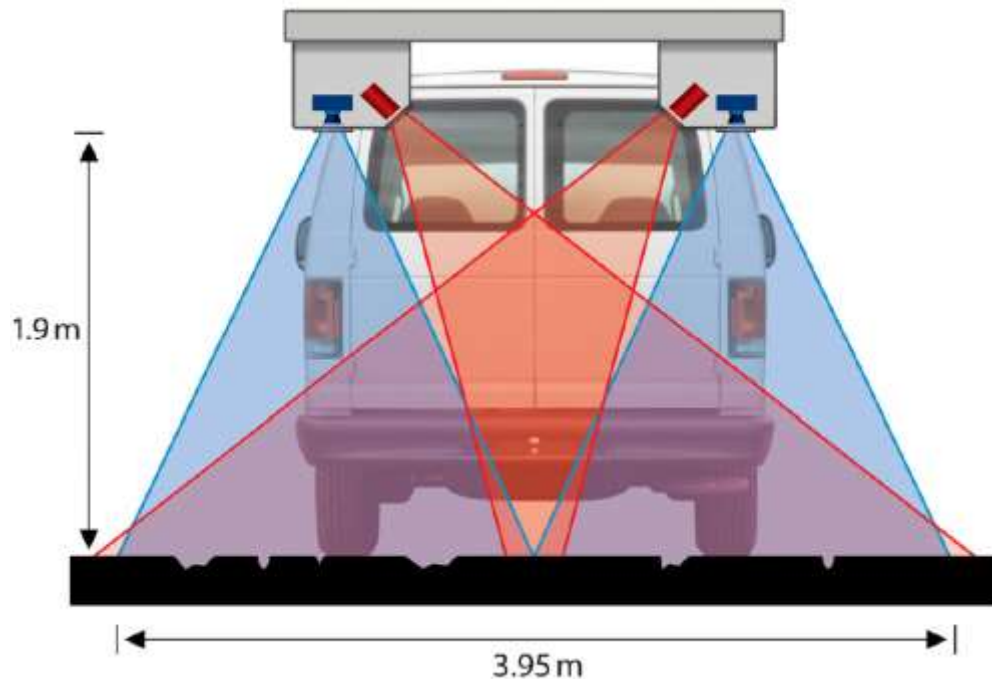
#### **2.1.4 LRIS Hardware**

The integrator company for the FDOT LRIS vehicle is the International Cybernetics Corporation (ICC) and they are responsible for resolving hardware issues, some of which could be addressed by routine maintenance. It is necessary that the hardware and software setup and “calibration” standards recommended by the LRIS equipment manufacturer (Pavemetrics) and the FDOT equipment integrator (ICC) be followed with regards to routine maintenance and calibration controls. The overall system maintenance and recalibration is recommended once a year. This includes checking the camera installed heights and the vehicle tire pressure to ensure the pavement surface is within the camera depth of field, where objects are in focus.

From the initial investigation of location referencing information by Fugro staff, there seems to be a software issue with determination of the location of each image across the length of the highway. When stitching the images together across the highway length, there are some gaps and some overlaps between consecutive images. The calculation of FromDist and ToDist parameters for each image needs to be revisited by FDOT staff to address this issue. For the purposes of this project, these values were manipulated by Fugro database experts to make sure the entire length of the images were visible in the Vision software to facilitate rating of the distresses. Image lengths were not affected by this manual correction, only the locations of the images were manipulated to align the edges of subsequent images.

- a. Distance measuring accuracy: the distance measuring instrument (DMI) needs to be inspected and calibrated on a routine basis as recommended by the manufacturer. A control section distance can be measured with the DOT reference device and the vehicle DMI measurements of the control section can be compared to the reference measurement.
- b. Latitude-Longitude accuracy: the global positioning system (GPS) devices need to be inspected and calibrated on a routine basis as recommended by the manufacturer. The vehicle needs to be parked at specific locations on the control section for about 15 minutes to establish a stable measurement. Then the GPS coordinates of those locations should be surveyed using total station equipment to check the vehicle GPS measurements. Depending on the number and model of the IMU units in the vehicle, acceptable errors could be found from the manufacturer website.

- c. LRIS platform stability: From the visual inspection by Fugro staff, no issues were found with platform stability. If there are loose connections in the platform, they need to be addressed as recommended by the manufacturer.



**Figure 25. Schematic of LRIS image collection system (Pavemetrics).**

### **2.1.5 Environmental Effects**

The effects of different lighting conditions (overcast, cloudy, or sunny) and vehicle speeds (25, 35, or 45 mph) have already been studied in a previous FDOT research project (documented in Report No. BD-544-11, chapter 2). It was found that the LRIS images are not significantly affected by different vehicle speeds and lighting conditions.

The LRIS user manual indicates that the equipment should not be operated at temperatures above 40 degrees Celsius (104 degrees Fahrenheit). It is recommended that protective covers be used when LRIS is not in use to protect against moisture and dust.

### **2.1.6 AASHTO Standard R86-18**

The following requirements in terms of minimum image quality acceptable for crack detection have been recommended in the American Association of State Highway and

Transportation Officials (AASHTO) provisional protocol (PP) number 68, which was later adopted as AASHTO Standard R86-18 (AASHTO 2018b):

*“4.3.1. The images must provide sufficient difference between data point values representing distressed and non-distressed areas that subsequent distress detection techniques can delineate a minimum of 33 percent of all cracks under 3 mm (0.12 in.), 60 percent of all cracks present from 3 mm (0.12 in.) and under 5 mm (0.2 in.) wide, and 85 percent of all cracks 5 mm (0.2 in.) wide or wider regardless of orientation or type. The determination of this capability will be made utilizing a minimum of ten 0.03-km (100-ft) samples containing an average of at least five such cracks per sample.*

*4.3.2. The images should be sufficiently void of erroneous differences between data point values that a section of pavement without distress, discontinuities, or pavement markings contains less than 3 m (10 ft) total length of detected false cracking in 50 m<sup>2</sup> (540 ft<sup>2</sup>) of pavement. The determination of this capability will be made utilizing a minimum of ten 0.03-km (100-ft) samples of various types that meet the criteria.”*

These image quality descriptions are extremely dependent on the crack detection algorithms that are used to evaluate whether the mentioned amount of cracks with specific width could be detected, or whether false positives are avoided. Therefore, these quality descriptors cannot be considered independent of the crack detection algorithm that is used by each agency. It is recommended that each agency uses their corresponding crack detection software to evaluate whether their collected images in combination with their software meet the requirements of the existing provisional protocol. Ideally however, the protocol needs to be modified to provide image quality requirements independent of the type of applied crack detection algorithm.

As detailed in Section 2.2.6, on average, the evaluated crack detection software was able to detect about 86% of the cracks in all orientations. This result was based on 24 sample images collected from 12 test sections in this study. The sample size satisfies the size requirements of PP-68. Therefore, it could be stated that if crack width is not considered, the image quality did satisfy the requirements of PP-68 in terms of crack detection (or lack of missed cracks). Due to the inherent noise in the images, a pre-processing step had to be conducted in order to filter out the noise. These filters tend to increase crack widths and therefore hinder accurate measurement of crack width. That is why the requirements of PP-68 were not evaluated for each group of crack widths.

With regards to false positives, sample images were evaluated from 12 test sections that met the requirements for sample size in PP-68. The results (which have been detailed in Section 2.2.6) indicate that 78% of the automatically detected distresses by length actually existed on the reference survey. This means that 22% of the detected distresses by length were false positives. The requirement of PP-68 is to have less than 10 feet of false positives in 540 ft<sup>2</sup> sample size (45 feet if the lane width is 12 ft), which

would translate into 22% (10/45). Therefore, it can be stated that the image quality did satisfy the requirements of PP-68 in terms of false positives.

### **2.1.7 Further Hardware Gap Analysis**

Following the next tasks of this research project and after establishing the appropriate automated crack detection algorithm and settings, the Fugro team could better identify potential impacts of LRIS hardware and image quality on crack detection results. If significant negative impacts are discovered manifested by missed cracks and false positives (as described in AASHTO PP-68), then potential remedies shall be suggested accordingly. Chapter 4 describes such additional investigations.

## **2.2 Evaluation of Existing Distress Survey Methods**

The evaluation of the existing distress survey methods was done in the following two steps:

1. Comparison of the overall cumulative quantities of various distress types found in the existing manual windshield survey, manual rating of the collected images (semi-automated survey through Fugro Vision), and a readily available automated software (Fugro WiseCrax)
2. Verification of the automatically detected distresses against the reference crack maps generated through a manual evaluation of the collected images (semi-automated survey)

The following sections will explain the applied distress survey protocol, the representative pavement test sections used for these evaluations, the manual windshield surveys, and the performance metrics considered for these evaluations.

### **2.2.1 Distress Survey Protocol**

In evaluating the existing methodologies, we must first examine what specific information is currently collected and how. Florida DOT's Rigid Pavement Condition Survey Handbook (2017) includes the following distress types and severities:

1. Transverse Cracking (count), Light-Moderate-Severe
2. Longitudinal Cracking (count), Light-Moderate-Severe



3. Spalling (linear feet), Moderate-Severe
4. Corner Cracking (count), Light-Moderate-Severe
5. Patching (sq. yards), Fair-Poor
6. Shattered Slabs (count), Moderate-Severe
7. Surface Deterioration (sq. feet), Moderate-Severe
8. Pumping (percentage range: Code 1 to 4), Light-Moderate-Severe
9. Joint Condition (partially sealed, not sealed)
10. Multiple Cracked Slabs (count)

These are considered the core distresses to be identified. In addition to the FDOT *Rigid Pavement Condition Survey Handbook* (2017) as the primary protocol, the more simplified approach of the AASHTO provisional protocol 67 for flexible pavements could be adopted for rigid pavements and considered for this evaluation. Using the AASHTO PP67 approach, the main distress types are longitudinal cracking, transverse cracking, and other pattern cracking which would include shattered slabs and corner cracking.

Guidelines are provided in the FDOT handbook for how the data is to be collected for establishing extent and severity of each distress type. These guidelines are reviewed with the designated FDOT raters each year to confirm they are current on their understanding of the guidelines and expectations. To improve consistency among the FDOT raters and to further clarify the protocol considerations of this experiment, a two-day distress raters' class was organized for both existing Florida DOT Raters and appropriate Fugro Roadware Staff August 25 to 26, 2015. The class included both classroom as well as field training exercises. The main objective of this workshop was for Fugro to understand how FDOT raters conduct rigid pavement condition surveys, and how some of the involved decisions on distress type, extent, and severity can be quantified for the automated algorithm to match FDOT raters' decisions.

The workshop started with a discussion of the various distresses included in the handbook. Then all the participants visited a nearby jointed concrete pavement section in Waldo, FL for a field exercise. Ten distress raters were divided into three groups, each having one experienced FDOT rater, one non-experienced FDOT rater, and one

Fugro rater. One of the groups had four raters. There were four test sections as follows. Each group rated one section, except for group 1 who rated two smaller sections:

- Section 01 rated by Group 1: 148th Ave to Earle St, R1 (inside lane)
- Section 02 rated by Group 1: 148th Ave to Earle St, R2 (outside lane)
- Section 03 rated by Group 2: Earle St to Seydel St, R1
- Section 04 rated by Group 3: Seydel St to End of PCC section

The average, standard deviation and coefficient of variation (COV) in amount of each distress type at each and all severity levels found on each test section has been documented in Appendix C. In addition, the graphs in Appendix C indicate the number of standard deviations that each rater (on each test section) was off from the average rating. Several images in Appendix C show the examples for each distress type found in the field.

Based on these results, there seems to be more agreement among the raters on some distresses than the others. For example, there seems to be about 80% agreement among the raters in detecting the total amount of transverse cracking, but only about 65% for spalling. Overall, there seems to be more agreement among the raters in detecting the total amount of each distress type rather than assigning the distress severity levels. The amount of agreement is defined as 100 minus the COV in percentage.

The results of this exercise do not provide adequate statistical information for the distress types and severity levels that were not frequent on the example test sections. For example, if there is only one shattered slab in a test section and all raters identify it, then there will be 100% agreement, but this level of agreement might not be representative of the actual level of agreement among the raters when they conduct state wide surveys. Another example would be the severe transverse cracks: if there are only two instances in a section and some raters assign them to moderate, then there will be a significant amount of variation (low agreement) among the raters. It was expected that in the subsequent evaluation with 10 test sections, there would be a higher amount of each distress type and severity level, so that the statistics would make more sense.

Based on the meeting discussions and the results of the field exercise (see Appendix C), several notes were recorded for consideration in the quantification process required

for software development. FDOT staff might discuss these notes to potentially include them for further clarity of the handbook. The following are the notes from those discussions.

**Overall Manual Distress Survey Notes:**

- The rated pavement surface is limited to the lane area between the inside edges of the two lane stripes, even if there are widened slabs
- When crack spalling is present on rigid pavements, crack width is measured at the bottom of the crack (as opposed to the pavement surface). So, spalling should not affect the crack width that is used for assigning severity levels.
- D cracking or map cracking are not rated according to FDOT protocol
- CRCP sections are not currently placed on Florida highways
- Bridges are not rated, also exclude the approach and leave slabs (when they are identified).
- Rehabilitation comments are made on the rating forms
- Rater comments are mainly used by the raters for the next survey
- Multiple cracked slabs (if the slab is shattered or NOT shattered but contains more than one crack of any type) are counted as well during the manual survey. This is used to determine Percent Cracked Slabs for HPMS/MAP-21 purposes.

**Surface Deterioration Notes:**

- Surface deterioration is not commonly encountered in the field.
- It is typically rated as square feet of deterioration per rated mile of pavement.
- The computer should measure this affected area and the final value should be divided by the length of rated pavement.

**Transverse Cracking Notes:**

- If there is a longitudinal joint within the rated lane, and two transverse cracks intersect that joint within a foot of each other, then the whole crack is counted as one transverse crack.
- It is possible to count multiple transverse cracks within a single slab.
- Severity is assigned according to the crack width that is present on the majority (more than 50 percent?) of the crack length. This needs to be clarified in the handbook.
- All sealed cracks are rated as low severity.

**Longitudinal Cracking Notes:**

- Cracks are counted per slab; if a longitudinal crack extends from one slab to the next, it will be counted as two longitudinal cracks
- It is possible to count multiple longitudinal cracks within a single slab.
- All sealed cracks are rated as low severity.

**Spalling Notes:**

- If both sides of a joint (but not cracks) are spalled, then both are counted independently.
- If the spalled area is sealed, it can affect the severity level if well sealed.
- Several small spalls within a crack/joint can be accumulated on the same crack/joint.
- A minimum spalling of 1 foot is claimed, if present, per crack/joint.
- If there is less than 4" of spalling on a crack/joint, then it is not typically recorded

**Corner Cracking Notes:**

- If there is loss of pavement material as a result of corner cracking, then it is counted as spalling and not corner cracking. The size of such material loss needs to be specified.
- Multiple corner cracks can occur within the same slab.
- If the points of intersection between the crack and the joints are very close to the corners (the LTPP Distress Identification Manual identifies it as less than 0.3 meters), the crack should be rated as spalling instead of corner cracking. This needs to be clarified in the handbook.
- Corner cracks must connect a transverse joint to a longitudinal joint. If a diagonal crack occurs at a long or transverse crack, it would be counted as an additional longitudinal or transverse crack (based on the orientation of the crack).

**Patching Notes:**

- Patching is recorded as Sq.Ft. in the field and summarized, then converted to square yards for recording.
- Note 2 reads: "If half or more of the slab is replaced, do not record as patching." This indicates full slab replacements are not counted as patching.
- Doesn't matter if the patching material is asphalt or concrete.
- The patching is rounded to the nearest square yard ( $<0.5 \text{ sq. Yd.} = 0$ )

**Shattered Slab Notes:**

- When a slab is rated as shattered slab, then no other distresses are recorded on that slab. However, if the slab is not shattered but contains more than one crack of any type, then it is counted as a multiple cracked slab. For calculating the HPMS/MAP-21 parameter Percent Cracked Slabs, the number of cracked slabs (shattered or not) is needed to divide by the total number of slabs.

**Joint Condition Notes:**

- The condition of the joints in a section is assigned based on the predominant condition. Does this mean more than 50% of the joints? This needs to be clarified in the handbook.

**2.2.2 Representative Test Sections**

To conduct an evaluation of the existing methods, FDOT engineers identified a set of 12 representative test sections that are each at least a standard evaluation length (0.1-mile-long) and contain several of the jointed concrete pavement distresses in them (making sure that all the distress types and severities are incorporated in at least a couple of the sections selected). In the selection of the representative test sections, the following major factors should be considered to the extent possible:

1. Existence of a variety of the cracking distresses
2. Existence of different severity levels for each crack type
3. Pavement surface texture (rough versus smooth)
4. Concrete tinning (or lack thereof)
5. Lighting conditions (with or without shades) and angle (going into or out of the sun)

A sample partial factorial is provided below as an example. While all cells need not be accounted for, by filling the bulk of them, the analysis should be able to account for potential or anticipated interactions and relationships. In this example, priority has been given to cracking distress types, because they are the focus of this project. Due to the project limitations, the pavement surface texture and concrete tinning factors were not considered in selection of the representative sections.

**Table 15. Example Partial Factorial Plan**

Lighting		Shade		Into Sun		Away from Sun	
Texture/Tinning		Heavy	Light	Heavy	Light	Heavy	Light
Distress Type and Severity	Low	SS	TC/LC	SP	CB	TC/LC	SS
	High	SP	CB	TC/LC	SS	CB	SP

LC/TC: Longitudinal and/or Transverse Cracking; CB: Corner Breaks; SS: Shattered Slabs; SP: Spalling

Table 16 shows a list of the 12 sections ultimately selected and some general properties of them.

**Table 16. Final Selected 12 Test Sections**

NO	CNTY	DIST	ROUTE	DIR	LN	BMP	LNPTH	DEFECTS_PRESENT
1	Orange	5	SR500/SR50	S	L2	13.070	0.155	TR, LNG, SPL, CNR, ODD SLABS & JOINTS
2	Orange	5	SR500/SR50	S	L2	12.744	0.148	TR, LNG, SPL, PT, ODD SLABS & JOINTS
3	Orange	5	SR500/SR50	S	L2	21.784	0.214	TR, LNG, SEALANT
4	Orange	5	SR15/600	N	R2	3.400	0.170	TR, LNG, SPL
5	Orange	5	SR15/600	N	R2	6.280	0.170	TR, LNG, CNR, SPL, SEALANT
6	Duval	2	SR139/SR15	SE	L2	3.826	0.120	TR, LNG, CNR, SPL, SHTRD SLB
7	Duval	2	SR139/SR15	SE	L2	3.706	0.121	TR, LNG, CNR, SPL, SHTRD SLB
8	Duval	2	SR139/SR15	SE	R2	3.596	0.098	TR, LNG, CNR, SPL
9	Duval	2	SR139/SR15	SE	R2	3.694	0.106	TR, LNG, CNR, SPL
10	Duval	2	I-95	SW	L3	4.344	0.134	TR, LNG, CNR, SPL
11	Alachua	2	SR24	SW	L2	0.110	0.141	TR, LNG, CNR, SPL, SHTRD SLB
12	Alachua	2	SR24	SW	L2	0.251	0.160	TR, LNG, CNR, SPL, SHTRD SLB

Images of these 12 test sections were collected both with the FDOT MPSV (2D LRIS) on December 1, 2015 and with a Fugro ARAN (3D LCMS) in October 2015. The main analyses were conducted using the LRIS images, but there could be a follow-up study showing the results of 3D analysis. Fugro staff created a SQL procedure to transfer LRIS images from the FDOT server folder structure to a SQL database format that is compatible with Fugro Vision software. This procedure has been documented in

Appendix M. it is imperative that any future data submission to Fugro be in the folder structure and format that has been identified in Appendix M. This would allow for the provided SQL code to create an appropriate instance of a Vision database corresponding to the collected MPSV images.

### **2.2.3 Manual Windshield Survey**

Three FDOT raters conducted a manual windshield distress survey of the 12 test sections according to the FDOT protocol. Care was taken not to aggregate the observations into one combined score, to avoid masking or obscuring differences in specific distress observations which may later be helpful in the gap analysis. The average, standard deviation and coefficient of variation (COV) in amount of each distress type at each and all severity levels found on each test section has been documented in Appendix D. In addition, the graphs in Appendix D indicate the number of standard deviations that each rater (on each test section) was off from the average rating.

The results from the different raters were analyzed to assess the variability among the raters. These analyses provide a clearer understanding of the distress definitions and areas of ambiguity (based on variability observed from the results of the experienced raters) that may merit evaluation prior to initiating the automation. The amount of agreement is defined as 100 minus the COV in percentage.

The results were similar to the results of the field workshop. There seems to be more agreement among the raters on some distresses than the others. For example, there seems to be about 82% agreement among the raters in detecting the total amount of transverse and longitudinal cracking, but only about 64% for spalling, 56% for corner cracking, and 71% for shattered slabs. This result was expected because there were some ambiguities in the protocol definitions of corner cracking and spalling as it was noted in section 2.2.1. Overall, there seems to be more agreement among the raters in detecting the total amount of each distress type rather than assigning the distress severity levels.

Considering the total amounts of all severity values for each distress type, the majority of ratings were under one standard deviation away from the average of all ratings for each test section. There were total of 36 ratings (12 sections each rated by three different FDOT raters). For transverse cracking, nine out of the 36 ratings in which any transverse cracking was recorded (25%) were more than one standard deviation away from the average. For longitudinal cracking, spalling, corner cracking, and shattered slabs, 10/36 (28%), 11/36 (30%), 5/23 (22%), and 7/27 (26%) ratings respectively were more than one standard deviation away from the average. These could be considered as outliers.



**Table 17. Overall Agreement Among Raters in Manual Windshield Survey (See Appendix D for Details)**

<b>Distress Type</b>	<b>Agreement Among Raters in Total Distress Amount (All Severities), 100 - COV (%)</b>	<b>Percentage of Ratings more than one STD away from AVG (outliers)</b>
Transverse Cracking	82%	25%
Longitudinal Cracking	82%	28%
Spalling	64%	30%
Corner Cracking	56%	22%
Shattered Slabs	71%	26%
Patching	74%	33%
Surface Deterioration	52%	45%

#### **2.2.4 Semi-Automated Survey**

With guidance from Fugro engineers, the same three FDOT raters conducted a semi-automated rating of the same 12 test sections using the LRIS images that were imported into the Vision software. Due to some malfunction in the FDOT MPSV unit, the data corresponding to one run of the collected images on section number 7 was not recorded properly and therefore, section 7 was only rated by two raters. There were total of 35 (12 sections with three runs each minus one missing run) ratings. The data was extracted from the Vision database and the results in terms of the average, standard deviation and coefficient of variation (COV) in amount of each distress type at each and all severity levels has been documented in Appendix E. In addition, the graphs in Appendix E indicate the number of standard deviations that each rater (on each test section) was off from the average rating.

On average, the agreement among the three raters is approximately 82% in terms of the total number of transverse cracks, 67% for longitudinal cracks, 62% for spalling, only 30% for corner cracks, and only 28% for shattered slabs. There seems to be less agreement among the raters in terms of the total amount of corner cracks and shattered slabs compared to longitudinal and transverse cracks. Overall, there seems to be less agreement among the raters using the semi-automated rating method compared to the manual windshield survey. This could be attributed to the years of experience of FDOT raters with the manual windshield survey compared to their unfamiliarity with the Vision software and the semi-automated method. This calls for more training and coordination among the raters in terms of software application.

Considering the total amounts of all severity values for each distress type, the majority of ratings were under one standard deviation away from the average of all ratings for each test section. For transverse cracking, seven out of the 35 ratings in which any transverse cracking was recorded (20%) were more than one standard deviation away from the average. For longitudinal cracking, spalling, corner cracking, and shattered slabs, 9/34 (26%), 10/35 (28%), 6/19 (32%), and 8/20 (40%) of ratings respectively

were more than one standard deviation away from the average. These could be considered as outliers.

**Table 18. Overall Agreement Among Raters in Semi-Automated Survey (See Appendix E for Details)**

<b>Distress Type</b>	<b>Agreement Among Raters in Total Distress Amount (All Severities), 100 – COV (%)</b>	<b>Percentage of Ratings more than 1 STD away from AVG (outliers)</b>
Transverse Cracking	82%	20%
Longitudinal Cracking	67%	26%
Spalling	62%	28%
Corner Cracking	30%	32%
Shattered Slabs	28%	40%
Patching	24%	47%
Surface Deterioration	62%	60%

### **2.2.5 Automated Survey**

The Vision automated algorithm (WiseCrax) was adjusted to correspond to the specified criteria in the handbook for the viable distresses and then run on sets of images collected from the pavement sections, which were evaluated by the group of experienced raters. As detailed in Section 2.3, the WiseCrax detection, classification, and rating parameters were investigated to select the optimum settings. The automated surveys on all the test sections were conducted using the same set of software settings (control parameters). The same algorithm was run as many times as there were raters (i.e. if three raters review each image, the algorithm was run three times). This provides for another set of analyses to compare reproducibility between each of the three sets of reviews, as well as the repeatability of the algorithm results within the multiple runs.

As detailed in Section 2.3, the WiseCrax algorithm, in its present form, is capable of only classifying joints, transverse cracks, and longitudinal cracks. New classification and rating routines are needed for corner cracking and shattered slabs, which will be addressed in Section 2.3. For identification of spalling and patching, there is a need for depth information and therefore 3D data would be required.

Also, as discussed in Section 2.3, filters were used to take the noise out of the images to improve results in terms of detecting wide joints and sealed cracks. The filtering process increases crack widths and therefore compromises the ability of the rating process to assign correct severity levels. Therefore, the results here are only expressed in terms of total distress amount in all severity levels. Section 2.3 will discuss future work to address this issue.

The algorithm results are based on length of the distresses and not count per slab as it is in the FDOT protocol. Therefore, a database SQL routine was developed to use the location of the detected joints to transform the total distress length by section to total distress counts per slab by section. This process is not final yet as there are issues with grouping the cracks together. As with any other automated detection routine, only segments of a crack are detected because of the inconsistencies in the intensity along the crack. Therefore, the multiple segments need to be grouped together to form the complete crack. WiseCrax currently has the option for grouping all distresses of the same type in each image frame, but that is not adequate for this project as there might be more than one slab in each image frame. WiseCrax also has other options for grouping according to a tile that encompasses multiple cracks, but the algorithm did not perform satisfactorily on the test sections. The algorithm needs to be improved in this regard. Section 2.3 will discuss future work to address this issue. Hence, the results are expressed both in terms of length and count in this evaluation.

## **2.2.6 Comparison of Different Rating Methods**

### **Success Metrics**

The three principal success metrics of any process are effectiveness, efficiency, and reliability. With respect to automated condition evaluations, these three metrics could be considered for two aspects of the process, first for the detection and classification of individual surface defects (cracks), and second for the overall evaluation and quantification of the pavement condition in a distinct section.

In the context of automated distress identification, effectiveness can be expressed in terms of accuracy of the crack detection software when compared to a reference baseline. Accuracy is a qualitative term referring to whether there is agreement between a measurement made on an object and its true (target or reference) value. Bias is a quantitative term describing the difference (or error) between the average of measurements made on the same object and its true value.

While systematic errors identified in the bias can be calibrated out, such evaluations must also address the random errors as well. The average results may be quite comparable, but individual results can deviate significantly. Efforts must also be made to control these deviations to produce results which can ultimately be classified as reliable. Reliability of automated distress surveys is often expressed in terms of precision. Precision is also a qualitative term describing the degree of repeatability of a measurement value. Variance and standard deviation of error are quantitative estimates of precision. Accuracy and precision (or the corresponding quantitative estimates: bias and variance) ultimately define how effective and reliable a system is as described in greater detail below.

Based on the overall cumulative amount of each distress among different test sections and multiple runs, the success metrics used to compare different rating methods are:

1. Average error (bias) was used to represent accuracy or effectiveness of each method. Accuracy can only be quantified with respect to a reference value.
2. Average standard deviation of error among 12 sections was used to represent precision of each method.
3. In order to represent reproducibility of manual and semi-automated methods, average standard deviation of error on the same test section and among the 3 raters was used. In order to represent repeatability of the automated algorithm, average standard deviation of error on the same test section and among 3 runs was used.
4. To use a measure of reliability independent of the reference survey, agreement among the three raters (or three runs) was also represented by 100 minus the coefficient of variation in the total amount of each distress type on each section among the three raters/runs. In addition, the number of outliers among the three raters/runs was represented by the number of section ratings that were more than one standard deviation away from the average of the three raters/runs.
5. To compare efficiency of the three methods, the time required for each survey method was estimated.

### **Reference Rating or “Ground Truth”**

Multiple research efforts in the past have introduced various methods to establish reference values or “ground truth” for pavement surface defects by using the “most appropriate” methodology available. The major types of reference values include:

1. Manual distress identification: In this method, professional (trained and experienced) distress raters identify the surface distresses on a set of pavement sections that are deemed representative of conditions across a network.
2. Semi-automated detection: This method is similar to the manual method, but the professional raters use the images collected by monitoring vehicle to identify the distresses.

3. Artificially fabricated distress: In this method, cracks are designed and fissured into steel plates or cut into an existing asphalt surface, so the precise dimensions of the defects are known. This method is mostly used to resolve image distortion issues caused by the camera lens or the image sensor.

Each method has its own advantages and limitations. The manual method simulates the actual distress identification process that has been in use by many state highway agencies (SHA) for a long period; however, there is a low degree of agreement among different professional raters which renders the “ground truth” as a highly variable measure.

The semi-automated option might be superior to the manual method for establishing “ground truth,” because the collected images are available for multiple raters to view in an office environment with less distraction from field traffic. However, some of the low severity cracks that are at initial stages of development might not be visible from the collected images. Increasing the number of raters could result in a more reliable ground truth.

After much deliberation, it was decided to use a semi-automated approach in which one run of the images for the 12 test sections were rated by one Fugro engineer and then completely reviewed and corrected by two other Fugro engineers. There are two advantages to this method, first that the rating was 100 percent controlled by two additional raters, and second that the raters were not FDOT experienced raters and therefore this reference can be used as an unbiased reference to evaluate all the three rating methods. FDOT raters and the Fugro software engineer did not have access to this reference rating.

### **Comparison Results on Overall Section Distress Quantities**

Table 19, Table 20, and Table 21 show the success metrics for manual field survey, semi-automated rating, and the automated algorithm, respectively, compared to the reference survey for the total amounts of each distress type (all severities) in each section. In these metrics, error is calculated as the difference between each value and the ground truth normalized to the ground truth and expressed in percentage.

As it was explained in Section 2.2.5, the automated algorithm was only used for transverse and longitudinal cracks and joints at this point. Also, as it was mentioned in Section 2.2.5, the algorithm is not producing counts of each distress per slab and the counts presented here are based on a database routine that is showing more cracks than existing.

**Table 19. Comparison of Manual Windshield Survey Rating to “Ground Truth”**

<b>Metric</b>	<b>Transverse Cracking (count)</b>	<b>Longitudinal Cracking (count)</b>	<b>Spalling (length)</b>	<b>Corner Cracking (count)</b>	<b>Patching (area)</b>	<b>Shattered Slabs (count)</b>
Bias (%)	25.3	-2.3	161.5	67.1	-18.5	30.0
STDEV of Error (%) among Sections	61.5	44.8	358.7	75.3	46.7	36.4
STDEV of Error (%) among Raters	27.3	14.7	103.8	30.9	43.9	22.4

**Table 20. Comparison of Semi-Automated Rating to “Ground Truth”**

<b>Metric</b>	<b>Transverse Cracking (count)</b>	<b>Longitudinal Cracking (count)</b>	<b>Spalling (length)</b>	<b>Corner Cracking (count)</b>	<b>Patching (area)</b>	<b>Shattered Slabs (count)</b>
Bias (%)	6.8	-2.4	129.9	15.5	487.6	-6.7
STDEV of Error (%) among Sections	47.9	52.7	261.2	76.5	887.4	29.0
STDEV of Error (%) among Raters	35.8	39.3	45.1	72.4	941.2	62.3

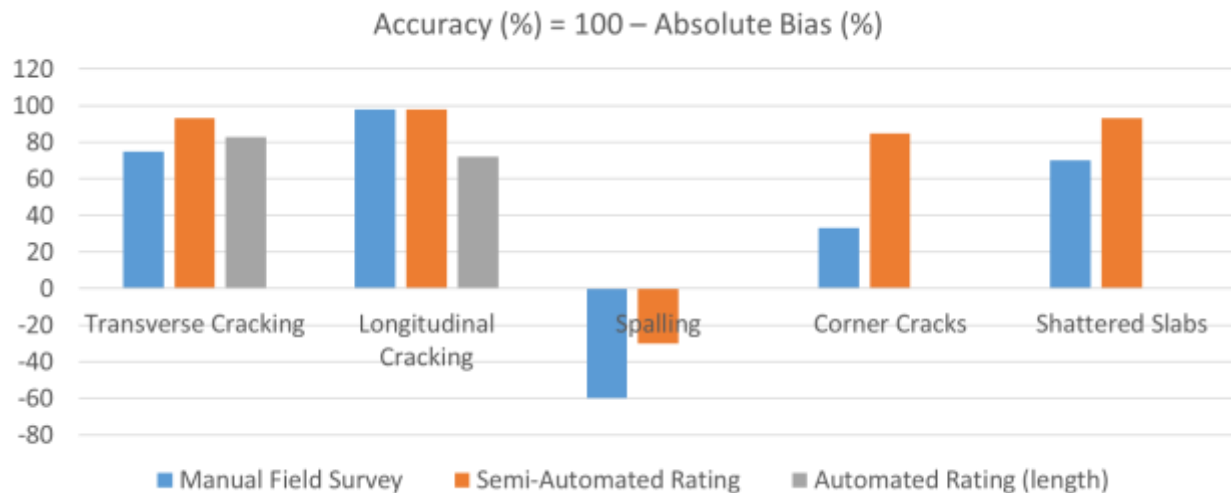
**Table 21. Comparison of Automated Rating to “Ground Truth” (Length and Count)**

<b>Metric</b>	<b>Transverse Cracking Length</b>	<b>Transverse Cracking Count</b>	<b>Longitudinal Cracking Length</b>	<b>Longitudinal Cracking Count</b>
Bias (%)	17.2	76.5	40.6	332.0
STDEV of Error (%) among Sections	89.3	98.0	95.2	278.9
STDEV of Error (%) among Multiple Runs	47.5	40.0	107.8	156.9

The results indicate that the automated routine is relatively more successful in detecting and identifying the length of transverse cracks (accuracy of 83%) compared to longitudinal cracks (accuracy of 60%). In fact, the accuracy of the automated routine in terms of the transverse cracks (83%) is comparable to the accuracy in the manual field surveys (75%), but it is lower compared to semi-automated surveys (93%). The reason for lower accuracy of the automated rating of longitudinal cracks is mainly because of

the longitudinal joints or lane stripes that are falsely being classified as cracks and therefore increasing the number of cracks (positive bias).

Figure 26 compares the accuracy of the three rating methods as calculated by 100 minus the absolute value of bias (%).



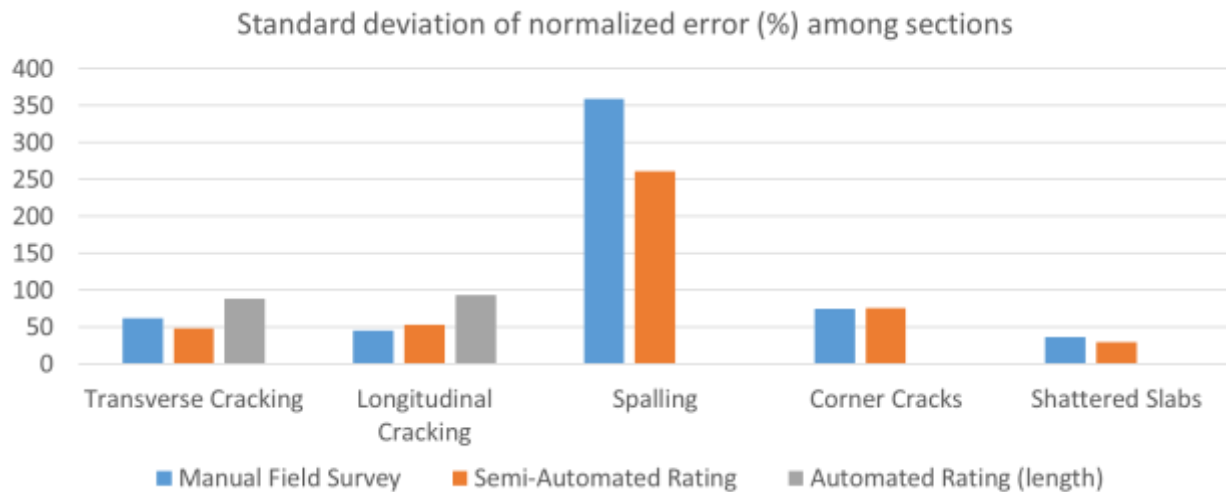
**Figure 26. Comparison of Different Methods in terms of Accuracy (100 - Absolute Bias(%))**

The semi-automated rating has the highest level of accuracy among the three methods for all distress types. The automated rating has a higher accuracy compared to the manual survey in terms of the total amount of transverse cracking. In contrast, the automated rating has lower accuracy compared to the manual survey in terms of the amount of longitudinal cracks. This is mainly because of the longitudinal joints and stripes that were incorrectly rated as longitudinal cracks.

Figure 27 shows a comparison among the methods in terms of precision as calculated by the standard deviation of error among 12 test sections. The automated rating is showing lower precision compared to the other rating methods. This is indicated by the higher amount of variation in the rating error among the 12 test sections. This is because the automated algorithm performed much better in some sections compared to the others. In test sections where any of the following defects exists, the automated algorithm had much higher errors causing the standard deviation of error among sections to be higher:

- Skewed transverse joints

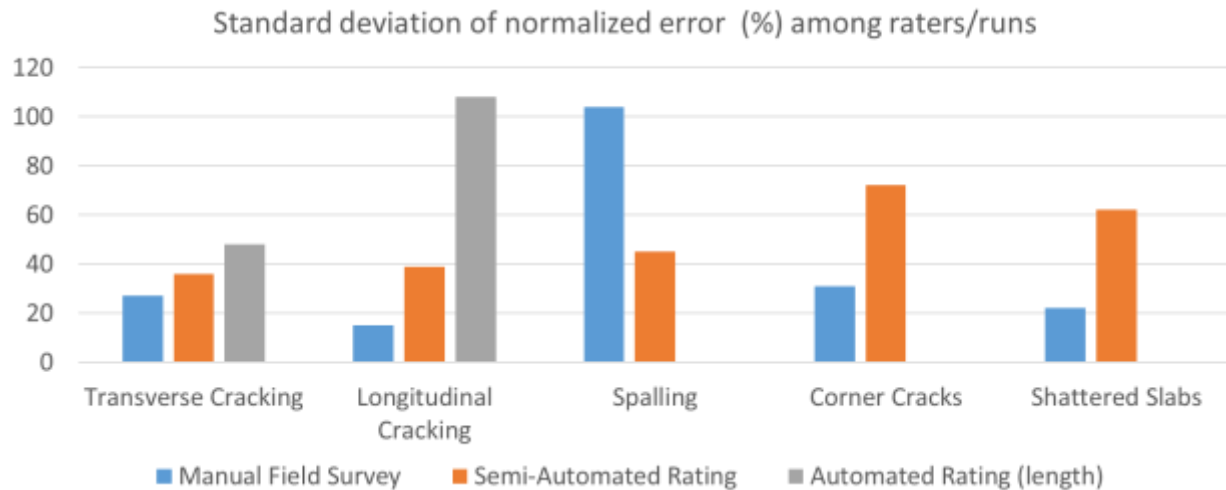
- Skewed longitudinal joints (or where a longitudinal joint crosses the pavement image diagonally)
- Sawed-in longitudinal joints that are not perfectly straight lines
- Pavement marking (white or black stripes within the lane)
- Traffic counters, and other surface scratch marks



**Figure 27. Comparison of Different Methods in terms of Precision (Standard Deviation of Normalized Error (%) Among 12 Sections)**

Figure 28 compares the reproducibility of the manual and semi-automated methods to the repeatability of the automated software using the standard deviation of error among the three raters/runs. The automated algorithm is showing much lower repeatability among multiple runs when compared to the reproducibility among multiple raters in the other rating methods. It should be noted that this is with different sets of images on each different run. This is because of the differences in levels of shades in multiple images of the same pavement section. If the same set of images are used, then there is zero variability among multiple runs of the software.

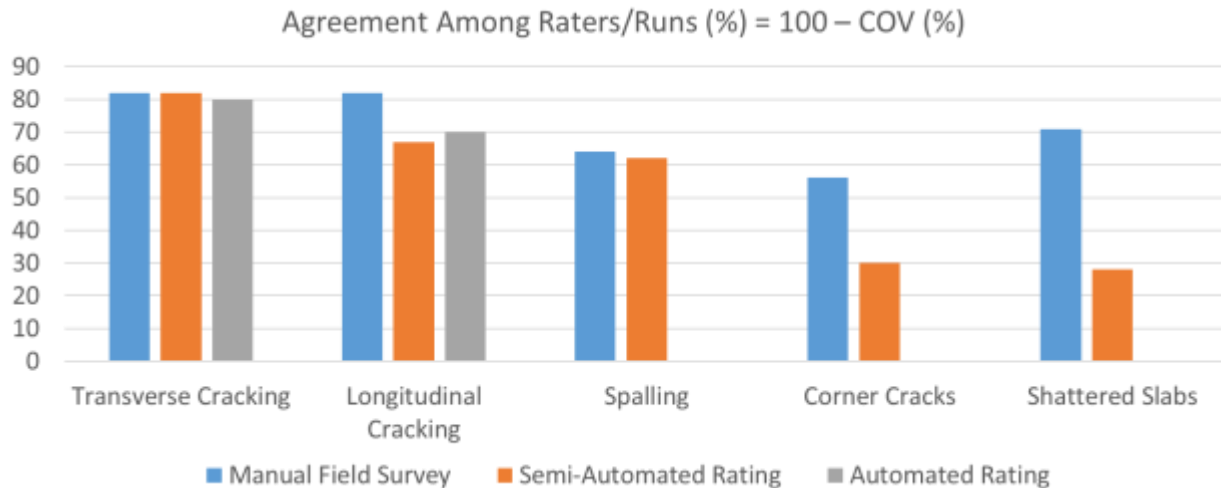




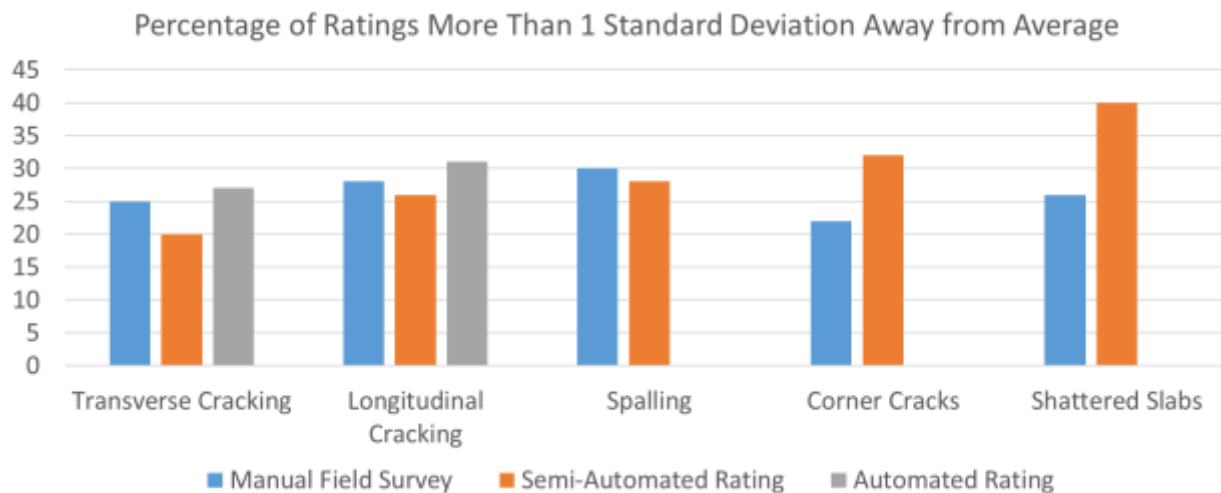
**Figure 28. Comparison of Different Methods in terms of Reliability (Standard Deviation of Normalized Error (%) Among 3 Raters/Runs)**

The semi-automated results show higher accuracy (lower bias) and higher precision (lower standard deviation among sections) compared to the manual field surveys in terms of most distress amounts. However, in agreement with what was presented in Section 2.2.4, the raters have lower agreement (higher standard deviation) in the semi-automated rating compared to field surveys. These results suggest that with further training and practice, the semi-automated results are going to have higher reproducibility in addition to the currently higher accuracy and precision compared to the manual field surveys.

As an alternative method to evaluate reliability of the different rating methods independent of the reference survey, Figure 29 and Figure 30 show the reproducibility results from the manual and semi-automated surveys (listed in Table 17 and Table 18, respectively), in addition to the repeatability results from the automated rating.



**Figure 29. Agreement Among Multiple Raters/Runs, A measure of Reproducibility/Repeatability**



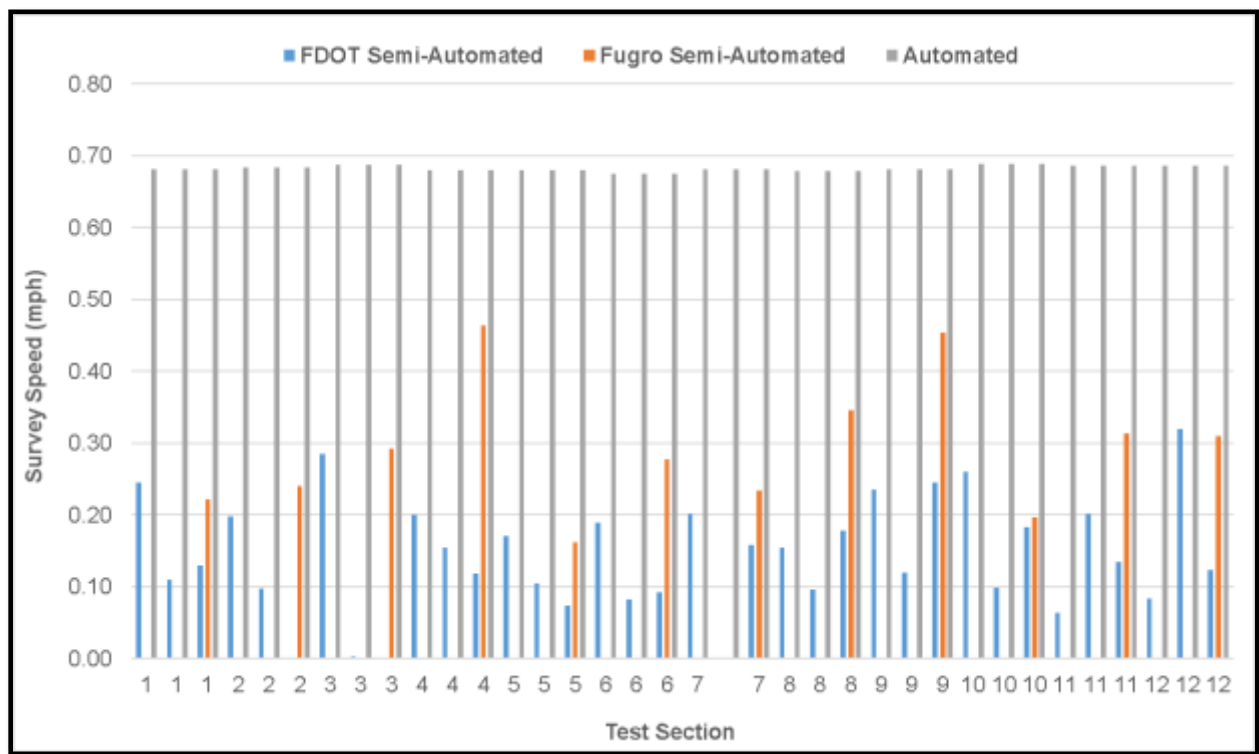
**Figure 30. Percentage of “Outlier” Ratings, A measure of Reproducibility/Repeatability**

In contrast to the results in Figure 28 (which are based on the variation of error compared to a reference survey), the results in Figure 29 and Figure 30 (which are based on the actual variation of distress amounts) indicate that the automated algorithm has a comparable repeatability to the manual and semi-automated methods.

The results indicate that for transverse cracking, there is more agreement among the raters and the least number of outliers in the semi-automated rating method. For longitudinal cracking however, there is more agreement among the raters in the manual survey, but the least number of outliers is in the semi-automated method.

Efficiency of the manual, semi-automated, and automated methods can be evaluated by the amount of time required to conduct each survey type. FDOT raters provided an estimate for the amount of time they spent in the field to conduct a windshield survey of the 12 test sections. Based on this crude estimate, the manual rating speed in doing windshield surveys while driving on the shoulder is about 1 to 3 miles per hour, depending on the amount of distresses present. It should be noted that for approximately 98% of the concrete pavements, they can drive on the shoulder.

The Vision software was used to extract the amount of time that each rater had spent on each test section to conduct a semi-automated survey. The automated detection, classification, and rating takes about 20 seconds per image frame. Therefore, the automated survey time is calculated through multiplying the number of image frames in each test section by 20 seconds. Figure 31 shows a comparison between the semi-automated and automated survey methods in terms of the survey speed in miles per hour for each test section and each rater/run.



**Figure 31. Comparison of the Efficiency (Speed) of Survey Methods**

Fugro raters (orange lines) have used the software more frequently for semi-automated rating and therefore had a higher speed (on average 0.29 mph) compared to FDOT raters (blue lines, on average 0.18 mph). The automated software has an average speed of 0.68 mph which is more than twice the efficiency of the semi-automated

method. The manual windshield survey is about twice faster than the automated survey. However, the automated survey does not require human intervention while running and only some QC is required after survey completion. Therefore, more computing power is needed rather than human intervention. In addition, the automated and semi-automated survey methods have the significant advantage of eliminating safety concerns for the raters who are driving or walking on highway shoulder.

### **Verification of Automatically Detected Distresses**

While the overall comparison of the quantities of each distress type between manual windshield survey and the automated algorithm results provide an indication of the strengths and weaknesses of the automated methodology, there is a need for a distress by distress verification of the software performance to identify the reasons behind the previously indicated weaknesses.

The reference (“ground truth”) rating used a point and trace methodology and manually rated the collected images to generate reference crack maps. Based on the reference semi-automated crack maps established, the following metrics are evaluated on a distress by distress basis:

- True Positives: correctly detected cracks (or distress)
- False Positives: detected cracks that don't exist in the reference survey
- False Negatives: Missed cracks
- Distress Validity (or Accuracy): an indicator to be calculated as the ratio of the correctly detected cracks (true positives) to the total detected cracks (true positives and false positives). This statistic indicates the percentage of the detected distress that was actually present in the reference survey, thereby expressing the validity of the distress detected by algorithms.
- Distress Sensitivity (or Recall): a parameter to be calculated as the ratio of the correctly detected cracks to the total actual cracks existing on the pavement surface (true positives and false negatives). This statistic represents the percentage of the distress in the reference survey that was detected by the automated method, thereby expressing the sensitivity of the algorithms to existing distress.
- Distress Classification Performance: a measure of the number of correctly classified cracks (according to the reference survey), divided by the number of correctly detected cracks (true positives). This statistic indicates the percentage of the detected distress that is correctly classified by the automated algorithm.

These metrics were evaluated on 24 sample image frames (two image frames randomly selected from each of the 12 test sections on run number 1) and the results can be found in Table 22. False positives are cracks that have been reported by the automated crack detection software, while no crack has been recorded in the “ground truth” at the same location. On the other hand, missed cracks are existing cracks that have been reported in the “ground truth”, but are not detected by the software (i.e. false negatives). As with the manual rating conducted in the field, the reference values on the computer may also have a range of agreement from professional raters in terms of how to measure crack width, severity, and in some cases crack extent.

**Table 22. Verification of Automatically Detected Distress on Sample Image Frames (Raw Data)**

Test Section	Image Frame	Length (ft)					Count	
		Ground Truth	True Positive		False Positive	False Negative	Ground Truth	Rating Result
			Correctly Rated	Not Correctly Rated				
Section 1	3P000019	23.048	9.304	7.936	8.992	5.808	2	9
Section 1	3P000020	23.828	21.786	0	4.432	2.042	3	7
Section 2	3P000115	22.615	18.994	0	14.87	3.621	2	7
Section 2	3P000116	11.425	10.747	0	0	0.678	1	2
Section 3	3P000029	48.97	41.272	3.688	4.426	4.01	3	7
Section 3	3P000022	22.464	20.424	0	3.166	2.04	2	5
Section 4	3P000014	22.43	18.746	0	14.114	3.686	2	6
Section 4	3P000024	20.312	10.38	0	44.74	9.932	1	9
Section 5	3P000767	26.592	4.289	20.202	1.316	2.101	2	6
Section 5	3P000768	41.112	13.019	19.635	6.924	8.458	4	12
Section 6	3P000022	6.581	0	6.581	1.158	0	1	2
Section 6	3P000023	44.261	36.852	2.906	3.68	7.408	7	8
Section 7	3P000062	16.819	11.751	0	1.829	5.068	2	4
Section 7	3P000061	17.59	11.206	3.409	0	2.107	2	4
Section 8	3P000006	17.398	13.974	1.388	0	2.836	2	4
Section 8	3P000010	17.472	10.627	0	0	6.845	2	2
Section 9	3P000031	8.63	5.02	0	5.265	2.61	1	5
Section 9	3P000038	13.757	8.67	0	2.084	5.187	2	4
Section 10	3P000052	10.518	10.488	0	3.018	0.3	1	3
Section 10	3P000053	33.57	31.498	0.552	0	1.52	3	9
Section 11	3P000044	30.744	30.744	0	30.094	0	2	9
Section 11	3P000045	43.781	43.381	0	24.051	0.4	5	14
Section 12	3P000087	46.934	34.682	0	6.165	12.252	4	9
Section 12	3P000088	30.578	30.578	0	20.006	0	2	7

The results clearly indicate the issue with crack counting as it was explained in Section 2.2.5. Since the detected segments of cracks were not appropriately grouped together, the total count of the cracks was much higher than existing. It is also evident that once a

crack is appropriately detected (within the true positives), the algorithm is doing a good job in terms of assigning the correct distress type (note the relatively small length of incorrectly rated cracks). In addition, the overall length of false positives and false negatives (missed cracks) are relatively comparable. However, there are some instances where there is a significant difference between the two. This relatively reasonable balance between the two extremes of aggressive detection (false positives) and missing cracks (false negatives) is an indication that appropriate detection settings have been used in the software. There needs to be an effort in the future development initiatives to maintain this balance and perhaps improve it. Details of the approach for selecting these settings have been explained in Section 2.3.

Based on the results in Table 22, the distress verification metrics were calculated in Table 23. The results indicate that on average, 78% of the automatically detected distresses actually existed on the reference survey, 84% of the distresses on the reference survey were detected via the automated algorithm, and 86% of the detected distresses were correctly classified into longitudinal or transverse cracking or joints.

**Table 23. Verification of Automatically Detected Distress on Sample Image Frames (Metrics)**

Test Section	Image Frame	Distress Validity (or Accuracy)	Distress Sensitivity (or Recall)	Distress Classification Performance
Section 1	3P000019	66%	75%	54%
Section 1	3P000020	83%	91%	100%
Section 2	3P000115	56%	84%	100%
Section 2	3P000116	100%	94%	100%
Section 3	3P000029	91%	92%	92%
Section 3	3P000022	87%	91%	100%
Section 4	3P000014	57%	84%	100%
Section 4	3P000024	19%	51%	100%
Section 5	3P000767	95%	92%	18%
Section 5	3P000768	83%	79%	40%
Section 6	3P000022	85%	100%	0%
Section 6	3P000023	92%	84%	93%
Section 7	3P000062	87%	70%	100%
Section 7	3P000061	100%	87%	77%
Section 8	3P000006	100%	84%	91%
Section 8	3P000010	100%	61%	100%
Section 9	3P000031	49%	66%	100%
Section 9	3P000038	81%	63%	100%
Section 10	3P000052	78%	97%	100%
Section 10	3P000053	100%	95%	98%
Section 11	3P000044	51%	100%	100%

Test Section	Image Frame	Distress Validity (or Accuracy)	Distress Sensitivity (or Recall)	Distress Classification Performance
Section 11	3P000045	64%	99%	100%
Section 12	3P000087	85%	74%	100%
Section 12	3P000088	60%	100%	100%
Average		78%	84%	86%

## 2.3 Appropriate Settings for Automated Survey

Fugro Vision software includes a distress identification application called WiseCrax. This application involves three main routines for distress identification:

1. Crack detection: during which any linear defects on pavement surface is detected and marked with lines. The performance of this step is highly dependent on the quality of the image, the exposure, lighting, the number of cracks and other defects present on the surface, the location of defects within the lane, etc.
2. Classification: during this step, all the detected defects are classified into one of the three categories of longitudinal defects, transverse defects, and other (or pattern) defects according to a changeable criterion for defect angle and density.
3. Rating: during this final step, the software assigns a distress type and severity to each of the classified defects according to a distress schema defined by the user. The user needs to select one or more criteria from a series of criteria such as angle, longitudinal and transverse extent, density, width, and others for each distress type and severity. Once the schema is setup and saved, this schema can be applied for network-level data collection.

### 2.3.1 Image Pre-Processing

After investigating multiple detection settings in the software, it was evident that the sealed joints with wider openings and sealed cracks were not appropriately detected. Therefore, it was decided that there was a need for image pre-processing with some filters to improve the crack detection results. A basic image processing operation was applied to eliminate the noise and texture in the images using an open source software called ImageJ. If it is determined that this pre-processing is essential with respect to other aspects of this project, a plugin can be developed in Vision which will include this open source routine for filtering out the noise.

Four types of filters were considered for removing the noise in the images:

1. Gaussian Filter
2. Median Filter
3. Haar Wavelet Filter
4. A Trous Wavelet Filter

Application of these filters was investigated with changing the involved parameters according to the following table. Sample test results are included in Appendix B, where crack detection results on the filtered images can be observed. The appropriate type and parameter settings for the filter depends on each specific image, and a filter that performs best for one image, could perform less desirable on another image. However, it is not feasible to select a different filter for each and every image. Therefore, the project team selected the filter type and parameter value that provided the best overall results among the sample selected representative images for the 12 test sections in this study. This selection was based on 24 sample image frames (two images from each of the 12 test sections), the length of which amounts to 480 feet which is about 5% of the total length of the 12 test sections. Based on this study and future studies, a pre-selected filter type could be applied to the images based on the pavement type, surface properties, lighting, etc.

After selecting a set of detection parameter settings suitable for the sample images (next section explains the adjustments of the detection settings), the filters were applied again to fine tune the required filter setting. Here are the results of this step of the investigation.



**Table 24. Image Pre-Processing Investigation Sample Test Results**

Filter Type	Tested Parameters	Example Detection Results in Appendix B
Gaussian	Radius 5	Frame: Section 11 3P000043 Figure 1
	Radius 10	Frame: Section 11 3P000043 Figure 2
	Radius 15	Frame: Section 11 3P000043 Figure 3
Median	Radius 5	Frame: Section 11 3P000043 Figure 4
	Radius 10	Frame: Section 11 3P000043 Figure 5
	Radius 15	Frame: Section 11 3P000043 Figure 6
Haar Wavelet	Coefficients: 10,10,10	Frame: Section 11 3P000043 Figure 7
A Trous Wavelet	Coefficients: 10,10,10	Frame: Section 11 3P000043 Figure 8
	Coefficients: 20, 20, 20	Frame: Section 11 3P000043 Figure 9
	Coefficients: 30,30,30	Frame: Section 11 3P000043 Figure 10
	Coefficients: 40, 30, 30	Frame: Section 11 3P000043 Figure 11

**Table 25. Image Pre-Processing Investigation Test Results After Fine-Tuning Detection Settings**

Filter Type	Tested Parameters	Detection Results in Appendix B
Gaussian	Radius 5	Frame: Section 11 3P000048 Figure 12 Frame: Section 12 3P000087 Figure 13
	Radius 10	Frame: Section 11 3P000048 Figure 14 Frame: Section 12 3P000087 Figure 15

It is clear that the application of the pre-processing filters improves the detection results. As shown in the sample test results, after application of 'A Trous filter' or Gaussian filter with smaller radius (5), the detection algorithm is more sensitive to the tiny cracks which are very narrow. Gaussian filter with larger radius (10) makes the detection of wider cracks, especially the sealed joint detection easier. Finally, the Gaussian filter with a radius of 10 pixels was selected to pre-process all the images. However, we may include the A Trous filter in future work.

The disadvantage of using these filters is that they result in the crack widths becoming larger and the detection routine will not be able to measure the actual crack width on the

pavement and therefore higher severity levels will be assigned in the rating process. In this preliminary evaluation, the WiseCrax option to detect sealed cracks was not enabled. Instead of filtering the images, the other option would be to separate detection of sealed cracks for detection of sealed joints. However, that option would also result in larger crack widths that affect severity ratings.

### **2.3.2 Detection Settings**

There are multiple detection parameters that can be adjusted for improved detection results. The following are the detection parameters and a short description of each:

- Crack Options
  - Crack Simplification: Higher numbers mean fewer details are stored for the crack trace
  - Extraction:
    - Transverse Cracking: Degree of transverse cracking in the pavement
    - Longitudinal Cracking: Degree of longitudinal cracking in the pavement
    - Crack Likelihood: Higher values suppress false positive at the expense of processing speed
    - Horizontal Bridging: Two adjacent cracks will be merged into one if the gap is less than X pixels
    - Vertical Bridging: Maximum vertical distance between two nodes before being split into two distinct cracks.
  - Pruning
    - Remove Short Distress: Discard cracks if below the minimum length

- Minimum Length (mm): Minimum length for reporting cracks in millimeters
- Remove Low Node-Count Distresses: Discard cracks if below the minimum number of nodes
- Minimum Node Count: The minimum node count required to keep a crack
- Remove Low-Cost Distress: Discard cracks below the cost threshold
- Remove 'Bright' Distress: Discard cracks above the intensity threshold
- Width
  - Maximum intensity to count a pixel as part of the crack
- Lane Options
  - Enable: Turn on lane detection
  - Detect Within Lanes: Only detect cracks within lanes. Will not be used for incremental/zone detection
- Sealed Crack Options: Defined sealed cracks detection parameters
  - Crack Simplification: Higher numbers mean fewer details are stored for the crack trace
  - Extraction:
    - Transverse Cracking: Degree of transverse cracking in the pavement

- Longitudinal Cracking: Degree of longitudinal cracking in the pavement
  - Crack Likelihood: Higher values suppress false positive at the expense of processing speed
  - Horizontal Bridging: Two adjacent cracks will be merged into one if the gap is less than X pixels
  - Vertical Bridging: Maximum vertical distance between two nodes before being split into two distinct cracks.
- Pruning
    - Remove Short Distress: Discard cracks if below the minimum length
    - Minimum Length (mm): Minimum length for reporting cracks in millimeters
    - Remove Low Node-Count Distresses: Discard cracks if below the minimum number of nodes
    - Minimum Node Count: The minimum node count required to keep a crack
    - Remove Low-Cost Distress: Discard cracks below the cost threshold
    - Remove 'Bright' Distress: Discard cracks above the intensity threshold
  - Width
    - Maximum intensity to count a pixel as part of the crack

At the first step, an investigation was conducted to determine the key detection parameters to which the detection results are most sensitive. This was evaluated by changing the parameters one by one and comparing the detection results against the default settings. There are 10 pre-set detection profiles in WiseCrax based on a range of pavement types and conditions that have been determined according to the years of experience of Fugro raters on various statewide projects. These settings can be found in Appendix B. From the results of this first step, the following parameters were found to influence the detection result significantly. The second step was to fine tune these key parameters to find the optimum detection profile. The following table describes how these key parameters were changed.

**Table 26. Investigation of Key Detection Parameters**

<b>Detection Parameter</b>	<b>Initial Default</b>	<b>Possible Range</b>	<b>Tested Values</b>
Expected Transverse Cracking (%)	15	0 to 100	10, 15, 20, 25, 35
Expected Longitudinal Cracking (%)	15	0 to 100	10, 15, 20, 25, 35
Horizontal Bridging	3	0 to 20	3,5,7,9
Vertical Bridging	5	0 to 20	3,5,7,9
Intensity Threshold	60	1 to 255	60,80,100,110,115,120

Sample detection results with different parameter settings on one example image frame are displayed in Appendix B to understand the impact of changing each parameter. Here are the observations from changing key detection parameters:

- Expected Transverse and Longitudinal Cracking (%): Number of pixels that are considered to be part of crack will increase if the expected cracking percentage is increased.
- Horizontal and Vertical Bridging: The continuity of the crack pixels would be increased if we increase the number of pixels used for bridging. Therefore, the chance of having cracks considered to be noise (short cracks) would be decreased.
- Intensity Threshold: By increasing this threshold from 60 to 120, width of the detected cracks became larger. Also, more crack pixels can be detected. However, increasing this value may cause more false positives.

**Table 27. Example Figures in Appendix B that Describe the Impact of Changing Key Detection Parameters**

Figure 154	Figure 155
Longitudinal Cracking (%) =15	Longitudinal Cracking (%) =30
Transverse Cracking (%) =15	Transverse Cracking (%) =30
Figure 156	Figure 157
Horizontal Bridging (%) =1	Horizontal Bridging (%) =3
Transverse Bridging (%) =3	Transverse Bridging (%) =5
Figure 158	Figure 159
Intensity Threshold: 120	Intensity Threshold: 60

The recommended parameter setting based on the sample images of the 12 test sections was found to be as in Figure 32.

**Detection Settings** [Advance]

- Detection**
  - WiseCrack Detection Settings**
    - Crack Options**
      - Crack Simplification: 2
      - Extraction**
        - Transverse Cracking [%]: 15
        - Longitudinal Cracking [%]: 15
        - Crack Likelihood: 2
        - Horizontal Bridging: 3
        - Vertical Bridging: 5
      - Pruning**
        - Remove Short Distresses: True
        - Minimum Length [mm]: 300
        - Remove Low Node-Count Distre: True
        - Minimum Node Count: 100
        - Remove Low-Cost Distresses: False
        - Remove 'Bright' Distresses: False
      - Width**
        - Intensity Threshold: 100
    - Default lane offset (meters): 0
    - Default lane width (meters): 3.6
    - Detection Profile Priority: Tag
    - Keep Detected Cracks: False
    - Keep Manual Cracks: False
    - Keep Previous Lanes: False
    - Lane Optimization: False
    - Lane Options**
      - Enabled: False
      - Detect within lanes: True
      - Lane set method: Detected/Always Default When Missing
    - Sealed Crack Options**
      - Crack Simplification: 1
      - Extraction**
        - Transverse Cracking [%]: 0
        - Longitudinal Cracking [%]: 0
        - Crack Likelihood: 3
        - Horizontal Bridging: 2
        - Vertical Bridging: 4
      - Pruning**
        - Remove Short Distresses: False
        - Remove Low Node-Count Distre: True
        - Minimum Node Count: 8
        - Remove Low-Cost Distresses: True
        - Minimum Cost Threshold: 10
        - Remove 'Bright' Distresses: True
        - Maximum Intensity Threshold: 100
      - Width**
        - Intensity Threshold: 100

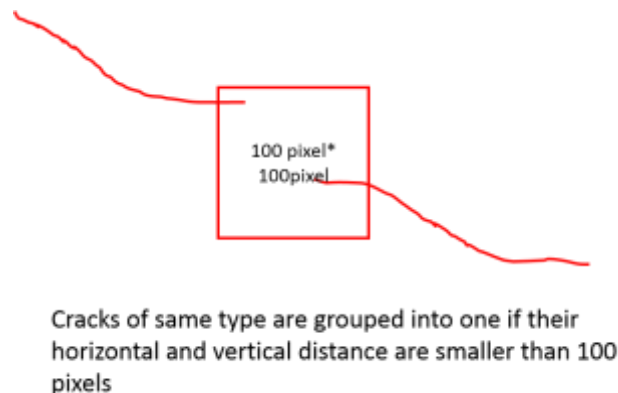
**Figure 32. Detection Parameter Settings for Evaluation of Existing Software**

### 2.3.3 Cracking classification

In the classification step, there are seven parameters that can be adjusted for suitable performance. The following values were used based on past experience.

**Table 28. Classification Parameter Settings**

Parameter	Description	Value Used
Classification Enable	Enables classification	TRUE
Separate Seal Classification	Classifies sealed cracks separately	FALSE
Degree Angle	Angle threshold differentiating between longitudinal and transverse defects	45
Tile Height	Tile used for calculating the density of defects in pattern distresses (such as alligator cracking)	50
Tile Width		50
Group Tile Height	Tile used for grouping defects together (see figure below)	100
Group Tile Width		100



**Figure 33 Group Tile Height/ Width**

Sample classification results are shown in the figures in Appendix B as referenced here.

On Section 12: image 87, after classification, several longitudinal cracks gathered into one group, as highlighted in Figure 161 in Appendix B.

Before classification	After classification (several individual longitudinal cracks gathered into one group)
Figure 160	Figure 161

On Section 11: image 43, after classification, several longitudinal cracks gathered into one group, as highlighted in Figure 163 in Appendix B.

Before classification	After classification (several longitudinal cracks gathered into one group)
Figure 162	Figure 163

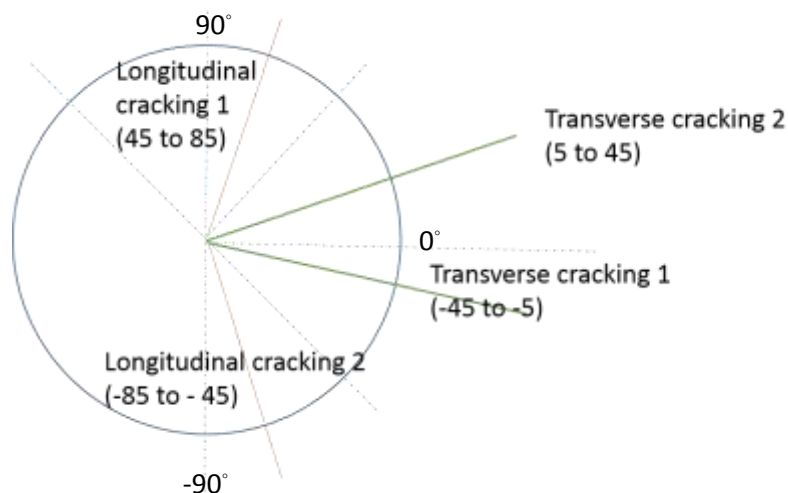
### 2.3.4 Distress Rating

The WiseCrax algorithm contains criteria such as angle, longitudinal and transverse extent, density, width, and others for assigning each distress type and severity. After considering all options, only transverse and longitudinal joints, and transverse and longitudinal cracks could be rated reliably. New classification and rating routines are needed for corner cracking and shattered slabs. For identification of spalling and patching, there is a need for depth data and therefore 3D data would be required for that purpose.

During the rating procedure, 'distress angle', the angle between a distress and the transverse direction, is adopted as one of the main parameters to distinguish joints from cracking: -5 to 5 degree for transverse joints, and 85 to 90 and -90 to -85 degree for longitudinal joints. Another parameter used in differentiating joints from cracks is distress extent. For longitudinal joints, its transverse extent should be less than 0.1 m. For transverse joints, its longitudinal extent should be less than 0.1m. Most of joints were successfully identified using this criterion. However, this criterion was not adequate for skewed transverse joints and some longitudinal joints where the imaging vehicle had changed lanes or transitioned from a ramp.

**Table 29. Settings used for Rating in WiseCrax**

Distress	Distress Angle (Degrees)	Distress Extent (Longitudinal) (m)	Distress Extent (Transverse) (m)
Transverse Joint	-5 to 5	0 to 0.1	NA
Longitudinal Joint	85 to 90 or -90 to -85	NA	0 to 0.1
Transverse Cracking	-45 to -5 or 5 to 45	NA	NA
Longitudinal Cracking	45 to 85 or -85 to -45	NA	NA



**Figure 34. Distress Angle Definitions**



The following figures in Appendix B display sample rating results:

Section 12: Image 87 in Figure 164

Section 11: Image 43 in Figure 165

Section 11: Image 44 in Figure 166

## **2.4 Gap Analysis and Design Considerations**

Accuracy and precision of the measured distress against the established reference values (“ground truth”) were evaluated to identify the systematic and random errors. The systematic error or bias could be addressed by calibration relative to the existing rating methodology, but the random errors need to be addressed by increasing the reliability of the crack detection and distress identification algorithm through various control parameters within the algorithm. Regarding the effect of error type in network-level pavement management decisions, it is believed that systematic errors in pavement condition data have a higher impact on the PMS outputs than random errors.

From these analyses, potential causes can be categorized to help with identification of prospective solutions. Initial categories of “potential causes” or “gaps” may include:

1. Human Random Errors (i.e. “oops, missed it”)
2. Human Systematic Errors (i.e. “that isn’t the way I interpreted the handbook”)
3. Software Systematic Errors (i.e. algorithm needs correction)
4. Hardware Issues (i.e. hardware settings or calibration are in question)
5. Limitation of Existing System

In this section of the report, the gaps in the performance of the automated rating algorithm are identified according to the success metrics observed in the previous section. In addition, a potential design consideration is offered as the solution to address each identified gap.

### **2.4.1 Human Random Errors**

Standard deviation of error among the different test sections should explain the degree of random error for each distress identification method. There is not much to be done to address human random errors. There seems to be higher standard deviation of error in the evaluated automated algorithm compared to the manual and semi-automated results which are relatively similar to each other. This higher variation of error for the automated results indicates that the algorithm performed much better in some test sections compared to the others. Therefore, this is not necessarily a random error and it could be a systematic issue. To address this gap, there needs to be a more robust crack detection, classification, and rating routine which will be discussed in the Section 2.4.3 on software systematic errors.

### **2.4.2 Human Systematic Errors**

The biases in the manual and semi-automated surveys represent human systematic errors. These errors seem to be relatively lower for the semi-automated rating compared to the manual field rating. In addition, there seems to be lower errors in terms of transverse and longitudinal cracking compared to corner cracks and shattered slabs. There seems to be a very high bias in terms of spalling and patching, but that could be attributed to the lower number of occurrences. To address this gap, it is recommended to improve the Distress Protocols, and/or their application and several notes have been provided in Section 2.2.1. Careful review, discussion and coordination needs to take place with FDOT staff to be certain the existing protocols are being interpreted and followed as closely as possible (and practical). During that coordination process, invariably “qualifiers” or editorial corrections are anticipated that will provide for more consistency in the application of the protocols for both manual and automated application.

### **2.4.3 Software Systematic Errors**

The following are the software systematic issues that have been identified and corresponding solutions that have been recommended by Fugro research team.

#### **Transverse and Longitudinal Joint Detection**

The WiseCrax software version 3.0 did not have a joint detection routine. In this preliminary exercise, the rating criteria (angle and extent) were used to classify transverse and longitudinal lines as joints. As it is evident in the higher number of longitudinal cracks compared to ground truth, which have caused higher bias and standard deviation of error for longitudinal cracks compared to transverse cracks, there seems to be some longitudinal joints at diagonal directions in the images which were mistakenly classified as longitudinal cracks. A review of the images confirms this observation. To avoid incorrectly considering these skewed joints as cracks, joints must be detected, and their surrounding pixels should be masked as non-crack area. Several

image-processing techniques, such as edge detection, contour detection and Hough line transform can be used for this task. The team recommends a joint detection plugin to be developed for the Vision software. It is perceived that much of the bias and standard error in automated detection of longitudinal and transverse cracks could be addressed by separating joints and lane markings from other surface defects.

### **Lane Marking Detection**

From a study of images, it was observed that several stripe edges were classified as longitudinal cracks. Since we mainly focus on pavement defects within lanes only, lane marking detection is vital to define the region of interest (ROI) for further operation executed with the pavement image. The algorithm for lane marking detection can still be improved. The computer vision-based technique for lane marking detection include thresholding and contour detection. Then the properties of contour can be studied, and the false positive detection can be filtered out.

### **Crack Severity Rating**

In this preliminary evaluation, severity rating was not considered. This is because of the noise in the images that needed to be removed using filters to detect sealed cracks. Filtering the images tends to increase crack widths and therefore impact the assignment of severity levels. In addition, when the WiseCrax option to enable detection of sealed cracks is used, the recorded crack widths are larger than what is measured and therefore not useful for severity rating. It is recommended that filtering is not used moving forward. This is because the non-sealed cracks have a higher priority for FDOT and because the crack width and severity assignment have higher priority than detection of sealed cracks.

It should be noted that the evaluation results show very low agreement among the raters in terms of identifying severity levels during manual and semi-automated surveys. This is evident in the results detailed in Appendices C, D, and E. It has been found to be very difficult to get consistency in severity levels regardless of the procedure used.

### **Crack Grouping and Count per Slab**

As it was explained in Section 2.2.5, a database routine was developed to count the number of cracks per slab. However, the results of the evaluation indicate much higher bias and lower precision in count values compared to length values. This is because multiple segments of one crack are counted as separate distresses thereby increasing the number of cracks. This issue can be addressed by developing an enhanced grouping process that would allow for grouping of cracks according to their location across the slab.

## **Corner Cracks**

After the joints are detected, each slab is defined. Corner cracks can be detected using coordinates of their start points and end points and their angle. There are four types of corner crack: bottom right, bottom left, top right, and top left.

## **Shattered Slabs**

Similar to the algorithm for corner cracking detection, the number of 'sub-slabs' can be acquired if coordinates of edges (longitudinal or transverse cracks) are given. The slab which are divided into more than four pieces are considered as Shattered slab. An alternative methodology could be based on crack counts per slab to simplify this process.

## **Spalling**

The evaluated software cannot detect spalling using the existing images. It is expected that depth (3D) data is required for detection of spalling at joint or crack edges.

## **Patching and Surface Deterioration**

Patching and surface deterioration continue to be two of the most challenging distresses to detect with an automated system. For these specific distresses of concern, alternative methods of identification will likely need to be identified or explored. However, it should be noted that the emphasis of this project is on cracking distresses.

### **2.4.4 Hardware Issues**

These typically include such items as camera settings, daily calibration checks and other fundamental controls that provide for more consistency in the use of the hardware being utilized. Initial and preliminary recommendations were made in Section 2, and Appendix A provides a draft guideline for annual calibration and check of the imaging hardware.

### **2.4.5 Limitation of the Existing System**

As it was mentioned, distresses such as spalling, or patching cannot be detected without 3D data. Images of the 12 test sections were collected both with the FDOT MPSV (2D LRIS) on December 1, 2015 and with a Fugro ARAN (3D LCMS) in October 2015. The main analyses in this study were conducted using the LRIS images as was within the scope of this study. Following completion of Task 3, FDOT will review the final evaluation results and if FDOT finds it beneficial, there could be a follow-up study showing the results of 3D analysis.

## 2.4.6 Recommended Design Solutions

Table 30 summarizes the identified gaps and corresponding recommended solutions.

**Table 30. Identified Gaps and Recommended Solutions**

Number	Category	Gap	Recommended Solution
1	Human Random Errors	High variation of rating results among test sections	N/A
2	Human Systematic Errors	High bias (average error) and high variation of rating results among multiple raters	Review and/or revise distress protocols
3	Software Systematic Errors	High bias in longitudinal cracking amount (high number of false positives)	Joint detection plugin and plugin for separating stripes
4		High variation of error among multiple test sections	Joint detection plugin and plugin for separating stripes
5		High variation of error among multiple runs (while reasonable variation in the actual values among multiple runs)	Joint detection plugin and plugin for separating stripes
6		High bias in crack counts	Improve crack grouping
7		Issue with rating of corner cracks	Corner crack plugin
8		Issue with rating of shattered slabs	Shattered slab plugin
9		Issue with crack width determination and severity rating	Do not use filters moving forward so that crack width can be measured
10	Hardware Limitations	distresses such as spalling, or patching cannot be detected without 3D data	Evaluate 3D data

Based on this gap analysis, the following development efforts are recommended for Task 3 of this project. The algorithm logic design is briefly explained for each development effort:

### 1) Transverse and longitudinal joint detection plugin

- a. First, an edge detection algorithm is used to detect the joint edges. Joint edges are detected by identifying points where the brightness changes

(decreases) sharply, based on the assumption that the other 'background' pixel brightness varies smoothly across the pavement image.

- b. Then, the non-straight line segments are filtered out by analyzing the shape of the contour line passing through the detected joint edges. The contour is a curve joining all the adjacent points along the edges. The elongation and orientation of the contour's shape is estimated. Elongation is calculated as  $[1 - W/L]$ , where  $W$  is the width of the rotated minimal bounding box (the rectangular enclosing the contour shape), and  $L$  is the length of the rotated minimal bounding box. The elongation of the contour should be large than a predefined threshold value to make sure the object is a linear feature. The angle between the line parallel to the length of the bounding box and the horizontal is representing the orientation of the contour shape. The orientation of the major axis of the contour should be close to 90 degrees or 0 degrees.
- c. Finally, the "straight" line is extracted using Hough Transform to fit a straight line through the joint edge points.

## 2) Lane marking detection plugin

- a. gray-level thresholding: We assume that the pixels of lane marking are brighter than the rest of the pixels in the image.
- b. contour analysis and filtering: Shape of the bounding box for the lane markings should be close to rectangle and its area should be larger than a predefined threshold value. Rectangularity is evaluated by the degree to which a contour shape fills its minimal bounding box (area of the object divided by area of the bounding box). Area is evaluated as the area enclosed by the contour of an object.

## 3) Plugin to improve crack grouping and count per slab

- a. group cracks based on the types of cracks (longitudinal or transverse)
  - i. detect the endpoints of the cracks and divide them into two groups based on the type of crack
  - ii. only connect the endpoint pair ( $P1(x_1, y_1)$ ,  $P2(x_2, y_2)$ ) if one of the following exists:

1. if both of the points in the pair belong to the category of longitudinal crack endpoint AND  $|x_1 - x_2|/|y_1 - y_2| > 1$  AND Euclidean distance between the pair is smaller than a threshold value (for example, 300 pixels) OR
  2. If both of the points in the pair belong to the category of transverse crack endpoint AND  $|x_1 - x_2|/|y_1 - y_2| \leq 1$  AND Euclidean distance between the pair is smaller than a threshold value (for example, 300 pixels)
- b. extract the corner points (vertices) of the slab and count the cracks in each slab based on the relationship of endpoints of crack and slab vertices:
- i. Assume crack endpoint P's coordinate is  $(x_p, y_p)$ , and the slab's upper left point is  $(x_1, y_1)$  and lower right point is  $(x_2, y_2)$ .
  - ii. if  $(x_p$  is between  $x_1$  and  $x_2)$  AND  $(y_p$  is between  $y_1$  and  $y_2)$ , then we consider the point  $(x_p, y_p)$  is inside the slab.
  - iii. If any crack endpoint is inside the slab, the crack is regarded as a 'crack in this slab'.

#### 4) Plugin to classify and rate corner cracks

- a. extract the corner cracks based on the relationship between endpoints of crack and slab edges (or joints); A corner crack should intersect with both transverse and longitudinal joints, and this point of intersection should be more than one foot apart from the slab corner on both the longitudinal and transverse joints. Based on its location, we classify corner cracks into four types: upper left, upper right, bottom left and bottom right.
- b. rate the corner crack based on its width:
  - i. light: width  $\leq 1/8$  inch
  - ii. moderate:  $1/8$  inch  $<$  width  $\leq 1/4$  inch

- iii. severe: width > 1/4 inch

5) Plugin to classify and rate shattered slabs

- a. count the number of regions bounded by the 'cracks inside the slab' and joints. If the number is greater than four, the slab is counted as shattered slab. Note that the grouping plugin should have satisfactory performance before this plugin can successfully classify shattered slabs.

- b. rate the shattered slab based on width of crack.

- i. moderate: width  $\leq$  1/4 inch

- ii. severe: width > 1/4 inch

## **2.5 Summary and Recommendations**

Results from the evaluations in Task 2 of this project provide the necessary tools to conduct appropriate analyses. Specifically:

1. Establish reference values
2. Determine acceptable range based on the variations observed during the evaluation of existing methods
3. Compare manual, semi-automated, and fully automated methods
4. Diagnose areas for improvement

### **2.5.1 Summary Observations**

The key observations from these evaluations were as follows:

1. While there was more agreement among the raters in manual field surveys compared to semi-automated rating, there seemed to be less bias (systematic errors) and higher precision (lower variation of each rater error among test sections) in the semi-automated results as opposed to field surveys.



2. There seemed to be more agreement among the raters in terms of transverse and longitudinal cracking compared to other distress types. A review of the distress identification protocol is recommended for increasing consistency among raters. Section 2.2.1 provided pertinent notes for the FDOT *Rigid Pavement Condition Survey Handbook* (2017) to be considered by FDOT staff.
3. The automated routine was relatively more successful in detecting and identifying the length of transverse cracks (83%) compared to longitudinal cracks (60%). In fact, the accuracy of the automated routine in terms of the transverse cracks (83%) was higher than the accuracy in the manual field surveys (75%). The reason was mainly because of the longitudinal joints or lane stripes that were falsely being classified as cracks and therefore increasing the number of cracks (positive bias). There is a need for proper joint detection.
4. In contrast to the reliability evaluation based on the variation of error compared to a reference survey, the evaluation based on the actual variation of distress amounts among multiple runs indicated that the automated algorithm had a comparable repeatability to the manual and semi-automated methods. It is perceived that by addressing the issues of joints and cracks, the variation among runs will decrease.
5. There was a need to filter out image noise to be able to detect sealed joints and wider cracks. As a result, crack widths were detected to be wider than actual and this compromised the ability of the software to assign proper severity levels. It is recommended that filtering is not used moving forward.
6. The evaluated software needs improvements in terms of the count of the distresses as opposed to the length. Proper grouping of detected crack segments is required.
7. Spalling could not be detected without depth (3D) data.

### **2.5.2 Recommendations for Task 3 Software Development**

For initial planning purposes, the following six subtasks are recommended for Task 3:

- 1) Transverse and longitudinal joint detection plugin,
- 2) Lane marking detection plugin,

- 3) Plugin to improve crack grouping and count per slab,
- 4) Plugin to classify and rate corner cracks,
- 5) Plugin to classify and rate shattered slabs,
- 6) Final evaluation results.

### **2.5.3 Future Analysis Recommendations**

The research team recommends the following analyses to be conducted in future to ensure an appropriate path forward with the software development and implementation:

- A. Conducting a Second Distress Workshop
- B. Confirming Detection Settings Using Additional Images
- C. Evaluating Automated Software Using 3D Data
- D. Evaluating a Second Alternative Software

The following segments provide the objectives, required activities, and the needed budget amounts for these additional activities. If FDOT approves these activities following Task 3, Fugro will prepare an updated proposal and request a corresponding time extension and budget modification to account for these additional tasks.

#### **A. Conducting a Second Distress Workshop**

After review of the FDOT *Rigid Pavement Condition Survey Handbook* (2017) during the preliminary distress workshop, it was determined that some of the distress definitions needed further clarification for consistent and reproducible distress rating results. In addition, review of the distress ratings conducted by FDOT experienced raters further highlighted the need for consensus building among the raters. There is a need for a second distress workshop with the following objectives:

1. Review the reference semi-automated distress rating (conducted by Fugro engineers) to arrive at a consensus among the FDOT experienced raters. This consensus survey will be used as the reference survey to evaluate accuracy and precision of the automated and manual distress ratings moving forward.

2. Review the notes from the first distress workshop on the FDOT *Rigid Pavement Condition Survey Handbook* (2017) and identify the required modifications to the handbook. This will also include clarifications of definitions for some distress types and severity levels to ensure corresponding software development.

The required activities for conducting the second distress workshop include the following:

- Activity 1: Pre-workshop coordination and preparation of presentation materials
- Activity 2: Attending and conducting the workshop
- Activity 3: Post-workshop review and action items

The estimated level of effort required to conduct a second distress workshop is about 120 hours of the consultant's time.

## **B. Confirming Detection Settings**

There is a need for further evaluation of the automated software settings on additional pavement images (of other textures, surface types and characteristics) with the following objectives:

1. Confirm whether a pre-processing filter is essential to filter out noise and identify the type and properties of the required filter based on additional images.
2. Investigate and confirm the crack detection parameter settings that provide the best compromise between false positives and missed cracks based on the initial test sections and the additional images.
3. Investigate the impacts of the selected filters and detection parameter settings on the width of the detected cracks and recommend path forward for proper assignment of severity levels

The required activities for confirming detection filters and settings include the following:

- Activity 1: coordinate with SMO to obtain about 120 images (30 images from four additional test sites of different surface types, textures and surface

characteristics), format received data into proper folder structure, and create Vision database

- Activity 2: investigate the necessity of filters based on four filter types and each with three different parameters (12 possible iterations) on a representative sample of the images (10%, about 12 images). Each iteration will take approximately five minutes to conduct and record. During this activity, the crack detection parameters will be fixed at the settings identified on the initial test sections.
- Activity 3: investigate the suitable crack detection parameter settings based on about 10 key parameters (the initial software evaluation found the detection results to be more sensitive to these key parameters) and each with three different values (30 possible iterations) on a representative sample of the existing and the additional images (existing 12 sections 40 images each, additional four sections 30 images each). About 10% of the images will be used for this exercise (60 images). Each iteration will take approximately five minutes to conduct and record. For each sampled image, the average pixel intensity can be calculated and a correlation with the selected settings could be investigated.
- Activity 4: obtain the FDOT manual survey results on the additional sections and compare total amounts of distress to confirm proper detection settings
- Activity 5: conduct a baseline semi-automated survey on the additional images to obtain crack maps and confirm proper detection settings

The estimated level of effort needed to conduct further analysis on detection settings is about 320 hours of consultant's time.

### **C. Evaluating Automated Software Using 3D Data**

Fugro has previously collected 3D LCMS images of the 12 test sections used in the initial software evaluation. However, the software evaluations were conducted based on the 2D LRIS images according to the proposal as the SMO MPSV unit collects 2D images only. Evaluation of the automated software on 3D images will benefit the project outcome as it will serve the following objectives:

1. Investigate whether the current limitations of the automated software results were due to hardware limitations

2. Provide insight into the limitations of 2D images and how a hardware upgrade would benefit SMO in distress identification

The required activities for evaluating the software on 3D images include the following:

- Activity 1: coordinate with FDOT to conduct semi-automated evaluations of the 3D images by FDOT experienced raters
- Activity 2: determine proper filters and detection parameter settings
- Activity 3: conduct classification and rating
- Activity 4: summarize the results and conduct comparisons
- Activity 5: prepare documentation

The estimated level of effort required to conduct an analysis of the 3D pavement images is about 350 hours of consultant's time.

#### **D. Evaluating a Second Alternative Software**

The analysis cited above was based on use of a software package that the research team had confidence and familiarity with. However, there are a host of other software available. A comparison with other software (which would meet the requirements of this project) will confirm whether the variability issues are due to the detection algorithm or due to hardware limitations.

The required activities for evaluating an alternative software on 2D images include the following:

- Activity 1: prepare the FDOT LRIS images to be used in the alternative software
- Activity 2: determine proper filters and detection parameter settings in the alternative software
- Activity 3: conduct classification and rating in the alternative software

- Activity 4: summarize the results and conduct comparisons
- Activity 5: prepare documentation

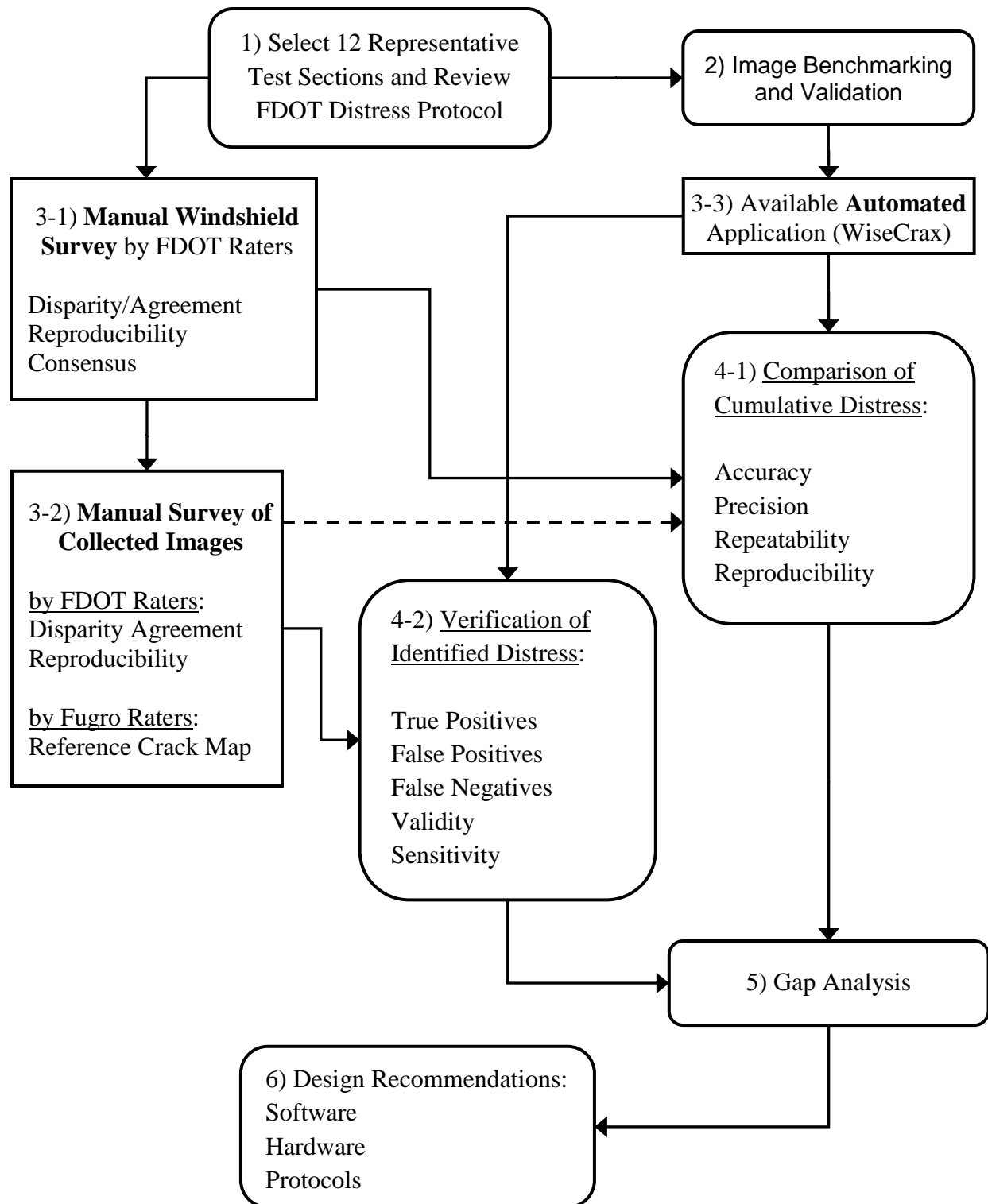
The estimated level of effort needed to conduct analyses using an alternative software is about 440 hours of consultant's time.

## **CHAPTER 3 – RIGID PAVEMENT APPLICATION DEVELOPMENT AND VALIDATION**

Task 3 of Phase I included the development of the FDOT Rigid Pavement Distress Application (FRPDA) for crack identification and quantification, and the corresponding validation testing of the application to evaluate its merit.

The preliminary experiment in Task 2 included: establishment of 12 validation test sites representing the typical crack types and severity encountered on Florida rigid pavements; validation of collected image quality and its adequacy for distress identification; ground truth measurements based on a manual rating of the collected LRIS images (reference survey); and comparison of accuracy and precision of the automated method to manual and semi-automated distress surveys using a comprehensive evaluation framework and established success metrics. Figure 35 illustrates the devised evaluation plan for conceptualization and design of the FRPDA algorithm. The previous chapter describes all these steps in detail.

This chapter describes the design solutions devised to address the gaps identified in Task 2. The design of these solutions was initiated in Task 2 and documented in the corresponding chapter. As the actual development effort started in Task 3, some of the solutions have been modified to better address the gaps. Section 3 describes the final algorithm in detail. Section 3.2 presents the results of automated distress identification using the developed solutions in terms of the same evaluation framework and success metrics that were established in Task 2. Finally, recommendations are provided in Section 3.3 on the path forward regarding implementation of the automated survey approach in practice.



**Figure 35. Framework for Evaluation and Design of Automated Pavement Distress Application**



### 3.1 Rigid Pavement Application Design Solutions

Table 31 summarizes the identified gaps in the preliminary evaluation of an available automated software application (WiseCrax) and corresponding recommended solutions based on the results of the gap analysis conducted in Task 2. Based on the gap analysis, the following development efforts were recommended and implemented in Task 3 of this project. The primary focus of this effort was on determining cracking distresses.

**Table 31. Identified Gaps in Automated Software System and Recommended Solutions**

Number	Gap	Recommended Solution
1	High bias in longitudinal cracking (high number of false positives, both count and length)	Develop joint detection algorithm and improvements for separating stripes
2	High variation of error among multiple test sections	
3	High bias in all crack counts (while reasonable bias in transverse crack length)	Improve crack grouping
4	Not rating corner cracks	Revise corner crack definition in FDOT protocol and develop corner crack algorithm
5	Not rating shattered slabs	Develop shattered slab algorithm
6	Issue with crack width determination (and therefore severity rating) after image filtering	Modify pixel intensity threshold for measuring crack width
7	Not rating spalling of crack and joint edges	Need depth data
8	Not rating patching	

Sections 3.1.1 and 3.1.2 describe the adjustments to the existing software (WiseCrax) based on the needs of this project. The adjusted routine first filters the images (see Section 3.1.1) and then detects surface defects (see Section 3.1.2). Both routines have been assembled into a single batch processor, which can be run from the Fugro Vision platform. Sections 3.1.3 to 3.1.7 explain the subroutines developed specifically for this project and embedded in the customized batch processor, which was named “*FDOT Rigid Pavement Distress Application*” (FRPDA).

The recommended procedure for automated identification and quantification of rigid pavement cracks is as follows. This process has been detailed in the *FDOT Rigid Pavement Distress Application User’s Guide* in Appendix G.

1. Run the automated lane assignment based on lane edge offset from image edge and specified lane width. Review and correct lane edges as needed to address any significant vehicle wander during data collection.
2. Run the automated batch processor for crack detection (based on WiseCrax), which filters the images and detects the surface defects for all sections in a project database.
3. Run the automated batch processor called “*FDOT Rigid Pavement Distress Application*” to:
  - a. Detect the joints for all sections in a project database;
4. Perform quality control (QC) of the joints, modify, add, or delete as appropriate for each section;
5. Run the automated batch processor called “*FDOT Rigid Pavement Distress Application*” to:
  - b. Conduct classification, which groups adjacent lines, assigns lines to slabs, and classifies lines into longitudinal and transverse based on their angle for all sections in a project database;
  - c. Rate the classified lines into corresponding crack types and severities for all sections in a project database;
6. Perform QC of the automated cracks, modify, add, or delete as appropriate for each section. Other non-cracking distress types can also be manually identified during this QC.

### **3.1.1 Pre-Filtering Images**

During Task 2 of Phase I, it became evident that filtering and down-sampling the collected images had a significant positive impact on the crack detection results. This was because the detection algorithm was not capable of differentiating between darker pixels within joints and sealed cracks that had a considerable width. It was also found that for the LRIS images collected on the 12 representative rigid pavement sections, the most suitable filter was a Gaussian filter with a radius of 10 pixels. This filter was selected since it provided the best compromise between detecting wider and narrower surface defects. This filter was applied to all the images from all the 12 test sections

using an open-source software called ImageJ. Of course, using an additional software for this purpose was considered a short-term solution at that stage of the research project to provide the final results. For production-level activities, this open-source code was embedded into the beginning of the WiseCrax detection routine, and the whole process can be accessed through a batch processor within the Fugro Vision platform.

### **3.1.2 Detection Profile Settings**

As was described in detail in Section 2.3, there are multiple detection parameters that can be adjusted for improved detection results. Based on the detailed investigation conducted in Task 2, the recommended parameter setting was established based on the sample images of the 12 test sections.

Filtering (down-sampling) the images tends to artificially increase crack widths and therefore adversely impact the assignment of severity levels. The reason is that the output of Gaussian Filtering is a 'weighted average' of each pixel's neighborhood, with the average weighed more towards the value of the central pixels. For this reason, the peak width of the intensity is increased. As a result, the crack width, which is measured by the number of darker pixels with an intensity less than the threshold value, would also increase in almost all cases.

It was recommended that a lower pixel intensity threshold (darker pixels) be used for determining the crack widths based on filtered images. This threshold is the maximum intensity (the lightest pixels) for a pixel to be counted as part of the crack width. An examination of different intensity thresholds (40, 45, 50, 55, 60, 65, 70, 75, 80, 85, 90, 95, 100) was conducted based on the sample images of the 12 test sections. The results of crack width determination with each of these thresholds were validated by measuring the actual crack widths based on non-filtered images. It was found that a threshold of 70 was yielding the most accurate width measurements for sealed cracks and a threshold of 80 was providing the best results for the width of non-sealed cracks. Therefore, an intensity threshold of 75 was implemented in the final application as the best compromise between sealed and non-sealed cracks.

The final detection settings are shown in Figure 36, and were applied to all images of the 12 test sections after pre-filtering. For detailed description of each detection control parameter, please refer to Section 2.3. The combination of the Gaussian filtering and surface defect detection was assembled into a single batch processor within the Fugro Vision platform.

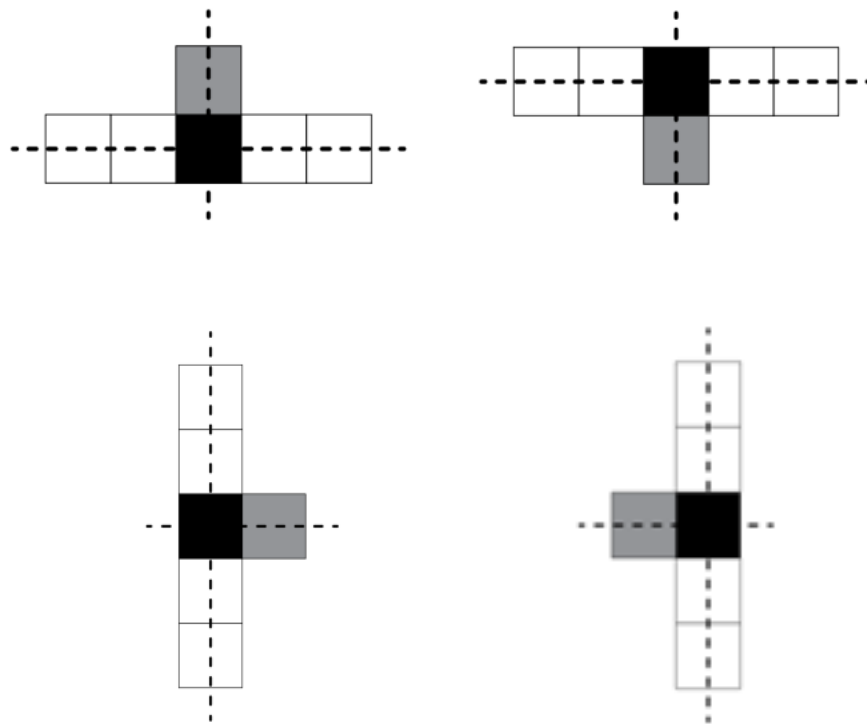
<b>Detection</b>	
WiseCrax Detection Settings	
Crack Options	
PavementType	Undefined
TrainingOpts	
Algorithm version	WISECRAX_V1
Crack Simplification	2
Extraction	
Transverse Cracking [%]	15
Longitudinal Cracking [%]	15
Crack Likelihood	2
Horizontal Bridging	3
Vertical Bridging	5
Pruning	
ApplyFeatureCombination	True
ApplySegmentFeatureCombination	True
Remove Short Distresses	True
Minimum Length [mm]	300
Remove Low Node-Count Distresses	True
Minimum Node Count	100
Remove Low-Cost Distresses	False
Remove 'Bright' Distresses	False
Remove 'Shallow' Distresses	False
Maximum Depth Threshold	128
Width	
Cost Threshold	10
Intensity Threshold	75
Detection Profile Priority	Tag
Keep Detected Cracks	False
Keep Manual Cracks	False
Lane Options	
Enabled	False
Detect within lanes	True
Lanes extraction	
LanesExtractionOptions	
Default lane offset (meters)	0
Default lane width (meters)	3
Keep Previous Lanes	False
Lane Optimization	True
Lane Optimization Frames Count	5
Lane set method	DetectedAlwaysDefaultWhenMissing

**Figure 36. Final Detection Parameter Settings Applied After Pre-Filtering**

### 3.1.3 Transverse and Longitudinal Joint Detection Routine

Since the initial crack detection software (WiseCrax) did not have an independent joint detection function at the time of this research project, a joint detection routine was specifically developed for this project. Note that this routine was designed to identify longitudinal and transverse joints that are approximately at right angles to the image frame, and the presence of skewed/diagonal joints was considered an exceptional rigid pavement design which is not frequently encountered. Since a concept of narrow windows is used to identify very straight lines as joints, naturally, the detected joints have a maximum angle of approximately 5 degrees from the horizontal or vertical.

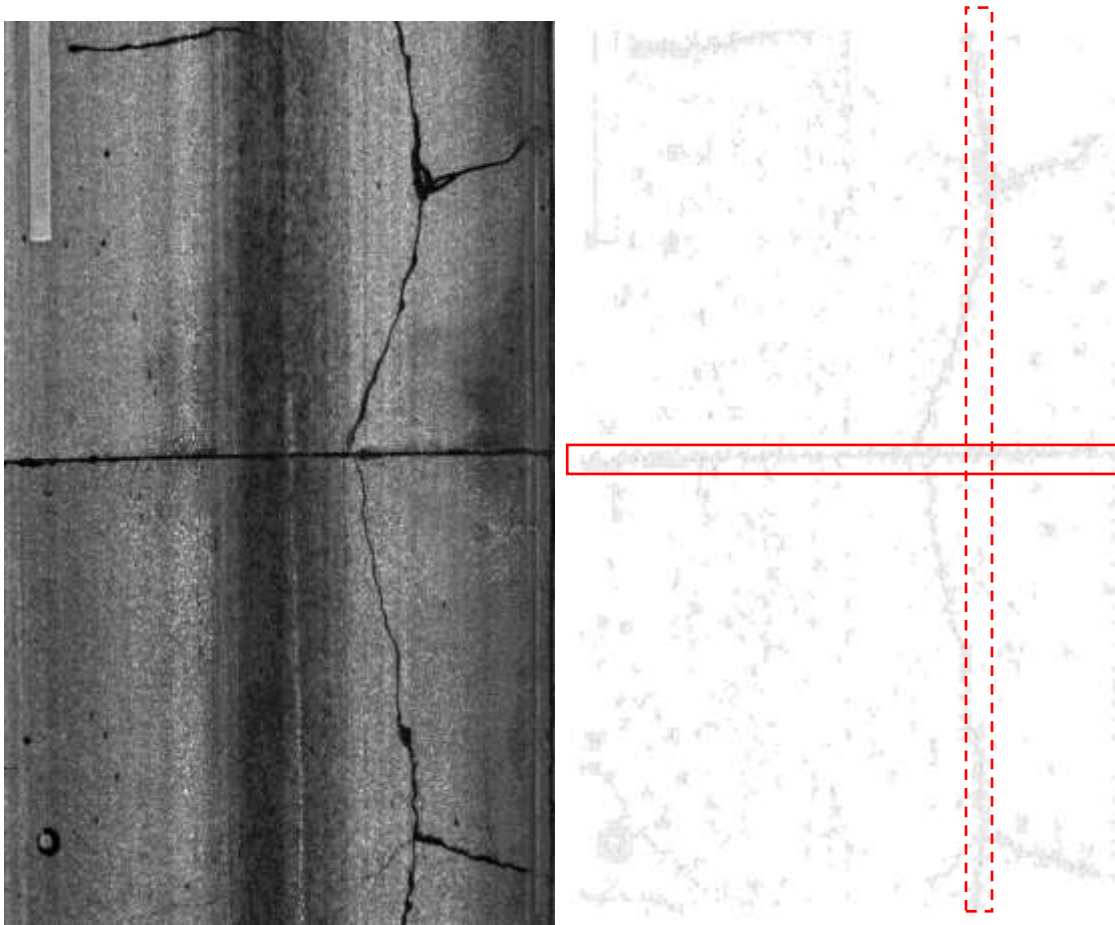
1. First, the image is downsized (the size of downsized image is  $0.25 \times 0.25$  of original image) to enable detection of wider (sealed) joint lines. Then the downsized image is divided into a matrix of cells. The size of each individual cell is 8 by 8 pixels. Then, the darkest pixel in each cell is detected and the information (i.e. intensity and x-y coordinates) of the darkest pixel is assigned to that cell. The existence of a joint cell is then detected by comparing its intensity with the intensity of adjacent cells using a contrast index. If the cell intensity is lower (i.e. darker) than adjacent cells, then the cell is a candidate “joint cell”. The adjacent “joint cells” are connected to form a candidate joint. Figure 37 shows example detected adjacent cells for longitudinal joints on the top and transverse joints on the bottom. The black and gray cells are candidate “joint cells”.



**Figure 37. Detecting Adjacent Candidate Joint Cells (Dark Cells, each 8 by 8 pixels)**

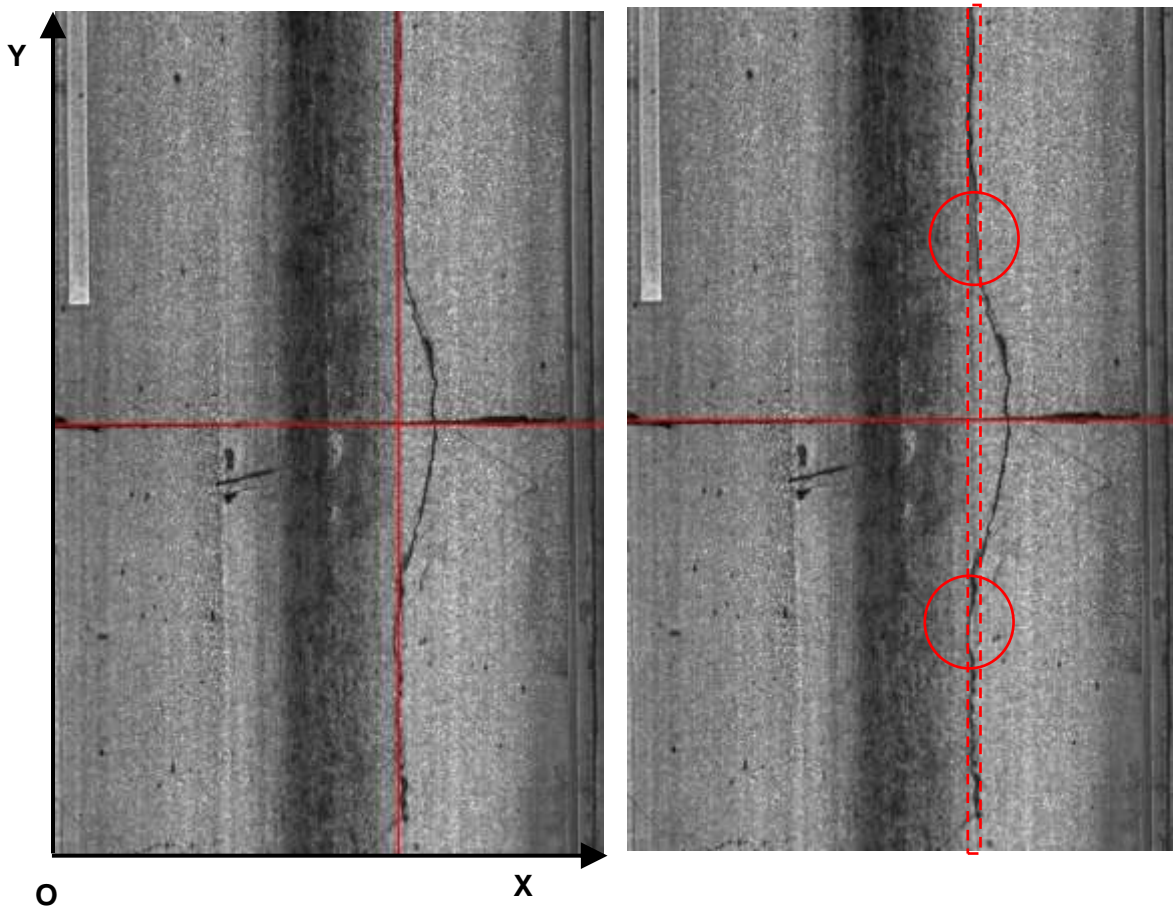
2. A narrow moving window (12 pixels wide) at 0 or 90 degrees (for transverse or longitudinal joints) is used to scan the whole candidate joint cell map, which only contains joint cells. Figure 38 shows an example of such narrow windows for both transverse and longitudinal joints. The number of cells that fall into this window is counted. If the number of cells is larger than a threshold number (we found that  $1/10$  of width or height of downsized image was the threshold that minimized the sum of false positives and false negatives.), then the candidate joint pixel detection result is probably a true positive and the centerline of the window is

considered as joint coordinates. Otherwise, the detection result is a false positive and would be excluded from further analysis.



**Figure 38. Narrow Window to Identify Joints from Detected Joint Cells**

3. Some crack cells (cells that belongs to a pavement crack) could be the source of false positives. A second narrow window (12 pixels wide) is used to filter out this kind of error. The gap between the candidate joint cells that fall within the narrow window is calculated and if this gap is higher than a specified threshold (64 pixels), then this is a meandering crack (going in and out of the narrow window) and not a straight joint. Figure 39 demonstrates an example of such false positive joints.
4. Finally, the selected joint coordinate (x coordinate for longitudinal joints and y coordinate for transverse joints) is recorded, and a line is drawn on the image. The coordinate information is also recorded in the SQL database for future assigning of cracks to specific slabs.



**Figure 39. Removing False Positive Joints According to the Gap Between Joint Cells**

Table 32 lists the preliminary results from the joint detection routine described above. For each of the 12 representative test sections (selected in Task 2), Table 32 is showing the number of correctly detected joints, with some exceptions, including falsely identified joints and missed joints. In addition, Table 32 provides summary statistics for detection rate and detection validity. Joint detection rate is calculated as the percentage of all existing joints that were successfully detected by the algorithm. Joint detection validity represents the percentage of detected joints that were actually existing on the pavement surface.

$$\text{Joint Detection Rate} = \frac{\text{Correctly Detected Joints}}{\text{All Actual Joints}}$$

$$\text{Joint Detection Validity} = \frac{\text{Correctly Detected Joints}}{\text{All Detected Joints}}$$

Both indicators show high percentages overall. However, there are a few exceptional situations that have resulted in missing some transverse joints and falsely detecting some longitudinal joints. Sections with considerable issues have been highlighted in yellow.

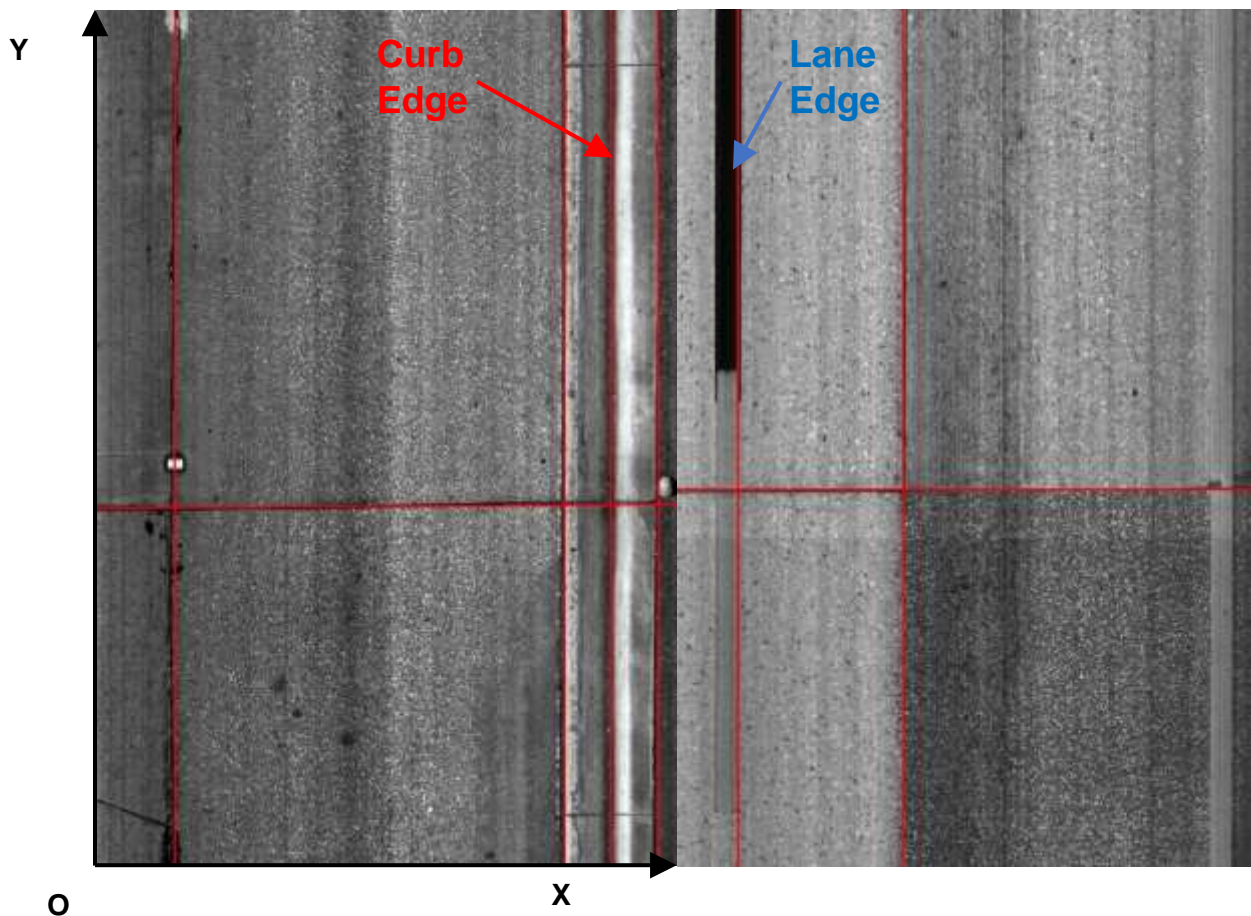
**Table 32. Preliminary Joint Detection Results**

Transverse Joints					
Section	Correct Joints	Exceptions		Detection Rate	Validity or Accuracy
		False Joints	Missed Joints	% of all existing joints	% of all detected joints
1	46	1	4	92.0	97.9
2	49	1	3	94.2	98.0
3	57	2	0	100.0	96.6
4	60	4	7	89.6	93.8
5	23	0	52	30.7	100.0
6	30	1	0	100.0	96.8
7	33	0	2	94.3	100.0
8	32	0	0	100.0	100.0
9	25	0	1	96.2	100.0
10	60	1	2	96.8	98.4
11	42	1	16	72.4	97.7
12	56	0	14	80.0	100.0
AVG	43	1	8	87.2	98.3
Longitudinal Joints					
Section	Correct Joints	Exceptions		Detection Rate	Validity or Accuracy
		False Joints	Missed Joints	% of all existing joints	% of all detected joints
1	16	0	9	64.0	100.0
2	34	0	7	82.9	100.0
3	51	33	0	100.0	60.7
4	40	10	6	87.0	80.0
5	65	2	16	80.2	97.0
6	71	14	0	100.0	83.5
7	87	31	2	97.8	73.7
8	57	14	2	96.6	80.3
9	59	14	0	100.0	80.8
10	59	0	3	95.2	100.0
11	34	19	2	94.4	64.2
12	48	20	0	100.0	70.6
AVG	52	13	4	91.5	82.6

Figure 40 shows two examples of exceptional situations resulting in falsely identified longitudinal joints. The image on the left shows a curb on the outer right edge that was falsely identified as an additional longitudinal joint. This and similar issues have been resolved by restricting the identification of multiple longitudinal joints closer to the image edges. The image on the right shows the black lane stripe that was falsely identified as a longitudinal joint. This and similar issues have been resolved by checking the pixel intensities of the adjacent 100 pixels in the original image, and thus removing dark or

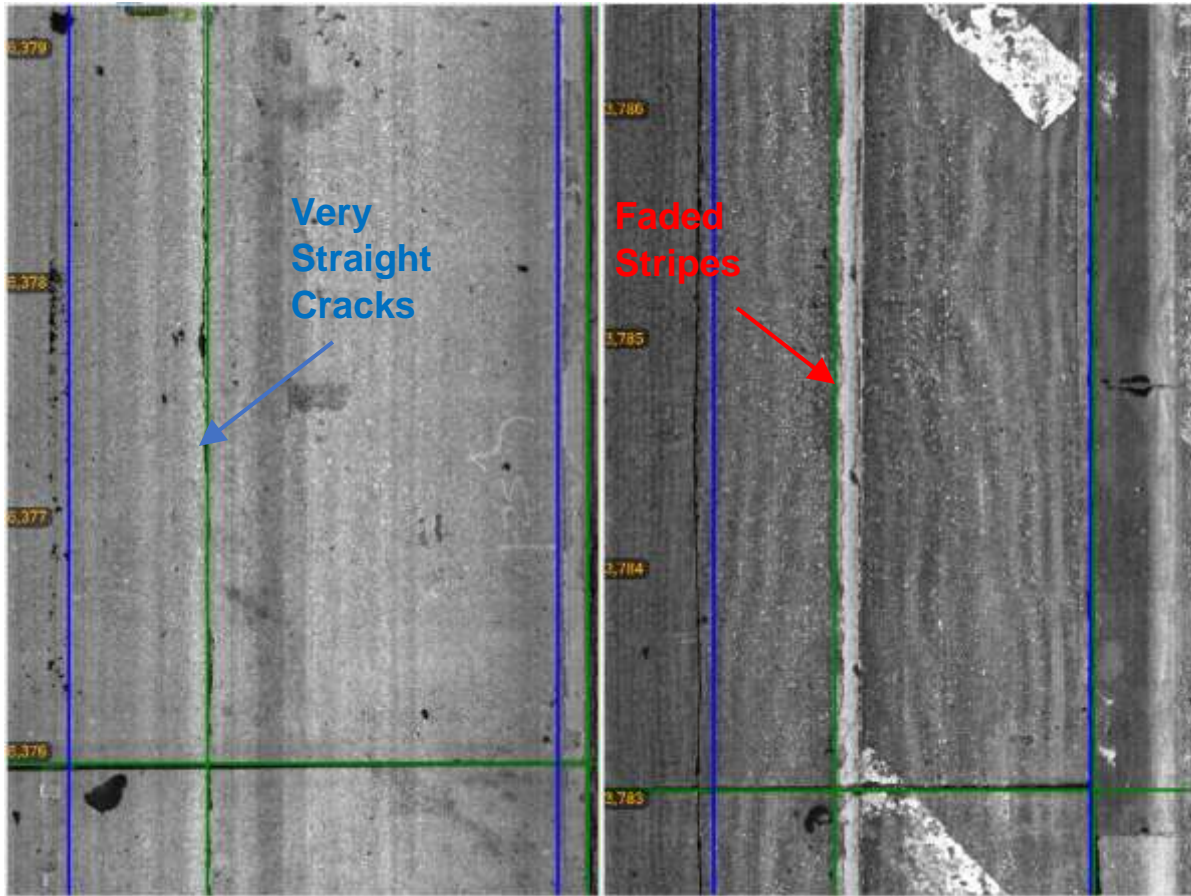


white stripes (if more than 30 pixels out of the 100 have lower than 30 or higher than 210 intensity) from the list of longitudinal joints.



**Figure 40. Examples of Exceptional Situations with Falsely Detected Longitudinal Joints (Curb Edge on the Left Image, and Lane Edge on the Right Image)**

It should be noted that this procedure was not successful in some sections (such as Section 9 on the right in Figure 41) due to the extensive presence of exceptional situations. Specifically, Section 9 had faded lane stripes in the middle of the images and were adding to the false positive joints. Therefore, Section 9 was excluded from the final evaluation. However, the faded lane stripes in Section 8 did not contribute to false positives, because those lane stripes were not in the middle of the images and this subroutine was able to disregard them as stripes. The image on the left in Figure 41 also shows another exceptional situation in Section 5, where extremely straight longitudinal cracks are falsely identified as longitudinal joints. This remains to be a gap in the developed application.



**Figure 41. (left) Very Straight Longitudinal Cracks Resulting in False Longitudinal Joints in Section 5; (right) Faded Lane Stripes in the Middle of Image Resulting in False Longitudinal Joints in Section 9**

While some of these issues have been resolved, it is very difficult if not impossible to identify every exception and address them all. It is possible to use machine learning algorithms to develop more robust routines that would learn to distinguish joints from other lines (this also applies to the identification of other distress). However, a machine learning algorithm will need to be trained effectively on a representative database that has an adequately large number of sample images with all the noted exceptions, and that has been manually and correctly marked. The performance of the machine learning algorithm depends heavily on the availability of such a database.

The automatically identified joints are displayed on the images using green lines. The user can then modify, delete, or add other joints if needed. It is recommended that a systematic QC protocol be established to review the results of the software, identify the common issues to be resolved in future efforts, and rectify the joint detection results before the identification of distresses. Following the implementation task of this project, there could be a routine developed that provides the raters with a randomly selected subset of the images to be manually controlled for quality.

Following the identification of the longitudinal and transverse joints and removing the falsely identified joints, concrete slabs are identified as areas surrounded by joints and lane or image edges. Each slab is assigned a unique SlabID to be able to assign each of the identified distresses to corresponding slabs. Table 33 shows examples of identified slabs, along with corresponding coordinates. In addition to the data fields shown in Table 33, the software also provides dimensions of the slab such as length, width, and area, which can be output into a comma-separated (csv) file format.

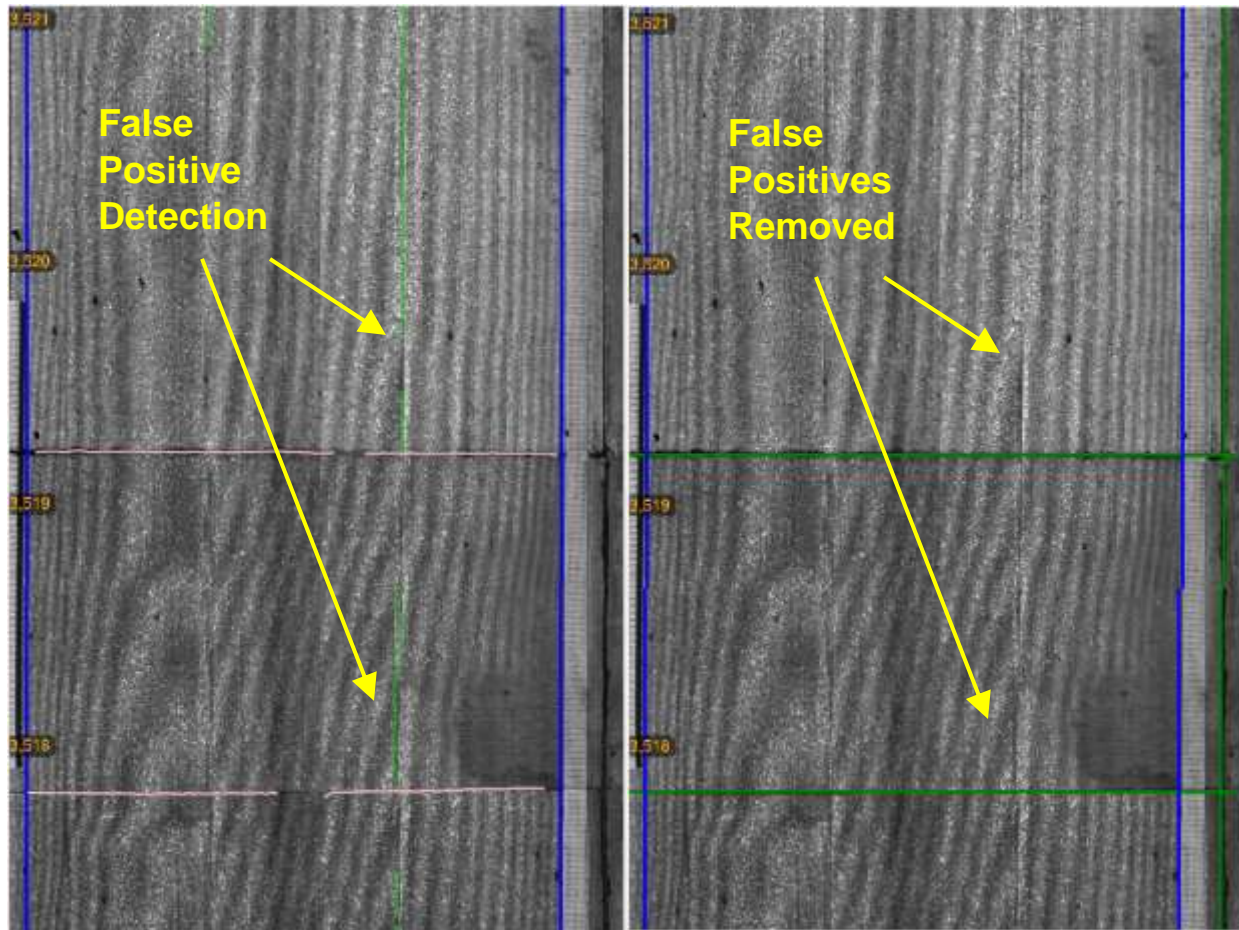
It should be noted that this segment of the routine can be run following the manual QC and modification of the identified joints so that the distresses are correctly assigned to corresponding slabs.

**Table 33. Example Slabs Identified Using Joints**

<b>IDSlab</b>	<b>MinX (meter)</b>	<b>MinY (meter)</b>	<b>MaxX (meter)</b>	<b>MaxY (meter)</b>
1	0	225.0125	1.283829	227.5494
2	1.283829	225.0125	3.430392	227.5494
3	0	228.8075	3.373903	231.8106
4	0.169465	234.9278	1.360859	237.8539
5	1.360859	234.9278	4.153444	237.8539
6	0	240.9556	1.473836	247.0091
7	1.473836	240.9556	4.153444	247.0091
8	0	247.0091	1.53546	253.0934
9	1.53546	247.0091	4.153444	253.0934
10	0	253.0934	3.89257	259.188

### **3.1.4 Routine to Remove False Positive Cracks**

Following the joint detection, there were still some straight lines such as skewed joints and lane markings and stripes that were incorrectly classified as cracks. Therefore, an additional routine was developed to remove straight lines that were not classified as joints in the joint detection procedure and were considered false positives for being cracks. This routine was successful in some cases more than the others. Figure 42 shows one example of the successful application of this routine, where the straight lines comprising false positive cracks have been removed after joint detection.



**Figure 42. Example Removing Straight Lines (False Positive Cracks) in Section 4**

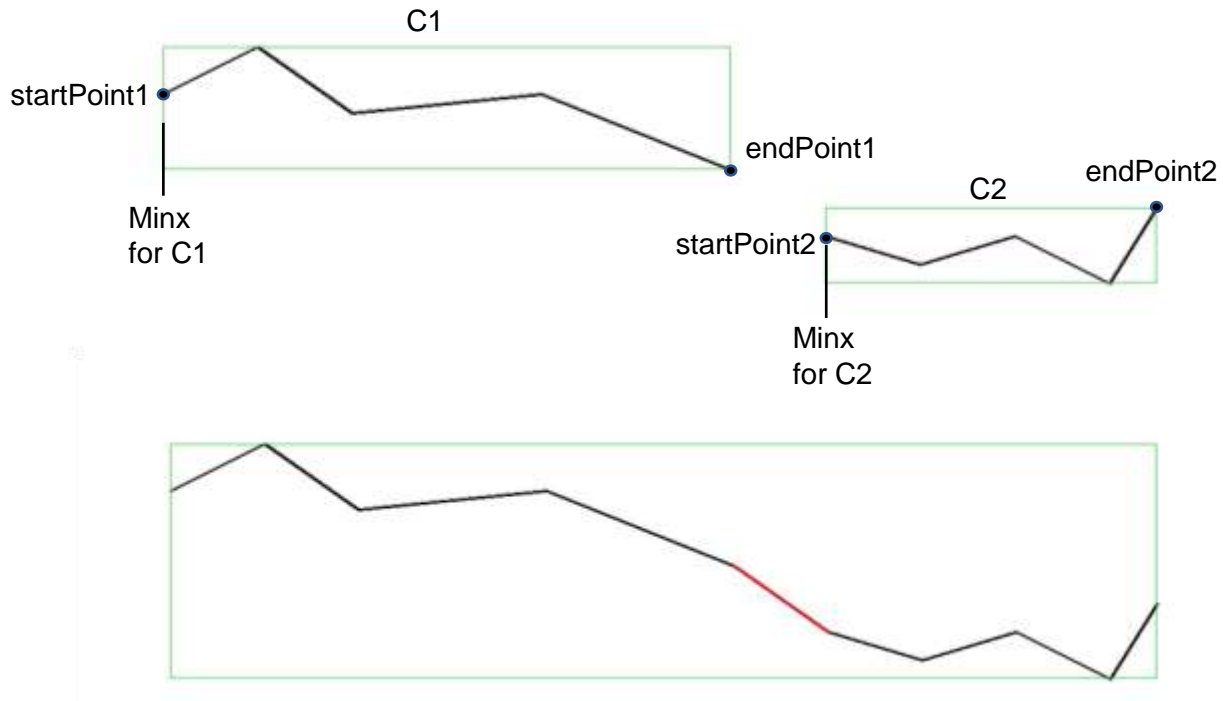
### **3.1.5 Routine to Improve Crack Grouping and Count per Slab**

The following steps describe the routine that was used to improve grouping of cracks that are close to one another and counting the cracks per slab:

1. The detected lines are grouped based on the types of lines (longitudinal or transverse)
2. The longitudinal lines are sorted based on minimum value of y coordinate (minY), and the transverse lines are sorted based on minimum value of x coordinate (minX)
3. The crack pair C1 [startPoint1(sx<sub>1</sub>,sy<sub>1</sub>), endPoint1 (ex<sub>1</sub>,ey<sub>1</sub>)] and C2 [startPoint2(sx<sub>2</sub>,sy<sub>2</sub>), endPoint2 (ex<sub>2</sub>,ey<sub>2</sub>)] are connected, if and only if one of the following exists:



- iii. Both lines belong to the category of longitudinal lines, where  $sy_1 < sy_2$  AND  $ey_1 < sy_2$  AND  $\frac{|sx_2 - ex_1|}{|sy_2 - ey_1|} \leq 1$  (the trajectory between the lines is also longitudinal) AND Euclidean distance between endPoint1 and startPoint2 is smaller than a threshold value (we used 500 pixels) OR
- iv. Both lines belong to the category of transverse lines, where  $sx_1 < sx_2$  AND  $ex_1 < sx_2$  AND  $\frac{|sx_2 - ex_1|}{|sy_2 - ey_1|} \geq 1$  (the trajectory between the lines is also transverse) AND Euclidean distance between endPoint1 and startPoint2 is smaller than a threshold value (we used 500 pixels)



**Figure 43. Example of Two Transverse Cracks Grouped into One Crack**

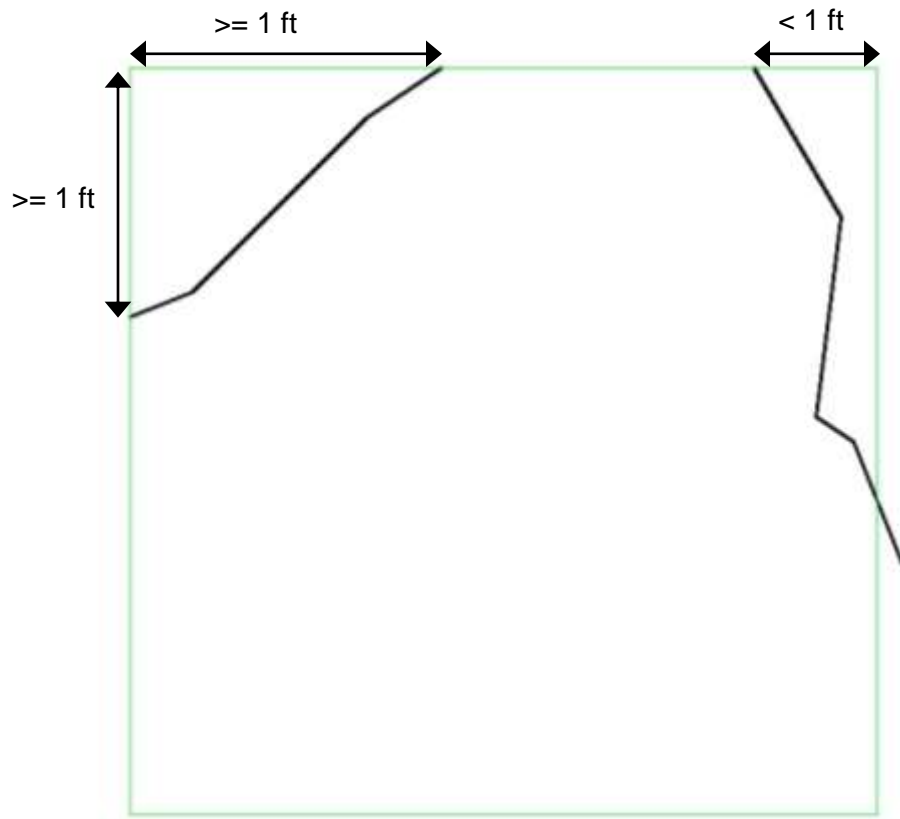
- 4. The corner points (vertices) of the slab are extracted, and the cracks in each slab are counted based on the relationship of crack ends and slab vertices:
  - i. Given the line startPoint (Xsp,Ysp) and endpoint (Xep,Yep) coordinates, and the slab's upper left point being (X1,Y1) and lower right point being (X2,Y2),

- ii. If (Xsp is between X1 and X2) AND (Ysp is between Y1 and Y2), then the startPoint (Xsp,Ysp) is considered inside the slab. If (Xep is between X1 and X2) AND (Yep is between Y1 and Y2), then the endpoint (Xep,Yep) is considered inside the slab.
- iii. If the bounding box of a crack intersects with a slab area, that crack is counted as a crack in that slab. So, a crack would be considered to be a crack in several slabs if it crosses several slabs, unless the length of its crossing is very small.

### **3.1.6 Routine to Classify and Rate Corner Cracks**

The corner cracks are extracted based on the relationship between end points of crack and slab edges (or joints):

1. A corner crack should intersect with both transverse and longitudinal joints, AND the distance from this point of intersection to the slab corner should be more than or equal to 1 foot and less than half the slab width or length (on both the transverse and longitudinal joints).
2. If a crack intersects a joint at a distance less than 1 foot from the corner, it is classified as spalling (Figure 44). Note that this crack should intersect the other joint as well.
3. Based on their location, corner cracks are classified into four types: upper left, upper right, bottom left, and bottom right.
4. The severity of corner cracks is rated based on their width:
  - i. Light: width  $\leq$  1/8 inch
  - ii. Moderate: 1/8 inch < width  $\leq$  1/4 inch
  - iii. Severe: width > 1/4 inch



**Figure 44. Example Corner Cracks and Spalling**

It should be noted that the spalling instances that are classified in this routine are only related to cases where the cracks were not fitting the definition of a corner crack but were intersecting both the transverse and longitudinal joints of one slab. In the absence of depth data, the spalling of cracks and joints are very difficult to detect. Therefore, this spalling number does not represent the entire amount of existing spalling and it is recommended that the manual QC process accounts for this.

### **3.1.7 Routine to Classify and Rate Shattered Slabs**

The following is the routine used for identifying shattered slabs:

1. The number of regions bounded by the 'cracks inside the slab' and joints are counted. If the number is greater than four, the slab is counted as a shattered slab. Note that the grouping routine should be first satisfied before a cracked slab can be successfully classified as a shattered slab.
2. The severity of the shattered slab is rated based on the average width of cracks in that slab:

- i. Moderate: width  $\leq 1/4$  inch
- ii. Severe: width  $> 1/4$  inch

However, no shattered slabs were identified on the 12 representative test sections. It should be noted that the total number of occurrences of this distress type was 10 shattered slabs in all test sections. There are potentially other alternative algorithms that can better classify shattered slabs, and further investigation is required in this regard. Therefore, this is a remaining gap that needs to be closed in future (please see Table 36).

### **3.2 Results of the Developed Rigid Pavement Distress Identification Application**

Similar to the experimental design in Task 2, the evaluation of the developed distress survey method was done in the following two steps:

- 3. Comparison of the overall cumulative quantities of various distress types found in the FDOT windshield survey, FDOT manual rating of the collected images (semi-automated survey), and the developed automated software (FRPDA).
- 4. Verification of the automatically detected distresses against the reference crack maps generated through a manual rating of the collected images (Fugro semi-automated survey).

The following sections will explain the success metrics considered for these evaluations, and the corresponding results.

#### **3.2.1 Success Metrics**

During the testing and comparison experiment designed in Task 2, the following success metrics were established for each category of the above evaluations. As detailed in Chapter 2, a semi-automated approach was used as the reference survey, in which all the images collected in one run for the 12 test sections (total of 509 images) were rated by one Fugro pavement engineer and then completely reviewed and corrected (according to FDOT protocol) by two other Fugro pavement engineers. There are two advantages to this method, first that the first semi-automated rating was 100 percent controlled by two additional raters, and second that the raters were not experienced FDOT raters and therefore this reference can be used as an unbiased reference to evaluate all the three rating methods. FDOT raters and the Fugro software developer did not have access to this reference rating.



**Based on the overall cumulative amount of each distress:**

1. Average error (bias) was used to represent **accuracy** or effectiveness of each method. Accuracy can only be quantified with respect to a reference value. The difference between each FDOT rater and the reference survey in determining the amount of each distress type was normalized (divided) to the amount identified in the reference survey. The average normalized error of the three raters (in percentage) across the 12 sections was used as the bias of the FDOT manual windshield and semi-automated rating methods. The average normalized error of the software in the three runs across the 12 sections was used as the bias of the automated method.
2. To represent **reproducibility** of manual and semi-automated methods, average standard deviation of error among the three FDOT raters (on the same test section) was used. Standard deviation of error among the three FDOT raters was calculated for each test section and then averaged across all sections.
3. The **repeatability** (or precision) of the automated algorithm is represented by the average standard deviation of error among three runs on the same test section. Standard deviation of error among the three runs was calculated for each test section and then averaged across all sections.
4. To use a measure of **reliability** independent of the reference survey, agreement among the three FDOT raters (for manual and semi-automated methods and among the three runs for the automated method) was represented by 100 minus the coefficient of variation in the total amount of each distress type on each section among the three raters/runs.
5. Average standard deviation of error among the 12 sections was used to evaluate the variability of each method across different situations.
6. To compare **efficiency** of the three methods (manual, semi-automated, and automated), the time required for each survey method was estimated.

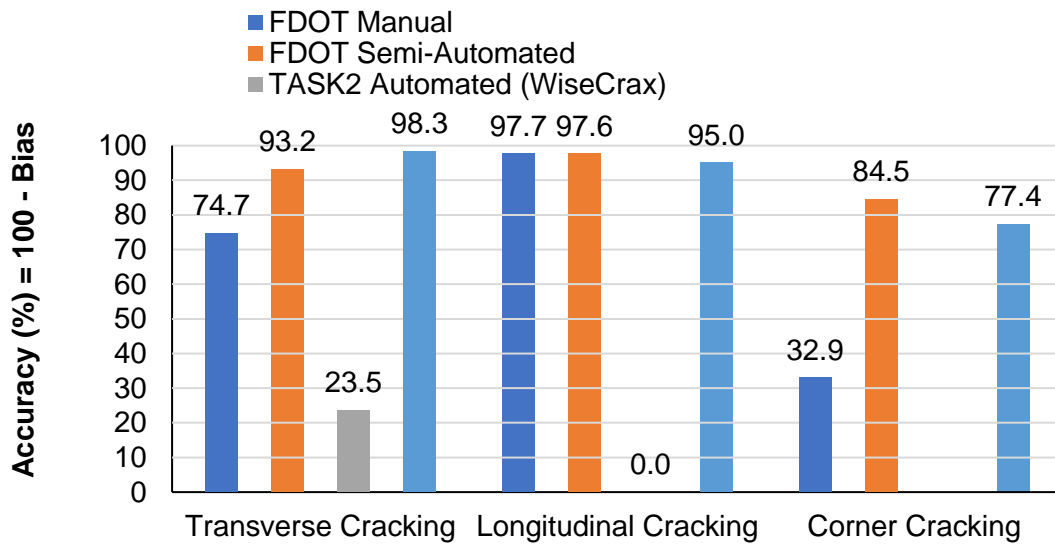
**On a distress by distress basis (based on length):**

- True Positives: correctly detected cracks
- False Positives: detected cracks that don't exist in the reference survey
- False Negatives: Missed cracks

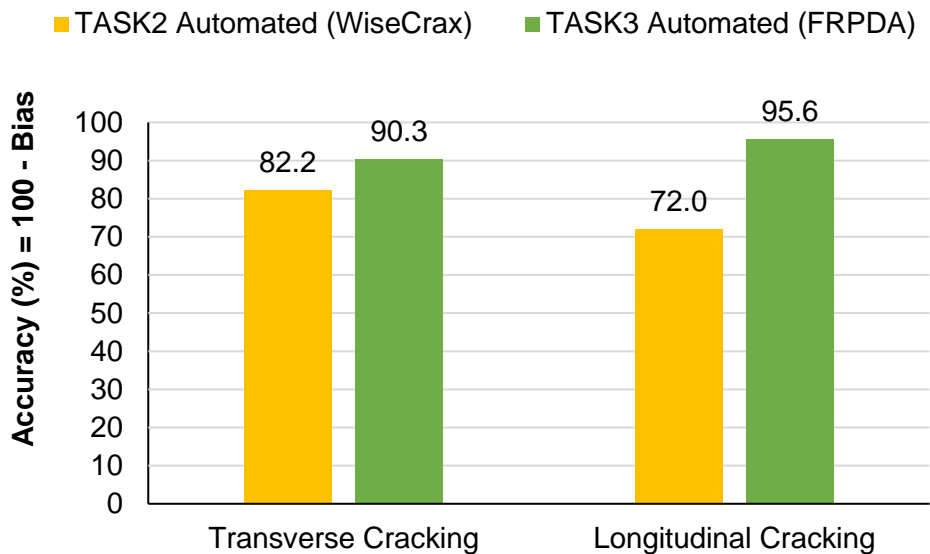
- Distress Validity (or Accuracy): an indicator to be calculated as the ratio of the correctly detected cracks (true positives) to the total detected cracks (true positives and false positives) multiplied by 100. This statistic indicates the percentage of the detected distress that was actually present in the reference survey, thereby expressing the validity of the distress detected by algorithms.
- Distress Sensitivity (or Recall): a parameter to be calculated as the ratio of the correctly detected cracks (true positives) to the total actual cracks existing on the pavement surface (true positives and false negatives) multiplied by 100. This statistic represents the percentage of the distress in the reference survey that was detected by the automated method, thereby expressing the sensitivity of the algorithms to existing distress.
- Distress Classification Performance: a measure of the number of correctly classified cracks (according to the reference survey), divided by the number of correctly detected cracks (true positives) multiplied by 100. This statistic indicates the percentage of the detected distress that is correctly classified by the automated algorithm. This metric does not incorporate severity of the distress.

### **3.2.2 Comparison Results on Overall Section Distress Quantities**

The chart in Figure 45 demonstrates the accuracy of the automated distress identification algorithm developed in Task 3 (FRPDA) in comparison to the previously available automated method in Task 2 (WiseCrax), and to the FDOT manual (windshield) and semi-automated methods. Accuracy is defined as 100 minus the bias (average error among three raters/runs across 12 sections) in identifying each distress type using each method. In addition to the evaluation of the total distress counts in Figure 45, Figure 46 shows the accuracy of the automated method in determining the total length of transverse and longitudinal cracks. It should be noted that the length of the cracks was only measured in the automated method and the manual and semi-automated methods only provided the number of cracks.



**Figure 45. Accuracy of Automated Methods in Identifying the Number of Cracks (higher bars are more accurate results)**

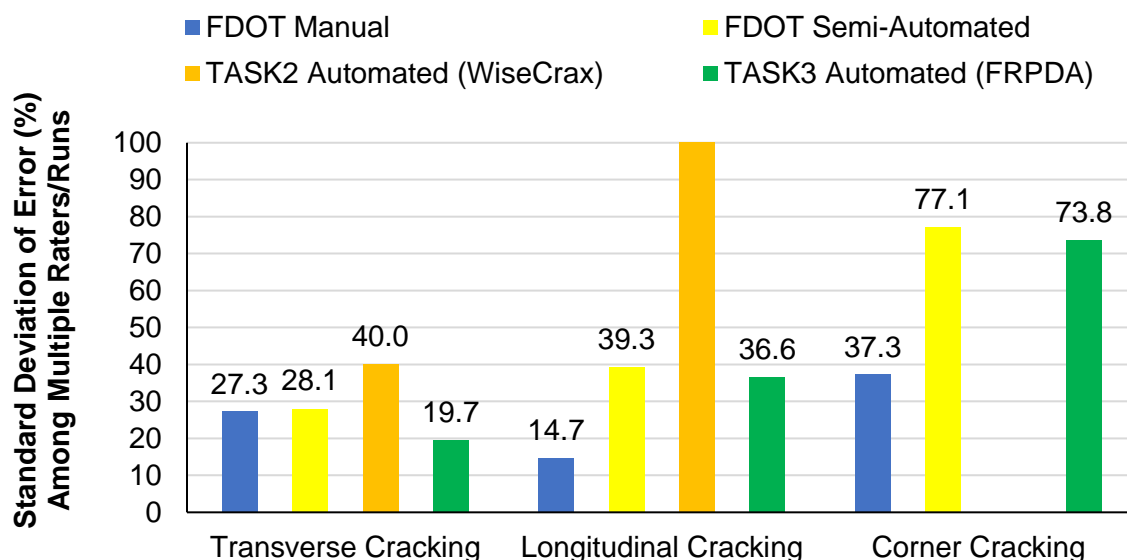


**Figure 46. Accuracy of Automated Methods in Identifying the Length of Cracks (higher bars are more accurate results)**

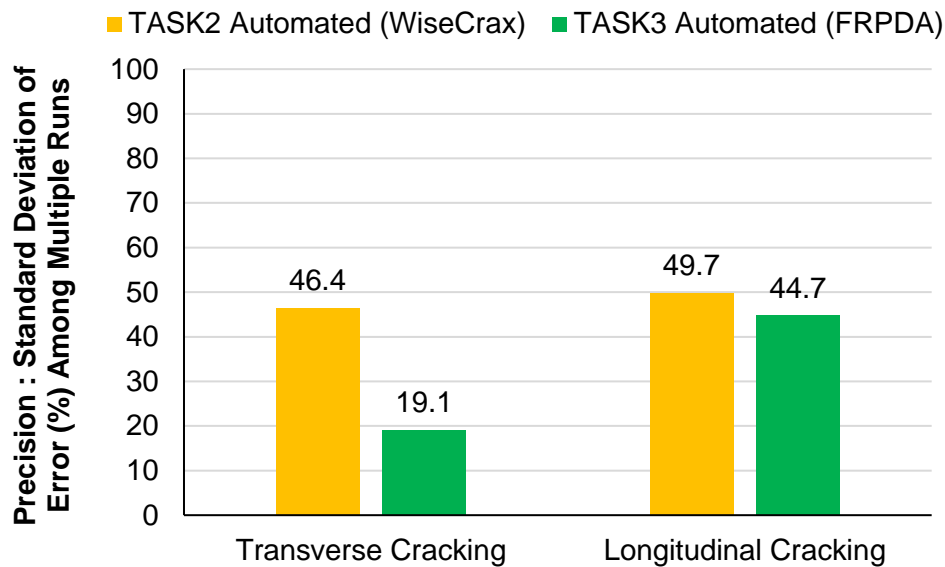
Figure 45 and Figure 46 show that the development efforts in Task 3 of this project have significantly increased the accuracy of the automated method in identifying both the count (80% on average) and the length (16% on average), respectively, of all distress types compared to the preliminary evaluation in Task 2. It should be noted that the preliminary automated method from Task 2 was not capable of classifying corner

cracks. All these improvements show that the gap analysis and the corresponding solution design have been successful. In addition, the accuracy of the improved automated method (FRPDA) is higher than the accuracy of the manual method (FDOT windshield survey) in terms of transverse cracks (by 23% in count) and corner cracks (by 44% in count), and comparable in terms of identifying longitudinal cracks (Figure 45).

The repeatability (precision) of the automated algorithm developed in Task 3 is significantly higher (lower standard deviation among three runs for each section) compared to the automated method used in the preliminary evaluation in Task 2 (Figure 47 and Figure 48). The repeatability of the automated method developed in Task 3 is higher than the reproducibility of the manual method in terms of transverse cracking and lower than the manual method in terms of longitudinal and corner cracking. As it was explained before, some of the exceptions regarding identification of longitudinal cracks can cause the repeatability to decrease from run to run. For example, a longitudinal line that was identified as a longitudinal crack in one run might be identified as a lane stripe in the other run due to the differences in image contrast and the different image boundaries caused by the wander of the imaging vehicle. In addition, it is worth to note that the repeatability of the improved automated results is comparable to the reproducibility of semi-automated results for longitudinal and corner cracking.

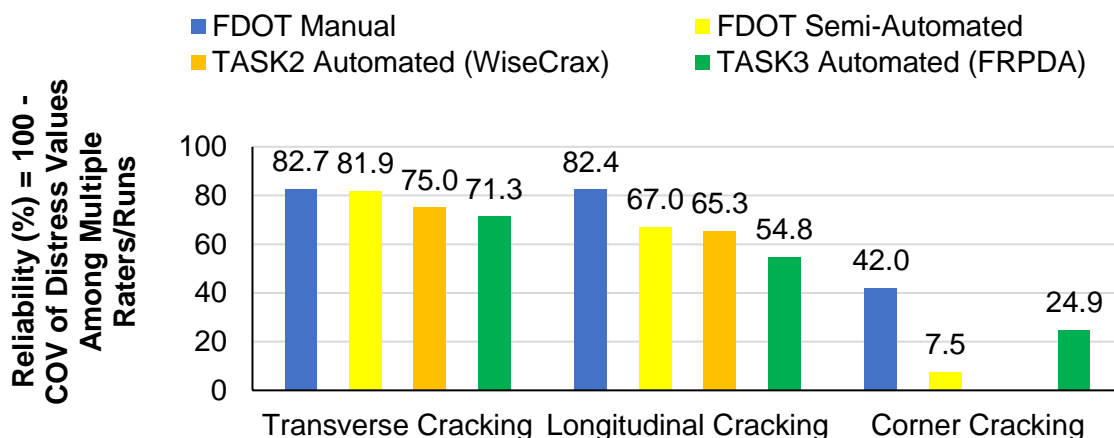


**Figure 47. Repeatability of Automated Methods Compared to Reproducibility of Manual and Semi-Automated Methods in Identifying the Number of Cracks (Standard Deviation of Error Among Multiple Runs/Raters: lower bars are more precise results)**

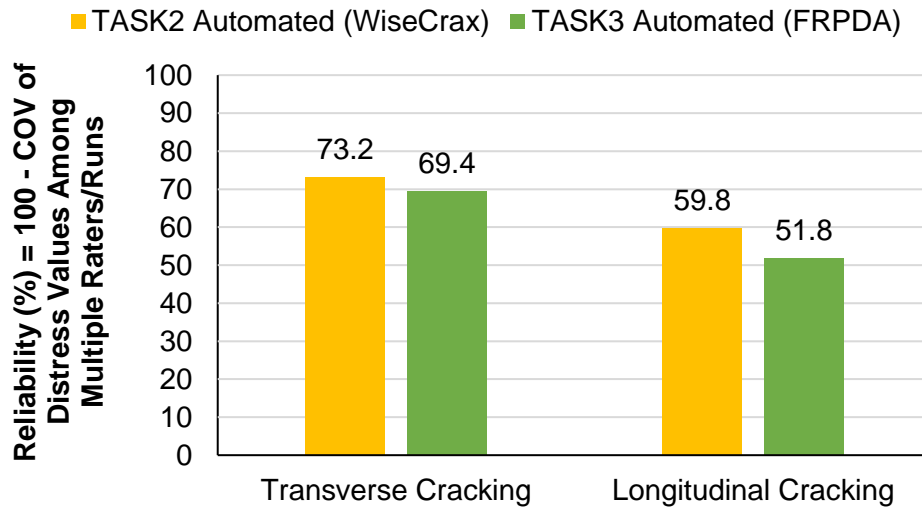


**Figure 48. Repeatability (Precision) of Automated Methods in Identifying the Length of Cracks (Standard Deviation of Error Among Multiple Runs/Raters: lower bars are more precise results)**

Figure 49 and Figure 50 show the reliability of the automated method in identifying the count and length of cracks, respectively. The reliability has been calculated as 100 minus the coefficient of variation in overall distress values among the multiple runs/raters. The Task 3 automated method has a lower reliability in identifying longitudinal cracks compared to identifying transverse cracks. Also, Task 3 automated method has a lower reliability than the original Task 2 automated method.

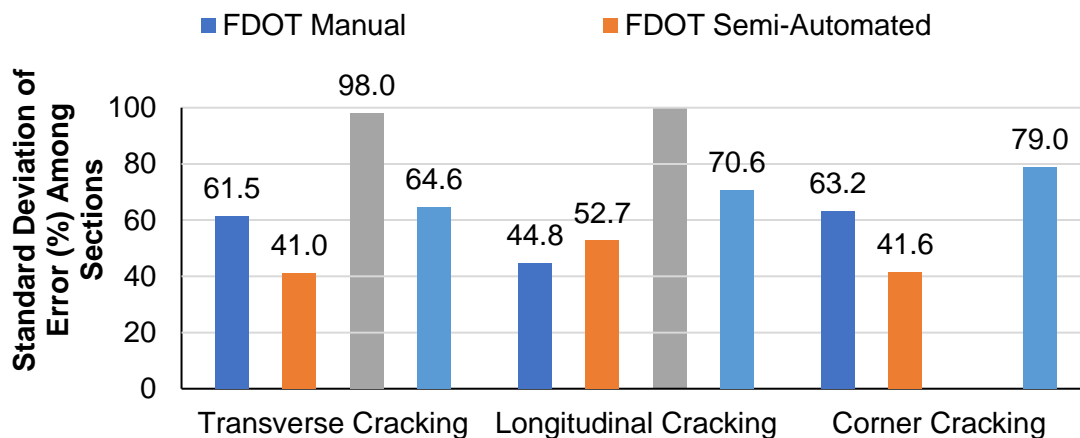


**Figure 49. Reliability of Automated Methods in Identifying the Number of Cracks (100 – Coefficient of Variation in Total Distress Amounts Among Multiple Runs/Raters: higher bars show more reliable results)**



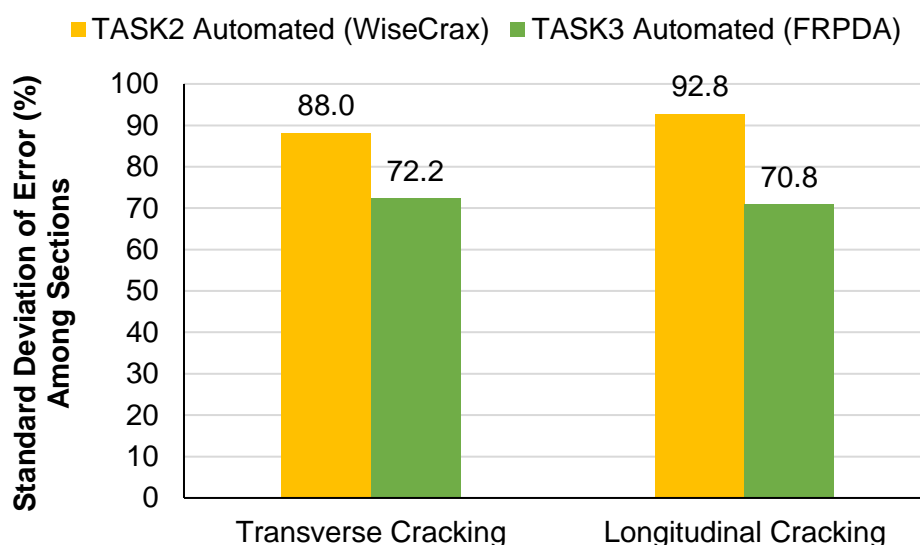
**Figure 50. Reliability of Automated Methods in Identifying the Length of Cracks (100 – Coefficient of Variation in Total Distress Amounts Among Multiple Runs/Raters: higher bars show more reliable results)**

The bar chart in Figure 51 shows a comparison among the different methods, in terms of the standard deviation of average error among different test sections. For each method, the average error is first calculated across all raters/runs for each section, and then the standard deviation of this average error among 12 sections is calculated. The development effort in Task 3 has resulted in a significant reduction in the standard deviation of average error among different sections, which proves that the developed algorithm (FRPDA) has a significantly lower variability compared to the algorithm used in Task 2 evaluations.



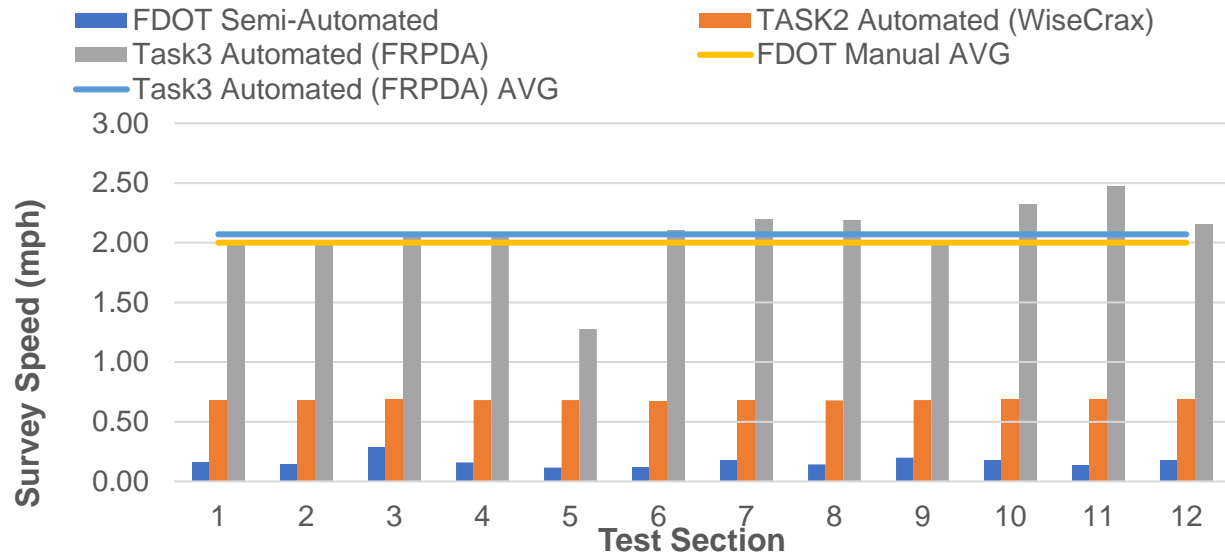
**Figure 51. Variability of Automated Methods in Identifying the Number of Cracks (Standard Deviation of Error Among Different Test Sections: lower bars mean less variable results)**

Although the variability of the automated method developed in Task 3 is comparable to the manual method in terms of transverse cracking, it is significantly higher (higher standard deviation) in terms of longitudinal cracking. Figure 52 shows a similar trend for the variability in identifying the overall length of each crack type. The difference in bias in identifying longitudinal cracks from one section to the other is due to the existence of exceptional circumstances in some sections as it was shown in Figure 41.



**Figure 52. Variability of Automated Methods in Identifying the Length of Cracks (Standard Deviation of Error Among Different Test Sections: lower bars mean less variable results)**

Figure 53 shows a comparison of efficiency (speed) of the automated method (running the detection batch processor followed by the FRPDA) for distress identification in comparison to other distress identification methods. Based on an estimation by FDOT raters, the manual distress surveys are typically conducted at an average speed of 2 mph (1 to 3 mph depending on the amount and severity of distresses present) and the survey speed for the automated method developed in Task 3 is slightly greater than that. Therefore, the automated survey can be conducted at the same efficiency, not to mention the significant improvement in safety of the FDOT staff.



**Figure 53. Comparison of Efficiency (Speed) of Automated to Semi-Automated Methods.**

Table 34 shows all the above success metrics for the FDOT manual (windshield), FDOT semi-automated, Task 2 automated (WiseCrax), and Task 3 automated (FRPDA) surveys.

**Table 34. Overall Success Metrics based on Cumulative Count Values**

Statistic	Crack Type	FDOT Manual	FDOT Semi-Automated	TASK2 Automated (WiseCrax)	TASK3 Automated (FRPDA)
Accuracy (%) = 100 - Bias	Transverse	75	93	24	98
	Longitudinal	98	98	0	95
	Corner	33	85	Not Rated	77
	Average	68	92	12	90
Repeatability/Reproducibility (%) = Standard Deviation of Error Among Multiple Runs/Raters	Transverse	27	28	40	20
	Longitudinal	15	39	157	37
	Corner	37	77	Not Rated	74
	Average	26	48	98	43
Reliability = 100 - COV of Distress Values Among Multiple Raters/Runs	Transverse	83	82	75	71
	Longitudinal	82	67	65	55
	Corner	42	7	Not Rated	25
	Average	69	52	70	50
Standard Deviation of Error (%) Among Sections	Transverse	61	41	98	65
	Longitudinal	45	53	279	71
	Corner	63	42	Not Rated	79
	Average	56	45	188	71
Efficiency = Speed (mph)	Average	2.0	0.2	0.7	2.1



### 3.2.3 Verification of Automatically Detected Cracks

Based on the results of the gap analysis conducted in Task 2, the majority of the development efforts in Task 3 focused on joint detection, and grouping, classification and rating of detected lines on pavement images (FRPDA). The surface lines (either cracks or joints or lane stripes or vehicle counter loops) on pavement images were detected using the same detection routine (based on WiseCrax) in both Task 2 and Task 3 efforts. Therefore, the results of crack detection in Task 3 have not substantially changed compared to the results from Task 2 (both conducted using WiseCrax on filtered images).

Table 35 shows the results of this verification, which was conducted again in Task 3 based on 24 sample images (5% of the total 509 images). Two images were selected from each of the 12 test sections, and the detected cracks were compared against the reference survey one by one. These 24 processed images have been provided in Appendix H for reference. In this table, the following success metrics have been evaluated. In these equations, true positives are the cracks that were detected and actually present on pavement surface. Correctly rated true positives are the true positives that were classified into the correct distress category (regardless of severity level).

$$Validity = \frac{\text{correctly detected}}{\text{all detected}} = \frac{\text{true positives}}{\text{true positives} + \text{false positives}}$$

$$Sensitivity = \frac{\text{correctly detected}}{\text{actual cracks}} = \frac{\text{true positives}}{\text{true positives} + \text{false negatives}}$$

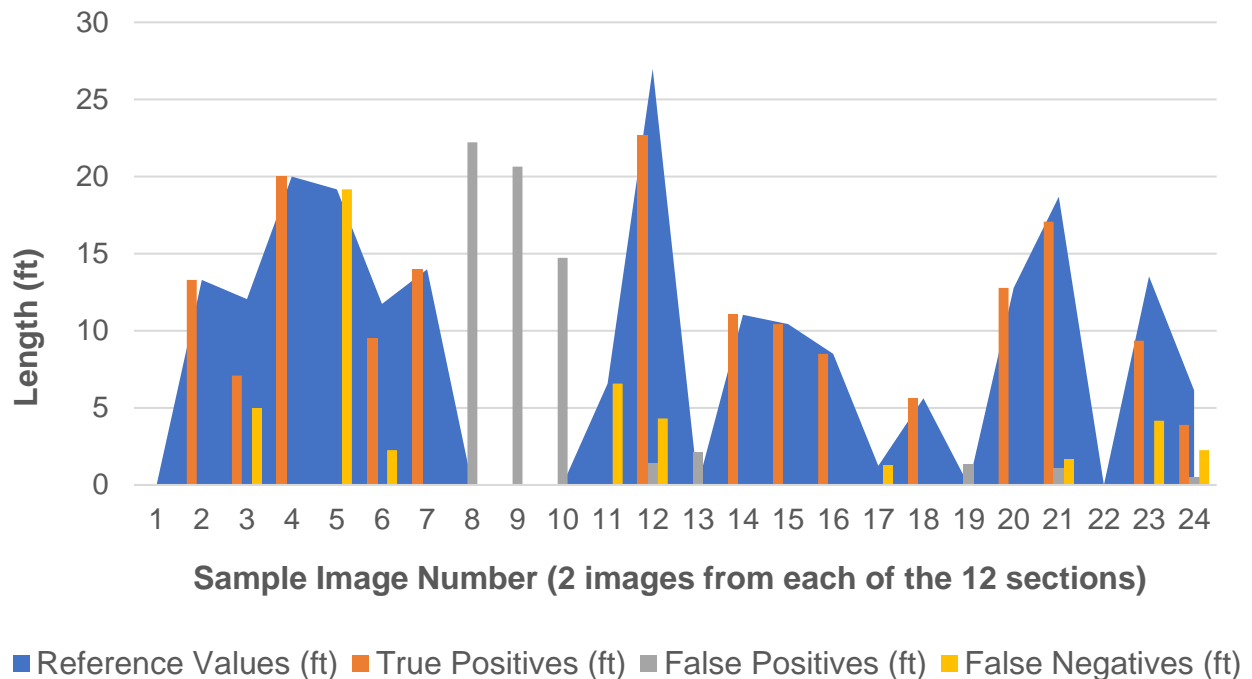
$$Classification\ Performance = \frac{\text{correctly classified}}{\text{true positives}}$$

**Table 35. Average Values for Crack Verification Metrics based on 24 Sample Images (based on length)**

	<b>Validity</b>	<b>Sensitivity (or Recall)</b>	<b>Classification Performance</b>
<b>Average</b>	72%	73%	86%
<b>Std Deviation</b>	45%	38%	36%

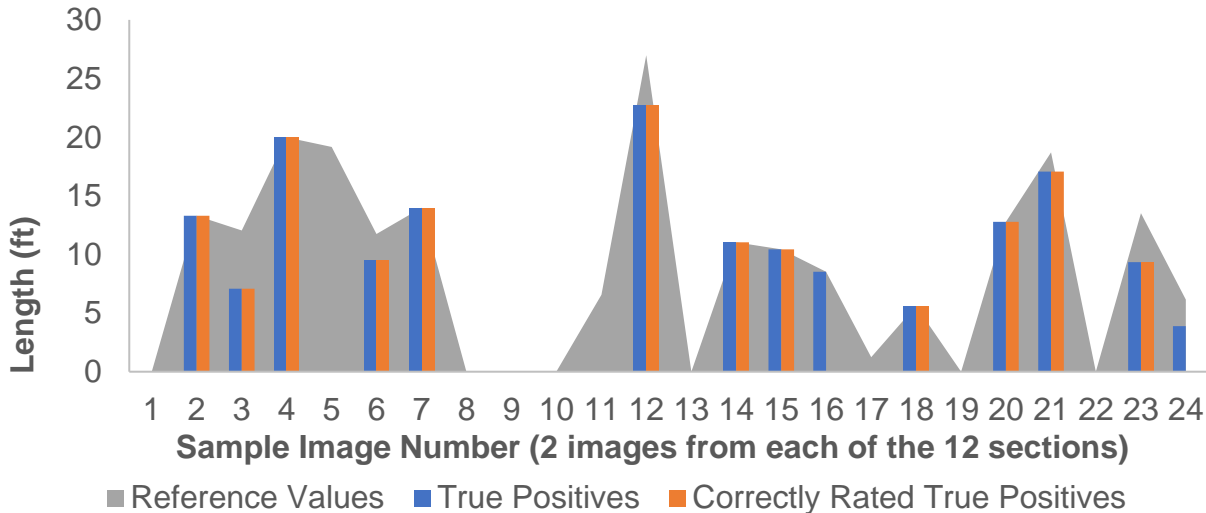
Figure 54 shows the length of cracks in the reference crack map, against the amount of true positive, false positive, and false negative. Except for Image 5 from Section 3 and Image 11 from Section 6, the detection process has identified true positives comparable to reference values. The amount of false positive is considerable (more than 5 feet) in Image 1 (Section 1), Image 8 (Section 4), and Images 9-10 (Section 5). The length of

missed cracks is significant only in Image 5 from Section 3 and Image 11 from Section 6. The reason for these isolated issues can be further investigated by examining the processed images that have been documented in Appendix H. For example, Image 5 of Section 3 and Image 11 from Section 6 have missed longitudinal cracks that were not detected by the detection routine. Image 8 from Section 4 shows straight lines from a vehicle counter loop that has been falsely identified as transverse joints. Images 9 and 10 of Section 5 have skewed joints that is a limitation for FRPDA and are falsely identified as cracks.



**Figure 54. Verification of Length of Automatically Detected Cracks Against Reference on Sample Images**

Figure 55 compares the amount of true positive and correctly detected true positives against the reference values. It seems like there were considerable difference between the length of true positives and correctly detected true positives in Image 16 (Section 8) and Image 24 (Section 12). Image 16 is showing a fairly straight transverse crack that was falsely rated as a transverse joint. Image 24 is showing a corner crack that has been identified as a transverse crack because part of the crack has not been detected.



**Figure 55. Verification of Length of Automatically Rated Cracks Against True Positives on Sample Images**

### 3.3 Summary and Recommendations for Implementation

During Task 3 of this research project, software routines were developed based on the gap analysis and solution design that was conducted in Task 2. This report presents the results of the final evaluation of the developed routines in identifying and quantifying the rigid pavement cracks. Based on this final evaluation, the following are the main observations:

- Following the development efforts in Task 3, the accuracy and repeatability of the automated algorithm (FRPDA) has increased significantly. This observation means that the gap analysis and the solution design were instrumental in addressing the issues with the preliminary automated method and therefore, further improvements are possible through a similar analysis.
- The accuracy of the automated algorithm (FRPDA) in identifying transverse and corner cracks (with respect to semi-automated reference values) is higher than the manual windshield survey method conducted by FDOT staff. The accuracy of the automated method is comparable to the manual method in terms of longitudinal cracks. This means that the automated method could be replacing the manual survey in identifying these three crack types. Other distress types (e.g. shattered slabs, spalling, and patching) could be identified using a semi-automated review of the collected images. This semi-automated review would be part of the QC process. It will be extensive and time consuming at the beginning of the implementation but will evolve towards more sampling and become more efficient after several years of implementation.

- The repeatability of the automated method (FRPDA) is higher than the reproducibility of the manual survey in identifying transverse cracks and lower in terms of other crack types. This means that the bias of the automated routine in identifying longitudinal and corner cracks can vary from run to run. It is worth to note that the repeatability of the automated results is comparable to the reproducibility of semi-automated results for longitudinal and corner cracking. The fact that both automated (FRPDA) and semi-automated surveys show lower repeatability for longitudinal and corner cracks could be due to the variations in image quality and vehicle wander from run to run. In another independent effort, Fugro has recently developed a code that can be used to remove some quality issues (including the typical streaks) from LRIS images. This code is currently a beta version and needs further acceptance testing before public release.
- The bias of the automated routine in identifying longitudinal cracks and corner cracks can vary from section to section depending on the exceptional circumstances that could result in false positives or missed cracks (Figure 41). Thus, a systematic quality control process is required.

There are several gaps that have been identified after the development and evaluation of the FRPDA in Task 3, which are listed in Table 36.

**Table 36. Remaining Gaps at Conclusion of Task 3**

Number	Remaining Gap	Recommended Solution
1	Very straight longitudinal cracks might be rated as longitudinal joints	Implement a data collection protocol to avoid lane stripes in the middle of images, Manual QC and intervention, these situations are not frequent
2	Partially faded, or non-straight and jagged longitudinal lane stripes in the middle of the lane might be rated as longitudinal cracks	
3	Skewed joints cannot be detected (even though they are not the predominant design anymore)	Manual QC and intervention, these situations are not frequent
4	Still some run to run variation (on different images of same section)	Implement a data collection protocol to avoid significant wander and variation between images
5	shattered slabs are not rated successfully	Revisit the algorithm, test other alternatives
6	Not rating spalling of crack and joint edges	Manual intervention in the short term, collect 3D data and use machine learning in the long-term
7	Not rating patching	

Based on these observations, the following recommendations are provided for FDOT to consider with respect to the annual condition surveys of rigid pavements:

- Use the developed automated algorithm (FRPDA) to automatically detect and identify the transverse, longitudinal, and corner cracks. Use a semi-automated routine to identify other distress types (e.g. shattered slabs, spalling, and patching) that have not been identified using the algorithm. This semi-automated routine should also be used for quality control of the results (specially to address the lower precision and repeatability in identifying longitudinal cracks).
- Develop a systematic procedure for implementing the results of this study for collecting, processing, and integrating pavement images; conducting image filtering; crack detection; and finally, crack classification and rating. This systematic procedure needs to also include a quality control and quality assurance protocol for each step.
- Following implementation of this automated distress survey procedure, further improvements to the automated algorithm can be designed based on further evaluations on actual surveys. These improvements can be implemented to enhance automated distress results and reduce the need for human intervention.
- If possible, using a 3D imaging technology can also significantly improve the results of crack detection and crack classification and rating. In the absence of 3D data, some distress types such as patching, and spalling cannot easily be detected. Spalling of cracks and joints are more pronounced in 3D images, because the technology darkens the areas that are lower than the nominal pavement surface. In addition, the 3D texture data can assist in recognizing the changes in pavement surface type, which can potentially automate identification of patched areas.

With proper implementation of the developed automated routine and a systematic quality control procedure, the annual condition evaluation for rigid pavements can become more effective, efficient, reliable, and safe.

## **CHAPTER 4 – LRIS FEASIBILITY ON FLEXIBLE PAVEMENTS**

Under Task 4, Fugro analyzed the viability of using 2D LRIS images to detect, quantify and classify cracks in flexible pavements. Fugro processed 2D LRIS images and data to be used in software evaluation. Fugro identified the potentials and the limitations of 2D pavement image technology for flexible pavements. The results from the analysis and recommendations are documented in this chapter.

Task 4 was subdivided into four (4) subtasks:

- 1) Data Collection was conducted by FDOT staff using their 2D LRIS equipment
- 2) Data Processing, including preparation and importing of LRIS data into the data viewing system, crack detection, and distress identification
- 3) Evaluation of the automatically detected cracks and identified distresses compared to the reference survey
- 4) Potentials and Limitations of the LRIS Technology for crack detection and distress identification

This chapter is organized in five sections. Section 4 provides a report on a data collection conducted by FDOT staff. Section 4.2 explains the data processing and data analysis details. Section 4.3 explains the evaluation of the automated distress survey results on 2D LRIS images and the corresponding potentials and limitations. Section 4.4 includes conclusions and recommendations.

### **4.1 Data Collection**

The 2D images were collected on 12 representative flexible pavement test sections by FDOT staff. Data collection for this task was completed in May 2017. This section describes what types of data were collected, the equipment used for collection, and where data was collected.

#### **4.1.1 Collected Data Elements**

All collected data is referenced geographically and linearly to FDOT's inventory based on the provided Location Referencing System (LRS). The collected data include the following:

- 2D pavement images using the Laser Road Imaging System (LRIS)
- Pavement longitudinal profile using an Inertial Profiler System (IPS)
- Pavement transverse profile using the Laser Rut Measurement System (LRMS)
- Differential Global Positioning System (GPS) data
- Distance Measuring Instrument (DMI) data integrated with GPS data

#### **4.1.2 Data Collection Equipment**

The 2D images and data were collected using the LRIS equipment manufactured by INO/Pavemetrics and integrated on an International Cybernetics Corporation (ICC) high-speed profiler host vehicle (Figure 56). It should be noted that as part of a separate purchase order, Fugro collected 3D images and data from the same locations using the LCMS equipment manufactured by INO/Pavemetrics and integrated on Fugro's Automatic Road Analyzer (ARAN) host vehicle. For more information on that effort, please refer to the Purchase Order Report included in Appendix I.



**Figure 56. FDOT LRIS Equipment**

### 4.1.3 Testing Locations

Similar to Phase I of this project, 12 representative flexible pavement test sections (Table 37) were selected by FDOT staff for Phase II evaluations. These representative test sections were selected in a manner that would include the key distress types and severity levels that are frequently encountered on Florida highways.

**Table 37. Representative Flexible Pavement Test Sections**

Index	County ID	Road	City	Lane	Direction	BMP	EMP	Length
1	02050000	SR 44	Crystal River	R2	East	0.000	0.604	0.604
2	02050000	SR 44	Crystal River	L2	West	0.000	0.604	0.604
3	11010000	SR 44	Leesburg	R2	East	0.000	1.592	1.592
4	11100000	SR 19	Umatilla	R2	North	3.816	4.906	1.090
5	11002000	SR 44	Leesburg	R2	East	1.183	2.276	1.093
6	11002000	SR 44	Leesburg	R2	East	3.184	4.514	1.330
7	11080000	SR 19	Howey in the Hills	R1	North	0.000	0.925	0.925
8	18020000	SR 50	Polk City	R1	East	5.356	6.421	1.065
9	26050000	SR 24	Gainesville	L2	South	3.367	6.095	2.728
10	26050000	SR 24	Gainesville	L2	South	6.095	7.670	1.575
11	10190000	SR 400 / I-4	Tampa	R3	East	11.098	12.332	1.234
12	10190000	SR 400 / I-4	Tampa	R3	East	20.407	21.476	1.069

## 4.2 Data Processing

This section provides a brief overview of the methodology behind some of the key processing steps conducted and any project specifications unique to this project.

### 4.2.1 Import Data

The LRIS data collected by FDOT staff had to be imported into a Vision database to be able to display and analyze the data in the Vision software. First, the quality of the data files needed to be evaluated since this data was not collected using the Fugro ARAN vehicles and were not always compatible with the Vision software.

#### Data Review

The purpose of this procedure is to review the contents of the data collected by the ICC Equipment provided by Florida DOT. This will review the existing information as well as look for needed information for importing the collected data to Fugro's Vision software.



The data provided by FDOT included nine folders, and each folder were named in the following format: 'County ID\_Route Name\_Pavement Type\_Start Mile Post-End Mile Post'. For example, a folder named 02050\_SR44\_AC\_0-0.604 includes data collected for test section 1 (out of 12), for which county ID is '02050000', route name is 'SR44', pavement type is asphalt concrete, start mile post is 0.0 and end mile post is 0.604.

The data collected for any adjacent sections (start point of one section is the end point of another) and any reverse sections (start points, and end points are the same but collection directions are opposite) are stored in the same folder.

Each folder includes two sub folders: Images and Profiler. The 'Images' folders hold all pavement images collected for the corresponding test sections, while the 'Profiler' folders provide information such as distance stamp of each image, and GPS coordinates recorded during the data collection.

After examination all files in the 'Profiler' folder, four files are identified as required for importing data to Vision database. Table 38 shows these files.

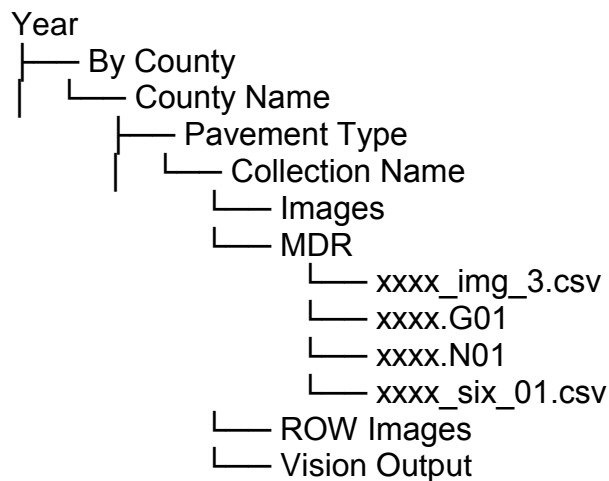
11. Image File: This file contains information, such as Distance stamp, GPS coordinates, county ID and file path of pavement images collected by the LRIS equipment. This file is stored in csv (comma-separated values) format in the file folder.
12. GPS File: This file provides more detailed GPS coordinates information of each pavement image collected. The GPS coordinates are updated every 0.2 seconds of UTC time. This file is stored in G01 format in the file folder.
13. Reference File: This file contains measurement information that are referenced from other files in the same folder.
14. Section File: This file includes section information, such as County ID, Route name, mile post of start points and end points of each section. This file is stored in csv format in the file folder.

**Table 38. Four Types of FDOT ICC Vehicle Files Used in Importing Process**

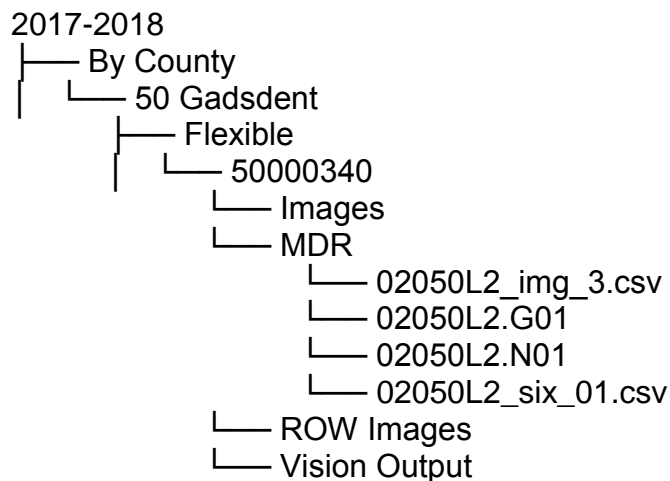
File Type	File Naming Rule	File Name Example
Image File	xxxx_img_3.csv	02050L2_img_3.csv
GPS File	xxxx.G01	02050L2.G01
Reference File	xxxx.N01	02050L2.N01
Section File	Xxxx_six_01.csv	02050L2_six_01.csv

## Standard Folder Structure

After thorough discussions, a new folder structure and file naming rules were agreed between FDOT and Fugro as the standard folder structure. The purpose for this standard folder structure is to minimize future need for changes in the SQL code that imports FDOT data into Fugro's Vision software. Figure 57 shows the standard folder structure and Figure 58 shows an example.



**Figure 57. Agreed Folder Structure**



**Figure 58. Folder Structure Example**

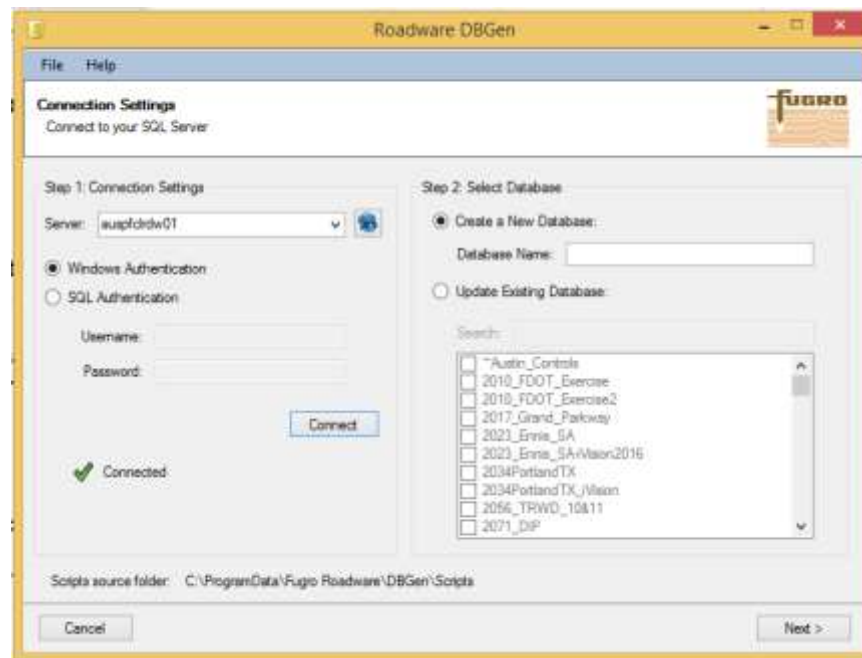
## Data Preprocessing Tool

During this stage, the raw data collected by ICC equipment are cleaned (remove redundancies), standardized, and transformed by the developed Java based data

preprocessing tool. The Java tool first renames the Image Information files, GPS files, reference files and section files to ensure: 1) files for the same sections have the same file name, and 2) files for the different sections have different file names, then separates the Image Information files and GPS files into one file per sub-section according to the section boundaries that have been provided by FDOT staff. This pre-processing has been described in Appendix M.

### Import Processed data to Vision Database

During this stage, the pre-processed data is imported into a Vision database. First, a blank Vision database is created using the DBGen tool provided in the Vision software package (Figure 59). Database objects such as tables, views, stored procedures, functions are loaded in the new created blank database, according to the database template in the DBGen tool.



**Figure 59. Fugro DBGen Software Interface for Creating Blank Vision Databases**

Then, the pre-processed data are uploaded into the Vision database with the developed SQL scripts, included in Appendix M of this report. Key information such as distance stamp, GPS coordinates, image file names are extracted from pre-processed data and loaded into the corresponding tables. With the data successfully integrated into the Vision database, the Vision software can connect to the database and display various information about road sections, locations and pavement images (Figure 60). Figure 61 is the database diagram illustrating the basic parts of tables, fields, key fields, and relationships in the Vision database.

36 / 36 location(s)

Section	County	RouteName	Direction	Lane	TestSection	RunNumber	Collection	Vehicle	Length
02050000	2	SR44	E	2	01	1	02050000ETR01R1		1,105.723
02050000	2	SR44	E	2	01	2	02050000ETR01R2		1,105.517
02050000	2	SR44	E	2	01	3	02050000ETR01R3		1,105.551
02050000	2	SR44	W	2	02	1	02050000WTL202R1		1,017.471
02050000	2	SR44	W	2	02	2	02050000WTL202R2		1,045.032
02050000	2	SR44	W	2	02	3	02050000WTL202R3		1,135.565
10190000	10	I-4	E	3	03	1	10190000ETR03R1		1,534.619
10190000	10	I-4	E	3	03	2	10190000ETR03R2		1,488.770
10190000	10	I-4	E	3	03	3	10190000ETR03R3		1,483.447
10190000	10	I-4	E	3	04	1	10190000ETR04R1		1,440.271
10190000	10	I-4	E	3	04	2	10190000ETR04R2		1,446.480
10190000	10	I-4	E	3	04	3	10190000ETR04R3		1,445.174
11002000	11	SR44	E	2	05	1	11002000ETR05R1		2,135.485
11002000	11	SR44	E	2	05	2	11002000ETR05R2		2,135.336
11002000	11	SR44	E	2	05	3	11002000ETR05R3		2,135.598
11002000	11	SR44	E	2	06	1	11002000ETR06R1		1,366.818
11002000	11	SR44	E	2	06	2	11002000ETR06R2		1,388.339
11002000	11	SR44	E	2	06	3	11002000ETR06R3		1,447.470
11010000	11	SR44	E	2	07	1	11010000ETR07R1		1,971.212
11010000	11	SR44	E	2	07	2	11010000ETR07R2		2,062.523
11010000	11	SR44	E	2	07	3	11010000ETR07R3		1,953.307
11080000	11	SR19	N	1	08	1	11080000ETR08R1		1,338.575

Total length: 59,983.761

Custom 10.0 Speed 12.020.56

Tagio-global/mz/zhao wuqin/rdw01 ROOT\_Traffic\_2D Blank Workspace

Figure 60. Fugro Vision Interface Showing the Imported Sections

## Identified Errors in Data Files

165

issues in the provided data files. Two typical errors have been identified in the provided data, which are documented here to avoid them in future:

1. Wrong start mile post and end mile post: In some examples, the same start and end mile posts were recorded for multiple rows in the saved data files, as seen in the example below (Figure 62).

A	B	C	D	E	F	G	H	I	J	K	L	M	N	O
Num	ImageNum	AdjDmi	FromDist	ToDist	Latitude	LatDir	Longitude	LongDir	Q	Sat	HDOP	Height	HeightI	Ge
143	3P000143	45226	3.9516211	3.9478293	25.81253041		-80.21530229		2	9	0.9	37.0922	F	
144	3P000144	45226	3.9516211	3.9478293	25.81253041		-80.21530229		2	9	0.9	37.0922	F	
145	3P000145	45226	3.9516211	3.9478293	25.81253041		-80.21530229		2	9	0.9	37.0922	F	
146	3P000146	45226	3.9516211	3.9478293	25.81253041		-80.21530229		2	9	0.9	37.0922	F	
147	3P000147	45226	3.9516211	3.9478293	25.81253041		-80.21530229		2	9	0.9	37.0922	F	
148	3P000148	45226	3.9516211	3.9478293	25.81253041		-80.21530229		2	9	0.9	37.0922	F	
149	3P000149	45226	3.9516211	3.9478293	25.81253041		-80.21530229		2	9	0.9	37.0922	F	
150	3P000150	45226	3.9516211	3.9478293	25.81253041		-80.21530229		2	9	0.9	37.0922	F	
151	3P000151	45226	3.9516211	3.9478293	25.81253041		-80.21530229		2	9	0.9	37.0922	F	
152	3P000152	45226	3.9516211	3.9478293	25.81253041		-80.21530229		2	9	0.9	37.0922	F	
153	3P000153	45226	3.9516211	3.9478293	25.81253041		-80.21530229		2	9	0.9	37.0922	F	
154	3P000154	45226	3.9516211	3.9478293	25.81253041		-80.21530229		2	9	0.9	37.0922	F	
155	3P000155	45226	3.9516211	3.9478293	25.81253041		-80.21530229		2	9	0.9	37.0922	F	
156	3P000156	45226	3.9516211	3.9478293	25.81253041		-80.21530229		2	9	0.9	37.0922	F	

**Figure 62. Typical Error in Mile Post Data**

2. Invalid length of test section: The length of test section should be longer than LRIS image height, which is 6.11 meter, approximately 0.004 mile. In some data files, the recorded length was less than this minimum.

## 4.2.2 Segmentation

Segmentation is the method of ensuring the data collected by the ICC equipment matches the geographic and linear references set up by FDOT. The segmentation process is completed to match the true start and stop locations of the road section to ensure that the collected data represents the exact location expected by FDOT. The matching of information was completed using Fugro's Vision and utilizing site information provided by FDOT.

Stationing for all routes was adjusted using a method called "rubber-banding", to match stationing provided by FDOT. All data collected prior to the start of the route are removed and the chainage of the beginning of the route is set to the FDOT value for that landmark. Chainages for all other landmarks on the route are adjusted to match length and location information provided by FDOT. In the "rubber-banding" process, data between each set landmark may be stretched or compressed accordingly to ensure station chainages match up.

### 4.2.3 Distress Data Analysis Process

The actual software development effort for this project was carried out during Task 6 of Phase II, and therefore at this stage of the analysis, the existing Fugro Vision software was used due to its availability with the integrated images and data. Therefore, the following software descriptions are the Vision software descriptions and not the descriptions for the FDOT customized application at this point of the project. Fugro Vision software includes an automated distress data analysis application, which involves the following main routines:

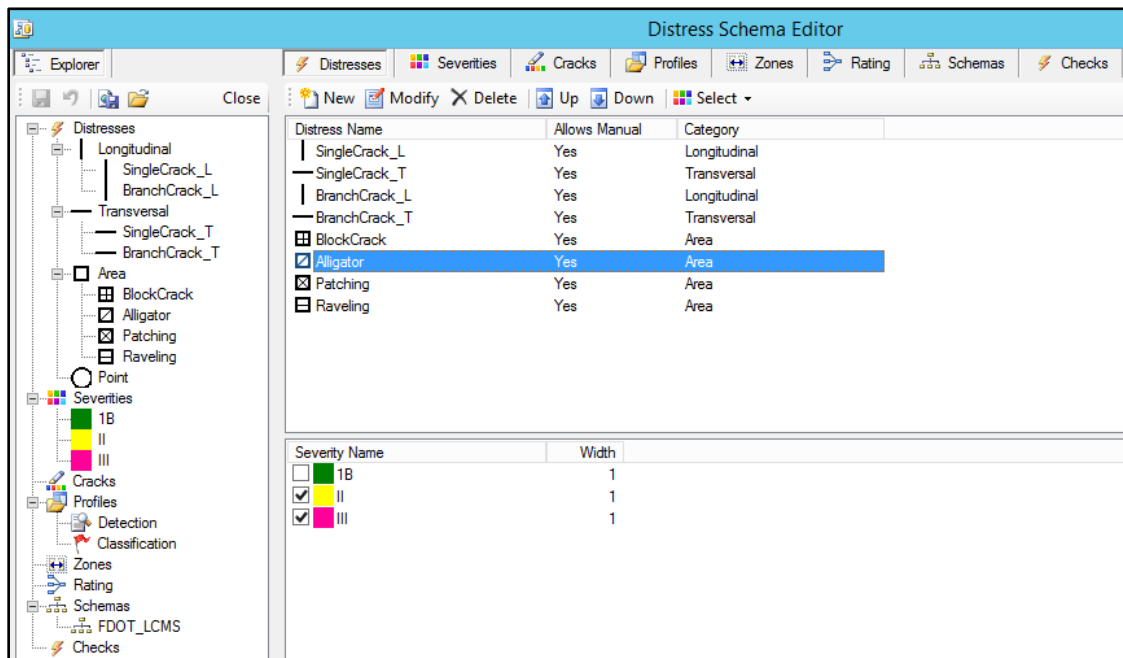
4. Lane Detection: during this step, lane boundaries are automatically detected and marked as blue lines on the pavement images.
5. Defect Detection: also called “Crack Detection,” during which any linear defects on pavement surface is detected and marked with lines.
6. Defect Classification: during this step, all the detected linear defects are classified into one of the three categories of longitudinal defects, transverse defects, and other (which will eventually be rated as alligator or block cracking) defects according to some criteria for defect angle and density, which can be changed by the user.
7. Distress Rating: during this final step, the software assigns a distress type and severity to each of the classified defects according to a distress schema defined by the user based on their experience. The user needs to select one or more criteria from a series of criteria such as angle, longitudinal and transverse extent, density, width, and others for each distress type and severity. Once the schema is established, this schema can be applied for network-level data collection.

### Distress Schema Specification

The performance of crack detection, classification and rating is highly dependent on a well-defined distress schema. The setting up of distress schema includes creation of Distress Type, Distress Severities, Crack Ranges, Detection Profile, Classification Profile, Road Zones and Rating Profile (Figure 63). In this project, the distress schema was setup according to the specified criteria for each distress type in the FDOT *Flexible Pavement Condition Survey Handbook* (2017). Once the schema is setup and saved, this schema can be applied for network-level data collection. The following segments describe how the details of the distress schema are setup.

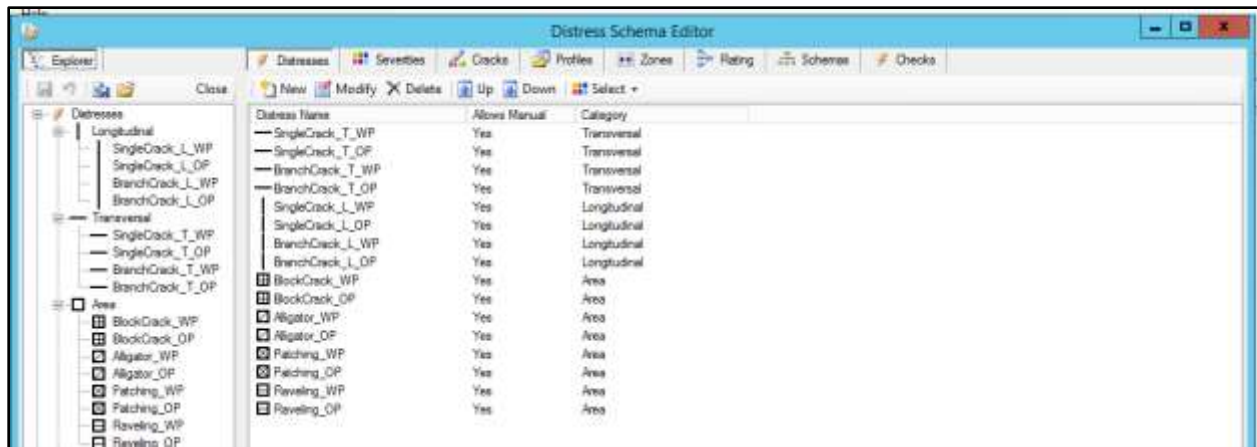
The Vision software provides two options for distinguishing distresses by zone location:

1. In the distress schema, only one distress type would be setup for both wheel path (WP) and outside wheel path (OP), but then they could be separated using a SQL code on the database based on the location information (Figure 63). This option is more flexible as it does not require reprocessing if it is decided to change the width of wheel path zones in the future. Specifically, if the images are going to be rated manually or if the automated distress needs manual QC and correction, this option is recommended. It is extremely tedious for the manual rater to draw separate distresses for the wheel path and non-wheel path areas (option 2). In this stage of the project, option number 1 was used for establishing the reference survey.
2. In the distress schema, separate distress types could be setup for WP and OP areas (Figure 64). This option is recommended when no manual correction of the automated process is needed. In this stage of the project, option number 2 was used for the automated distress survey.



**Figure 63. Vision Distress Schema Editor Interface with One Distress Type for Both Wheel Path and Outside Wheel Path Zones (Option 1)**





**Figure 64. Vision Distress Schema Editor Interface with Separate Distress Types Defined for Wheel Path and Outside Wheel Path Zones (Option 2)**

### ***Distress Type and Severity***

Distress types are defined under the 'Distresses' tab and the severities under the 'Severities' tab. Then, each distress type is assigned the possible severity options. FDOT's *Flexible Pavement Condition Survey Handbook* (2017) includes the following distress types and severities:

15. Single Cracks (linear length, feet), Class 1B or Class II or Class III
16. Branch Cracks (linear length, feet), Class 1B or Class II or Class III
17. Block Cracks (area, sq. feet), Class II or Class III
18. Alligator or Fatigue Cracks (area, sq. feet), Class II or Class III
19. Patching (area, sq. feet), no severity levels
20. Raveling (area, sq. feet), Light or Moderate or Severe

During the distress rating process, these distress types are identified and quantified individually and then they are added up to generate the total amount of cracking in each one of the Class 1B, Class II, and Class III cracks. All linear distress types are recorded in two groups of longitudinal and transverse to differentiate their orientation and facilitate

quality control, but they are added up for each distress type (for example, branch cracks or single cracks) following the survey.

Following the distress survey, two categories of distress will be recorded for each of these distress types: within the wheel paths (CW), and outside the wheel paths (CO). For automated survey results, this differentiation was made in the schema setup (option 2). For the reference survey, this differentiation was conducted using a SQL code (option 1). This is required for the final calculation of the amount of distress in each class within and outside the wheel paths, because the deduct values are higher for distresses within the wheel paths.

The total area for patching and raveling is added to the total amount of Class III cracks. The details of each distress type and severity are recorded to keep a permanent record that facilitates quality control and quality assurance initiatives. All the summation happens on the recorded data in the SQL database.

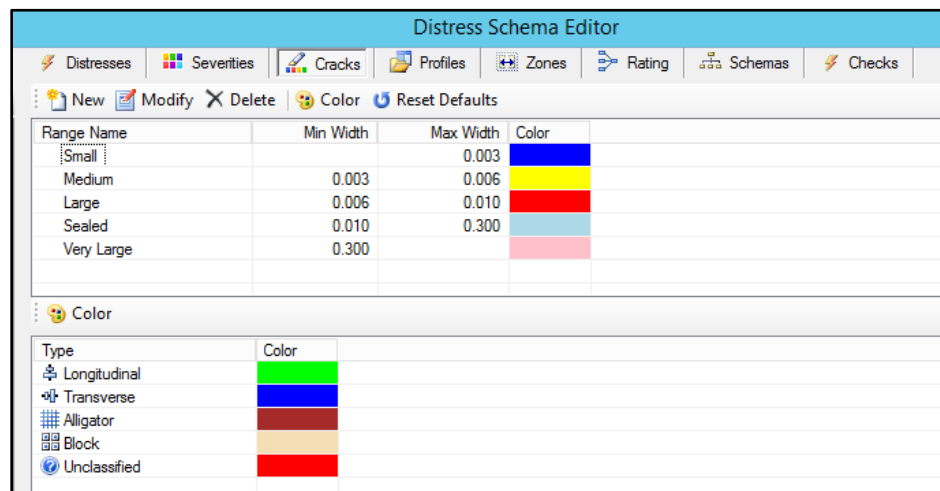
### ***Crack Range***

Under the 'Cracks' tab in the Distress Schema Editor, a coloring scheme is defined for identification of the detected cracks/defects on the pavement image according to crack width (Figure 65). The following crack ranges were determined for this project as they correspond to the severity levels identified in the FDOT manual:

1. Small cracks with crack width less than 3.18 mm are identified with blue color lines (later assigned to Class 1B category in distress rating)
2. Medium cracks with crack width equal to or greater than 3.18 and less than 6.35 mm are identified with yellow color lines (later assigned to Class II category in distress rating)
3. Large cracks with crack width equal to or greater than 6.35 mm are identified with a red color lines (later assigned to Class III category in distress rating)

The "Max Width" in Figure 65 means "less than" and the "Min Width" indicates "equal to or greater than". As previously noted, this is NOT the FDOT customized application. At this stage, we are using the existing Vision software to compare 2D versus 3D data. The FDOT customized application will be developed during Task 6 (development). Also patching and raveling are "distresses" and NOT "cracks". This menu is ONLY showing cracks. After the distresses are identified in the "rating" process, patching and raveling can be added.

Following the crack detection process, the detected cracks are displayed on top of the pavement images with the colors corresponding to their width. As shown in Figure 65, the Cracks menu also allows selection of specific coloring scheme for the classification categories of Longitudinal, Transverse, Alligator, Block, and Unclassified categories. Following the classification process, each class of cracks are identified on top of pavement images using the corresponding colors. These colors help with quality control of the detection and classification process.



**Figure 65. Cracks Menu in the Distress Schema Editor**

The default crack color displayed in the user interface shows the width range of the crack. For example, the widths of cracks in green color are less than or equal to 3.18 mm. The colors can also be changed to represent the type of crack using the drop menu as shown in Figure 66.



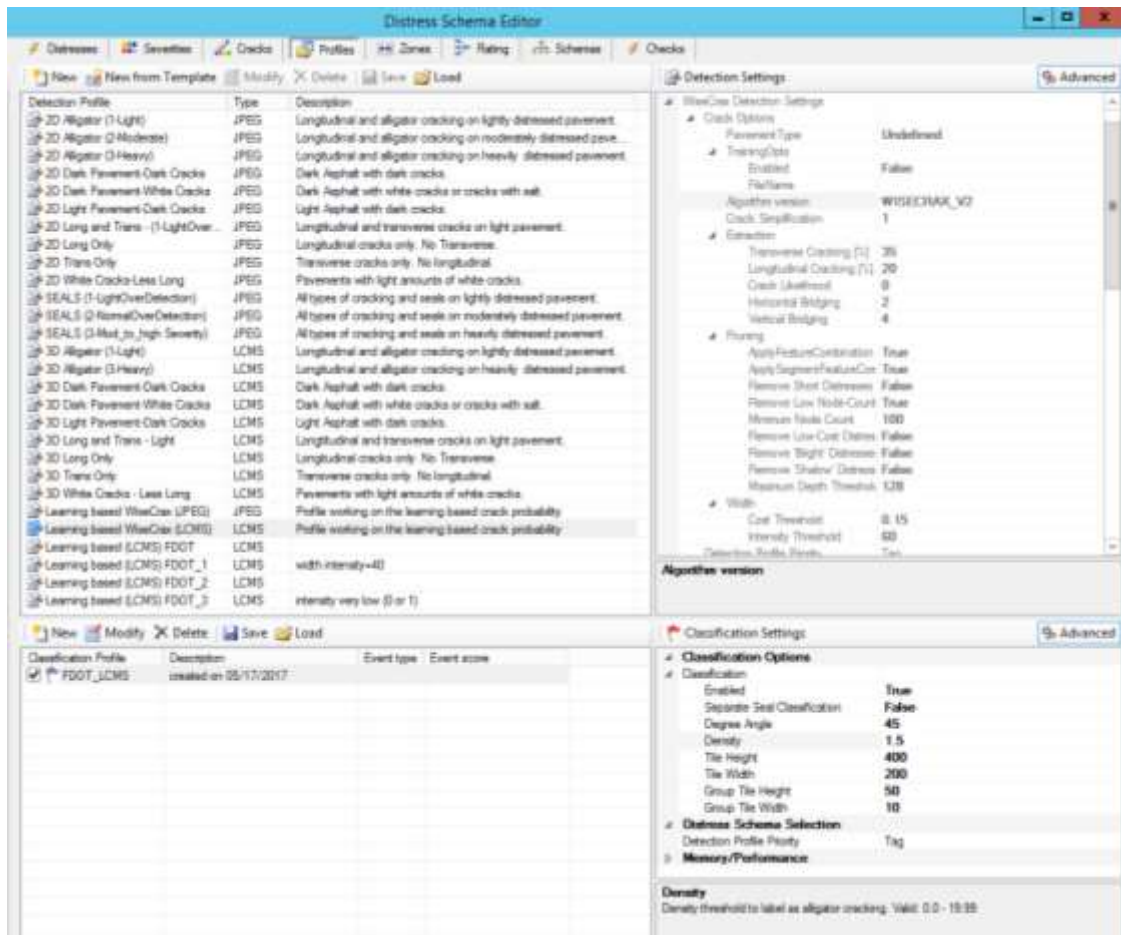
**Figure 66. Changing the Colors of the Displayed Cracks**

The same color cannot be used for cracks of the same type or same width ranges, but there are no conflicts if the same color is used for 'Range' and 'Type'.

### ***Detection and Classification Profiles***

Under the 'Profiles' tab in the Distress Schema Editor, the control parameters for the crack detection and classification processes are determined. The software typically

shows the default values for these control parameters that have been set based on empirical experience. In the Task 2 report for this project, various control parameters for the detection of cracks from 2D images and for the classification of detected cracks into transverse and longitudinal categories were introduced and the impacts on software performance of changing each control parameter were explained in detail. Figure 67 shows the 'Profiles' tab, which allows for customization of the control parameters for the crack detection and classification processes.



**Figure 67. Detection and Classification Profiles in the Distress Schema Editor**

Vision provides two alternative automated crack detection algorithms to choose from when running this process on 2D images:

1. WiseCrack Crack Detection: This automated crack detection algorithm was developed by Fugro and used in Phase I of this project. This algorithm detects cracks based on image pixel intensities. For details of this methodology please refer to Task 2 report.

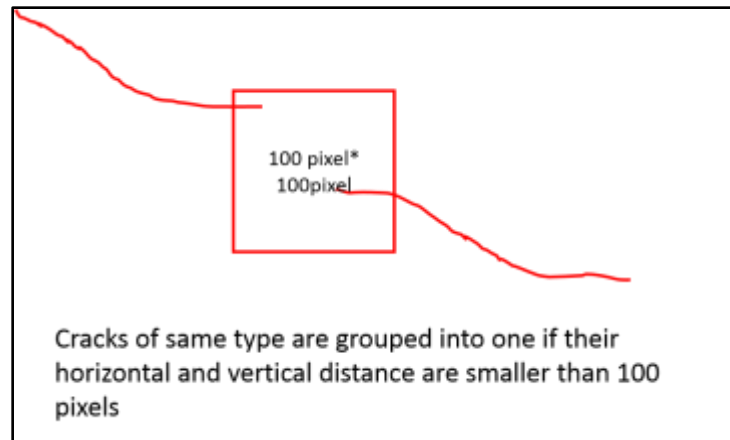
2. Fugro Machine Learning Crack Detection: This machine learning automated crack detection algorithm was recently developed by Fugro engineers, based on a large database of semi-automated evaluation of 2D images.

The Fugro machine learning based 2D crack detection algorithm has been tested on numerous pavement surface images and its corresponding control parameters have been optimized in the latest version of Vision software. As a result, it is recommended that the detection parameters are not changed. Due to superior performance on multiple recent statewide projects, the machine learning algorithm was used for this analysis.

In the classification step, there are several parameters that can be changed to improve the classification results (Table 39). For this phase of the project, eight classification profiles using eight different control parameter sets were used, and the final classification profile was selected based on the best results among these profiles.

**Table 39. Classification Parameter Settings**

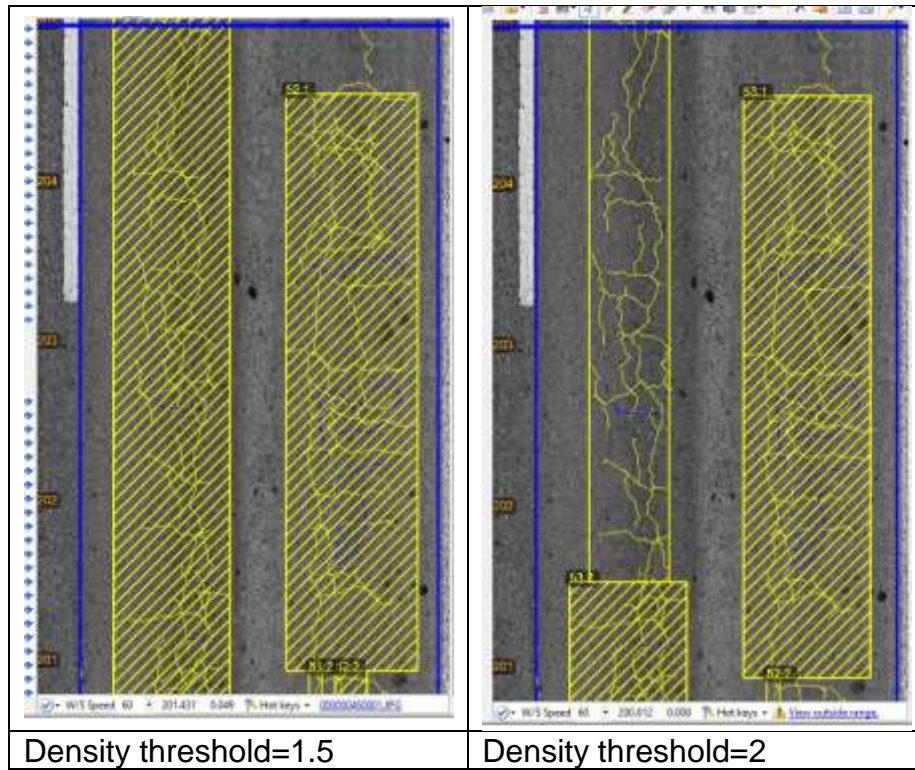
Parameter	Description	Value Used
Classification Enabled	Enables classification	TRUE
Separate Seal Classification	Classifies sealed cracks separately	FALSE
Degree Angle	Angle threshold differentiating between longitudinal and transverse defects, this is the angle for the best fit line across the crack nodes	45
Density	The density threshold beyond which there are enough cracks within a tile to count the tile area as alligator cracking area and not individual cracks.	1.5
Tile Height (pixels)	Tile used for calculating the density of the alligator or block categories	400
Tile Width (pixels)		200
Group Tile Height (pixels)	Tile used for grouping defects together (see Figure 68). Cracks that fall within these grouping tiles and are of the same classification will be grouped together to make one crack set or group of cracks.	50
Group Tile Width (pixels)		10



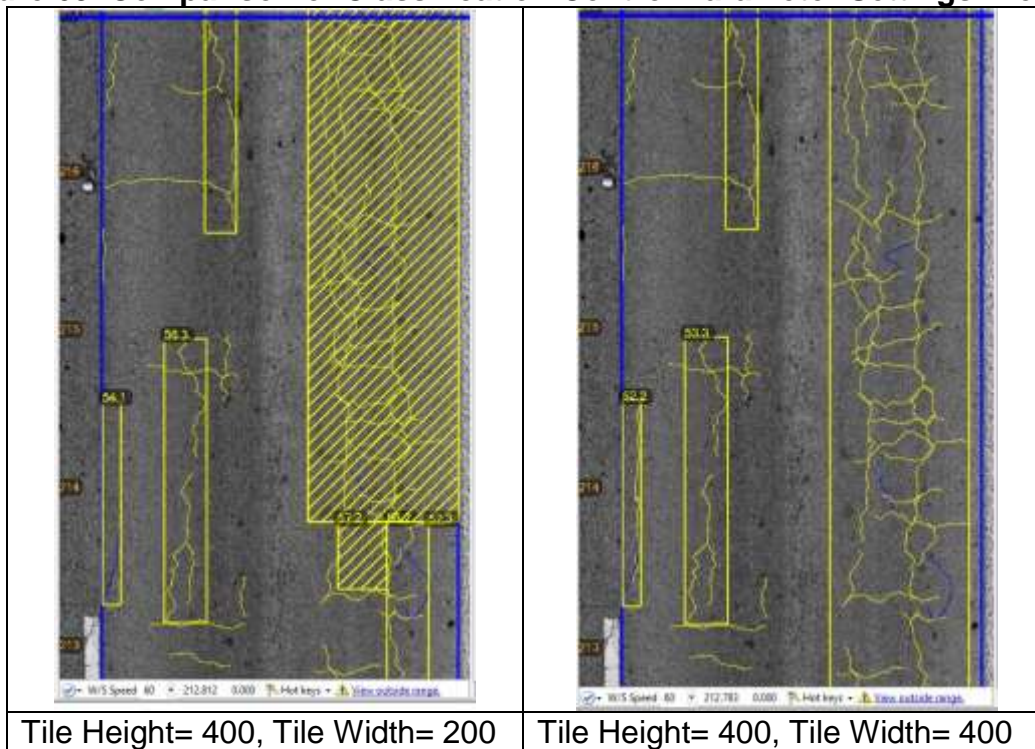
**Figure 68. Group Tile Height and Width**

The tuning of the classification control parameters was conducted by changing the parameters one by one and comparing the one classification result against the other. Figure 69 shows a comparison of the classification results when changing the density threshold that defines when cracks become alligator cracks. To compute crack density, the bounding box of a crack is divided into grids of tiles of user input size. If the density threshold is increased, there will be less distresses classified as alligator cracking. Figure 69 shows a comparison of classification results when changing the dimensions of the Tile used for calculating the density of the alligator or block categories. It is obvious that the larger the tile size, the smaller the density of the cracks. As a result, if the density threshold is fixed but the tile size is increased, there will be less distresses classified into alligator category. In this example, the crack set are rated as alligator when density threshold is 1.5. When the density threshold is increased to 2.0, this crack set is rated as longitudinal crack, which is actually not true. This parameter was tested on three sections which contained a larger amount of alligator cracking, and finally selected 1.5 as the optimum density threshold.



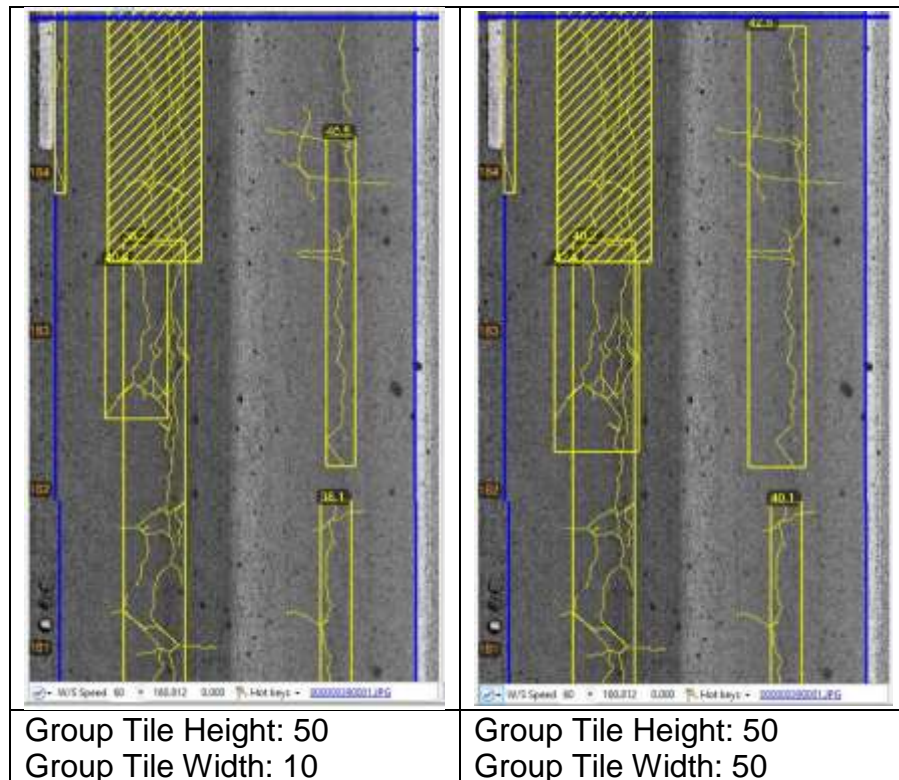


**Figure 69. Comparison of Classification Control Parameter Settings: Density**



**Figure 70. Comparison of Classification Control Parameter Settings: Tile Height and Width**

During the classification, the detected cracks are grouped into crack sets based on their proximity to each other. The distances between each crack bounding box are checked; if the horizontal distance between two adjacent bounding boxes is smaller than the group tile width and the longitudinal distance between the boxes is smaller than group tile height, then the two cracks are merged into one crack set. Each crack set will be rated as one distress. Figure 71 shows a comparison of the classification results when changing the dimensions of the Group Tile used for grouping defects together (see Figure 68).



**Figure 71. Comparison of Classification Control Parameter Settings: Group Tile Height and Width**

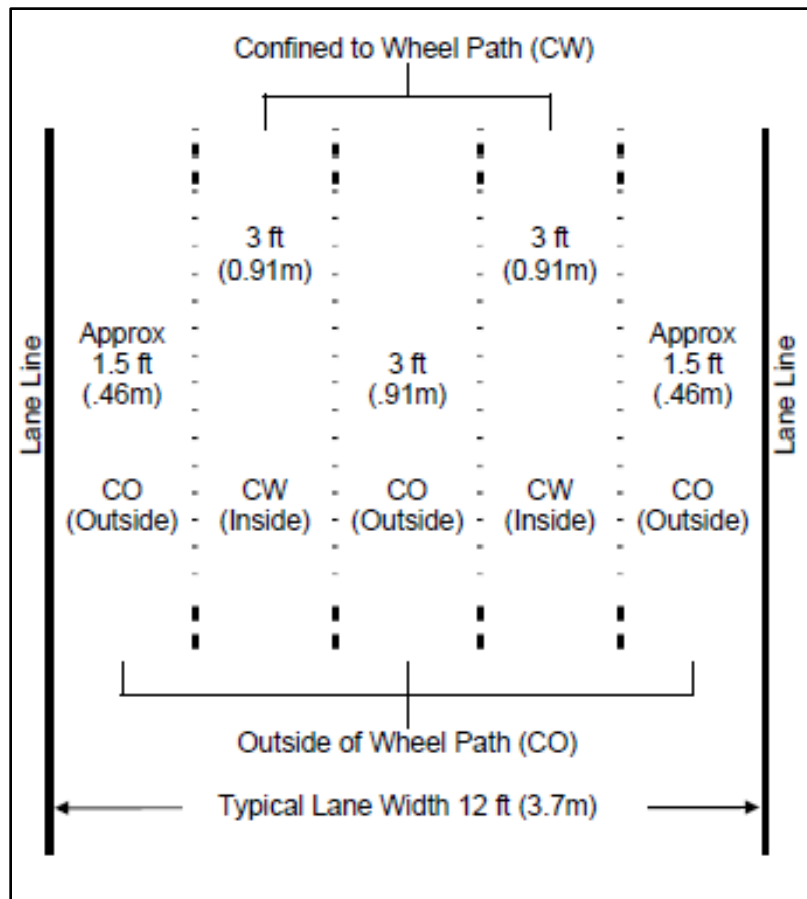
### ***Road Zone***

Road zone describes the portion of the road that is in the wheel paths and what is outside the wheel paths. The road zones were customized according to the Florida DOT specification of each wheel path being three feet wide (the FHWA HPMS Field Manual of December 2016 specifies one meter) and the center zone being three feet (0.91 meters) wide (Figure 72 and Figure 73):




1. Left Exterior: 0 meters offset from the Left Edge to -1.365 meters offset from the Center



2. Left Wheel Path: -1.365 to -0.455 meters offset from the Center
3. Center: -0.455 to 0.455 meters offset from the Center
4. Right Wheel Path: 0.455 to 1.365 meters offset from the Center
5. Right Exterior: 1.365 meters offset from the Center to 0 meters offset from the Right Edge



**Figure 72. Wheel Path Designation in FDOT Flexible Distress Handbook (2017)**

 New  Modify  Delete						
#	Road Zone	Left Anchor	Offset	Right Anchor	Offset	
1	Left Exterior	LeftEdge	0.000	Centre	-1.365	
2	Left WheelPath	Centre	-1.365	Centre	-0.455	
3	Center	Centre	-0.455	Centre	0.455	
4	Right Wheelpath	Centre	0.455	Centre	1.365	
5	Right Exterior	Centre	1.365	RightEdge	0.000	

**Figure 73. Road Zone Settings**

### ***Rating Profile***

The Rating Profile is used for assigning a distress type and severity to each of the detected and classified surface defects. This profile contains several components including profile name, profile description and rating rules. The rating rules configuration include distress rule set up and severity rule set up. While the Distress Rules specify classification of crack, the road zone, and distress metrics to be calculated, the Severity Rules determine detailed constraints on distresses that will be rated into each severity.

*Distress Rules* are setup based on the following:

1. Crack Classification: following detection and classification, all cracks are classified into Longitudinal, Transverse, Alligator, or Block. As previously noted, there are two options for distinguishing distresses by zone location. Table 40 and Table 41 show the distress types that were considered for this project and their corresponding crack classification for option 1 and option 2, respectively. As it was noted before, these distress types are used for documenting the distresses in a permanent record to facilitate quality control.

**Table 40. Distress Types and Corresponding Crack Classification and Severity Levels (option 1 corresponding to Figure 63 used for the reference survey)**

Distress Name	Crack Classification	Severity Levels
SingleCrack_L	Longitudinal	1B, II, III
SingleCrack_T	Transverse	1B, II, III
BranchCrack_L	Longitudinal	1B, II, III
BranchCrack_T	Transverse	1B, II, III
BlockCrack	Block	II, III
AlligatorCrack	Alligator	II, III
Raveling	NA	III
Patching	NA	III

**Table 41. Distress Types and Corresponding Crack Classification and Severity Levels (option 2 corresponding to Figure 64 used for automated results)**

<b>Distress Name</b>	<b>Crack Classification</b>	<b>Severity Levels</b>
SingleCrack_L_WP	Longitudinal	1B, II, III
SingleCrack_L_OP	Longitudinal	1B, II, III
SingleCrack_T_WP	Transverse	1B, II, III
SingleCrack_T_OP	Transverse	1B, II, III
BranchCrack_L_WP	Longitudinal	1B, II, III
BranchCrack_L_OP	Longitudinal	1B, II, III
BranchCrack_T_WP	Transverse	1B, II, III
BranchCrack_T_OP	Transverse	1B, II, III
BlockCrack_WP	Block	II, III
BlockCrack_OP	Block	II, III
AlligatorCrack_WP	Alligator	II, III
AlligatorCrack_OP	Alligator	II, III
Raveling_WP	NA	III
Raveling_OP	NA	III
Patching_WP	NA	III
Patching_OP	NA	III

2. **Lane Type**: Used only with option 2 (Table 41 and Figure 64), this refers to the road zones to be included in the process of identifying a selected Distress Type. For wheel path distresses, the 'Left Wheel Path' and 'Right Wheel Path' zones created in the 'Road Zone' menu of the Schema Editor can be selected. For non-wheel path distresses, the 'Left Exterior', 'Center', and 'Right Exterior' zones created in the 'Road Zone' menu of the Schema Editor are selected. For the reference survey in which manual correction of the automated results was required, this feature was disabled and instead wheel path and non-wheel path distresses were recorded in the same distress type and separated using an SQL code on the database (option 1). In this manner, if the road zone widths change in the future, the data can easily be reprocessed and there would be no need for conducting the manual distress rating again.
  
3. **Metric**: These include metrics to be reported for a selected Distress Type after automated identification and quantification. The following metrics were selected in the created rating rules. They will be calculated and recorded in the Vision Database.
  - 1) Crack Count - Number of Cracks that make up a Crack Group
  - 2) Crack Area - Area that contains all Cracks (all cracks in Crack Group)
  - 3) Crack Length - Actual length along all cracks in a Crack Group

- 4) Crack Extent - Longitudinal length of cracks in a Crack Group (Length in y-axis)
- 5) Transverse Extent - Horizontal length of cracks in a Crack Group (Length in x-axis)
- 6) Width - Width of Crack (Average width of cracks in Crack Group)
- 7) Diagonal - Length from bottom left to top right of every distress bounding box

*Severity Rules* are setup based on the following (In current version of Vision software, the unit used in parameter settings is meter):

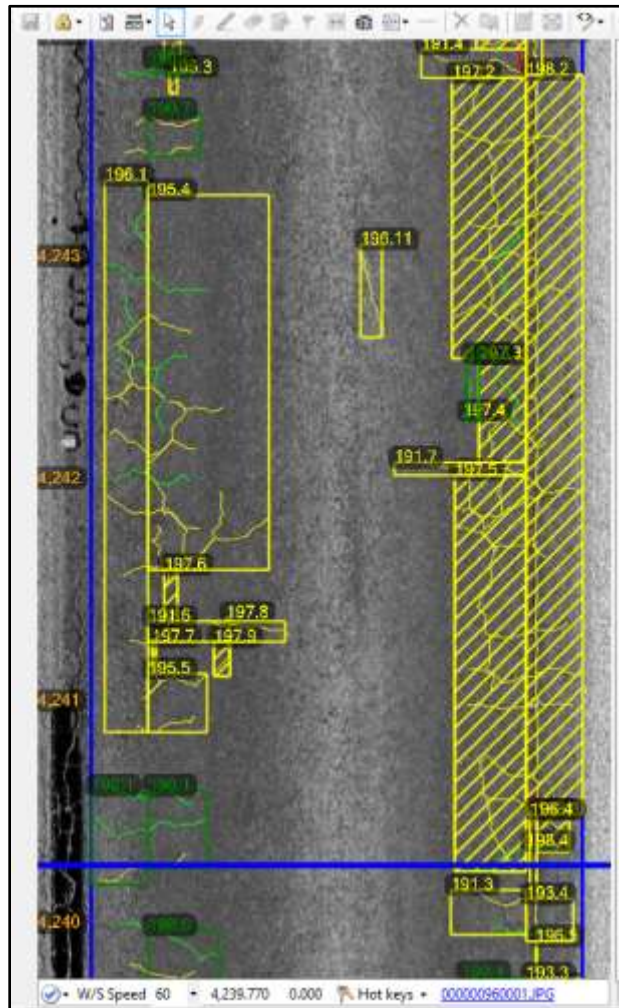
1. Crack Width: a crack width range is used as a constraint for selected severity levels in this project as demonstrated in Table 42.

**Table 42. Crack Width Range**

Severity Level	Crack Width Range (mm)
Class 1B	Less than 3.18
Class II	Greater than or equal to 3.18 and less than 6.35
Class III	Greater than or equal to 6.35 and less than 1000

2. Crack Length: a minimum extent of 0.3 meter (1.0 ft) is used as a constraint for identifying distresses (this was selected based on past experience):
  - a. Transverse Extent is used for transverse single and branch cracks
  - b. Longitudinal Extent is used for longitudinal single and branch cracks
  - c. No extent limitation was considered for alligator or block cracks
3. Road Zone: Used only with option 2 (Table 41 and Figure 64), this refers to the road zones to be included in the process of rating a selected Distress Severity. For wheel path distresses, the 'Left Wheel Path' and 'Right Wheel Path' zones created in the 'Road Zone' menu of the Schema Editor can be selected. For non-wheel path distresses, the 'Left Exterior', 'Center', and 'Right Exterior' zones created in the 'Road Zone' menu of the Schema Editor are selected. This results

in only the portion of detected cracks within specified zones to be included in each severity rating. This was only used for the fully automated survey. For example, Figure 74 shows that Distress number 195 shows longitudinal cracking in the wheel path and Distress number 196 shows the adjacent longitudinal cracking outside the wheel path. Similarly, Distress number 197 shows alligator cracking in the wheel path, while Distress number 198 indicates the adjacent alligator cracking outside the wheel path.



**Figure 74. Automatically Separated Wheel Path and Non-Wheel Path Distress Rating**

#### **Automated Pavement Distress Identification**

Fugro Vision software includes batch processors for automated lane detection, crack detection, classification and rating as identified in Table 43. These batch processors can be executed individually or all together. The JPEG Crack Detection Processor is Fugro's

solution for detecting surface defects using machine learning algorithms on 2D or 3D pavement images.

**Table 43. Batch Processor**

Batch Processor	Function
JPEG Lane Detection Processor	Lane Detection
JPEG Crack Detection Processor	Crack Detection from 2D or 3D Images
Classification Processor	Classification
Rating Processor	Rating

### ***JPEG Lane Detection Processor***

After this processor is completed, the lane boundary is shown as blue vertical lines in the user interface. Also, the location of detected lane is recorded in the Vision database.

### ***JPEG Crack Detection Processor***

After this processor is completed, cracks are detected from pavement images and are shown in the 'Range color' in the user interface. The crack information, such as Type, Chainage, Offset (in), Crack Length (ft), Crack Width, Cracks (count), Sealed Count, Crack Density (%), Crack Angle (degree), and Crack Depth (in) is listed in the 'Cracks' table (Figure 75). All the cracks are categorized as 'Unclassified' as they are still not classified yet at this stage.

Σ Summary Show Crack List Width ▾										
Type	Chainage	Offset (in)	CrackLength (ft)	CrackWidth (in)	Cracks (c...	SealedCount	CrackDensity (%)	CrackAngle ...	Crack...	
Unclassified	0.601	59.467	0.838	0.08022	1	0	0.39102	88.7567	0.0000	
Unclassified	0.603	4.293	4.994	0.07606	1	0	0.54072	88.4852	0.0000	
Unclassified	0.601	59.361	1.431	0.06328	1	0	0.37927	88.1778	0.0000	
Unclassified	0.603	58.458	0.997	0.06413	1	0	0.18128	84.1695	0.0000	
Unclassified	0.602	104.077	0.967	0.09442	1	0	0.32044	83.8512	0.0000	
Unclassified	0.600	59.021	0.874	0.07299	1	0	0.38295	80.8504	0.0000	
Unclassified	0.603	35.382	0.721	0.06620	1	0	0.21655	80.6297	0.0000	
Unclassified	0.603	2.843	0.724	0.11060	1	0	0.73312	0.1670	0.0000	
Unclassified	0.602	109.329	0.725	0.07743	1	0	0.44750	-79.6964	0.0000	
Unclassified	0.600	58.460	1.390	0.07738	1	0	0.36697	-83.1224	0.0000	
Unclassified	0.601	59.386	1.065	0.07644	1	0	0.33670	-84.9768	0.0000	
Unclassified	0.602	59.264	0.882	0.06163	1	0	0.32125	-85.9339	0.0000	
Unclassified	0.600	105.324	1.046	0.06900	1	0	0.36750	-86.0183	0.0000	
Unclassified	0.602	57.298	0.942	0.05428	1	0	0.30138	-87.1886	0.0000	
Unclassified	0.603	150.471	0.773	0.09578	1	0	0.21977	-89.8435	0.0000	

**Figure 75. Crack Table**

## **Classification Processor**

After this processor is completed, the cracks are classified and grouped into crack sets. The Crack table is updated to Crack Set table (Figure 76). Each Crack Set includes one or more cracks.

Type	Chainage	Offset (in)	CrackLength (ft)	CrackWidth (in)	Cracks (count)	SealedCount	CrackDensity (%)	CrackAngle (°)	CrackDepth (in)
⚙️ Longitudinal	0.602	57.298	0.942	0.05428	1	0	0.30138	-87.1886	0.0000
⚙️ Longitudinal	0.602	59.264	0.882	0.06163	1	0	0.32125	-85.9339	0.0000
⚙️ Longitudinal	0.603	58.458	0.997	0.06413	1	0	0.18128	84.1695	0.0000
⚙️ Longitudinal	0.603	35.382	0.721	0.06620	1	0	0.21655	80.6297	0.0000
⚙️ Longitudinal	0.600	105.324	1.046	0.06900	1	0	0.36750	-86.0183	0.0000
⚙️ Longitudinal	0.601	59.361	2.270	0.06954	2	0	0.38361	-89.7959	0.0000
⚙️ Longitudinal	0.600	58.460	2.264	0.07568	2	0	0.37314	-87.0319	0.0000
⚙️ Longitudinal	0.603	4.293	4.994	0.07606	1	0	0.54072	88.4852	0.0000
⚙️ Longitudinal	0.601	59.386	1.065	0.07644	1	0	0.33670	-84.9768	0.0000
⚙️ Longitudinal	0.602	109.329	0.725	0.07743	1	0	0.44750	-79.6964	0.0000
⚙️ Longitudinal	0.602	104.077	0.967	0.09442	1	0	0.32044	83.8512	0.0000
⚙️ Longitudinal	0.603	150.471	0.773	0.09578	1	0	0.21977	-89.8435	0.0000
⚙️ Transverse	0.603	2.843	0.724	0.11060	1	0	0.73312	0.1670	0.0000

**Figure 76. Crack Set Table**

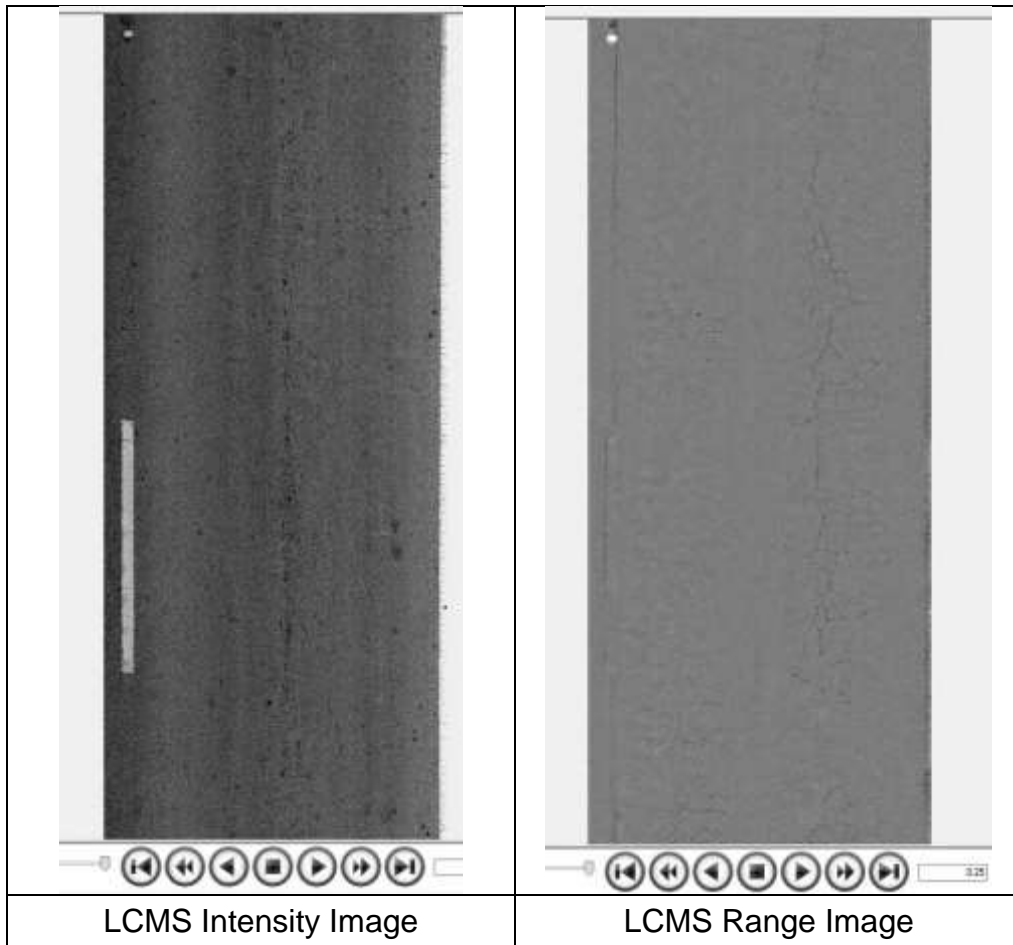
## **Rating Processor**

During the rating procedure, crack sets are rated. Severity levels and types are assigned to distresses.

### **Semi-Automated Pavement Distress Identification**

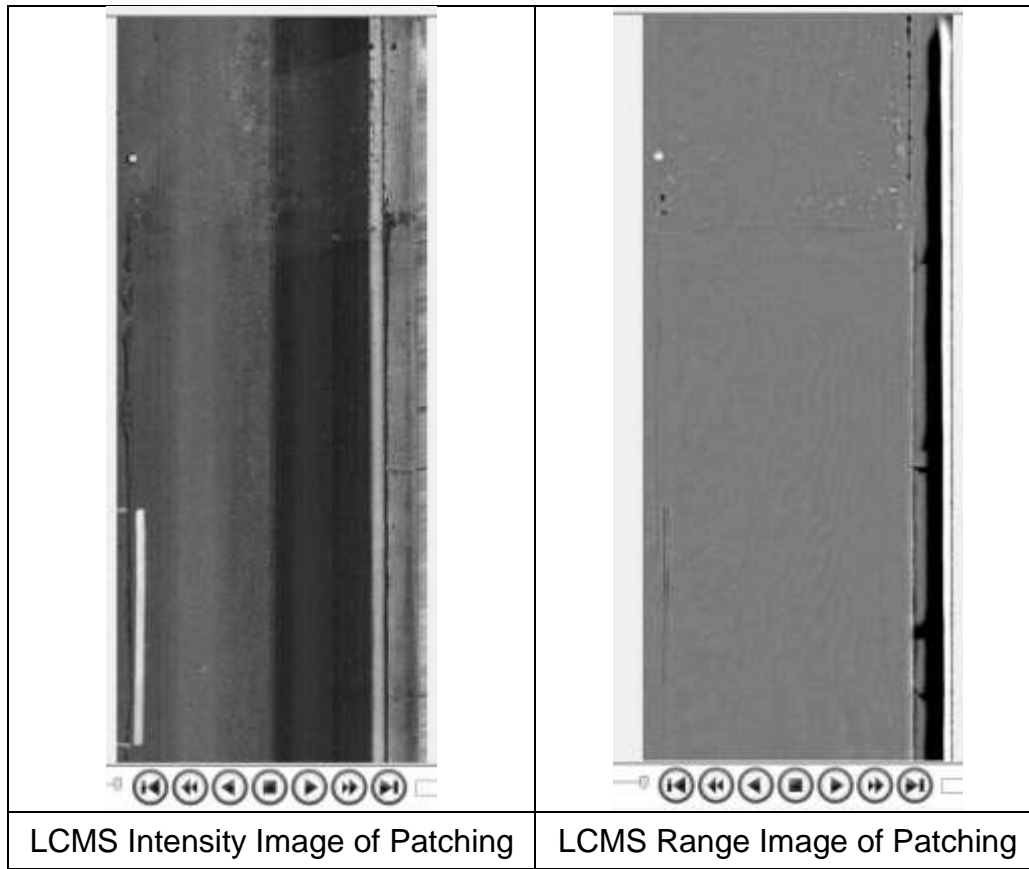
A Fugro rater conducted a semi-automated rating on one run of the images for the 12 test sections using 3D LCMS images that were collected on the same test sections and imported into the Vision software. Then another Fugro rater reviewed the results of the first rater to reach consensus on the reference survey ("Ground Truth"). During this procedure, linear distresses and area distresses (boxes) are manually drawn on top of the collected pavement images. The results of the crack detection process, including the color-coded cracks were used by raters as guidance to assign severity levels based on crack width.

Due to the lack of range images and ROW video data, the LRIS data is inappropriate to be used for creating a reference close to ground truth. The following examples have been provided to demonstrate the superiority of the 3D LCMS data over 2D LRIS data for generating the reference survey. In Example 1 (Figure 77), cracks can be missed if the detection is solely dependent on the intensity image. In Example 2 (Figure 78), the patching boundary can be falsely rated as transverse crack, if there is no ROW image (Figure 79).



**Figure 77. Demonstrating the Reason for Using 3D Images for Reference Survey: Example 1**





**Figure 78. Demonstrating the Reason for Using 3D Images for Reference Survey: Example 2**



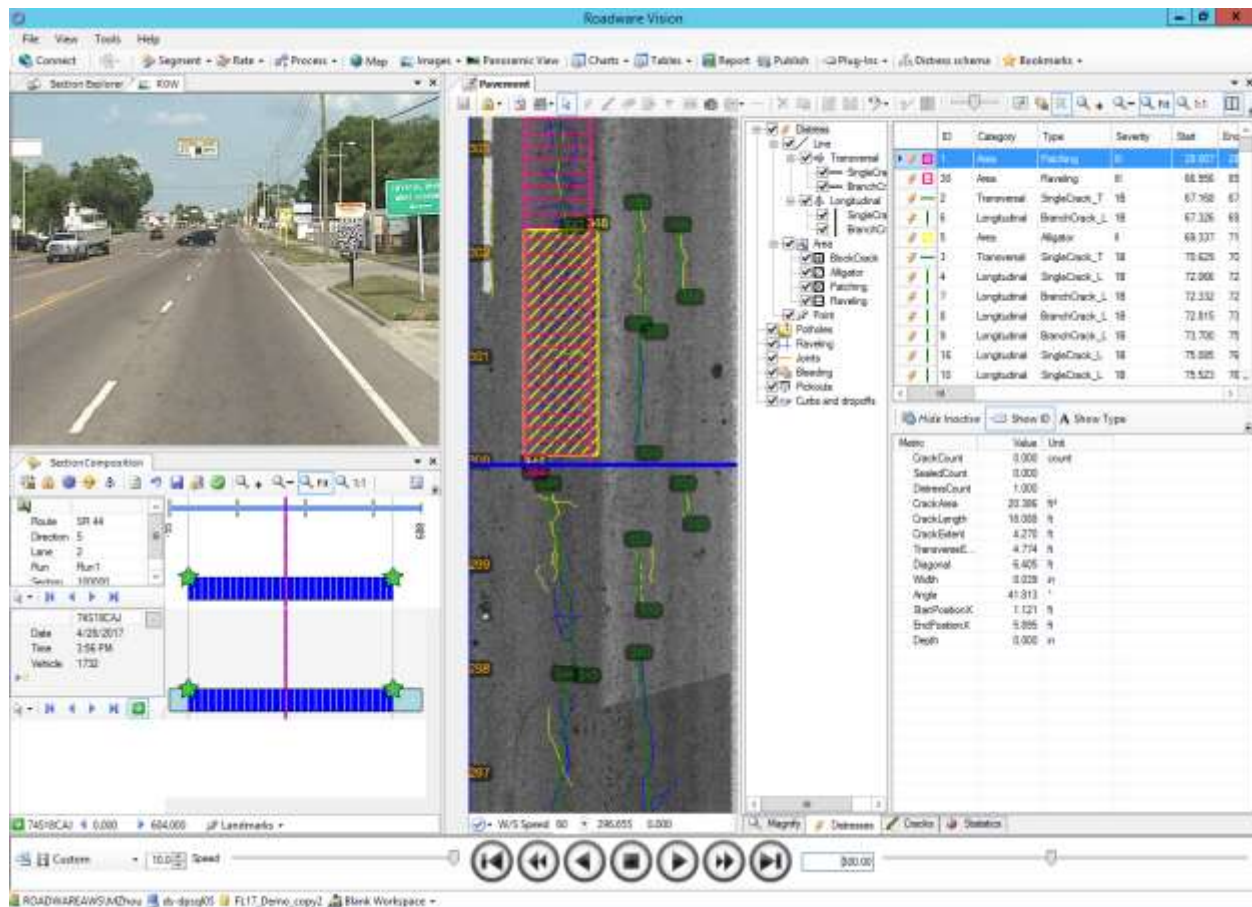
**Figure 79. ROW Image of Patching Area**

It is noted that LRIS data are collected in the order of county ID, while the Section ID in the reference LCMS data are sorted in the order of site ID. Table 44 documents the relation between the session IDs in the reference database and the LRIS database to avoid confusion. To facilitate the data comparison between 2D database and 3D reference database, this information was imported as a table into the 2D database.

**Table 44. Relation Between the 2D Database and the 3D Reference Database**

Site ID	ID Session in Reference Database	Section ID in LRIS Database	ID Session Section ID in LRIS Database		
			Run1	Run2	Run2
1	15	1	1	2	3
2	19	2	4	5	6
3	24	7	19	20	21
4	38	9	25	26	27
5	31	5	13	14	15
6	34	6	16	17	18
7	44	8	22	23	24
8	45	10	28	29	30
9	13	12	34	35	36
10	14	11	31	32	33
11	49	3	7	8	9
12	55	4	10	11	12

As shown in Figure 80, the Vision Pavement rating module allows the analyst to simultaneously view both the ROW and pavement images while marking and rating pavement distresses. This feature facilitates the semi-automated distress identification.



**Figure 80. Vision Pavement Rating Module for Semi-Automated Distress Survey**

The two stages for creating reference data are introduced in Section 4.3.2.

### 4.3 Evaluation of the LRIS Technology for Crack Detection and Distress Identification

In this chapter of the report, the results of crack detection and distress identification using the 2D LRIS images are evaluated. The 2D data collection was conducted by FDOT using their LRIS equipment and the data were analyzed by Fugro staff during Task 4 of this project. The following will describe the success metrics, the reference values, and the results, which will be analyzed to conclude on feasibility of using 2D LRIS technology in identification and quantification of flexible pavement distresses.

#### 4.3.1 Success Metrics

The three principal success metrics of any process are effectiveness, efficiency, and reliability. In the context of automated distress identification, effectiveness can be expressed in terms of accuracy of the crack detection software when compared to a

reference baseline. Accuracy is a qualitative term referring to whether there is agreement between a measurement made on an object and its true (target or reference) value. Bias is a quantitative term describing the difference (or error) between the average of measurements made on the same object and its true value.

While systematic errors identified in the bias can be calibrated out, such evaluations must address the random errors as well. The average results may be quite comparable, but individual results can deviate significantly. Efforts must be made to control these deviations to produce results which can ultimately be classified as reliable. Reliability of automated distress surveys is often expressed in terms of precision. Precision is a qualitative term that can describe the degree of repeatability of a measurement value on the same sample, or consistency in accuracy of measurement on different samples. Coefficient of variation of actual measurement values on the same sample is a quantitative estimate of repeatability. Standard deviation of error (standard error) is a quantitative estimate of consistency. Accuracy and precision (or the corresponding quantitative estimates: bias, variance, and standard error) ultimately define how effective and reliable a system is as described in greater detail below. The efficiency of the system is typically measured by the time it takes to conduct these measurements.

With respect to automated condition evaluations, the success metrics could be considered for two aspects of the process, first for the detection of individual surface defects (cracks), and second for the identification and quantification of the distresses in a distinct section.

The following are the success metrics used for evaluating the crack detection results:

- True Positives: length of correctly detected cracking
- False Positives: length of detected cracking that don't exist in the reference survey
- False Negatives: length of missed cracking
- Crack Validity: an indicator to be calculated as the ratio of the correctly detected cracks (true positives) to the total detected cracks (true positives and false positives). This statistic indicates the percentage of the detected cracks that was actually present in the reference survey, thereby expressing the validity of the cracks detected by algorithms.

$$\text{Validity (\%)} = 100 \times \frac{\text{correctly detected}}{\text{all detected}} = 100 \times \frac{\text{true positives}}{\text{true positives} + \text{false positives}}$$

- Crack Sensitivity (or Recall): a parameter to be calculated as the ratio of the correctly detected cracks to the total actual cracks existing on the pavement surface (true positives and false negatives). This statistic represents the percentage of the cracks in the reference survey that was detected by the automated method, thereby expressing the sensitivity of the algorithms to existing cracks.

$$\text{Sensitivity (\%)} = 100 \times \frac{\text{correctly detected}}{\text{actual cracks}} = 100 \times \frac{\text{true positives}}{\text{true positives} + \text{false negatives}}$$

- Crack Detection Accuracy: based on average normalized error (bias) of automatically detected crack length compared to the reference. Accuracy (%) = 100 – Bias (%)
- Crack Detection Repeatability: based on coefficient of variation (COV) of detected crack length among three runs (independent of the reference and averaged among the sections). Repeatability (%) = 100 – COV (%)
- Crack Detection Consistency: based on coefficient of variation (COV) of crack detection accuracy among 12 test sections. Consistency (%) = 100 – [Standard Deviation of Accuracy (%) / Average Accuracy (%)]
- Crack Detection Efficiency: based on the time required for the automated crack detection. Efficiency (second per foot) = time for cracking detection divided by the total length

Based on the overall cumulative amount of each distress among different test sections and multiple runs, the success metrics used to evaluate the feasibility of using 2D images are:

1. Distress Identification Accuracy: based on average error (bias) with respect to the reference distress survey values for each distress type. Accuracy (%) = 100 – Bias (%)
2. Distress Identification Repeatability: based on coefficient of variation (COV) of automatically identified distresses among three runs for each distress type

(independent of the reference and averaged among the sections). Repeatability (%) =  $100 - \text{COV} (\%)$

3. Distress Identification Consistency: based on coefficient of variation (COV) of distress identification accuracy among 12 sections for each distress type. Consistency (%) =  $100 - [\text{Standard Deviation of Accuracy} (\%) / \text{Average Accuracy} (\%)]$
4. Distress Identification Efficiency: based on the time required for the automated distress survey. Efficiency (second per foot) = time for cracking detection, classification, and rating divided by the total length.

#### **4.3.2 Reference Rating or “Ground Truth”**

Both Crack Detection Reference and Distress Identification Reference were created for this evaluation based on the 3D LCMS data that were collected as part of Purchase Order No. PR10026557 for this research project (see Appendix I):

1. Crack Detection Reference: the Pavemetrics LCMS crack detection routine was used to generate a baseline crack map and then a Fugro data technician reviewed all the images in one run of the 12 test sections and modified the crack maps. New cracks were added for missed cracks, false positives were deleted, and some cracks with wrong extent were modified to reflect the actual cracks that can be seen on the 3D intensity and range (depth) images and with assistance from the ROW images.
2. Distress Identification Reference: as it was explained in the semi-automated distress survey part, a reference survey was created by one Fugro engineer and another Fugro technician reviewed the results to reach a consensus for the reference survey. This reference survey was created using the 3D images because they provide both intensity and range (depth) views, along with the ROW images. Therefore, comprehensive sources of data are available in the 3D database for creating this reference survey.

#### **4.3.3 2D Crack Detection Results**

Table 45 shows the true positives, false positives, false negatives, validity, and sensitivity of the automated crack detection using Fugro’s machine learning algorithm on 2D images. This table indicates that only about 25 percent of the automatically detected cracks from 2D images were actually present on the pavement surface (Validity). Also, only about 18 percent of the cracks in the ground truth were automatically detected from 2D images (Sensitivity).

In Table 45, the yellow highlighted cells indicate significant false positives (more than 50% of the reference) and the orange colored cells indicate significant amounts of missed cracks (more than 50% of the reference). It is evident that in Sections number 3, 7, and 9, there is a significant number of false positives. This is due to two reasons. First, some patching area boundaries and Automated Vehicle Counter (AVC) loops and Weigh-In-Motion (WIM) devices being falsely detected as cracks. Second, the amount of cracking in the semi-automated reference survey for these three sections is lower compared to other sections and as a result, the errors seem higher. From Table 45, it is also evident that the 2D method has missed a significant amount of the cracks and only detected about 18 percent of the existing cracks in the reference.

**Table 45. Verification of Crack Detection on 2D images Using Fugro Machine Learning Algorithm**

Test Section	Ground Truth (ft)	Crack Detection Results			Crack Validity (%)	Crack Sensitivity (%)
		True Positives (ft)	False Positives (ft)	False Negatives (ft)		
1	22,944.22	1,162.61	3,337.93	21,781.61	25.83	5.07
2	26,741.89	824.98	3,727.55	25,916.91	18.12	3.08
3	132.74	42.55	16,471.86	90.19	0.26	32.06
4	14,823.69	3,659.58	4,199.93	11,164.11	46.56	24.69
5	68,726.86	6,226.68	10,005.31	62,500.18	38.36	9.06
6	112,892.60	7,139.73	10,005.56	105,752.87	41.64	6.32
7	809.34	523.47	13,969.35	285.87	3.61	64.68
8	27,185.46	5,184.47	13,606.25	22,000.99	27.59	19.07
9	3,993.09	807.72	19,550.12	3,185.37	3.97	20.23
10	36,631.86	1,718.52	12,621.25	34,913.34	11.98	4.69
11	30,517.80	3,507.70	6,274.08	27,010.10	35.86	11.49
12	29,327.95	3,003.47	3,539.88	26,324.48	45.90	10.24
					<b>24.97</b>	<b>17.56</b>

In addition to the crack detection verification results in Table 45, other crack detection success metrics including normalized error, average error (bias), variation between multiple runs (repeatability), and variation among 12 test sections (consistency) of the automated crack detection algorithms from 2D images have been listed in Table 46.

The three test sections number 3, 7, and 9 have been highlighted in yellow to indicate the sections that have the greatest number of false positives. The bias has been provided as the average normalized crack detection error both on all the test sections and excluding the three outliers. When excluding the outliers, Table 46 indicates that the accuracy (100 - Bias) of the automated crack detection from 2D images is only about 32 percent.

The automated detection from 2D images has demonstrated a sufficiently high run-to-run repeatability. Ten out of twelve sections have more 90 percent agreement among runs, while the average repeatability of all 12 sections is about 93 percent. The 2D crack detection is showing poor consistency of results on different sections, as it has about 39 percent agreement in crack detection accuracy among 12 sections.

**Table 46. Accuracy, Repeatability, and Consistency of Crack Detection based on 2D Images**

Test Section	Ground Truth (ft)	Detected Crack Length			Normalized Error			100 - AVG ABS Error (%)	Repeatability (%)
		Run 1 (ft)	Run 2 (ft)	Run 3 (ft)	Run1 (%)	Run2 (%)	Run3 (%)		
1	22,944.2	4,500.5	4,564.0	4,090.5	-80.4	-80.1	-82.2	19.1	94.1
2	26,741.9	4,552.5	3,864.7	3,843.5	-83.0	-85.6	-85.6	15.3	90.1
3	132.7	16,514.4	14,055.8	15,632.5	12341.2	10489.0	11676.8	-11402.3	91.9
4	14,823.7	7,859.5	7,699.6	7,906.2	-47.0	-48.1	-46.7	52.8	98.6
5	68,726.9	16,232.0	13,279.2	10,427.5	-76.4	-80.7	-84.8	19.4	78.2
6	112,892.6	17,145.3	18,010.4	17,739.2	-84.8	-84.0	-84.3	15.6	97.5
7	809.3	14,492.8	13,748.8	14,703.7	1690.7	1598.8	1716.8	-1568.7	96.5
8	27,185.5	18,790.7	19,884.4	19,572.2	-30.9	-26.9	-28.0	71.4	97.1
9	3,993.1	20,357.8	19,751.2	20,089.8	409.8	394.6	403.1	-302.5	98.5
10	36,631.9	14,339.8	14,077.4	11,809.3	-60.8	-61.6	-67.8	36.6	89.6
11	30,517.8	9,781.8	9,506.5	9,133.1	-67.9	-68.8	-70.1	31.0	96.6
12	29,328.0	6,543.4	6,448.3	6,702.6	-77.7	-78.0	-77.2	22.4	98.0
<b>Bias (%)</b>								<b>1079.8</b>	<b>93.3</b>
<b>Bias Excluding Outliers (%)</b>								<b>-68.5</b>	
<b>Accuracy (%) = 100 - Absolute Bias</b>								<b>31.5</b>	
<b>Consistency (%) = 100 - COV(Accuracy)</b>								<b>38.8</b>	

#### 4.3.4 2D Distress Identification Results

In this section, the results of automated distress identification (performance of classification and rating algorithm) from 2D images are evaluated. As it was demonstrated in the previous section, the crack detection from 2D images is missing a significant amount of cracking and as a result, there is a significant negative bias in the distress identification results for the 2D methodology.

It should also be noted that the automated algorithm used crack angle to differentiate between longitudinal and transverse cracks, and crack density in a given area to differentiate between single linear cracks and an area of alligator cracking. Therefore, the error compared to ground truth is estimated by comparing the total amount of automatically identified longitudinal and transverse cracks to the sum of the single and branch cracks manually identified in the reference survey. Similarly, the total amount of



automatically identified alligator cracking is compared to the sum of the alligator and block cracks manually identified in the reference survey.

### Evaluation of Automatically Identified Longitudinal, Transverse, and Alligator Cracking from 2D LRIS Images

Table 47 shows the success metrics for automatically identifying Longitudinal cracks from 2D images. In this table, test sections where there was minimal amount of longitudinal cracking in the reference survey, have been highlighted as outliers. Excluding the outliers, the automated distress identification from 2D images has demonstrated about 46 percent accuracy in identifying longitudinal cracking. The results show a negative bias indicating less automatically identified longitudinal cracks from 2D images, compared to the reference survey. However, the 2D results show a significantly higher amount of longitudinal cracking identified compared to the reference survey in the three outlier test sections where the reference survey showed lower cracking.

On average, there is about 89 percent run-to-run agreement among the three runs in the length of automatically identified longitudinal cracks from 2D images. There is about 45 percent section-to-section agreement among the 12 sections in the normalized error (compared to the reference survey) in automatically identifying the length of longitudinal cracks from 2D images.

**Table 47. Accuracy, Repeatability, and Consistency of Longitudinal Cracks based on 2D Images**

Test Section	Ground Truth (ft)	Automatically Identified Longitudinal Cracks			Normalized Error			100 - AVG ABS Error (%)	Repeatability (%)
		Run 1 (ft)	Run 2 (ft)	Run 3 (ft)	Run1 (%)	Run2 (%)	Run3 (%)		
1	3,596.8	1,310.3	1,260.2	1,126.8	-63.6	-65.0	-68.7	34.3	92.3
2	2,138.4	921.8	794.5	813.3	-56.9	-62.8	-62.0	39.4	91.8
3	9.8	5,845.5	3,380.4	3,256.0	59608.6	34428.9	33158.0	-42298.5	64.9
4	2,744.9	2,492.6	2,629.6	2,541.8	-9.2	-4.2	-7.4	93.1	97.3
5	8,468.6	5,782.1	4,822.6	3,559.0	-31.7	-43.0	-58.0	55.8	76.4
6	9,148.4	4,937.9	5,869.4	5,263.9	-46.0	-35.8	-42.5	58.6	91.2
7	481.8	1,812.0	1,629.8	1,967.1	276.1	238.3	308.3	-174.2	90.6
8	7,717.2	3,996.3	4,238.6	4,446.6	-48.2	-45.1	-42.4	54.8	94.7
9	807.5	1,454.5	1,181.4	1,254.1	80.1	46.3	55.3	39.4	89.1
10	6,599.3	3,914.4	3,497.8	2,383.0	-40.7	-47.0	-63.9	49.5	75.8
11	10,103.9	1,817.9	1,921.7	2,195.5	-82.0	-81.0	-78.3	19.6	90.1
12	19,775.8	1,030.8	979.4	1,151.6	-94.8	-95.0	-94.2	5.3	91.6
Bias (%)								3520.3	89.0
Bias Excluding Outliers (%)								-54.4	
Accuracy (%) = 100 - Absolute Bias								45.6	
Consistency (%) = 100 - COV(Accuracy)								44.7	

Table 48 shows the success metrics for automatically identifying Transverse cracks from 2D images. In this table, test sections where there was minimal amount of

transverse cracking in the reference survey, have been highlighted as outliers. Excluding the outliers, the automated distress identification from 2D images has demonstrated about 24 percent accuracy in identifying transverse cracking. The results show a negative bias indicating less automatically identified transverse cracks compared to the reference survey.

On average, there is about 91 percent run-to-run agreement among the three runs in the length of automatically identified transverse cracks from 2D images. There is about 6 percent section-to-section agreement among the 12 sections in the normalized error (compared to the reference survey) in automatically identifying the length of transverse cracks from 2D images.

**Table 48. Accuracy, Repeatability, and Consistency of Transverse Cracks based on 2D Images**

Test Section	Ground Truth (ft)	Automatically Identified Transverse Cracks			Normalized Error				Repeatability (%)
		Run 1 (ft)	Run 2 (ft)	Run 3 (ft)	Run1 (%)	Run2 (%)	Run3 (%)	100 - AVG ABS Error (%)	
1	276.9	30.6	29.1	30.5	-89.0	-89.5	-89.0	10.8	97.2
2	273.0	51.0	52.4	55.6	-81.3	-80.8	-79.6	19.4	95.5
3	10.9	0.0	0.0	0.0	-100.0	-100.0	-100.0	0.0	100.0
4	256.7	17.4	18.2	18.6	-93.2	-92.9	-92.8	7.0	96.7
5	109.4	65.5	66.4	63.1	-40.1	-39.3	-42.3	59.4	97.4
6	157.2	68.6	73.1	71.6	-56.3	-53.5	-54.5	45.2	96.8
7	16.5	4.7	1.0	2.3	-71.6	-93.7	-86.1	16.2	30.6
8	965.3	42.6	41.0	39.6	-95.6	-95.8	-95.9	4.2	96.4
9	21.6	115.1	124.4	123.3	433.1	476.0	470.8	-360.0	95.8
10	2,306.4	22.5	18.9	12.8	-99.0	-99.2	-99.4	0.8	72.8
11	170.7	99.3	90.2	93.0	-41.8	-47.1	-45.5	55.2	95.1
12	590.6	101.4	106.8	64.1	-82.8	-81.9	-89.2	15.4	74.4
Bias (%)								-33.9	91.4
Bias Excluding Outliers (%)								-75.8	
Accuracy (%) = 100 - Absolute Bias								24.2	
Consistency (%) = 100 - COV(Accuracy)								5.6	

Table 49 shows the success metrics for automatically identifying Alligator cracks from 2D images. In this table, test sections where there was zero amount of alligator cracking in the reference survey, have been highlighted as outliers. Excluding the outliers, the automated distress identification from 2D images has demonstrated about 0.01 percent accuracy in identifying alligator cracking.

The results show a significant amount of negative bias, indicating that the 2D distress identification has failed in identifying areas with alligator cracking. This is mainly due to the large amount of missed cracking in 2D crack detection, which in turn results in

cracking areas with such low density that cannot be identified by the computer as alligator cracking areas.

On average, there is about 16 percent run-to-run agreement among the 3 runs in the automatically identified alligator cracking area from 2D images. There is about -140 percent section-to-section agreement among the 12 sections in the normalized error (compared to the reference survey) in automatically identifying the area of alligator cracking from 2D images.

**Table 49. Accuracy, Repeatability, and Consistency of Alligator Cracks based on 2D Images**

Test Section	Ground Truth (Sq Ft)	Automatically Identified Alligator Cracks			Normalized Error			100 - AVG ABS Error (%)	Repeatability (%)
		Run 1 (Sq Ft)	Run 2 (Sq Ft)	Run 3 (Sq Ft)	Run1 (%)	Run2 (%)	Run3 (%)		
1	5,846.8	0.0	0.0	0.0	-100.0	-100.0	-100.0	0.0	100.0
2	9,482.9	14.2	0.0	0.0	-99.8	-100.0	-100.0	0.05	-73.2
3	0.0	0.0	0.0	0.0					100.0
4	3,100.2	0.2	0.0	0.0	-99.9	-100.0	-100.0	0.0	-73.2
5	18,795.1	0.1	0.0	0.0	-100.0	-100.0	-100.0	0.0	-73.2
6	27,372.5	0.0	0.0	0.0	-100.0	-100.0	-100.0	0.0	100.0
7	0.0	0.0	0.0	0.0					100.0
8	4,223.7	0.0	0.0	0.0	-100.0	-100.0	-100.0	0.0	100.0
9	0.0	0.0	0.0	0.0					100.0
10	6,567.4	0.0	0.0	0.0	-100.0	-100.0	-100.0	0.0	-73.2
11	1,533.7	0.2	0.2	0.01	-99.9	-99.9	-100.0	0.01	34.3
12	900.1	0.0	0.0	0.0	-100.0	-100.0	-100.0	0.0	100.0
Bias (%)								-99.9	15.7
Bias Excluding Outliers (%)								-99.9	
Accuracy (%) = 100 - Absolute Bias								0.01	
Consistency (%) = 100 - COV(Accuracy)								-139.8	

The Vision software records the amount of time that each batch processor had spent on each test section to conduct an automated survey. The automated detection, classification, and rating took about 26 seconds per image frame for the 2D images. The main contributor to slower speed is the crack detection time and the classification and distress identification processes take only about 0.05 seconds per image frame.

#### **Evaluation of Automatically Identified Wheel Path and Non-Wheel Path Cracking from 2D LRIS Images**

In this section, the semi-automated reference rating results were converted to cracking within the wheel path (WP) and outside the wheel path (OP) using a SQL code (see option 1 in Section 4.2.3). The automated distress identification results were already available in WP and OP format, because the distress schema was setup accordingly (see option 2 in Section 4.2.3). The total amount of cracking within the wheel paths (CW) was calculated by adding the longitudinal, transverse, and alligator cracking

areas. The longitudinal and transverse cracking areas were calculated by multiplying their length by one foot, as specified in the FDOT *Flexible Pavement Condition Survey Handbook* (2017).

Table 50 and Table 51 show the automated distress identification results for CO and CW distresses from 2D images, respectively. The accuracy in determining the CO distresses from 2D images is about 33 percent. The run-to-run repeatability in determining the CO distresses from 2D images is about 86 percent. The section-to-section consistency in determining the CO distresses from 2D images is about 34 percent.

**Table 50. Accuracy, Repeatability, and Consistency of Cracking Outside Wheel Paths (CO) Based on 2D Images**

Test Section	Ground Truth (Sq Ft)	Automatically Identified Cracking			Normalized Error			100 - AVG ABS Error (%)	Repeatability (%)
		Run 1 (Sq Ft)	Run 2 (Sq Ft)	Run 3 (Sq Ft)	Run1 (%)	Run2 (%)	Run3 (%)		
1	2,269.16	413.16	332.64	276.57	-81.79	-85.34	-87.81	15.02	79.85
2	2,929.56	326.82	267.14	349.21	-88.84	-90.88	-88.08	10.73	86.51
3	11.98	5,845.47	3,380.38	3,255.96	48,693.57	28,116.86	27,078.30	-34529.58	100.00
4	3,452.35	1,675.19	1,837.38	1,755.16	-51.48	-46.78	-49.16	50.86	95.38
5	13,550.71	4,981.47	3,890.31	2,891.53	-63.24	-71.29	-78.66	28.94	73.34
6	15,456.96	3,289.52	3,959.84	3,622.93	-78.72	-74.38	-76.56	23.45	90.75
7	296.23	1,807.72	1,626.94	1,962.51	510.24	449.22	562.50	-407.32	90.66
8	4,232.96	2,919.43	3,178.08	3,411.57	-31.03	-24.92	-19.40	74.88	92.23
9	249.79	1,369.37	1,063.21	1,164.95	448.21	325.64	366.37	-280.07	87.00
10	6,584.24	3,900.46	3,461.47	2,344.54	-40.76	-47.43	-64.39	49.14	75.21
11	4,653.28	1,678.48	1,732.75	2,033.89	-63.93	-62.76	-56.29	39.01	89.45
12	11,403.25	990.18	940.88	1,061.73	-91.32	-91.75	-90.69	8.75	93.91
Bias (%)								<b>2909.81</b>	<b>86.29</b>
Bias Excluding Outliers (%)								<b>-66.58</b>	
Accuracy (%) = 100 - Absolute Bias								<b>33.42</b>	
Consistency (%) = 100 - COV(Accuracy)								<b>34.07</b>	

The accuracy in determining the CW distresses from 2D images is about nine percent. The run-to-run repeatability in determining the CW distresses from 2D images is about 91 percent. The section-to-section consistency in determining the CO distresses from 2D images is about 0.4 percent.

**Table 51. Accuracy, Repeatability, and Consistency of Cracking Within Wheel Paths (CW) Based on 2D Images**

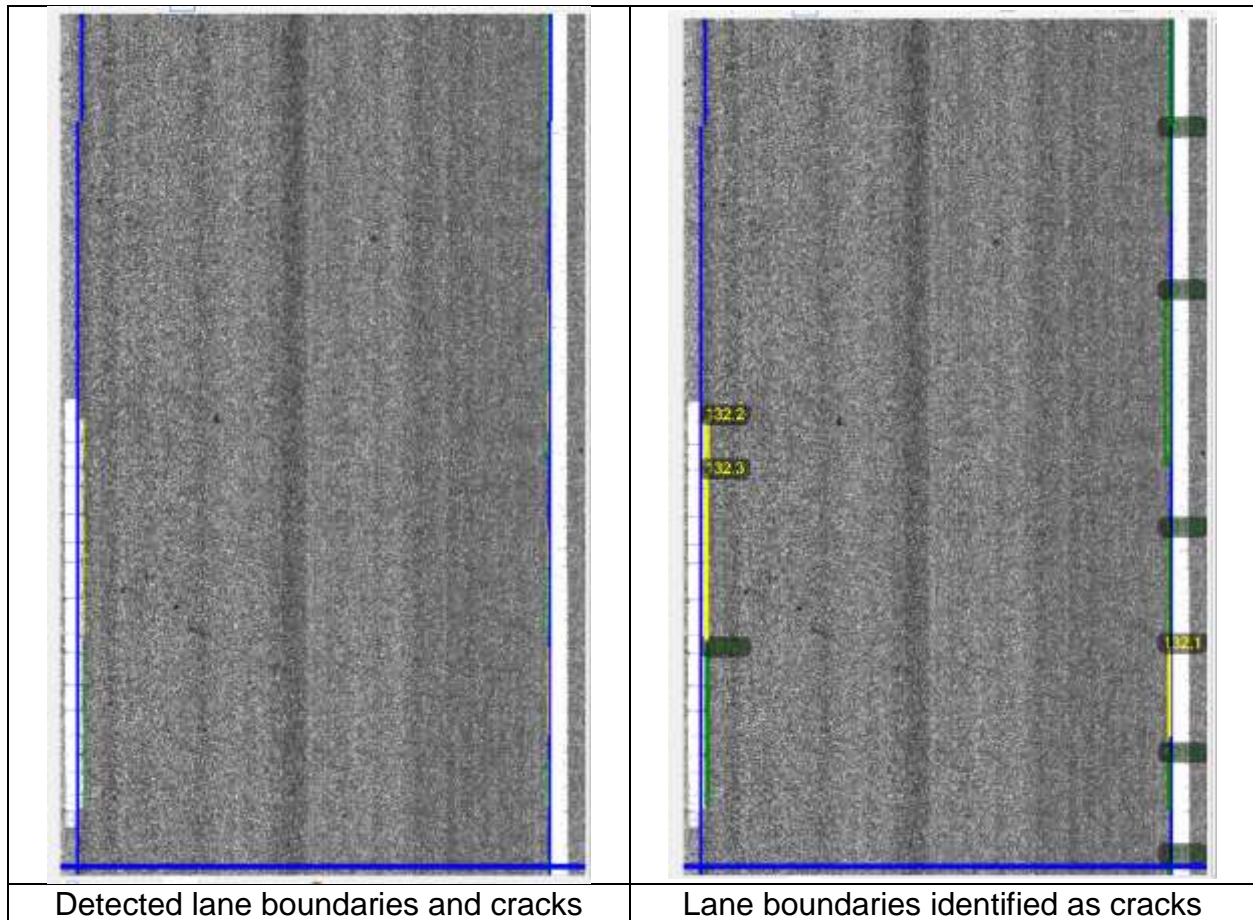
Test Section	Ground Truth (Sq Ft)	Automatically Identified Cracking			Normalized Error			100 - AVG ABS Error (%)	Repeatability (%)
		Run 1 (Sq Ft)	Run 2 (Sq Ft)	Run 3 (Sq Ft)	Run1 (%)	Run2 (%)	Run3 (%)		
1	7,451.30	927.65	956.62	880.79	-87.55	-87.16	-88.18	12.37	95.85
2	8,964.78	660.09	579.74	519.69	-92.64	-93.53	-94.20	6.54	87.99
3	8.74	0.00	0.00	0.00	-100.00	-100.00	-100.00	0.00	100.00
4	2,649.44	835.01	810.36	805.19	-68.48	-69.41	-69.61	30.83	98.05
5	13,822.31	866.24	998.70	730.53	-93.73	-92.77	-94.71	6.26	84.50
6	21,221.13	1,717.08	1,982.63	1,712.50	-91.91	-90.66	-91.93	8.50	91.43
7	202.05	9.02	3.91	6.91	-95.54	-98.06	-96.58	3.27	61.17
8	8,673.24	1,119.50	1,101.42	1,074.67	-87.09	-87.30	-87.61	12.67	97.95
9	579.29	200.31	242.65	212.42	-65.42	-58.11	-63.33	37.71	90.02
10	8,888.91	36.51	55.22	51.26	-99.59	-99.38	-99.42	0.54	79.31
11	7,155.08	238.93	279.39	254.64	-96.66	-96.10	-96.44	3.60	92.08
12	9,863.21	142.03	145.32	153.92	-98.56	-98.53	-98.44	1.49	95.83
Bias (%)								<b>-89.68</b>	<b>91.44</b>
Bias Excluding Outliers (%)								<b>-90.80</b>	
Accuracy (%) = 100 - Absolute Bias								<b>9.20</b>	
Consistency (%) = 100 - COV(Accuracy)								<b>0.38</b>	

#### 4.3.5 Results Analysis

##### False Positive Analysis

It is evident that in Sections number 3, 7, and 9, the 2D method has demonstrated a significant number of false positives (more than 50% compared to the reference). This is due to two reasons:

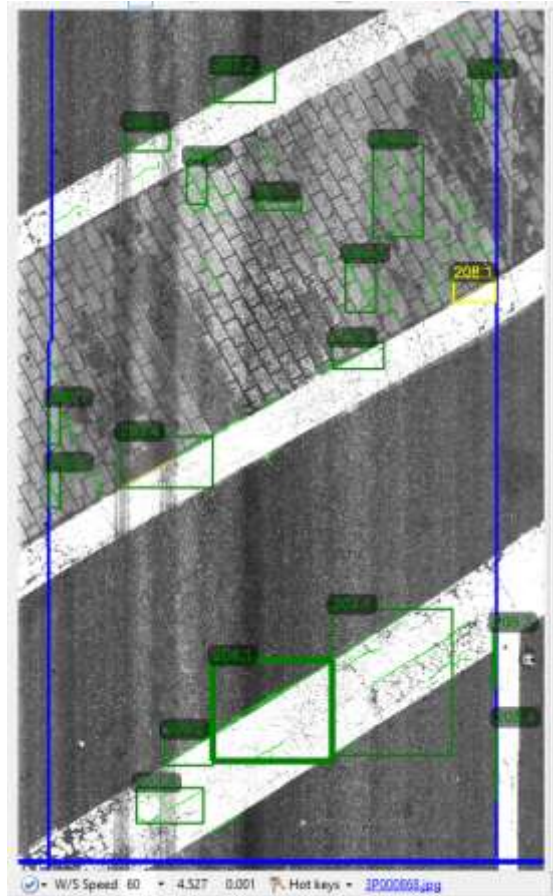
First, some road lane markings are falsely identified as cracks. The existing Vision road lane detection system detects the lane marking boundaries as vertical lines and records x coordinates of these detected lines in the database. All cracks of which x coordinates are less than or equals to x coordinate of left lane, or greater than or equal to x coordinate of right lane are not considered for distress rating. However, in some pavement images, the lane marking may not be completely vertical. The image pixels within the detected lanes can be falsely identified as crack pixel due to its high contrast with the adjacent pixels (see Figure 81).



**Figure 81. Lane boundaries identified as cracks**

Second, patching boundaries, pavement markings, joints of brick paving are other typical causes of false positives. See Figure 82 for an example.



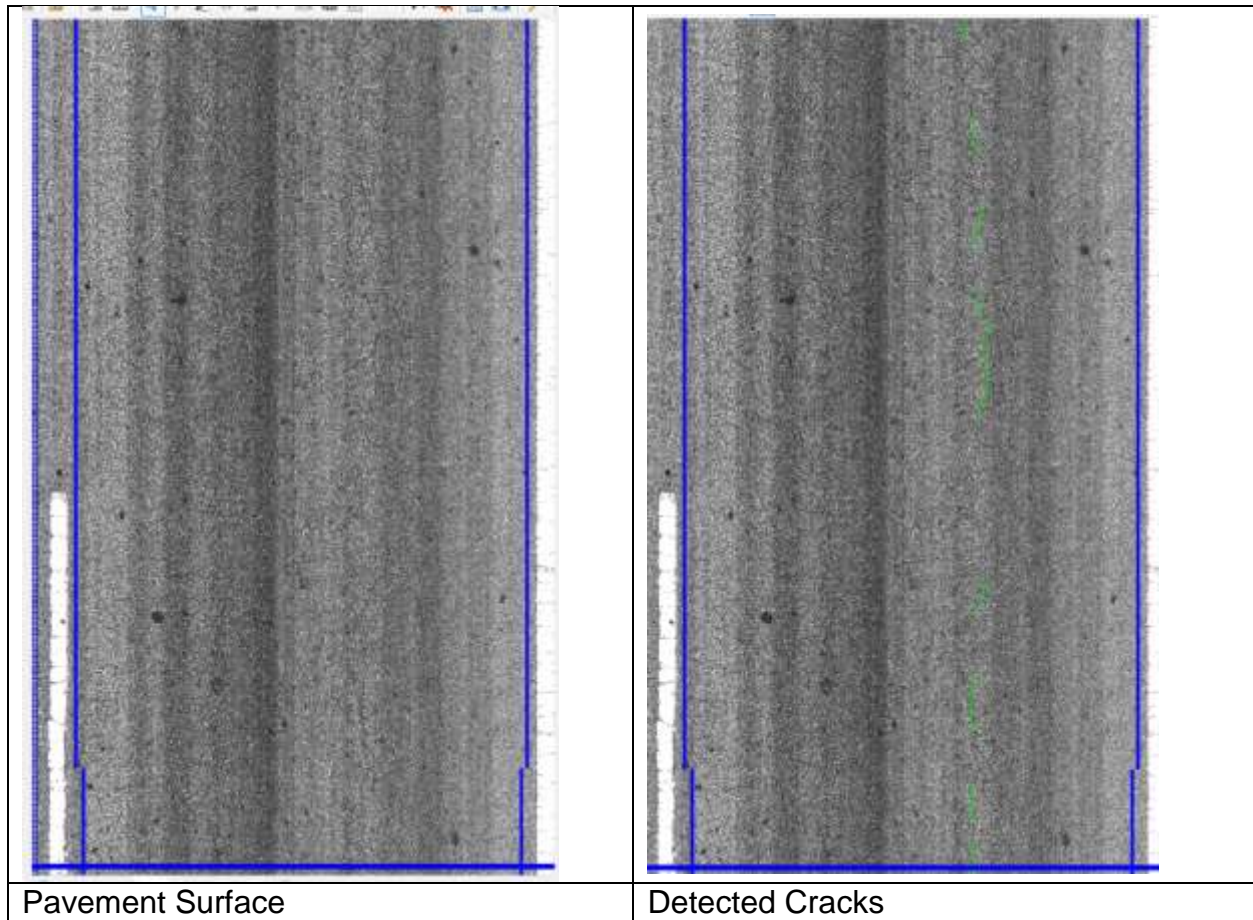


**Figure 82. Other Features Falsely Detected as Cracks**

### **False Negative Analysis**

The significant amount of missed cracking has resulted in poor accuracy of the 2D technology in identifying transverse and alligator cracking distress types. This type of false negative arises for two reasons:

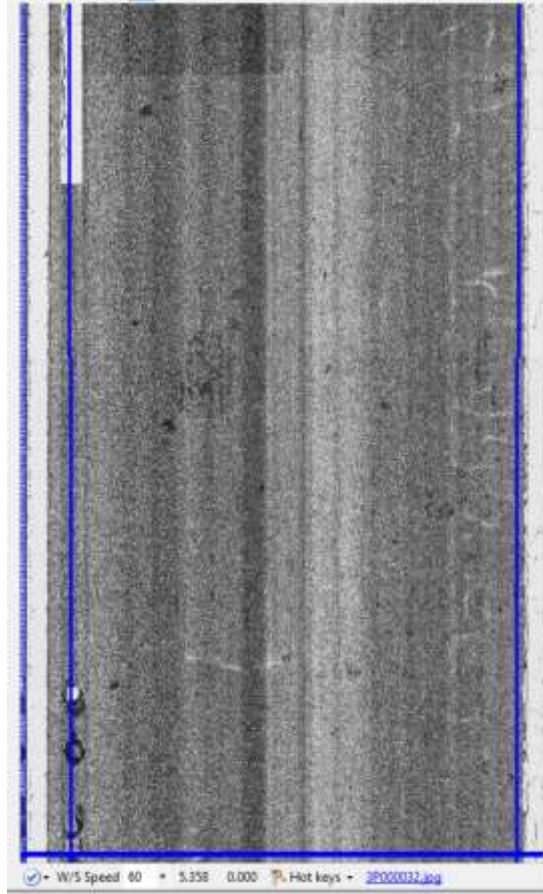
First, the sensitivity of crack detection algorithm is significantly impacted by the lighting condition when the pavement images are collected. In a lower lighting condition, the contrast between crack pixels and surrounding pavement surface pixels is reduced, therefore, small cracks are difficult to be detected (Figure 83).



**Figure 83. Low Contrast Between Crack and Surrounding Pixels Resulting in Missed Cracks**

Second, the crack detection algorithm may also fail to detect bright cracks on dark pavement surface (Figure 84) and cracks of thick width.





**Figure 84. White Alligator Cracks on Dark Pavement**

#### **4.3.6 Potentials and Limitations of the LRIS Technology**

The 2D LRIS technology has the following potentials:

1. The LRIS equipment is more affordable than the 3D LCMS equipment.
2. The run-to-run repeatability of crack detection from 2D images is acceptable.

However, there are several important limitations of the 2D LRIS technology:

1. The accuracy of crack detection from 2D images is very low (31 percent), as evidenced by the crack detection algorithm only detecting 18 percent of the cracks that were in the reference survey. Also, only 25 percent of the cracks detected from the 2D images were actually present in the reference survey.

2. The section-to-section consistency of crack detection from 2D images is very low.
3. Even excluding some outliers, significant amount of missed cracking has resulted in poor accuracy of the 2D technology in identifying cracking distress types.
4. When the pavement surface is damp, the area around the crack edges become darker in the 2D images and as a result, the crack detection algorithms result in exaggerated crack width measurements based on pixel intensities. This issue negatively impacts severity rating of cracking distresses.

#### **4.4 Conclusion and Recommendations**

This chapter described the efforts undertaken in Task 4 of this FDOT research project to evaluate the feasibility of the 2D LRIS technology for crack detection and distress identification. The findings of this effort can be summarized as follows:

1. While the results of 2D crack detection were comparable from run to run, there were a significant number of missed cracks when compared to the ground truth.
2. While the run-to-run repeatability of the 2D technology was acceptable in identifying the length of longitudinal and transverse cracks in most cases, the accuracy compared to the ground truth and section-to-section consistency of the 2D technology was very poor in identifying any type of cracking.

Based on the noted evaluation results, it is recommended that alternative technologies are considered for detection of cracks and the corresponding identification and quantification of flexible pavement surface distresses.

## CHAPTER 5 – FLEXIBLE PAVEMENT APPLICATION DESIGN

Task 5 of this research project included an evaluation of the existing survey methods, a gap analysis of the existing automated software, and the development of design recommendations for addressing identified gaps. This chapter is organized into five sections. Following this introduction, Section 5 describes the test sections used throughout the flexible pavement survey evaluation and software design process. Section 5.2 and Section 5.3 describe the manual windshield survey and the existing automated software results, respectively. The results of the two survey methods are compared in Section 5.4. Last, the gap analysis and design considerations for the automated flexible pavement distress identification software are described in Section 5.5.

Please note the following reference phrases in this chapter:

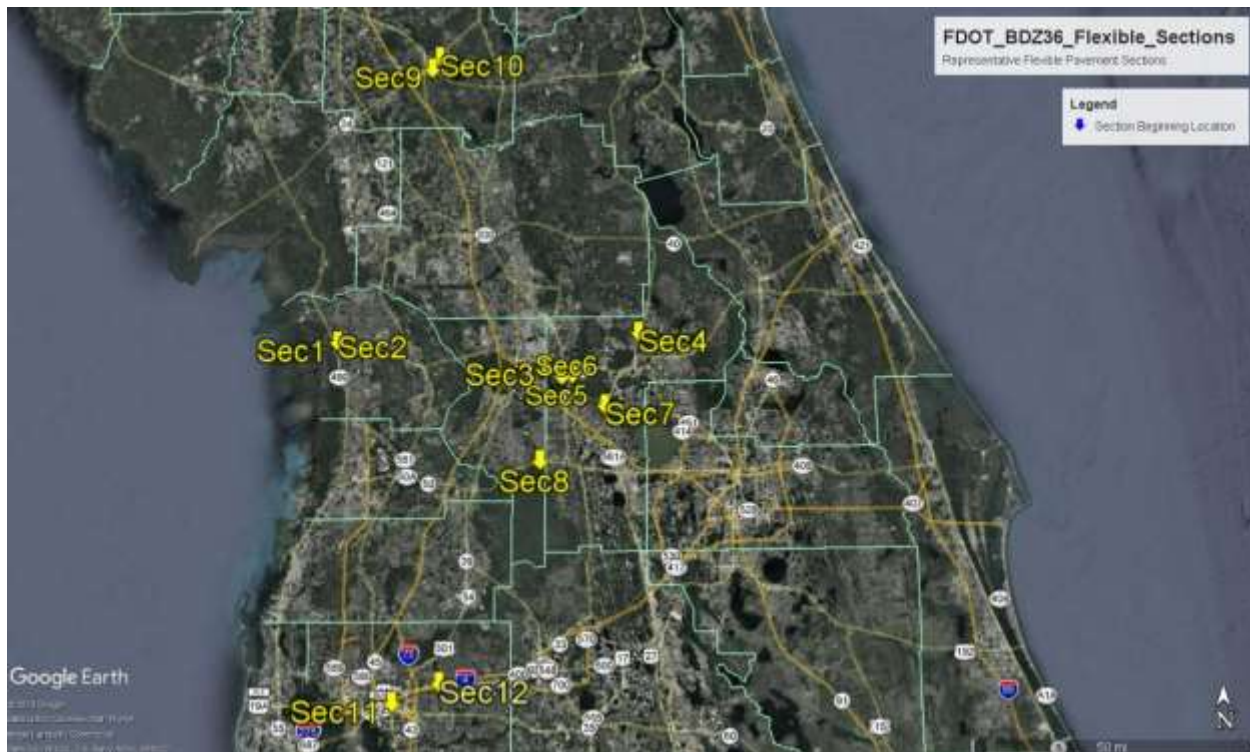
- “*Vision 3.1*”: this refers to Fugro’s Vision 3.1 software, which includes a machine learning algorithm for crack detection and an automated routine for distress classification and rating. This existing automated software was evaluated in Task 5 and the existing gaps were identified so that the software development activities in Task 6 could address these gaps.
- “crack detection”: this refers to the process of locating and marking the pavement surface defects from the collected imagery.
- “crack classification”: this refers to the process of classifying each detected crack into a specific crack type and assigning a severity level to it.
- “reference survey”: this refers to the semi-automated surveys conducted on one run of the collected pavement images, which serve as benchmarks when evaluating the automated software results. There are two reference surveys: one serving as benchmark for crack detection and one for crack classification and severity rating.

### 5.1 Representative Test Sections

The evaluation of the existing two distress survey methods included a comparison of the overall cumulative quantities of various distress types found in the existing FDOT manual windshield survey and a readily available existing automated software (Vision 3.1). To conduct this evaluation, FDOT engineers identified a set of 12 representative test sections that are each at least a standard evaluation length (0.1-mile-long) and contain several of the flexible pavement distresses in them. Table 16 and Figure 85 show the selected 12 flexible pavement sections.

**Table 52. Selected 12 Flexible Pavement Test Sections**

NO	COUNTY	SECTION ID	ROUTE	DIR	LANE	BMP	EMP	LNGTH
1	Baker	02050000	SR44	E	R2	0	0.604	0.604
2	Baker	02050000	SR44	W	L2	0	0.604	0.604
3	Collier	11010000	SR44	E	R2	0	1.592	1.592
4	Collier	11100000	SR19	N	R2	3.816	4.906	1.09
5	Collier	11002000	SR44	E	R2	1.183	2.276	1.093
6	Collier	11002000	SR44	E	R2	3.184	4.514	1.33
7	Collier	11080000	SR19	N	R1	0	0.925	0.925
8	Flagler	18020000	SR50	E	R1	5.356	6.421	1.065
9	Hendry	26050000	SR24	S	L2	3.367	6.095	2.728
10	Hendry	26050000	SR24	S	L2	6.095	7.67	1.575
11	Clay	10190000	SR400	E	R3	11.098	12.332	1.234
12	Clay	10190000	SR400	E	R3	20.407	21.476	1.069



**Figure 85. Selected 12 Flexible Pavement Test Sections**

## 5.2 Manual Windshield Survey

Three FDOT raters conducted a manual windshield distress survey of the 12 test sections according to the FDOT protocol. Each rater conducted the manual distress survey separately in a separate vehicle and according to the FDOT *Flexible Pavement*

*Condition Survey Handbook* (2017). The average, standard deviation, and coefficient of variation (COV) of each distress type at each severity level found on each test section has been documented in Appendix J.

A summary of the overall agreement among raters is presented in Table 53. The summary statistics show that there was a low level of agreement for any individual distress and severity. Some test sections exhibited minimal amounts of a particular distress type, and variation among raters for distress types with small quantities led to high values of COV and low levels of agreement. The results also show a higher level of agreement among the three raters when adding the quantities of class IB, class II, and class III cracks. This demonstrates the additional variability that is introduced to the survey when assigning distress severities to particular distress types.

**Table 53. Overall Agreement Among Raters in Manual Windshield Survey (See Appendix J for Details)**

Distress Type	Agreement Among Raters in Total Distress Amount, 100 - COV (%)	
	CW (Wheel Path Cracking)	CO (Cracking Outside Wheel Paths)
Class IB	-6%	-2%
Class II	11%	3%
Class III	3%	10%
Class IB + Class II + Class III	46%	34%
Raveling	-19%	1%
Patching	7%	0%

## 5.3 Automated Distress Survey Using Vision 3.1

In this chapter of the report, the results of crack detection and crack classification and severity rating using 3D pavement images are evaluated. The 3D data collection was conducted by Fugro using the Automatic Road Analyzer (ARAN) Laser Crack Measurement System (LCMS) equipment and the data were analyzed by Fugro staff using the readily available existing automated software (Vision 3.1) as part of the required activities for Purchase Order (PO) 10026557. For further information on the automated data collection and processing methodology, please refer to the final PO report in Appendix I. The following sections will describe the success metrics, the reference values, and the evaluation results.

### 5.3.1 Success Metrics

In the context of automated distress identification, effectiveness can be expressed in terms of accuracy of the software results when compared to a reference baseline, which

can be quantified by bias or average normalized error. Reliability of automated distress surveys is often expressed in terms of precision. Precision is a qualitative term that can describe the degree of repeatability of a measurement value on the same sample, or consistency in accuracy of measurement on different samples. Coefficient of variation of actual measurement values on the same sample is a quantitative estimate of repeatability. Standard deviation of error (standard error) is a quantitative estimate of consistency. The efficiency of each method is typically measured by the time it takes to conduct these measurements.

With respect to automated condition evaluations, the success metrics could be considered for two aspects of the process, first for the detection of individual surface defects (cracks), and second for the identification and quantification of the distresses in a distinct section.

The following are the success metrics used for evaluating the crack detection results:

- True Positives: length of correctly detected cracks
- False Positives: length of detected cracks that don't exist in the reference survey
- False Negatives: length of missed cracks
- Crack Validity: This statistic indicates the percentage of the detected cracks that was actually present in the reference survey, thereby expressing the validity of the cracks detected by algorithms.

$$Validity (\%) = 100 \times \frac{\text{correctly detected}}{\text{all detected}} = 100 \times \frac{\text{true positives}}{\text{true positives} + \text{false positives}}$$

- Crack Sensitivity (or Recall): This statistic represents the percentage of the cracks in the reference survey that was detected by the automated method, thereby expressing the sensitivity of the algorithms to existing cracks.

$$Sensitivity (\%) = 100 \times \frac{\text{correctly detected}}{\text{actual cracks}} = 100 \times \frac{\text{true positives}}{\text{true positives} + \text{false negatives}}$$

- Crack Detection Accuracy: This statistic is evaluated based on average normalized error (bias) of automatically detected crack length compared to the reference.  $\text{Accuracy (\%)} = 100 - \text{Bias (\%)}$
- Crack Detection Repeatability: This statistic is evaluated based on coefficient of variation (COV) of detected crack length among three runs (independent of the reference and averaged among the sections).  $\text{Repeatability (\%)} = 100 - \text{COV (\%)}$
- Crack Detection Consistency: This statistic is evaluated based on coefficient of variation (COV) of crack detection accuracy among 12 test sections.  $\text{Consistency (\%)} = 100 - [\text{Standard Deviation of Accuracy (\%)} / \text{Average Accuracy (\%)}]$
- Crack Detection Efficiency: This statistic is evaluated based on the time required for the automated crack detection.  $\text{Efficiency (second per foot)} = \text{time for cracking detection} / \text{total length}$

The following are the success metrics used for evaluating the crack classification and severity rating results based on the overall cumulative amount of each crack type among different test sections and multiple runs:

1. Crack Classification Accuracy: This statistic is evaluated based on average error (bias) with respect to the reference distress survey values for each crack type.

$$\text{Accuracy (\%)} = 100 - \text{Bias (\%)}$$

2. Crack Classification Repeatability: This statistic is evaluated based on coefficient of variation (COV) of automatically identified cracking among three runs for each crack type (independent of the reference and averaged among the sections).

$$\text{Repeatability (\%)} = 100 - \text{COV (\%)}$$

3. Crack Classification Consistency: This statistic is evaluated based on coefficient of variation (COV) of crack classification accuracy among 12 sections for each crack type.

$$\text{Consistency (\%)} = 100 - [\text{Standard Deviation of Accuracy (\%)} / \text{Average Accuracy (\%)}]$$

4. Crack Classification Efficiency: This statistic is evaluated based on the time required for the automated distress survey.

Efficiency (second per foot) = time for cracking detection, classification, and rating divided by the total length.

### 5.3.2 Reference Surveys

Two reference surveys were created for this evaluation:

1. Crack Detection Reference: the Pavemetrics LCMS crack detection algorithm was used to generate a baseline crack map and then a Fugro data technician reviewed all the images in one run (run number 1 out of the three collected runs) of the 12 test sections and modified the crack maps. False negatives (missed cracks) were mapped, false positives were deleted, and cracks with incorrect extent (length or area) were modified to reflect the actual cracks that can be seen on the 3D intensity and range (depth) images and with assistance from the ROW images.
2. Crack Classification Reference: a reference distress survey was manually created by one Fugro engineer using the collected images, and another Fugro technician reviewed the results to reach a consensus for the reference survey.

The crack detection reference was used to evaluate the effectiveness of the crack detection algorithm and the crack classification reference was used to evaluate the effectiveness of the distress classification and rating routine.

### 5.3.3 Evaluation Limitations

The evaluation was conducted considering the following limitations of this analysis:

1. The 12 test sections were selected as representative of the actual pavement surfaces found across Florida. With such a small sample, it is possible that not all the actual pavement network is represented in this study. Every effort was made to select a representative sample. However, the budgetary and schedule limitations of this project would not allow for collection and processing of data across a wider network.
2. Vision 3.1 as it stands does not exactly differentiate between the crack types as defined in the FDOT *Flexible Pavement Condition Survey Handbook* (2017), because those definitions were originally intended for human raters and not for



computers. Vision 3.1 uses crack angle to differentiate between longitudinal and transverse cracks, and crack density in a given area to differentiate between single linear cracks and an area of alligator cracking. Therefore, the error compared to the reference is estimated by comparing the total amount of automatically identified longitudinal and transverse cracks to the sum of the single and branch cracks manually identified in the reference survey. Similarly, the total amount of automatically identified alligator cracking is compared to the total area of the alligator cracks manually identified in the reference survey.

3. This study is mainly focused on cracking distresses and patching and raveling were not considered in this evaluation. The 3D technology provides pavement surface macro-texture measurements which could potentially be used for identifying raveling. However, these texture measurements need to be calibrated to corresponding areas of raveling identified by experienced raters.

#### **5.3.4 Evaluation of Automatically Detected Crack Quantities**

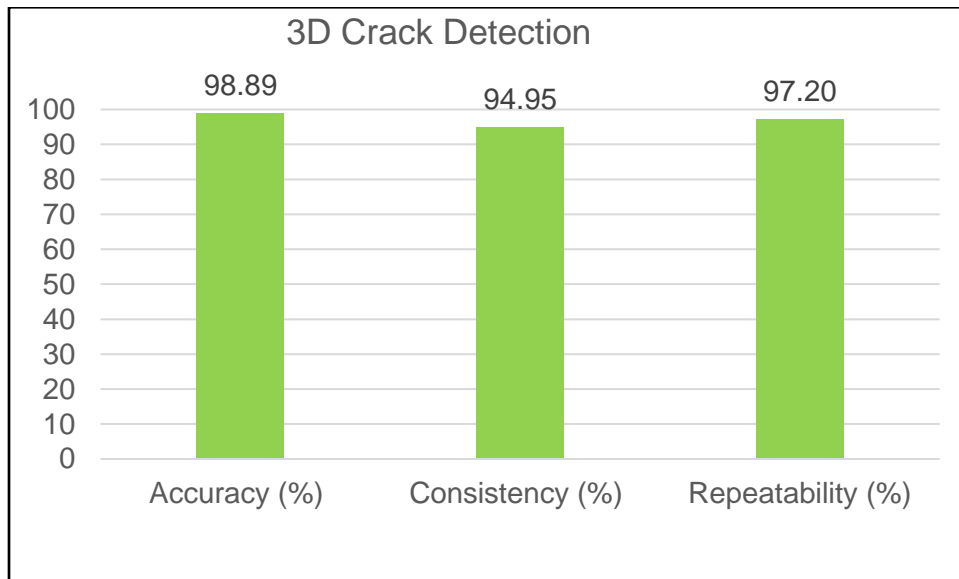
Table 54 shows the true positives, false positives, false negatives, validity, and sensitivity of the automated crack detection using the Vision 3.1 (machine learning algorithm) on 3D images. This table includes the crack detection results on run number 1 of the 3 runs. This table indicates that on average, about 75 percent of the automatically detected cracks were actually present on the pavement surface (Validity). Also, on average, about 89 percent of the cracks in the reference crack map were automatically detected from 3D images (Sensitivity).

In Table 54, the yellow highlighted cells indicate outlier test sections with significant false positives (more than 50% of the reference). It is evident that in sections number 3, 7, and 9, Vision 3.1 has demonstrated a significant amount of false positive. This is due to two reasons. First, some patching area boundaries and Automated Vehicle Counter (AVC) loops and Weigh-In-Motion (WIM) devices being falsely detected as cracks. Second, the amount of cracking in the reference survey for these three sections is lower compared to other sections and as a result, the errors seem higher. Excluding sections 3, 7, and 9, crack detection validity is about 91 percent and crack detection sensitivity is approximately 91 percent.

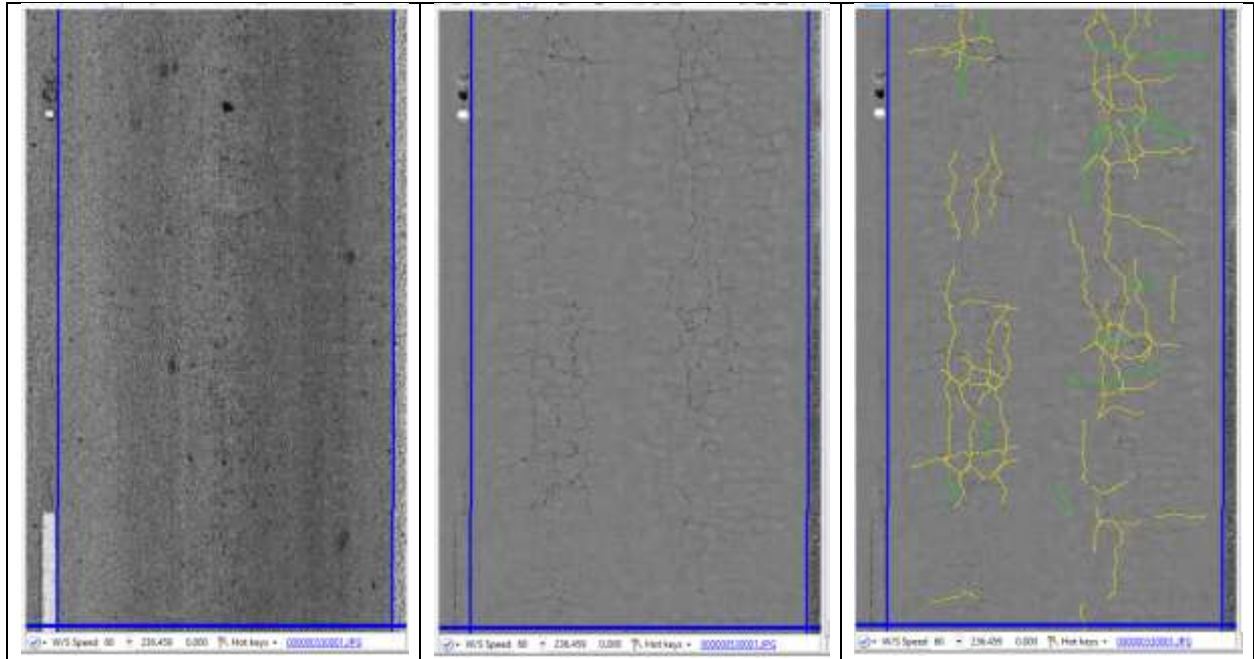
In addition to the crack detection verification results in Table 54, other crack detection success metrics including accuracy, consistency, and repeatability of Vision 3.1 are illustrated in Figure 86. When excluding the outlier sections (sections 3, 7, and 9), the accuracy (100 - Bias) of Vision 3.1 in crack detection is about 99 percent. The run-to-run repeatability exhibited 97 percent agreement among runs. Vision 3.1 is showing high consistency of results on different sections, about 95 percent agreement in crack detection accuracy among 12 sections.

**Table 54. Verification of Crack Detection on 3D images Using Vision 3.1**

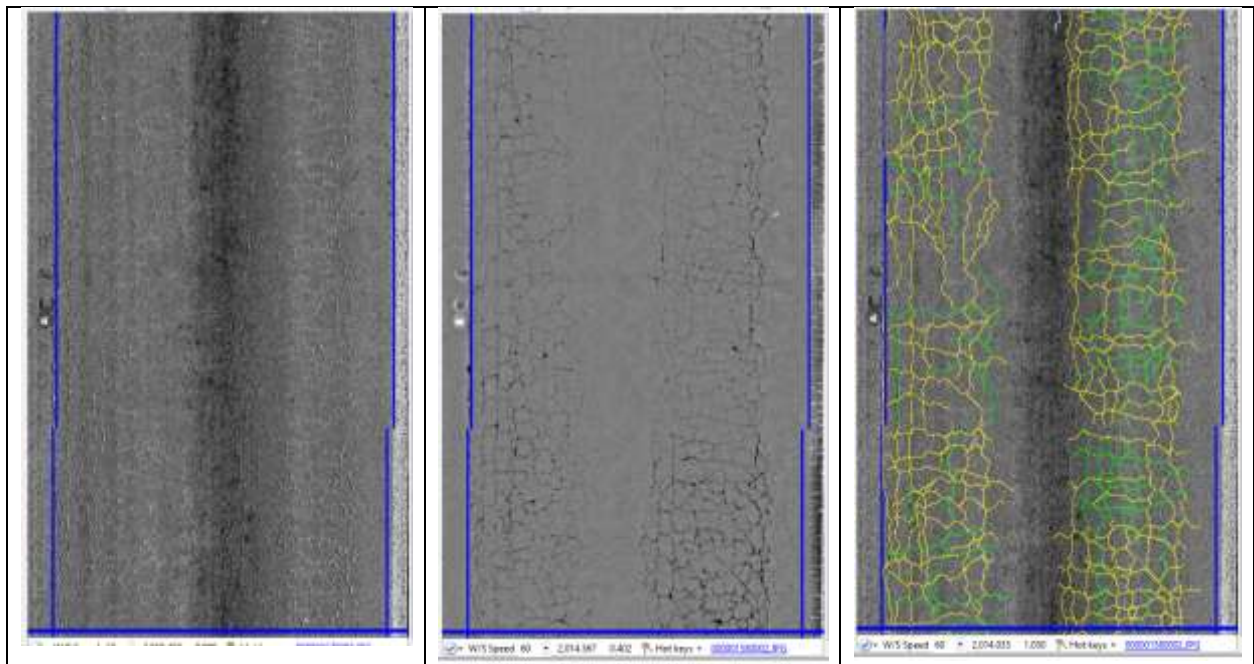
Test Section	Reference (ft)	Crack Detection Results			Crack Validity (%)	Crack Sensitivity (%)
		True Positives (ft)	False Positives (ft)	False Negatives (ft)		
1	22,944.22	18,464.62	2,762.11	4,479.60	86.99	80.48
2	26,741.89	24,873.49	1,217.80	1,868.40	95.33	93.01
3	132.74	126.10	824.84	6.64	13.26	94.99
4	14,823.69	12,015.20	1,429.99	2,808.49	89.36	81.05
5	68,726.86	65,286.40	3,453.19	3,440.46	94.98	94.99
6	112,892.60	102,199.75	11,059.70	10,692.85	90.24	90.53
7	809.34	687.92	1,820.47	121.42	27.42	85.00
8	27,185.46	23,990.87	2,097.65	3,194.59	91.96	88.25
9	3,993.09	2,881.59	6,082.98	1,111.50	32.14	72.16
10	36,631.86	38,825.92	1,803.39	(2,194.06)	95.56	105.99
11	30,517.80	27,386.58	4,025.66	3,131.22	87.18	89.74
12	29,327.95	28,174.06	3,057.05	1,153.89	90.21	96.07
Total Average					74.55	89.36
Average Excluding Sections 3, 7, and 9					91.31	91.12

**Figure 86. Crack Detection Success Metrics for Vision 3.1**

To better demonstrate the capability of 3D technology in detecting surface cracks, two example locations have been selected. Figure 87 and Figure 88 show the 3D crack detection results for the two example locations.



**Figure 87. Example LCMS Intensity (left), Range (center), and Detected Crack Map (right)**



**Figure 88. Example LCMS Intensity (left), Range (center), and Detected Crack Map (right)**

### **5.3.5 Evaluation of Automatically Classified Cracking Quantities**

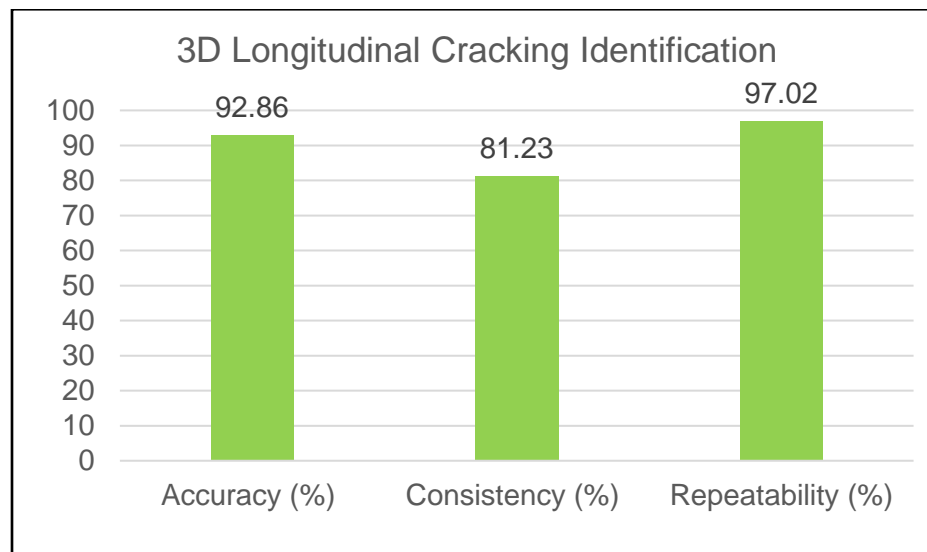
In this section, the results of Vision 3.1 in terms of crack classification are evaluated. Vision 3.1 records the amount of time that each batch processor had spent on each test

section to conduct an automated survey. The automated crack detection, crack classification, and severity rating took about 6 seconds per image frame for the 3D images. The majority of the processing time is consumed during the crack detection time. The classification and severity rating processes take only about 0.05 seconds per image frame. These time records have been achieved with an Intel Core i5 3.3GHz CPU and an 8GB RAM, with a Windows 10 64-bit operating system.

### Evaluation of Automatically Identified Longitudinal, Transverse, and Alligator Cracking

In this section, the evaluation is conducted based on the amount of automatically identified Longitudinal, Transverse, and Alligator cracking. It should be noted that Vision 3.1 uses crack angle to differentiate between longitudinal and transverse cracks, and crack density in a given area to differentiate between single linear cracks and an area of alligator cracking. Therefore, the normalized error compared to the reference survey is estimated by comparing the total amount of automatically identified longitudinal or transverse cracks to the sum of single and branch cracks (manually identified in the reference survey) that are positioned longitudinally or transversely. Similarly, the total amount of automatically identified alligator cracking is compared to the sum of alligator and block cracks manually identified in the reference survey.

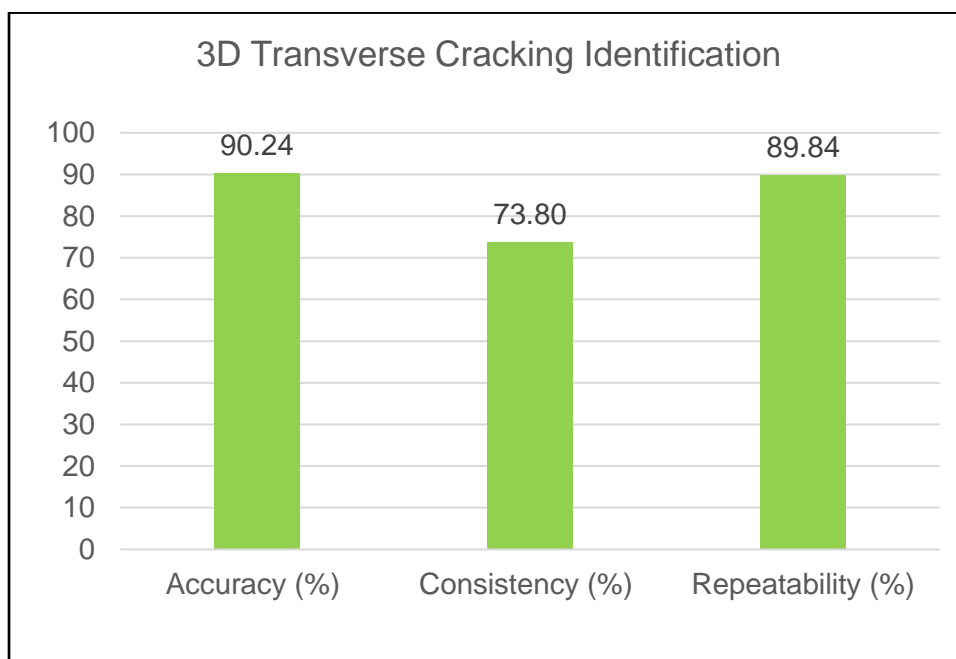
Figure 89 shows the success metrics for automatically identifying Longitudinal cracks. Excluding the outlier sections (test sections with minimal amount of longitudinal cracking in the reference survey: sections 3, 7, and 9), the automated longitudinal cracking identification has demonstrated about 93 percent accuracy. The results show a positive bias (on average +7%; see PO 10026557 Report in Appendix I for details) indicating more automatically identified longitudinal cracks compared to the reference survey.



**Figure 89. Longitudinal Cracking Success Metrics for Vision 3.1**

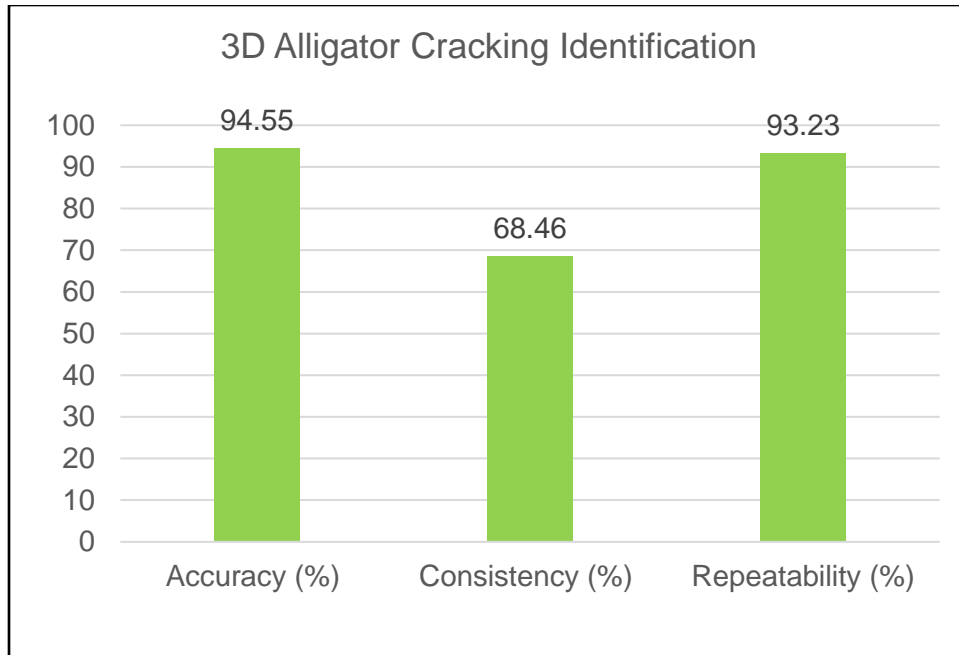
On average, there is about 97 percent run-to-run repeatability in the length of automatically identified longitudinal cracks. There is about 81 percent section-to-section consistency in the accuracy in automatically identifying the length of longitudinal cracks.

Figure 90 shows the success metrics for automatically identifying Transverse cracks. Excluding the outlier sections (test sections with minimal amount of transverse cracking in the reference survey: sections 3, 7, and 9), the automated transverse cracking identification have demonstrated about 90 percent accuracy. The results show a negative bias (on average -10%; see PO 10026557 Report in Appendix I for details) indicating less automatically identified transverse cracks compared to the reference survey. On average, there is about 90 percent run-to-run repeatability in the length of automatically identified transverse cracks. There is about 74 percent section-to-section consistency in the accuracy in identifying transverse cracking.



**Figure 90. Transverse Cracking Success Metrics for Vision 3.1**

Figure 91 shows the success metrics for automatically identifying Alligator cracks. Excluding the outlier sections (test sections free of alligator cracking: sections 3, 7, and 9), the automated alligator cracking identification has demonstrated about 95 percent accuracy. The results show a negative bias (on average -5%; see PO 10026557 Report in Appendix I for details) indicating less automatically identified alligator cracks compared to the reference survey. On average, there is about 93 percent run-to-run repeatability in the automatically identified alligator cracking areas. There is about 68 percent section-to-section consistency in the accuracy in automatically identifying the area of alligator cracks.



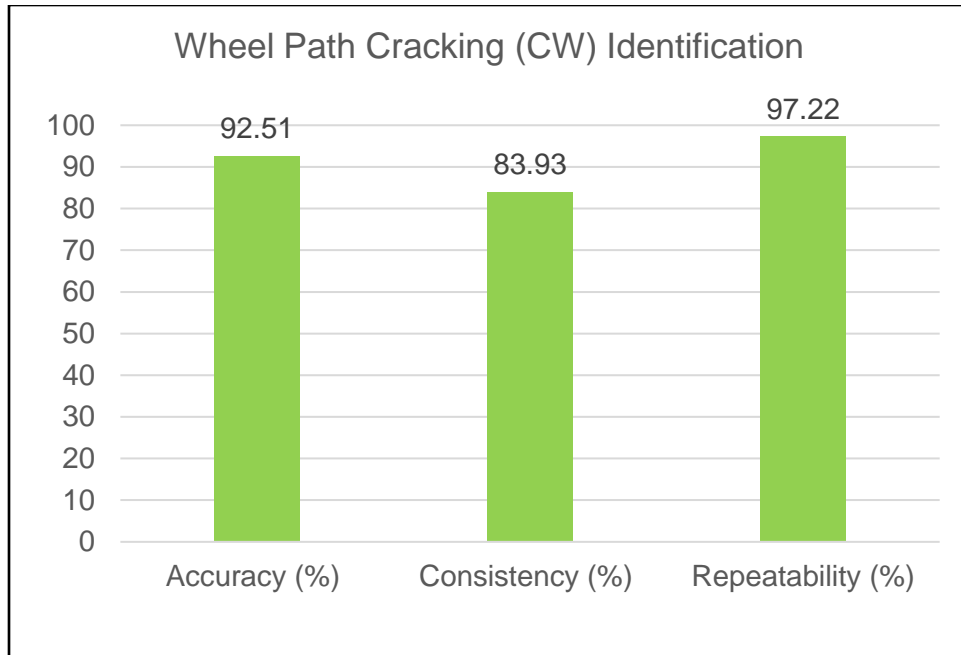
**Figure 91. Alligator Cracking Success Metrics for Vision 3.1**

#### **Evaluation of Automatically Identified Wheel Path and Non-Wheel Path Cracking**

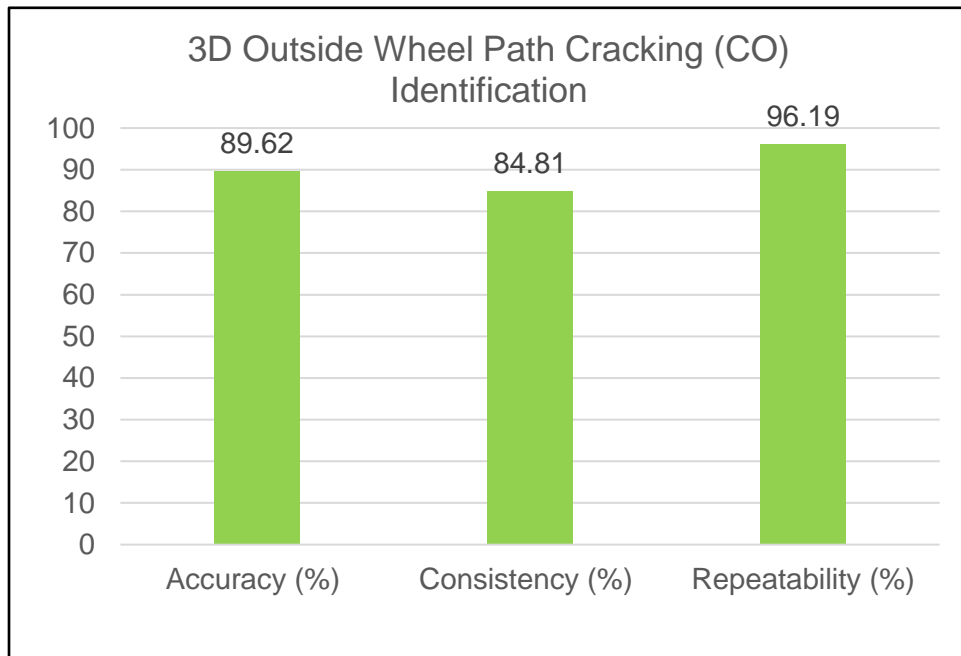
In this section, the reference rating results were converted to cracking within the wheel path (CW) and outside the wheel path (CO) using a SQL code. The total amount of cracking within the wheel paths (CW) was calculated by adding the longitudinal, transverse, and alligator cracking areas. The longitudinal and transverse cracking areas were calculated by multiplying their length by one foot, as specified in the *FDOT Flexible Pavement Condition Survey Handbook* (2017).

Figure 92 shows Vision 3.1 results for CW distresses from 3D images. The accuracy in determining the CW distresses is about 92 percent. The results show a negative bias (on average -7%; see PO 10026557 Report in Appendix I for details) indicating less automatically identified CW cracks compared to the reference survey. The run-to-run repeatability in determining the CW distresses is about 97 percent. The section-to-section consistency in determining the CW distresses is about 84 percent.

Figure 93 shows Vision 3.1 results for CO distresses from 3D images. The accuracy in determining the CO distresses is about 89 percent. The results show a negative bias (on average -10%; see PO 10026557 Report in Appendix I for details) indicating less automatically identified CO cracks compared to the reference survey. The run-to-run repeatability in determining the CO distresses is about 96 percent. The section-to-section consistency in determining the CO distresses is about 85 percent.



**Figure 92. Wheel Path Cracking (CW) Success Metrics for Vision 3.1**



**Figure 93. Outside Wheel Path Cracking (CO) Success Metrics for Vision 3.1**

## Automatically Identified Cracking Summary

Table 55 provides the summary statistics for the automated distress survey results using Vision 3.1 on 3D images. As it is evident from this table, the average accuracy compared to the reference survey and the run-to-run repeatability of Vision 3.1 in identifying cracking distress types are above 90% in almost all cases. One reason for the high accuracy and repeatability is that cracks from all severity levels are categorized in the same group based on crack type. However, there is less consistency in Vision 3.1 results across the multiple test sections, especially regarding alligator cracking.

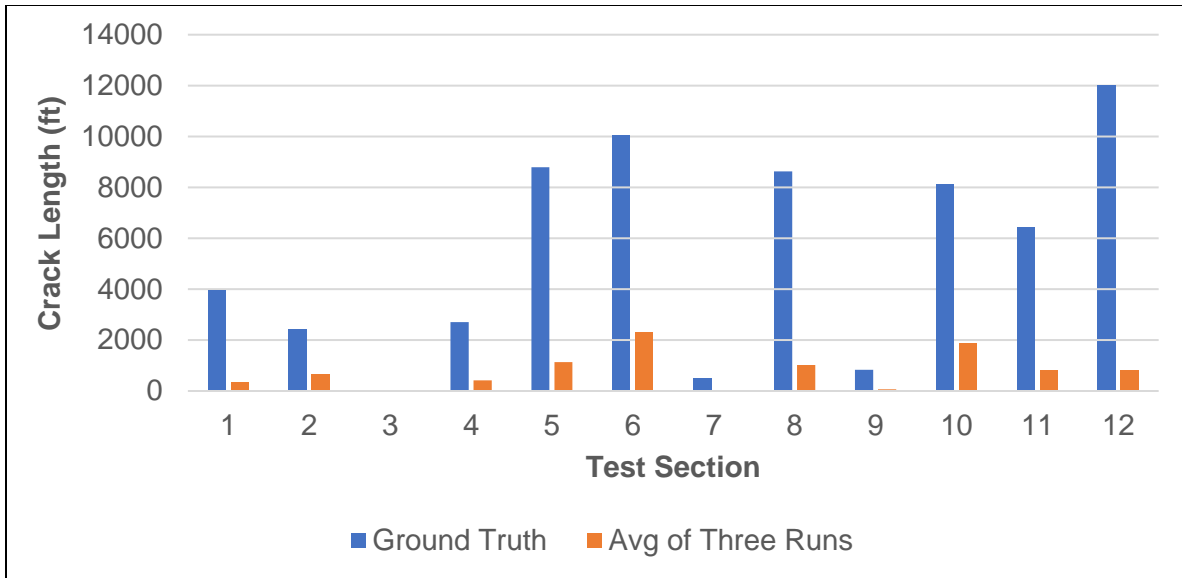
**Table 55. Summary Statistics for Vision 3.1 Results from 3D Images**

<b>Distress</b>	<b>Accuracy (%)</b>	<b>Section-To-Section Consistency (%)</b>	<b>Run-To-Run Repeatability (%)</b>
Longitudinal Cracking	92.86	81.23	97.02
Transverse Cracking	90.24	73.80	89.84
Alligator Cracking	94.55	68.46	93.23
Wheel Path Cracking (CW)	92.51	83.93	97.22
Non-Wheel Path Cracking (CO)	89.62	84.81	96.19

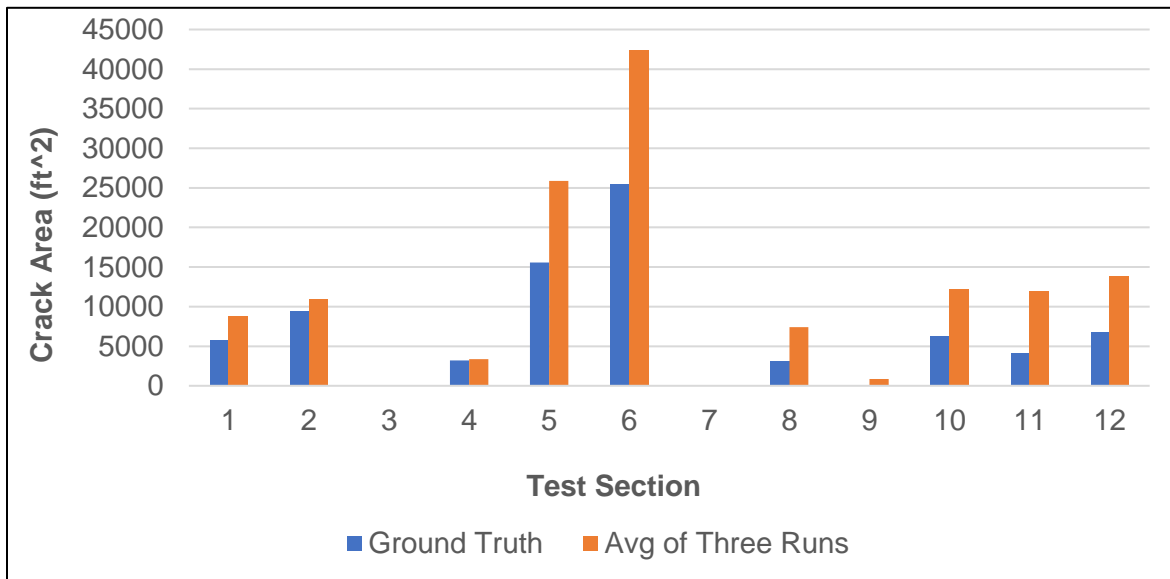
### 5.3.6 Evaluation of Automatically Rated Crack Severities

Vision 3.1 was used to automatically rate the crack severities for each of the 12 test sections. Vision 3.1 uses average crack width measurement to determine crack severities according to the FDOT *Flexible Pavement Condition Survey Handbook* (2017). Figure 94, Figure 95, and Figure 96 compare Vision 3.1 results to those of the reference survey for severity levels 1B, II, and III, respectively (note: vertical axis ranges vary). Class 1B are hairline cracks that are less than or equal to  $\frac{1}{8}$  inch (3.18 mm) wide, Class II are cracks greater than  $\frac{1}{8}$  inch (3.18 mm) and less than or equal to  $\frac{1}{4}$  inch (6.35 mm) wide, and Class III are cracks greater than  $\frac{1}{4}$  inch (6.35 mm) wide. Note that the extent of Class 1B cracks is the sum of the length of single and branch cracks. But the extent of the Class II and Class III cracks is the sum of the area of single, branch, and alligator cracks, where the single and branch cracks are assumed to have a width of one foot.





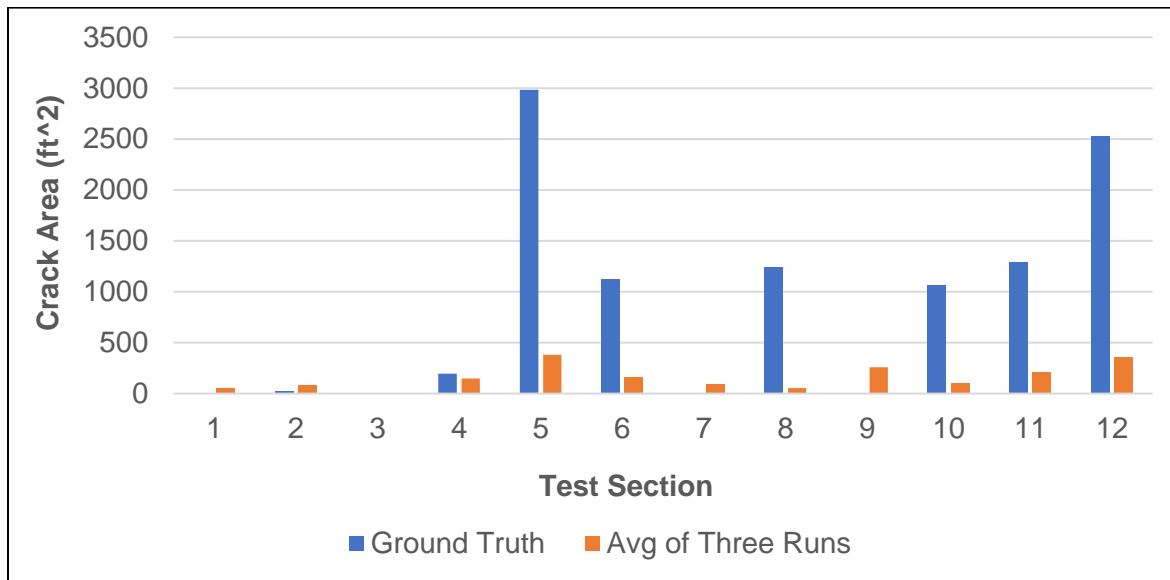
**Figure 94. Severity Level 1B Rating Results for Vision 3.1**



**Figure 95. Severity Level II Rating Results for Vision 3.1**

The figures demonstrate that Vision 3.1 rates the majority of cracks as severity level II. It should be noted that the manual assignment of severity levels in the reference survey is always more subjective than classification of cracks into single, branch, and alligator distress types. This is because it is easier to visually differentiate between single, branch, and alligator cracks than it is to visually differentiate between various crack widths. In the reference survey, the rater can use the measurement tool in Vision 3.1 to get familiar with the visual representation of various crack widths on the image. The

rater then relies on this visual representation to manually rate the severity levels of each identified cracking distress.



**Figure 96. Severity Level III Rating Results for Vision 3.1**

## 5.4 Comparison of Different Survey Methods

This section compares the results of the manual windshield surveys conducted by FDOT distress raters, Vision 3.1 on 3D images, and the reference survey described in Section 5.3.2. The results compared in this section include percent wheel path cracking (CW) and percent non-wheel path cracking (CO). While patching and raveling are typically included in the total cracking percentages, Vision 3.1 results presented do not include patching or raveling. The outlier test sections discussed previously (sections 3, 7, and 9) were excluded from this analysis as well.

### 5.4.1 Success Metrics

The following are the success metrics used for comparing different survey methods based on the overall cumulative amount of each crack type among different test sections and multiple runs:

1. Crack Classification Accuracy: This statistic is evaluated based on average error (bias) with respect to the reference distress survey values for each crack type.

$$\text{Accuracy (\%)} = 100 - \text{Bias (\%)}$$

2. Manual Windshield Survey Reproducibility: This statistic is evaluated based on coefficient of variation (COV) of manually identified cracking among three raters for each crack type (independent of the reference and averaged among the sections).

$$\text{Reproducibility (\%)} = 100 - \text{COV (\%)}$$

3. Automated Crack Classification Repeatability: This statistic is evaluated based on coefficient of variation (COV) of automatically identified cracking among three runs for each crack type (independent of the reference and averaged among the sections).

$$\text{Repeatability (\%)} = 100 - \text{COV (\%)}$$

4. Crack Classification Consistency: This statistic is evaluated based on coefficient of variation (COV) of crack classification accuracy among 12 sections for each crack type.

$$\text{Consistency (\%)} = 100 - [\text{Standard Deviation of Accuracy (\%)} / \text{Average Accuracy (\%)}]$$

#### 5.4.2 Comparison Results on Overall Section Cracking Quantities

Table 56 and Table 57 show the success metrics for the manual windshield survey and Vision 3.1, respectively, compared to the reference survey for the total amounts of CW and CO cracking (all severities) in each section.

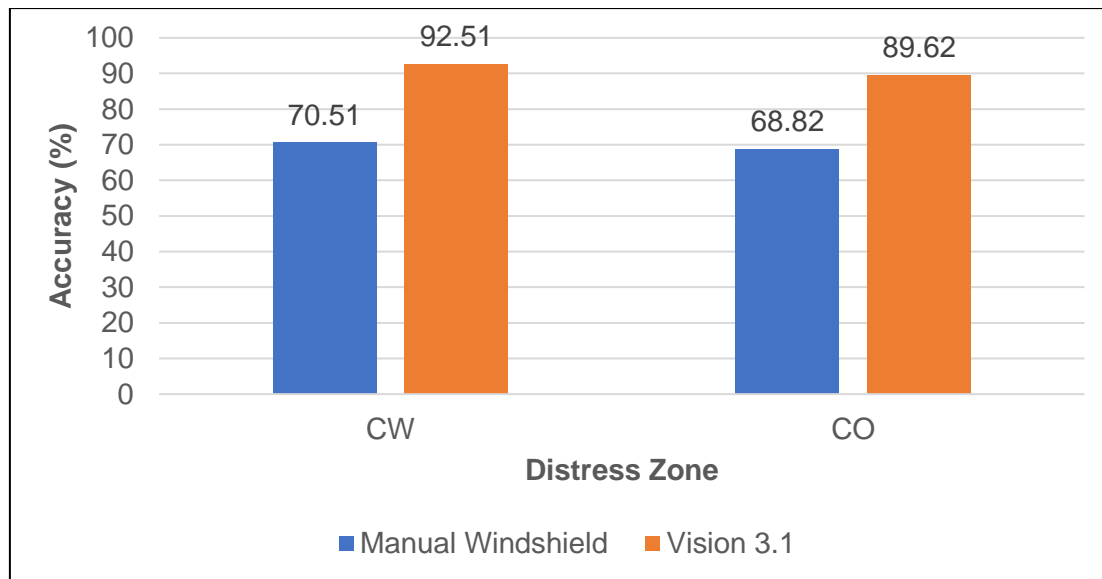
**Table 56. Comparison of Manual Windshield Survey Rating to the Reference Survey**

Metric	CW	CO
Accuracy (%)	70.51	68.82
Section-To-Section Consistency (%)	98.48	98.61
Rater-To-Rater Reproducibility (%)	50.71	37.36

**Table 57. Comparison of Vision 3.1 Rating to the Reference Survey**

Metric	CW	CO
Accuracy (%)	92.51	89.62
Section-To-Section Consistency (%)	99.85	99.85
Run-To-Run Repeatability (%)	97.22	96.19

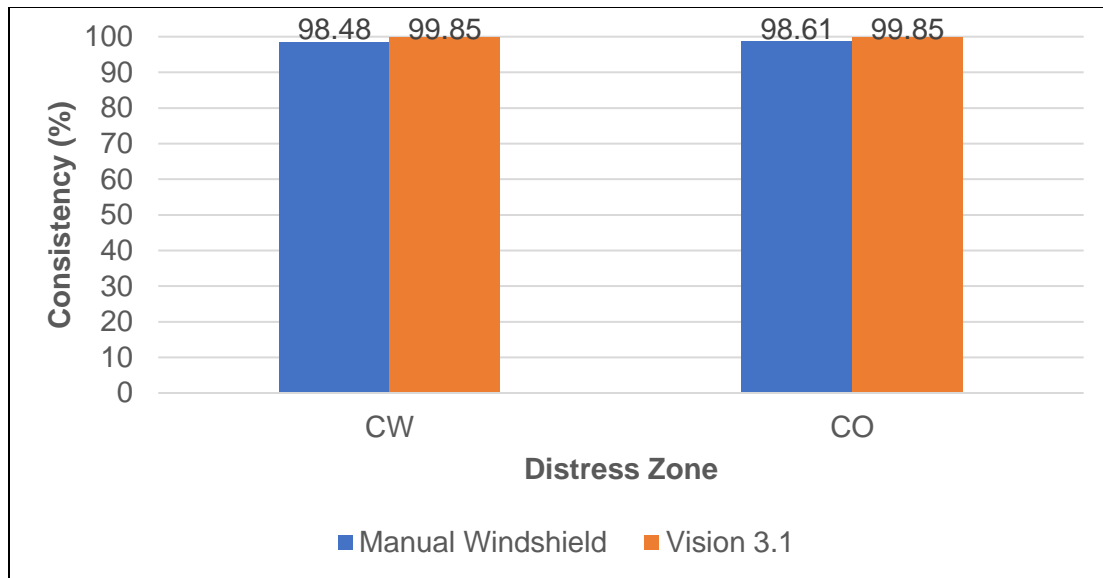
Figure 97 compares the accuracy of the two rating methods as calculated by 100 minus the absolute value of bias (%).



**Figure 97. Comparison of Different Methods in terms of Accuracy**

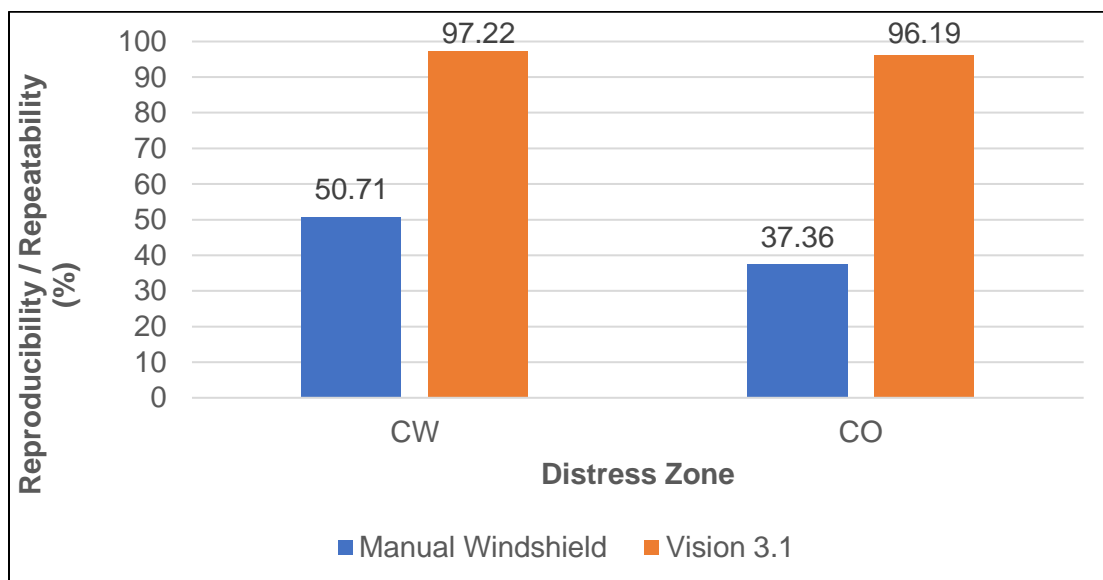
The results indicate that Vision 3.1 is relatively more successful in detecting and identifying the extent of CW cracking (accuracy 93%) compared to CO cracking (accuracy of 90%). The accuracy of Vision 3.1 for both CW and CO cracking (93% and 90%, respectively) is higher than that of the manual windshield survey (71% and 69%, respectively).

Figure 98 shows a comparison among the methods in terms of consistency as calculated by 100 minus the coefficient of variation of accuracy among 12 test sections. The manual windshield survey is showing a slightly lower consistency compared to Vision 3.1. However, both methods show high consistency among the test sections, excluding the outliers (sections 3, 7, and 9).



**Figure 98. Comparison of Different Methods in terms of Consistency**

Figure 99 compares the reproducibility of the manual windshield survey to the repeatability of Vision 3.1 using 100 minus the coefficient of variation of distress amounts among the three raters/runs. Vision 3.1 is showing much higher repeatability among multiple runs when compared to the reproducibility among multiple raters in the manual windshield survey.



**Figure 99. Comparison of the Reproducibility of Manual Windshield Survey to the Repeatability of Vision 3.1 Results**

## **5.5 Gap Analysis and Design Considerations**

In this section of the report, the gaps in the performance of Vision 3.1 are identified. In addition, a potential design consideration is offered as the solution to address each identified gap.

### **5.5.1 Identified Gaps**

Based on the results of Vision 3.1 evaluations on 3D images, it is evident that Vision 3.1 has an adequate performance in detecting pavement surface cracks, but it is not performing well regarding classification and rating of the detected cracks into corresponding distress types and severities according to the FDOT *Flexible Pavement Condition Survey Handbook* (2017). Regarding crack detection, it should be noted that on three test sections (number 3, 7, and 9), the total length of false positives was more than 50% of the length of actual existing cracks in the reference. But the length of actual existing cracks in the reference was itself very low.

#### **Setup Parameters**

To utilize the classification and rating functions of Vision 3.1, many parameters must be input by the user. The reason for this was that by design, this software was supposed to have the flexibility to be used on a variety of pavement surfaces in various conditions across the world. A wide range of setup parameters could not only introduce inconsistency to results if different parameters are selected by different users, but it could also make the analysis seem overly complicated and challenging. Fugro will develop a batch processor for FDOT crack classification and rating, which will require a minimal number of setup parameters. Additionally, the batch processor will eliminate the need to establish a distress schema in Vision 3.1 since the batch processor would be tailored to the FDOT distress identification protocol.

#### **Crack Classification Issues**

Vision 3.1 classifies crack types based on a table of coordinates for each crack node. Vision 3.1 uses the table to determine the crack angle to differentiate longitudinal from transverse cracks and uses density of cracking in a given area to identify alligator cracking areas. While the software displays a crack map on the user interface, the crack map is not used for distress classification purposes. Fugro will develop a crack map, which can be used for the distress classification process.

Vision 3.1 does not include the “Branch Crack” crack type, and it does not have the capability of classifying branch cracks. Using a crack map, single and branch crack distress types can be identified based on geometric properties in addition to crack angle. Also, alligator cracking can be detected using characteristics other than crack

density. Developing a crack map will enable new algorithms to increase the accuracy and consistency of distress classification.

While there may be potential to improve the block cracking classification capabilities of Vision 3.1, block cracking will not be included in FDOT automated classification processors. Due to a limited amount of block cracking across Florida highways, there are currently no test sections that exhibit sufficient block cracking, with which to evaluate automatic results.

### **Crack Severity Rating Issues**

As illustrated in Section 5.3.6, the automatically rated crack severities do not align well with the severities determined using the reference survey. Since distress severities are primarily dependent on crack width, the crack width determined using Vision 3.1 is likely insufficient for effectively rating distress severities according to the FDOT protocol. Fugro will improve the crack width detection algorithm to improve the automatic rating results.

### **5.5.2 Recommended Design Solutions**

Table 58 summarizes the identified gaps in Vision 3.1 and corresponding recommended solutions. Based on this gap analysis, the following development efforts will be considered for Task 6 of this project. The algorithm logic design is briefly explained for each development effort.

**Table 58. Identified Gaps and Recommended Solutions**

<b>Number</b>	<b>Gap in Vision 3.1</b>	<b>Recommended Solution</b>
1	Numerous setup parameters	Develop batch processor with minimal setup parameters
2	Distress classification based on crack angle and density has issues with classifying alligator cracks Vision 3.1 cannot classify branch cracks	Develop crack map for use during distress classification Develop methodology to classify alligator cracks based on closed cells Develop methodology to classify branch cracks based on joint pixels
3	Block crack classification is not available	No recommendation due to lack of test sections which exhibit block cracking
4	Inaccurate distress severity rating	Develop improved crack width algorithm for distress severity rating purposes

## Batch Processor Development

A batch processor is designed to be developed as a plugin for Vision 3.1. The batch processor shall include the improvements described below and developed in Task 6 of this project. The batch processor shall be tailored to the FDOT distress rating protocol.

### Crack Map

1. Create a binary image using the detected crack node coordinates in which white pixels represent cracks and all other pixels are black based.
2. The binary image includes redundant information which can be reduced using the following morphological processes (see Figure 100):
  - i. Resizing: keeps the essential information but improves the processing speed by reducing the size and number of pixels.
  - ii. Dilation: enlarges the boundaries of regions of white pixels. This process reduces the size of gaps within each region, and some gaps are filled completely to establish closed crack cells that can be categorized as alligator cracking.
  - iii. Skeletonizing: reduces the white regions in the binary image to a skeletal remnant that preserves the extent and connectivity of the original. The thickness of features in the skeleton is one pixel.

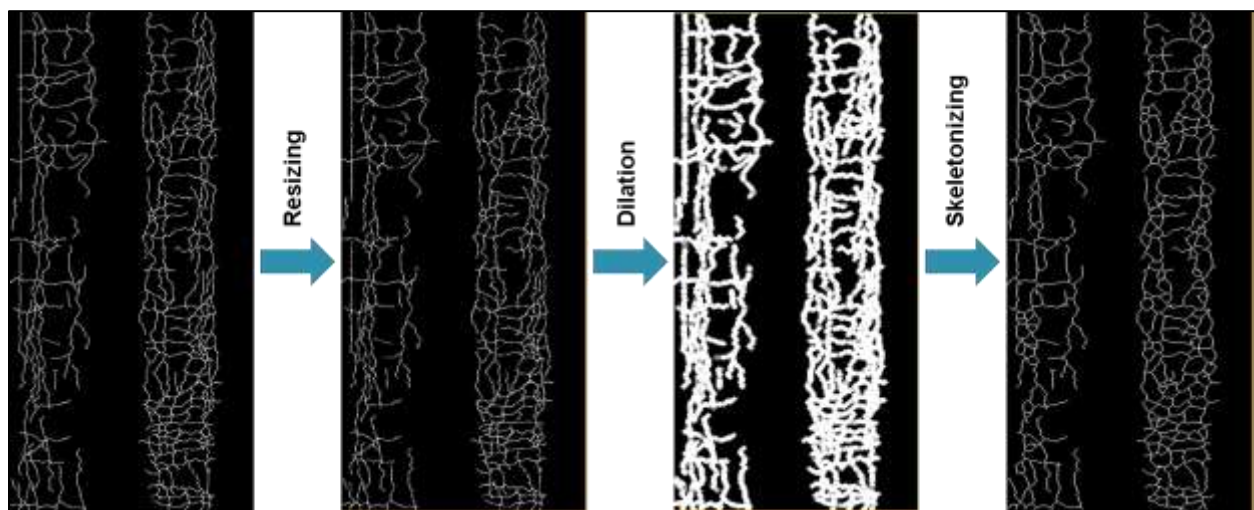
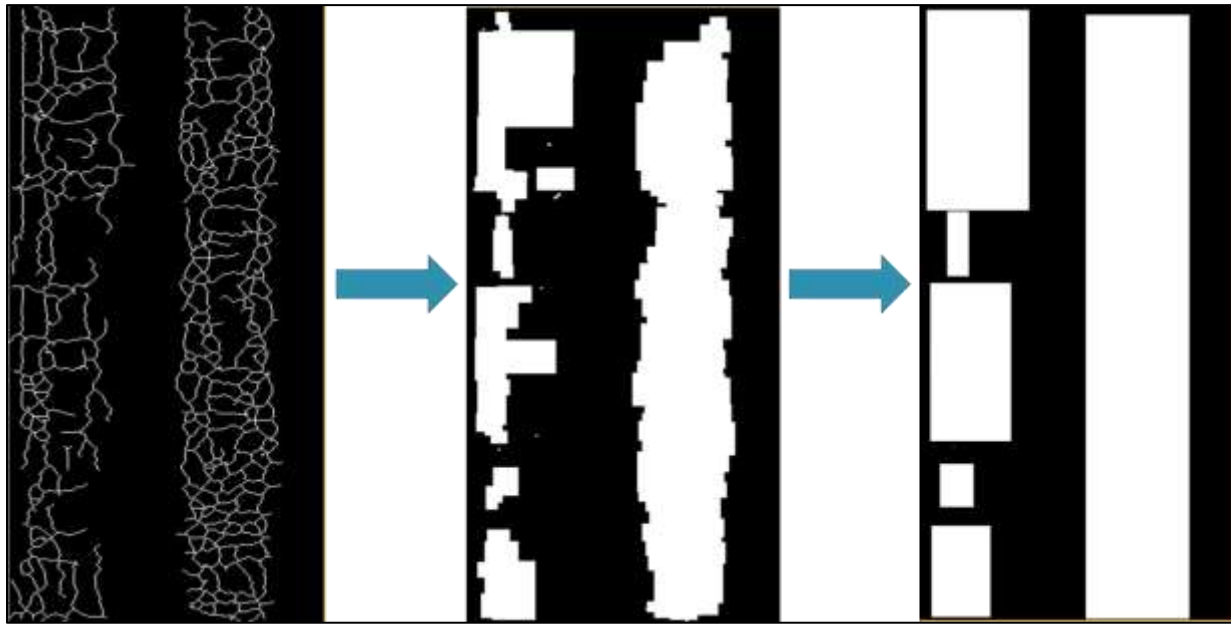


Figure 100. Example Showing Resizing, Dilation, and Skeletonizing to Create Crack Map



### Alligator Cracking Classification

The crack map is analyzed to locate all regions in which the cracks have formed a closed cell. Connected closed-cell regions are combined into a bounding box which represents the area of alligator cracking (see Figure 101).



**Figure 101. Example Showing Extraction of Alligator Cracking Areas from the Crack Map**

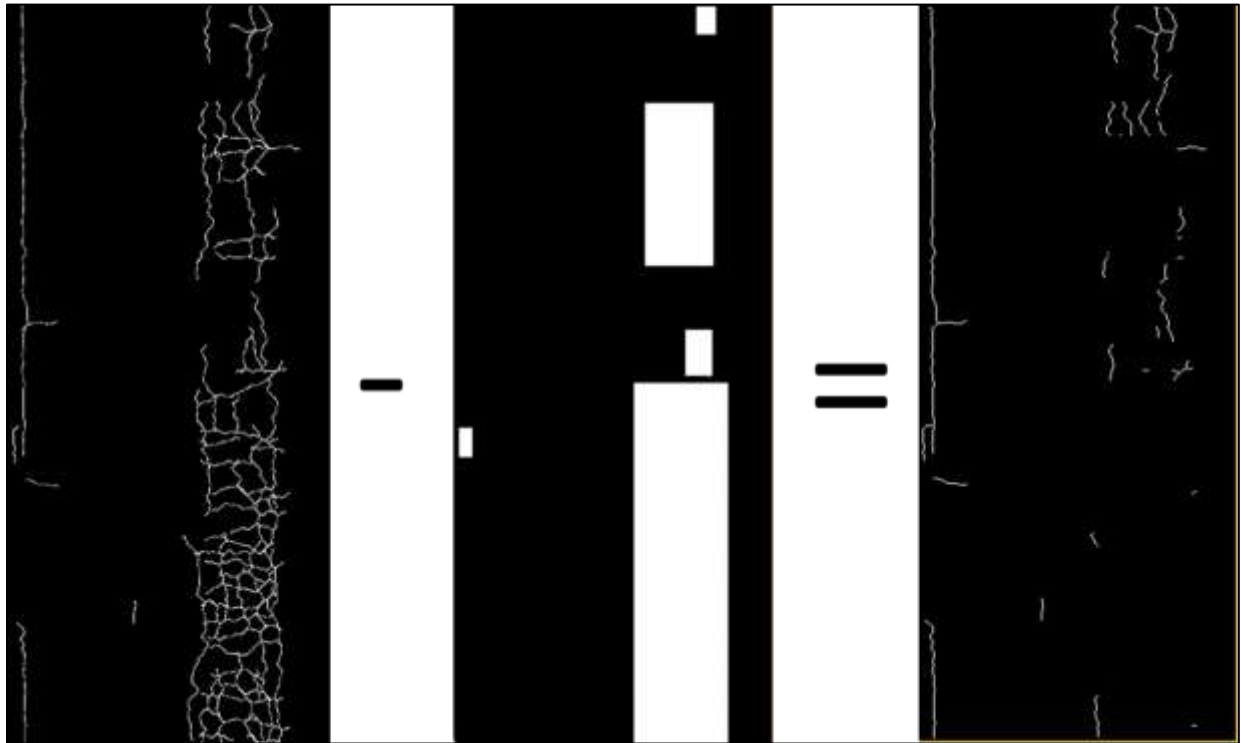
### Single and Branch Cracking Classification

Any cracks in the crack map that do not fall within alligator cracking bounding boxes are considered linear or branch cracks (see Figure 102).

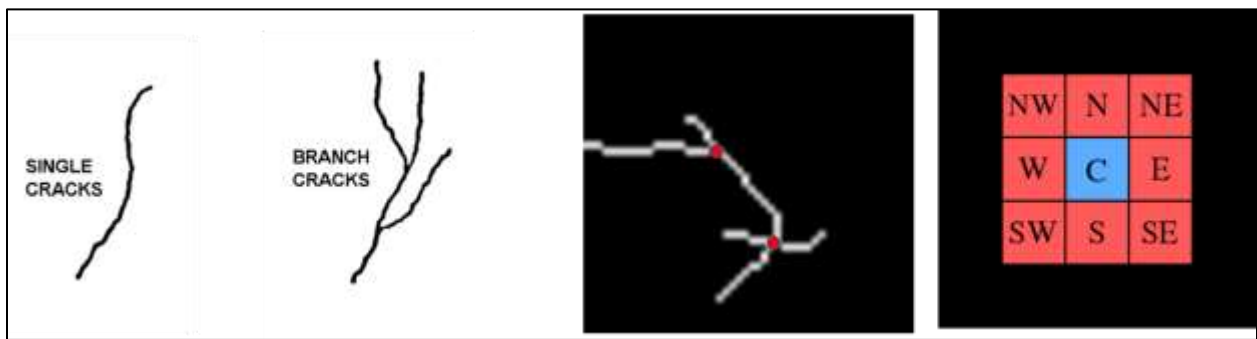
Branch cracks will be distinguished from linear cracks based on the number of adjoining pixels. In a skeletonized image, there are three types of pixels:

- i. End pixels which have one adjoining pixel
- ii. Center pixels which have two adjoining pixels
- iii. Joint pixels which have more than two adjoining pixels

A branch crack is an element in the crack map with at least one joint pixel (see Figure 103).



**Figure 102. Example Showing Extraction of Single and Branch Cracks from the Crack Map**



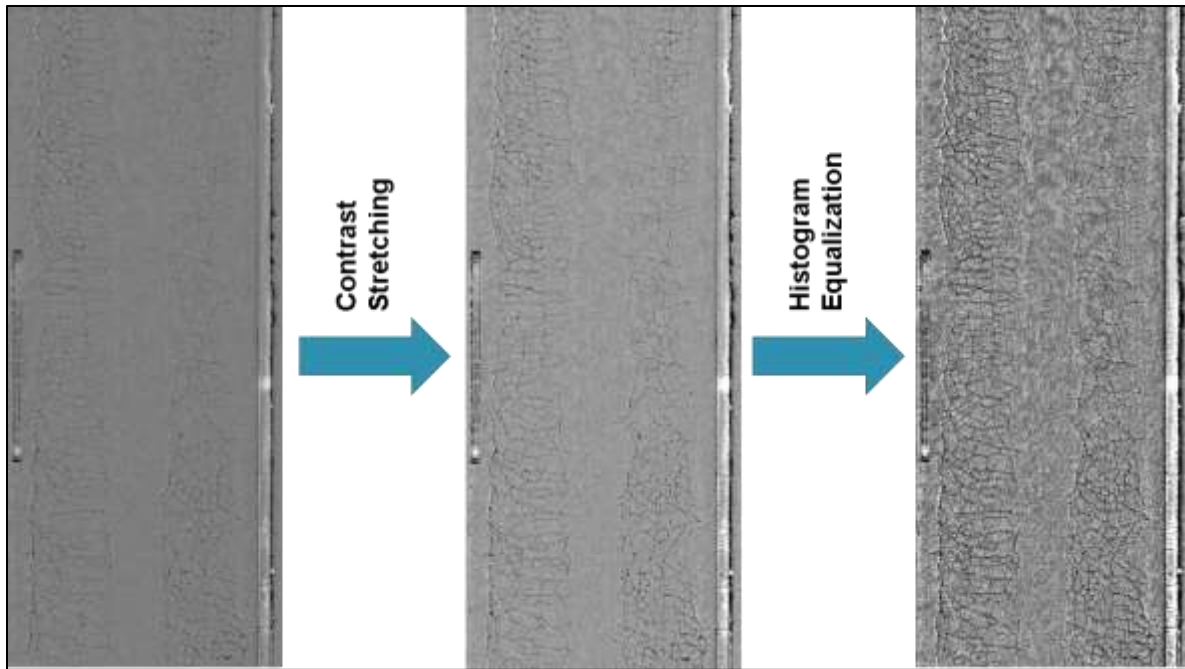
**Figure 103. Joint Pixels and Branch Cracks**

#### **Develop Improved Crack Width Algorithm**

1. Create a binary image using the range image, which includes the 3D depth data.  
The crack map and binary image developed in the classification development

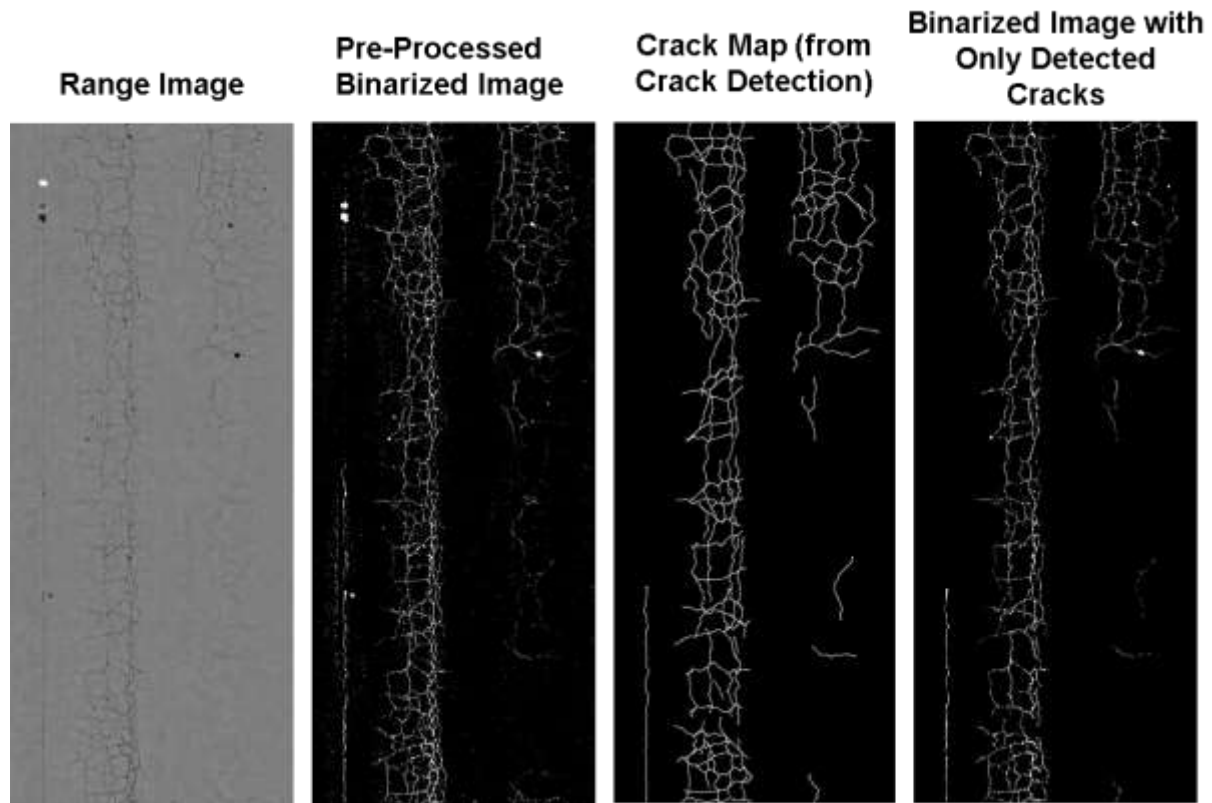
effort was based on the intensity image and contain crack locations, but they do not contain width information.

- i. Pre-process the range image using contrast stretching and histogram equalization techniques. The grayscale range image will produce a better binary image if it exhibits high contrast rather than low contrast (see Figure 104).



**Figure 104. Example Preprocessing of 3D Range Image**

- ii. Extract the binary image from the pre-processed range image using an edge-detection thresholding algorithm.
- iii. Remove extraneous information from the binary image. The binary image will contain white pixels which do not correspond to cracks that were detected or included on the crack map. The crack map can be overlaid on the range binary image to keep only white pixels which correspond to a detected crack (see Figure 105).



**Figure 105. Example Development of Enhanced Crack Map for Crack Width Determination**

2. Determine crack width using the range binary image.
  - i. Overlay the bounding boxes from the classification results onto the range binary image.
  - ii. Sum the number of white pixels within each bounding box.
  - iii. Average crack width for each bounding box =  $\frac{\text{Number of white pixels}}{\text{Crack length}}$

## CHAPTER 6 – FLEXIBLE PAVEMENT APPLICATION DEVELOPMENT AND VALIDATION

Task 6 of this research project included the development of the FDOT Flexible Pavement Distress Application (FFPDA) according to the algorithm design, which was devised during Task 5 for addressing identified gaps. This chapter is organized into four sections. Following this introduction, Section 6.1 summarizes the algorithm design and the application development efforts. Section 6.2 describes the experiment design for validation of the developed application. Section 6.3 presents the results of the validation experiment. Finally, Section 6.4 summarizes the results and provides pertinent recommendations for implementation of the developed application in future data collection and processing activities. In addition, Appendix L provides a Reference Manual for FDOT staff to conduct automated distress identification using the developed application and perform quality control on the results.

Please note the following reference phrases in this report:

- “*Vision 3.1*”: this refers to Fugro’s Vision 3.1 software, which includes a machine learning algorithm for crack detection and an automated routine for distress classification and rating. This existing automated software was evaluated in Task 5 and the existing gaps were identified so that the software development activities in Task 6 could address these gaps.
- “crack detection”: this refers to the process of locating and marking the pavement surface defects from the collected imagery.
- “crack classification”: this refers to the process of classifying each detected crack into a specific crack type and assigning a severity level to it.
- “reference survey”: this refers to the semi-automated survey conducted on one run of the collected pavement images, which serves as a benchmark when evaluating the automated software results.

### 6.1 Application Development

Based on the results of Vision 3.1 evaluations in Task 5, it was evident that Vision 3.1 had an adequate performance in detecting pavement surface cracks, but it was not performing well regarding classification and rating of the detected cracks into corresponding crack types and severities according to the FDOT *Flexible Pavement Condition Survey Handbook* (2017). Table 59 summarizes the identified gaps and corresponding recommended solutions. Based on this gap analysis that was performed

in Task 5, the following development efforts were conducted for Task 6 of this project. The algorithm logic design is briefly explained for each development effort.

**Table 59. Identified Gaps and Recommended Solutions**

<b>Number</b>	<b>Gap</b>	<b>Recommended Solution</b>
1	Numerous setup parameters	Develop batch processors with minimal setup parameters
2	Crack classification based on crack angle and density has issues with classifying Alligator cracks	Develop improved crack map for use during crack classification Develop methodology to classify Alligator cracks based on closed cells
3	Inability to classify Branch cracks	Develop methodology to differentiate Branch cracks from Single cracks based on joint pixels
4	Single and Branch cracks in proximity of each other and Alligator cracks are classified separately	Develop methodology to group cracks that are in proximity to each other
5	Vision 3.1 requires wheel path and non-wheel path cracks to be defined in the distress schema ahead of distress survey	Develop methodology to automatically differentiate wheel path cracks from non-wheel path cracks after automated survey and manual QC
6	Block crack classification is not accurate enough	No recommendation due to lack of test sections which exhibit Block cracking
7	Inaccurate crack severity rating	Develop improved crack width algorithm for distress severity rating purposes
8	Need to output summary data in the FDOT protocol format	Develop batch processor to summarize the results of automated survey and manual QC in output file

### **6.1.1 Batch Processor Development**

Two batch processors were developed as plugins for Vision 3.1:

1. 'FDOT Flexible Pavement Distress Application (FFPDA)' which takes the results of automated crack detection as an input, classifies the cracks as single, branch, and alligator, and then assigns a severity level of 1B, II, or III based on crack classification and width. This processor addresses gaps number 1, 2, 3, 4, 5, and 7.

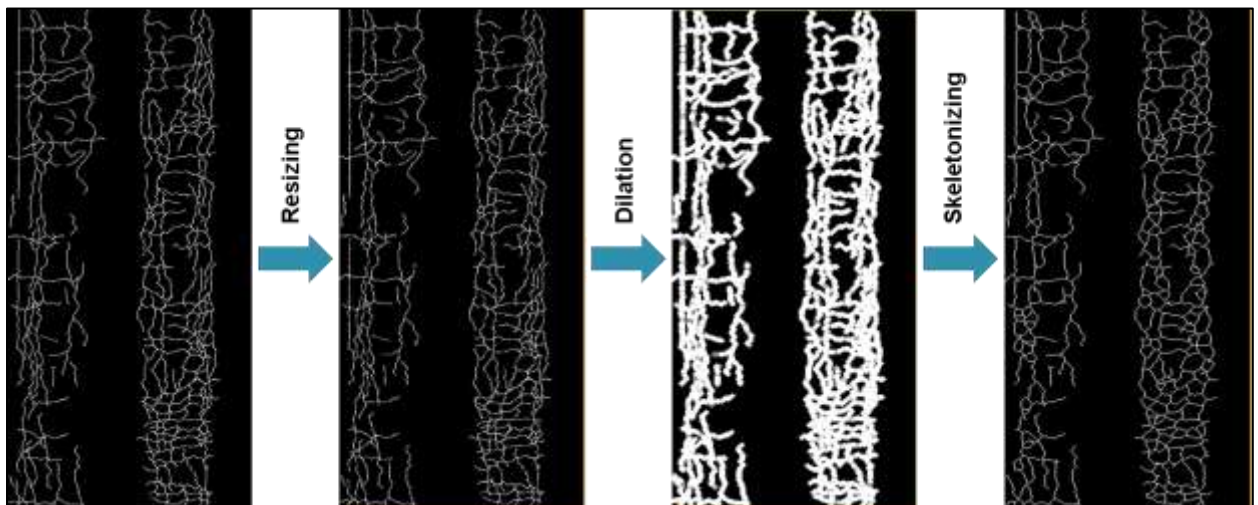
2. 'FDOT Flexible Pavement Rating Results Summary' which takes the results of FFPDA and any QC (manually drawing or modifying distresses on the images), differentiates wheel path from non-wheel path cracks, and summarizes all the distress information into comma separated value (csv) files. This processor addresses gap number 8.

The batch processors include the improvements described below and developed in Task 6 of this project. The batch processors are tailored to the FDOT distress rating protocol. This built-in customization will eliminate the need for numerous setup parameters and user-defined distress schemas.

### 6.1.2 Improved Crack Map Development

The following steps describe how the FFPDA algorithm was developed to generate an improved crack map based on the automated crack detection results:

1. Create a binary image using the detected crack node coordinates, in which white pixels represent cracks and all other pixels are black (see first image from left in Figure 106)
2. The binary image includes redundant information, which can be reduced using the following morphological processes (see Figure 106):
  - i. Resizing: keeps the essential information but improves the processing speed by reducing the size and number of pixels.
  - ii. Dilation: enlarges the boundaries of regions of white pixels. This process reduces the size of gaps within each region, and some gaps are filled completely (Szeliski 2010).



**Figure 106. Example Showing Resizing, Dilation, and Skeletonizing to Create Improved Crack Map**

The dilation operator takes two pieces of data as inputs. The first is the binary image (crack map) which is to be dilated. The second is a (usually small) set of coordinate points known as a structuring element (also known as a kernel). It is this structuring element (see Figure 107 for example) that determines the precise effect of the dilation on the input image.

The mathematical definition of dilation for binary images is as follows:

Suppose that  $X$  is the set of Euclidean coordinates corresponding to the input binary image, and that  $K$  is the set of coordinates for the structuring element.

Let  $K_x$  denote the translation of  $K$  so that its origin is at  $x$ .

Then, the dilation of  $X$  by  $K$  is simply the set of all points in  $X$  such that the intersection of  $K_x$  with  $X$  is non-empty.

As an example of binary dilation, suppose that the structuring element is a  $3 \times 3$  square, with the origin at its center, as shown in Figure 107. Note that in this and subsequent diagrams, foreground (white) pixels are represented by 1's and background (black) pixels by 0's.

1	1	1
1	1	1
1	1	1

**Figure 107. A  $3 \times 3$  Square Structuring Element**

To compute the dilation of a binary input image by this structuring element, each of the *background* (black) pixels in the input image is considered in turn. For each background pixel (called the *input pixel*), the structuring element is superimposed on top of the input image, so that the origin of the structuring element coincides with the input pixel position. If *at least one* pixel in the structuring element coincides with a foreground (white) pixel in the image underneath, then the input pixel is set to the foreground (white) value. If all the corresponding pixels in the image are background, however, the input pixel is left at the background value.



For the example 3×3 structuring element in Figure 107, the effect of this operation is to change any black pixels that have a neighboring white pixel to the white color. Such pixels must lie at the edges of white regions, and so the practical upshot is that foreground regions grow (and holes inside a region shrink).

- iii. Skeletonizing: reduces the white regions in the binary image to a skeletal remnant that largely preserves the extent and connectivity of the original region. The thickness of any linear feature in the skeleton is one pixel. The skeleton of the binary image is acquired using the *Zhang-Suen Thinning Algorithm* (Zhang and Suen 1984). The details of this algorithm are described as following:

The algorithm operates on all white pixels P1 that can have eight neighbors. The neighbors are arranged in a clock-wise sequence as indicated in Figure 108. Obviously, the boundary pixels of the image cannot have the full eight neighbors.

P9	P2	P3
P8	<b>P1</b>	P4
P7	P6	P5

**Figure 108. The Pixel Arrangement in the Zhang-Suen Thinning Algorithm**

Define  $\{A(P1)\}$  = the number of transitions from black to white, (0 to 1) when moving in the clock-wise sequence P2 to P3 to P4 to P5 to P6 to P7 to P8 to P9 back to P2. (Note the extra P2 at the end - it is circular).

Define  $\{B(P1)\}$  = The number of white pixel neighbors of P1 = (sum(P2 .. P9))

Step 1: All pixels are tested and pixels satisfying all the following conditions (simultaneously) are set to black:

- 1) The P1 pixel is white and has eight neighbors
- 2)  $\{2 \leq B(P1) \leq 6\}$  in other words, P1 has between 2 to 6 white pixel neighbors
- 3)  $A(P1) = 1$  in other words, there is only one transition from black to white when moving in the clock-wise sequence above

4) At least one of P2 and P4 and P6 is black

5) At least one of P4 and P6 and P8 is black

Step 2: All pixels are tested again and pixels satisfying all the following conditions (simultaneously) are set to black:

1) The pixel is white and has eight neighbors

2)  $\{2 \leq B(P1) \leq 6\}$  in other words, P1 has between 2 to 6 white pixel neighbors

3)  $A(P1) = 1$  in other words, there is only one transition from black to white when moving in the clock-wise sequence above

4) At least one of P2 and P4 and P8 is black

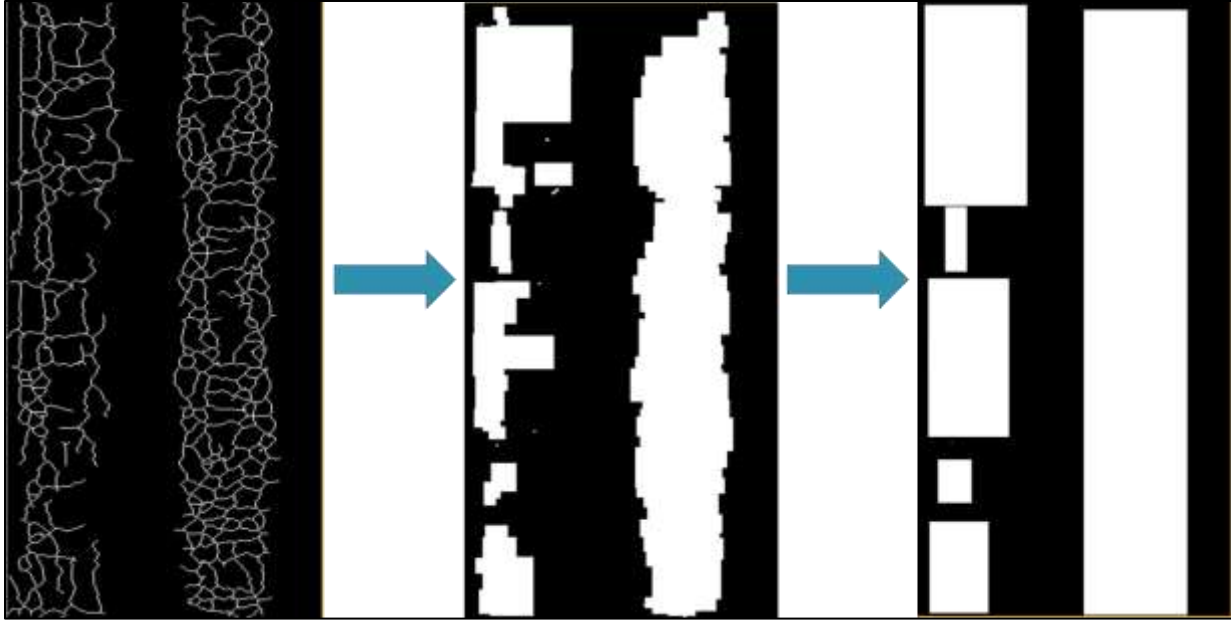
5) At least one of P2 and P6 and P8 is black

Iteration: Steps one and two are repeated until image pixels are no longer changed

Figure 106 shows the results of the three morphological processes of resizing, dilation, and skeletonizing on an example pavement image.

### **6.1.3 Alligator Cracking Classification**

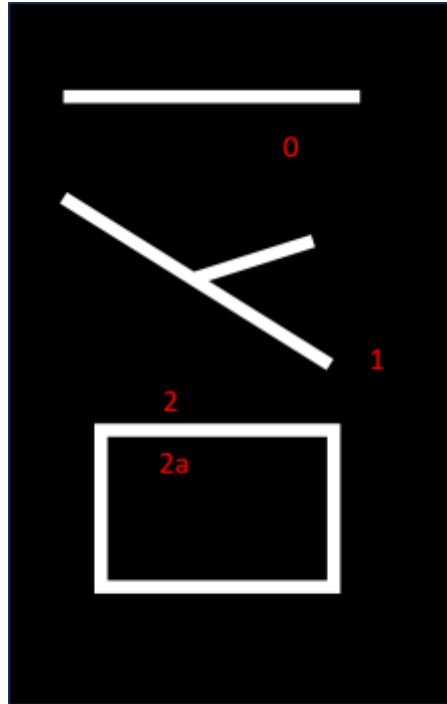
The improved crack map is analyzed to locate all regions in which the cracks have formed a closed cell. Connected closed-cell regions are combined into a bounding box which represents the area of alligator cracking (see Figure 109).



**Figure 109. Example Showing Extraction of Alligator Cracking Areas from the Crack Map**

The locations of closed cells are acquired by *Contour Hierarchy Analysis* (Suzuki and Abe 1985). Contours can be explained simply as a curve joining all the continuous points (along the boundary), having the same color or intensity. In some cases, some contours are inside other contours; the outer ones are called parents and inner ones are called children. This way, contours in an image have some relationship to each other. And we can specify how one contour is connected to another, is it a child of some other contour, or is it a parent. Representation of this relationship is called the *Hierarchy*.

Consider the example image shown in Figure 110. Contour lines 2 and 2a denote the external and internal contours of the outermost box. Here, contours 0, 1, and 2 are external or outermost. We can say, they are in hierarchy-0 or simply they are in the same hierarchy level. Next comes contour 2a. It can be considered as a child of contour 2 (or in opposite way, contour 2 is parent of contour 2a). So, let contour 2a be in hierarchy-1. A closed cell is an indication of alligator cracking and closed cells are detected if a contour has at least one child (for example, contour 2). In the case of multiple contours inside each other, the outermost parent contour defines the boundaries of the alligator cracking area.



**Figure 110. Schematic Description of Contour Hierarchy Analysis**

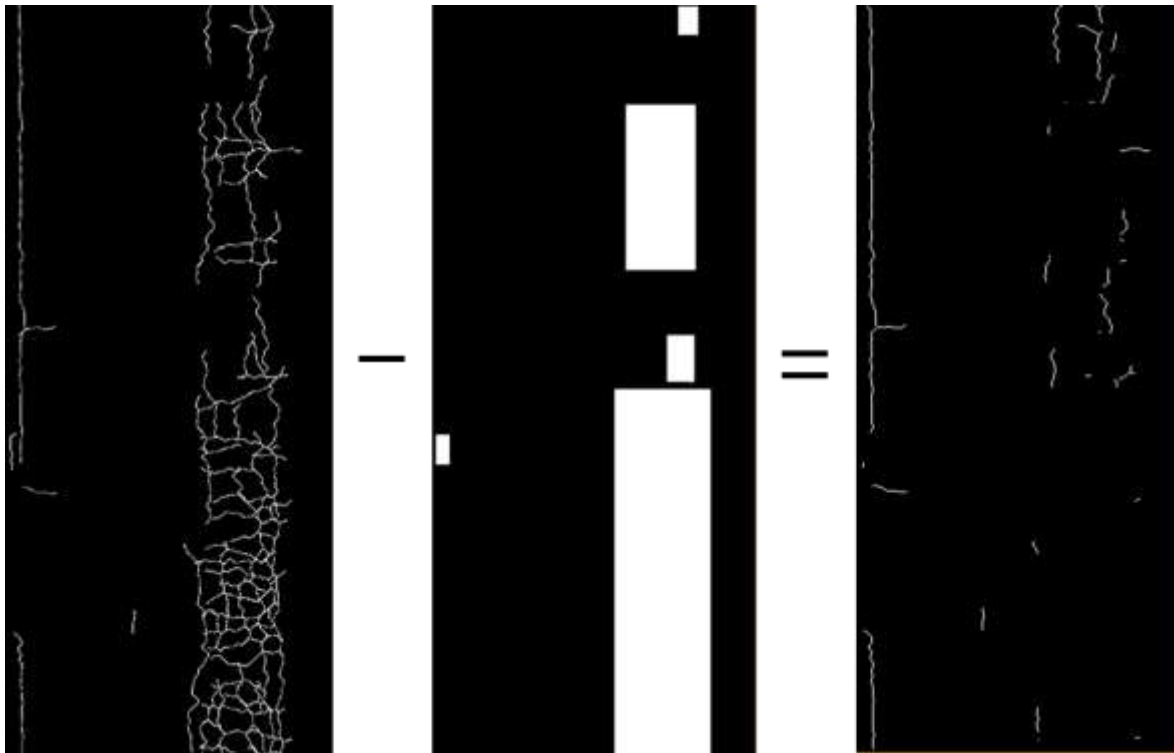
#### **6.1.4 Single and Branch Cracking Classification**

Any cracks in the crack map that do not fall within alligator cracking bounding boxes are considered single or branch cracks (see Figure 111).

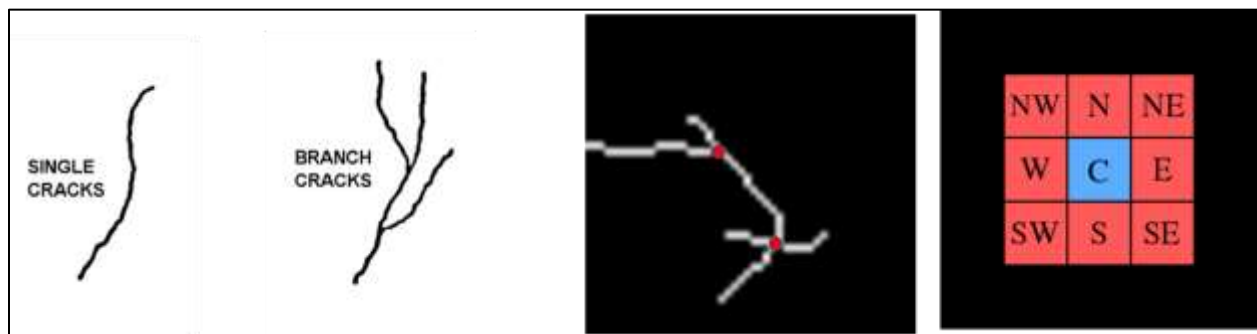
Branch cracks were distinguished from single cracks based on the number of adjoining pixels. In a skeletonized image, there are three types of pixels:

- i. End pixels which have one adjoining pixel
- ii. Center pixels which have two adjoining pixels
- iii. Joint pixels which have more than two adjoining pixels

A branch crack is defined as an element in the crack map with at least one joint pixel (see Figure 112) if the branch stemming from that joint pixel is longer than 1 foot.



**Figure 111. Example Showing Extraction of Single and Branch Cracks from the Crack Map**

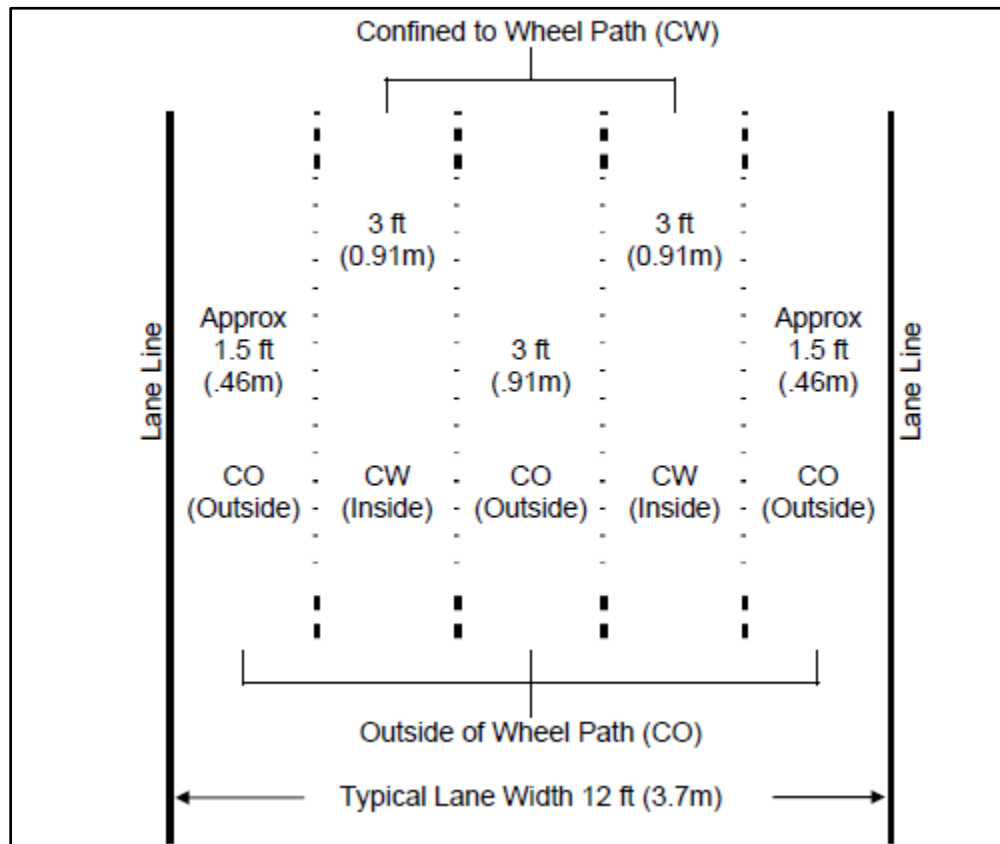


**Figure 112. Joint Pixels and Branch Cracks**

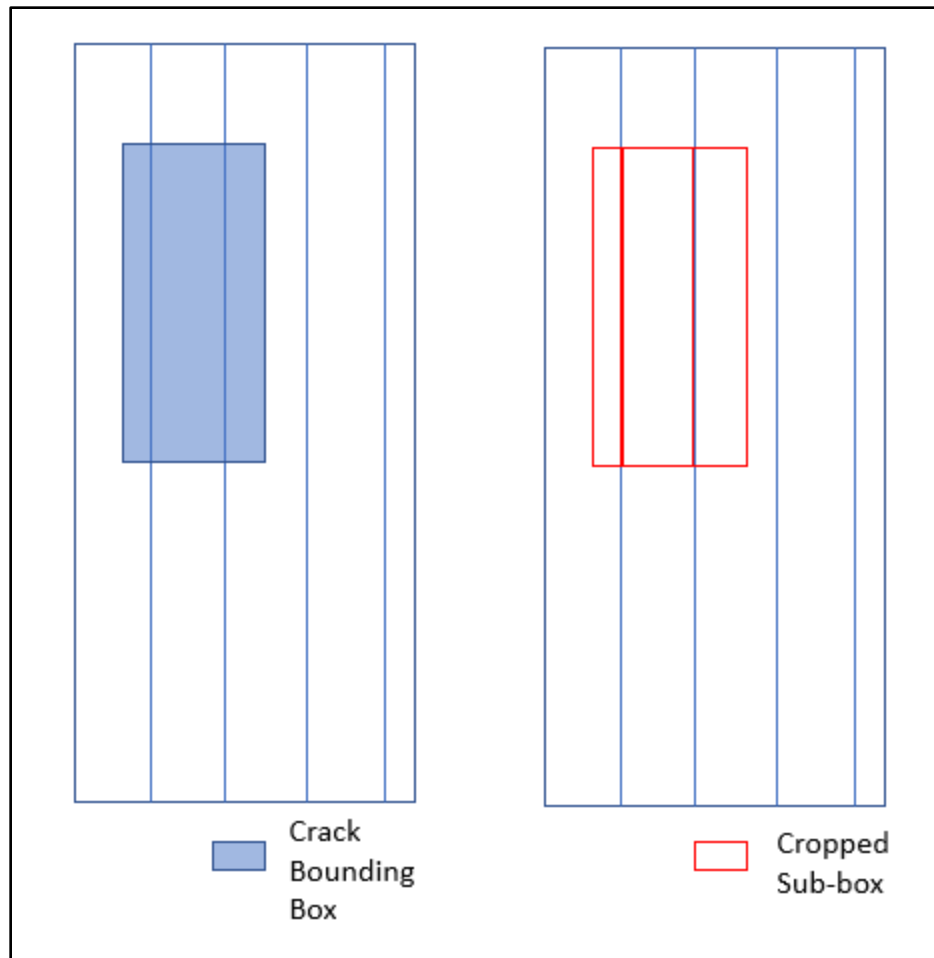
### 6.1.5 Wheel-Path and Non-Wheel-Path Cracking

During the classification, the cracks are assigned with different crack types: alligator, branch or single. The cracks are then further classified into wheel-path cracks and non-wheel-path cracks based on the location across the lane width, more specifically, its x coordinate.

For any identified distress, if the corresponding bounding boxes crossed any boundaries of the five road zones shown in Figure 113 (and defined in the 2017 FDOT *Flexible Pavement Condition Survey Handbook*), those bounding boxes were cropped into multiple sub-boxes as shown in Figure 114. The original bounding boxes can span multiple road zones, but these final sub-boxes can only exist in one road zone. In this manner, the identified cracking can be divided between wheel-path and outside wheel-path zones.



**Figure 113. FDOT Defined Road Zones Across the Lane Width**

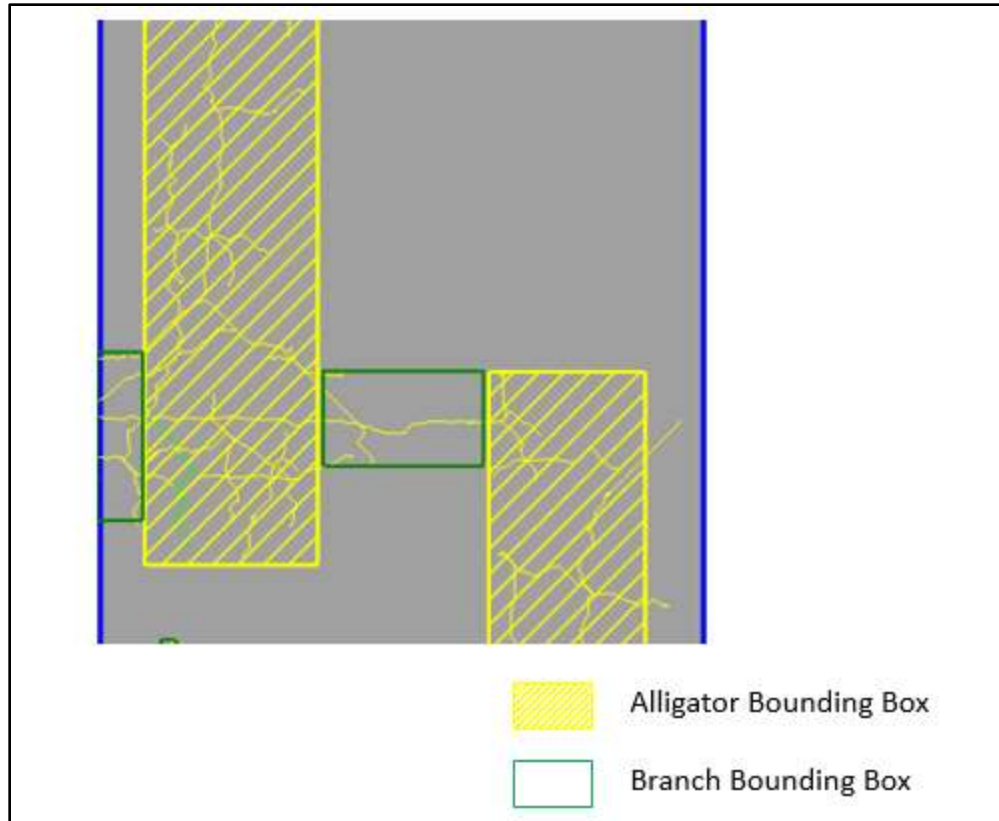


**Figure 114. Cropping Bounding Box into Sub-Boxes According to Road Zone**

### 6.1.6 Bounding Box Grouping

Three types of groupings are performed on the bounding boxes (cropped sub-boxes). If the minimum longitudinal (y) distance between an alligator cracking bounding box and a branch cracking bounding box is less than or equal to 1ft, they are merged as one alligator cracking bounding box. Similarly, if the minimum y distance between a branch cracking bounding box and a single crack bounding box is less than or equal to 1ft, they are merged as one branch cracking bounding box. Also, if the minimum y distance between an alligator cracking bounding box and a single crack bounding box is less than or equal to 1ft, they are merged as one alligator cracking bounding box. Figure 115 shows an example of the results of bounding box grouping.

Crack bounding boxes are finalized in this step, cracks in the same crack bounding boxes are grouped as one crack set. After width information is assigned to these crack sets, crack sets are converted to distresses.



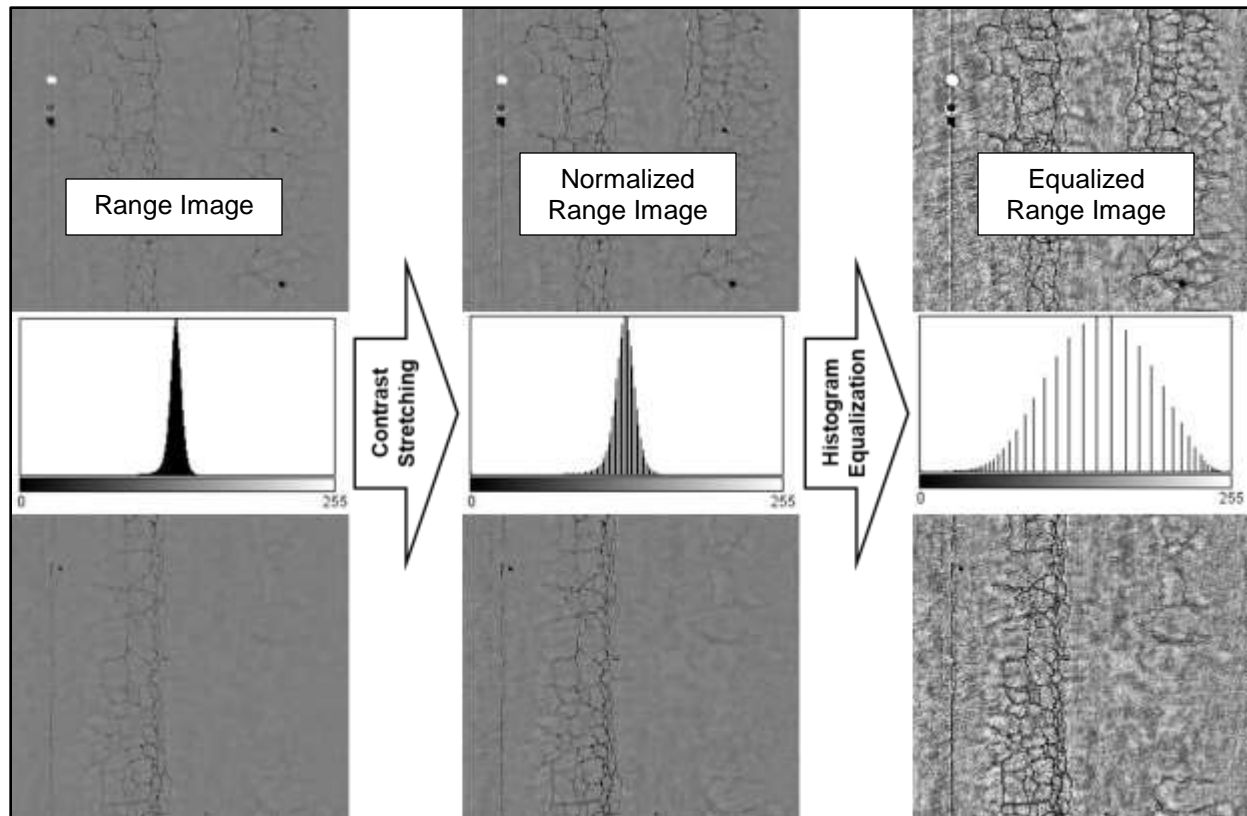
**Figure 115. Grouped Bounding Box**

#### **6.1.7 Improved Crack Width Identification**

There was a need to improve the estimation of crack width to improve the accuracy of the software in assigning severity levels to cracks. The crack map and binary image developed in the classification development effort contain crack locations, but they do not contain width information. The following explains the development efforts to create a binary image using the range image (which includes the 3D depth data), and the estimation of crack width:

1. Pre-process the range image using contrast stretching and histogram equalization techniques. The grayscale range image will produce a better binary image if it exhibits high contrast rather than low contrast (see Figure 116).





**Figure 116. Example Preprocessing of 3D Range Image**

- i. Contrast Stretching: Often called normalization, this is a simple image enhancement technique that attempts to improve the contrast in an image by 'stretching' the range of intensity values it contains to span a desired range of values, e.g. the full range of pixel values that the image type concerned allows (Kaur and Choudhary 2012).

Before the stretching can be performed, it is necessary to specify the upper and lower pixel value limits over which the image is to be normalized. Often these limits will just be the minimum and maximum pixel values that the image type concerned allows. For example, for 8-bit gray level images, the lower and upper limits might be 0 and 255. Call the lower and the upper limits  $a$  and  $b$  respectively.

The contrast stretching algorithm then scans the image to find the lowest and highest pixel values currently present in the image. Call these  $c$  and  $d$ . Then each pixel  $P$  is scaled using the following function:

$$P_{out} = (P_{in} - c) \left( \frac{b - a}{d - c} \right) + a$$

Values below 0 are set to 0 and values above 255 are set to 255.

- ii. Histogram Equalization: is a method that improves the contrast in an image, to stretch out the intensity range (Szeliski 2010). In Figure 116, the pixels in the intensity histogram of the center image seem clustered around the middle of the available range of intensities. What Histogram Equalization does is to stretch out this range. The tails of this histogram indicate the underpopulated intensities. After applying the equalization, the histogram for the image on the right shows that pixels in the resulting image have intensities that are more evenly distributed across the spectrum.
2. Extract the binary image from the pre-processed range image using a *Multi-Threshold Maximum Entropy Algorithm* (Apro et al. 2011). The Maximum Entropy is an automatic thresholding (classification) method where the optimal threshold value (for differentiating pixels in two classes of cracks and non-cracks) can be found by maximizing the entropy (minimizing the homogeneity) of the resulting classes. This thresholding technique is called a bi-level approach, where a unique threshold value is defined to differentiate the two classes. The bi-level thresholding techniques give satisfactory results on the images with clear foreground-background differentiation. But for the segmentation of complex images, a multi-thresholding approach is more suitable. A multi-thresholding technique converts the different types of regions of the image into regions having the optimal number of grey-level pixels.

Suppose that  $h(i)$  is a value in a normalized histogram. Typically,  $i$  takes integer values from 0 to 255 (for 8-bit depth images).  $h(i)$  is the number of pixels that have the intensity  $i$ . It is assumed that  $h(i)$  is normalized, meaning the total area under the frequency distribution histogram is equal to 1:

$$\sum_{i=0}^{i_{\max}} h(i) = 1$$

The entropy of black (background) pixels is defined as:

$$H_B(t) = - \sum_{i=0}^t \frac{h(i)}{\sum_{j=0}^t h(j)} \log \frac{h(i)}{\sum_{j=0}^t h(j)}$$

The entropy of white (foreground) pixels is defined as:

$$H_W(t) = - \sum_{i=t+1}^{i_{\max}} \frac{h(i)}{\sum_{j=t+1}^{i_{\max}} h(j)} \log \frac{h(i)}{\sum_{j=t+1}^{i_{\max}} h(j)}$$

The optimal threshold can be selected by maximizing the sum of foreground and background entropies as:

$$T_{opt} = \underset{t=0 \dots i_{\max}}{\text{ArgMax}} [H_B(t) + H_W(t)]$$

The above formula for optimal threshold value (bi-level thresholding) can be extended to multi-level thresholding of an image. Assuming that there are n thresholds dividing the original image into n+1 classes, the optimal thresholds  $\{T_1, T_2, \dots, T_n\}$  are chosen by maximizing the sum of entropies as follows

$$\{T_1, \dots, T_n\} = \underset{t_1 < \dots < t_n}{\text{ArgMax}} [H(-1, t_1) + H(t_1, t_2) + \dots + H(t_n, i_{\max})]$$

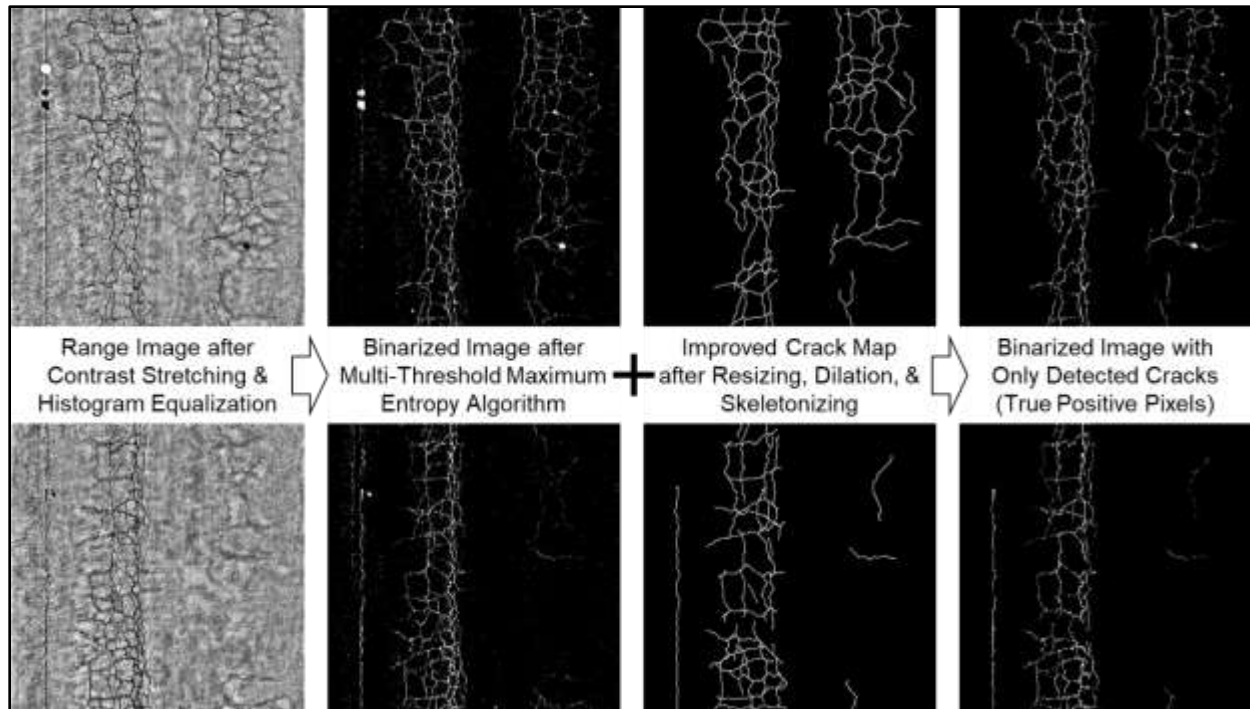
where:

$$H(t_k, t_{k+1}) = - \sum_{i=t_k+1}^{t_{k+1}} \frac{h(i)}{\sum_{j=t_k+1}^{t_{k+1}} h(j)} \log \frac{h(i)}{\sum_{j=t_k+1}^{t_{k+1}} h(j)}$$

In this project, the n is set to be 2. In other words, two thresholding values are obtained and applied to the pre-processed range image. The pre-processed gray-scale range images are converted to binary images (see Figure 117).

3. Remove extraneous information from the binary image. The binary image will contain white pixels which do not correspond to cracks that were

detected or included on the crack map. The width of the cracks in the skeletonized crack map (see Figure 106) is increased from one to 20 pixels, and then this crack map is overlaid on the pre-processed binarized image from step 3 to keep only white pixels in the binary image that correspond to detected cracks (see Figure 117).



**Figure 117. Example Development of Enhanced Crack Map for Crack Width Determination**

4. Determine crack width using the final range binary image (see Figure 117).
  - i. Overlay the bounding boxes from the classification results onto the range binary image.
  - ii. Sum the number of white pixels within each bounding box. The width of each pixel in the LCMS image is very close to 1 mm.
  - iii. 
$$\text{Average crack width in millimeter for each bounding box} = \frac{\text{Number of white pixels}}{\text{Crack length (mm)}}$$

### **6.1.8 Improving Crack Severity Level Assignment**

If the average crack width for a branch cracking area is less than or equal to  $\frac{1}{8}$  inch (3.18 mm) wide, that area would be assigned a Class 1B severity level. However, during the manual distress workshop conducted with the FDOT raters, it was discovered that if the same area had a lot of branching (no closed cells that would indicate alligator cracking), then the FDOT raters would bump its severity level to Class II.

Since the automated software is supposed to replace the manual windshield survey for the annual pavement condition survey (PCS), it was decided that this practice needs to be incorporated into the software. Therefore, the following algorithm was developed in this regard:

1. If a crack group is classified as branch cracking, and
2. the average crack width is less than or equal to  $\frac{1}{8}$  inch (3.18 mm), and
3. in every 10 feet of the crack length, there are at least 5 branches of minimum 1 foot each,
4. then the cracking is assigned as Class II.

## **6.2 Validation Experiment Design**

The following sections will describe the experiment test sections, the success metrics, the reference values, and the evaluation limitations.

### **6.2.1 Experiment Test Sections**

To conduct this validation experiment, FDOT engineers identified a set of 12 representative test sections that are each at least a standard evaluation length (0.1-mile-long) and contain several of the flexible pavement distresses in them. Table 52 and Figure 85 show the selected 12 flexible pavement sections.

### **6.2.2 Manual Windshield Survey**

Three FDOT raters conducted a manual windshield distress survey of the 12 test sections according to the FDOT protocol. Each rater conducted the manual distress survey separately in a separate vehicle and according to the FDOT *Flexible Pavement Condition Survey Handbook* (2017).

### 6.2.3 Automated Survey

The 3D data collection was conducted by Fugro using the Automatic Road Analyzer (ARAN) Laser Crack Measurement System (LCMS) equipment and the data were analyzed by Fugro staff using the readily available Vision 3.1 software. The ARAN collected 3 repeated runs on each of the 12 test sections. Surface defects were detected using the machine learning algorithm in Vision 3.1. Then the FFPDA batch processor developed in Task 6 was used to classify and rate the detected cracks according to the FDOT *Flexible Pavement Condition Survey Handbook* (2017).

### 6.2.4 Success Metrics

The following are the success metrics used for evaluating the crack classification and severity rating results based on the overall cumulative amount of each crack type among different test sections and multiple runs:

1. Crack Classification Accuracy: This statistic is evaluated based on average error (bias) with respect to the reference distress survey values for each crack type.

$$\text{Accuracy (\%)} = 100 - \text{Bias (\%)}$$

2. Manual Windshield Survey Reproducibility: This statistic is evaluated based on coefficient of variation (COV) of manually identified cracking among three raters for each crack type (independent of the reference and averaged among the sections).

$$\text{Reproducibility (\%)} = 100 - \text{COV (\%)}$$

3. Automated Crack Classification Repeatability: This statistic is evaluated based on coefficient of variation (COV) of automatically identified cracking among three runs for each crack type (independent of the reference and averaged among the sections).

$$\text{Repeatability (\%)} = 100 - \text{COV (\%)}$$

4. Crack Classification Consistency: This statistic is evaluated based on coefficient of variation (COV) of crack classification accuracy among 12 sections for each crack type.

$$\text{Consistency (\%)} = 100 - [\text{Standard Deviation of Accuracy (\%)} / \text{Average Accuracy (\%)}]$$

5. Crack Classification Efficiency: This statistic is evaluated based on the time required for the automated distress survey.

Efficiency (second per foot) = time for crack detection, classification, and rating divided by the total length.

### **6.2.5 Reference Survey**

A reference distress survey was manually created by one Fugro engineer using the collected images from one automated run (run number 1), and another Fugro technician reviewed the results to reach a consensus for the reference survey. This reference survey was used to evaluate the effectiveness of the crack classification and rating routine.

### **6.2.6 Evaluation Limitations**

The evaluation was conducted considering the following limitations of this analysis:

1. The 12 test sections were selected as representative of the actual pavement surfaces found across Florida. With such a small sample, it is possible that not all of the actual pavement network is represented in this study. Every effort was made to select a representative sample. However, the budgetary and schedule limitations of this project would not allow for collection and processing of data across a wider network. For example, there were not a significant amount of block cracking present in the selected sections.
2. This study is mainly focused on cracking distresses; patching and raveling were not considered in this evaluation.

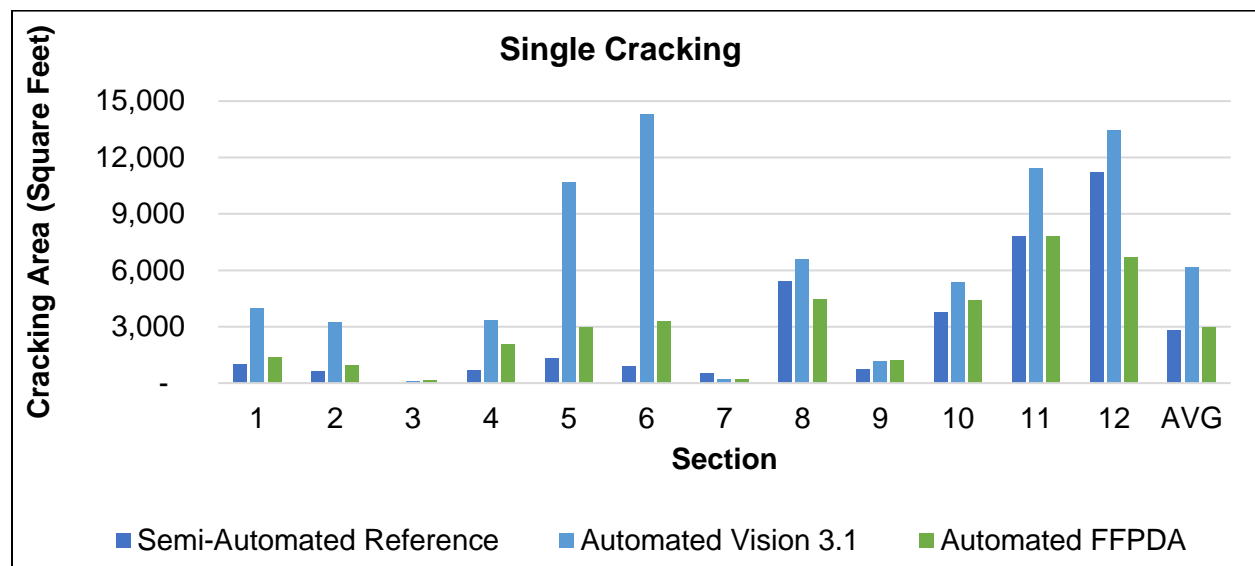
## **6.3 Validation Experiment Results**

The results of the validation experiment are presented according to the experiment design described in the previous section. The amount of cracking automatically identified using FFPDA after the development effort is compared to that using Vision 3.1, the manual windshield survey by FDOT raters and the semi-automated reference survey by Fugro staff. The automated results are averaged among the three runs and the manual results are averaged among the three raters. The automated results were for cracking found between the lanes after lane detection. No manual quality control was conducted after the automated runs.

### 6.3.1 Automatically Identified Crack Types

In this section, the evaluation is conducted based on the amount of automatically identified Single, Branch, and Alligator cracking. The following results are for cracking in all 5 road zones between the lane markings. FDOT raters report only the predominant crack type and severity in CW and CO, when performing the PCS windshield survey. Therefore, a direct comparison of their results to the automated results could not be conducted for crack type.

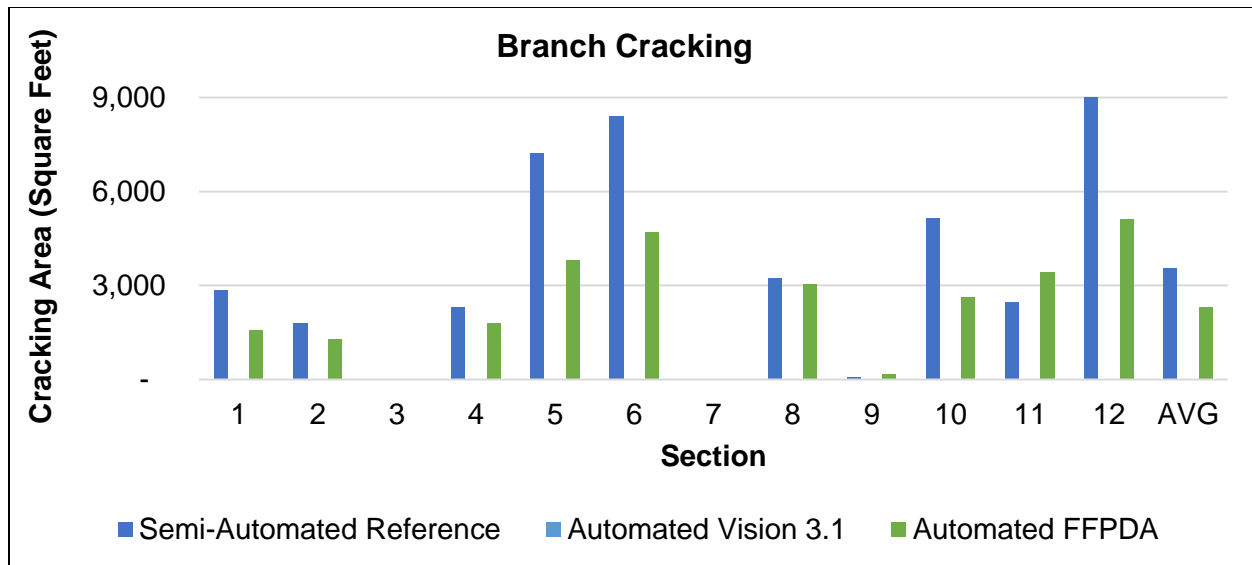
Figure 118 shows the amount of automatically identified Single cracks in each of the 12 sections, compared to the reference survey. Compared to Vision 3.1, FFPDA has resulted in less amount of identified single cracking. This is because Vision 3.1 was not capable of classifying branch cracks and was identifying all branch cracks as single cracks.



**Figure 118. Comparison of Automatically Identified Single Cracks to Reference Survey**

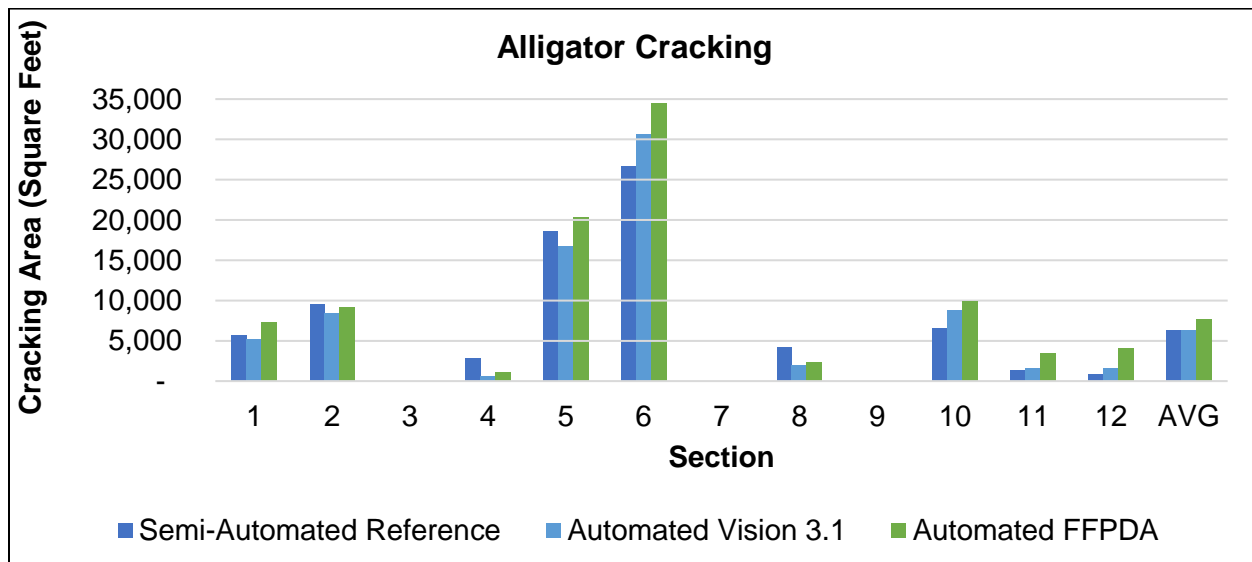
Figure 119 shows the amount of automatically identified Branch cracks on each of the 12 sections, compared to the reference survey. Vision 3.1 was not capable of identifying branch cracking but FFPDA has identified branch cracks at a relatively lower extent compared to the reference survey.





**Figure 119. Comparison of Automatically Identified Branch Cracks to Reference Survey**

Figure 120 shows the amount of automatically identified Alligator cracks on each of the 12 sections, compared to the reference survey. Compared to the reference and the Vision 3.1, FFPDA has resulted in higher amount of identified alligator cracking. This is because of the grouping mechanism that was devised in FFPDA to group cracking areas that are in proximity to each other. The grouping mechanism was incorporated to better match the practice of FDOT manual raters.



**Figure 120. Comparison of Automatically Identified Alligator Cracking to Reference Survey**

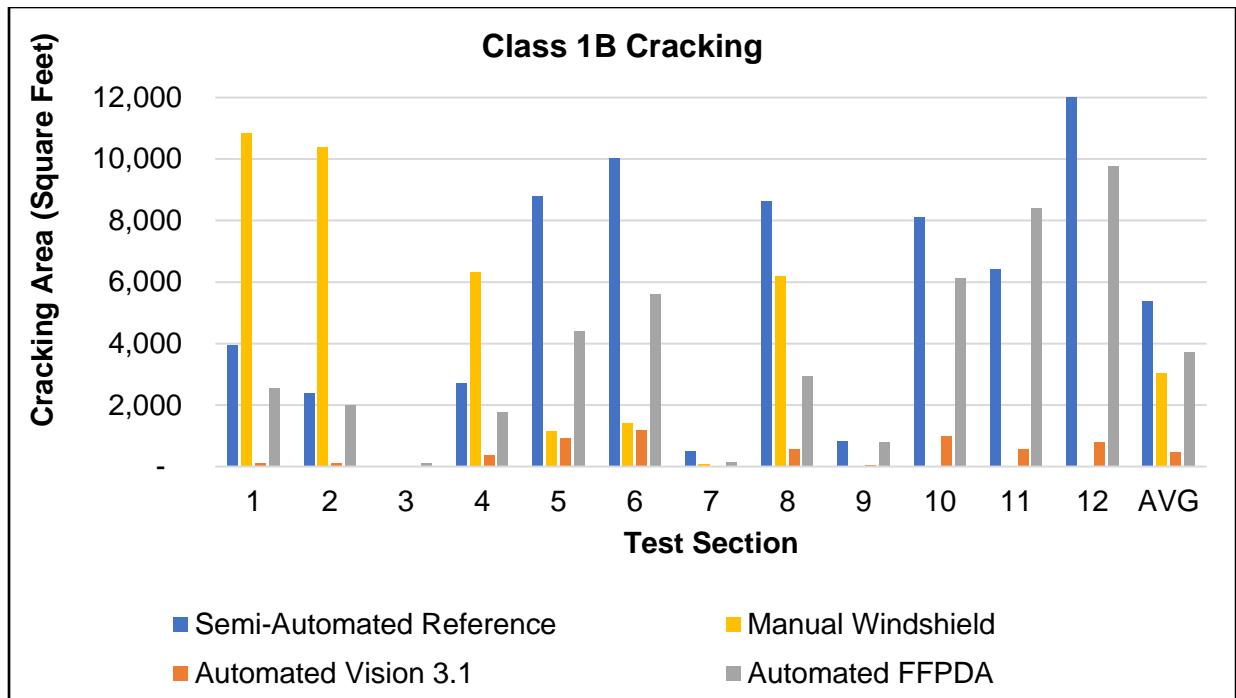
### 6.3.2 Automatically Rated Crack Severities

Both Vision 3.1 and FFPDA use average crack width measurements to determine crack severities according to the FDOT *Flexible Pavement Condition Survey Handbook* (2017). However, FFPDA has an improved methodology as described in Section 6.1.7.

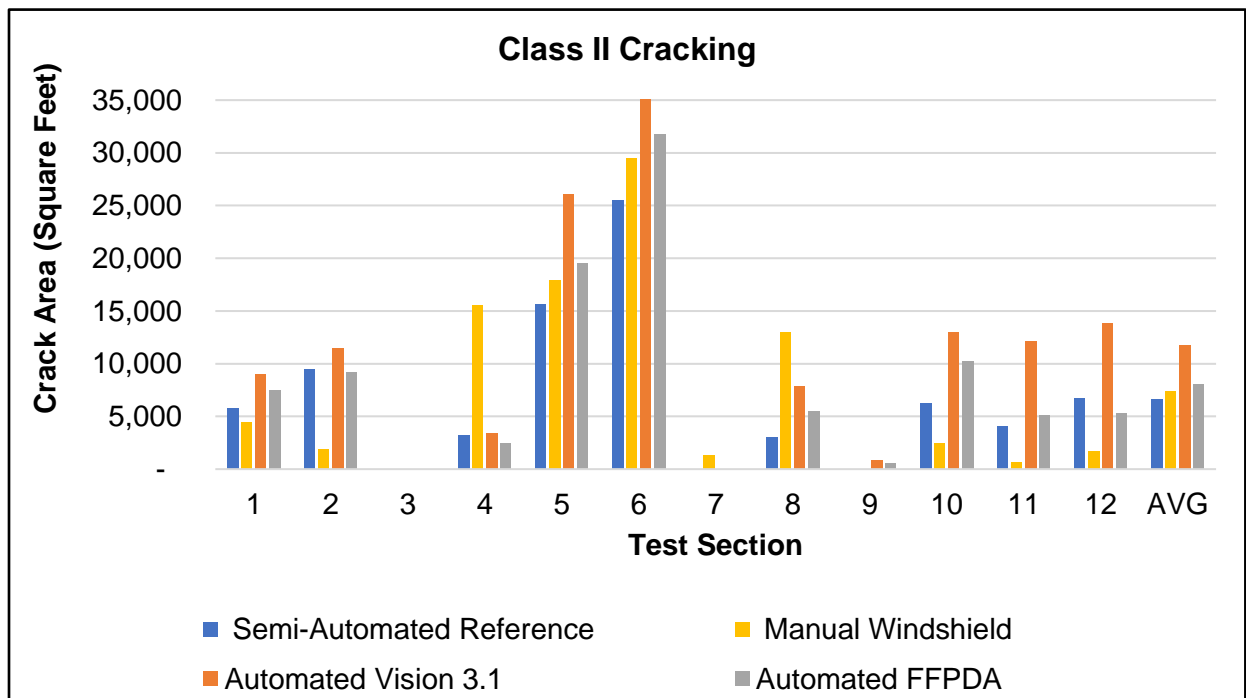
Class IB are hairline cracks that are less than or equal to  $\frac{1}{8}$  inch (3.18 mm) wide, Class II are cracks greater than  $\frac{1}{8}$  inch (3.18 mm) and less than or equal to  $\frac{1}{4}$  inch (6.35 mm) wide, and Class III are cracks greater than  $\frac{1}{4}$  inch (6.35 mm) wide. Note that the extent of Class 1B cracks is the sum of the length of single and branch cracks. But the extent of the Class II and Class III cracks is the sum of the area of single, branch, and alligator cracks, where the single and branch cracks are assumed to have a width of one foot.

It should be noted that the manual assignment of severity levels in the reference survey is always more subjective than classification of cracks into single, branch, and alligator crack types. This is because it is easier to visually differentiate between single, branch, and alligator cracks than it is to visually differentiate between various crack severities. In the reference survey, the rater can use the measurement tool in Vision 3.1 to get familiar with the visual representation of various crack widths on the image. The rater then relies on this visual representation to manually rate the severity levels of each identified cracking distress. This is very similar to the subjectivity observed in the manual windshield survey results. For the manual windshield survey, the cracking area is averaged among the three raters for each crack type.

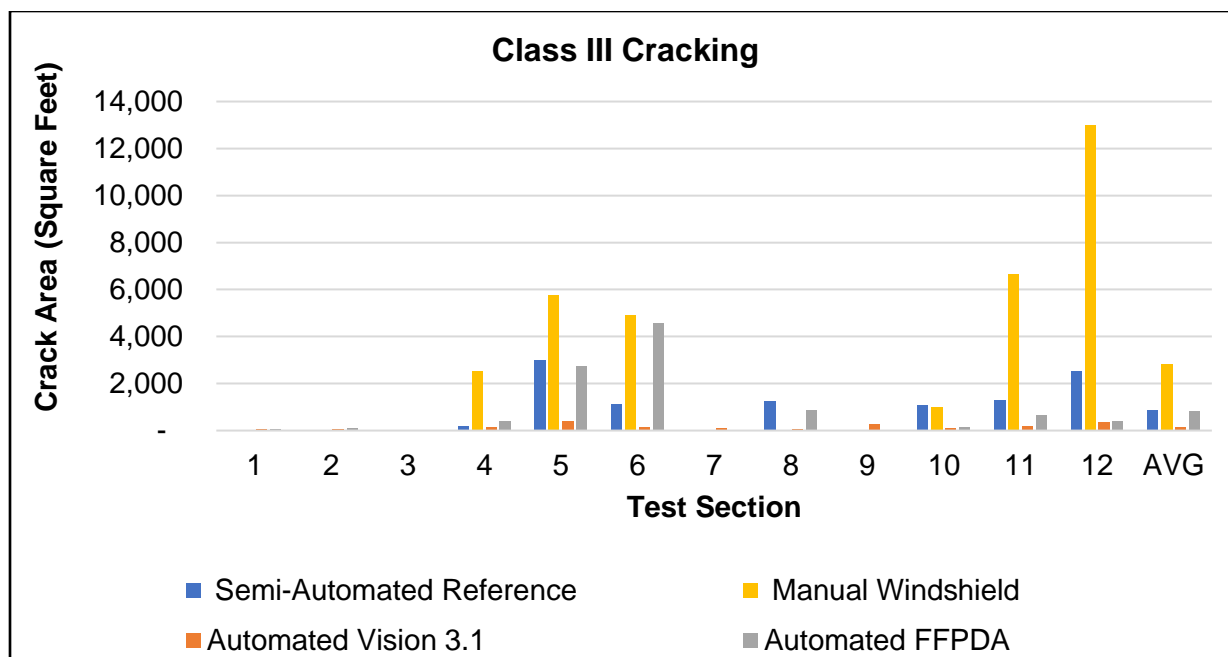
Figure 121, Figure 122, and Figure 123 compare the automatically rated results to those of the manual windshield survey and the reference survey for Class 1B, Class II, and Class III cracks, respectively (note: vertical axis ranges vary). FFPDA has resulted in a higher amount of Class 1B cracking compared to Vision 3.1, which compares better against the reference survey. On the other hand, FFPDA has resulted in a lower amount of Class II cracking compared to Vision 3.1, which compares very well against both the reference survey and the manual windshield survey results. FFPDA has also improved the amount of identified Class III cracking compared to Vision 3.1.



**Figure 121. Comparison of Automatically Identified Class 1B Cracks to the Manual Windshield and Reference Surveys**



**Figure 122. Comparison of Automatically Identified Class II Cracks to the Manual Windshield and Reference Surveys**

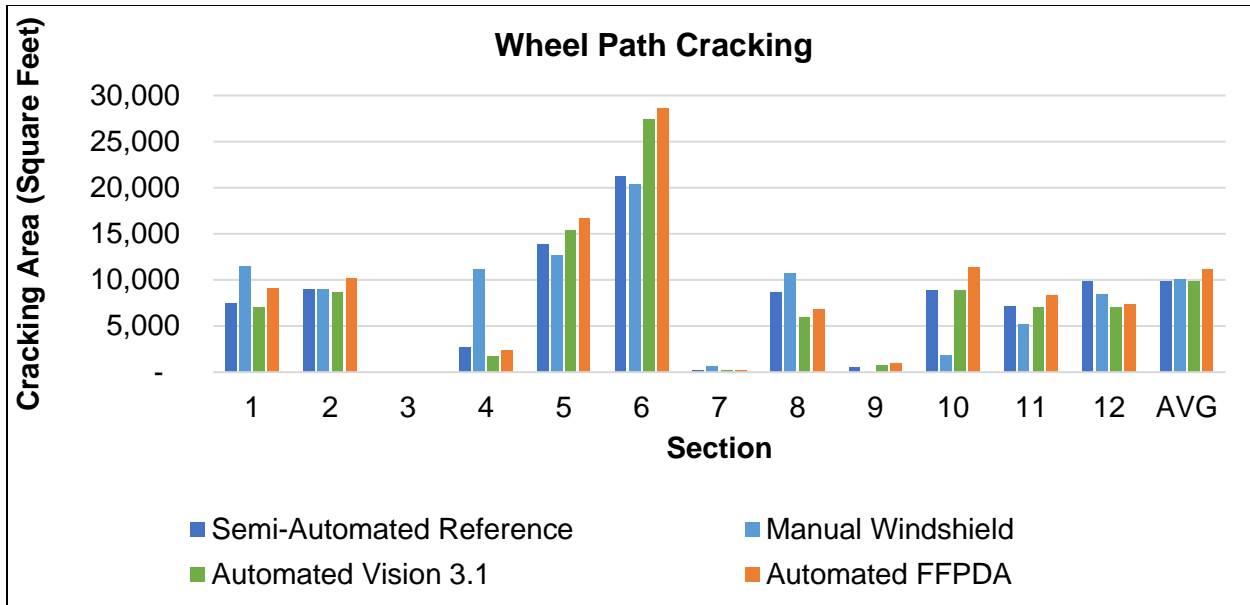


**Figure 123. Comparison of Automatically Identified Class III Cracks to the Manual Windshield and Reference Surveys**

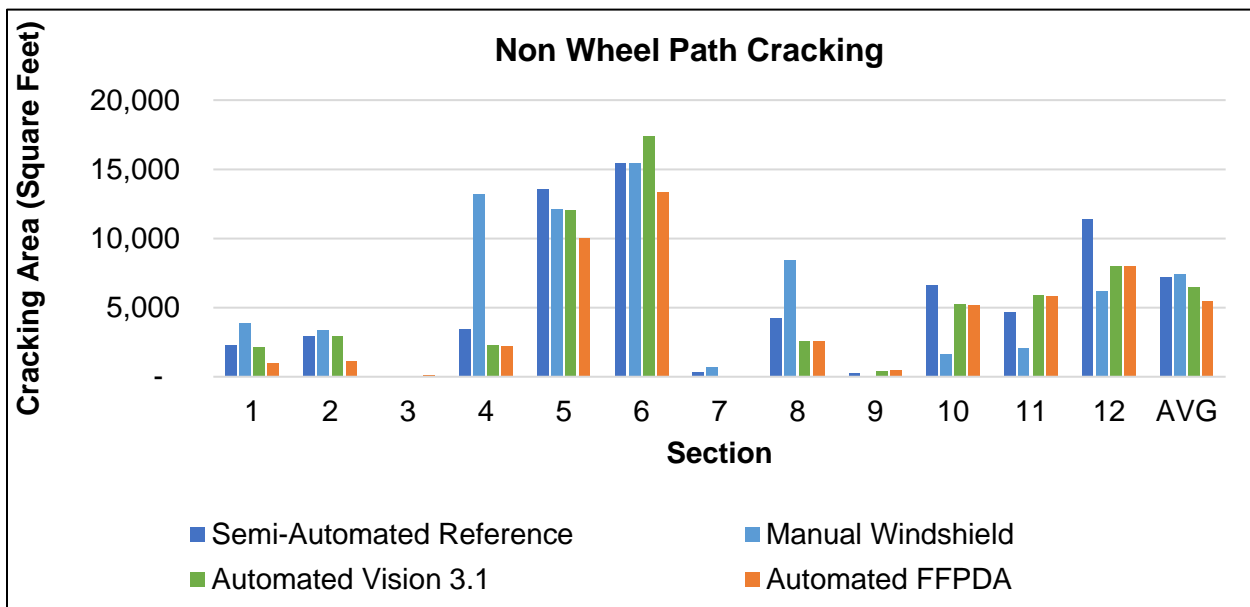
Overall, the performance of the FFPDA is acceptable compared to the reference and the manual windshield survey regarding Class 1B and Class II cracks. But the same cannot be stated regarding Class III cracks. The caveat in all these comparisons is that the FFPDA has a more systematic methodology for measuring crack width and assigning severity levels compared to the subjective visual methodology of the manual windshield survey and the semi-automated reference survey.

### 6.3.3 Automatically Identified Wheel Path and Non-Wheel Path Cracking

In this section, the rating results were converted to cracking within the wheel path and outside the wheel path according to the FDOT *Flexible Pavement Condition Survey Handbook* (2017). Figure 124 and Figure 125 show a comparison of the automated Vision 3.1 and FFPDA software to the manual windshield and reference surveys for wheel path and non- wheel path cracking, respectively.



**Figure 124. Comparison of Automatically Identified Wheel Path Cracking to the Manual Windshield and Reference Surveys**



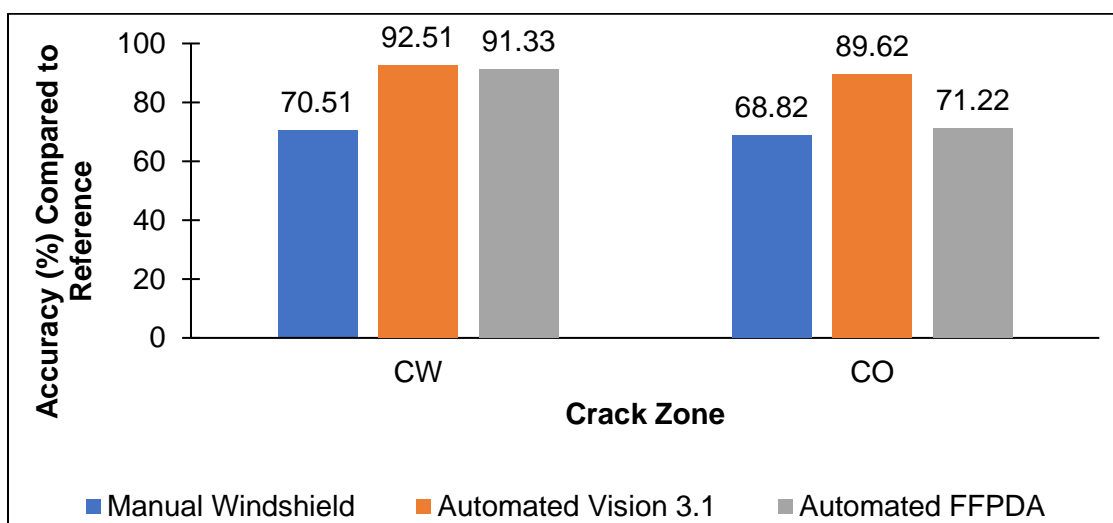
**Figure 125. Comparison of Automatically Identified Non- Wheel Path Cracking to the Manual Windshield and Reference Surveys**

#### 6.3.4 Comparison of Different Rating Methods

This section compares the results of the manual windshield surveys conducted by FDOT distress raters, the fully automated distress surveys using Vision 3.1 and FFPDA,

and the semi-automated reference survey described in Section 5.3.2, according to the success metrics described in Section 6.2.4. The results compared in this section include percent wheel path cracking (CW) and percent non-wheel path cracking (CO). The outlier test sections with minimal amount of cracking (sections 3, 7, and 9) were excluded from this analysis.

Figure 126 compares the accuracy of the three rating methods of manual windshield, automated Vision 3.1, and automated FFPDA, compared to the reference survey. FFPDA is showing a lower accuracy compared to Vision 3.1, but it is closer to the manual windshield results. This is mainly because of the grouping mechanism that was developed in Task 6 for the automated results to better reflect the practice of the FDOT raters in the field.

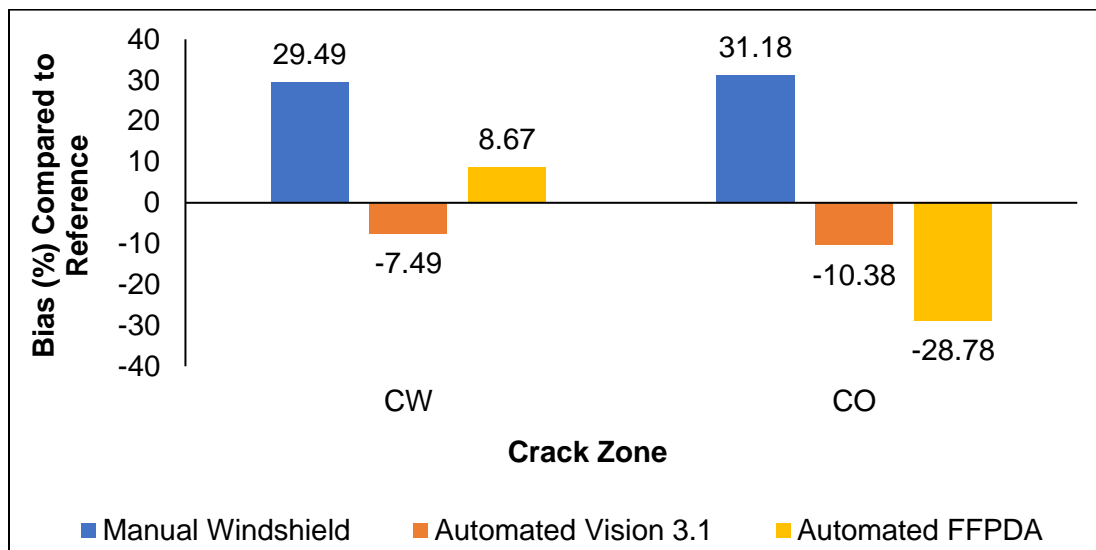


**Figure 126. Comparison of Different Methods in terms of Accuracy**

Figure 127 compares the bias of the three rating methods. Compared to the reference survey, FFPDA over-estimates CW and under-estimates CO. The bias of FFPDA compared to the reference survey is in the same direction as the manual windshield survey for CW but in the opposite direction for CO. Vision 3.1 has a bias in the opposite direction of the manual windshield survey results for both CW and CO. Since the bias of FFPDA is positive for CW and negative for CO, this means that the total amount of cracking identified by FFPDA is closer to the reference survey compared to the Vision 3.1 or the manual windshield survey results.

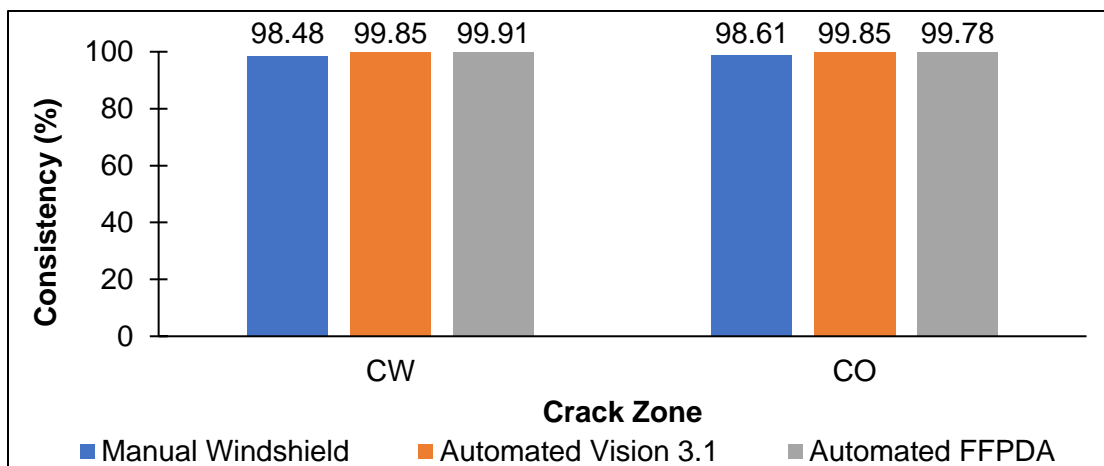
This means that compared to the reference survey, FDOT manual raters tend to over-estimate cracking, while FFPDA tends to over-estimate cracking in the wheel path zones (CW) and under-estimate cracking outside of the wheel path zones (CO). Wheel path cracking is an indication of fatigue in the pavement structure, and it has a higher importance compared to non-wheel path cracking in overall pavement condition

evaluation. FFPDA and manual windshield methods show better agreement in terms of wheel path cracking compared to non-wheel path cracking.



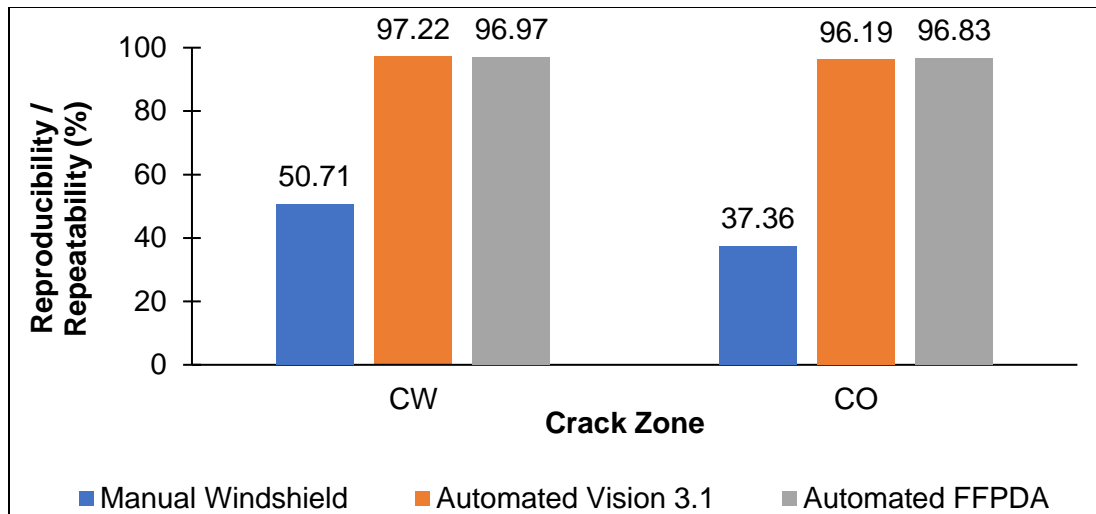
**Figure 127. Comparison of Different Methods in terms of Bias**

Figure 128 shows a comparison among the methods in terms of section-to-section consistency of the results. All three methods are comparable in this regard.



**Figure 128. Comparison of Different Methods in terms of Consistency**

Figure 129 compares the reproducibility of the manual windshield method to the repeatability of the two automated software, independent of the reference survey. The automated methods are showing much higher repeatability among multiple runs when compared to the reproducibility among multiple raters in the manual rating method.



**Figure 129. Comparison of Different Methods in terms of Repeatability/Reproducibility**

### 6.3.5 Comparison of FFPDA to Manual Windshield Survey

Since the ultimate objective of developing FFPDA is to replace the existing manual windshield surveys for the annual pavement condition survey (PCS), this section will compare the results of the two methods in terms of decision making. In this section, the rating results were converted to crack rating according to the FDOT *Flexible Pavement Condition Survey Handbook* (2017). In this evaluation, the raveling and patching areas were ignored, because the focus of the study was on cracking areas.

Figure 130 shows a comparison of FFPDA crack rating results to the results of the manual windshield survey. The box plots show the statistics for all runs on each of the 12 test sections. The X signs show the mean of the 3 runs/raters and the circles show the median of them. Except for section number 9, in all other test sections, the FFPDA shows no variation in crack rating values among the 3 runs. For the sections where the FFPDA shows no variation in crack rating values, the X sign for the mean, the circle for the median, and the box limits are in the same location. In contrast, in almost all sections, there is variation in crack rating values among the 3 raters. Due to the subjectivity of visual raters in assigning severity levels to the visible cracks (measuring crack width with the naked eye from a moving vehicle), such variability in the crack rating found in the manual windshield survey is expected.



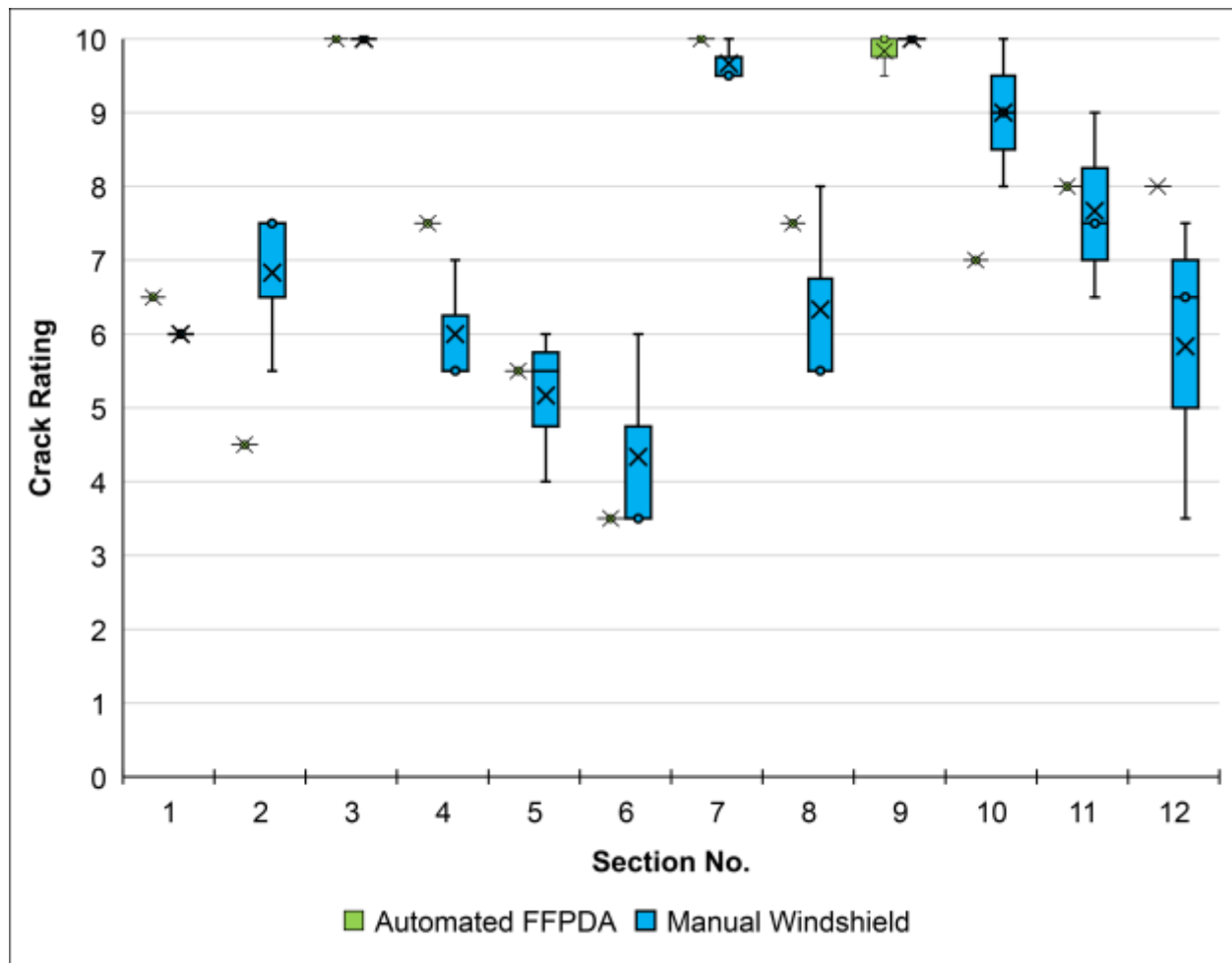
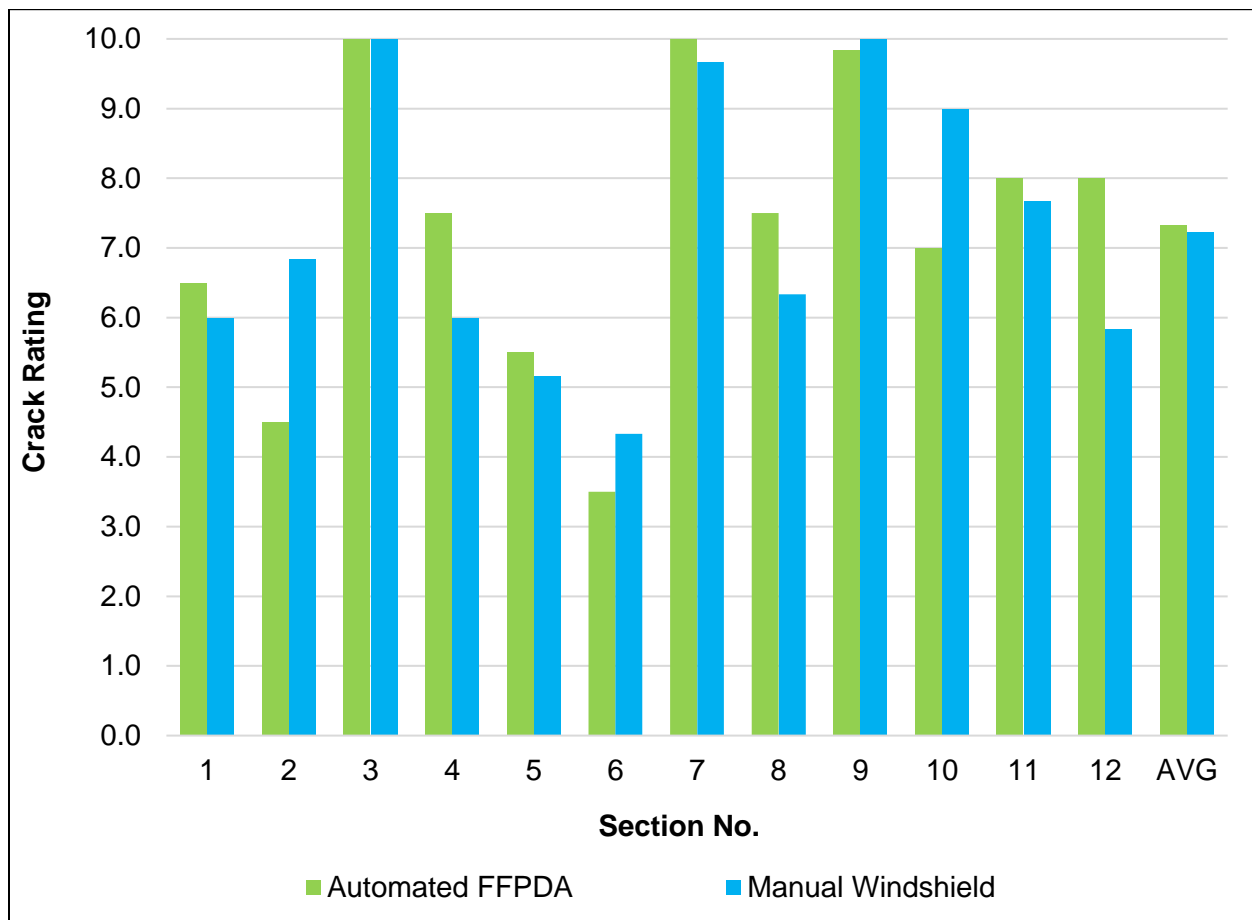


Figure 130. Comparison of FFPDA to Manual Windshield Survey Crack Rating Statistics

Figure 131 shows a comparison of the crack rating averaged among the 3 raters for the manual windshield survey and averaged among the 3 runs for the FFPDA results. On average, FFPDA and the manual windshield survey show acceptable agreement in terms of the overall crack rating.



**Figure 131. Comparison of FFPDA to Manual Windshield Survey Crack Rating Averages**

## 6.4 Summary and Recommendations for Implementation

Task 6 of this project involved development of the FFPDA to address the gaps that were discovered in Task 5, and validation of the FFPDA results according to the experiment design. The following conclusions can be made:

1. FFPDA demonstrates higher repeatability compared to the manual windshield survey. This was expected due to the subjectivity of the manual windshield survey (i.e. visual rating with the naked eye from a moving vehicle).
2. FFPDA demonstrates higher accuracy compared to the manual windshield survey. Accuracy is measured according to the bias compared to the reference survey and is a relatively subjective metric in this case.
3. FFPDA and the manual windshield survey have similar section-to-section consistency in the rating results.
4. FFPDA results showed better agreement with the manual windshield survey results than the previously tested Vision 3.1 software. This is because the FFPDA addressed the issues with Branch cracking, Alligator cracking, and severity level assignment that were found with Vision 3.1.
5. FFPDA and manual windshield methods have more agreement in terms of wheel path cracking compared to non-wheel path cracking.
6. The manual raters are often documenting more cracking compared to the reference survey in both the wheel paths and outside the wheel paths. However, the FFPDA is finding more cracking compared to the reference survey in the wheel paths and less cracking compared to the reference survey in non-wheel path zones.

According to the observations in the software validation results, the following are the recommendations for implementation:

1. Use FFPDA on a larger database of highway sections to determine if there are any systematic errors in software results. Use the semi-automated rating (manual rating of pavement images) to QC the results of FFPDA and potentially discover any remaining systematic errors.

2. Using the larger database of representative test sections, compare the results of FFPDA and the manual windshield ratings to determine a calibration equation between the two methodologies. This equation can be used to transform the FFPDA cracking results to a similar scale as the manual windshield results to ensure smooth pavement deterioration trends before and after implementation of an automated approach. In the long term, the deduct values for the combined condition index might need to be revisited as a result of this exercise.

The semi-automated rating method should also be used to determine pavement areas affected by raveling and patching. The developed software can automatically add these semi-automated rating results to the automated cracking results of FFPDA and provide the final combined condition index for every pavement section.

## CHAPTER 7 – AUTOMATED APPLICATION IMPLEMENTATION

Task 7 of this research project involved technical support to implement the validated automated distress identification applications for both rigid and flexible pavements into the annual Pavement Condition Survey (PCS) process. This implementation was completed during two phases:

1. Phase I: after completion of Task 3, Fugro provided support to implement the validated FDOT Rigid Pavement Distress Application (FRPDA)
2. Phase II: after completion of Task 6, Fugro provided support to implement the validated FDOT Flexible Pavement Distress Application (FFPDA)

This document is organized into five sections. Following this introduction, Section 7.1 summarizes the implementation activities for FRPDA. Section 7.2 describes the implementation activities conducted for FFPDA. Section 7.3 presents a suggested data quality management program. Finally, Section 7.4 summarizes the efforts and provides pertinent recommendations for future data collection and processing activities.

### 7.1 Implementation Activities for FDOT Rigid Pavement Distress Application (FRPDA)

This section of the report summarizes the activities conducted for implementation of the FRPDA into the annual PCS process.

#### 7.1.1 Data Collection

The sample data for identification and quantification of distresses for rigid pavements was collected using the FDOT multi-purpose survey vehicle (MPSV), which is equipped with the Laser Road Imaging System (LRIS). In Task 2, Fugro staff conducted an investigation to determine whether the collected two-dimensional (2D) pavement images are of acceptable quality for crack detection and how FDOT can potentially measure various image quality indicators in future. As a result, Fugro developed a **Hardware Maintenance Protocol** to be used by FDOT staff in order to ensure long term image quality and consistency. This protocol was submitted as an appendix to the Task 2 Report.

During Task 2 of this research project, a two-day distress raters' class was organized for both existing FDOT raters and appropriate Fugro staff on August 25 to 26, 2015. The class included both classroom as well as field training exercises. The main objective of this workshop was for Fugro to understand how FDOT raters conduct rigid pavement condition surveys, and how some of the involved decisions on distress type, extent, and severity can be quantified for the automated algorithm to match FDOT raters' decisions. Based on the meeting discussions and the results of the field exercise, several notes were recorded for consideration in the quantification process required for software development. FDOT staff might discuss these notes to potentially include them for further clarity of the handbook.

### 7.1.2 Data Processing

Fugro developed a workflow to load the collected 2D LRIS images into the Vision software tool used for this research project. This workflow has two fundamental elements:

1. Location and format of the collected data
2. Structured Query Language (SQL) code that fetches data from the stored location and puts it in the required database format to be used by Vision software

This workflow was first submitted as Appendix G of the Task 2 Report. The latest version of this workflow is documented in Appendix A of this report. If the fundamental elements of this workflow are followed, LRIS data following the same format and structure can be imported into Vision software using this workflow.

In addition, Fugro developed the **FRPDA User's Guide** for image filtering, crack detection, joint detection, and crack classification and rating. This guide was delivered in Appendix A of the Task 3 Report. Appendix C of the Task 3 Report was a software installation guide.

At the conclusion of Phase I, Fugro held a meeting on February 22, 2017 at FDOT State Materials Office (SMO), during which the developed software (FRPDA version 1.0) and corresponding recommendations were demonstrated to FDOT staff. In addition, the software was installed and tested on several desktop computers for FDOT staff to use and test. On June 8, 2017, a hands-on FRPDA training class was held in a computer instruction room at the FDOT SMO.

### 7.1.3 Data Analysis and Reporting

In Appendix B of the Task 3 Report, Fugro provided a guide to use basic Vision functions for viewing images and manual rating of the pavement images. This semi-automated distress survey was recommended for quality control of the automated results and for adding other non-cracking pavement surface distress types such as spalling, surface deterioration, and patching.

After running the FRPDA, the results of joint detection and cracking identification are stored in comma-separated values (csv) files. The contents of these files can easily be used to develop reports in a meaningful format to be used for pavement management and treatment design purposes.

### 7.1.4 Data Quality Management

Chapter 4 of this document provides a suggested framework for data quality management.

## 7.2 Implementation Activates for FDOT Flexible Pavement Distress Application (FFPDA)

This section of the report summarizes the activities conducted for implementation of the FFPDA into the annual PCS process.

### 7.2.1 Data Collection

The sample data for identification and quantification of distresses for flexible pavements was collected using a Fugro Automatic Roadway Analyzer (ARAN) vehicle equipped with the three-dimensional (3D) Laser Crack Measurement System (LCMS). At the time of the conclusion of this research project, FDOT had not purchased a 3D data collection system. However, FDOT had contracted the collection of the pavement condition data on Florida Interstate Highways to a Data Collection Contractor who operated an LCMS vehicle.

On June 7 to 8, 2017, a two-day distress raters' class was organized for both existing FDOT raters and appropriate Fugro staff. The class included both classroom as well as field training exercises. The main objective of this workshop was for Fugro to understand how FDOT raters conduct flexible pavement condition surveys, and how some of the involved decisions on distress type, extent, and severity can be quantified for the automated algorithm to match FDOT raters' decisions.

### 7.2.2 Data Processing

Fugro developed a workflow to load the 3D LCMS images and data collected by the Data Collection Contractor into the Vision software tool used for this research project. This workflow has two fundamental elements:

1. Location and format of the collected data
2. Structured Query Language (SQL) code that fetches data from the stored location and puts it in the required database format to be used by Vision software

This workflow is documented in Appendix B of this report. If the fundamental elements of this workflow are followed, LCMS data following the same format and structure can be imported into Vision software using this workflow. In addition, a user interface was created for facilitating the application of this SQL code for data transfer (see details in Appendix B).

In addition, Fugro developed the **FFPDA Reference Manual** for crack detection, and crack classification and rating. This guide was delivered as Appendix B of the Task 6 Report. This Reference Manual included a software installation guide and a Quick Start Guide.

At the conclusion of Task 6, Fugro held a meeting on June 25 to 26, 2018 at FDOT SMO during which the developed software and corresponding recommendations were demonstrated to FDOT staff. In addition, the software was installed and tested on several desktop computers for FDOT staff to use and test. The testing by FDOT staff revealed some issues in Vision 3.4 that compromised the performance of FFPDA. Therefore, the FFPDA was revised to match Vision 3.1, the most recent reliable version of the platform.

### 7.2.3 Data Analysis and Reporting

In the Reference Manual submitted as an appendix to the Task 6 Report, Fugro provided instructions to use a semi-automated distress survey for quality control of the automated results and for adding other non-cracking pavement surface distress types such as raveling and patching.

After running the FFPDA, the results of cracking identification and section crack rating are stored in csv files. The contents of these files can easily be used to develop reports in a meaningful format to be used for pavement management and treatment design purposes.

## 7.2.4 Data Quality Management

Chapter 4 of this document provides a suggested framework for data quality management.

## 7.3 Data Quality Management Program

This chapter presents a suggested data quality management program. FDOT staff may choose to adopt this program within their existing processes for quality management.

### 7.3.1 Definitions

The following are definitions of terms, abbreviations, and acronyms used in this quality management program.

**Table 60. Definition of Quality Terms**

<b>Term</b>	<b>Definition</b>
Quality	The degree to which a set of inherent characteristics of a product or service fulfill requirements.
Quality Standards	Quantitative and qualitative characteristics of product or service that are used to determine the quality of each deliverable. Examples include accuracy, precision, resolution, etc.
Accuracy	Accuracy is a qualitative term referring to whether there is agreement between a measurement made on an object and its true (target or reference) value, indicating measurement effectiveness. Bias is a quantitative term describing the difference (or error) between the average of measurements made on the same object and its true value.
Precision	Precision is a qualitative term describing the degree of repeatability of a measurement value, indicating measurement reliability. Variance and standard deviation of error are quantitative estimates of precision.
Resolution	Data reporting format corresponding to measurement methodology and specific application by the user.
Quality Management	The overarching system of policies and procedures that govern the performance of quality control and acceptance activities.
Quality Control	A series of measurements and corresponding corrective actions to ensure that a desired level of quality is obtained for the developed product or service.



Quality Acceptance	The criteria to confirm that the quality of the developed product or service is indeed acceptable for application by the user.
Quality Assurance	Reporting, training, and process improvement activities to increase the ability of the development process to fulfill quality requirements for the product or service being provided.

### 7.3.2 Quality Management Approach

A pavement performance Data Quality Management Program (DQMP) is recommended with the following objectives:

- Evaluation and updates of data collection, processing, and reporting standards and protocols considering agency goals and objectives
- Better compliance with data standards and protocols
- Improved completeness, accuracy, and consistency of data
- Increased data credibility within the organization
- Cost savings from more appropriate data-driven treatment recommendations
- Increased accuracy of budget need determinations
- Better integration with other internal agency data
- Compliance with FHWA MAP-21/FAST Act requirements

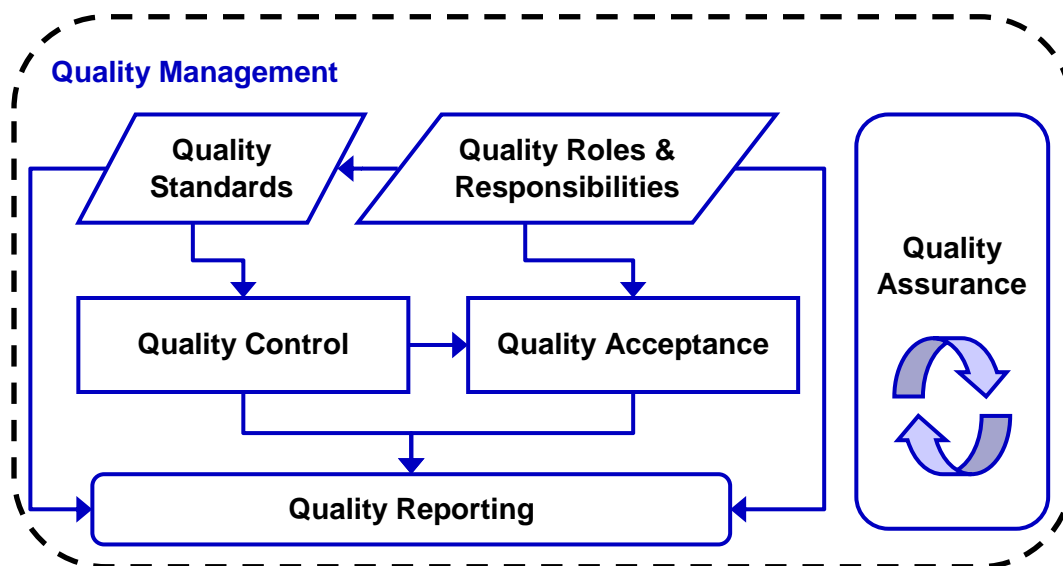
The FHWA *Practical Guide for Quality Management of Pavement Condition Data Collection* (Pierce et al. 2013) was consulted in the development of this DQMP. At a minimum, every quality management system shall include:

- Quality standards, including data collection, processing, and reporting methodology
- Routine data quality control (QC) measures, checklists, and criteria
- Error tracking and resolution system
- Periodic quality assurance (QA) procedures to ensure the data collection and processing system is producing data conforming to the quality standards
- Quality acceptance and reporting
- Identification of roles and responsibilities

FDOT collects highway inventory and condition data using internal resources to the furthest extent possible. In addition, FDOT procures services from qualified Data Collection Contractors when the need arises. Regardless of the in-house or contracted data collection approach, quality management is administered by the FDOT staff. FDOT may require the Data Collection Contractors to submit a Quality Control Plan which complies with and complements this DQMP.

The flow chart in Figure 132 demonstrates the various aspects of the quality management approach. The quality standards, roles, and responsibilities should be set in the DQMP. For in-house collection, quality control shall be conducted by FDOT staff. For contracted collection, the

Data Collection Contractor should conduct quality control activities according to the submitted Quality Control Plan. FDOT staff shall review the QC results and conduct quality acceptance audits. The whole quality management process and findings should be documented through the quality reporting plan. All of the involved processes shall be reviewed according to the findings and any relevant process improvements shall be identified and implemented through continuous quality assurance.



**Figure 132. Quality Management Approach**

The key activities, processes, and procedures for quality management of the pavement performance data are briefly described in Table 61, with more in-depth information provided in the sections that follow.

**Table 61. Contents of the Data Quality Management Program**

<b>Data Collection Protocols and Quality Standards</b>	The data collection deliverables subject to quality review, protocols used to collect, and quality standards that are the measures used to determine a successful outcome for a deliverable. Deliverables are evaluated against these criteria before they are formally approved.
<b>Data Quality Control (QC) Measures</b>	The QC activities conducted by either FDOT staff (for in-house collection) or the Data Collection Contractor that monitor, provide feedback, and verify that the data collection deliverables meet the defined quality standards.
<b>Data Quality Acceptance Criteria</b>	The acceptance testing that will be used to determine if quality criteria are met and corrective actions that will be taken for any deliverables not meeting criteria.

<b>Quality Assurance (QA) Plan</b>	The plan for training of the involved staff, and using the QC results for the improvement of corresponding data collection and QC processes.
<b>Quality Reporting Plan</b>	The documentation of key quality management activities, including QC log and acceptance log, and the format of the final quality management report.
<b>Roles and Responsibilities</b>	The quality-related responsibilities of the data collection team.

### 7.3.3 Data Collection Protocols and Quality Standards

The latest version of the FHWA *Highway Performance Monitoring System (HPMS) Field Manual* (December 2016) is to be used for the collection and processing of data that will be submitted to the FHWA. The HPMS Field Manual references various AASHTO protocols for calibration of equipment and collection of data. For non-HPMS data, the latest version of the FDOT *Rigid Pavement Condition Survey Handbook* (September 2017) and *Flexible Pavement Condition Survey Handbook* (October 2017) will be used for distress data. HPMS and non-HPMS data can be collected in-house or by the Data Collection Contractor at the discretion of FDOT.

#### Deliverables, Protocols, and Quality Standards

The data elements that need to be submitted to the FHWA HPMS for 0.1-mile segments are included in

Table 62. This list includes the corresponding protocol for data collection and processing. The list also includes recommended quality standards for accuracy, precision, and resolution that need to be reviewed by FDOT staff to determine whether they are acceptable.

The data elements beyond what is submitted to the HPMS and need to be collected for FDOT's pavement management purposes are listed in Table 63. This list includes the corresponding protocol for data collection and processing, and the recommended quality standards for accuracy, precision, and resolution that need to be reviewed by FDOT staff to determine whether they are acceptable.

In these tables, accuracy can be measured as the average error compared to reference values (normalized errors in percentage and absolute errors in corresponding measurement units), and precision can be estimated as the run-to-run repeatability out of 3 repeated runs (variation from mean of 3 repeated runs). Both accuracy and precision shall be evaluated on control sites, where reference values are documented according to a methodology approved by FDOT (see section on Reference Measurements). Precision shall also be evaluated on verification sites (see section on Control and Verification Sites). Accuracy and precision shall be evaluated based on a 95% confidence level; meaning 95% of the collected data needs to be within acceptable tolerance from the reference and from the mean of the repeat runs. In addition to checking the data on control and verification sites, the quality standards of accuracy and precision can also be used in a random blind sampling of every batch of data delivered for acceptance testing (see section 7.3.5).

In this case, the reference values used for evaluating accuracy can be the previous measurements on that test section.

The recommended quality standards of accuracy and precision in

Table 62 and Table 63 are based on the measurement resolution, and past experience in capabilities of current measurement technology. For example, the current automated survey technology has a higher rate of success in estimating the amount of cracking as opposed to non-cracking surface defects; as a result, the quality standards set for cracking distress types are tighter than that set for non-cracking surface defects. In majority of the data elements, the quality standard set for precision is tighter than that set for accuracy. This is because reference values used for evaluating accuracy might be measured with a different technology, but precision is an estimate of the repeatability of multiple measurements with the same technology.

**Table 62. Recommended Protocols and Quality Standards for HPMS Data**

<b>Deliverable</b>	<b>Protocol</b>	<b>Resolution &amp; Reporting</b>	<b>Accuracy (compared to reference)</b>	<b>Repeatability (out of 3 runs)</b>
International Roughness Index (IRI)	Collection of Longitudinal Profile: AASHTO R57-14 Quantification of IRI: AASHTO R43-13	Nearest 1 inch per mile Report MRI (average of left and right IRI) a	± 10%	± 5%
Rut Depth	Collection of Transverse Profile: AASHTO R88-18 Rut Depth: AASHTO R87-18	Nearest 0.01 inch Report average rut depth of two wheel paths a	± 0.1 inches	± 0.05 inches
Faulting	Measurement and Quantification: AASHTO R36-17	Nearest 0.01 inch Report average absolute faulting of all joints in the right wheel path, including zero values a	± 0.1 inches	± 0.05 inches
Percent Cracking	Image Collection: AASHTO R86-18 Cracking Estimation: AASHTO R85-18	Nearest 1% Report Percent Cracking b,a	The higher of ± 25% or ± 5 points in Percent Cracking	The higher of ± 15% or ± 3 points in Percent Cracking
Present Serviceability Rating (PSR)	HPMS Field Manual, Agreement with FHWA Division Office on approach	Nearest 0.1 point Report PSR from 0.1 to 5.0 a	± 0.5 points	± 0.5 points

<b>Deliverable</b>	<b>Protocol</b>	<b>Resolution &amp; Reporting</b>	<b>Accuracy (compared to reference)</b>	<b>Repeatability (out of 3 runs)</b>
Horizontal Curvature	HPMS Field Manual	Horizontal curvature category	Matching degree of curve from construction plans $\pm 0.3$	$\pm 0.1$ degree
Grade	HPMS Field Manual	Vertical curvature category	Matching grade from construction plans $\pm 0.3$	$\pm 0.1$ percent

a Report one number for 0.1-mile segments, full extent, one lane, one direction.

b AC: Total area of cracked wheel path divided by total section area; JPCP: Percentage of slabs with at least one transverse crack > 1/2 lane width; CRCP: Cracking (exclude transverse) area divided by total section area.

**Table 63. Recommended Protocols and Quality Standards for FDOT Pavement Management Data**

<b>Deliverable</b>	<b>Protocol</b>	<b>Resolution &amp; Reporting</b>	<b>Accuracy (compared to reference)</b>	<b>Repeatability (out of 3 runs)</b>
<b>Pavement Condition Data: Flexible Pavements</b>				
Cracking Confined to Wheel Paths	FDOT Flexible Pavement Condition Survey Handbook (October 2017)	Percent of wheel path area affected at 3 severity levels: Class 1B, Class II, Class III	± 10%	± 10%
Cracking Outside of Wheel Paths		Percent of non-wheel path area affected at 3 severity levels: Class 1B, Class II, Class III	± 10%	± 10%
Dominant Crack Type		Alligator (A), Block (B), and Combination (C)	N/A	N/A
Patching Confined to Wheel Paths b		Percent of wheel path area affected	± 25%	± 15%
Patching Outside of Wheel Paths b		Percent of non-wheel path area affected	± 25%	± 15%
Raveling Confined to Wheel Paths b		Percent of wheel path area affected at 3 severity levels: Light, Moderate, Severe	± 25%	± 15%
Raveling Outside of Wheel Paths b		Percent of non-wheel path area affected at 3 severity levels: Light, Moderate, Severe	± 25%	± 15%
Crack Rating		Between 0 and 10 with a resolution of 0.5	± 0.5 points	± 0.5 points
Ride Rating		Between 1 and 10 with a resolution of 0.1	± 0.3 points	± 0.1 points
Rut Depth		Nearest 0.125 inches	± 0.125 inches	± 0.125 inches
Rut Rating		Between 0 and 10 with a resolution of 1	± 1 point	± 1 point
International Roughness Index (IRI)	ASTM E1926	Nearest 1 inch per mile, average of the left and right wheel paths	± 10%	± 5%
Ride Number (RN)	ASTM E1489	Between 0 and 5, Nearest 0.01, average of the left and right wheel paths	± 10%	± 5%

<b>Deliverable</b>	<b>Protocol</b>	<b>Resolution &amp; Reporting</b>	<b>Accuracy (compared to reference)</b>	<b>Repeatability (out of 3 runs)</b>
<b>Pavement Condition Data: Rigid Pavements</b>				
Transverse Cracking	FDOT Rigid Pavement Condition Survey Handbook (September 2017)	Count occurrence at 3 severity levels	± 10%	± 5%
Longitudinal Cracking		Count occurrence at 3 severity levels	± 10%	± 5%
Corner Cracking		Count occurrence at 3 severity levels	± 15%	± 10%
Joint Condition b		Partially Sealed or Not Sealed, representative severity within the rated section	N/A	N/A
Surface Deterioration b		Area extent at 2 severity levels	± 25%	± 15%
Spalling b		Length extent at 2 severity levels	± 25%	± 15%
Patching b		Area extent at 2 severity levels	± 25%	± 15%
Pumping b		percent within the rated section at 3 severity levels	± 25%	± 15%
Shattered Slab b		Number of affected slabs at 2 severity levels	N/A	N/A
Fault Index (FI)		Nearest 1	± 2	± 1
Faulting	AASHTO R36-17	Nearest 0.03 (1/32) inch, report average absolute faulting of all joints in the right wheel path, including zero values	± 0.1 inches	± 0.05 inches
Slab Length	N/A	Approximate slab length in feet	± 5%	± 5%
Slab Count	N/A	Count slabs	± 5%	± 5%
Cracked Slab Count	HPMS Field Manual	Number of affected slabs	± 10%	± 5%

<b>Deliverable</b>	<b>Protocol</b>	<b>Resolution &amp; Reporting</b>	<b>Accuracy (compared to reference)</b>	<b>Repeatability (out of 3 runs)</b>
<b>General, Location, and Geometric Data</b>				
Pavement Images	AASHTO R86-18	4096 pixels across 12 feet lane width; able to collect 2 mm wide cracks at highway speeds	Uniform illumination; color balanced and clear; proper image stitching	
Right of Way (ROW) Images	N/A	1920 x 1080 pixels; covering 120 degree viewing angle	Free of distortion and over-exposure; color balanced and clear; synchronized with other image/data; allow length and width measurements of assets	
GPS Coordinates	N/A	Nearest 0.0000001 degree	± 15 feet	± 0.00001 degrees
GPS Elevation	N/A	Nearest 0.1 meter	± 0.1 meter	± 0.1 meter
Chainage (LRS)	N/A	Nearest 0.001 mile	± 15% compared to walking wheel	± 5%
PAVE_TYPE b	HPMS Field Manual	Asphalt, PCC, CRC, or Composite	Matching FDOT Inventory data	N/A
Macrotexture	ASTM E1845	Nearest 0.001 inch Mean Texture Depth (MTD), RMS, and Error for each wheel path	N/A	± 15%
Friction Number	ASTM E274 ASTM E501 ASTM E524	Nearest 0.1 for each wheel path	N/A	N/A
Cross Fall	N/A	Nearest 0.1 percent	N/A	± 15%
Horizontal Radius of Curvature	N/A	Nearest 1 meter	N/A	± 15%
Grade	N/A	Nearest 0.1 percent	N/A	± 0.1 percent
Edge Drop-off	N/A	Count occurrence and height to nearest 1 mm	N/A	± 15%

b Currently, these data elements can only be estimated by manual rating of the collected pavement images.



## Reference or “Ground Truth” Measurement

It is recommended to establish control sites (see Section on Control and Verification Sites) and collect reference data on them. The reference data should be collected on the control sites at least once every 2 years.

For collecting reference sensor data (roughness, rut depth, faulting, grade, cross slope), the reference data can be collected with a certified equipment that matches the description of a reference profiler in AASHTO R56-14 Standard. Several commercial versions of these reference profilers are available through ICC, ARRB, and SSI companies. Fugro owns and operates an ICC version.

The AASHTO R56-14 Standard was developed for certification of inertial profiling systems, and it contains guidelines for establishing a reference longitudinal profile using a reference profiler. This reference longitudinal profile can be used to quantify the reference values for IRI, RN, faulting, and grade data.

The AASHTO R88-18 Standard for collecting transverse profile data also includes guidelines for collecting reference transverse profile data using a reference profiler with similar descriptions to that noted in the AASHTO R56-14 Standard. This reference transverse profile can be used to quantify the reference values for rut depth and cross slope data.

The sensor data shall be collected with the reference profiler multiple times until 3 repeatable runs (the correlation of all data among the 3 runs is equal to or higher than 0.98) are achieved. Then one of those 3 repeatable runs would be used as reference.

For horizontal curvature data, a sample of the HPMS sections that are categorized as D, E, or F can be used as control sections, on which construction plans are used as reference values. After this verification of curvature data in the base year, this sample data can be used as historical reference for the following years.

For establishing reference distress data, it is recommended that at least 3 certified distress raters would first review the distress type, severity, and extent guidelines in the *FDOT Rigid Pavement Condition Survey Handbook* (September 2017) and *Flexible Pavement Condition Survey Handbook* (October 2017), and review example historical data. The raters would then conduct a semi-automated survey to identify distresses on pavement images. Following the semi-automated survey, the raters will compare notes and arrive at a consensus for all distress types, severity, and extent to document the reference (“ground truth”) distress survey.

On any site other than the control sites, the most recent accepted data should be used as reference measurements.

## Control and Verification Sites

The recommended number and length of control and verification sites are listed in Table 64. The control sites are used for vehicle calibration checks and certification and shall be visited once every month (during data collection season), including the entry and exit controls. Additionally, in the event data collection vehicles or data collection components undergo repair or replacement, the affected system(s) will need to be recalibrated and then verified using the control sites. The

verification sites are used for weekly calibration checks during data collection and are planned to be scattered across the state to the extent possible to avoid traveling back and forth between a data collection district and the central office. The control sites can also be used for verification.

The control and verification site data shall be shipped to the office to be compared against the reference data to evaluate accuracy. The reference data on the control sections should be collected at a 2-year frequency (see Section on Reference Measurement) and for the verification sites, the last cycle of data collection can be used as reference data. The repeatability among 3 repeated runs on these sites will be used to evaluate precision. If multiple data collection vehicles are used, the verification sites need to be used for evaluating reproducibility of the sensor data across multiple vehicles.

There are sites already established for Distance Measuring Instrument (DMI) calibration, which can be used as control and verification sections for sensor data. Ideally, these sites should have minimal surface distress to avoid complications in establishing reference sensor data. For flexible pavements, it is recommended to have two control sites, one smooth and one relatively rough to evaluate the accuracy and repeatability of the equipment on different ride quality situations. Due to the limited length of rigid pavements across Florida, only one control site is recommended.

The control sections for distress data need to have an adequate amount of each distress type to the extent feasible. That is why the control sites for distress data and those for sensor data need to be separate. If the data collection crew (FDOT or Contractor) conduct daily quality control of the collected pavement images, there is no need for weekly verification of distress data and the monthly evaluation of accuracy and precision on the control sites will suffice. Therefore, no verification sites are recommended for distress data.

**Table 64. Planned Control and Verification Sites**

Site Purpose	Pavement Type	District	Route	Direction	Length b
<b>Control and Verification Sites for Sensor Data</b>					
Control/Verification	AC	District 2	TBD	TBD	500 ft
Control/Verification	AC	District 2	TBD	TBD	500 ft
Control/Verification	PCC	District 2	TBD	TBD	500 ft
Verification	AC	District 1	TBD	TBD	500 ft
Verification	AC	District 3	TBD	TBD	500 ft
Verification	AC	District 4	TBD	TBD	500 ft
Verification	AC	District 5	TBD	TBD	500 ft
Verification	AC	District 6	TBD	TBD	500 ft
<b>Control Sites for Distress Data</b>					
Control	AC	District 2	TBD	TBD	500 ft
Control	PCC	District 2	TBD	TBD	1000 ft

b 0.1-mile segments are typically adequate for both control and verification sections. The recommended length for the rigid distress control section is longer due to the limited density of observed distress on concrete pavements.

## Equipment Calibration and Certification Protocols

Table 65 lists the available national standards for calibration and certification of data collection equipment. National standards are under development for calibration and certification of some of the equipment.

**Table 65. Available Equipment Calibration and Certification Protocols**

<b>Data Element</b>	<b>Data Collection Equipment</b>	<b>Equipment Calibration Protocol</b>	<b>Comments</b>
Longitudinal profile	Inertial profilers	Collection System: AASHTO M328-14 Equipment Certification: AASHTO R56-14	National Standard Available
Transverse profile	Laser sensors	AASHTO R48-10 or AASHTO R88-18	National Standard Under Development
Faulting of concrete joints	Profilers or 3D images	AASHTO R36-17	National Standard Under Development
Pavement distress	2D or 3D imaging technology	AASHTO R86-18	National Standard Under Development

For FDOT in-house data collection, the Data Collection Vehicle Provider is responsible for annual preventive maintenance, calibration, and certification of the equipment installed and integrated on the vehicle. The following is a general overview of the tasks conducted during annual vehicle certification, depending on the specific equipment integrated on the vehicle:

- Central Data Acquisition Computer (CDAC) checkup and updates
- Smart Video Controller (SVC) checkup and updates
- AC BOX and DC BOX checkup and maintenance
- Distribution Enclosure checkup and maintenance
- Cables / Racks / Dog House / Miscellaneous checkup and maintenance
- DMI checkup and calibration
- Chassis / Generator / Inverter / Charger checkup and maintenance
- Laser South Dakota Profiler (LSDP) and Texture sensor checkup, maintenance, and calibration (including static test, bounce test, and repeat runs for verification)
- Laser Rut Measurement System (LRMS) checkup, maintenance, and calibration (including static test, cross-fall rolling test, dynamic repeat runs for verification)
- Grade and pitch sensors checkup, maintenance, and calibration (including static and bounce tests and repeat runs for verification)
- POSLV PCS (Position and Orientation System) checkup and software updates
- Right-Of-Way (ROW) forward and backward cameras checkup and maintenance

- Pavement Laser Road Imaging System (LRIS) or Laser Crack Measurement System (LCMS) checkup, maintenance, and calibration

For contracted data collection, the Data Collection Contractor shall be required to submit equipment calibration and certification information including a regular maintenance and testing program as part of their Quality Control Plan.

### **Certification of Equipment Operators and Persons Performing Manual Data Collection**

Typically, the reference distress survey on the control sites would be conducted manually or semi-automated (manual rating of collected images). FDOT shall hold workshops for the distress raters to collectively review the definitions and sample images and potentially conduct an exam rating to certify the distress raters.

For FDOT in-house data collection, the equipment operators shall receive annual training and certification, a record of which shall be documented. This training shall include the following topics regarding vehicle operation:

- Driver safety and proactive driving practice
- Mechanical checkup and maintenance (refer to Data Collection Vehicle Provider)
- Overall equipment operation (refer to Data Collection Vehicle Provider)
- Daily/weekly/monthly equipment/sensor checks and preventive maintenance
- DMI calibration and verification
- Repeat runs and verification testing for sensor data

For contracted data collection, the Data Collection Contractor should be required to submit current documentation indicating training and certification of equipment operators as part of their Quality Control Plan. Some of the pavement surface distress types may be manually identified on the collected images using desktop software (semi-automated survey). The Data Collection Contractor is responsible for training and certification of corresponding staff.

### 7.3.4 Data Quality Control Measures

For in-house data collection, FDOT staff are responsible for quality control (QC) activities before, during, and after data collection. For contracted data collection, the conduct of QC procedures and measurements are the responsibility of the Data Collection Contractor. The QC steps are conducted according to the Quality Control Plan submitted by the Data Collection Contractor and approved by FDOT. Regardless of in-house or contracted data collection, the following includes the key procedures and corresponding frequency for data quality control measurements during three stages of data preparation.

#### Quality Control Activities Conducted Before Data Collection

These QC activities include calibration and periodic checks of data collection equipment and the first visit to the control sites. Table 66 includes an overview of these activities. In addition to the recommendations provided in Table 66, QC activities should be performed in accordance with equipment manufacturer recommendations.

**Table 66. Quality Control Activities Conducted Before Data Collection**

Deliverable	Quality Expectations	QC Activity	Frequency
All Pavement Data	Completeness	Plan collection route	Once, prior to data collection.
		Routing QC to match FDOT supplied info b	Once, prior to data collection.
		Define equipment configuration b	Once, prior to data collection.
		Verify equipment configuration b	Once, prior to collection. Also conducted after any equipment changes.
	Accuracy and Repeatability	Equipment calibration	Once, prior to collection. Also conducted after any equipment changes.
		DMI calibration	Once, prior to data collection. Also conducted during and after data collection.
		Data collection and data processing personnel certification	Once, prior to data collection.
Distress and Sensor Data	Accuracy and Repeatability	Control sites measurements	Once, prior to data collection. Also conducted during and after data collection.

b These activities are only conducted for contracted data collection.

### Quality Control Activities Conducted During Data Collection

Table 67 lists the QC activities during data collection used to continuously monitor the data being collected and a schedule of daily/monthly checks. It also includes the monitoring of ambient conditions and corresponding actions to address issues. In addition to the recommendations provided in Table 67, QC activities should be performed in accordance with equipment manufacturer recommendations.

**Table 67. Quality Control Activities Conducted During Data Collection**

Deliverable	Quality Expectations	QC Activity	Frequency
All Pavement Data	Safety/Efficiency	Mechanical inspection	Daily
		Preventative maintenance program	Annual
	Completeness	Field activity report including the collection location info	Daily for contracted and Weekly for in-house
	Accuracy	Subsystem checks (sensors, computers, software)	Daily
		Real-time quality monitoring (monitor images and data streams during collection)	Daily
		End of day verification (review sample of data and images from day's collection)	Daily
		DMI calibration	Monthly
Distress and Sensor Data	Accuracy and Repeatability	Control sites	Monthly
		Verifications sites	Weekly

### Quality Control Activities Conducted After Data Collection

A list of QC activities after data collection is included in Table 68, including review and checking of data for completeness, reasonableness, logic, acceptable range, accuracy and precision. In addition to the recommendations provided in Table 68, QC activities should be performed in accordance with equipment manufacturer recommendations.

**Table 68. Quality Control Activities Conducted After Data Collection**

<b>Deliverable</b>	<b>Quality Expectations</b>	<b>QC Activity</b>	<b>Frequency</b>
All Pavement Data	Accuracy and Repeatability	DMI calibration	Once, after data collection is complete
	Accuracy	Field collection comment review	Each batch
		Location/GPS checks	Each batch
	Data within acceptable range	Range checks	Each processing batch
	Completeness And reasonableness	Completeness checks	Each processing batch
		Pilot test delivery b	Once, first 100 miles
		Segmenting chainage checks b	Each batch
		Data analysis inventory/ locator checks (inventory information matches DOT specified information) b	Each processing batch
		Database hierarchical relationship checks	Each processing batch
Pavement/ ROW Images	Quality	Image quality checks (brightness, contrast, clarity)	Each weekly data import
	Logic	Image sequence checks	Each weekly data import
Sensor Data	Accuracy and Repeatability	Control sites measurements	After data collection is complete
Distress Data	Accuracy and Repeatability	Control sites measurements	Prior to distress rating
	Accuracy and Data within acceptable range	Distress rating personnel certification	Once, prior to data processing
		Distress year to year comparison	Each distress batch
	Logic	Data analysis pavement type check (pavement specific distresses are only rated on appropriate pavement types)	Each processing batch

b These activities are only conducted for contracted data collection.

Note: A batch is a group of collected sections or miles that flows through a process at the same time. Rather than performing a complete process on each section individually, processes are performed on batches of many sections to improve efficiency. Each data batch should typically be delivered on a monthly basis or from each collection District.

### **Error Tracking and Resolution Procedure**

All identified issues and errors need to be documented in a QC Log (see Section 7.3.7), including the corresponding resolution. Tracking errors and resolutions using the QC Log will help identify resolution techniques for known frequently occurring errors. Errors could be systematic or random. This procedure is primarily concerned with systematic errors, which should mostly be identified through the QC measurements before, during, and after data collection. The QC Log needs to be submitted along with every data delivery batch to FDOT.



### **7.3.5 Data Quality Acceptance Criteria**

This chapter recommends procedures and criteria for FDOT acceptance of the data delivered either by FDOT staff or by the Data Collection Contractor for both HPMS and PCS purposes. FDOT staff shall conduct quality acceptance procedures which include data completeness, range, type, consistency, logic, and reasonableness checks. An overview of typical quality acceptance activities is provided in Table 69, which includes initial automated data checks, in-depth review of flagged data, and review of data distributions for HPMS delivery.

Furthermore, it is recommended that FDOT staff conduct a 5% sampling and review of the pavement performance data in each delivery. A stratified random sampling approach is recommended, in which an equal number of samples would be randomly selected from different areas of the probability distribution curve for each data element. In this manner, pavement sections in poor, fair, and good conditions would be sampled at a uniform rate. The performance measures on these samples would be reviewed to be within an acceptable tolerance compared to the historic values. This sampling and review process shall only be fully implemented after final approval and allocation of corresponding resources.

The data deliverables shall be submitted on a monthly basis, along with the results of the QC measurements for each delivery (QC Log). The SQL database of each delivery batch should not be larger than 4 terabytes (TB) to avoid slower data processing speeds caused by larger databases. FDOT staff shall review each delivery and report any inconsistencies in a preliminary Acceptance Log to the FDOT data collection staff or the Data Collection Contractor's Project Manager for relevant action (correction, re-processing, or re-collection). After any re-submittal, FDOT will conduct a second review and issue an updated Acceptance Log, which indicates whether that data delivery batch can be accepted by FDOT. For a data delivery batch to be accepted by FDOT, it needs to pass all the requirements noted in Table 69. In addition, all the QC issues identified during the quality control measurements (QC Log) need to be resolved.

**Table 69. Recommended Quality Acceptance Procedures and Criteria**

<b>Quality Expectation</b>	<b>Acceptance (Percent within the Limits)</b>	<b>Acceptance Testing</b>	<b>Action if Criteria Not Met</b>
<b>Initial Automated Data Checks</b>			
No blanks	100%	Check for critical cells to not be blank	Correction or Re-Collection
Correct data type and format	100%	Data type (integer, string, etc.) and format check according to data dictionary	Correction
Data completeness	98%	Matching FDOT supplied routing package to ensure all identified routes have been collected if possible	Correction or Re-Collection
Image completeness	98%	Check every data record to have corresponding ROW and pavement images	Re-Collection
Accurate location information	98%	GPS coordinates within acceptable accuracy compared to FDOT values for each section; unique GPS coordinates for each data record (no duplicates); data alignment check	Re-Collection
Correct data according to surface type	98%	Collected data matching pavement type (e.g. no faulting on flexible pavements, etc.)	Correction or Re-Process
Individual data fields within acceptable range	98%	Check individual data values to be within acceptable range established by FDOT based on data measurement method and other logic checks	Re-Collection Re-Process
Combination of data fields within acceptable range	95%	Logic check of related data fields (e.g. sum of distresses to match section length or area)	Correction or Re-Process
<b>Review Flagged Data</b>			
Reasonable IRI Data	98%	Flag data with the following <ul style="list-style-type: none"> <li>➤ Collection Speed &lt; 40 mph</li> <li>➤ IRI zero or null values</li> <li>➤ IRI value difference &gt; 30% from left to right wheel path</li> </ul>	Review and if not justified, send for Re-Collection or Re-Process

<b>Quality Expectation</b>	<b>Acceptance (Percent within the Limits)</b>	<b>Acceptance Testing</b>	<b>Action if Criteria Not Met</b>
Reasonable Rut Depth Data	98%	Flag data with Rut value difference > 30% from left to right wheel path	Review and if not justified, send for Re-Collection or Re-Process
Reasonable Faulting Data	98%	Flag data with Fault value > 1 inch for any wheel path	Review and if not justified, send for Re-Collection or Re-Process
Reasonable Curve Data	98%	Check curve data classified in categories D, E and F against construction plans	Review and if not justified, send for Re-Collection or Re-Process
<b>Review of Data Distribution for HPMS Delivery</b>			
Reasonable Distribution of IRI Data	98%	Check distribution of IRI data according to historical network distributions.	Review and if not justified, send for Re-Collection or Re-Process
Reasonable Distribution of Rut Depth Data	98%	Check distribution of rut depth data according to historical network distributions. Flag for verification if more than 40% of sections have zero rutting. Flag for verification if more than 0.00% of sections have rutting > 1in.	Review and if not justified, send for Re-Collection or Re-Process
Reasonable Distribution of Faulting Data	98%	Check distribution of faulting data according to historical network distributions. Flag for verification if more than 90% of sections have zero faulting. Flag for verification if more than 0.00% of sections have faulting > 1 in.	Review and if not justified, send for Re-Collection or Re-Process

<b>Quality Expectation</b>	<b>Acceptance (Percent within the Limits)</b>	<b>Acceptance Testing</b>	<b>Action if Criteria Not Met</b>
Reasonable Distribution of Percent Cracking Data	98%	Check distribution of percent cracking data according to historical network distributions. Flag for verification if more than 90% of sections have zero percent cracking. Flag for verification if more than 30% of sections have percent cracking between 0 and 1%. Flag for verification if more than 0.00% of sections have percent cracking more than 54%.	Review and if not justified, send for Re-Collection or Re-Process
<b>5% Random Sampling and Review Checks</b>			
IRI data within 10% of historical values	95%	IRI sample data audits	Re-Collection Re-Process
Rut depth within 0.1 inch of historical values	95%	Rut depth sample data audits	Re-Collection Re-Process
Faulting data within 0.1 inch of historical values	95%	Faulting sample data audits	Re-Collection Re-Process
Correct Lane Marking	100%	Lane marking sample data review	Correction or Re-Process
Correct Joint Location	100%	Joint location sample data review	Correction or Re-Process
Correct Crack Detection	98%	Flag sections when more than 20% cracking misdetection	Re-Process
Cracking Distress Types within 15% of historical values	95%	Distress sample data audits	Re-Collection Re-Process
Non-Cracking Distress Types within 25% of historical values	95%	Distress sample data audits	Re-Collection Re-Process
Geometric Properties within 15% of historical values	95%	Geometric properties sample data audits	Re-Collection Re-Process
Quality ROW and Pavement Images	98%	ROW and pavement sample images visual checks	Re-Collection

### **7.3.6 Quality Assurance Plan**

This chapter covers the periodic quality assurance (QA) procedures to ensure the data collection and processing system is producing data conforming to the quality standards and protocols. The results of the routine QC measurements and FDOT quality acceptance audits on the produced data are fed into the QA procedures.

#### **Training**

As part of their Quality Control Plan, the Data Collection Contractor validates that the corresponding staff are properly trained and certified in maintenance and operation of data collection equipment, and operation of the data processing software. In addition, corresponding staff need to be trained on the relevant FDOT guidelines.

Moreover, any FDOT staff who are collecting data or conducting the review and audit of the submitted data should also be trained and certified in maintenance and operation of data collection equipment, as well as the operation of the data processing software.

Standard Operating Procedures (SOPs) are key documents that should be frequently updated and made available to all relevant staff for training purposes.

#### **Process Improvement**

As a result of all quality management activities, areas for improvement should be identified in the data collection, processing, and quality control procedures. These process improvements should be designed to enhance data quality and should be reflected in the updated SOPs.

The existing agency protocols for collection, processing, and reporting of pavement performance data should be updated in line with the corresponding advances in data collection technologies. The FDOT staff shall review all the existing protocols, considering their specific objectives, and recommend any changes or updates in concert with newer data collection technologies.

### 7.3.7 Quality Reporting Plan

This chapter covers the documentation of all quality management activities with the objective of staff training, identification of gaps, and process improvement.

#### QC Log

A QC Log should be submitted with every data delivery batch either by FDOT staff or the Data Collection Contractor. Table 70 shows an example format of this QC Log, which should include any exceptions found as a result of the QC activities and a corresponding resolution.

**Table 70. Example QC Log Format**

QC Log						
ID Number	Review Date	Deliverable Reviewed	Location Information	Findings	Resolution	Resolution Date
12500	7/20/18	ROW Imagery	US-27	ROW images exhibit water spots	Cleaned camera windshield	7/21/18

#### Acceptance Log

The results of the quality review and audit by FDOT staff of each data delivery are documented in the Acceptance Log, an example format of which is presented in Table 71.

**Table 71. Example Acceptance Log Format**

Acceptance Log					
ID Number	Review Date	Deliverable Reviewed	Findings	Resolution	Resolution Date
302	8/05/18	July 18 Pavement Data	Section 302681 missing pavement images	Recollect section 302681	8/20/18

#### QA Log

Table 72 shows an example format for documenting the process improvements identified through various quality management activities.

**Table 72. Example QA Log Format**

QA Log					
ID Number	Corresponding QC Log Number	Process	Identified Improvement	Implementation Approach	Implementation Date
802	12500	ROW Image Collection	Clean camera windshield after	Update collection protocol	7/27/18

QA Log					
ID Number	Corresponding QC Log Number	Process	Identified Improvement	Implementation Approach	Implementation Date
			inclement weather		

### 7.3.8 Roles and Responsibilities

Table 73 identifies the recommended staff categories that should be involved in quality management activities and their corresponding responsibilities. In addition, a contingency plan needs to be identified to ensure continuous conduct of quality management and process improvement.

**Table 73. Recommended Quality Team Roles and Responsibilities**

Team Role	Quality Management Responsibilities
FDOT Project Manager	<ul style="list-style-type: none"> <li>➤ Set quality standards, acceptance criteria, and corrective actions</li> <li>➤ Review and approve Contractor's Quality Control Plan</li> <li>➤ Review Contractor's equipment and training certifications</li> <li>➤ Review weekly updates from Contractor's PM</li> <li>➤ Review Contractor's QC Log and approve resolution of quality issues</li> <li>➤ Supervise acceptance checks and finalize Acceptance Log</li> <li>➤ Submit Acceptance Log with feedback to Contractor's PM</li> <li>➤ Monitor resolution of quality exceptions and submit the re-delivery Acceptance Log to Contractor's PM</li> <li>➤ Prepare quality management report</li> <li>➤ Recommend improvements to quality processes</li> </ul>
FDOT Quality Management Engineer	<ul style="list-style-type: none"> <li>➤ Supervise manual measurements of control sites, establish reference values, and maintain its records</li> <li>➤ Review Contractor's QC Plan</li> <li>➤ Learn Contractor's data viewing software</li> <li>➤ Approve the entry control site report</li> <li>➤ Review monthly control site reports</li> <li>➤ Approve the exit control site report</li> <li>➤ Conduct data QC for in-house collection</li> </ul>

Team Role	Quality Management Responsibilities
	<ul style="list-style-type: none"> <li>➤ Review data delivery report and issue resolution method in the QC Log</li> <li>➤ Conduct quality acceptance checks on each data delivery batch</li> <li>➤ Summarize acceptance check results and initiate Acceptance Log</li> <li>➤ Review Contractor response and conduct corresponding acceptance checks on re-delivery</li> <li>➤ Update Acceptance Log</li> <li>➤ Recommend improvements to quality processes</li> </ul>
FDOT In-House Data Collection Supervisor	<ul style="list-style-type: none"> <li>➤ Establish control and verification sites</li> <li>➤ Maintain and calibrate in-house equipment</li> <li>➤ Train and certify in-house equipment operators</li> <li>➤ Conduct QC activities before and during in-house collection</li> <li>➤ Recommend improvements to quality processes</li> </ul>
Data Collection Contractor Project Manager	<ul style="list-style-type: none"> <li>➤ Submit Quality Control Plan</li> <li>➤ Ensure staff training and certification</li> <li>➤ Review vehicle configuration and calibration reports</li> <li>➤ Coordinate and submit vehicle certification at third party location</li> <li>➤ Coordinate first control site visit (entry) and report results</li> <li>➤ Review routing plan and resolve discrepancy with FDOT inventory</li> <li>➤ Review daily/weekly/monthly equipment checks</li> <li>➤ Submit weekly verification site checks along with a summary of daily checks</li> <li>➤ Communicate weekly with FDOT PM to provide status and schedule update</li> <li>➤ Submit monthly control site checks</li> <li>➤ Diagnose and resolve any issues from daily/weekly/monthly checks</li> <li>➤ Review data QC checks and diagnose issues in QC Log</li> <li>➤ Ensure QC issues are addressed</li> <li>➤ Submit monthly data delivery batch along with QC Log</li> <li>➤ Review Acceptance Log feedback from FDOT PM</li> </ul>



Team Role	Quality Management Responsibilities
	<ul style="list-style-type: none"> <li>➤ Diagnose and address issues with each delivery and resubmit along with QC and Acceptance Logs</li> <li>➤ Coordinate last control site visit (exit) and report results</li> <li>➤ Conduct lessons learned meeting and identify process improvements to be documented in QA Log</li> </ul>

### Vendor Dispute Resolution

The FDOT PM and Data Collection Contractor's PM shall work to minimize any conflicts on the front end by clearly defining the project goals, deliverables (contract, scope, schedule, and budget), quality standards, roles, and responsibilities during project initiation. However, if any issues or discrepancies should arise during the project, the following are the recommended steps to be undertaken:

1. The issue or disagreement shall be clearly identified by both the FDOT PM and Data Collection Contractor's PM.
2. A review of the project contract and initial project plan shall be conducted by the Data Collection Contractor's PM and reviewed by the FDOT PM. If the contract or project plan clearly addresses the issue, the Data Collection Contractor's PM and the FDOT PM will both be required to acknowledge the fact before proceeding to the next step.
3. The first tier of resolution options to be explored are those that do not negatively impact the project contract, budget, or schedule. The second tier of resolution options to be explored are those that may impact schedule, contract and/or budgets. All resolution options will be reviewed and discussed to ensure all parties are clear on each option's impact on the project deliverables, timelines, and budget.
4. After all resolution options have been presented and all FDOT questions have been answered to their satisfaction, the FDOT PM shall commit to an option that resolves the issue with minimal impact. Upon identification of an acceptable resolution option, the Data Collection Contractor's PM should adjust the project plan to reflect the changes.

## 7.4 Recommendations for Further Implementation

Task 7 of this research project involved technical support to implement the validated automated distress identification applications for both rigid and flexible pavements into the annual Pavement Condition Survey (PCS) process. At the time of completion of this research project, FDOT was yet to purchase a new vehicle for data collection. However, FDOT commissioned collection of LCMS data on the Florida Interstate Highway System. According to the observations during software implementation, the following are the recommendations for further implementation:

1. For the historical LRIS data from the FDOT MPSV, the workflow in Appendix A can be used to transfer the data to Vision. For FDOT contracted data, Fugro staff have developed and tested the workflow in Appendix B, which can be used to transfer the LCMS data into Vision. The workflow in Appendix B includes a user interface that facilitates the execution of the SQL code to transfer the data.
2. It is recommended to use FRPDA and FFPDA on a larger database of highway sections to determine if there are any systematic errors in software results. It is also recommended to use the semi-automated rating (manual rating of pavement images) to QC the results of FRPDA and FFPDA and potentially discover any remaining systematic errors.
3. The semi-automated rating method should also be used to determine rigid and flexible pavement areas affected by non-cracking distress types. The developed software can automatically add these semi-automated rating results to the automated cracking results of FFPDA and provide the final combined condition index for every pavement section. The process of combining semi-automated rating results with automated cracking results should be validated before implementation.
4. Using a larger database of representative test sections, compare the results of FRPDA and FFPDA to the manual windshield Crack Ratings to determine a calibration equation between the two methodologies. This equation can be used to transform the FFPDA cracking results to a similar scale as the manual windshield results to ensure smooth pavement deterioration trends before and after implementation of an automated approach. In the long term, the deduct values for the calculation of Crack Rating might need to be revisited as a result of this exercise.
5. It is recommended that the FDOT *Rigid Pavement Condition Survey Handbook* and *Flexible Pavement Condition Survey Handbook* be reviewed considering the capabilities of the automated software. These guidelines were developed for visual windshield surveys and need to be evaluated and updated as necessary. It is recommended that the distress types, their definitions, and measurement method be reviewed in meetings with the data stakeholders such as the pavement management staff.
6. The recommended quality management program should be reviewed and evaluated by FDOT staff to be eventually implemented within the annual PCS process.

## CHAPTER 8 – TECHNOLOGY NEEDS AND GAPS ASSESSMENT

In Task 8 of this research project, the project team reviewed the results and findings from the tasks completed under Phase I and Phase II to identify gaps in functionality of the FDOT data collection hardware and the automated computer applications for automated crack identification and quantification on flexible and rigid pavements to meet FDOT's short- and long-term needs. The team also identified the necessary support resources (staffing, hardware and software) to support these needs. The team developed recommendations to bridge these gaps in the form of a suggested technical solution along with an estimated level of effort and time schedule.

This document is organized into five sections. Following this introduction, Section 8.1 summarizes the identified gaps in functionality of the FDOT data collection hardware and the recommended features for the new FDOT data collection vehicle. Section 8.2 describes the remaining gaps in the FDOT Rigid Pavement Distress Application (FRPDA) to meet the FDOT needs and the corresponding recommended remedies. Section 8.3 lists the remaining gaps in the FDOT Flexible Pavement Distress Application (FFPDA) and the pertinent solutions. Finally, Section 8.4 summarizes the key remaining gaps and their corresponding solutions for future data collection and processing activities.

### 8.1 Remaining Gaps in the Data Collection Equipment

This section of the report describes the remaining gaps in the FDOT data collection equipment and some recommended solutions to bridge those gaps. Some of these gaps were identified during the application of collected data and images in Phase I of this research project to detect and quantify surface cracking on rigid pavements. During Task 4 of Phase II, several important limitations of the existing equipment in detection and quantification of cracking on flexible pavements were also identified.

#### 8.1.1 Hardware Gaps Identified in Phase I

The sample data for identification and quantification of cracking on rigid pavements was collected using FDOT multi-purpose survey vehicle (MPSV), which is equipped with the Laser Road Imaging System (LRIS). In Task 2, Fugro staff conducted an investigation to determine whether the collected two-dimensional (2D) pavement images are of acceptable quality for crack detection and how FDOT can potentially measure various image quality indicators in future. This investigation concluded that the LRIS data met the requirements for pavement images to be used in crack detection according to the AASHTO provisional protocol that later became the AASHTO Standard Designation R 86-18. However, as noted in the Task 2 report, the requirements in this standard are dependent on the crack detection algorithms that are used to evaluate whether the minimum amount of cracking with specific width could be detected, or whether false positives are avoided.

It was found that the LRIS images and data were of acceptable quality for crack detection on rigid pavements if certain quality control procedures were followed. As a result, Fugro developed a **Hardware Maintenance Protocol** to be used by FDOT staff to ensure long term image quality and consistency. This protocol was submitted as an appendix to the Task 2 Report.

When considering other non-cracking types of rigid pavement distress such as surface deterioration, patching, and spalling, having access to the 3D depth data can provide useful information.

### **8.1.2 Hardware Gaps Identified in Phase II**

In Task 4 of Phase II, the research team analyzed the viability of using 2D LRIS images to detect, quantify and classify cracks on flexible pavements. The 2D LRIS technology was found to have the following potentials:

3. The LRIS equipment is more affordable than the three-dimensional (3D) equipment.
4. The run-to-run repeatability of crack detection from 2D images is acceptable.

However, there are several important limitations of the 2D LRIS technology:

5. The section-to-section consistency of crack detection from 2D images was 39% which is very low.
6. The accuracy of crack detection from 2D images was very low, as evidenced by the crack detection algorithm only detecting 18 percent of the cracks that were in the reference survey. Also, only 25 percent of the cracks detected from the 2D images were actually present in the reference survey.

When the flexible pavement surface is damp, the area around the crack edges become darker in the 2D images and as a result, the crack detection algorithms result in exaggerated crack width measurements based on pixel intensities. This issue negatively impacts severity rating of cracking distress types.

Since FDOT did not own 3D imaging equipment, the sample data for identification and quantification of distresses for flexible pavements was collected using a Fugro Automatic Roadway Analyzer (ARAN) vehicle equipped with the 3D Laser Crack Measurement System (LCMS). At the time of the conclusion of this research project, FDOT had not yet purchased a 3D data collection vehicle. However, FDOT had contracted the collection of the pavement condition data on Florida Interstate Highways to a Data Collection Contractor who operated an LCMS vehicle.

Based on a systematic evaluation framework and pertinent success metrics, it was found that the 3D technology is superior to the 2D technology in the following areas:

1. 67% increase in the crack detection accuracy, which translates into 71% more in percentage of detected crack length from the ground truth, and 50% more in percentage of the correctly detected cracks.
2. 83% increase in accuracy in identifying wheel path cracking (CW) and 56% more accuracy in identifying cracking outside the wheel paths (CO).
3. 6% more run-to-run repeatability in identifying wheel path cracking (CW) and 10% more repeatability in identifying cracking outside the wheel paths (CO).
4. 83% more section-to-section consistency in identifying wheel path cracking (CW) and 51% more consistency in identifying cracks outside the wheel paths (CO).

5. 6 seconds faster in crack detection per image frame.

The following advantages are based on thousands of miles collected with 2D LRIS and 3D LCMS technologies:

1. The 3D technology is less prone to crack width exaggeration on damp pavement surfaces and thereby produces more robust severity rating.
2. The 3D technology provides an area-based surface macro-texture measurement which can potentially be used for identifying raveling. Since these measurements are area-based, they have shown a significantly higher run-to-run repeatability compared to the macro-texture measurements with point laser sensors, which are line based and sensitive to vehicle wander.

The 3D technology was used for automated identification and quantification of flexible pavement distresses in Phase II of this research project. Detecting pavement surface cracks and identifying the corresponding distress with superior accuracy, consistency, repeatability, and efficiency of the 3D technology.

### **8.1.3 Recommended Data Collection Hardware Specifications**

This section presents an overview of key components the research team recommend for the next FDOT data collection vehicle. These specifications are according to the experience of Fugro in data collection and processing, and in line with the latest available and proven technology at the time of this research project.

#### **Requirements for the Data Collection Vehicle Integrator**

The integrated data collection system shall be a new, currently advertised production model. This model or line of equipment and post-processing software shall specifically have at least five years or more of prior assembly, operational, service support, and maintenance experience in North America. A reference list, with complete names, addresses, and telephone numbers of at least five (5) different active State agencies in the United States who purchased directly from the manufacturer and who own the same Model of the manufacturer's equipment, including their relevant representative(s) in the United States, shall be provided by the manufacturer to ascertain quality assurance, ensure non-prototype integrity of equipment model, and to confirm the capacity of the manufacturer to deliver and support the equipment exactly to these specifications.

The provider company shall offer a multi-year support service agreement with the following components:

1. Frequent training and certification of FDOT staff designated for vehicle operation and equipment maintenance
2. Support of FDOT in setup of equipment calibration and control sites
3. Annual visit to FDOT offices for equipment maintenance and calibration certification
4. On-demand customer support services, including online remote access and diagnostics for resolution of any potential issues

## **Requirements for the Vehicle**

A Mercedes made Sprinter model, or a Ford made Transit 350 model are the recommended chassis that would allow for the required equipment to be seamlessly integrated. Advantages of using a Mercedes Sprinter are the superior line of sight via windows for the driver, better suspension system, longer lasting chassis. After including the preferred options, the two models are similar in pricing. However, dependent on the location, Mercedes maintenance costs might be higher than that of Ford.

It is recommended to upgrade the alternator so that the inverter can be used for generating additional power. It is important in the mechanical drawings to ensure the weight and center of gravity is in adherence with corresponding DOT design requirements. Auto Start and Stop capability is also recommended.

## **Requirements for the Data Collection Equipment on the Vehicle**

The System shall meet or exceed the specifications set forth by the following industry standards:

- The Inertial Profiling System for measuring the longitudinal profile:
  - The minimum precision and bias requirements for Equipment Classification 1 in accordance with ASTM E950M, Standard Test Method for Measuring the Longitudinal Profile of Traveled Surfaces with an Accelerometer Established Inertial Profiling Reference
  - ASTM E2560, Standard Specification for Data Format for pavement Profile.
  - AASHTO M328-10, Standard Specification for Inertial Profiler.
  - AASHTO R56-10, Certification of Inertial Profiling Systems.
  - AASHTO R36-17, Standard Practice for Evaluating Faulting of Concrete Pavements.
- Pavement Imaging System for crack detection and measuring the transverse profile:
  - A 3D system such as the Pavemetrics LCMS is required.
  - AASHTO R86-18, Standard Practice for Collecting Images of Pavement Surfaces for Distress Detection.
  - AASHTO R88-18, Standard Practice for Collecting the Transverse Pavement Profile.
- High Definition (HD) cameras for right-of-way (ROW) images:
  - HD resolution.
  - Adequate shutter speed for crisp images.
  - Automated adjustment to abrupt changes in lighting condition, e.g. under tunnels and bridges.

## **Requirements for the Integration System**

The integration system needs to be designed with state-of-the-practice features: Tight and shock resistant computer rack enclosures, easy access to electronics and connections, detailed wiring and electronics schematics and on-board labeling for ease in troubleshooting by FDOT technicians, all cabling and connections hidden in flooring and paneling providing a clean and safe internal operational environment, redundant solid state hard drive storage for extended data collection length before having to change hard drives, hot swappable hard drives, National Electrical Manufacturers Association (NEMA) rating of all electronics, computers, etc. for shock and vibrations typical of a moving vehicle.

The system needs to be designed so that the maintenance is available to be completed by State Staff. Each wire and connection must be properly labeled, and schematics provided to ensure that cabling and connections as well as other components are easily identifiable and swappable. The system requires heat sinking and shock mounting enclosures. Fully independent air conditioning for the computer system is recommended.

## **Requirements for Data Collection and Processing Software**

The following are the recommended features for the data collection software onboard the vehicle:

- Real Time vehicle route planning and mapping.
- Auto-sectioning of data collected in the vehicle with an on-board GIS base map.
- Data verification tools for in-field operator use, e.g. missing element finder, duplicate element, GPS gap with data checks, image count and resolution detection based on preset storage parameters.
- On-line help menus and error detection help.
- Remote Wi-Fi access for troubleshooting.
- Verbal and keyboard “event” marking for operator selection of events, e.g. speed limit low/high thresholds, etc.
- All data sets are stored in an SQL database that allows for easy export to user defined reporting and uploading into PMS or other software programs. Utilizing this SQL database avoids challenges associated with using multiple data files for each road segment (e.g. one for DMI, one for GPS, one for IRI, one for rutting, etc.).

The following are the recommended features for the data processing software in the office:

- All data should be uploaded by batch and into a SQL database.
- Upload control into single synchronized software, which then allows for segmenting, processing, analysis, and reporting all from one location.
- Modular design and scalable product.
- Designate road zones to meet HPMS and FDOT requirements.
- Automated lane detection from pavement striping.

- Automated joint detection and slab assignment.
- Automated crack detection.
- Automated crack classification and rating according to HPMS and FDOT requirements.
- User defined roughness and rutting processing and reporting tools: all raw data is stored for every road segment allowing for processing of ride and rut statistics using multiple processing and reporting parameters. So, the single set of data can be used for network level, project level, and research level analysis.
- Stitched together panoramic view of multiple distinct camera feeds.
- Fully synchronized view of the collection route map, raw and processed data tables, charts, graphs, filterable by any field in the data set
- Batch data processing allows the user to reprocess each data element separately, e.g. reprocess for longitudinal profile and not have to reprocess for distress. Batch processing should be available to process one or multiple sections.
- Built-in reports for specific standard requirements such as the FHWA HPMS reporting and customizable reports as required by the end user.
- Ability to share data through email links, or location reference for review by others.

### **Requirements for Data Cloud Storage and Online Sharing**

The following are the recommended requirements for data cloud storage and online sharing:

- Cloud storage and web access of data, reports, mapping, etc. A professional provider with established data safety (multiple backups) and security (following standard protocols) background should be used. An example is the Amazon Web Services (AWS).
- Access can be given to any user via a web browser, without the need to local software installation or local PC minimum hardware/software specifications.
- Simultaneous and linked data viewing from plots, tables, and map presentations of the data allowing the user to view data streamed from any given one point of a roadway to any other given point on the roadway. This feature also allows the user to perform a “one click” view on a map of a PMS section and automatically view the tabled data, plot of the data, along with synchronized photo-logging images collected for the point selected.
- Ability to filter on locators – e.g. District, route, route number, intersection description, milepost, etc.
- Ability to share data via web links, ability to share location of specific events or details with other users.
- Year over year data review and synchronization of images and data using precise GPS data. Side by side review for engineers and analysts to explain trend dynamics, e.g. does the improvement in pavement condition from one year to the other correspond with a treatment.



- Use image thumbnails to increase playback speed over slower connections. Full resolution image should appear when playback is stopped.
- Offset the distress categories and marking so users can see the pavement defects for quality control.
- Reporting functions and data export capabilities.

### Estimated Budget

Based on latest similar vehicles, the team estimates that FDOT should budget for approximately \$900,000.00 to \$1,250,000.00 for a data collection vehicle with the aforementioned requirements to be purchased in 2019. This includes the cost of purchasing the vehicle, the equipment that is integrated on the vehicle, the corresponding data collection and processing software, cloud data storage and online sharing platform, and a 5-year support service agreement. Of course, prices are dependent on a variety of factors such as availability of vehicle and equipment parts, geographic location of assembly, international trade agreements, etc. and the provided ballpark estimate is for general information only.

## 8.2 Remaining Gaps in the FDOT Rigid Pavement Distress Application (FRPDA)

There are several gaps that were identified after the development and evaluation of the FRPDA in Task 3, which are listed in Table 74 along with a corresponding recommended solution.

**Table 74. Remaining Gaps in FRPDA and Recommended Solutions**

Gap No.	Remaining Gap Description	Recommended Solution
1	Very straight longitudinal cracks might be rated as longitudinal joints	Implement a data collection protocol to avoid lane stripes in the middle of images; Manual QC and intervention; these situations are not frequent
2	Partially faded, or non-straight and jagged longitudinal lane stripes in the middle of the lane might be rated as longitudinal cracks	
3	Skewed joints cannot be detected (even though they are not the predominant design anymore)	Manual QC and intervention; these situations are not frequent
4	Some run to run variation (on different images of same section)	Implement a data collection protocol to avoid significant wander and variation between images
5	Shattered slabs are not identified successfully	Manual rating of images in the short term to build training database; use machine learning in the long-term
6	Not identifying spalling of crack and joint edges but has low deduct values	Manual rating of images in the short term to build training database;

7	Not identifying patching but has low deduct values	collect 3D data and use machine learning in the long-term
8	Not identifying surface deterioration but has low deduct values	
9	Not identifying pumping but it is an infrequent distress	
10	Not identifying joint condition	

The identified gaps can be classified into the following categories:

1. Gaps that are infrequent issues; these gaps can be addressed via proper quality control after data collection or quality assurance precautions before and during collection. Gaps number 1 through 4, and number 9 in Table 74 are of this category.
2. Gaps that are frequent issues but not significantly impacting the survey results; these gaps can be addressed with proper quality control in the short term; machine learning can be used in the long term, but it might not be worth the effort. Gaps number 6 through 8 in Table 74 are of this category.
3. Gaps that are frequent and have significant impacts on the survey results; for these gaps, manual rating of pavement images is strongly recommended to build a training database for machine learning algorithms. Gaps number 5 and 10 in Table 74 are of this category.

### 8.2.1 Recommended Development Initiatives and Level of Effort

In this section of the report, some recommendations are listed for the gaps that were categorized as being frequent issues (categories 2 and 3 above). These development initiatives and their estimated crude level of effort are listed in Table 75.

**Table 75. Recommended Development Initiatives for FRPDA and the Level of Effort**

Gap No.	Remaining Gap Description	Development Initiative	Level of Effort
5	Shattered slabs	Identify representative test sections that have an adequate number of shattered slabs and cracked slabs that are not shattered	40 staff-hours
		Manual rating of images to build training database	960 staff-hours
		Train and test machine learning algorithm	320 staff-hours
6	Spalling of cracks and joints	Identify representative test sections that have an adequate number of spalled cracks/joints	40 staff-hours
		Manual rating of images to build training database; 3D spalling depth data required for identification and severity levels	960 staff-hours
		Train and test machine learning algorithm	320 staff-hours

7	Patching	Identify representative test sections that have an adequate amount of patching	40 staff-hours
		Manual rating of images to build training database; 3D texture data required	960 staff-hours
		Train and test machine learning algorithm	320 staff-hours
8	Surface deterioration	Identify representative test sections that have an adequate amount of surface deterioration	40 staff-hours
		Manual rating of images to build training database; 3D texture data required	960 staff-hours
		Train and test machine learning algorithm	320 staff-hours
9	Pumping	Identify representative test sections that have an adequate amount of pumping (challenging)	40 staff-hours
		Manual rating of images to build training database	960 staff-hours
		Train and test machine learning algorithm	320 staff-hours
10	Joint condition	Identify representative test sections that have an adequate number of sealed, non-sealed, and partially sealed joints	40 staff-hours
		Manual rating of images to build training database; 3D depth data required	960 staff-hours
		Train and test machine learning algorithm	320 staff-hours

Using a 3D imaging technology can significantly improve the results of crack detection and crack classification. In the absence of 3D data, some distress types such as patching and spalling cannot easily be detected. Spalling of cracks and joints are more pronounced in 3D images, because the technology darkens the areas that are lower than the nominal pavement surface. In addition, the 3D texture data can assist in recognizing the changes in pavement surface type, which can potentially automate identification of patched areas. It is important to determine the extent of these gaps and their individual relative impact on the overall pavement condition rating.

For most of these remaining gaps, it is challenging for the computer software to identify these distress types based on logical algorithms. Therefore, it is recommended to build a database of manually rated images to be used in training of machine learning algorithms. The first step is to identify representative test sections that have an adequate amount of the specific distress, and instances that can be false positives (e.g. slabs broken into three pieces can be falsely identified as shattered slabs). This could be challenging in the case of infrequent distress types such as pumping. FDOT staff need to determine the viability of such development initiatives for infrequent distress types in terms of the return on the invested level of effort.

The second step is to develop the training database. One component is the automatically collected data such as the pixel intensities and 3D depth and texture data. The other component is the human identification of distress types, extent, and severity levels corresponding to the automatically collected data in specific locations. This requires the most significant level of effort in the recommended solutions, because the machine learning results can only be as good as the

quality of the training data. It is very important that multiple raters be trained on the distress classification and rating guidelines, so that they would be able to cross-check each other's work for the best quality. An independent quality auditor is recommended to check random blind samples of data for adherence to the corresponding guidelines.

The provided level of effort is a ball park estimate for each development effort in terms of staff hours. The assumption is that one staff would be assigned to look for representative test sections for a week (40 hours). Three staff members would be assigned for the manual rating of the images (two manual raters and one quality auditor) for two months (960 hours). Finally, two software developers (one for development and another for continuous testing) would be working on the training and test initiatives for four weeks (320 hours). Ample computing time allocated for the development effort depending on the size of the training database. Some of these initiatives can be conducted in parallel if the same test sections can be representative sections for multiple distress types.

### 8.3 Remaining Gaps in the FDOT Flexible Pavement Distress Application (FFPDA)

Several gaps were identified after the development and evaluation of the FFPDA in Task 6, which are listed in Table 76 along with a corresponding recommended solution.

**Table 76. Remaining Gaps in FFPDA and Recommended Solutions**

Gap No.	Remaining Gap Description	Recommended Solution
1	Partially faded, or non-straight and jagged longitudinal lane stripes might be rated as longitudinal cracks	Manual QC and intervention; these situations are not frequent
2	Block cracks are not differentiated from other crack types	Manual QC and intervention; these situations are not frequent, and it does not impact the Crack Rating
3	Not identifying raveling	Manual rating of images in the short term to build training database; collect 3D data and relate macrotexture to raveling in the long-term
4	Not identifying patching	Manual rating of images in the short term to build training database, collect 3D data and use machine learning in the long-term

The identified gaps can be classified into the following categories:

1. Gaps that are infrequent issues; these gaps can be addressed via proper quality control after data collection or quality assurance precautions before and during collection. Gap number 1 in Table 76 is of this category.
2. Gaps that are frequent issues but not significantly impacting the survey results; these gaps can be addressed with proper quality control in the short term; machine learning can be used in the long term, but it might not be worth the effort. Gap number 2 in Table 76 is of this category.
3. Gaps that are frequent and have significant impacts on the survey results; for these gaps, manual rating of pavement images is strongly recommended to build a training database for machine learning algorithms. Gap numbers 3 and 4 in Table 76 are of this category.

### 8.3.1 Recommended Development Initiatives and Level of Effort

In this section of the report, some recommendations are listed for the gaps that were categorized as being frequent issues (categories 2 and 3 above). These development initiatives and their estimated crude level of effort are listed in Table 77.

**Table 77. Recommended Development Initiatives for FRPDA and the Level of Effort**

Gap No.	Remaining Gap Description	Development Initiative	Level of Effort
2	Block cracks	Identify representative test sections that have an adequate amount of block cracking, and longitudinal/transverse cracks (challenging)	40 staff-hours
		Manual rating of images to build training database	960 staff-hours
		Train and test machine learning algorithm	320 staff-hours
3	Raveling	Identify representative test sections that have an adequate amount of raveling, and open graded surfaces that could be false positives	40 staff-hours
		Manual rating of images to build training database; 3D texture data required for identification and severity levels	960 staff-hours
		Train and test machine learning algorithm	320 staff-hours
4	Patching	Identify representative test sections that have an adequate amount of patching	40 staff-hours
		Manual rating of images to build training database; 3D texture data required	960 staff-hours
		Train and test machine learning algorithm	320 staff-hours

The 3D technology provides an area-based surface macro-texture measurement which can potentially be used for identifying raveling. Since these measurements are area-based, they have shown a significantly higher run-to-run repeatability compared to macro-texture measurements with point laser sensors, which are line based and sensitive to vehicle wander. These robust 3D texture measurements can be used to identify changes in pavement surface type, areas of raveling, and quality control of open graded friction courses or chip seal surfaces. The Pavemetrics LCMS processor provides the texture values and a corresponding Raveling Index which is directly proportional to mean texture depth (MPD). However, this Raveling Index has not been calibrated to manual ratings of surface raveling and therefore a high Raveling Index might just be an indicator of open graded friction courses or chip seal surfaces. There is a need to explore the relative values of MPD and root mean square (RMS) of texture between the wheel paths and adjacent areas to see whether the relative difference in texture can be correlated with manual rating of raveling areas. In addition, 3D texture data can assist in recognizing changes in pavement surface type, which can potentially automate identification of patched areas.

For most of these gaps, it is challenging for the computer software to identify these distress types based on logical algorithms. Therefore, it is recommended to build a database of manually rated images to be used in training of machine learning algorithms. The first step is to identify representative test sections that have an adequate amount of the specific distress, and instances that can be false positives (e.g. combinations of transverse and longitudinal cracks can be falsely identified as block cracking). This could be challenging in the case of infrequent distress types such as block cracking. FDOT staff need to determine the viability of such development initiatives for infrequent distress types in terms of the return on the invested level of effort.

The second step is to develop the training database. One component is the automatically collected data such as the pixel intensities and 3D depth and texture data. The other component is the human identification of distress types, extent, and severity levels corresponding to the automatically collected data in specific locations. This requires the most significant level of effort in the recommended solutions, because the machine learning results can only be as good as the quality of the training data. It is very important that multiple raters be trained on the distress classification and rating guidelines, so that they would be able to cross-check each other's work for the best quality. An independent quality auditor is recommended to check random blind samples of data for adherence to the corresponding guidelines.

The provided level of effort is a ball park estimate for each development effort in terms of staff hours. The assumption is that one staff would be assigned to look for representative test sections for a week (40 hours). Three staff members would be assigned for the manual rating of the images (two manual raters and one quality auditor) for two months (960 hours). Finally, two software developers (one for development and another for continuous testing) would be working on the training and test initiatives for four weeks (320 hours). There should be ample computing time allocated for the development effort depending on the size of the training database. Some of these initiatives can be conducted in parallel if the same test sections can be representative sections for multiple distress types.

## 8.4 Summary of Key Remaining Gaps and Pertinent Solutions

Task 8 of this research project involved identification of the remaining gaps and pertinent solutions for the automated distress identification applications for both rigid and flexible pavements. The research team identified the following as the key software gaps that are both frequent issues and have a significant impact on the distress survey results:

1. FRPDA key gaps and recommended solutions
  - a. Shattered slabs: use machine learning trained based on the manual ratings to differentiate cracked slabs that are broken into four or more pieces.
  - b. Patching: use machine learning to relate the manual rating of patching to the texture and possibly intensity of pavement areas.
  - c. Joint condition: use machine learning to relate the manual rating of joint conditions to the depth of joints measured with 3D technology.
2. FFPDA key gaps and recommended solutions
  - a. Raveling: use machine learning to relate the manual rating of raveling to the difference in texture between wheel paths and areas outside the wheel paths.
  - b. Patching: use machine learning to relate the manual rating of patching to the texture and possibly intensity of pavement areas.

It is recommended that the FDOT *Rigid Pavement Condition Survey Handbook* and *Flexible Pavement Condition Survey Handbook* be reviewed considering the capabilities of the automated software and the requirements of data stakeholders. These guidelines were developed for visual windshield surveys and need to be evaluated and updated if necessary. It is recommended that the distress types, their definitions, and measurement method be reviewed in meetings with the data stakeholders such as the pavement management staff. This evaluation needs to be conducted before any future development initiatives are considered for addressing the gaps.



## REFERENCES

AASHTO (2013). "Standard Practice for Quantifying Roughness of Pavements," AASHTO Designation R 43-13, American Association of State Highway and Transportation Officials, Washington, D.C.

AASHTO. (2014a). "Standard Practice for Collecting Images of Pavement Surfaces for Distress Detection, AASHTO Designation PP 68-10." Standard Specification for Transportation Materials of Sampling and Testing, American Association of State Highway and Transportation Officials, Washington, D.C., PP 68-1-PP 68-5.

AASHTO. (2014b). "Standard Practice for Quantifying Cracks in Asphalt Pavement Surfaces from Collected Images Utilizing Automated Methods, AASHTO Designation PP 67-14." Standard Specification for Transportation Materials of Sampling and Testing, American Association of State Highway and Transportation Officials, Washington, D.C., PP 67-1-PP 67-6.

AASHTO (2014c). "Standard Practice for Certification of Inertial Profiling Systems," AASHTO Designation R 56-14, American Association of State Highway and Transportation Officials, Washington, D.C.

AASHTO (2014d). "Standard Practice for Operating Inertial Profiling Systems," AASHTO Designation R 57-14, American Association of State Highway and Transportation Officials, Washington, D.C.

AASHTO (2017). "Standard Practice for Evaluating Faulting of Concrete Pavements," AASHTO Designation R 36-17, American Association of State Highway and Transportation Officials, Washington, D.C.

AASHTO (2018a). "Standard Practice for Quantifying Cracks in Asphalt Pavement Surfaces from Collected Pavement Images Utilizing Automated Methods," AASHTO Designation R 85-18, American Association of State Highway and Transportation Officials, Washington, D.C.

AASHTO (2018b). "Standard Practice for Collecting Images of Pavement Surfaces for Distress Detection," AASHTO Designation R 86-18, American Association of State Highway and Transportation Officials, Washington, D.C.

AASHTO (2018c). "Standard Practice for Determining Pavement Deformation Parameters and Cross Slope from Collected Transverse Profiles," AASHTO

Designation R 87-18, American Association of State Highway and Transportation Officials, Washington, D.C.

AASHTO (2018d). "Standard Practice for Collecting the Transverse Pavement Profile," AASHTO Designation R 88-18, American Association of State Highway and Transportation Officials, Washington, D.C.

ASTM (2013). "Standard Practice for Computing Ride Number of Roads from Longitudinal Profile Measurements Made by an Inertial Profile Measuring Device," Standard Designation: E1489-08 (Reapproved 2013), American Society for Testing and Materials International, West Conshohocken, PA.

Adhara Systems. (n.d.). "uniAMS: UniAnalyze." [http://www.adharasys.com/uniams\\_analyze\\_main.html](http://www.adharasys.com/uniams_analyze_main.html) (06/01, 2015).

Ahmed, M. F. M., and Haas, C. (2010). "The Potential of Low Cost Close Range Photogrammetry towards Unified Automatic Pavement Distress Surveying." Proceedings of the 89th Annual Meeting of the Transportation Research Board, Transportation Research Board, Washington, D.C., 11-15.

Aijo, J. (2005). "Automated Crack Measurement Test in Finland 2004." Finnra Reports 2005.

Amarasiri, S., Gunaratne, M. & Sarkar, S., 2010. Modeling of Crack Depths in Digital Images of Concrete Pavements Using Optical Reflection Properties. ASCE Journal of Transportation Engineering, 136(6), pp. 489-499.

Apro, M., Pal, S., and Dedijer, S. (2011). "Evaluation of Single and Multi-Threshold Entropy-Based Algorithms for Folded Substrate Analysis," *Journal for the Faculty of Technical Sciences - Graphic Engineering and Design*, Vol. 2, No. 2, pp. 2-3.

ASTM (1998). Standard Practice for Use of the Terms Precision and Bias in ASTM Test Methods, Annual Book of ASTM Standards, Vol. 14.02, Designation E 177-90a, American Society for Testing and Materials, West Conshohocken, PA.

ASTM (2005). "Standard Practice for Calculating Pavement Macrottexture Mean Profile Depth," Standard Designation: E1845-01 (Reapproved 2005), American Society for Testing and Materials International, West Conshohocken, PA.

ASTM (2008a). "Standard Specification for Standard Rib Tire for Pavement Skid-Resistance Tests," Standard Designation: E501-08, American Society for Testing and Materials International, West Conshohocken, PA.

ASTM (2008b). "Standard Specification for Standard Smooth Tire for Pavement Skid-Resistance Tests," Standard Designation: E524-08, American Society for Testing and Materials International, West Conshohocken, PA.

ASTM (2008c). "Standard Practice for Computing International Roughness Index of Roads from Longitudinal Profile Measurements," Standard Designation: E1926-08, American Society for Testing and Materials International, West Conshohocken, PA.

ASTM (2011). "Standard Test Method for Skid Resistance of Paved Surfaces Using a Full-Scale Tire," Standard Designation: E274-11, American Society for Testing and Materials International, West Conshohocken, PA.

ASTM (2017). "Standard Specification for Data Format for pavement Profile," Standard Designation E2560-17, American Society for Testing and Materials International, West Conshohocken, PA.

ASTM (2018). "Standard Test Method for Measuring the Longitudinal Profile of Traveled Surfaces with an Accelerometer-Established Inertial Profiling Reference," Standard Designation E950M-09, American Society for Testing and Materials International, West Conshohocken, PA.

Attoh-Okine, N., and Adarkwa, O. (2013). "Pavement Condition Surveys-Overview of Current Practices." Rep. No. DCT 245, Delaware Center for Transportation, Newark, DE.

Ayenu-Prah, A., and Attoh-Okine, N. (2008). "Evaluating Pavement Cracks with Bidimensional Empirical Mode Decomposition." EURASIP Journal on Advances in Signal Processing, 2008(1), 1-7.

Cheng, H., and Glazier, C. (2007). "Automated Real-Time Pavement Crack Detection and Classification System." Final Report for Highway IDEA Project 106, Transportation Research Board of the National Academies, Washington, D.C.

FDOT (2017). *Flexible Pavement Condition Survey Handbook*. State Materials Office, Florida Department of Transportation.

FDOT (2017). *Rigid Pavement Condition Survey Handbook*. State Materials Office, Florida Department of Transportation.

FHWA (2015). "National Performance Management Measures; Assessing Pavement Condition for the National Highway Performance Program and Bridge Condition for the National Highway Performance Program; Proposed Rule," 23 CFR Part 490, Federal Register, Vol. 80, No. 2, Federal Highway Administration, Department of Transportation.

FHWA (2016). *Highway Performance Monitoring System Field Manual*. Federal Highway Administration, Washington, D.C.

Fieguth, P. W., and Sinha, S. K. (1999). "Automated Analysis and Detection of Cracks in Underground Scanned Pipes." Image Processing, 1999. ICIP 99. Proceedings. 1999 International Conference on, IEEE, Cairo, Egypt, 395-399.

Flintsch, G. W., and McGhee, K. K. (2009). NCHRP Synthesis 401: Quality Management of Pavement Condition Data Collection. Transportation Research Board of the National Academies, Washington, D.C.

Fugro Roadware. (2012). Pave 3D System. Fugro Roadware Inc., n.p.

Fugro Roadware. (2004). Deploying Videolog - Receiving the Best Value for Your Investment. Fugro Roadware Inc., n.p.

Fundakowski, R. A. (1991). "Video Image Processing for Evaluating Pavement Surface Distress." Rep. No. Final Report of NCHRP Project 1-27, Transportation Research Board, Washington, D.C.

Gao, J. (2009). Digital Analysis of Remotely Sensed Imagery. McGraw-Hill Professional, New York, NY.

Gavilán, M., Balcones, D., Marcos, O., Llorca, D. F., Sotelo, M. A., Parra, I., Ocaña, M., Aliseda, P., Yarza, P., and Amírola, A. (2011). "Adaptive Road Crack Detection System by Pavement Classification." *Sensors*, 11(10), 9628-9657.

Groeger, J. L., Stephanos, P., and Dorsey, P. (2003a). "Evaluation of AASHTO Cracking Protocol: Quantifying Distress in Asphalt Pavement Surfaces." 82nd Annual Meeting of the Transportation Research Board, Washington, DC, Transportation Research Board, Washington, D.C., 1-18.

Groeger, J. L., Stephanos, P., Dorsey, P., and Chapman, M. (2003b). "Implementation of Automated Network-Level Crack Detection Processes in Maryland." *Transportation Research Record: Journal of the Transportation Research Board*, 1860(1), 109-116.

Gunaratne, M., Mraz, A., Sokolic, I., and Nazef, A. (2003). "Development of Florida's Comprehensive Pavement Evaluation Vehicle." *Proceedings of 82th Annual Meeting of the Transportation Research Board*, Transportation Research Board, Washington, D.C., 1-21.

Gunaratne, M., Amarasiri, S., and Nasser, S. (2008). "Investigation of Automated and Interactive Crack Measurement Systems." Rep. No. BD544-36, University of South Florida, Florida Department of Transportation, Tampa, FL.

Habel, R., Laurent, J., Francois, J., and Fox-Ivey, R. (2014). "Use of 3D Scanning Technology for Automated Inspection of Multi-modal Transportation Infrastructure." Pavemetrics System Inc., n.p., 1-20.

Haykin, S. (1998). *Neural Networks: A comprehensive Foundation*, 2nd Edition. Prentice Hall, Hoboken, NJ.

Huang, Y., and Xu B. (2006). "Automatic Inspection of Pavement Cracking Distress." Report No. FHWA/TX-06/5-4975-01-1, Federal Highway Administration, Washington, D.C.

INO. (2014). "Laser Road Imaging System (LRIS)." [http://www.ino.ca/en/examples/laser-road-imaging-system-\(Iris\)/](http://www.ino.ca/en/examples/laser-road-imaging-system-(Iris)/) (5/29, 2015).

International Cybernetics. (2015). "Automatic Crack Detection." [http://www.intlcybernetics.com/automated\\_crack\\_detection.html](http://www.intlcybernetics.com/automated_crack_detection.html) (6/1, 2015).

ISO. (2005). *ISO 9000: 2005 Quality Management Systems-Fundamentals and Vocabulary*. International Standards Organisation, Geneva, Switzerland.

Kargah-Ostadi, N. & Stoffels, S. M., 2015. Framework for Development and Comprehensive Comparison of Empirical Pavement Performance Models. *ASCE Journal of Transportation Engineering*, Volume 04015012.

Kaur, J. and Choudhary, A. (2012). "Comparison of Several Contrast Stretching Techniques on Acute Leukemia Images," *International Journal of Engineering and Innovative Technology*, Vol. 2, No. 1, p. 333.

Kim, J. Y. (2008). "Development of New Automated Crack Measurement Algorithm using Laser Images of Pavement Surface". Ph.D. dissertation. The University of Iowa, Iowa City, IA.

Lee, H. (1991). "Accuracy, Precision, Repeatability, and Compatibility of the Pavedex PAS 1 Automated Distress Measuring Device." *Transportation Research Board*, 1311(1), 136-143.

Lee, H., Lee B. (2004). "Position-Invariant Neural Network for Digital Pavement Crack Analysis." *Computer-Aided Civil and Infrastructure Engineering*, 19 (2004), 105-118

Lu, J. J., Mei, X., and Gunaratne, M. (2002). "Development of an Automatic Detection System for Measuring Pavement Crack Depth on Florida Roadways." *University of South Florida, Florida Department of Transportation, Tampa, FL.*

Mathavan, S., Rahman, M., and Kamal, K. (2013). "Crack Detection in Pavement Images Using Texture Analysis and Unsupervised Learning." *Proceedings of 92nd Annual Meeting of the Transportation Research Board, Transportation Research Board, Washington, D.C., .*

McGhee, K. H. (2004). *NCHRP Synthesis 334: Automated Pavement Distress Collection Techniques*. Transportation Research Board of the National Academies, Washington, D.C.

McNeil, S. and F. Humplick, (1991), "Evaluation of Errors in Automated Pavement-distress Data Acquisition," *Journal of Transportation Engineering*, Vol. 117, No. 2, pp. 224–241.

Miller, J. S., and Bellinger, W. Y. (2014). "Distress Identification Manual for the Long-Term Pavement Performance Program (Fifth Revised Edition)." Rep. No. FHWA-HRT-13-092, Federal Highway Administration, Washington, D.C.

Mullis, C., Shippen, N., Brooks, E., and Reid, J. (2005). "Automated Data Collection Equipment for Monitoring Highway Condition." Rep. No. FHWA-OR-RD-05-10, Oregon Department of Transportation, Federal Highway Administration, Salem, OR.

Najarian, S., Dargahi, J., Darbemamieh, G., and Farkoush, S. H. (2011). *Mechatronics in Medicine A Biomedical Engineering Approach*. McGraw-Hill Professional, New York, NY.

National Park Service, Road Inventory Program—Quality Assurance Manual, Federal Highway Administration, Lakewood, Colo., 2003.

North Carolina DOT. (2011). *NCDOT Digital Imaginary Distress Evaluation Handbook, Version 1.0*. North Carolina Department of Transportation, Raleigh, NC.

Oklahoma DOT. (2005). *Pavement Management Distress Rating Guide*. Oklahoma Department of Transportation, Oklahoma City, OK.

Oliveira, H., and Correia, P. L. (2008). "Supervised Strategies for Crack Detection in Images of Road Pavement Flexible Surfaces." *European Signal Processing Conference (EUSIPCO'08)*, Ecole Polytechnique Federale de Lausanne, Lausanne, Switzerland, 25-29.

Omer, R., and Fu, L. (2010). "An Automatic Image Recognition System for Winter Road Surface Condition Classification." *Intelligent transportation systems (itsc), 2010 13th international IEEE conference on*, IEEE, Madeira Island, Portugal, 1375-1379.

Ong, G., Noureldin, S. & Sinha, K. C., 2010. *Automated Pavement Condition Data Collection Quality Control, Quality Assurance and Reliability*, Indianapolis: Indiana Department of Transportation.

Papagiannakis, A. T., Gharaibeh, N. G., Weissmann, J., and Wimsatt, A. J. (2009). "Pavement Scores Synthesis." Rep. No. FHWA/TX-09/0-6386-1, Texas Transportation Institute and Texas Department of Transportation, Austin, TX.

Pavement Management Services (2015), *Pavement Condition and Complete Roadside Inventory*, Brochure obtained through <http://pavement.com.au/wp-content/uploads/2014/11/ARAN-LRMS.pdf> (6/1, 2015).

Pavemetrics Inc. (2015). "LCSMTM Laser Crack Measurement System." <http://www.pavemetrics.com/en/lcms.html> (6/1, 2015).

Peng, B., Wang, K. C. P., and Chen, C. (2014). "Automatic Crack Detection by Multi-Seeding Fusion on 1mm Resolution 3D Pavement Images." Second Transportation & Development Congress 2014, American Society of Civil Engineers, Orlando, FL, 543-552.

Pennsylvania DOT. (2015a). "Automated Pavement Condition Survey Field Manual, Publication 336." Rep. No. PUB 336 (4-15), Pennsylvania Department of Transportation, Harrisburg, PA.

Pennsylvania DOT. (2015b). "Video Logging."  
<http://www.dot.state.pa.us/Internet/Bureaus/pdBOMO.nsf/infoRMRIVideo> (5/28, 2015).

Pierce, L.M., G. McGovern, and K.A. Zimmerman. (2013). "Practical Guide for Quality Management of Pavement Condition Data Collection," Report No. FHWA-HIF-14-006, Federal Highway Administration, Washington, D.C.

Rada, G. R., Simpson, A. L. & Elkins, G. E., 2007. Updated LTPP Manual Distress Data Bias and Precision Estimates. Washington, D.C., Transportation Research Board.

Rada, G. R. et al., 1999. Study of LTPP Distress Data Variability, Volume I, McLean, Virginia: Federal Highway Administration.

Raman, M., M. Hossain, R.W. Miller, G. Cumberledge, D.H. Lee, and J.K. Kihyoung (2004), "Assessment of Image-Based Data Collection and the AASHTO Provisional Standard for Cracking on Asphalt-Surfaced Pavements," Transportation Research Record: Journal of the Transportation Research Board, No. 1889, Transportation Research Board of the National Academies, Washington, D.C., pp. 116–125.

Saliminejad, S., and Gharaibeh, N. G. (2013). "Impact of Error in Pavement Condition Data on the Output of Network-Level Pavement Management Systems." Transportation Research Record: Journal of the Transportation Research Board, 2366(1), 110-119.

Schnebele, E., Tanyu, B. F., Cervone, G., and Waters, N. (2015). "Review of Remote Sensing Methodologies for Pavement Management and Assessment." European Transport Research Review, 7(2), 1-19.

Serigos, P. A., Prozzi, J. A., De Fortier, A., and Murphy, M. (2015). "Evaluation of 3D Automated Systems for the Measurement of Pavement Surface Cracking." 95nd Annual Meeting of the Transportation Research Board, Transportation Research Board, Washington, D.C., 1-15.



Selezneva, O.I., G. Mladenovic, R. Speir, J. Amenta, and J. Kennedy, (2004), "National Park Service Road Inventory Program—Quality Assurance Sampling Considerations for Automated Collection and Processing of Distress Data," Transportation Research Record: Journal of the Transportation Research Board, No. 1889, Transportation Research Board of the National Academies, Washington, D.C., pp. 106–115.

Shah, R., Wingate, T., Nash-Gardner, P., Buehlman, T., and Beasley, H. (2010). "Automated Pavement Condition Collection Vehicle for City of Houston." Esri International User Conference, Esri, San Diego, CA, 1-9.

Smola, A. J., and Schölkopf, B. (2004). "A tutorial on Support Vector Regression." Statistics and Computing, 14(3), 199-222.

Sokolic, I. (2004). "Criteria to Evaluate the Quality of Pavement Camera Systems in Automated Evaluation Vehicles". Ph.D. dissertation. University of South Florida, Tampa, FL.

Stoffels, S.M., D. Morian, D. Frith, and C.D. Larson, (2001), "Quality Analysis Methods for Pavement Distress Data," Presented at the 80th Annual Meeting of the Transportation Research Board, Washington, D.C.

Subirats, P., Dumoulin, J., Legeay, V., and Barba, D. (2006). "Automation of Pavement Surface Crack Detection using the Continuous Wavelet Transform." Image Processing, 2006 IEEE International Conference on, IEEE, Atlanta, GA, 3037-3040.

Suzuki, S. and Abe, K. (1985). "Topological Structural Analysis of Digitized Binary Images by Border Following," *Computer Vision, Graphics, and Image Processing*, Vol. 30, No. 1, pp. 32-46.

Szeliski, Richard (2010). *Computer Vision: Algorithms and Applications*, Springer, London, UK.

Sy, N. T., Avila, M., Begot, S., and Bardet, J. (2008). "Detection of Defects in Road Surface by a Vision System." Electrotechnical Conference, 2008. MELECON 2008. The 14th IEEE Mediterranean, IEEE, Ajaccio, France, 847-851.

Tighe, S.L., L. Ningyuan, and T.J. Kazmierowski, (2008), "Evaluation of Semiautomated and Automated Pavement Distress Collection for Network-Level Pavement Management," Transportation Research Record: Journal of the Transportation Research Board, No. 2084, Transportation Research Board of the National Academies, Washington, D.C., pp. 11–17.

Timm, D. H., and McQueen, J. M. (2004). "A Study Of Manual Vs Automated Pavement Condition Surveys." Rep. No. IR-04-01, Highway Research Center, Auburn University, Alabama.

Timm, D. H., and Turochy, R. E. (2014). "Pavement Condition Model Based on Automated Pavement Distress Surveys." Rep. No. Final Report ALDOT Project 930-758, Alabama Department of Transportation, Montgomery, AL.

TRB. (2009). "Glossary of Highway Quality Assurance Terms, 4th update." Rep. No. Transportation Research Circular E-C137, Transportation Research Board, Washington, D.C.

Tsai, Y. & Li, F., 2012. Critical Assessment of Detecting Asphalt Pavement Cracks under Different Lighting and Low Intensity Contrast Conditions Using Emerging 3D Laser Technology. ASCE Journal of Transportation Engineering, 138(5), pp. 649-656.

Tsai, Y. & Wang, Z., 2014. A Remote Sensing and GIS-Enabled Asset Management System (RS-GAMS), Phase 2 Final Report, s.l.: US Department of Transportation.

Tsai, Y., Jiang, C. & Huang, Y., 2014. Multiscale Crack Fundamental Element Model for Real-World Pavement Crack Classification. ASCE Journal of Computing in Civil Engineering, 28(4).

UK Roads Board, 2009. SCANNER Surveys for Local Roads User Guide and Specification Volume 5: Technical Requirements for SCANNER Survey Parameters and Accreditation, s.l.: UK Department of Transport.

Virginia DOT. (2012). A Guide to Evaluating Pavement Distress through the Use of Digital Images (Version 2.6). Virginia Department of Transportation, Richmond, VA.

Wang, K. C. P. (2004). "Automated Pavement Distress Survey through Stereovision." Rep. No. Final Report for Highway IDEA Project 88, Transportation Research Board of the National Academies, Washington, D.C.

Wang, K.C.P., R.P. Elliott, A. Meadors, and M. Evans (2004). "Application and Validation of an Automated Cracking Survey System," 6th International Conference on Managing Pavements, Brisbane, Queensland, Australia, Oct. 19–24.

Wang, K. C. P. (2011). "Potential for Comprehensive Evaluation of Pavement Surface with 3D Laser Imaging." The 23rd Annual Road Profile Users' Group (RPUG) Meeting, Stateline, NV, 1-27.

Wang, K. C. P., and Gong, W. (2007). "Automated Real-Time Pavement Crack Detection and Classification." Rep. No. IDEA Final Project Report NCHRP-111, IDEA Program, Transportation Research Board, Fayetteville, AR.

Wang, K. C., and Smadi, O. (2011). Transportation Research Circular Number E-C156: Automated Imaging Technologies for Pavement Distress Surveys. Transportation Research Board of the National Academies, Washington, D.C.

Wang, K., Hou, Z. & Williams, S., 2011. Precision Test of Cracking Surveys with the Automated Distress Analyzer. ASCE Journal of Transportation Engineering, 137(8), p. 571–579.

Wang, K., Qiu, S. & Wang, W., 2015. A Comprehensive System for AASHTO PP67-10 Based Pavement Crack Evaluation. Washington, D.C., Transportation Research Board.

Warren, G., Wix, R., and Leschinski, R. (2013). "Assessment of Pavement Cracking in Real Time Using Three-Dimensional (3D) Laser Technology and Advanced Image Analysis Algorithms." 92nd Annual Meeting of the Transportation Research Board, Transportation Research Board, Washington, D.C., 1-12.

Xu, B., and Huang, Y. (2003). "Automated Pavement Cracking Rating System: A Summary." Rep. No. Project Summary Report 7-4975-S, Center for Transportation Research The University of Texas at Austin, Austin, TX.

Ying, L. (2009). "Beamlet Transform based Technique for Pavement Image Processing and Classification". Ph.D. dissertation. The University of Toledo, Toledo, OH.

Zhang, T. Y. and Suen, C. Y. (1984). "A Fast Parallel Algorithm for Thinning Digital Patterns," *Communications of the ACM*, Vol. 27, No. 3, pp. 236-239.

Zhang, W., Zhang, Z., Qi, D., and Liu, Y. (2014). "Automatic Crack Detection and Classification Method for Subway Tunnel Safety Monitoring." *Sensors*, 14(10), 19307-19328.

Zhu, Z., German, S., and Brilakis, I. (2011). "Visual Retrieval of Concrete Crack Properties for Automated Post-Earthquake Structural Safety Evaluation." *Automation in Construction*, 20(7), 874-883.

Zou, Q., Cao, Y., Li, Q., Mao, Q., and Wang, S. (2012). "CrackTree: Automatic Crack Detection from Pavement Images." *Pattern Recognition Letters*, 33(3), 227-238.

## APPENDICES

## **A. RECOMMENDED PROTOCOL FOR FDOT LRIS HARDWARE MAINTENANCE**

Fugro staff conducted an investigation to determine whether the collected pavement images are of acceptable quality for crack detection and how FDOT can potentially measure various image quality indicators in future. As a result of this study, Fugro developed a hardware maintenance protocol to be used by FDOT staff in order to ensure long term image quality and consistency.

The equipment integrator (International Cybernetics Corporation), the LRIS vendor (Pavemetrics Systems), and the LRIS manufacturer (INO) should provide corresponding guidelines for maintenance and calibration of the LRIS. According to Pavemetrics guidelines, the overall system maintenance and recalibration is recommended once a year.

NOTE: Please carefully review all the safety precautions provided by the equipment vendor to avoid fire or personal injury.

Fugro is NOT responsible for providing such guidelines and their application. The following are general recommendations by Fugro staff based on their experience with the LRIS system.

### **A.1 General Image Properties**

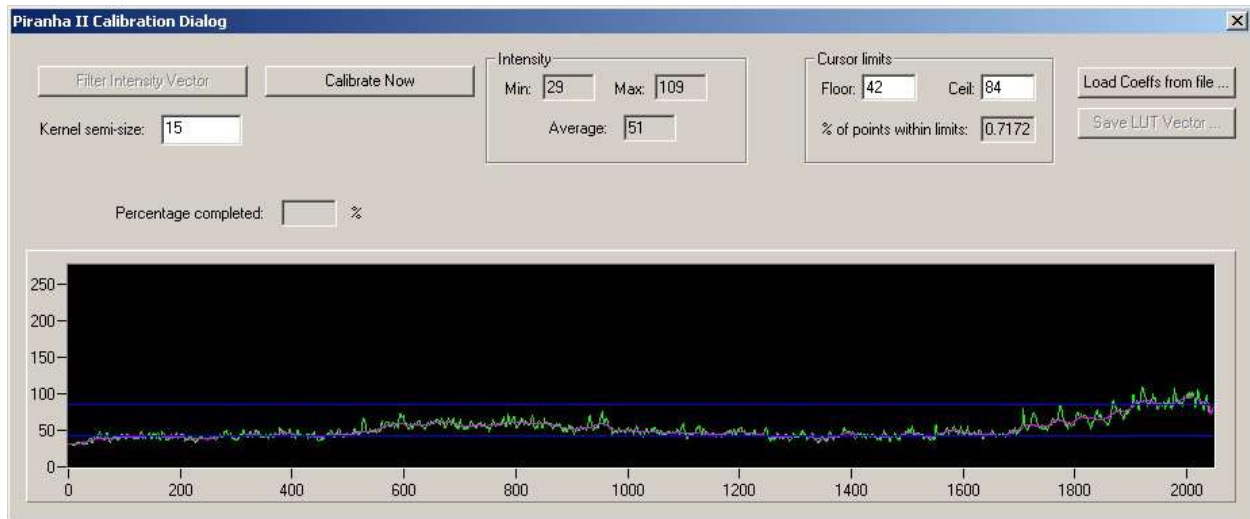
The typical state of the practice regarding these image properties is a subjective evaluation by an experienced human interpreter.

#### **A.1.1 Resolution: no need for checks**

The FDOT LRIS images have about 4,044 pixels, which is deemed as adequate for crack detection. The produced image resolution is NOT expected to change over time. Therefore, there is no need for frequent control.

#### **A.1.2 Exposure: Check and Calibrate Annually**

Adequate level of exposure is a very subjective matter and typically it is evaluated by an experienced engineer/technician. While executing the INO calibration procedure for LRIS (the application RoadCrack.exe displayed in the below screen capture), the calibration software will try to adjust pixel coefficients based on the non-uniformity found in the reference image, and when the expert is satisfied with the image displayed in the graphical interface, they should press Stop.



**Figure 133. Calibration dialog box.**

The following steps should be conducted once every year:

1. Start the application RoadCrack.exe and initialize both sensors (keep it simple, don't use the external trigger check box)
2. Set the operation mode to UnCalibrated
3. Start the acquisition and grab some images in Uncalibrated mode. Ideally, the calibration should be done using real road images, otherwise it is difficult to find a surface that has the same reflective properties as the pavement. The calibration uses the last uncalibrated image that has been grabbed and try to adjust the per pixel coefficients based on that image. The images used for calibration should not contain any defects like large cracks, shoulders, drop-off, marking, etc... They should also be acquired on a road section that is as uniform as possible. Finally, it is also better to use images acquired while the vehicle is moving (could be moving slow), this gives a more representative intensity profile vector (small defects are averaged). Remember that the uncalibrated image is used as a reference, and the calibration software will try to adjust pixel coefficients based on the non-uniformity found in that image.
4. When you are ready to calibrate, that is when you are satisfied with the image displayed in the graphical interface, you press Stop.

5. Then, you choose Calibrate Left/Right camera from the camera menu. The average intensity profile will be computed, and another window will be called. The average intensity profile will then be displayed in the new window.
6. Before popping up the new window, the software will ask you to save the reference image. It is a good idea to save that image as a future reference.
7. Drag and drop the blue cursors so that most of the average intensity profile is within the two cursors (see the BlueCursor.jpg image).
8. Press on Filter Intensity vector, and then Calibrate Now. This process should take about two minutes. This is the time to download the coefficients into camera's memory. Once it is done, you will be asked to save the resulting coefficients. It could be a good idea to save them for future reference. (tip: before pushing Calibrate now, you can also try changing the size of the filtering kernel. Edit the kernel size and press Enter. This would result in a more or less smooth profile. We may want to try using a larger kernel size (smoother profile)).
9. When it is done, close that window and return to the main interface.
10. At this step, you can check the result of the calibration by setting the Operation Mode to Calibrated and grab some images

**NOTE:** When switching from calibrated to uncalibrated, the image may become almost totally black. Changing the gains will correct that problem (set new gains and press enter). The mouse wheel can also be used to adjust the gain.

11. Set back the Operation mode to Uncalibrated, grab some images and proceed with the calibration for right sensor.

**KNOWN BUG:** Because the calibration process uses the last image that has been grabbed, it may happen that the image used for calibration is incomplete (there could be a black section in the images). This is not critical for the calibration since it has no effect on the average intensity profile. However, if you want to fix that bug anyway, simply set BreakEffect = FINISH in the Piranha2FixedLineRate.cam file.

If you need assistance with the above procedure, please send INO Uncalibrated images used as reference as well as the resulting coefficients that have been uploaded to the cameras. You can also send us the resulting calibrated images grabbed with your application.



### **A.1.3 Dynamic Range: no need for checks**

Dynamic range determines the level of detailed information contained in the image regarding the full spectrum of color or gray scale. The higher the dynamic range, the more levels of differences exist in the digital values of image pixels. In the 8-bit dynamic range of the FDOT LRIS images (which is currently widely used in the industry), there are 256 levels on the spectrum which translates into 256 shades of gray in a black and white image. The dynamic range is NOT expected to change over time. Therefore, there is no need for frequent control.

### **A.1.4 White balance: Check and Calibrate Annually**

It is recommended that a wide uniform standard 18% gray carpet be used for calibration of the white balance. The ICC software includes a routine for such calibration.

## **A.2 Image Issues**

These are issues that could be caused by defective hardware and/or unsuitable hardware settings. These issues could impact crack detection by increasing the potential for false positives.

### **A.2.1 Alignment: Check and Calibrate Annually**

There are settings parameter files that control the angle and overlap of stitching of the left and right images. These settings are adjusted according to a visual examination of the images of the target site. The images should show the diamond stripes as they appear on the actual site. It is recommended that the images of the target site be controlled at least once every year that the MPSV is in service.

### **A.2.2 Streaks: Clean Daily**

A disadvantage to the LRIS system is that because it creates images line by line any dirt or dust on the camera lens can create streaks in the image. These streaks result in black lines appearing in the images and can cause difficulty with automated crack detection software that uses the light and dark contrast to identify cracks.



**Figure 134. Example LRIS pavement image (right) showing intensity streaks that cannot be seen on the ROW image (left)**

Every morning before data collection, all windows on the LRIS units should be cleaned with a soft fabric using isopropanol or methanol. Avoid scratches that could damage the optical quality of windows and affect system performances. The controller and the sensor's body should be cleaned with a soft fabric using water only. Appropriate precautions should be taken to make sure that the isopropanol or methanol is not used over the different labels that are affixed on the sensors and on the controller. It is recommended to protect the external windows with covers when the LRIS is not in use.

**NOTE:** The LRIS sensors have not been designed to resist to powerful water jets. You should not use a high-pressure hose or water gun to clean them.

### **A.3 Image Feature Capturing (optical distortion)**

These properties are related to misrepresentation of actual pavement features due to inherent optical distortions in the camera and the wide-angle lens. These issues could impact crack detection by increasing the potential for detecting erroneous crack lengths and widths.

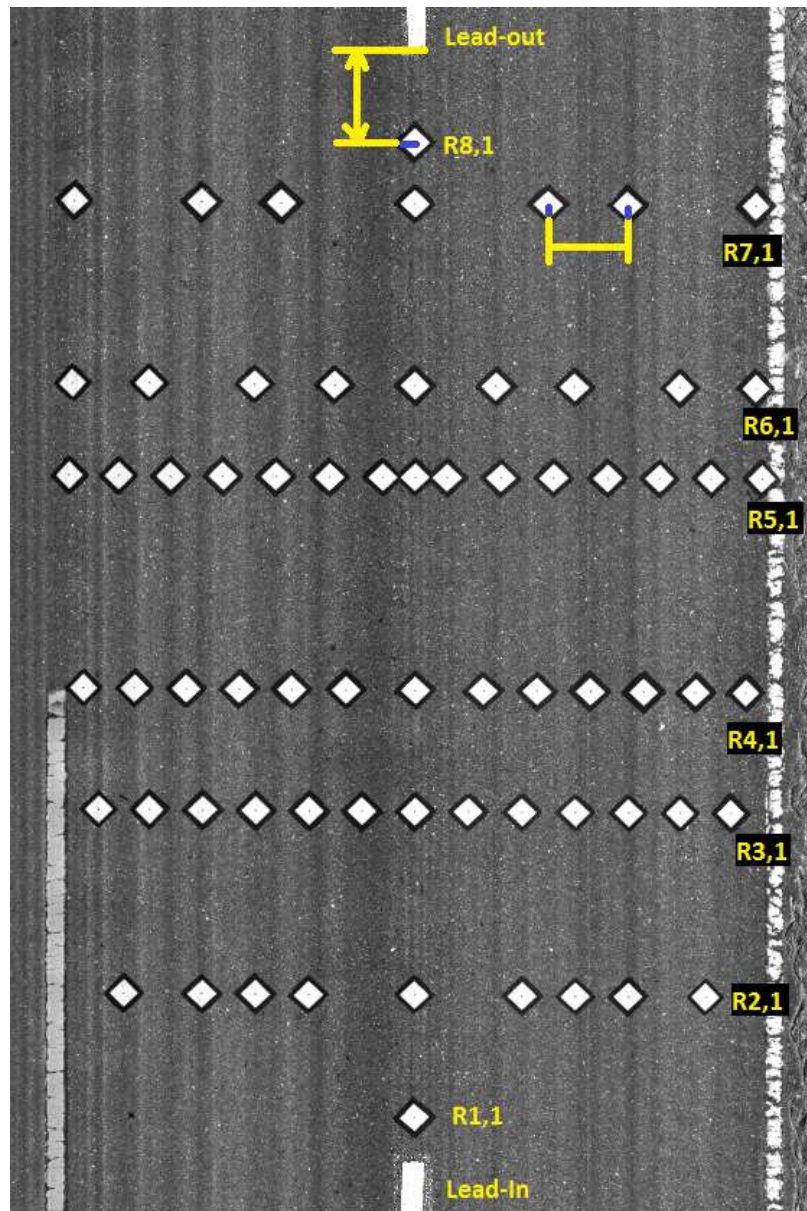
#### **A.3.1 Crack Length: Check Annually**

FDOT has set up an imaging target site with diamond shaped stripes as indicated in Figure 135.



**Figure 135. Pavement section with optical distortion study points.**

Figure 136 depicts the target site setup and Table 78 shows the reference measurement patches that are considered for this evaluation.



**Figure 136. LRIS 2D image of FDOT target site.**

In the transverse direction, all the distances between consecutive diamond stripes are measured in each row. For the longitudinal and diagonal directions, a sample of the distances are measured in the field.

**Table 78. Reference points for measurements**

TRANSVERSE											
Row	Patch Number	Row	Patch Number	Row	Patch Number	Row	Patch Number	Row	Patch Number	Row	Patch Number
R2	1 - 2	R3	1 - 2	R4	1 - 2	R5	1 - 2	R6	1 - 2	R7	1 - 2
	2 - 3		2 - 3		2 - 3		2 - 3		2 - 3		2 - 3
	3 - 4		3 - 4		3 - 4		3 - 4		3 - 4		3 - 4
	4 - 5		4 - 5		4 - 5		4 - 5		4 - 5		4 - 5
	5 - 6		5 - 6		5 - 6		5 - 6		5 - 6		5 - 6
	6 - 7		6 - 7		6 - 7		6 - 7		6 - 7		6 - 7
	7 - 8		7 - 8		7 - 8		7 - 8		7 - 8		
	8 - 9		8 - 9		8 - 9		8 - 9		8 - 9		
			9 - 10		9 - 10		9 - 10				
			10 - 11		10 - 11		10 - 11				
			11 - 12		11 - 12		11 - 12				
			12 - 13		12 - 13		12 - 13				
							13 - 14				
							14 - 15				

LONGITUDINAL	DIAGONAL
Patch Number	Patch Number
R1,1 - R2,5	R1,1 - R3,9
R2,5 - R3,7	R1,1 - R3,3
R3,7 - R4,7	R6,7 - R7,4
R4,7 - R5,8	R7,4 - R6,6
R5,8 - R6,5	R8,1 - R6,3
R6,5 - R7,4	R3,7 - R6,7
R7,4 - R8,1	

The optical distortion of a camera system is NOT expected to change over time; however, it could easily be checked annually to detect any other system issues that might change with time and impact the measured distortion. The following exercise is recommended to be conducted annually to ensure optical distortions are not increasing with time:

1. FDOT staff should conduct 3 measurements per patch and the average of those measurements is considered as the field reference measurement ("ground truth") to estimate the error in image measurements due to optical distortions. All field measurements are done to the nearest full millimetre.
2. The same distances should be measured on LRIS 2D images. The width of LRIS 2D images are typically 4044 pixels. This depends on the amount of overlap between the left and right camera images during stitching. Each pixel can be assumed as 1 mm (which might not always be true but is the best estimate).



3. The normalized error between field measurements and image measured distances on the FDOT imaging target site should be evaluated in the transverse, longitudinal and diagonal directions.
4. The average percentage of errors (normalized to field measurements) in longitudinal, transverse, and diagonal directions should be calculated and compared to the values listed in Table 79. These values were estimated during a research study in 2016 and it is expected that the optical distortion errors should fall within the recommended range in every annual estimation.

**Table 79. Recommended Range for Annual Error Estimation based on Previous Estimation of Average and Standard Deviation of Error Compared to Field Measurements**

Direction	2016 Error Estimation		Recommended Normalized Error Range
	Average Error (%)	Standard Deviation of Error (%)	
Transverse	3.12	2.92	0 to 6 %
Longitudinal	-2.30	0.46	-3 to -2 %
Diagonal	-0.92	0.81	-2 to 0%

### **A.3.2 Crack Width: no need for checks**

Unlike length measurements which are very objective, crack width measurements are subjective due to the gray areas in the images and subjectivity in visual field inspections. In addition, the small magnitudes of crack width make it a challenge (if not impossible) to measure the errors which are in sub millimeters, while the image resolution is at 1 mm.

### **A.3.3 Image Focus and Signal-to-Noise Ratio: Check Annually**

This is a traditional quantitative measure representing the ratio of the amount of undistorted features captured in an image (signal) to the distortion errors (noise) in detecting features, expressed in decibels. Therefore, this measure and similar measures such as mean squared error (MSE) require a reference “undistorted” image. An estimate of the signal to noise ratio (SNR) can be approximated as the average value of the image pixels (0 to 255 for 8-bit images) divided by the standard deviation of the image intensity values. This approximation eliminates the need for a reference image, but an image with a high SNR value approximated through this method does not necessarily remain faithful to the reality.

The SNR of a camera system is NOT expected to change over time; however, it could easily be checked annually to detect any other system issues that might change with

time and impact the measured SNR. The following exercise is recommended to be conducted annually to ensure signal to noise ratio is not increasing with time:

1. An SNR target should be synthetically manufactured. Figure 137 shows two sample target images used as a reference for evaluating the signal to noise ratio. They are composed of black and white areas.
2. An image of the synthetic target should be taken with the LRIS under proper lighting conditions (around noon on a clear sunny day so that there are no shades on the target) while the MPSV is stationary to serve as the reference undistorted image. The pixel intensity values (0 to 255 for 8-bit images) should be measured for the black and white areas of the image. These measurements can be done using open source software such as ImageJ.
3. A picture of the target taken by the LRIS camera while moving at collection speed should be used to evaluate the SNR of the captured image as compared to the reference. The pixel intensity values should be measured for the black and white areas of the image. It is recommended that at least 3 images be taken and the average of the 3 be used for comparison.
4. To evaluate camera focus, the contrast (difference) between the average pixel intensity values of the brighter (white) and darker (black) areas should be maximized. Therefore, this contrast should be measured for the reference stationary image and the images taken while the vehicle is moving. The average contrast for the collected images should be within 5% of the reference image.

$$Contrast_{Ref} = \mu_{White} - \mu_{Black} \geq 200$$

$$Contrast_{moving} = \mu_{White} - \mu_{Black}$$

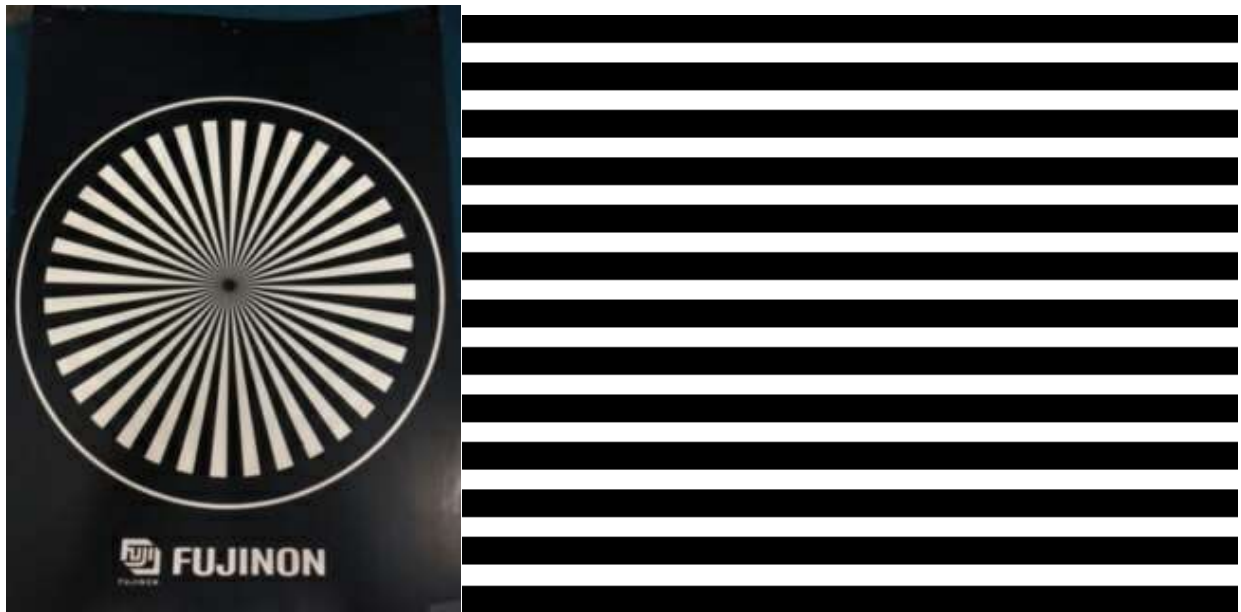
$$\frac{|Contrast_{Ref} - Contrast_{moving}|}{Contrast_{Ref}} \leq 5\%$$

5. To evaluate signal to noise ratio, the relative metric of average intensity divided by the standard deviation of intensity should be calculated for the brighter and darker pixels. This calculation should be conducted for the reference stationary image and the images taken while the vehicle is moving. The average of this relative SNR measure for the collected images should be within 5% of the reference image for both brighter and darker pixels.

$$SNR_{Black}^{Ref} = \frac{\mu_{Black}}{\sigma_{Black}}, SNR_{White}^{Ref} = \frac{\mu_{White}}{\sigma_{White}}$$

$$SNR_{Black}^{moving} = \frac{\mu_{Black}}{\sigma_{Black}}, SNR_{White}^{moving} = \frac{\mu_{White}}{\sigma_{White}}$$

$$\frac{|SNR_{Black}^{Ref} - SNR_{Black}^{moving}|}{SNR_{Black}^{Ref}} \leq 5\%, \frac{|SNR_{White}^{Ref} - SNR_{White}^{moving}|}{SNR_{White}^{Ref}} \leq 5\%$$



**Figure 137. Sample Target Images used as a Reference for Evaluating Signal to Noise Ratio**

Detailed investigation of SNR values was conducted in a previous FDOT study and it is documented in Report No. BD-544-11. It is recommended that a similar target image be used for annual control checks of the SNR values.

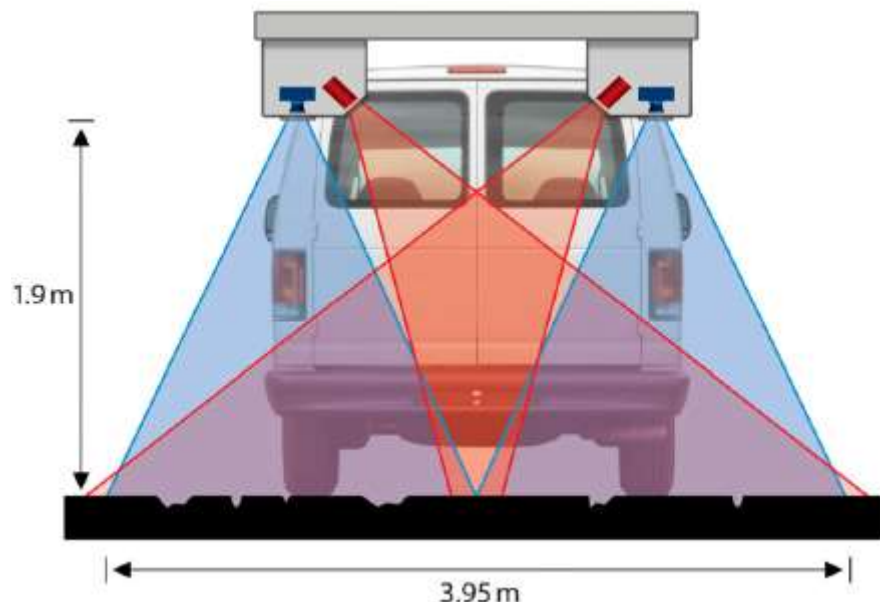
#### **A.4 LRIS Hardware: Check Annually**

The integrator company for the FDOT LRIS vehicle is the International Cybernetics Corporation (ICC) and they are responsible for resolving hardware issues, some of which could be addressed by routine maintenance. It is necessary that the hardware and software setup and “calibration” standards recommended by the LRIS equipment manufacturer (Pavemetrics) and the FDOT equipment integrator (ICC) be followed with regards to routine maintenance and calibration controls. The overall system maintenance and recalibration is recommended once a year. This includes checking the camera installed heights and the vehicle tire pressure to ensure the pavement surface is



within the camera depth of field, where objects are in focus. As described in the previous section, the image is in focus if the contrast between the bright and dark areas are maximized.

- a) Distance measuring accuracy: the distance measuring instrument (DMI) needs to be inspected and calibrated on a routine basis as recommended by the manufacturer. A control section distance can be measured with the DOT reference device and the vehicle DMI measurements of the control section can be compared to the reference measurement.
- b) Latitude-Longitude accuracy: the global positioning system (GPS) devices need to be inspected and calibrated on a routine basis as recommended by the manufacturer. The vehicle needs to be parked at specific locations on the control section for about 15 minutes to establish a stable measurement. Then the GPS coordinates of those locations should be surveyed using total station equipment in order to check the vehicle GPS measurements. Depending on the number and model of the IMU units in the vehicle, acceptable errors could be found from the manufacturer website.
- c) LRIS platform stability: If there are loose connections in the platform, they need to be addressed as recommended by the manufacturer.



**Figure 138. Schematic of image collection concept.**

## **A.5 Environmental Effects: no need for checks**

The effects of different lighting conditions (overcast, cloudy, or sunny) and vehicle speeds (25, 35, or 45 mph) have already been studied in a previous FDOT research project (documented in Report No. BD-544-11, chapter 2). It was found that the LRIS images are not significantly affected by different vehicle speeds and lighting conditions. The LRIS user manual indicates that the equipment should not be operated at temperatures above 40 degrees Celsius (104 degrees Fahrenheit).

- a. Performance at various lighting conditions
- b. Temperature, humidity, and wind
- c. Performance at varying speeds

## B. DETERMINATION OF SUITABLE AUTOMATED SETTINGS FOR PROCESSING LRIS IMAGES FOR RIGID PAVEMENT DISTRESS IN THE EXISTING AUTOMATED SOFTWARE

**Table 80. Settings for WiseCrax pre-set detection profiles**

Detection		1	2	3	4	5	6
Profile Name		longitudinal and alligator cracks on lightly distressed pavement	longitudinal and alligator cracks on moderately distressed pavement	longitudinal and alligator cracks on heavily distressed pavement	Dark Asphalt with dark crack	Dark Asphalt with white crack or crack with salt	Light Asphalt with dark crack
Crack Types		longitudinal and alligator cracks	longitudinal and alligator cracks	longitudinal and alligator cracks			
Crack Color					dark	white	dark
Pavement Color					dark	dark	light
Pavement Material							asphalt
Defection Degree		lightly	moderate	heavily			
Crack Options							
	Crack Simplification	1	1	1	1	2	1
	Extraction						
	Transverse Cracking	15	12	25	50	30	80
	Longitudinal Cracking	15	12	25	50	30	80
	Crack Likelihood	2	1	1	2	1	3
	Horizontal Bridging	3	3	3	3	2	3
	Vertical Bridging	5	5	5	5	9	5
	Pruning						
	Remove Short Distress	TRUE	TRUE	TRUE	TRUE	TRUE	TRUE
	Minimum Length (mm)	100	100	100	150	150	140
	Remove Low Node-Count Distresses	TRUE	TRUE	TRUE	FALSE	TRUE	TRUE

Detection		1	2	3	4	5	6
	Minimum Node Count	50	50	50	N/A	100	60
	Remove Low-Cost Distresses	FALSE	FALSE	FALSE	TRUE	FALSE	FALSE
	Minimum Cost Threshold	N/A	N/A	N/A	50	N/A	N/A
	Remove 'Bright' Distresses	FALSE	FALSE	FALSE	TRUE	TRUE	FALSE
	Maximum Intensity Threshold	N/A	N/A	N/A	110	115	N/A
Width							
	Intensity Threshold	60	60	60	60	60	60
Lane Options							
	Enabled	TRUE	TRUE	TRUE	TRUE	TRUE	TRUE
	Detect within lanes	TRUE	TRUE	TRUE	TRUE	TRUE	TRUE
	Scale	0.5	0.5	0.5	0.5	0.5	0.5
	Threshold	50	50	50	50	50	50
	Slice height	200	200	200	200	200	200
	Smooth width	10	10	10	10	10	10
	Minimum marker width	50	50	50	50	50	50
	Maximum marker width	250	250	250	250	250	250
Lane set method							
Sealed Crack Options							
Crack Simplification		1	1	1	1	1	1
Extraction							
	Transverse Cracking	0	17.5	0	0	0	0
	Longitudinal Cracking	0	17.5	0	0	0	0
	Crack Likelihood	3	3	3	3	3	3

Detection		1	2	3	4	5	6
	Horizontal Bridging	2	2	2	2	2	2
	Vertical Bridging	4	4	4	4	4	4
	Pruning						
	Remove Short Distresses	FALSE	FALSE	FALSE	FALSE	FALSE	FALSE
	Remove Low Node-Count	TRUE	TRUE	TRUE	TRUE	TRUE	TRUE
	Minimum Node Count	8	8	8	8	8	8
	Remove Low-Cost	TRUE	TRUE	TRUE	TRUE	TRUE	TRUE
	Minimum Cost Threshold	10	10	10	10	10	10
	Remove 'Bright'	TRUE	TRUE	TRUE	TRUE	TRUE	TRUE
	Maximum Intensity	80	80	80	80	80	80
	Intensity Threshold	80	80	80	80	80	80





**Table 81. Settings for WiseCrax pre-set detection profiles (continued)**

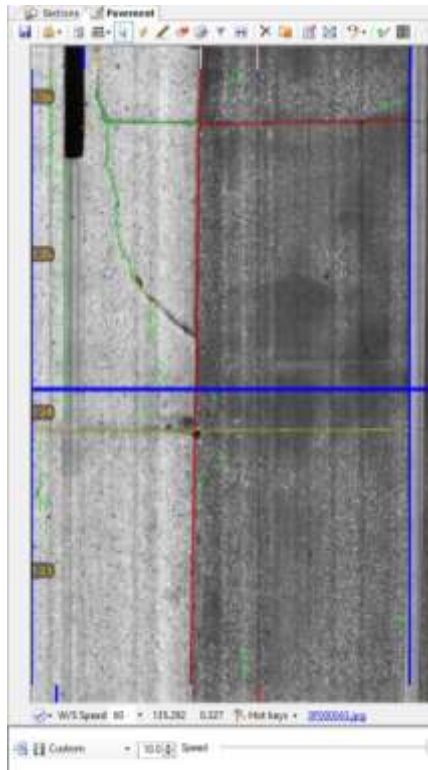
Detection			7	8	9	10
Profile Name			longitudinal and transverse cracks on light pavement	longitudinal crack	Transverse crack	Pavements with light number of white cracks
Crack Types			longitudinal and transverse cracks	longitudinal crack	Transverse crack	
Crack Color						white (light amount)
Pavement Color			light			
Pavement Material						
Defection Degree						
Crack Options						
	2		2	1	2	1
	10	0	10	30	25	50
	10	37.5	5	10	25	50
	2	2	2	1	1	2
	3	3	3	2	3	3

Detection		7	8	9	10
5	5	5	9	5	5
	TRUE	TRUE	TRUE	TRUE	TRUE
	125	125	150	150	100
	FALSE	FALSE	TRUE	TRUE	TRUE
	N/A	N/A	75	100	50
	FALSE	FALSE	FALSE	FALSE	FALSE
	N/A	N/A	N/A	N/A	N/A
	FALSE	FALSE	FALSE	TRUE	FALSE
	N/A	N/A	N/A	115	N/A
60	60	60	60	60	60
Lane Options					
TRUE		TRUE	TRUE	TRUE	TRUE
TRUE		TRUE	TRUE	TRUE	TRUE
0.5		0.5	0.5	0.5	0.5
50		50	50	50	50
200		200	200	200	200
10		10	10	10	10
50		50	50	50	50
250		250	250	250	250
Sealed Crack Options					
Crack Simplification		1	1	1	1
0	0	0	0	0	0
0	0	0	0	0	0
3	3	3	3	3	3

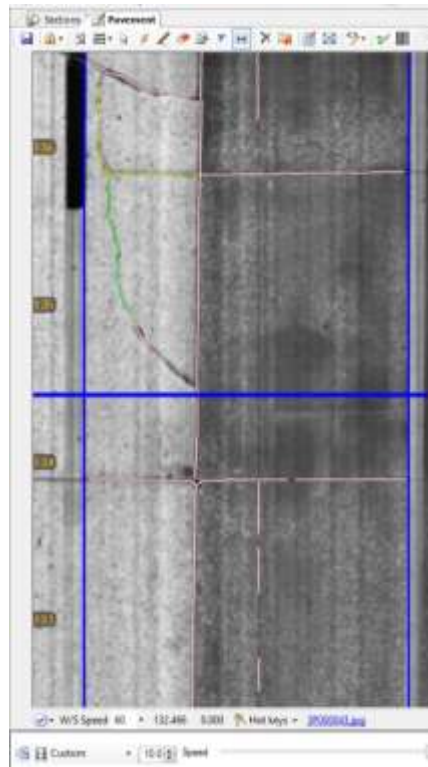
Detection			7	8	9	10
	2	2	2	2	2	2
	3	3	3	3	4	4
	FALSE	FALSE	FALSE	FALSE	FALSE	FALSE
	TRUE	TRUE	TRUE	TRUE	TRUE	TRUE
	10	10	10	10	8	8
	TRUE	TRUE	TRUE	TRUE	TRUE	TRUE
	120	120	120	120	10	10
	TRUE	TRUE	TRUE	TRUE	TRUE	TRUE
	60	60	60	60	80	80
					80	80

**Table 82. Crack Detection Legend for Figure 139 through Figure 163**

Range Name	Min Width	Max Width	Color
Small		0.118	
Medium	0.118	0.236	
Large	0.236	0.394	
Very Large	0.394		

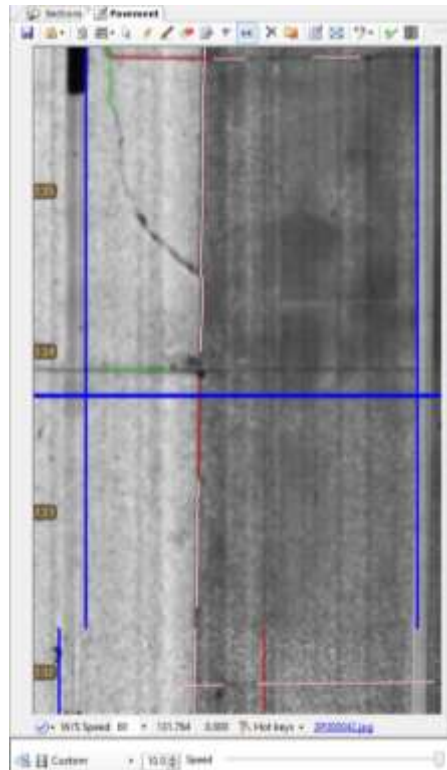


**Figure 139. Crack Detection Sample Image Number 1**

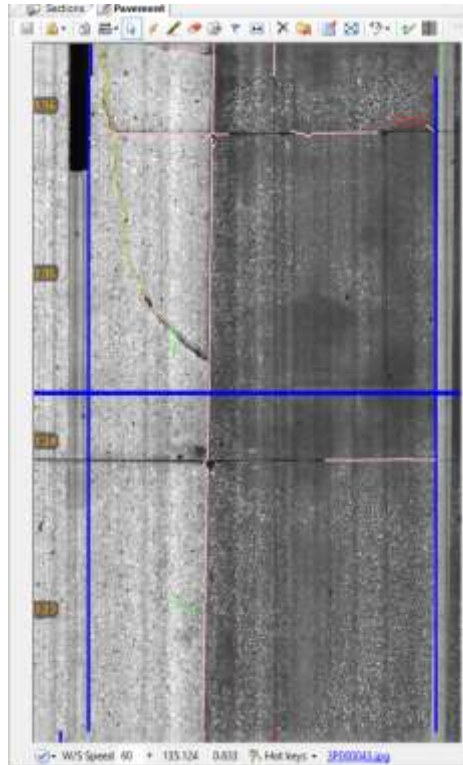


**Figure 140. Crack Detection Sample Image Number 2**

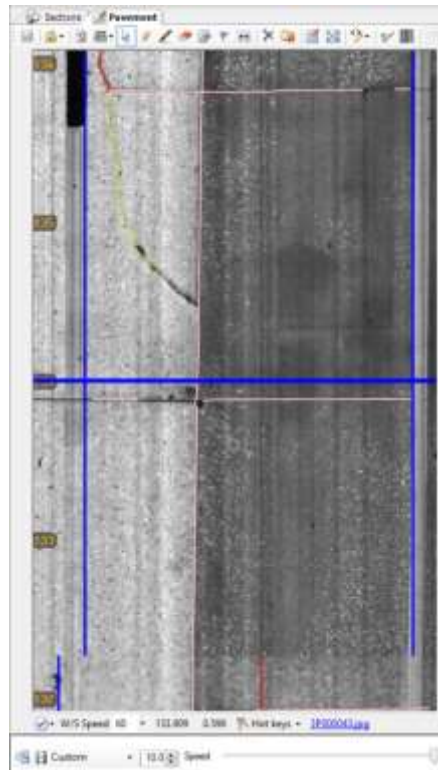




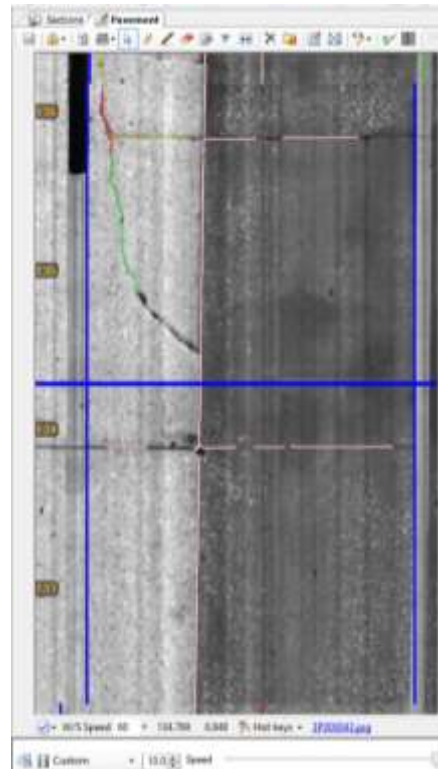
**Figure 141. Crack Detection Sample Image Number 3**



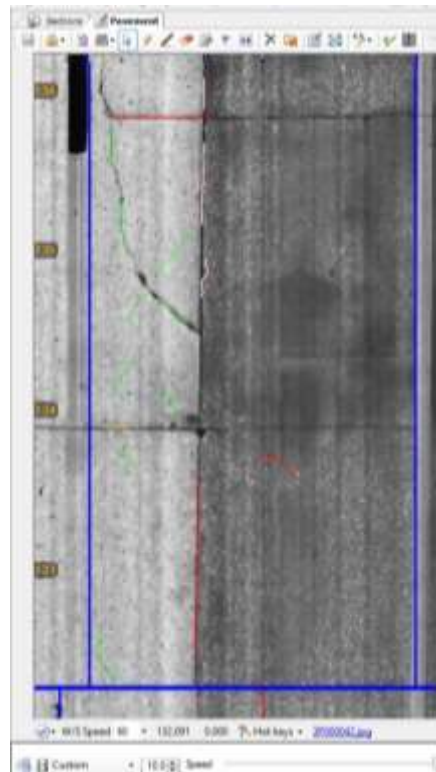
**Figure 142. Crack Detection Sample Image Number 4**



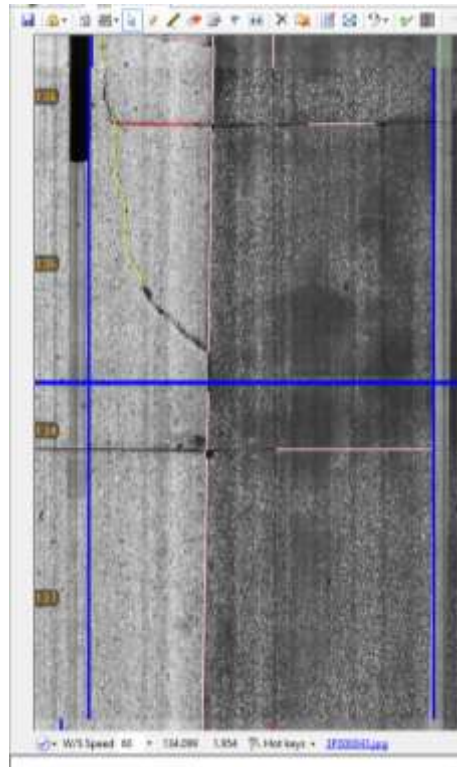
**Figure 143. Crack Detection Sample Image Number 5**



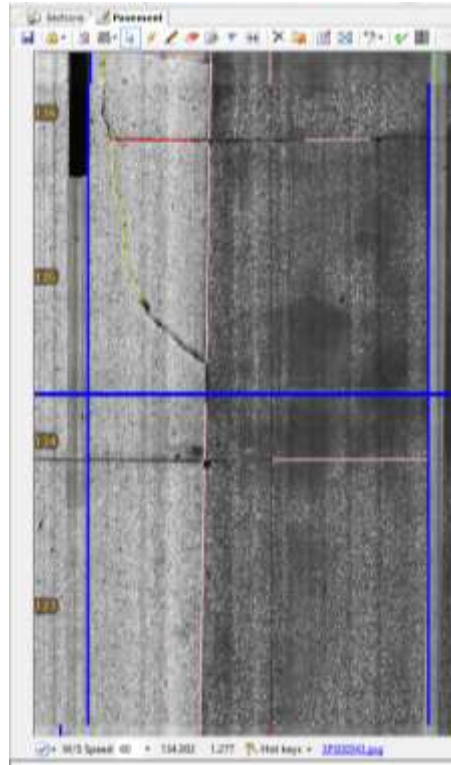
**Figure 144. Crack Detection Sample Image Number 6**



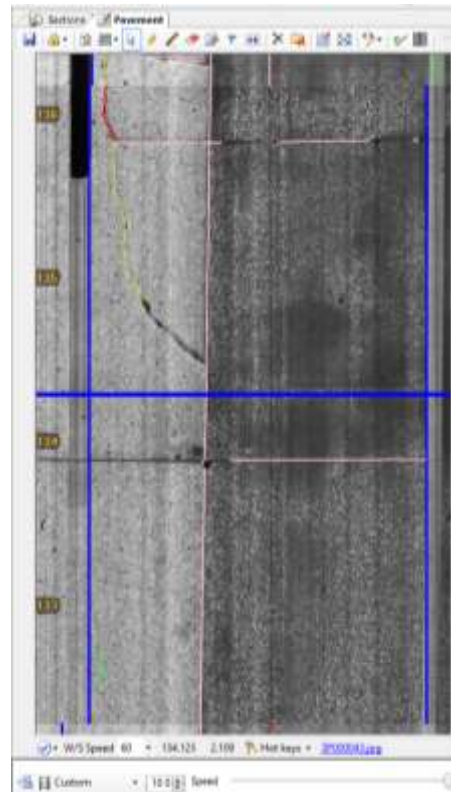
**Figure 145. Crack Detection Sample Image Number 7**



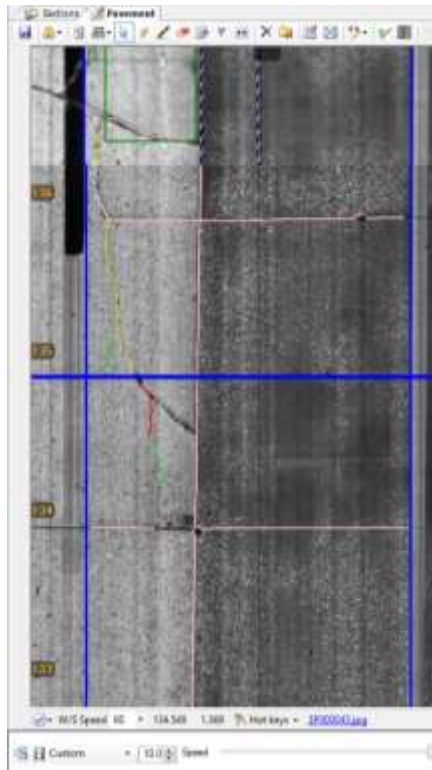
**Figure 146. Crack Detection Sample Image Number 8**



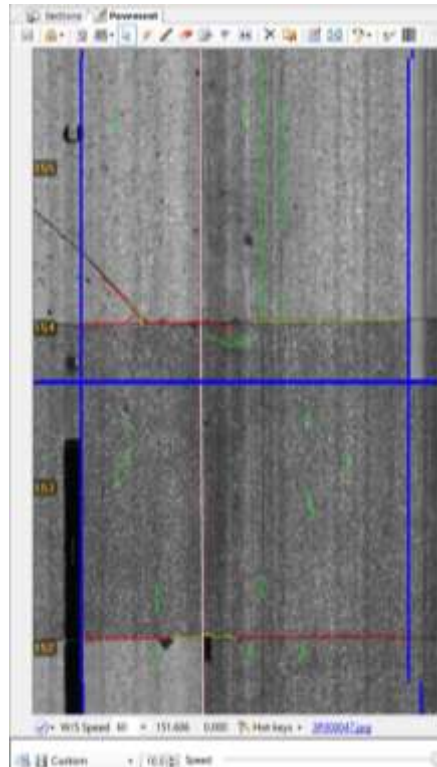
**Figure 147. Crack Detection Sample Image Number 9**



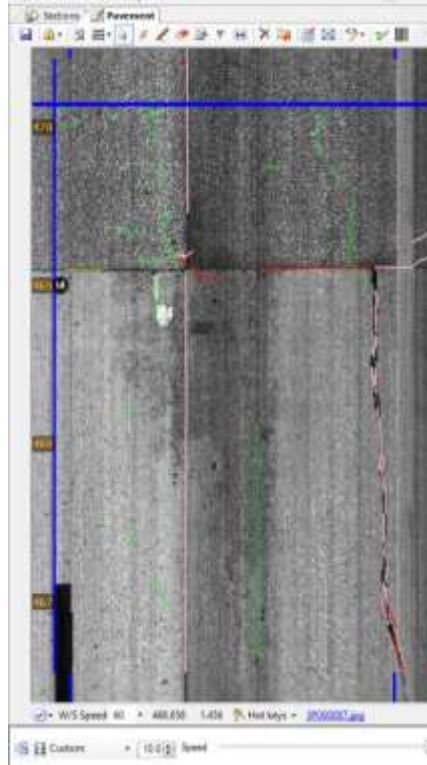
**Figure 148. Crack Detection Sample Image Number 10**



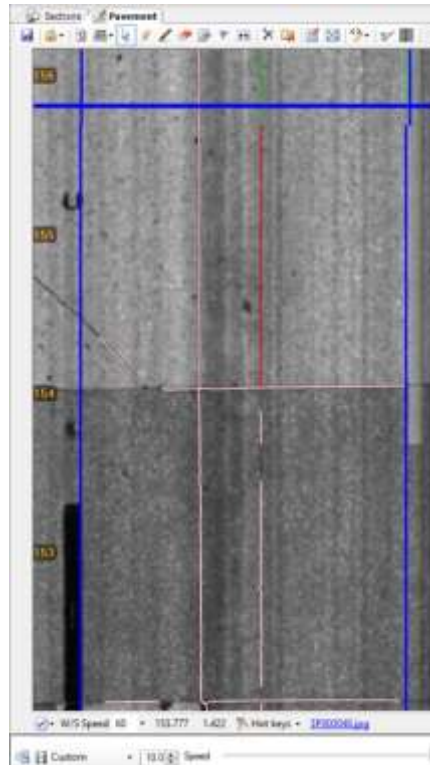
**Figure 149. Crack Detection Sample Image Number 11**



**Figure 150. Crack Detection Sample Image Number 12**



**Figure 151. Crack Detection Sample Image Number 13**



**Figure 152. Crack Detection Sample Image Number 14**





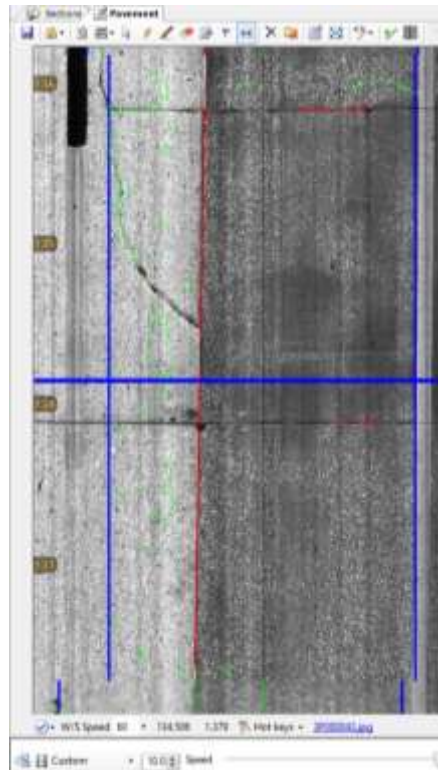


Figure 155. Crack Detection Sample Image Number 17

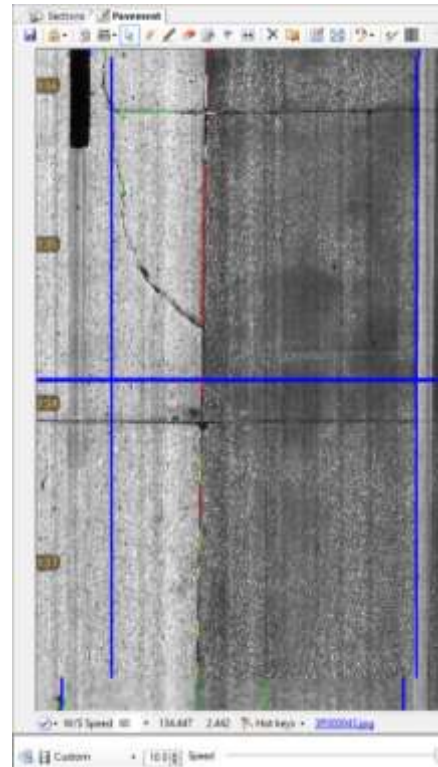
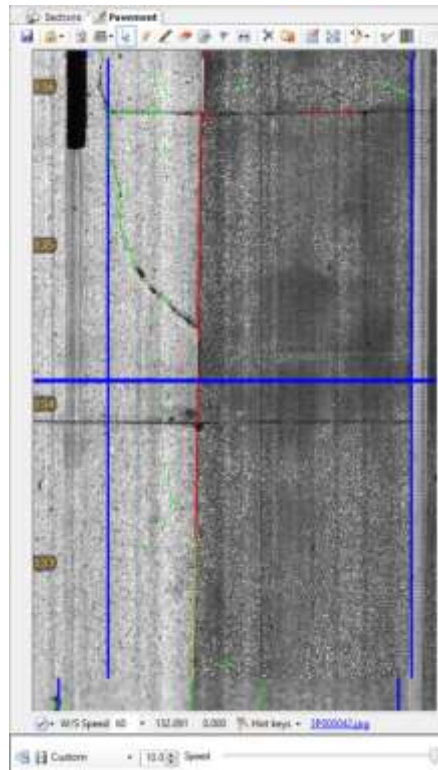
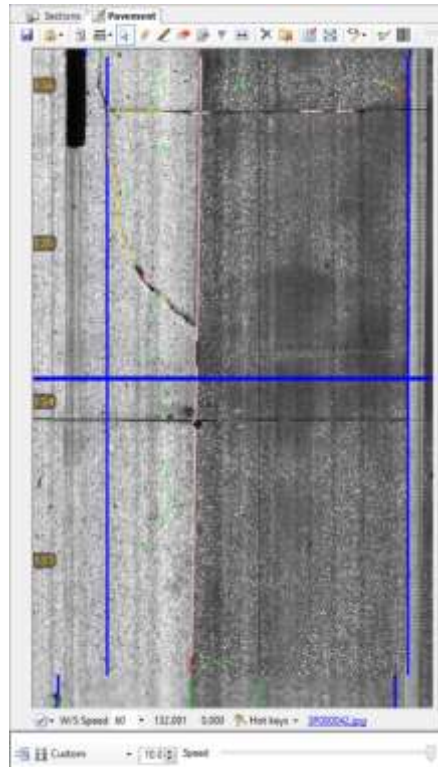


Figure 156. Crack Detection Sample Image Number 18

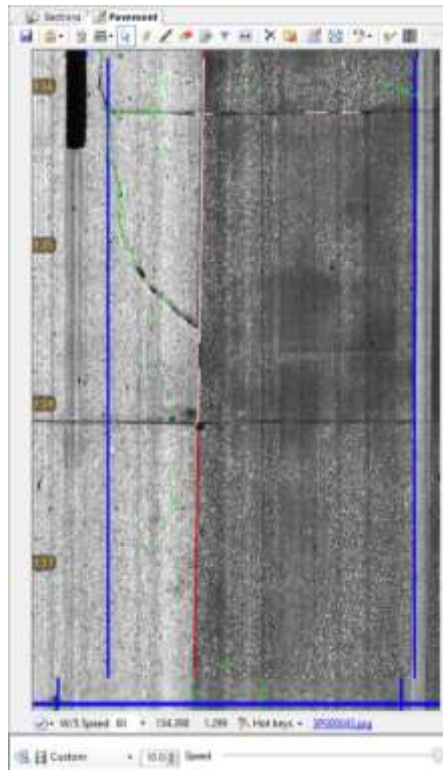




**Figure 157. Crack Detection Sample Image Number 19**



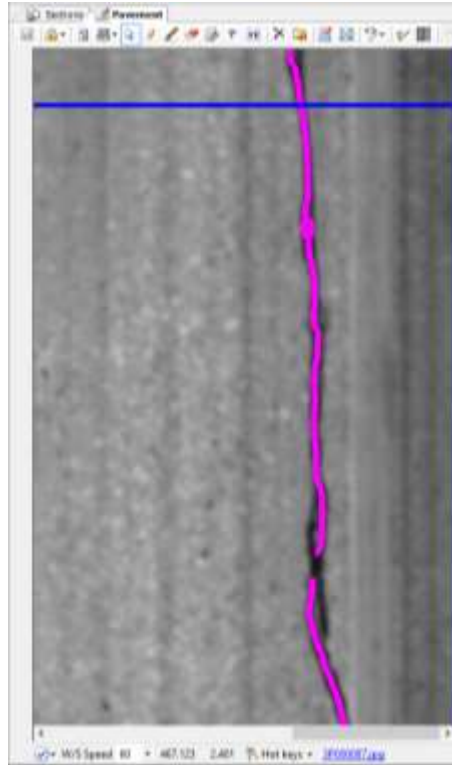
**Figure 158. Crack Detection Sample Image Number 20**



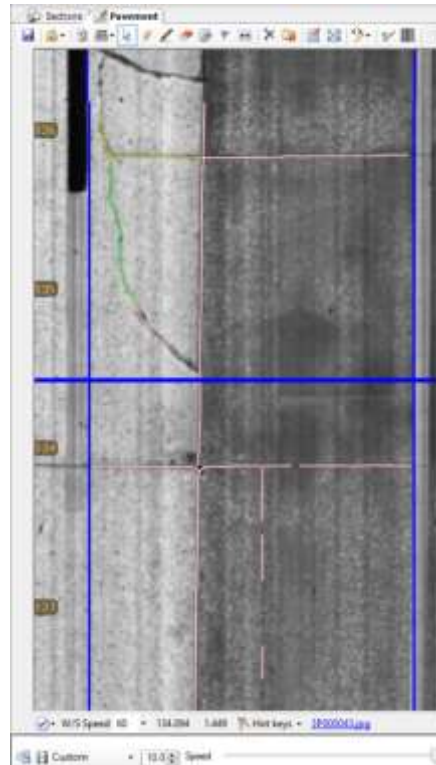
**Figure 159. Crack Detection Sample Image Number 21**



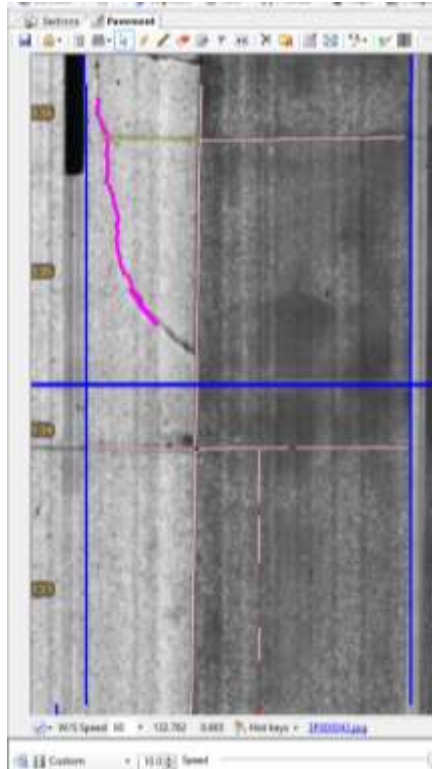
**Figure 160. Crack Detection Sample Image Number 22**



**Figure 161. Crack Detection Sample Image Number 23**




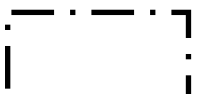



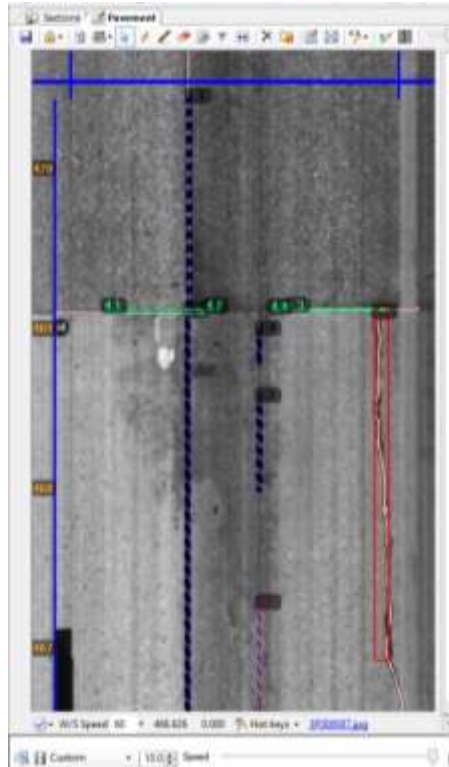
**Figure 162. Crack Detection Sample Image Number 24**



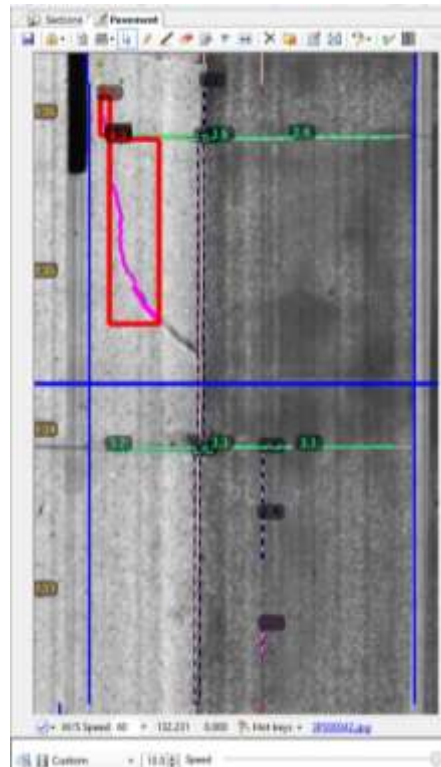
**Figure 163. Crack Detection Sample Image Number 25**

**Table 83. Distress Identification Legend for Figure 164 through Figure 166**

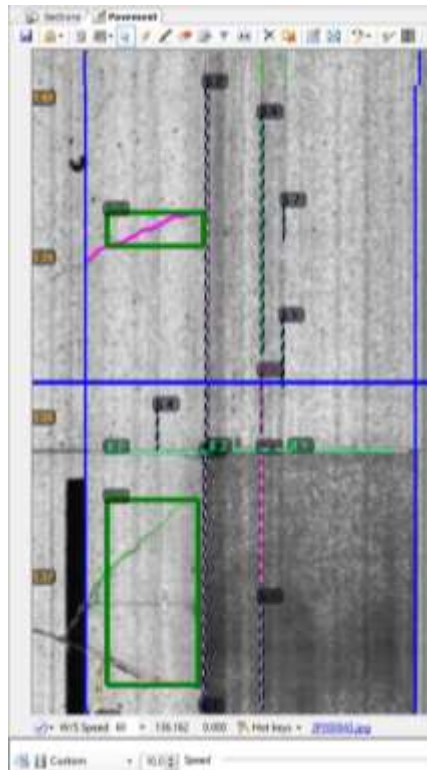
Transverse Distress	
Longitudinal Distress	
Transverse Joint	
Longitudinal Joint (87-90)	
Longitudinal Joint (-90--87)	



**Figure 164. Crack Classification Sample Image Number 1**



**Figure 165. Crack Classification Sample Image Number 2**



**Figure 166. Crack Classification Sample Image Number 3**

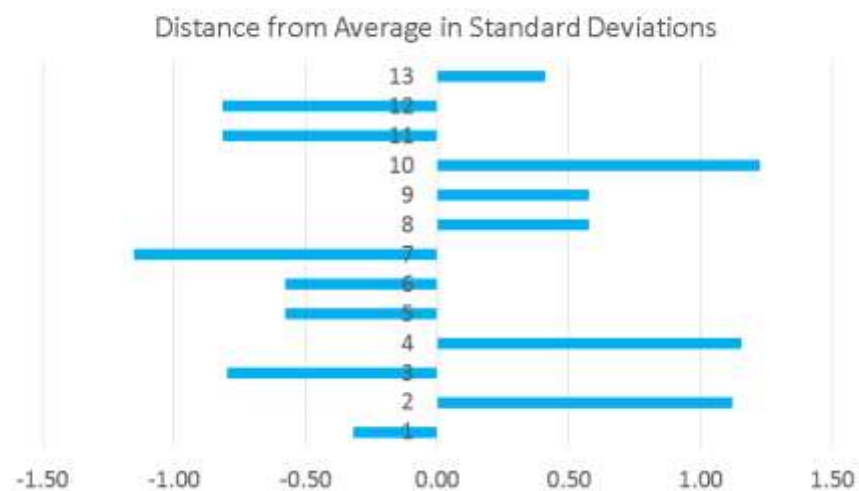
## C. RESULTS FROM FIELD DISTRESS WORKSHOP ON RIGID PAVEMENTS

In the following tables, highlighted values indicate more than 50% variation or less than 50% agreement among the raters.

**Table 84. Statistics of transverse cracking at different severity level**

Section ID	Statistic	Transverse Cracking (count)				
		Light	Moderate	Severe	Total	
01	AVG	8.67	1.67	0.33	10.67	
02	AVG	6.00	2.00	1.33	9.33	
03	AVG	21.00	2.00	2.00	25.00	
04	AVG	10.25	3.50	1.25	15.00	
01	(Min,Max)	(8,9)	(0,3)	(0,1)	(9,13)	
02	(Min,Max)	(4,7)	(0,4)	(1,2)	(8,12)	
03	(Min,Max)	(19,23)	(0,4)	(0,5)	(19,28)	
04	(Min,Max)	(6,17)	(1,6)	(0,3)	(13,18)	
01	COV (%)	6.66	91.65	173.21	19.52	
02	COV (%)	28.87	100.00	43.30	24.74	
03	COV (%)	9.52	100.00	132.29	20.78	
04	COV (%)	48.70	68.01	120.00	16.33	
OVERALL VARIATION (%)		AVG(COV)	23.44	89.92	117.20	20.34
OVERALL PRECISION (%)		100-AVG(COV)	76.56	10.08	-17.20	79.66

### Transverse Cracking (count), Light-Moderate-Severe



**Figure 167. Distance from average in standard deviation (transverse cracking).**





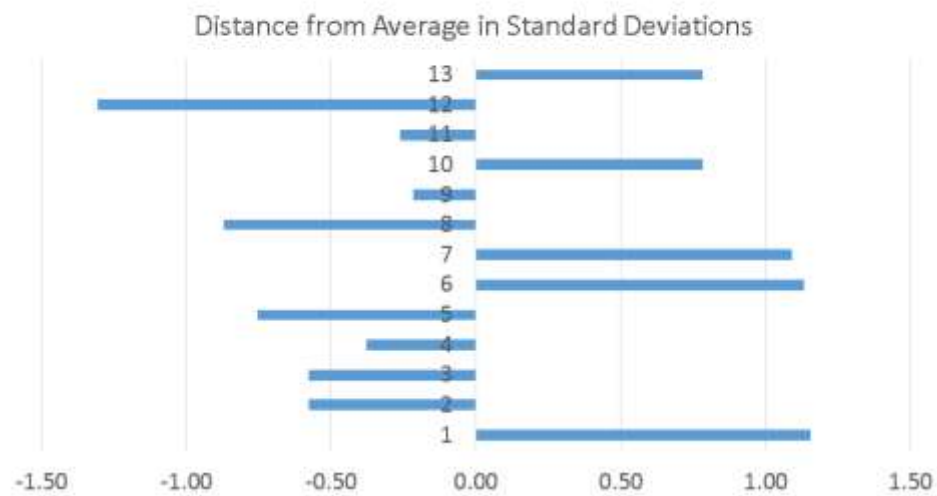
Figure 168. Transverse cracking on rigid pavements.

Table 85. Statistics of longitudinal cracking at different severity level

Section ID	Statistic	Longitudinal Cracking (count)				
		Light	Moderate	Severe	Total	
01	AVG	1.00	0.33	0.00	1.33	
02	AVG	10.00	4.00	1.00	15.00	
03	AVG	2.33	0.67	0.33	3.33	
04	AVG	1.25	0.75	0.25	2.25	
01	(Min,Max)	(1,1)	(0,1)	(0,0)	(1,2)	
02	(Min,Max)	(7,16)	(0,6)	(0,2)	(13,18)	
03	(Min,Max)	(0,5)	(0,1)	(0,1)	(2,5)	
04	(Min,Max)	(0,3)	(0,2)	(0,1)	(1,3)	
01	COV (%)	0.00	173.21	0.00	43.30	
02	COV (%)	51.96	86.60	100.00	17.64	
03	COV (%)	107.85	86.60	173.21	45.83	
04	COV (%)	100.66	127.66	200.00	42.55	
OVERALL VARIATION (%)		AVG(COV)	65.12	118.52	118.30	37.33
OVERALL PRECISION (%)		100-AVG(COV)	34.88	-18.52	-18.30	62.67



## Longitudinal Cracking (count), Light-Moderate-Severe



**Figure 169. Distance from average in standard deviation (longitudinal cracking).**

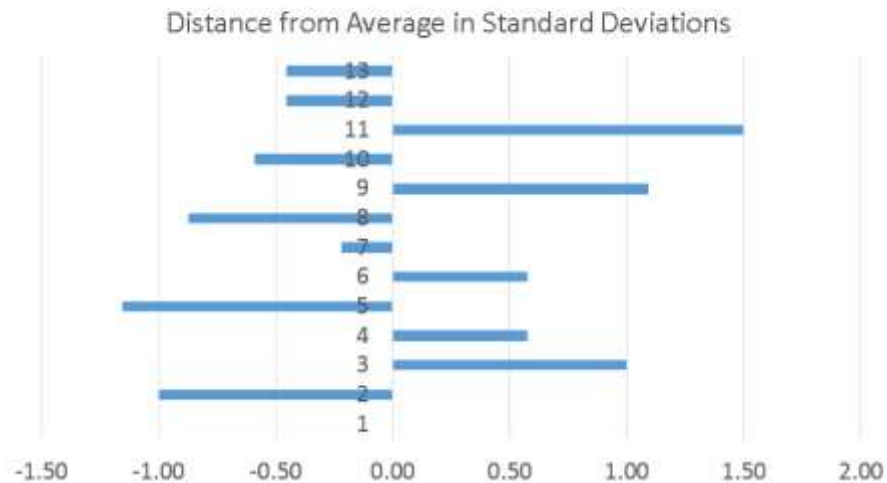


**Figure 170. Longitudinal cracking on rigid pavement.**

**Table 86. Statistics of spalling at different severity level**

Section ID	Statistic	Spalling (ft)		
		Moderate	Severe	Total
01	AVG	13.33	0.67	14.00
02	AVG	8.00	0.33	8.33
03	AVG	20.67	1.00	21.67
04	AVG	4.50	5.75	10.25
01	(Min,Max)	(11,17)	(0,2)	(11,17)
02	(Min,Max)	(7,9)	(0,1)	(7,9)
03	(Min,Max)	(13,29)	(0,2)	(15,30)
04	(Min,Max)	(3,6)	(1,16)	(6,21)
01	COV (%)	24.11	173.21	21.43
02	COV (%)	12.50	173.21	13.86
03	COV (%)	38.81	100.00	35.25
04	COV (%)	28.69	120.80	70.07
<b>OVERALL VARIATION (%)</b>		<b>AVG(COV)</b>	26.03	141.80
<b>OVERALL PRECISION (%)</b>		<b>100-AVG(COV)</b>	73.97	-41.80

## Spalling (linear feet), Moderate-Severe



**Figure 171. Distance from average in standard deviation (spalling).**

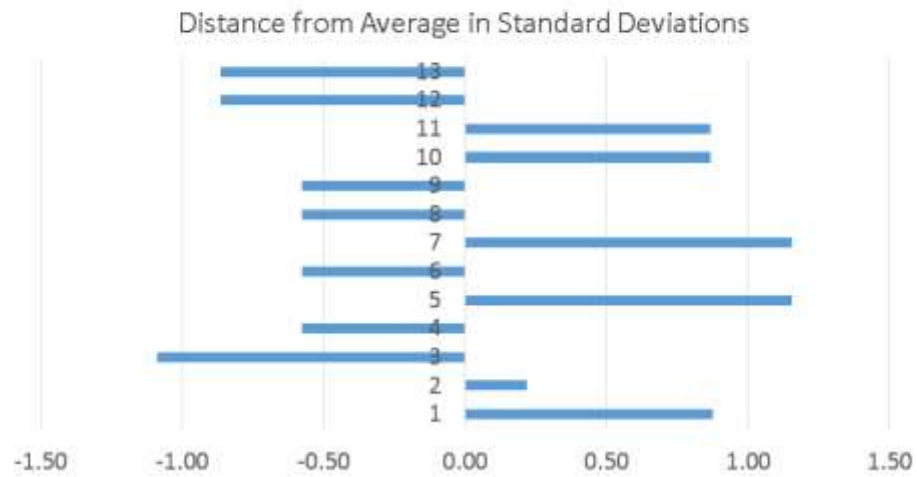


Figure 172. Spalling on rigid pavements.

Table 87. Statistics of corner cracking at different severity level

Section ID	Statistic	Corner Cracking (count)				
		Light	Moderate	Severe	Total	
01	AVG	1.67	0.00	0.00	1.67	
02	AVG	0.67	1.00	3.00	4.67	
03	AVG	0.33	0.00	0.00	0.33	
04	AVG	1.25	0.00	0.25	1.50	
01	(Min,Max)	(0,3)	(0,0)	(0,0)	(0,3)	
02	(Min,Max)	(0,1)	(0,2)	(3,3)	(4,6)	
03	(Min,Max)	(0,1)	(0,0)	(0,0)	(0,1)	
04	(Min,Max)	(0,3)	(0,0)	(0,1)	(0,3)	
01	COV (%)	91.65	0.00	0.00	91.65	
02	COV (%)	86.60	100.00	0.00	24.74	
03	COV (%)	173.21	0.00	0.00	173.21	
04	COV (%)	120.00	0.00	200.00	115.47	
OVERALL VARIATION (%)		AVG(COV)	117.86	25.00	50.00	101.27
OVERALL PRECISION (%)		100-AVG(COV)	-17.86	75.00	50.00	-1.27

## Corner Cracking (count), Light-Moderate-Severe



**Figure 173. Distance from average in standard deviation (corner cracking).**



**Figure 174. Corner cracking on rigid pavement.**

**Table 88. Statistics of patching at different severity level**

Section ID	Statistic	Patching (sq yd)		
		Fair	Poor	Total
01	AVG	0.00	0.00	0.00
02	AVG	0.00	0.00	0.00
03	AVG	4.00	0.00	4.00
04	AVG	1.00	0.25	1.25
01	(Min,Max)	(0,0)	(0,0)	(0,0)
02	(Min,Max)	(0,0)	(0,0)	(0,0)
03	(Min,Max)	(1,10)	(0,0)	(1,10)
04	(Min,Max)	(0,4)	(0,1)	(0,4)
01	COV (%)	0.00	0.00	0.00
02	COV (%)	0.00	0.00	0.00
03	COV (%)	129.90	0.00	129.90
04	COV (%)	200.00	200.00	151.44
<b>OVERALL VARIATION (%)</b>		<b>AVG(COV)</b>		
		82.48	50.00	70.34
<b>OVERALL PRECISION (%)</b>		<b>100-AVG(COV)</b>		
		17.52	50.00	29.66

**Table 89. Statistics of shattered slabs**

Section ID	Statistic	Shattered Slabs (count)		
		Moderate	Severe	Total
01	AVG	1.00	0.00	1.00
02	AVG	1.00	0.00	1.00
03	AVG	0.00	0.00	0.00
04	AVG	0.00	0.00	0.00
01	(Min,Max)	(1,1)	(0,0)	(1,1)
02	(Min,Max)	(1,1)	(0,0)	(1,1)
03	(Min,Max)	(0,0)	(0,0)	(0,0)
04	(Min,Max)	(0,0)	(0,0)	(0,0)
01	COV (%)	0.00	0.00	0.00
02	COV (%)	0.00	0.00	0.00
03	COV (%)	0.00	0.00	0.00
04	COV (%)	0.00	0.00	0.00
<b>OVERALL VARIATION (%)</b>		<b>AVG(COV)</b>		
		0.00	0.00	0.00
<b>OVERALL PRECISION (%)</b>		<b>100-AVG(COV)</b>		
		100.00	100.00	100.00



Figure 175. Shattered slab of rigid pavement.

Table 90. Statistics of surface deterioration

Section ID	Statistic	Surface Deterioration (sq ft)			
		Moderate	Severe	Total	
01	AVG	0.00	0.00	0.00	
02	AVG	0.00	0.00	0.00	
03	AVG	0.00	0.00	0.00	
04	AVG	0.50	0.00	0.50	
01	(Min,Max)	(0,0)	(0,0)	(0,0)	
02	(Min,Max)	(0,0)	(0,0)	(0,0)	
03	(Min,Max)	(0,0)	(0,0)	(0,0)	
04	(Min,Max)	(0,1)	(0,0)	(0,1)	
01	COV (%)	0.00	0.00	0.00	
02	COV (%)	0.00	0.00	0.00	
03	COV (%)	0.00	0.00	0.00	
04	COV (%)	115.47	0.00	115.47	
OVERALL VARIATION (%)		AVG(COV)	28.87	0.00	28.87
OVERALL PRECISION (%)		100-AVG(COV)	71.13	100.00	71.13

**Table 91. Statistics of pumping**

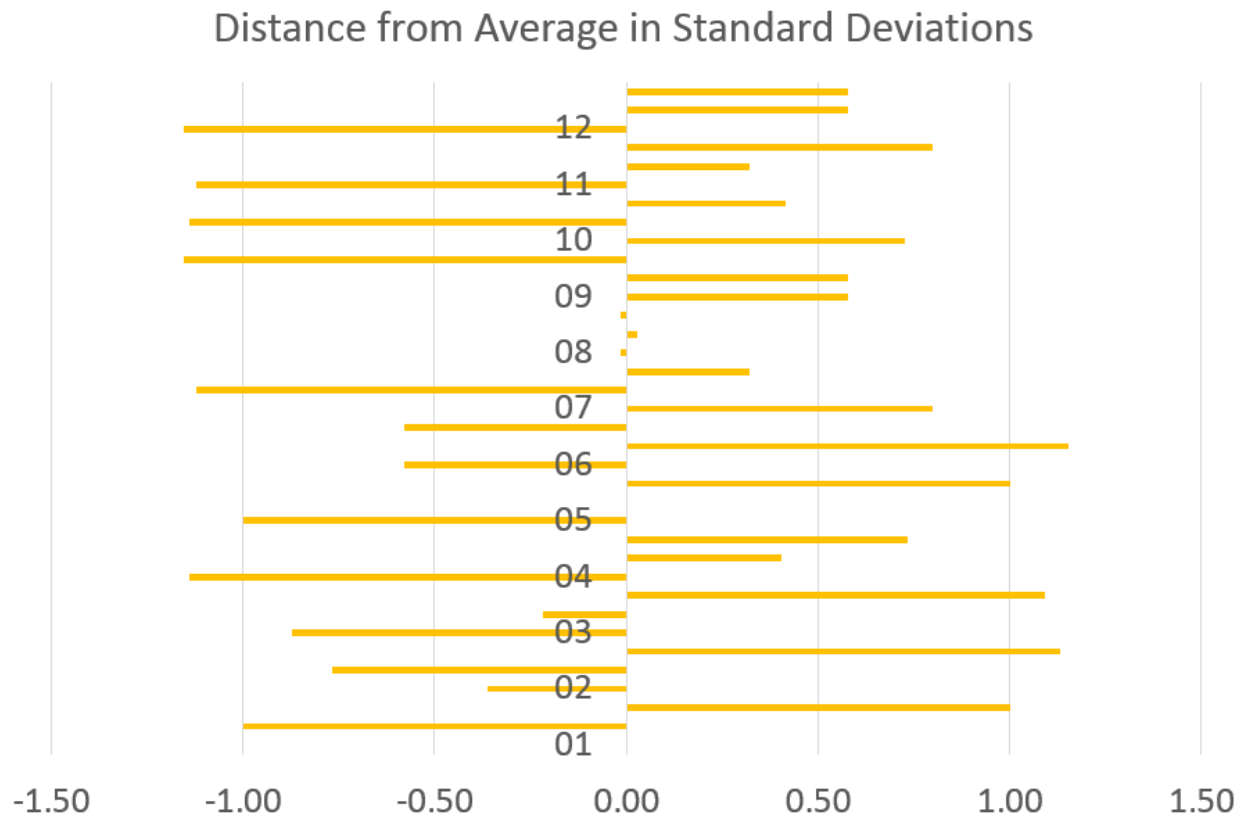
Section ID	Statistic	Pumping (code 1 to 4)			
		Light	Moderate	Severe	Total
01	AVG	0.00	0.00	0.00	0.00
02	AVG	0.00	0.00	0.00	0.00
03	AVG	0.00	0.00	0.00	0.00
04	AVG	0.00	0.00	0.00	0.00
01	(Min,Max)	(0,0)	(0,0)	(0,0)	(0,0)
02	(Min,Max)	(0,0)	(0,0)	(0,0)	(0,0)
03	(Min,Max)	(0,0)	(0,0)	(0,0)	(0,0)
04	(Min,Max)	(0,0)	(0,0)	(0,0)	(0,0)
01	COV (%)	0.00	0.00	0.00	0.00
02	COV (%)	0.00	0.00	0.00	0.00
03	COV (%)	0.00	0.00	0.00	0.00
04	COV (%)	0.00	0.00	0.00	0.00
<b>OVERALL VARIATION (%)</b>		<b>AVG(COV)</b>	0.00	0.00	0.00
<b>OVERALL PRECISION (%)</b>		<b>100-AVG(COV)</b>	100.00	100.00	100.00

## D. MANUAL WINDSHIELD SURVEY RESULTS ON RIGID PAVEMENTS

Table 92. Transverse cracking (count): light, moderate, and severe

Section ID	Statistic	Light	Moderate	Severe	Total	
01	AVG	11.00	0.00	0.00	11.00	
02	AVG	15.67	0.00	0.00	15.67	
03	AVG	6.67	2.00	10.67	19.33	
04	AVG	17.00	2.33	1.00	20.33	
05	AVG	5.00	0.00	0.00	5.00	
06	AVG	6.67	1.33	2.33	10.33	
07	AVG	15.00	8.33	8.00	31.33	
08	AVG	9.67	6.33	7.33	23.33	
09	AVG	13.67	0.33	1.67	15.67	
10	AVG	1.67	3.00	4.00	8.67	
11	AVG	8.67	2.33	0.33	11.33	
12	AVG	19.67	2.67	2.00	24.33	
01	(Min,Max)	(10,12)	(0,0)	(0,0)	(10,12)	
02	(Min,Max)	(10,24)	(0,0)	(0,0)	(10,24)	
03	(Min,Max)	(2,10)	(0,5)	(10,11)	(18,21)	
04	(Min,Max)	(7,23)	(0,4)	(0,3)	(10,27)	
05	(Min,Max)	(4,6)	(0,0)	(0,0)	(4,6)	
06	(Min,Max)	(6,8)	(1,2)	(1,3)	(10,11)	
07	(Min,Max)	(14,16)	(6,10)	(5,10)	(29,33)	
08	(Min,Max)	(7,11)	(5,7)	(6,9)	(23,24)	
09	(Min,Max)	(13,14)	(0,1)	(1,2)	(15,16)	
10	(Min,Max)	(0,3)	(0,6)	(2,8)	(5,11)	
11	(Min,Max)	(4,11)	(1,4)	(0,1)	(9,13)	
12	(Min,Max)	(17,23)	(1,4)	(1,3)	(23,25)	
01	COV (%)	9.09	0.00	0.00	9.09	
02	COV (%)	47.05	0.00	0.00	47.05	
03	COV (%)	62.45	132.29	5.41	7.90	
04	COV (%)	51.28	89.21	173.21	44.63	
05	COV (%)	20.00	0.00	0.00	20.00	
06	COV (%)	17.32	43.30	49.49	5.59	
07	COV (%)	6.67	24.98	33.07	6.64	
08	COV (%)	23.89	18.23	20.83	2.47	
09	COV (%)	4.22	173.21	34.64	3.69	
10	COV (%)	91.65	100.00	86.60	37.09	
11	COV (%)	46.63	65.47	173.21	18.37	
12	COV (%)	15.53	57.28	50.00	4.75	
OVERALL VARIATION (%)		AVG(COV)	32.98	58.66	52.20	17.27
OVERALL PRECISION (%)		100-AVG(COV)	67.02	41.34	47.80	82.73

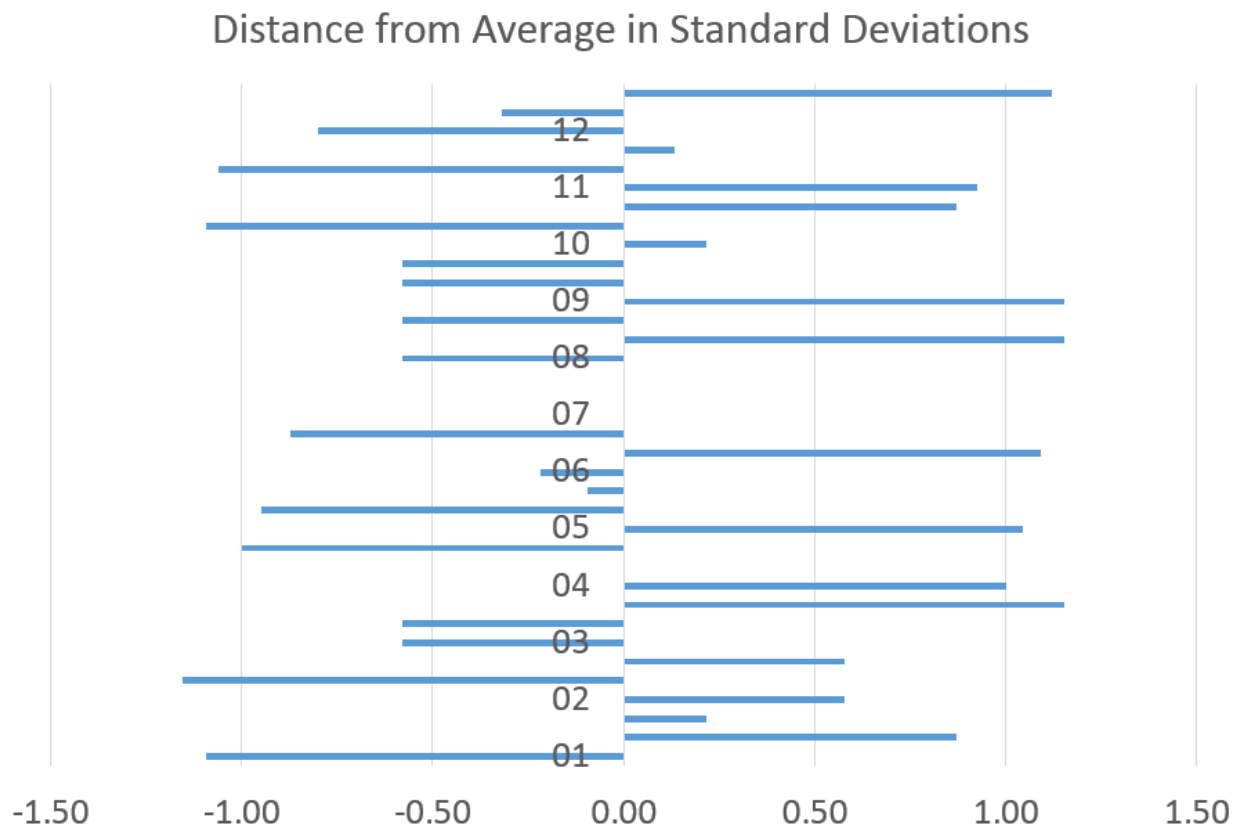




**Figure 176. Distance from average in standard deviation (transverse cracking).**

**Table 93. Longitudinal cracking (count): light, moderate, and severe**

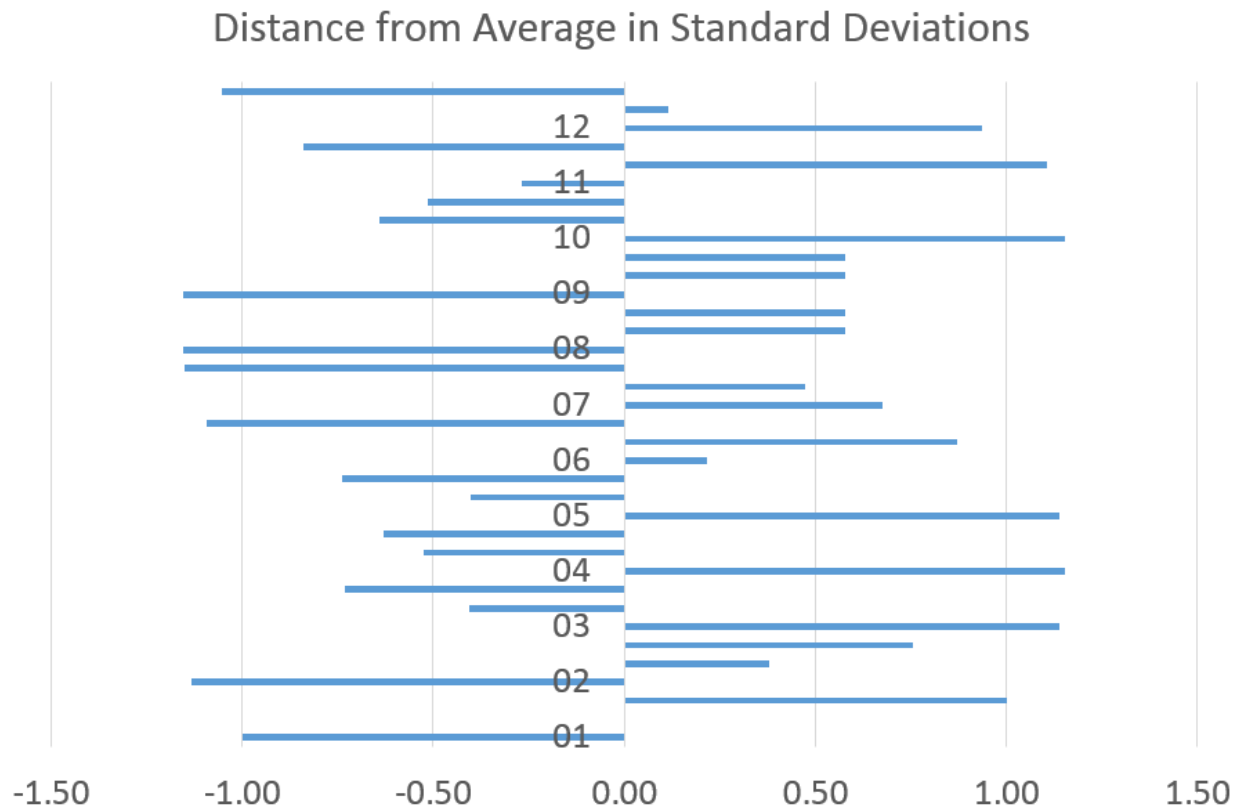
Section ID	Statistic	Light	Moderate	Severe	Total	
01	AVG	11.67	0.00	0.00	11.67	
02	AVG	7.67	0.00	0.00	7.67	
03	AVG	18.00	1.67	0.67	20.33	
04	AVG	6.67	2.33	1.00	10.00	
05	AVG	1.33	30.00	0.00	31.33	
06	AVG	2.33	0.67	1.33	4.33	
07	AVG	0.67	1.33	1.00	3.00	
08	AVG	2.00	0.00	0.33	2.33	
09	AVG	0.67	3.00	0.67	4.33	
10	AVG	0.67	1.00	1.00	2.67	
11	AVG	17.67	1.67	1.00	20.33	
12	AVG	16.33	0.33	2.00	18.67	
01	(Min,Max)	(10,13)	(0,0)	(0,0)	(10,13)	
02	(Min,Max)	(7,8)	(0,0)	(0,0)	(7,8)	
03	(Min,Max)	(15,20)	(1,3)	(0,2)	(20,21)	
04	(Min,Max)	(4,10)	(0,4)	(0,3)	(9,11)	
05	(Min,Max)	(0,4)	(24,35)	(0,0)	(28,35)	
06	(Min,Max)	(1,4)	(0,1)	(1,2)	(3,6)	
07	(Min,Max)	(0,2)	(0,2)	(1,1)	(3,3)	
08	(Min,Max)	(2,2)	(0,0)	(0,1)	(2,3)	
09	(Min,Max)	(0,2)	(2,4)	(0,1)	(4,5)	
10	(Min,Max)	(0,1)	(0,2)	(0,2)	(1,4)	
11	(Min,Max)	(15,19)	(0,4)	(0,2)	(15,25)	
12	(Min,Max)	(14,18)	(0,1)	(1,3)	(17,21)	
01	COV (%)	13.09	0.00	0.00	13.09	
02	COV (%)	7.53	0.00	0.00	7.53	
03	COV (%)	14.70	69.28	173.21	2.84	
04	COV (%)	45.83	89.21	173.21	10.00	
05	COV (%)	173.21	18.56	0.00	11.21	
06	COV (%)	65.47	86.60	43.30	35.25	
07	COV (%)	173.21	86.60	0.00	0.00	
08	COV (%)	0.00	0.00	173.21	24.74	
09	COV (%)	173.21	33.33	86.60	13.32	
10	COV (%)	86.60	100.00	100.00	57.28	
11	COV (%)	13.07	124.90	100.00	24.75	
12	COV (%)	12.74	173.21	50.00	11.15	
OVERALL VARIATION (%)		AVG(COV)	64.89	65.14	74.96	17.60
OVERALL PRECISION (%)		100-AVG(COV)	35.11	34.86	25.04	82.40



**Figure 177. Distance from average in standard deviation (longitudinal cracking).**

**Table 94. Spalling (linear feet): moderate and severe**

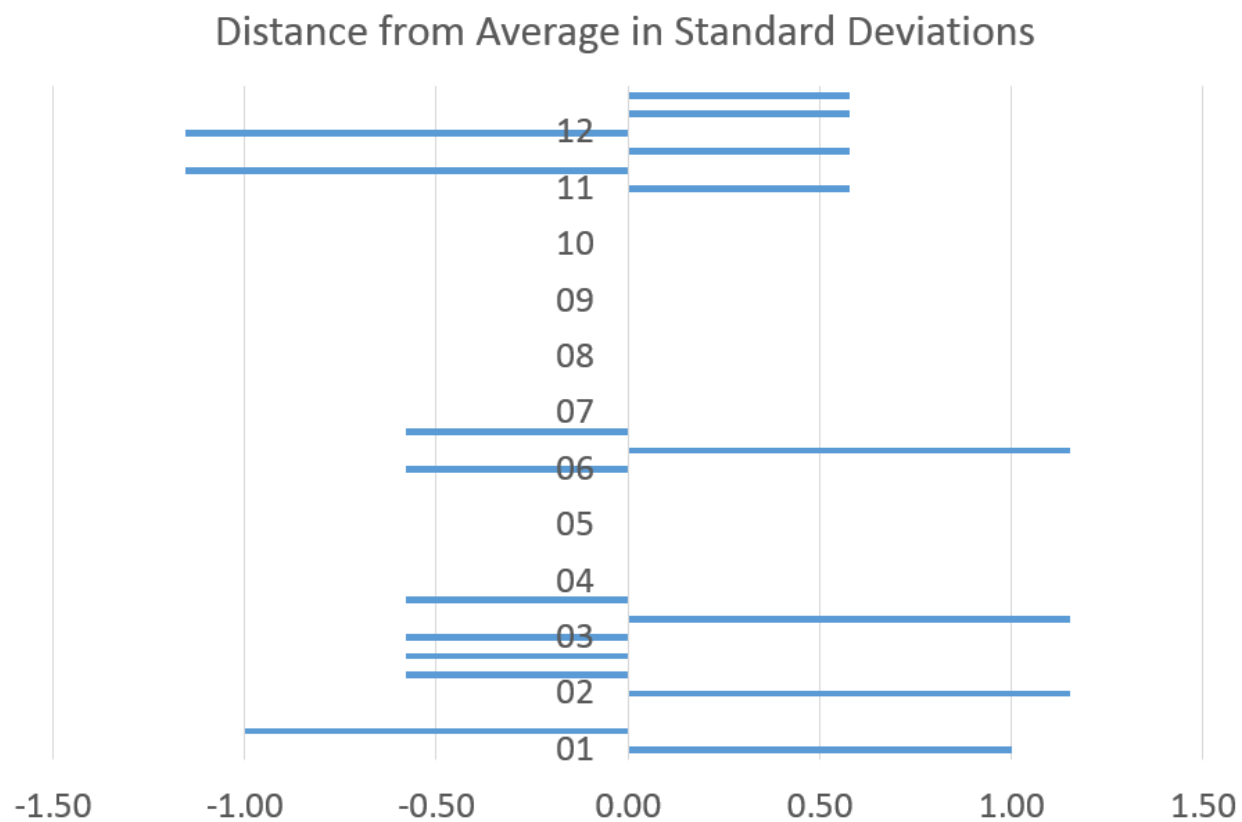
Section ID	Statistic	Moderate	Severe	Total
01	AVG	5.67	0.33	6.00
02	AVG	8.00	0.00	8.00
03	AVG	14.33	9.67	24.00
04	AVG	14.33	9.67	24.00
05	AVG	15.67	5.33	21.00
06	AVG	4.00	13.67	17.67
07	AVG	19.33	8.33	27.67
08	AVG	11.33	7.67	19.00
09	AVG	7.00	2.33	9.33
10	AVG	16.00	10.00	26.00
11	AVG	14.00	4.33	18.33
12	AVG	22.00	14.00	36.00
01	(Min,Max)	(2,10)	(0,1)	(2,10)
02	(Min,Max)	(5,10)	(0,0)	(5,10)
03	(Min,Max)	(12,17)	(1,21)	(15,38)
04	(Min,Max)	(12,18)	(6,17)	(18,35)
05	(Min,Max)	(10,23)	(0,15)	(10,38)
06	(Min,Max)	(3,5)	(13,14)	(16,19)
07	(Min,Max)	(17,21)	(5,11)	(22,31)
08	(Min,Max)	(9,14)	(6,9)	(17,20)
09	(Min,Max)	(2,10)	(1,4)	(6,11)
10	(Min,Max)	(15,18)	(4,20)	(21,35)
11	(Min,Max)	(9,19)	(2,9)	(11,28)
12	(Min,Max)	(16,26)	(11,20)	(27,44)
01	COV (%)	71.32	173.21	66.67
02	COV (%)	33.07	0.00	33.07
03	COV (%)	17.56	106.17	51.20
04	COV (%)	22.43	65.70	39.75
05	COV (%)	42.50	157.25	71.11
06	COV (%)	25.00	4.22	8.65
07	COV (%)	10.77	36.66	17.83
08	COV (%)	22.21	19.92	9.12
09	COV (%)	62.27	65.47	30.93
10	COV (%)	10.83	87.18	30.04
11	COV (%)	35.71	93.26	47.66
12	COV (%)	24.05	37.12	23.73
OVERALL VARIATION (%)		AVG(COV)	70.51	35.81
OVERALL PRECISION (%)		100-AVG(COV)	29.49	64.19



**Figure 178. Distance from average in standard deviation (spalling).**

**Table 95. Corner cracking (count): light, moderate, and severe**

Section ID	Statistic	Light	Moderate	Severe	Total
01	AVG	1.00	0.00	0.00	1.00
02	AVG	0.33	0.00	0.00	0.33
03	AVG	0.33	0.00	0.00	0.33
04	AVG	0.00	0.00	0.00	0.00
05	AVG	1.00	0.00	0.00	1.00
06	AVG	0.33	0.00	2.33	2.67
07	AVG	0.00	0.67	2.33	3.00
08	AVG	0.00	0.00	0.00	0.00
09	AVG	0.00	0.00	0.00	0.00
10	AVG	0.00	0.00	1.00	1.00
11	AVG	1.67	2.00	0.67	4.33
12	AVG	4.67	3.00	3.00	10.67
01	(Min,Max)	(0,2)	(0,0)	(0,0)	(0,2)
02	(Min,Max)	(0,1)	(0,0)	(0,0)	(0,1)
03	(Min,Max)	(0,1)	(0,0)	(0,0)	(0,1)
04	(Min,Max)	(0,0)	(0,0)	(0,0)	(0,0)
05	(Min,Max)	(1,1)	(0,0)	(0,0)	(1,1)
06	(Min,Max)	(0,1)	(0,0)	(2,3)	(2,4)
07	(Min,Max)	(0,0)	(0,2)	(1,3)	(3,3)
08	(Min,Max)	(0,0)	(0,0)	(0,0)	(0,0)
09	(Min,Max)	(0,0)	(0,0)	(0,0)	(0,0)
10	(Min,Max)	(0,0)	(0,0)	(1,1)	(1,1)
11	(Min,Max)	(1,2)	(0,4)	(0,1)	(3,5)
12	(Min,Max)	(3,6)	(2,4)	(2,4)	(10,11)
01	COV (%)	100.00	0.00	0.00	100.00
02	COV (%)	173.21	0.00	0.00	173.21
03	COV (%)	173.21	0.00	0.00	173.21
04	COV (%)	0.00	0.00	0.00	0.00
05	COV (%)	0.00	0.00	0.00	0.00
06	COV (%)	173.21	0.00	24.74	43.30
07	COV (%)	0.00	173.21	49.49	0.00
08	COV (%)	0.00	0.00	0.00	0.00
09	COV (%)	0.00	0.00	0.00	0.00
10	COV (%)	0.00	0.00	0.00	0.00
11	COV (%)	34.64	100.00	86.60	26.65
12	COV (%)	32.73	33.33	33.33	5.41
<b>OVERALL VARIATION (%)</b>		<b>AVG(COV)</b>			
			57.25	25.54	16.18
<b>OVERALL PRECISION (%)</b>		<b>100-AVG(COV)</b>			
			42.75	74.46	83.82
					56.52

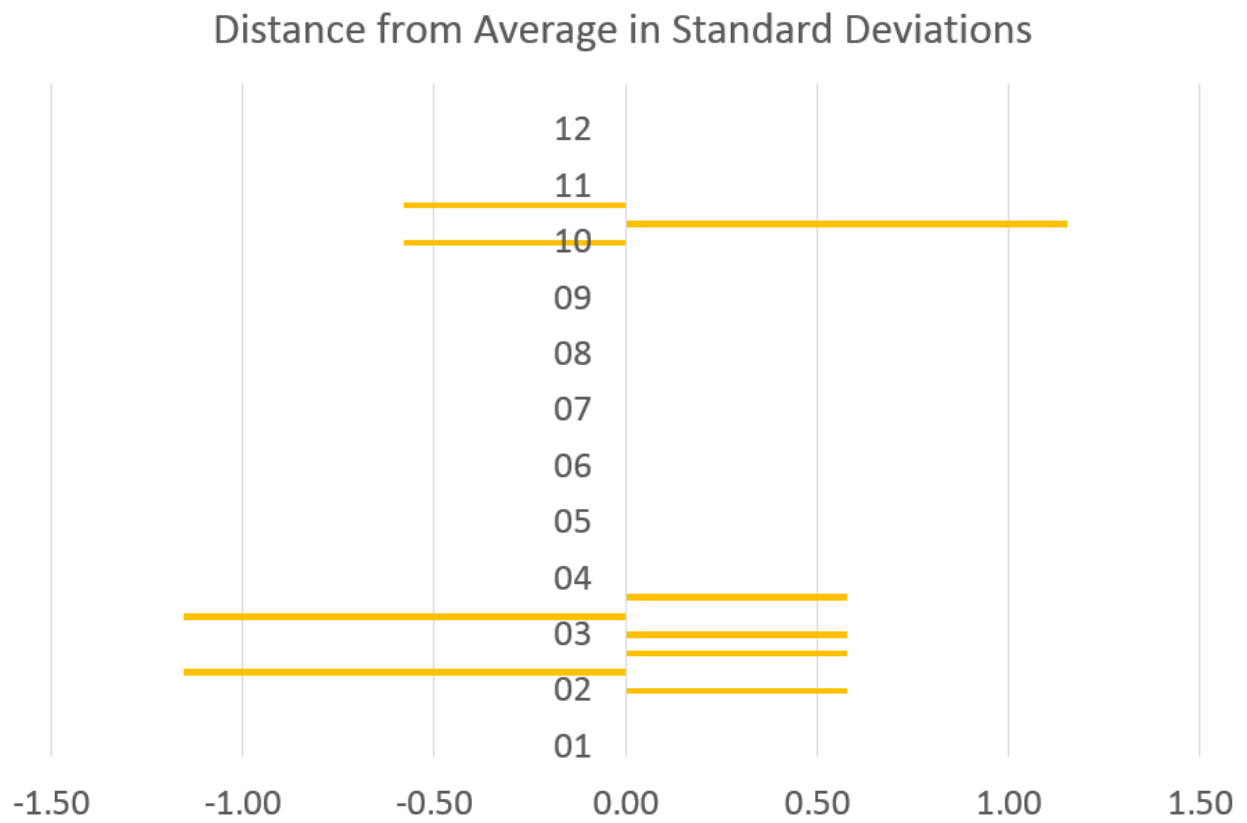


**Figure 179. Distance from average in standard deviation (corner cracking).**

**Table 96. Patching (sq. yards): fair and poor**

Section ID	Statistic	Fair	Poor	Total	
01	AVG	0.00	0.00	0.00	
02	AVG	1.33	0.00	1.33	
03	AVG	2.00	2.67	4.67	
04	AVG	0.00	0.00	0.00	
05	AVG	0.00	0.00	0.00	
06	AVG	0.00	1.00	1.00	
07	AVG	0.00	0.00	0.00	
08	AVG	0.00	0.00	0.00	
09	AVG	0.00	0.00	0.00	
10	AVG	0.00	1.00	1.00	
11	AVG	0.00	0.00	0.00	
12	AVG	0.00	0.00	0.00	
01	(Min,Max)	(0,0)	(0,0)	(0,0)	
02	(Min,Max)	(0,2)	(0,0)	(0,2)	
03	(Min,Max)	(0,3)	(2,3)	(2,6)	
04	(Min,Max)	(0,0)	(0,0)	(0,0)	
05	(Min,Max)	(0,0)	(0,0)	(0,0)	
06	(Min,Max)	(0,0)	(1,1)	(1,1)	
07	(Min,Max)	(0,0)	(0,0)	(0,0)	
08	(Min,Max)	(0,0)	(0,0)	(0,0)	
09	(Min,Max)	(0,0)	(0,0)	(0,0)	
10	(Min,Max)	(0,0)	(0,3)	(0,3)	
11	(Min,Max)	(0,0)	(0,0)	(0,0)	
12	(Min,Max)	(0,0)	(0,0)	(0,0)	
01	COV (%)	0.00	0.00	0.00	
02	COV (%)	86.60	0.00	86.60	
03	COV (%)	86.60	21.65	49.49	
04	COV (%)	0.00	0.00	0.00	
05	COV (%)	0.00	0.00	0.00	
06	COV (%)	0.00	0.00	0.00	
07	COV (%)	0.00	0.00	0.00	
08	COV (%)	0.00	0.00	0.00	
09	COV (%)	0.00	0.00	0.00	
10	COV (%)	0.00	173.21	173.21	
11	COV (%)	0.00	0.00	0.00	
12	COV (%)	0.00	0.00	0.00	
OVERALL VARIATION (%)		AVG(COV)	14.43	16.24	25.77
OVERALL PRECISION (%)		100-AVG(COV)	85.57	83.76	74.23

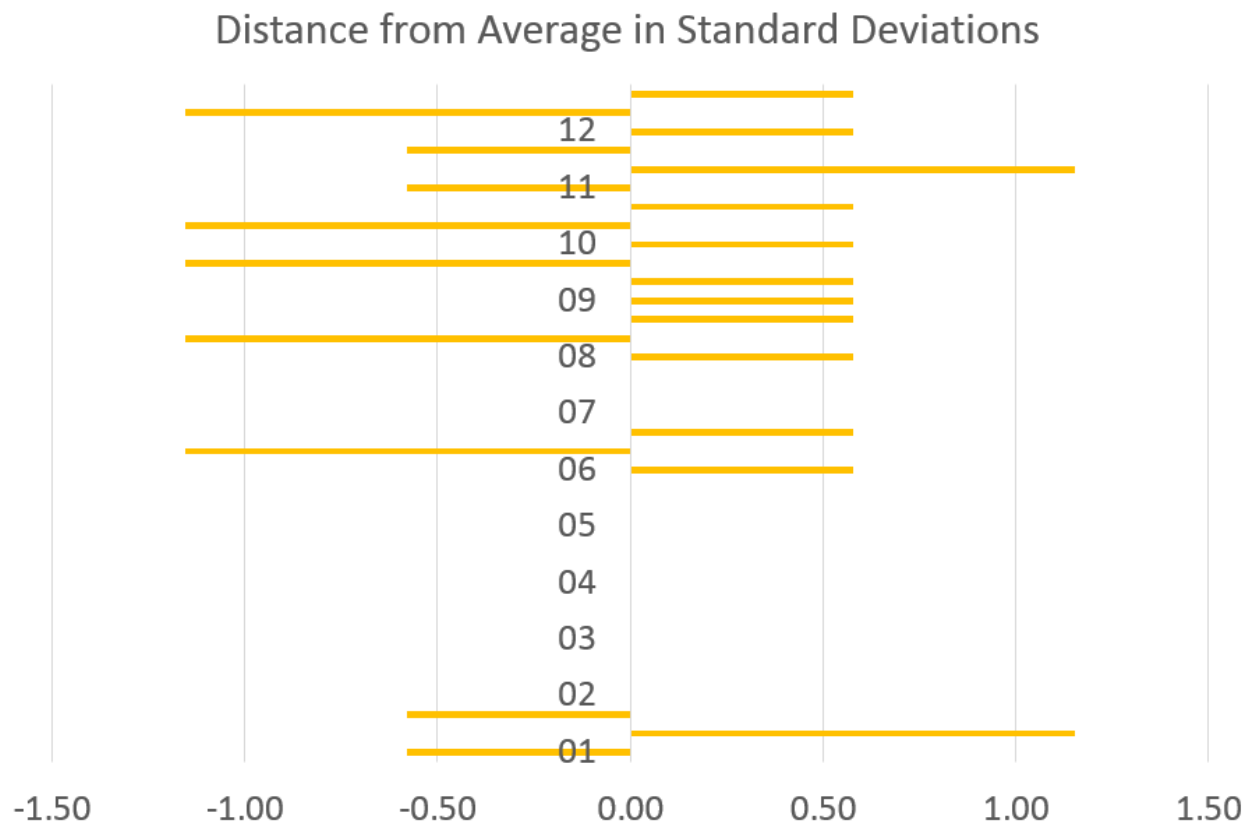




**Figure 180. Distance from average in standard deviation (patching).**

**Table 97. Shattered slab (count): moderate and severe**

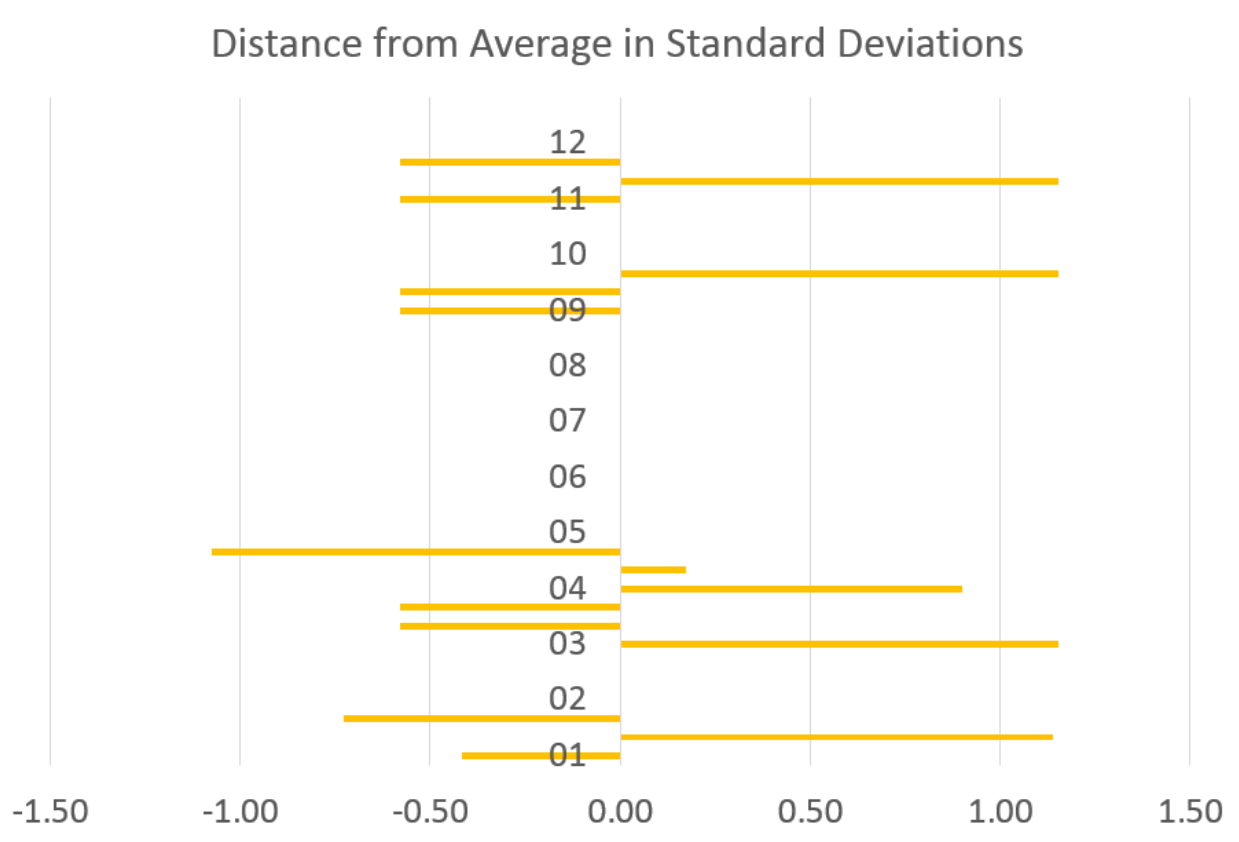
Section ID	Statistic	Moderate	Severe	Total
01	AVG	1.33	0.00	1.33
02	AVG	0.00	0.00	0.00
03	AVG	0.33	0.67	1.00
04	AVG	1.00	0.00	1.00
05	AVG	0.00	0.00	0.00
06	AVG	0.67	4.00	4.67
07	AVG	0.00	1.00	1.00
08	AVG	0.67	0.00	0.67
09	AVG	0.67	0.00	0.67
10	AVG	0.00	0.67	0.67
11	AVG	2.33	1.00	3.33
12	AVG	1.33	2.33	3.67
01	(Min,Max)	(1,2)	(0,0)	(1,2)
02	(Min,Max)	(0,0)	(0,0)	(0,0)
03	(Min,Max)	(0,1)	(0,1)	(1,1)
04	(Min,Max)	(1,1)	(0,0)	(1,1)
05	(Min,Max)	(0,0)	(0,0)	(0,0)
06	(Min,Max)	(0,1)	(4,4)	(4,5)
07	(Min,Max)	(0,0)	(1,1)	(1,1)
08	(Min,Max)	(0,1)	(0,0)	(0,1)
09	(Min,Max)	(0,1)	(0,0)	(0,1)
10	(Min,Max)	(0,0)	(0,1)	(0,1)
11	(Min,Max)	(2,3)	(1,1)	(3,4)
12	(Min,Max)	(1,2)	(1,3)	(3,4)
01	COV (%)	43.30	0.00	43.30
02	COV (%)	0.00	0.00	0.00
03	COV (%)	173.21	86.60	0.00
04	COV (%)	0.00	0.00	0.00
05	COV (%)	0.00	0.00	0.00
06	COV (%)	86.60	0.00	12.37
07	COV (%)	0.00	0.00	0.00
08	COV (%)	86.60	0.00	86.60
09	COV (%)	86.60	0.00	86.60
10	COV (%)	0.00	86.60	86.60
11	COV (%)	24.74	0.00	17.32
12	COV (%)	43.30	49.49	15.75
<b>OVERALL VARIATION (%)</b>		<b>AVG(COV)</b>	45.36	18.56
<b>OVERALL PRECISION (%)</b>		<b>100-AVG(COV)</b>	54.64	81.44
				70.95



**Figure 181. Distance from average in standard deviation (shattered slab).**

**Table 98. Surface deterioration (sq. feet): moderate and severe**

Section ID	Statistic	Moderate	Severe	Total
01	AVG	5.33	1.33	6.67
02	AVG	0.00	0.00	0.00
03	AVG	13.67	0.00	13.67
04	AVG	29.67	0.00	29.67
05	AVG	0.00	0.00	0.00
06	AVG	0.00	0.00	0.00
07	AVG	0.00	0.00	0.00
08	AVG	0.00	0.00	0.00
09	AVG	0.33	0.00	0.33
10	AVG	0.00	0.00	0.00
11	AVG	0.33	0.00	0.33
12	AVG	0.00	0.00	0.00
01	(Min,Max)	(0,14)	(0,2)	(2,14)
02	(Min,Max)	(0,0)	(0,0)	(0,0)
03	(Min,Max)	(10,21)	(0,0)	(10,21)
04	(Min,Max)	(3,52)	(0,0)	(3,52)
05	(Min,Max)	(0,0)	(0,0)	(0,0)
06	(Min,Max)	(0,0)	(0,0)	(0,0)
07	(Min,Max)	(0,0)	(0,0)	(0,0)
08	(Min,Max)	(0,0)	(0,0)	(0,0)
09	(Min,Max)	(0,1)	(0,0)	(0,1)
10	(Min,Max)	(0,0)	(0,0)	(0,0)
11	(Min,Max)	(0,1)	(0,0)	(0,1)
12	(Min,Max)	(0,0)	(0,0)	(0,0)
01	COV (%)	141.97	86.60	96.44
02	COV (%)	0.00	0.00	0.00
03	COV (%)	46.47	0.00	46.47
04	COV (%)	83.55	0.00	83.55
05	COV (%)	0.00	0.00	0.00
06	COV (%)	0.00	0.00	0.00
07	COV (%)	0.00	0.00	0.00
08	COV (%)	0.00	0.00	0.00
09	COV (%)	173.21	0.00	173.21
10	COV (%)	0.00	0.00	0.00
11	COV (%)	173.21	0.00	173.21
12	COV (%)	0.00	0.00	0.00
<b>OVERALL VARIATION (%)</b>		<b>AVG(COV)</b>	7.22	47.74
<b>OVERALL PRECISION (%)</b>		<b>100-AVG(COV)</b>	92.78	52.26

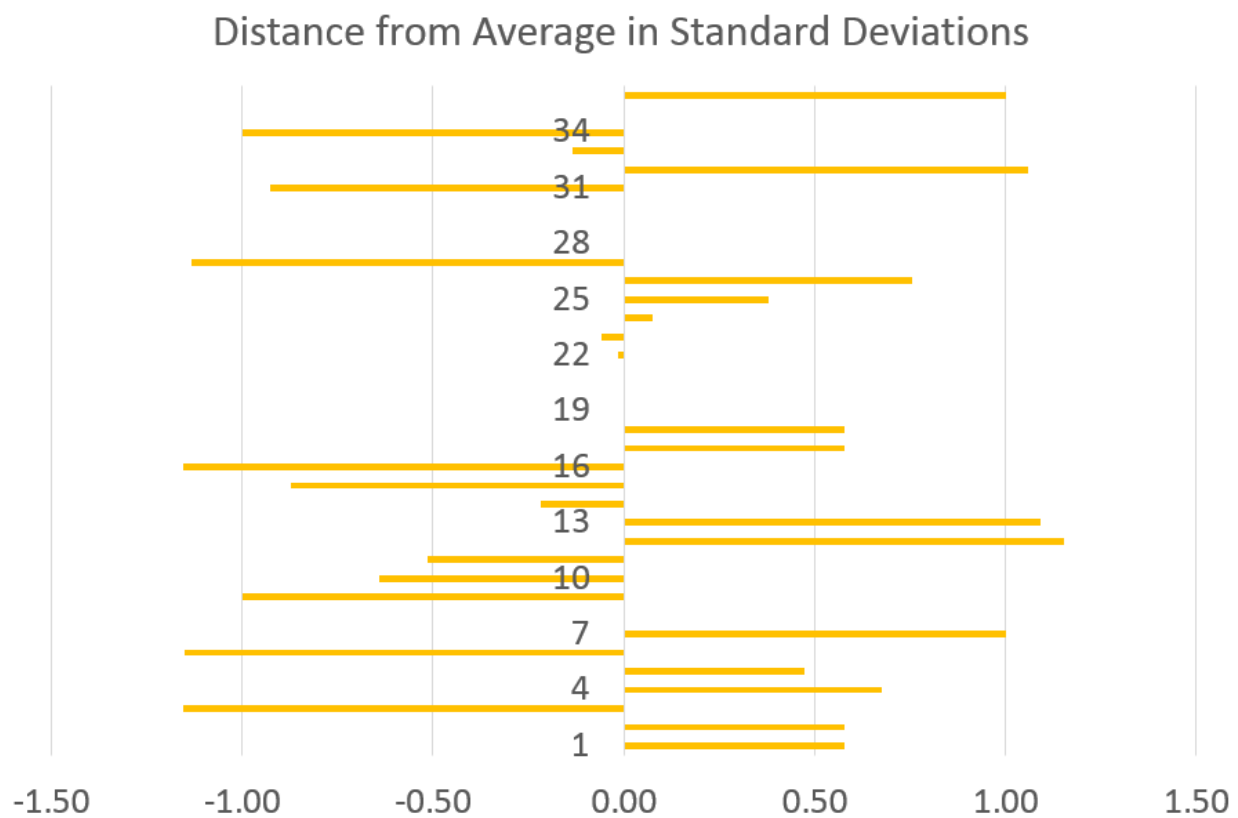


**Figure 182. Distance from average in standard deviation (surface deterioration).**

## E. SEMI-AUTOMATED SURVEY RESULTS ON RIGID PAVEMENTS

Table 99. Transverse cracking (count): light, moderate, and severe

Section ID	Statistic	Light	Moderate	Severe	Total	
01	AVG	9.67	0.00	0.00	9.67	
02	AVG	13.67	0.00	0.00	13.67	
03	AVG	7.67	4.33	5.00	17.00	
04	AVG	9.33	2.67	2.00	14.00	
05	AVG	3.33	1.33	0.67	5.33	
06	AVG	7.33	1.00	5.33	13.67	
07	AVG	11.00	7.00	8.00	26.00	
08	AVG	10.67	6.33	5.33	22.33	
09	AVG	8.00	0.33	1.67	10.00	
10	AVG	4.67	3.67	0.67	9.00	
11	AVG	11.67	0.67	0.00	12.33	
12	AVG	16.33	5.67	1.00	23.00	
01	(Min,Max)	(7,11)	(0,0)	(0,0)	(7,11)	
02	(Min,Max)	(8,17)	(0,0)	(0,0)	(8,17)	
03	(Min,Max)	(7,8)	(2,9)	(0,9)	(16,18)	
04	(Min,Max)	(2,21)	(2,4)	(0,5)	(9,23)	
05	(Min,Max)	(3,4)	(0,2)	(0,2)	(4,7)	
06	(Min,Max)	(4,10)	(0,2)	(4,7)	(13,14)	
07	(Min,Max)	(8,14)	(5,9)	(3,13)	(26,26)	
08	(Min,Max)	(7,17)	(2,9)	(4,7)	(21,24)	
09	(Min,Max)	(7,10)	(0,1)	(0,4)	(7,12)	
10	(Min,Max)	(0,9)	(0,8)	(0,1)	(9,9)	
11	(Min,Max)	(9,14)	(0,1)	(0,0)	(10,15)	
12	(Min,Max)	(10,22)	(1,11)	(0,2)	(21,25)	
01	COV (%)	23.89	0.00	0.00	23.89	
02	COV (%)	36.09	0.00	0.00	36.09	
03	COV (%)	7.53	93.26	91.65	5.88	
04	COV (%)	109.44	43.30	132.29	55.79	
05	COV (%)	17.32	86.60	173.21	28.64	
06	COV (%)	41.66	100.00	28.64	4.22	
07	COV (%)	38.57	40.41	88.39	0.00	
08	COV (%)	51.63	59.78	28.64	6.84	
09	COV (%)	21.65	173.21	124.90	26.46	
10	COV (%)	96.63	110.22	86.60	0.00	
11	COV (%)	21.57	86.60	0.00	20.40	
12	COV (%)	36.90	88.82	100.00	8.70	
OVERALL VARIATION (%)		AVG(COV)	41.91	73.52	71.19	18.08
OVERALL PRECISION (%)		100-AVG(COV)	58.09	26.48	28.81	81.92

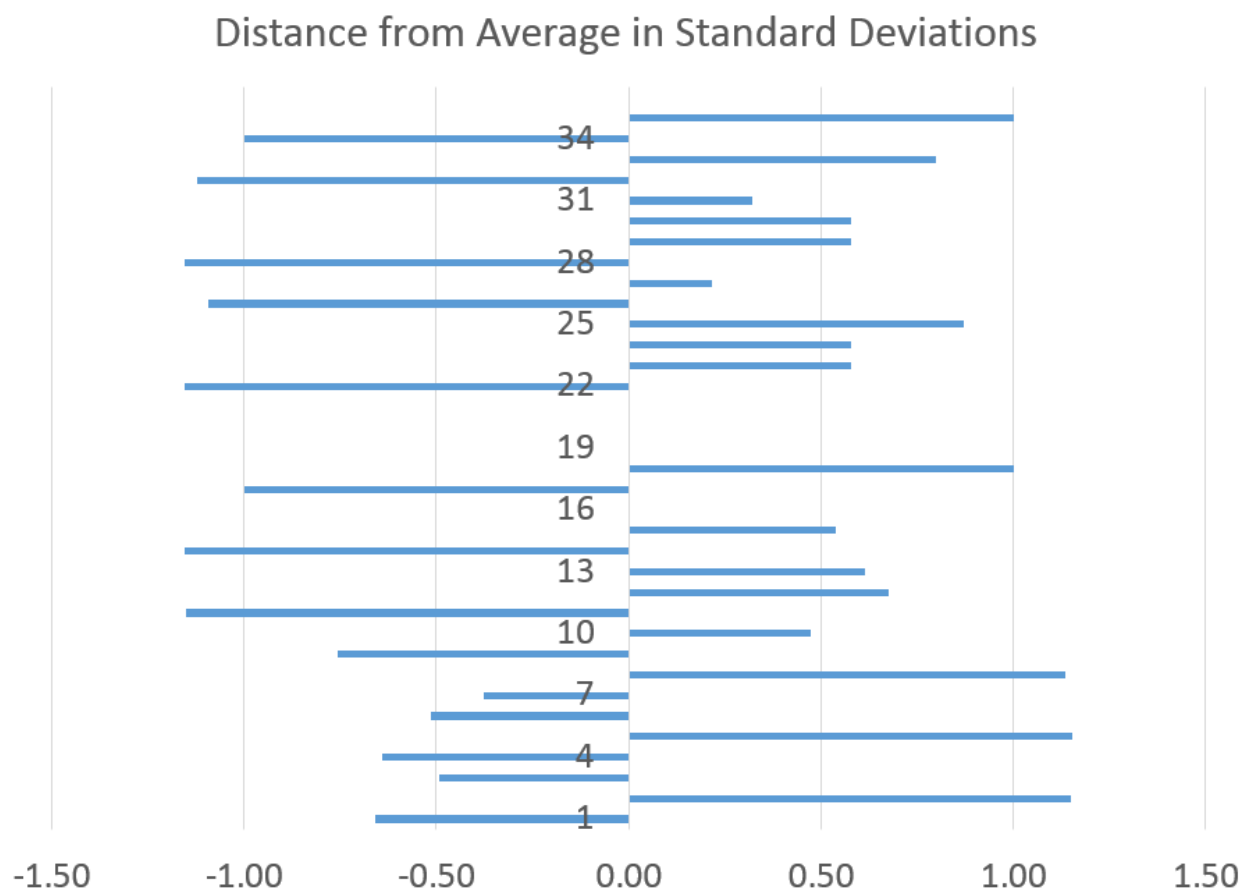


**Figure 183. Distance from average in standard deviation (transverse cracking).**

**Table 100. Longitudinal cracking (count): light, moderate, and severe**

Section ID	Statistic	Light	Moderate	Severe	Total	
01	AVG	17.00	0.00	0.00	17.00	
02	AVG	11.00	0.00	0.00	11.00	
03	AVG	19.33	0.33	0.33	20.00	
04	AVG	9.00	1.00	0.67	10.67	
05	AVG	6.33	14.00	13.33	33.67	
06	AVG	1.67	1.67	0.67	4.00	
07	AVG	1.00	0.50	1.50	3.00	
08	AVG	2.00	0.33	0.33	2.67	
09	AVG	0.67	0.67	0.33	1.67	
10	AVG	3.33	0.67	0.67	4.67	
11	AVG	15.00	0.33	0.00	15.33	
12	AVG	14.00	1.00	1.00	16.00	
01	(Min,Max)	(13,24)	(0,0)	(0,0)	(13,24)	
02	(Min,Max)	(6,20)	(0,0)	(0,0)	(6,20)	
03	(Min,Max)	(18,22)	(0,1)	(0,1)	(18,23)	
04	(Min,Max)	(5,14)	(0,3)	(0,2)	(5,14)	
05	(Min,Max)	(1,16)	(0,40)	(0,40)	(18,42)	
06	(Min,Max)	(1,2)	(1,2)	(0,1)	(3,5)	
07	(Min,Max)	(0,2)	(0,1)	(1,2)	(3,3)	
08	(Min,Max)	(2,2)	(0,1)	(0,1)	(2,3)	
09	(Min,Max)	(0,1)	(0,1)	(0,1)	(0,3)	
10	(Min,Max)	(0,5)	(0,2)	(0,2)	(4,5)	
11	(Min,Max)	(13,16)	(0,1)	(0,0)	(13,17)	
12	(Min,Max)	(12,17)	(0,2)	(0,2)	(12,20)	
01	COV (%)	35.78	0.00	0.00	35.78	
02	COV (%)	71.00	0.00	0.00	71.00	
03	COV (%)	11.95	173.21	173.21	13.23	
04	COV (%)	50.92	173.21	173.21	46.25	
05	COV (%)	132.42	160.99	173.21	40.33	
06	COV (%)	34.64	34.64	86.60	25.00	
07	COV (%)	141.42	141.42	47.14	0.00	
08	COV (%)	0.00	173.21	173.21	21.65	
09	COV (%)	86.60	86.60	173.21	91.65	
10	COV (%)	86.60	173.21	173.21	12.37	
11	COV (%)	11.55	173.21	0.00	13.58	
12	COV (%)	18.90	100.00	100.00	25.00	
OVERALL VARIATION (%)		AVG(COV)	56.81	115.81	106.08	32.99
OVERALL PRECISION (%)		100-AVG(COV)	43.19	-15.81	-6.08	67.01

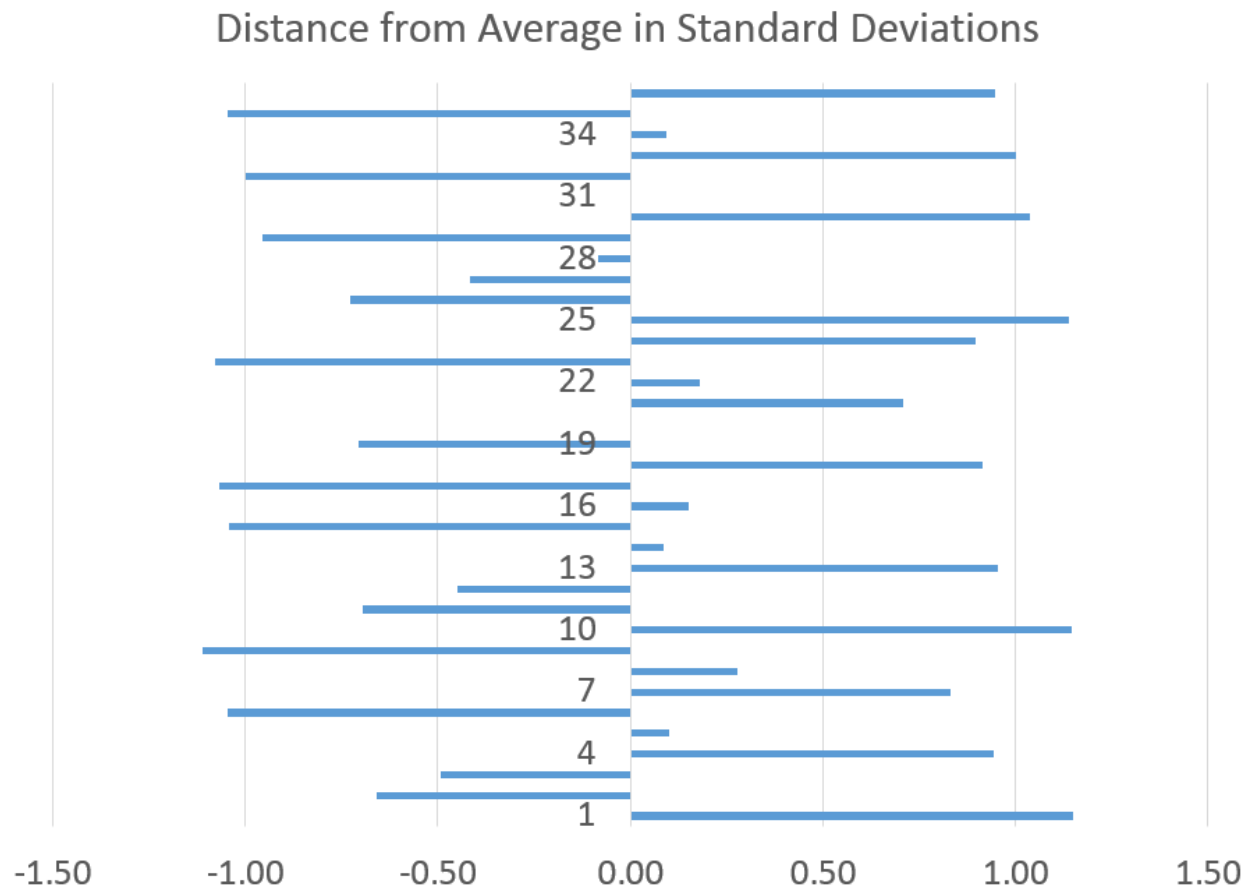




**Figure 184. Distance from average in standard deviation (longitudinal cracking).**

**Table 101. Spalling (linear feet): moderate and severe**

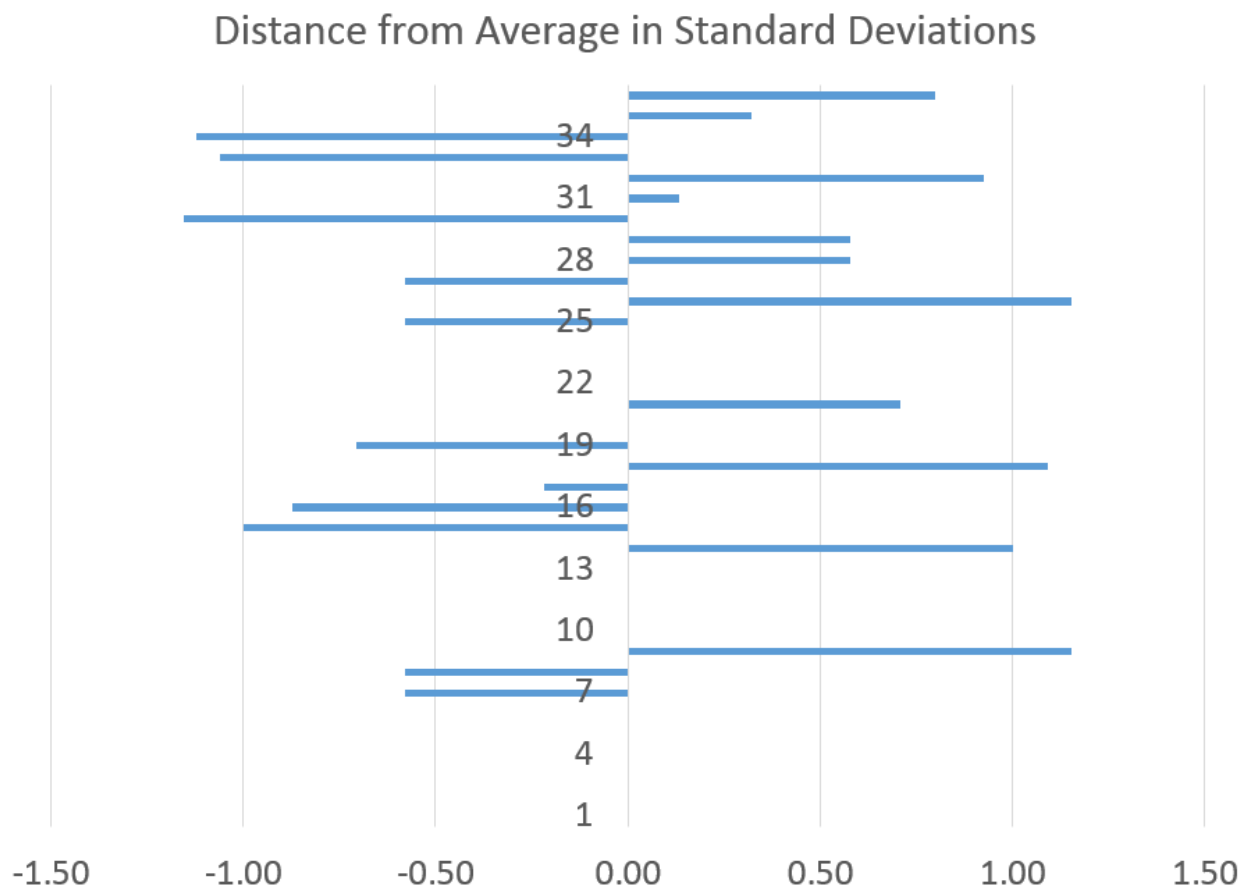
Section ID	Statistic	Moderate	Severe	Total
01	AVG	15.00	0.00	15.00
02	AVG	20.00	0.67	20.67
03	AVG	16.67	3.33	20.00
04	AVG	28.67	14.00	42.67
05	AVG	37.67	3.33	41.00
06	AVG	14.33	6.67	21.00
07	AVG	37.00	11.50	48.50
08	AVG	15.00	7.00	22.00
09	AVG	9.00	1.67	10.67
10	AVG	32.00	2.67	34.67
11	AVG	18.33	0.67	19.00
12	AVG	27.33	3.00	30.33
01	(Min,Max)	(7,29)	(0,0)	(7,29)
02	(Min,Max)	(7,31)	(0,2)	(7,33)
03	(Min,Max)	(11,21)	(0,5)	(16,23)
04	(Min,Max)	(27,30)	(7,25)	(37,52)
05	(Min,Max)	(17,53)	(0,10)	(17,63)
06	(Min,Max)	(11,16)	(3,11)	(14,27)
07	(Min,Max)	(34,40)	(8,15)	(42,55)
08	(Min,Max)	(8,20)	(2,12)	(10,32)
09	(Min,Max)	(6,15)	(0,3)	(6,18)
10	(Min,Max)	(27,36)	(0,7)	(27,43)
11	(Min,Max)	(17,20)	(0,1)	(17,21)
12	(Min,Max)	(20,31)	(0,6)	(23,37)
01	COV (%)	81.10	0.00	81.10
02	COV (%)	60.62	173.21	63.15
03	COV (%)	30.79	86.60	18.03
04	COV (%)	5.33	68.88	19.09
05	COV (%)	49.34	173.21	56.26
06	COV (%)	20.14	60.62	31.23
07	COV (%)	11.47	43.04	18.95
08	COV (%)	41.63	71.43	50.62
09	COV (%)	57.74	91.65	60.27
10	COV (%)	14.32	141.97	23.14
11	COV (%)	8.33	86.60	10.53
12	COV (%)	23.23	100.00	23.16
OVERALL VARIATION (%)		AVG(COV)	33.67	91.43
OVERALL PRECISION (%)		100-AVG(COV)	66.33	8.57



**Figure 185. Distance from average in standard deviation (spalling).**

**Table 102. Corner cracking (count): light, moderate, and severe**

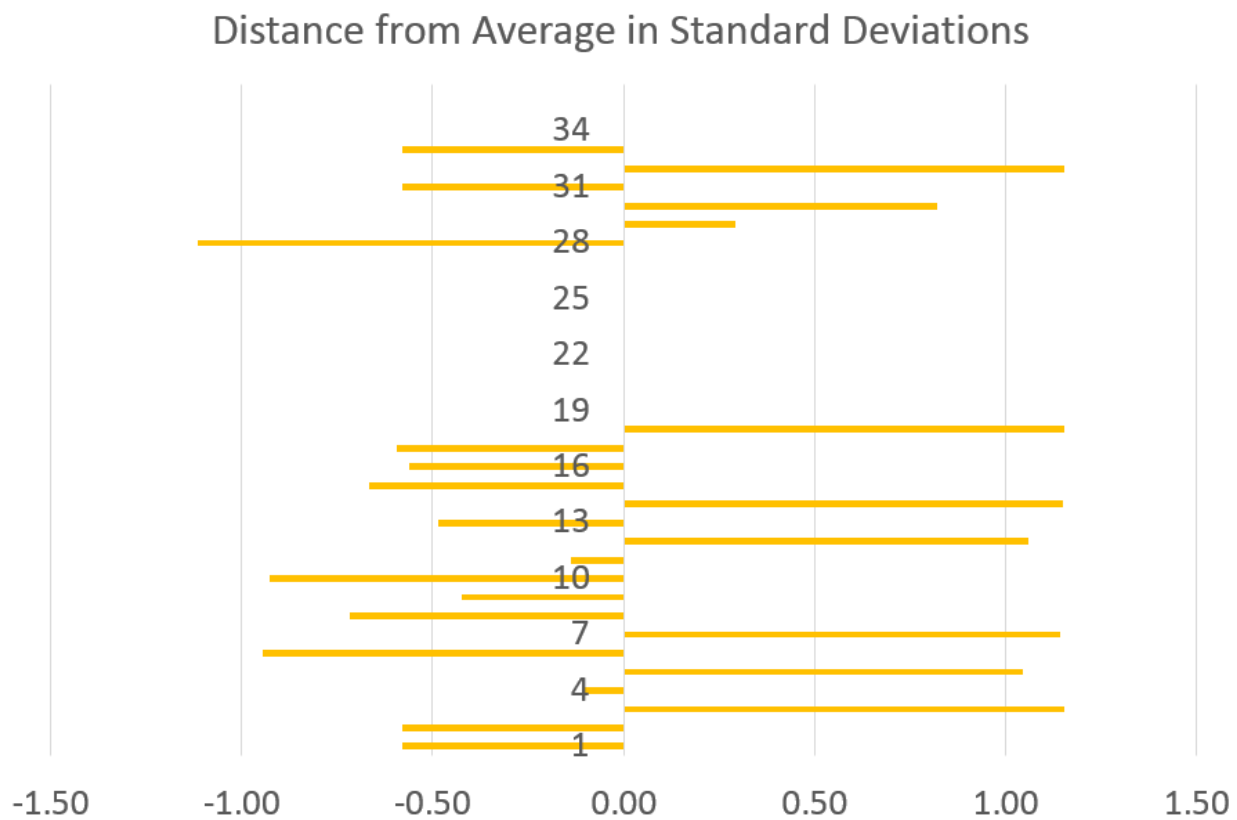
Section ID	Statistic	Light	Moderate	Severe	Total	
01	AVG	1.00	0.00	0.00	1.00	
02	AVG	0.00	0.00	0.00	0.00	
03	AVG	0.33	0.00	0.00	0.33	
04	AVG	0.00	0.00	0.00	0.00	
05	AVG	0.67	0.00	0.33	1.00	
06	AVG	1.00	0.33	1.00	2.33	
07	AVG	0.50	0.50	0.50	1.50	
08	AVG	0.00	0.00	0.00	0.00	
09	AVG	0.33	0.00	0.00	0.33	
10	AVG	0.00	0.33	0.33	0.67	
11	AVG	3.33	1.00	0.33	4.67	
12	AVG	3.00	1.67	0.67	5.33	
01	(Min,Max)	(1,1)	(0,0)	(0,0)	(1,1)	
02	(Min,Max)	(0,0)	(0,0)	(0,0)	(0,0)	
03	(Min,Max)	(0,1)	(0,0)	(0,0)	(0,1)	
04	(Min,Max)	(0,0)	(0,0)	(0,0)	(0,0)	
05	(Min,Max)	(0,2)	(0,0)	(0,1)	(0,2)	
06	(Min,Max)	(0,2)	(0,1)	(0,3)	(1,4)	
07	(Min,Max)	(0,1)	(0,1)	(0,1)	(0,3)	
08	(Min,Max)	(0,0)	(0,0)	(0,0)	(0,0)	
09	(Min,Max)	(0,1)	(0,0)	(0,0)	(0,1)	
10	(Min,Max)	(0,0)	(0,1)	(0,1)	(0,1)	
11	(Min,Max)	(1,5)	(0,3)	(0,1)	(2,7)	
12	(Min,Max)	(2,4)	(1,2)	(0,1)	(3,7)	
01	COV (%)	0.00	0.00	0.00	0.00	
02	COV (%)	0.00	0.00	0.00	0.00	
03	COV (%)	173.21	0.00	0.00	173.21	
04	COV (%)	0.00	0.00	0.00	0.00	
05	COV (%)	173.21	0.00	173.21	100.00	
06	COV (%)	100.00	173.21	173.21	65.47	
07	COV (%)	141.42	141.42	141.42	141.42	
08	COV (%)	0.00	0.00	0.00	0.00	
09	COV (%)	173.21	0.00	0.00	173.21	
10	COV (%)	0.00	173.21	173.21	86.60	
11	COV (%)	62.45	173.21	173.21	53.93	
12	COV (%)	33.33	34.64	86.60	39.03	
OVERALL VARIATION (%)		AVG(COV)	71.40	57.97	76.74	69.40
OVERALL PRECISION (%)		100-AVG(COV)	28.60	42.03	23.26	30.60



**Figure 186. Distance from average in standard deviation (corner cracking).**

**Table 103. Patching (sq. yard): fair and poor**

Section ID	Statistic	Fair	Poor	Total	
01	AVG	0.00	0.03	0.03	
02	AVG	1.37	0.00	1.37	
03	AVG	1.95	2.03	3.97	
04	AVG	0.04	0.03	0.07	
05	AVG	0.79	0.01	0.81	
06	AVG	12.41	0.58	12.99	
07	AVG	0.00	0.00	0.00	
08	AVG	0.00	0.00	0.00	
09	AVG	0.00	0.00	0.00	
10	AVG	0.06	1.82	1.88	
11	AVG	0.01	0.00	0.01	
12	AVG	0.00	0.00	0.00	
01	(Min,Max)	(0,0)	(0,0.09)	(0,0.09)	
02	(Min,Max)	(1.27,2.43)	(0,0)	(1.27,2.43)	
03	(Min,Max)	(1.74,2.51)	(1.45,2.37)	(3.96,4)	
04	(Min,Max)	(0,0.06)	(0,0.08)	(0,0.14)	
05	(Min,Max)	(0.17,2.21)	(0,0.04)	(0.22,2.21)	
06	(Min,Max)	(0,37.23)	(0,1.09)	(0,38.32)	
07	(Min,Max)	(0,0)	(0,0)	(0,0)	
08	(Min,Max)	(0,0)	(0,0)	(0,0)	
09	(Min,Max)	(0,0)	(0,0)	(0,0)	
10	(Min,Max)	(0,0.19)	(0.64,2.79)	(0.64,2.79)	
11	(Min,Max)	(0,0.03)	(0,0)	(0,0.03)	
12	(Min,Max)	(0,0)	(0,0)	(0,0)	
01	COV (%)	0.00	173.21	173.21	
02	COV (%)	73.93	0.00	73.93	
03	COV (%)	25.21	24.87	0.64	
04	COV (%)	86.65	173.21	108.16	
05	COV (%)	154.73	173.21	150.56	
06	COV (%)	173.21	93.94	168.80	
07	COV (%)	0.00	0.00	0.00	
08	COV (%)	0.00	0.00	0.00	
09	COV (%)	0.00	0.00	0.00	
10	COV (%)	173.21	59.79	59.00	
11	COV (%)	173.21	0.00	173.21	
12	COV (%)	0.00	0.00	0.00	
OVERALL VARIATION (%)		AVG(COV)	71.68	58.18	75.62
OVERALL PRECISION (%)		100-AVG(COV)	28.32	41.82	24.38

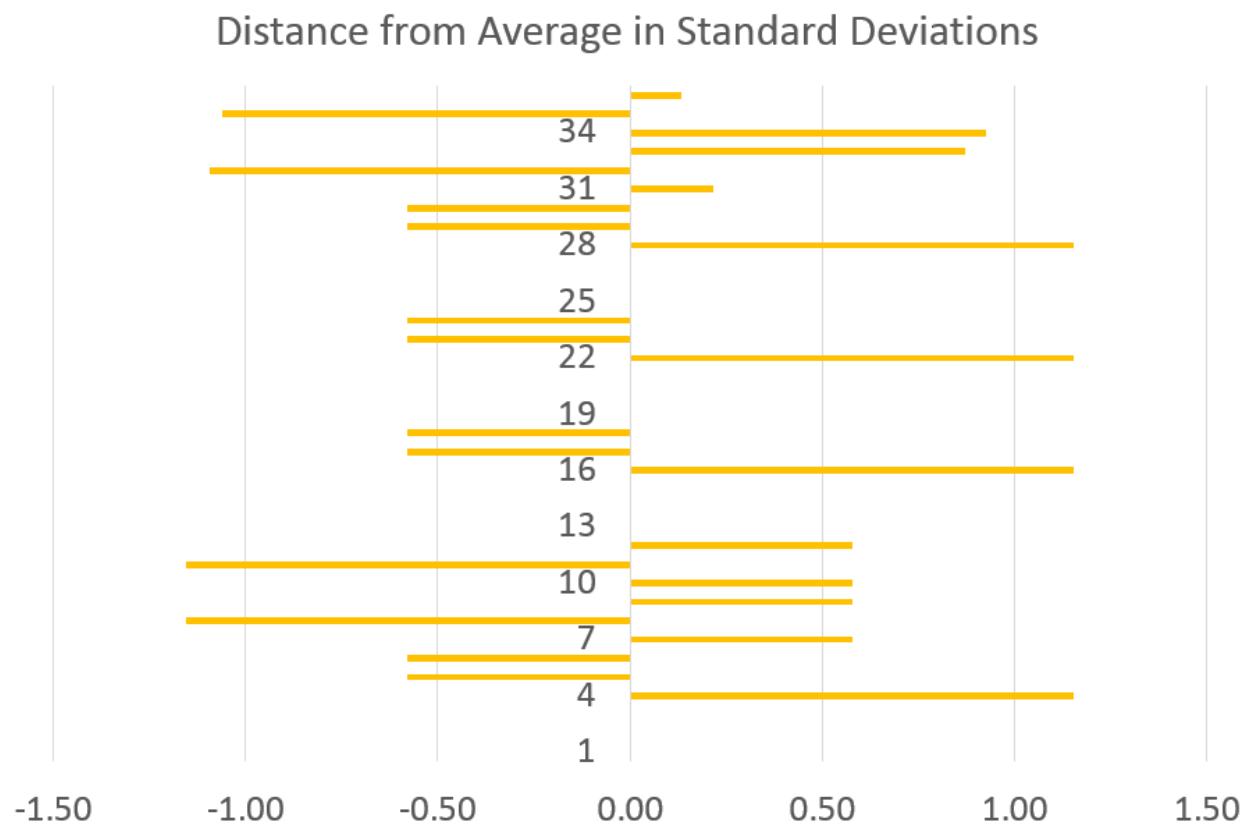


**Figure 187. Distance from average in standard deviation (patching).**

**Table 104. Shattered slab (count): moderate and severe**

Section ID	Statistic	Moderate	Severe	Total	
01	AVG	1.00	0.00	1.00	
02	AVG	0.33	0.00	0.33	
03	AVG	0.67	0.00	0.67	
04	AVG	0.67	0.00	0.67	
05	AVG	0.00	0.00	0.00	
06	AVG	0.33	3.00	3.33	
07	AVG	0.00	1.00	1.00	
08	AVG	0.00	0.33	0.33	
09	AVG	0.00	0.00	0.00	
10	AVG	0.00	0.33	0.33	
11	AVG	2.00	0.67	2.67	
12	AVG	1.67	1.00	2.67	
01	(Min,Max)	(1,1)	(0,0)	(1,1)	
02	(Min,Max)	(0,1)	(0,0)	(0,1)	
03	(Min,Max)	(0,1)	(0,0)	(0,1)	
04	(Min,Max)	(0,1)	(0,0)	(0,1)	
05	(Min,Max)	(0,0)	(0,0)	(0,0)	
06	(Min,Max)	(0,1)	(2,4)	(3,4)	
07	(Min,Max)	(0,0)	(1,1)	(1,1)	
08	(Min,Max)	(0,0)	(0,1)	(0,1)	
09	(Min,Max)	(0,0)	(0,0)	(0,0)	
10	(Min,Max)	(0,0)	(0,1)	(0,1)	
11	(Min,Max)	(1,3)	(0,2)	(1,4)	
12	(Min,Max)	(0,3)	(0,2)	(0,5)	
01	COV (%)	0.00	0.00	0.00	
02	COV (%)	173.21	0.00	173.21	
03	COV (%)		0.00		
04	COV (%)		0.00		
05	COV (%)	0.00	0.00	0.00	
06	COV (%)	173.21	33.33	17.32	
07	COV (%)	0.00	0.00	0.00	
08	COV (%)	0.00	173.21	173.21	
09	COV (%)	0.00	0.00	0.00	
10	COV (%)	0.00	173.21	173.21	
11	COV (%)	50.00	173.21	57.28	
12	COV (%)	91.65	100.00	94.37	
OVERALL VARIATION (%)		AVG(COV)	55.11	54.41	71.82
OVERALL PRECISION (%)		100-AVG(COV)	44.89	45.59	28.18

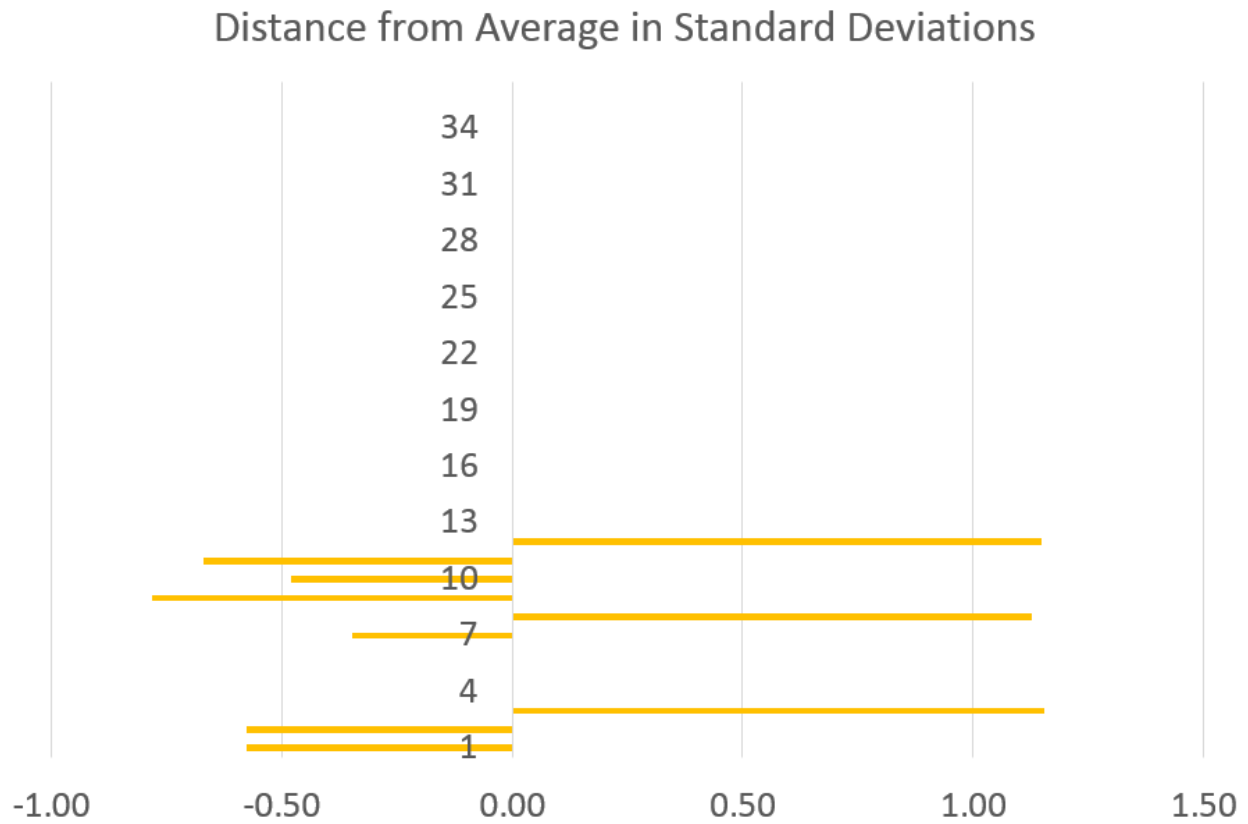




**Figure 188. Distance from average in standard deviation (shattered slab).**

**Table 105. Surface deterioration (sq. feet): moderate and severe**

Section ID	Statistic	Moderate	Severe	Total	
01	AVG	0.11	0.00	0.11	
02	AVG	0.00	0.00	0.00	
03	AVG	0.08	0.00	0.08	
04	AVG	0.52	0.00	0.52	
05	AVG	0.00	0.00	0.00	
06	AVG	0.00	0.00	0.00	
07	AVG	0.00	0.00	0.00	
08	AVG	0.00	0.00	0.00	
09	AVG	0.00	0.00	0.00	
10	AVG	0.00	0.00	0.00	
11	AVG	0.00	0.00	0.00	
12	AVG	0.00	0.00	0.00	
01	(Min,Max)	(0,0.33)	(0,0)	(0,0.33)	
02	(Min,Max)	(0,0)	(0,0)	(0,0)	
03	(Min,Max)	(0,0.18)	(0,0)	(0,0.18)	
04	(Min,Max)	(0,1.41)	(0,0)	(0,1.41)	
05	(Min,Max)	(0,0)	(0,0)	(0,0)	
06	(Min,Max)	(0,0)	(0,0)	(0,0)	
07	(Min,Max)	(0,0)	(0,0)	(0,0)	
08	(Min,Max)	(0,0)	(0,0)	(0,0)	
09	(Min,Max)	(0,0)	(0,0)	(0,0)	
10	(Min,Max)	(0,0)	(0,0)	(0,0)	
11	(Min,Max)	(0,0)	(0,0)	(0,0)	
12	(Min,Max)	(0,0)	(0,0)	(0,0)	
01	COV (%)	173.21	0.00	173.21	
02	COV (%)	0.00	0.00	0.00	
03	COV (%)	128.01	0.00	128.01	
04	COV (%)	149.29	0.00	149.29	
05	COV (%)	0.00	0.00	0.00	
06	COV (%)	0.00	0.00	0.00	
07	COV (%)	0.00	0.00	0.00	
08	COV (%)	0.00	0.00	0.00	
09	COV (%)	0.00	0.00	0.00	
10	COV (%)	0.00	0.00	0.00	
11	COV (%)	0.00	0.00	0.00	
12	COV (%)	0.00	0.00	0.00	
OVERALL VARIATION (%)		AVG(COV)	37.54	0.00	37.54
OVERALL PRECISION (%)		100-AVG(COV)	62.46	100.00	62.46

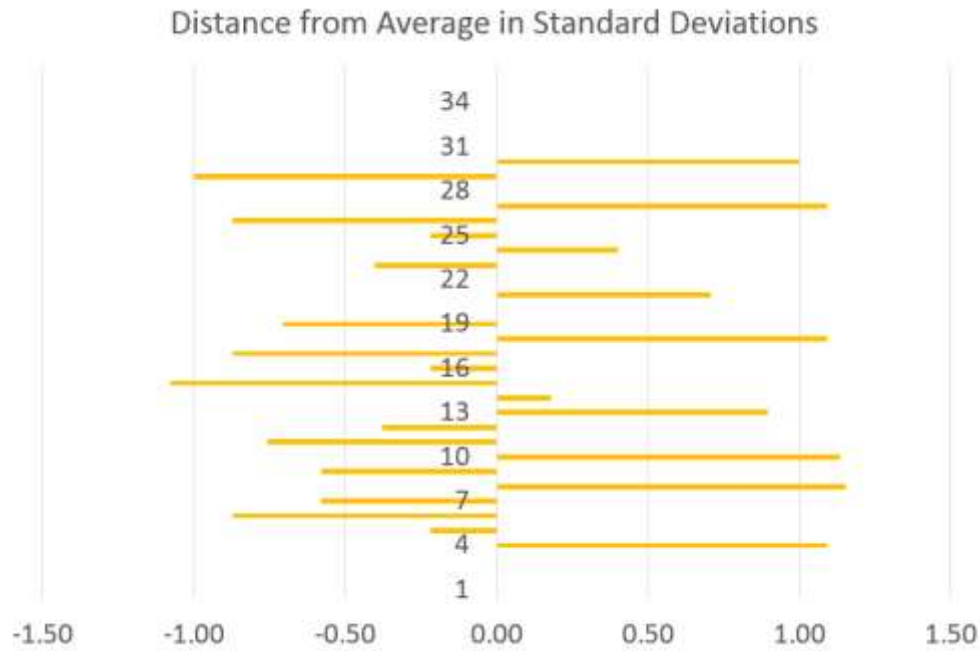


**Figure 189. Distance from average in standard deviation (surface deterioration).**

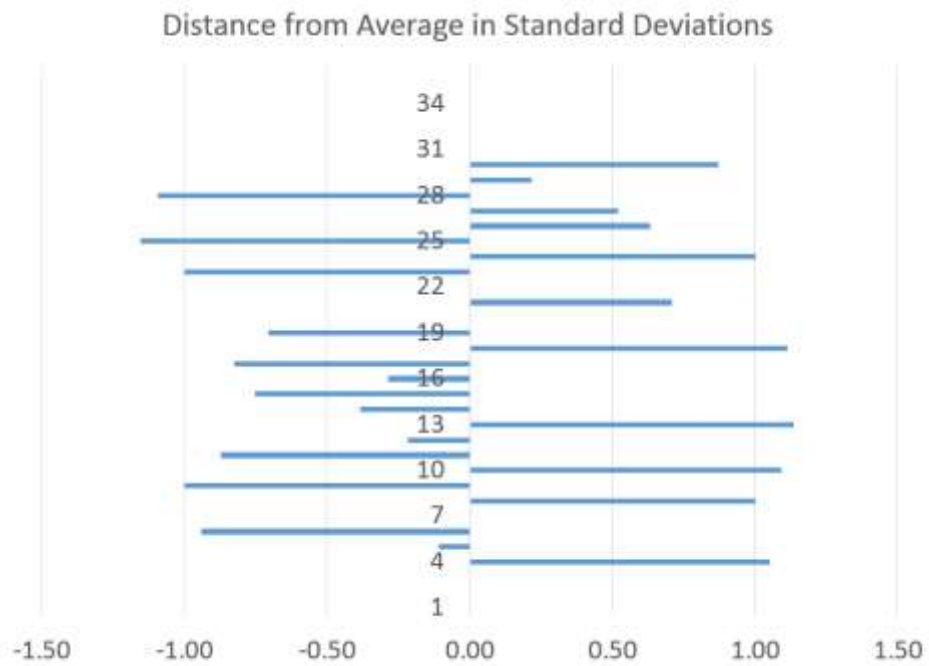
## F. AUTOMATED SURVEY RESULTS ON RIGID PAVEMENTS USING THE EXISTING SOFTWARE

Table 106. Transverse and longitudinal cracking (count)

		Transverse Cracking (count)	Longitudinal Cracking (count)
Section ID	Statistic	Total	Total
02	AVG	18.33	41.67
03	AVG	21.00	56.00
04	AVG	32.00	29.67
05	AVG	10.00	43.33
06	AVG	17.33	22.67
07	AVG	35.00	23.00
08	AVG	20.00	6.00
09	AVG	12.67	28.33
10	AVG	14.00	13.33
02	(Min,Max)	(17,20)	(36,48)
03	(Min,Max)	(18,27)	(53,59)
04	(Min,Max)	(28,38)	(23,38)
05	(Min,Max)	(4,15)	(27,68)
06	(Min,Max)	(16,19)	(15,33)
07	(Min,Max)	(27,43)	(6,40)
08	(Min,Max)	(12,28)	(5,7)
09	(Min,Max)	(10,16)	(18,34)
10	(Min,Max)	(12,16)	(10,16)
02	COV (%)	8.33	14.47
03	COV (%)	24.74	5.36
04	COV (%)	16.54	25.74
05	COV (%)	55.68	50.15
06	COV (%)	8.81	40.99
07	COV (%)	32.32	104.53
08	COV (%)	40.00	16.67
09	COV (%)	24.12	31.63
10	COV (%)	14.29	22.91
OVERALL VARIATION (%)	AVG(COV)	24.98	34.72
OVERALL PRECISION (%)	100-AVG(COV)	75.02	65.28



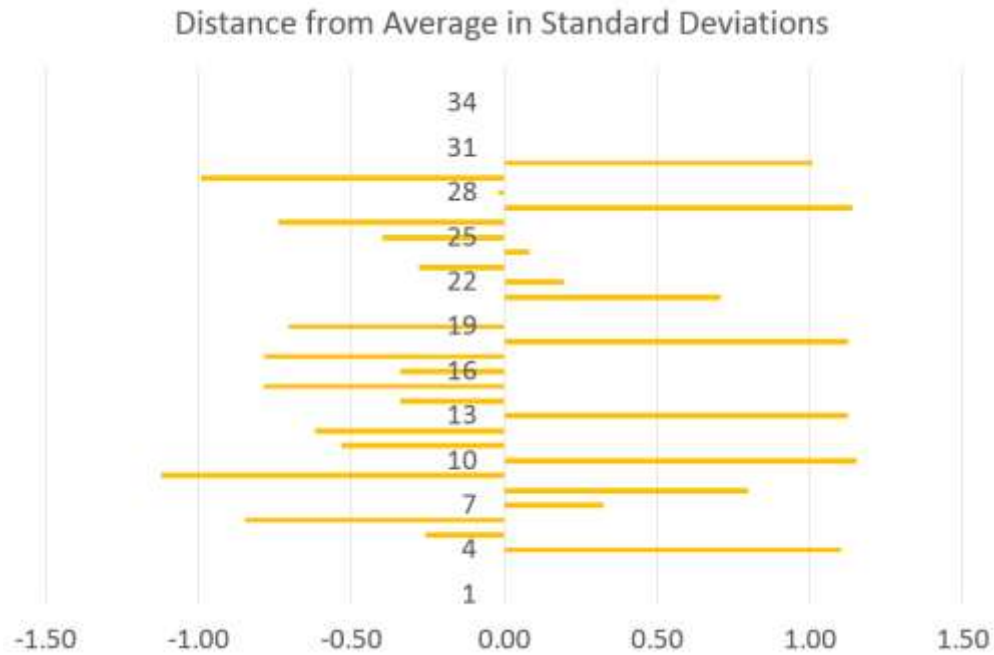
**Figure 190. Distance from average in standard deviation (transverse cracking count)**



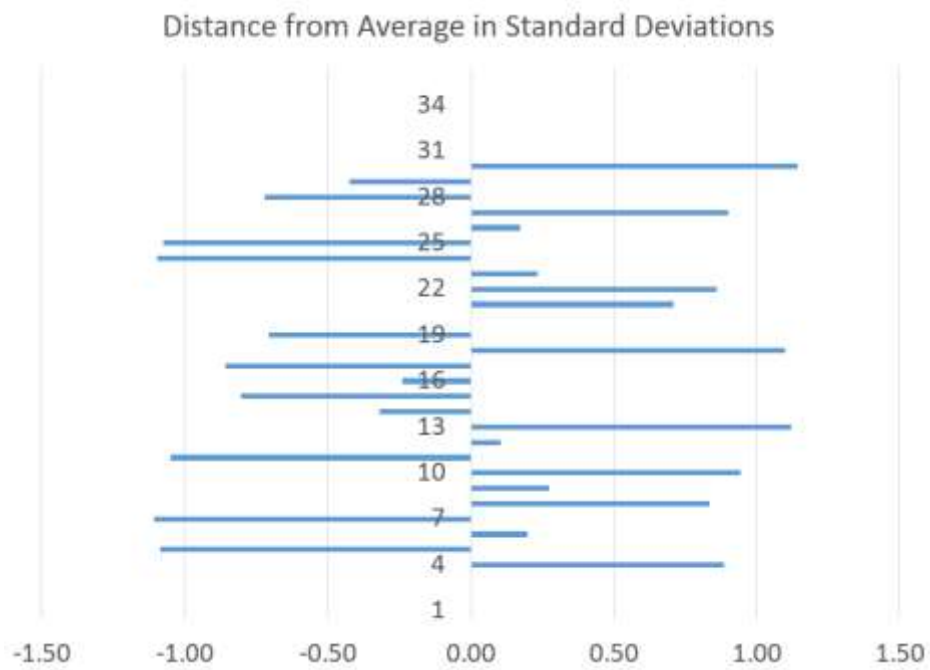
**Figure 191. Distance from average in standard deviation (longitudinal cracking count)**

**Table 107. Transverse and longitudinal cracking (linear feet)**

		Transverse Cracking Length (ft)	Longitudinal Cracking Length (ft)
Section ID	Statistic	Total	Total
02	AVG	101.36	151.70
03	AVG	111.49	260.08
04	AVG	146.39	87.62
05	AVG	54.30	273.26
06	AVG	89.80	69.19
07	AVG	139.63	33.53
08	AVG	73.92	3.98
09	AVG	43.12	142.42
10	AVG	93.47	28.49
02	(Min,Max)	(90.29,115.79)	(142.95,158.86)
03	(Min,Max)	(85.31,130.11)	(240.59,274.77)
04	(Min,Max)	(134.9,167.76)	(61.85,110.84)
05	(Min,Max)	(13.92,112.13)	(143.91,453.86)
06	(Min,Max)	(75.06,110.91)	(41.58,104.53)
07	(Min,Max)	(131.73,147.52)	(19.38,47.69)
08	(Min,Max)	(53.34,88.26)	(0,7.11)
09	(Min,Max)	(39.05,49.39)	(63.09,208.95)
10	(Min,Max)	(62.44,125.11)	(25.67,32.97)
02	COV (%)	12.90	5.32
03	COV (%)	20.93	6.76
04	COV (%)	12.66	28.07
05	COV (%)	94.62	59.00
06	COV (%)	20.88	46.50
07	COV (%)	7.99	59.69
08	COV (%)	24.72	91.17
09	COV (%)	12.79	51.79
10	COV (%)	33.53	13.76
OVERALL VARIATION (%)		AVG(COV)	26.78
OVERALL PRECISION (%)		100-AVG(COV)	73.22
			59.77



**Figure 192. Distance from average in standard deviation (transverse cracking length).**



**Figure 193. Distance from average in standard deviation (longitudinal cracking length).**

## **G. FDOT RIGID PAVEMENT DISTRESS APPLICATION (FRPDA) USER'S GUIDE**

The developed application (FRPDA) is executed by running a batch processor from the Fugro Vision platform, which is used for data monitoring, processing, and reporting. Previously, FDOT raters used the same platform to conduct the semi-automated surveys. It is recommended that the new users review the guide on Using Basic Vision Functions, which has been included at the end of this Appendix to become familiar with the Vision platform before conducting distress surveys. Fugro also maintains more detailed User Manual and Training Modules for users to learn and adjust to the Vision platform. The Installation Guidelines for the Fugro Vision platform and the FRPDA batch processor are also included in this Appendix.

The outline of the recommended procedure for automated identification and quantification of pavement distress is as follows:

1. Run the automated lane assignment based on lane edge offset from image edge and specified lane width. Review and correct lane edges as needed to address any significant vehicle wander during data collection.
2. Run the automated batch processor for crack detection (based on WiseCrax), which filters the images and detects the surface defects for all sections in a project database. This processor is mainly based on the existing Fugro software and not the development efforts in this project. Therefore, it has been organized in a separate processor to protect the pertinent intellectual property (IP).
3. Run the automated batch processor called “*FDOT Rigid Pavement Distress Application*” to:
  - a. Detect the joints for all sections in a project database;
4. Perform quality control (QC) of the joints, modify, add, or delete as appropriate for each section using the Vision platform;
5. Run the automated batch processor called “*FDOT Rigid Pavement Distress Application*” to:
  - b. Conduct classification, which groups adjacent lines, assigns lines to slabs, and classifies lines into longitudinal and transverse based on their angle for all sections in a project database;

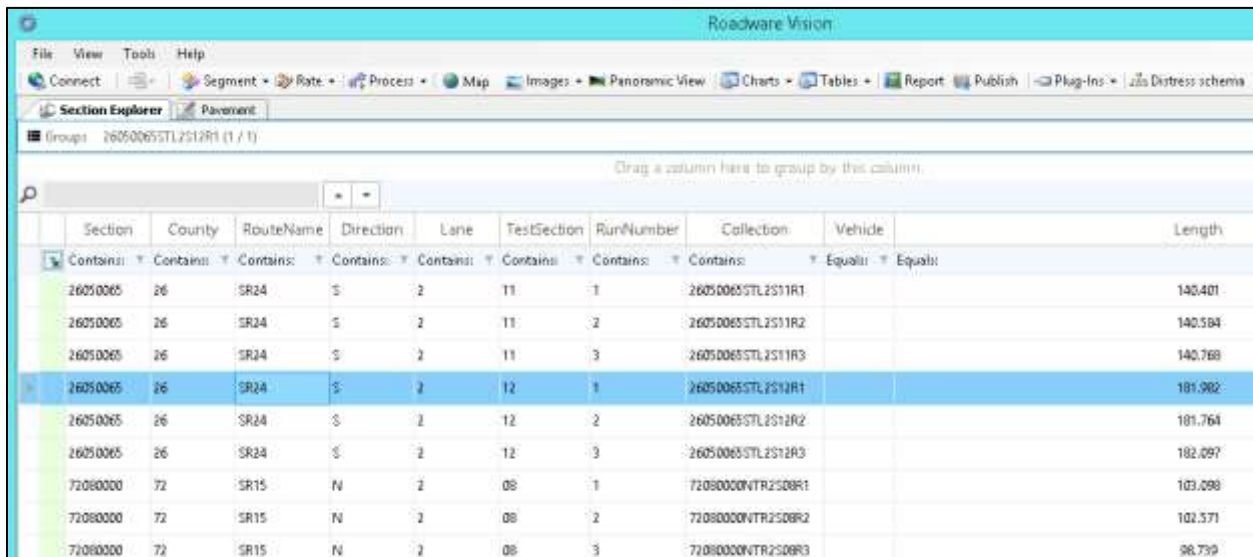


- c. Rate the classified lines into corresponding crack types and severities for all sections in a project database;
6. Perform QC of the automated cracks, modify, add, or delete as appropriate for each section using the Vision platform. Other non-cracking distress types can also be manually identified during this QC.

The following sections explain each of the above steps in more detail.

## G.1. Preliminary Adjustments

The pavement sections are organized in 'sessions', where images are stored. The user will need to double click on a session in the 'Section Explorer' to highlight it. Only one session can be highlighted at a time. After highlighting a session, lock the session so you can work on it manually. This will stop other users from accessing and processing data from that section. The section on Using Basic Vision Functions includes details on how to lock or unlock a session. Even if you start from locking one section, you can still run the batch processor for an automated survey of multiple sections at the same time. As a general rule, automated processes can be executed without locking sessions, but any manual adjustments would require you to lock the session.

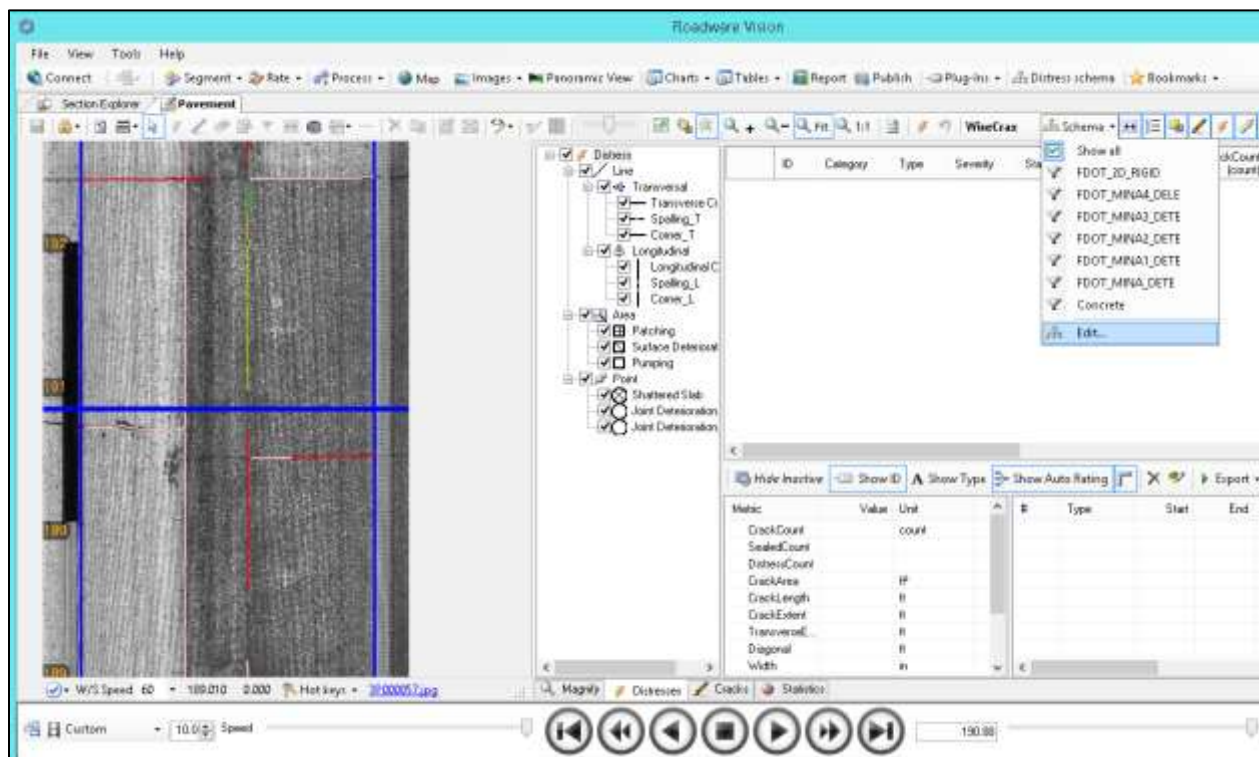


Section	County	RouteName	Direction	Lane	TestSection	RunNumber	Collection	Vehicle	Length
26050065	26	SR24	S	2	11	1	26050065STL2S11R1		140.401
26050065	26	SR24	S	2	11	2	26050065STL2S11R2		140.584
26050065	26	SR24	S	2	11	3	26050065STL2S11R3		140.768
26050065	26	SR24	S	2	12	1	26050065STL2S12R1		181.902
26050065	26	SR24	S	2	12	2	26050065STL2S12R2		181.764
26050065	26	SR24	S	2	12	3	26050065STL2S12R3		182.097
72080000	72	SR15	N	2	08	1	72080000NTR2S08R1		103.098
72080000	72	SR15	N	2	08	2	72080000NTR2S08R2		102.571
72080000	72	SR15	N	2	08	3	72080000NTR2S08R3		98.750

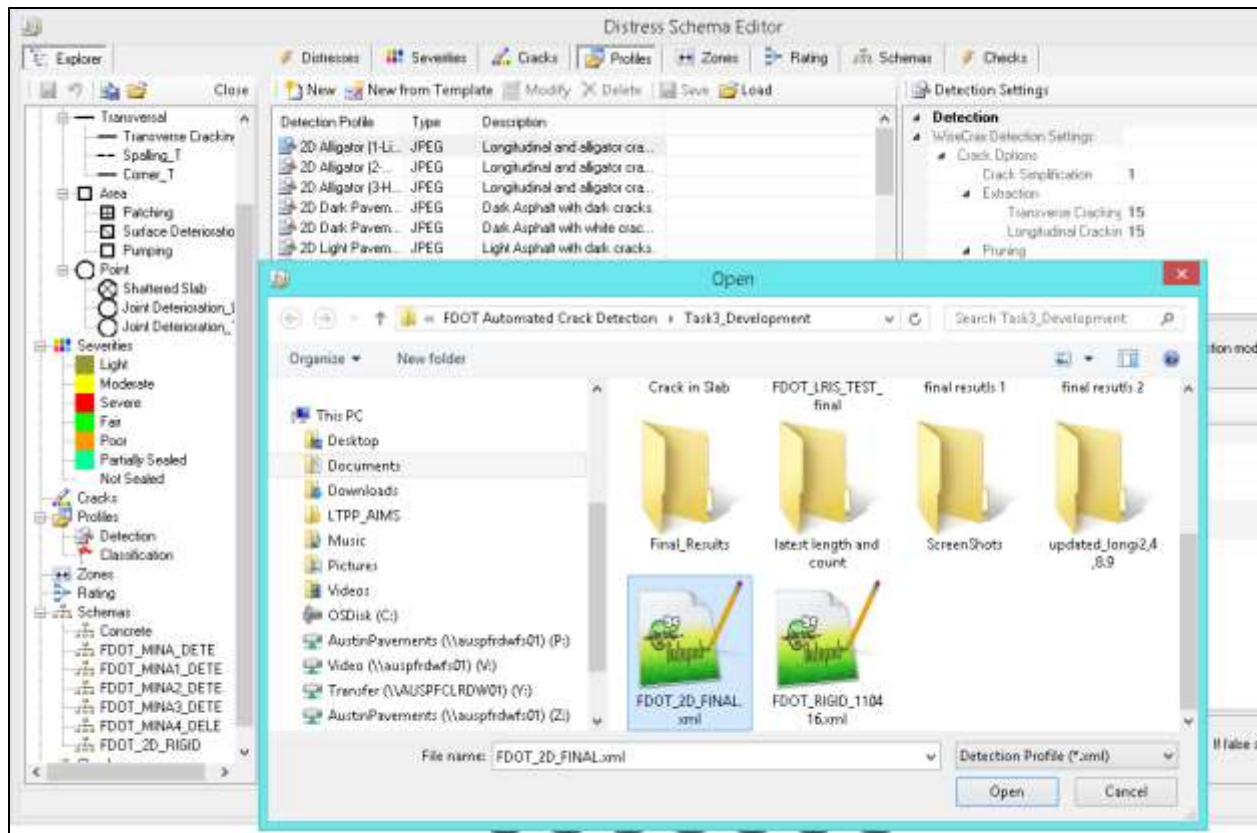
The correct 'Distress Schema' needs to be loaded before running the application. The schema specifies the included distress types and their severities. Fugro engineers create project specific schema that can be saved, emailed, and loaded. If you do not have a distress schema, or if you would like to create one for a specific different project, then you need to use the process for 'Setting Up a Schema,' which is explained at the end of this Appendix. It is recommended that the new users would refrain from creating

or modifying distress schema, unless approved by a more professional user. Different profiles will impact the detection results a lot, because each profile contains different parameter settings for the detection process. It is very important that you use the detection profile specifically created for you by a professional user. Once a schema is loaded for a project, other users can access it. Therefore, it is recommended that a professional user loads the schema.

The following screen captures show where the professional user can load a previously saved schema. Go to the 'Schema' drop-down menu and select 'Edit'.

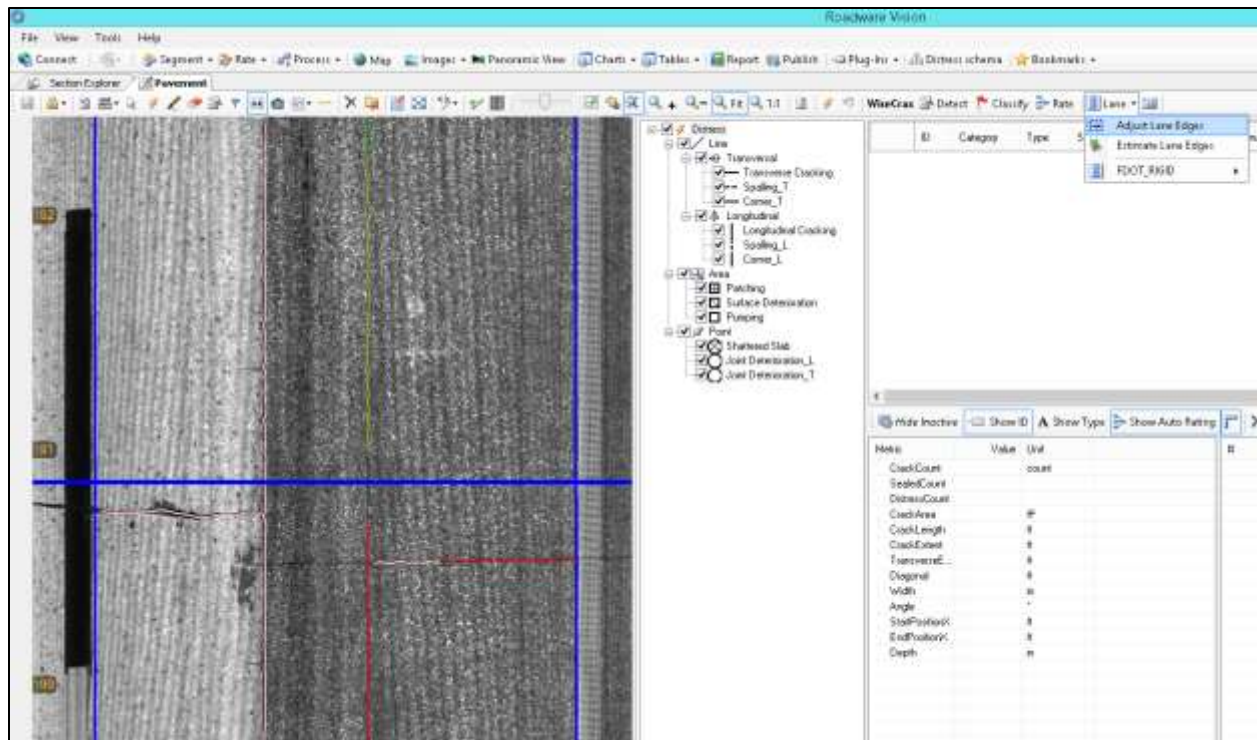


Then go to the 'Profiles' tab, and load the schema file from the saved location on your hard drive or server.



## G.2. Lane Edge Adjustments

Before the user can conduct automated distress surveys, they need to setup lane edges. Lane edges can be drawn separately for each image, which is approximately 20 feet long. The Vision platform allows you to automatically setup all the lane edges for all the images in each session by specifying the offset of one lane edge and the lane width. Select "Lane" then select "Adjust Lane Edges":



The following window will show up, where you can automatically setup all the lane edges for all the images in each session, by specifying the offset of one lane edge and the lane width (note: only Metric units are available at this time). You can either select one or multiple images in each session to setup their lane edges.

**Lane Adjustment Editor**

**Lane Width**  Change +/-

**Lane Offset**  Change +/-

**Change Scope**  
☒ **Current frame** ☐ Apply to selection

**Adjustment Propagation**  
☒ Change values ☐ Apply change values (+/-)

**Make Current** **Go** Clear Restore

Frame	Chainage	Lane Width	Offset
000000100000.fis	-0.162	?	?
000000110000.fis	6.052	?	?
000000120000.fis	12.266	?	?
000000130000.fis	18.480	?	?
000000140000.fis	24.693	?	?
000000150000.fis	30.907	?	?
000000160000.fis	37.121	?	?
000000170000.fis	43.334	3.337	-0.205
<b>000000180000.fis</b>	49.548	?	?
000000190000.fis	55.762	?	?

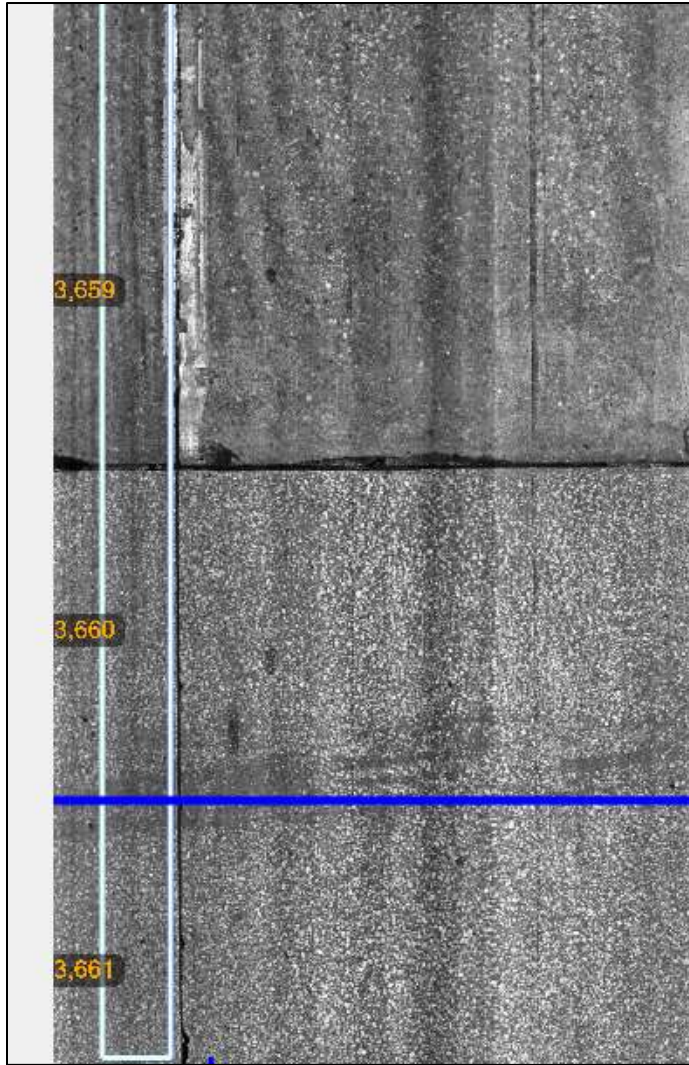
☒ Recalculate ratings OK Cancel

Note that due to vehicle wander and lane departures, this automated lane edge assignment might not be very accurate. It is recommended that the results of this automated lane edge assignment be reviewed and adjusted manually. To manually adjust the lane edges after you have locked the session, click on the lane icon (see screen below) to adjust lane edge on pavement images.

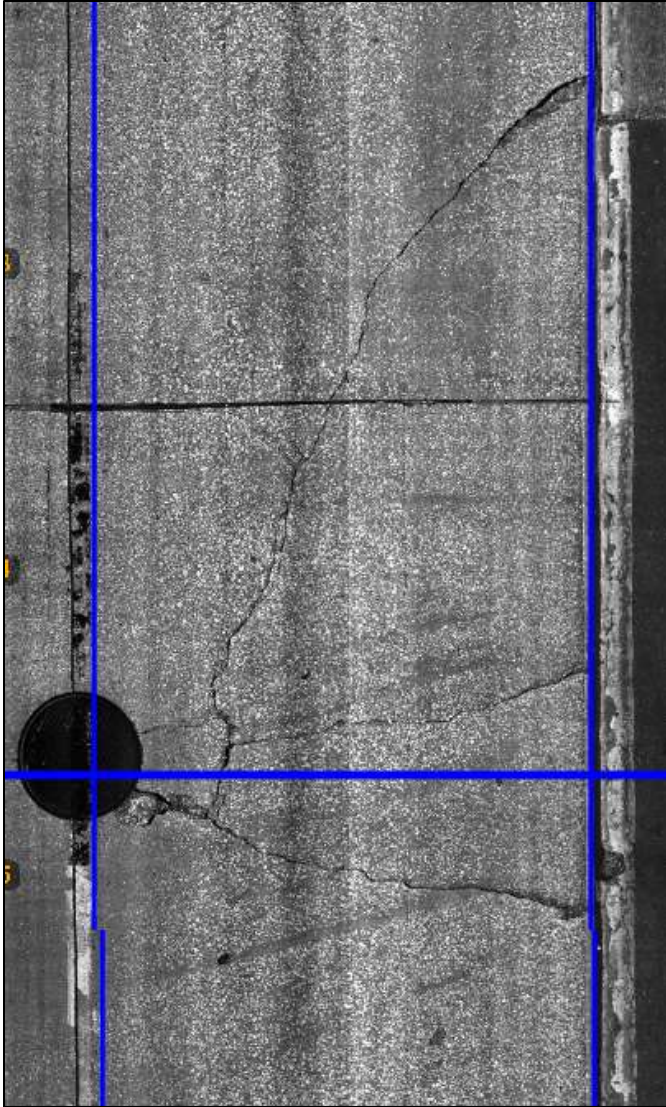


Click on left/right half of the image, left click your mouse and select 'Adjust Lane Edge (left/right)':





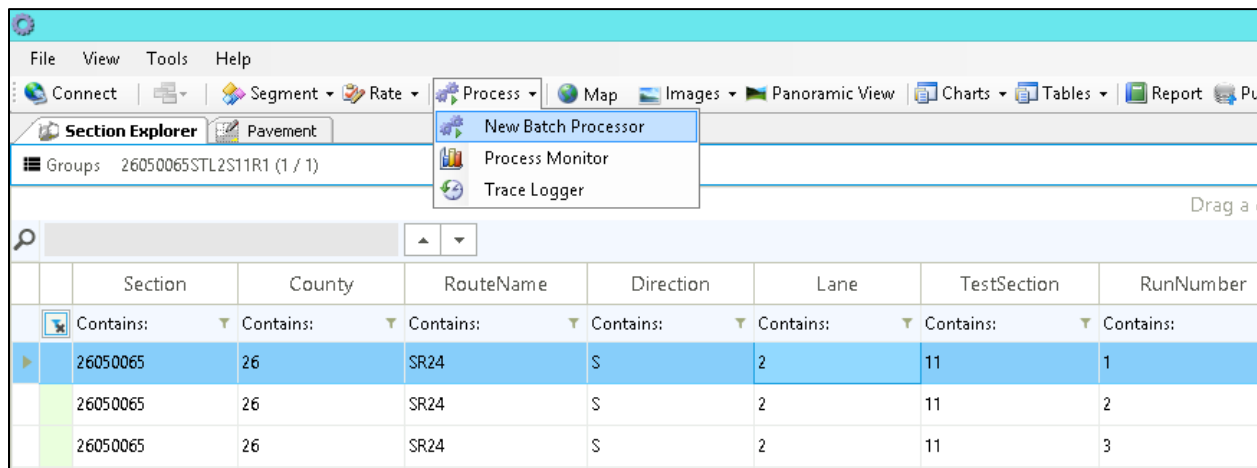
The following is an example of adjusted lane edge:



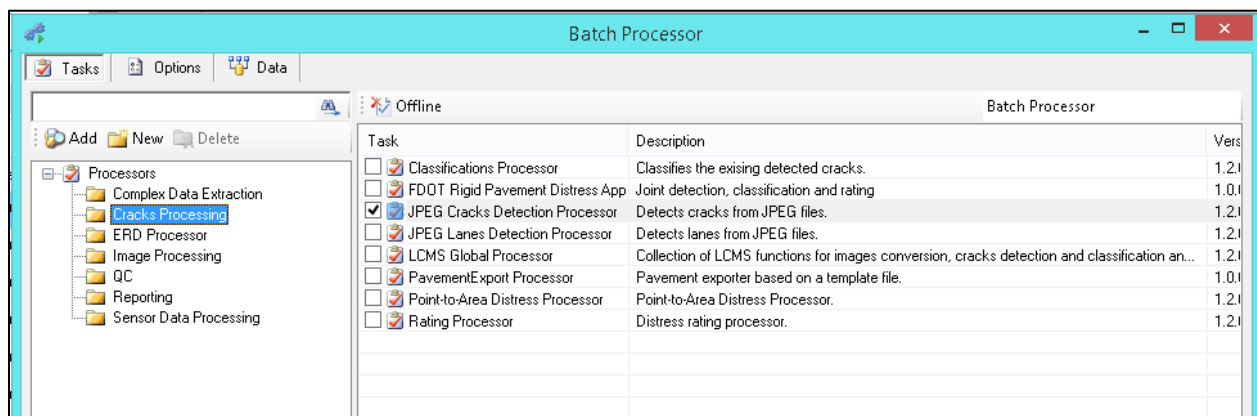


### G.3. Automated Pre-Filtering and Crack Detection

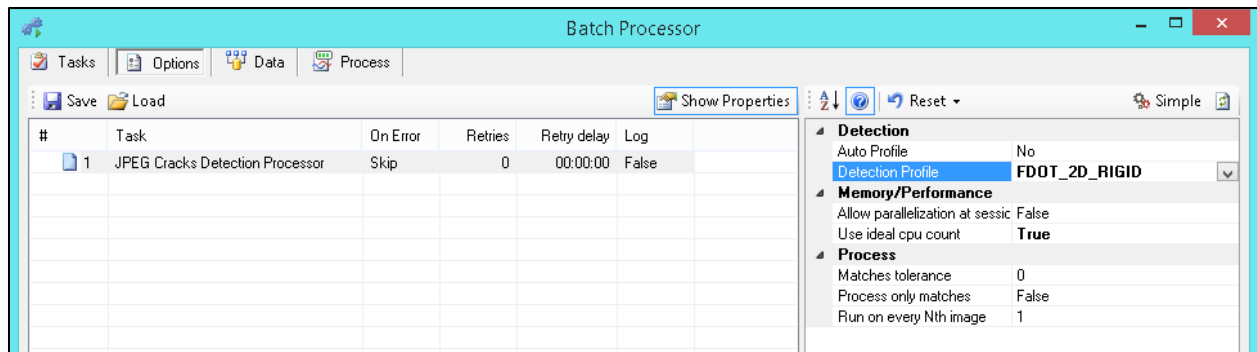
The existing batch processor for detection of pavement surface defects (based on WiseCrax algorithm) has been slightly adjusted to include pre-filtering with a Gaussian filter using the ImageJ open-sourec code. Select the 'Process' tab, and click on the 'New Batch Processor' from the drop-down menu:



Select the 'Cracks Processing' group of processors from the left hand side folders, and then select the 'JPEG Cracks Detection Processor' from the list:



After selecting this processor from the 'Tasks' menu, go to the 'Options' menu on top, and choose the 'Detection Profile' called "FDOT\_2D\_RIGID" (Fugro engineers will provide the correct profile for you.). You must select the detection profile, or the processor won't run.



Go to the 'Data' menu on top to select the session(s) that you would like to process. Note that in this menu, all of the available sessions will be loaded. The session numbers will be based on the 'Collection' data field in the list of sections (Section Explorer). In order to choose your desired session(s), you need to remove the unwanted sessions. First select the desired session to highlight it in blue. You can select multiple sessions by holding down the Ctrl key and left-clicking on multiple sessions (in the following example, all the sessions with their name ending in R1 corresponding to run number 1 have been selected). Then, click on the check box on the top left and from the drop-down menu, select 'Invert'.

Batch Processor							
Tasks Options Data Process							
X Remove Go Search							
#	All		Date	Vehicle	Collected	Matched	%
1	Invert	2S11R1	2015-12-17 11:44	0	140	140	100
2	Clear	2S11R2	2015-12-17 11:50	0	141	141	100
3		26050005TL2S11R3	2015-12-17 11:54	0	141	141	100
4		26050005TL2S12R1	2015-12-17 11:44	0	182	182	100
5		26050005TL2S12R2	2015-12-17 11:50	0	182	182	100
6		26050005TL2S12R3	2015-12-17 11:54	0	182	182	100
7		72080000NTR2S08R1	2015-12-02 01:44	0	103	103	100
8		72080000NTR2S08R2	2015-12-02 01:52	0	103	103	100
9		72080000NTR2S08R3	2015-12-02 01:55	0	99	99	100
10		72080000NTR2S08R4	2015-12-02 02:06	0	98	98	100
11		72080000NTR2S09R1	2015-12-02 01:44	0	113	113	100
12		72080000NTR2S09R2	2015-12-02 01:52	0	110	110	100
13		72080000NTR2S09R3	2015-12-02 01:55	0	113	113	100
14		72080000NTR2S09R4	2015-12-02 02:06	0	122	122	100
15		72080000TL2S08R1	2015-12-02 01:54	0	121	121	100
16		72080000TL2S08R2	2015-12-02 02:03	0	121	121	100
17		72080000TL2S08R3	2015-12-02 02:11	0	121	121	100
18		72080000TL2S07R1	2015-12-02 01:54	0	126	126	100
19		72080000TL2S07R3	2015-12-02 02:11	0	122	122	100
20		72290000TL3S10R1	2015-12-10 12:27	0	139	139	100
21		72290000TL3S10R2	2015-12-10 12:42	0	140	140	100
22		72290000TL3S10R3	2015-12-10 12:56	0	139	139	100
23		75010000TL2S01R1	2015-12-03 11:50	0	163	163	100
24		75010000TL2S01R2	2015-12-03 12:15	0	163	163	100
25		75010000TL2S01R3	2015-12-03 12:26	0	163	163	100
26		75010000TL2S01R4	2015-12-03 12:41	0	744	0	0
27		75010000TL2S02R1	2015-12-03 11:50	0	152	152	100
28		75010000TL2S02R2	2015-12-03 12:15	0	152	152	100
29		75010000TL2S02R3	2015-12-03 12:26	0	152	152	100
30		75010000TL2S02R4	2015-12-03 12:41	0	744	0	0
31		75020000TL2S03R1	2015-12-03 10:50	0	213	213	100
32		75020000TL2S03R2	2015-12-03 10:53	0	213	213	100
33		75020000TL2S03R3	2015-12-03 10:56	0	213	213	100
34		75030000NTR2S04R1	2015-12-03 01:29	0	174	174	100
35		75030000NTR2S04R2	2015-12-03 02:02	0	171	171	100
36		75030000NTR2S04R3	2015-12-03 02:28	0	171	171	100
37		75030000NTR2S05R1	2015-12-03 01:29	0	302	302	100
38		75030000NTR2S05R2	2015-12-03 02:02	0	261	261	100
39		75030000NTR2S05R3	2015-12-03 02:28	0	261	261	100

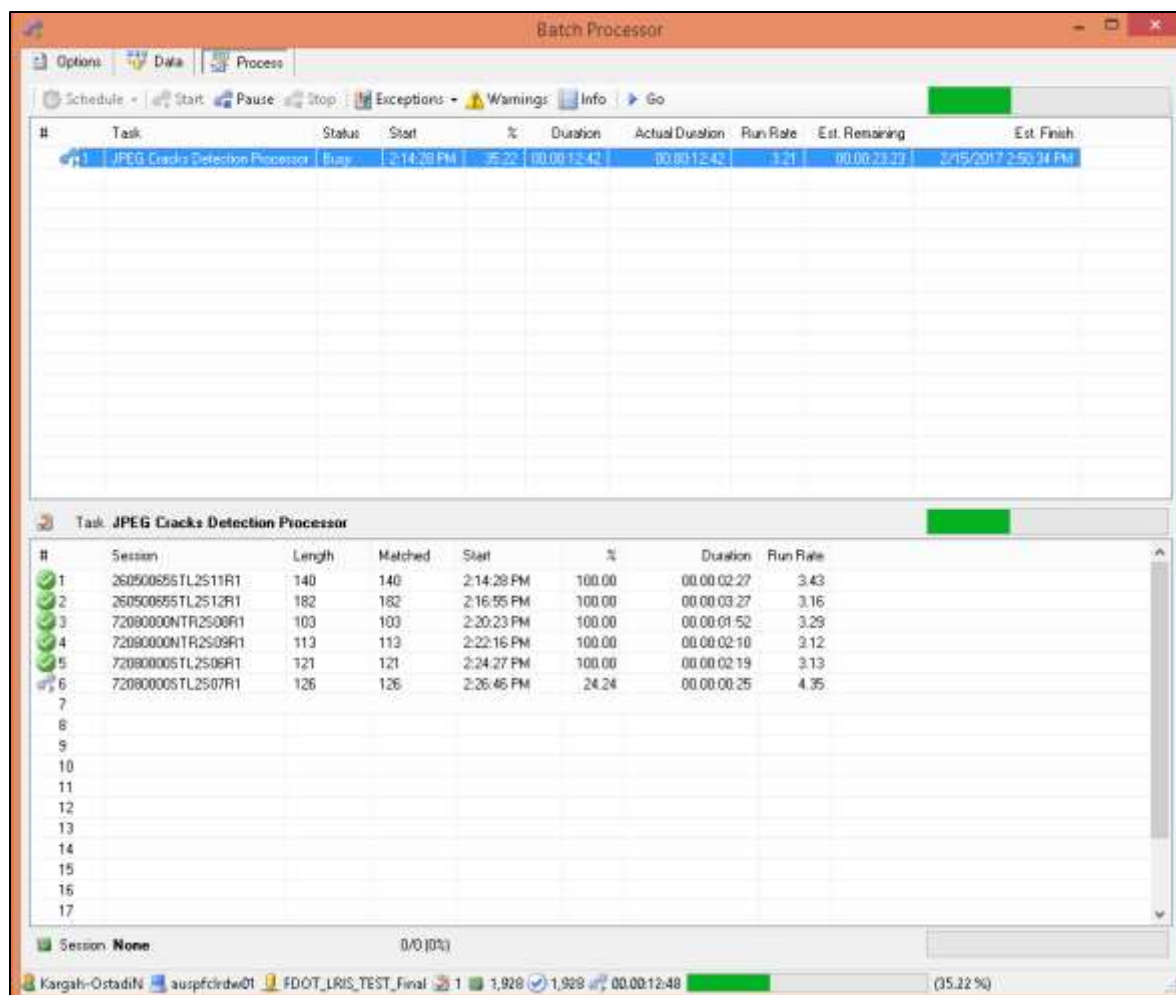
This will result in all the other unwanted sessions to be highlighted in blue.

Batch Processor						
Tasks Options Data Process						
Remove Go Search						
#	Session	Date	Vehicle	Collected	Matched	%
1	260500655TL2511R1	2015-12-17 11:44	0	140	140	100
2	260500655TL2511R2	2015-12-17 11:50	0	141	141	100
3	260500655TL2511R3	2015-12-17 11:54	0	141	141	100
4	260500655TL2512R1	2015-12-17 11:44	0	182	182	100
5	260500655TL2512R2	2015-12-17 11:50	0	182	182	100
6	260500655TL2512R3	2015-12-17 11:54	0	182	182	100
7	72080000NTR2509R1	2015-12-02 01:44	0	103	103	100
8	72080000NTR2509R2	2015-12-02 01:52	0	103	103	100
9	72080000NTR2509R3	2015-12-02 01:55	0	99	99	100
10	72080000NTR2509R4	2015-12-02 02:06	0	99	99	100
11	72080000NTR2509R1	2015-12-02 01:44	0	113	113	100
12	72080000NTR2509R2	2015-12-02 01:52	0	110	110	100
13	72080000NTR2509R3	2015-12-02 01:55	0	113	113	100
14	72080000NTR2509R4	2015-12-02 02:06	0	122	122	100
15	720800005TL2506R1	2015-12-02 01:54	0	121	121	100
16	720800005TL2506R2	2015-12-02 02:03	0	121	121	100
17	720800005TL2506R3	2015-12-02 02:11	0	121	121	100
18	720800005TL2507R1	2015-12-02 01:54	0	126	126	100
19	720800005TL2507R2	2015-12-02 02:11	0	122	122	100
20	722900005TL3510R1	2015-12-10 12:27	0	139	139	100
21	722900005TL3510R2	2015-12-10 12:42	0	140	140	100
22	722900005TL3510R3	2015-12-10 12:56	0	139	139	100
23	750100005TL2501R1	2015-12-03 11:50	0	163	163	100
24	750100005TL2501R2	2015-12-03 12:15	0	163	163	100
25	750100005TL2501R3	2015-12-03 12:36	0	163	163	100
26	750100005TL2501R4	2015-12-03 12:41	0	744	0	0
27	750100005TL2502R1	2015-12-03 11:50	0	152	152	100
28	750100005TL2502R2	2015-12-03 12:15	0	152	152	100
29	750100005TL2502R3	2015-12-03 12:26	0	152	152	100
30	750100005TL2502R4	2015-12-03 12:41	0	744	0	0
31	750200005TL2503R1	2015-12-03 10:50	0	212	212	100
32	750200005TL2503R2	2015-12-03 10:53	0	213	213	100
33	750200005TL2503R3	2015-12-03 10:56	0	213	213	100
34	75030000NTR2504R1	2015-12-03 01:29	0	174	174	100
35	75030000NTR2504R2	2015-12-03 02:02	0	171	171	100
36	75030000NTR2504R3	2015-12-03 02:29	0	171	171	100
37	75030000NTR2505R1	2015-12-03 01:29	0	302	302	100
38	75030000NTR2505R2	2015-12-03 02:02	0	261	261	100
39	75030000NTR2505R3	2015-12-03 02:29	0	261	261	100

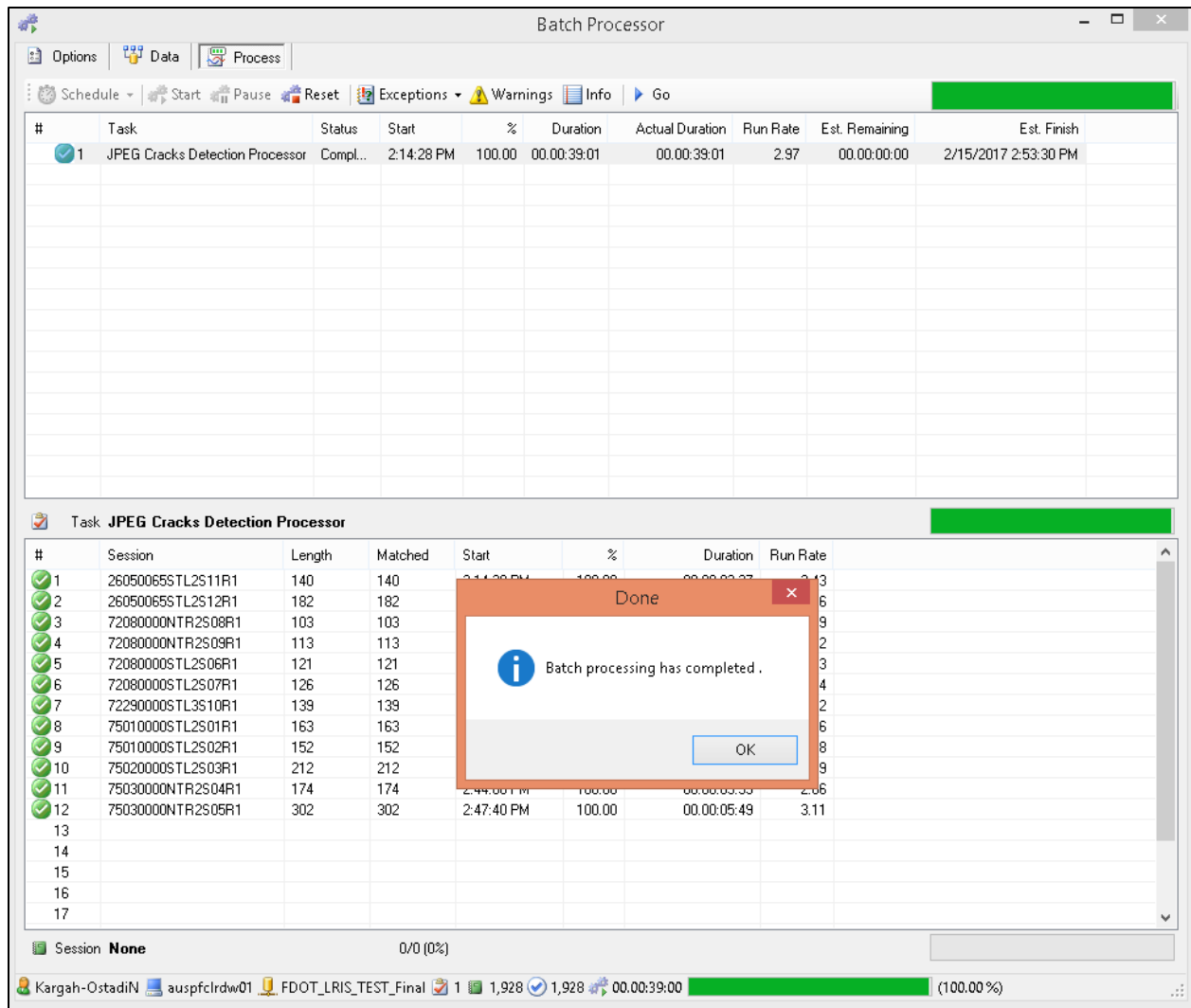
Now, you can click to 'Remove' the unwanted sessions. If you remove the incorrect sessions by mistake, you can click on the undo icon on top left to reload all the available sessions in this project.

Batch Processor						
Tasks Options Data Process						
Remove     Go  Search						
#	Session	Date	Vehicle	Collected	Matched	%
1	26050065STL2S11R1	2015-12-17 11:44	0	140	140	100
2	26050065STL2S12R1	2015-12-17 11:44	0	182	182	100
3	72080000NTR2S08R1	2015-12-02 01:44	0	103	103	100
4	72080000NTR2S09R1	2015-12-02 01:44	0	113	113	100
5	72080000STL2S06R1	2015-12-02 01:54	0	121	121	100
6	72080000STL2S07R1	2015-12-02 01:54	0	126	126	100
7	72290000STL3S10R1	2015-12-10 12:27	0	139	139	100
8	75010000STL2S01R1	2015-12-03 11:50	0	163	163	100
9	75010000STL2S02R1	2015-12-03 11:50	0	152	152	100
10	75020000STL2S03R1	2015-12-03 10:50	0	212	212	100
11	75030000NTR2S04R1	2015-12-03 01:29	0	174	174	100
12	75030000NTR2S05R1	2015-12-03 01:29	0	302	302	100

In order to run the processor on the selected session(s), go to the 'Process' menu on top and select 'Start'. The 'Process' menu will show you the progress of the processing on each and all of the selected sessions. You can select 'Pause' or 'Stop' at any time during the process:

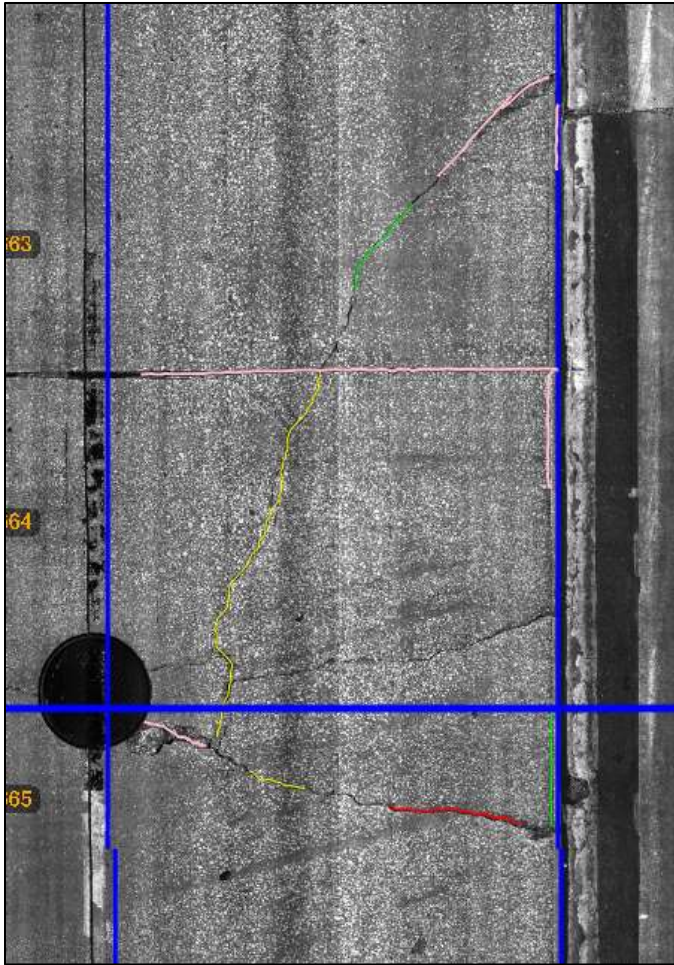


After the processing has been completed for all the selected sessions, a message box will let you know that the batch processing is complete. Click on OK button to continue.



In order to see the detection results on any session that was already selected (highlighted in the 'Section Explorer' menu) before the batch processing, you need to double click to highlight another session and then come vback and double click the desired session. This process refreshes the view of the session and you can see the changes that took effect as a result of the batch processor. This screen capture shows an example image after the detection process has been executed and the surface defects have been detected:





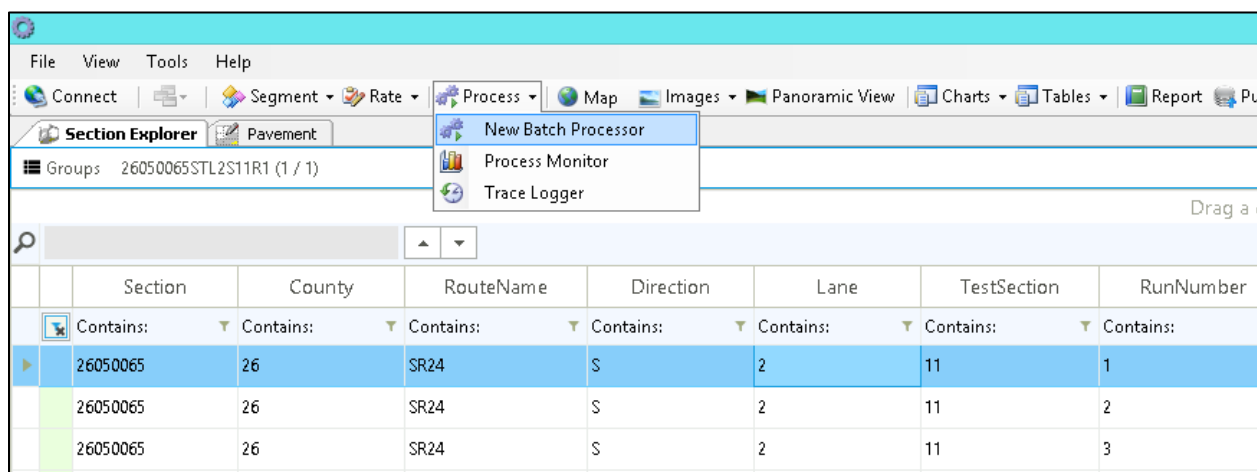


## G.4. FDOT Rigid Pavement Distress Application: FRPDA

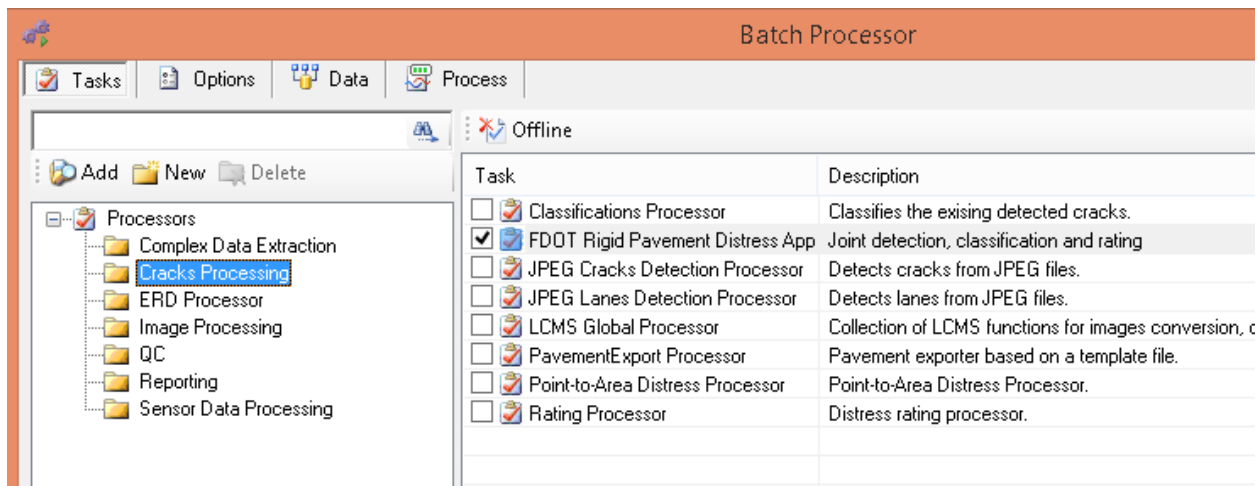
This application is developed specifically for FDOT, and it contains the following functions:

1. Detection of joints from 2-D pavement surface images,
2. Classification of lines (that have been detected by the previous batch processor) into longitudinal and transverse orientations based on their angle; grouping of adjacent cracks based on their type and proximity to one another; and assigning the detected cracks to the correct slab, based on their locations relative to the joints of the slabs;
3. Rating of the cracks into longitudinal, transverse, or corner cracking, and shattered slabs; and assigning a severity level based on the width of cracks.

Select the 'Process' tab, and click on the 'New Batch Processor' from the drop-down menu:

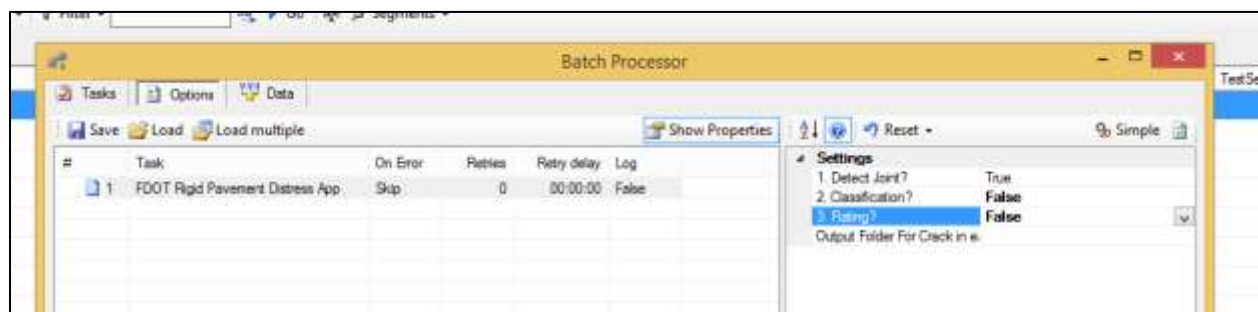


Select the 'Cracks Processing' group of processors from the left-hand side folders, and then select the 'FDOT Rigid Pavement Distress App' from the list:



#### G.4.1. Joint Detection and QC

Go to the 'Options' menu on top. In the 'Settings' for the 'FDOT Rigid Pavement Distress App', you can specify which process you would like to run: joint detection, classification, or rating. If you just want to detect the joints from pavement images, set the 'Detect Joint' as True, and 'Classification' and 'Rating' as False:



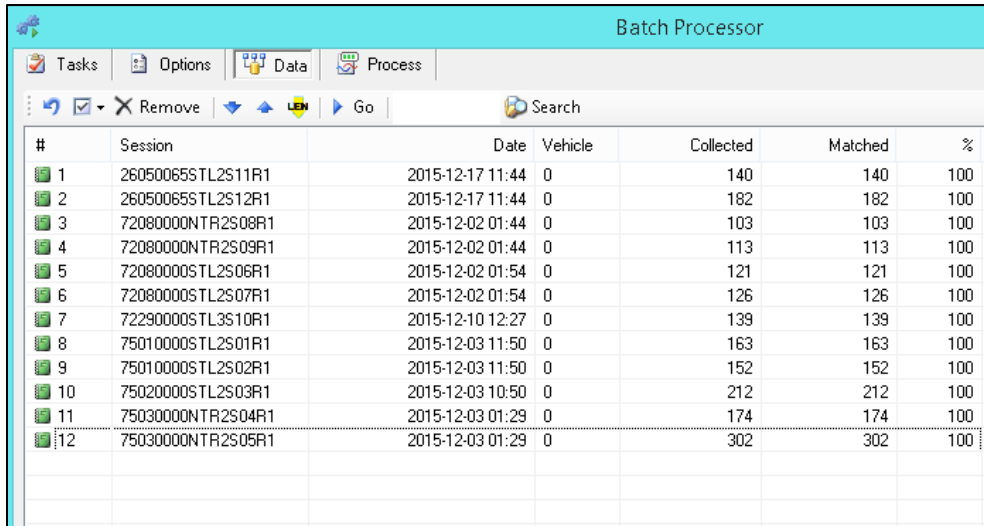
Select the 'Data' (sessions) you would like to process. The default data to be processed is pavement images from all sessions. Go to the 'Data' menu on top to select the session(s) that you would like to process. Note that in this menu, all of the available sessions will be loaded. The session numbers will be based on the 'Collection' data field in the list of sections (Section Explorer). In order to choose your desired session(s), you need to remove the unwanted sessions. First select the desired session to highlight it in blue. You can select multiple sessions by holding down the Ctrl key and left-clicking on multiple sessions (in the following example, all the sessions with their name ending in R1 corresponding to run number 1 have been selected). Then, click on the check box on the top left and from the drop-down menu, select 'Invert'.

Batch Processor							
Tasks Options Data Process							
X Remove Go Search							
#	All		Date	Vehicle	Collected	Matched	%
1	Invert	2S11R1	2015-12-17 11:44	0	140	140	100
2	Clear	2S11R2	2015-12-17 11:50	0	141	141	100
3		260500655TL2S11R3	2015-12-17 11:54	0	141	141	100
4		260500655TL2S12R1	2015-12-17 11:44	0	182	182	100
5		260500655TL2S12R2	2015-12-17 11:50	0	182	182	100
6		260500655TL2S12R3	2015-12-17 11:54	0	182	182	100
7		72080000NTR2S08R1	2015-12-02 01:44	0	103	103	100
8		72080000NTR2S08R2	2015-12-02 01:52	0	103	103	100
9		72080000NTR2S08R3	2015-12-02 01:55	0	99	99	100
10		72080000NTR2S08R4	2015-12-02 02:06	0	98	98	100
11		72080000NTR2S09R1	2015-12-02 01:44	0	113	113	100
12		72080000NTR2S09R2	2015-12-02 01:52	0	110	110	100
13		72080000NTR2S09R3	2015-12-02 01:55	0	113	113	100
14		72080000NTR2S09R4	2015-12-02 02:06	0	122	122	100
15		72080000NTR2S09R1	2015-12-02 01:54	0	121	121	100
16		72080000NTR2S08R2	2015-12-02 02:03	0	121	121	100
17		72080000NTR2S08R3	2015-12-02 02:11	0	121	121	100
18		72080000NTR2S07R1	2015-12-02 01:54	0	126	126	100
19		72080000NTR2S07R3	2015-12-02 02:11	0	122	122	100
20		72290000NTR2S10R1	2015-12-10 12:27	0	139	139	100
21		72290000NTR2S10R2	2015-12-10 12:42	0	140	140	100
22		72290000NTR2S10R3	2015-12-10 12:56	0	139	139	100
23		75010000NTR2S01R1	2015-12-03 11:50	0	163	163	100
24		75010000NTR2S01R2	2015-12-03 12:15	0	163	163	100
25		75010000NTR2S01R3	2015-12-03 12:26	0	163	163	100
26		75010000NTR2S01R4	2015-12-03 12:41	0	744	0	0
27		75010000NTR2S02R1	2015-12-03 11:50	0	152	152	100
28		75010000NTR2S02R2	2015-12-03 12:15	0	152	152	100
29		75010000NTR2S02R3	2015-12-03 12:26	0	152	152	100
30		75010000NTR2S02R4	2015-12-03 12:41	0	744	0	0
31		75020000NTR2S03R1	2015-12-03 10:50	0	213	213	100
32		75020000NTR2S03R2	2015-12-03 10:53	0	213	213	100
33		75020000NTR2S03R3	2015-12-03 10:56	0	213	213	100
34		75030000NTR2S04R1	2015-12-03 01:29	0	174	174	100
35		75030000NTR2S04R2	2015-12-03 02:02	0	171	171	100
36		75030000NTR2S04R3	2015-12-03 02:28	0	171	171	100
37		75030000NTR2S05R1	2015-12-03 01:29	0	302	302	100
38		75030000NTR2S05R2	2015-12-03 02:02	0	261	261	100
39		75030000NTR2S05R3	2015-12-03 02:28	0	261	261	100

This will result in all the other unwanted sessions to be highlighted in blue.

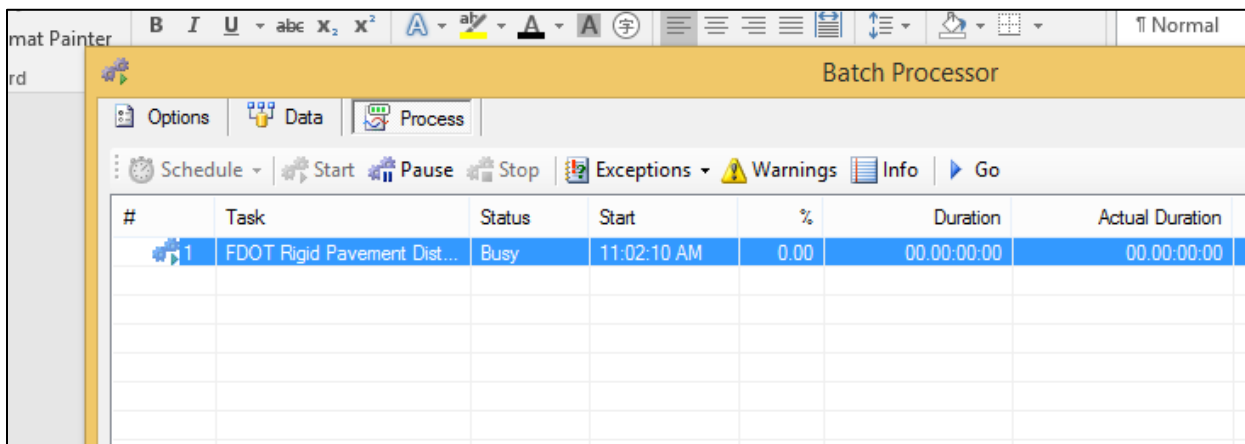
Batch Processor						
Tasks Options Data Process						
Remove Go Search						
#	Session	Date	Vehicle	Collected	Matched	%
1	260500655TL2511R1	2015-12-17 11:44	0	140	140	100
2	260500655TL2511R2	2015-12-17 11:50	0	141	141	100
3	260500655TL2511R3	2015-12-17 11:54	0	141	141	100
4	260500655TL2512R1	2015-12-17 11:44	0	182	182	100
5	260500655TL2512R2	2015-12-17 11:50	0	182	182	100
6	260500655TL2512R3	2015-12-17 11:54	0	182	182	100
7	72080000NTR2509R1	2015-12-02 01:44	0	103	103	100
8	72080000NTR2509R2	2015-12-02 01:52	0	103	103	100
9	72080000NTR2509R3	2015-12-02 01:55	0	99	99	100
10	72080000NTR2509R4	2015-12-02 02:06	0	99	99	100
11	72080000NTR2509R1	2015-12-02 01:44	0	113	113	100
12	72080000NTR2509R2	2015-12-02 01:52	0	110	110	100
13	72080000NTR2509R3	2015-12-02 01:55	0	113	113	100
14	72080000NTR2509R4	2015-12-02 02:06	0	122	122	100
15	720800005TL2506R1	2015-12-02 01:54	0	121	121	100
16	720800005TL2506R2	2015-12-02 02:03	0	121	121	100
17	720800005TL2506R3	2015-12-02 02:11	0	121	121	100
18	720800005TL2507R1	2015-12-02 01:54	0	126	126	100
19	720800005TL2507R2	2015-12-02 02:11	0	122	122	100
20	722900005TL3510R1	2015-12-10 12:27	0	139	139	100
21	722900005TL3510R2	2015-12-10 12:42	0	140	140	100
22	722900005TL3510R3	2015-12-10 12:56	0	139	139	100
23	750100005TL2501R1	2015-12-03 11:50	0	163	163	100
24	750100005TL2501R2	2015-12-03 12:15	0	163	163	100
25	750100005TL2501R3	2015-12-03 12:36	0	163	163	100
26	750100005TL2501R4	2015-12-03 12:41	0	744	0	0
27	750100005TL2502R1	2015-12-03 11:50	0	152	152	100
28	750100005TL2502R2	2015-12-03 12:15	0	152	152	100
29	750100005TL2502R3	2015-12-03 12:26	0	152	152	100
30	750100005TL2502R4	2015-12-03 12:41	0	744	0	0
31	750200005TL2503R1	2015-12-03 10:50	0	212	212	100
32	750200005TL2503R2	2015-12-03 10:53	0	213	213	100
33	750200005TL2503R3	2015-12-03 10:56	0	213	213	100
34	75030000NTR2504R1	2015-12-03 01:29	0	174	174	100
35	75030000NTR2504R2	2015-12-03 02:02	0	171	171	100
36	75030000NTR2504R3	2015-12-03 02:29	0	171	171	100
37	75030000NTR2505R1	2015-12-03 01:29	0	302	302	100
38	75030000NTR2505R2	2015-12-03 02:02	0	261	261	100
39	75030000NTR2505R3	2015-12-03 02:29	0	261	261	100

Now, you can click to 'Remove' the unwanted sessions. If you remove the incorrect sessions by mistake, you can click on the undo icon on top left to reload all the available sessions in this project.



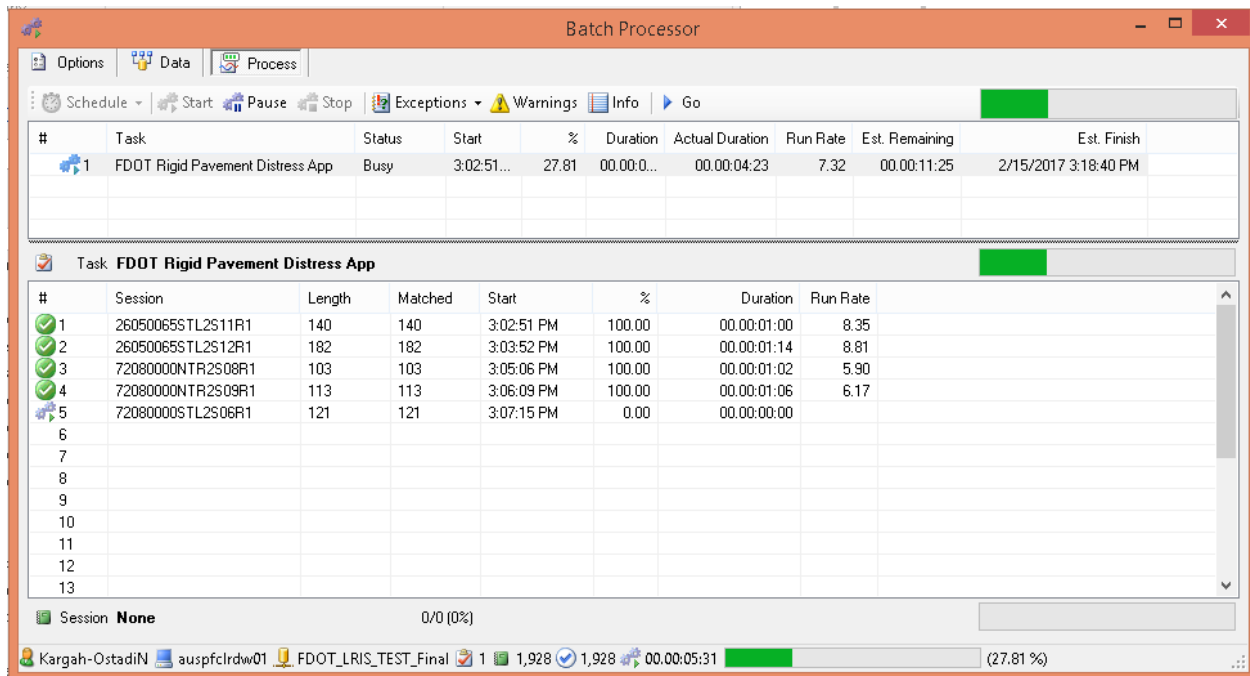
#	Session	Date	Vehicle	Collected	Matched	%
1	260500655TL2S11R1	2015-12-17 11:44	0	140	140	100
2	260500655TL2S12R1	2015-12-17 11:44	0	182	182	100
3	72080000NTR2S08R1	2015-12-02 01:44	0	103	103	100
4	72080000NTR2S09R1	2015-12-02 01:44	0	113	113	100
5	72080000TL2S06R1	2015-12-02 01:54	0	121	121	100
6	72080000TL2S07R1	2015-12-02 01:54	0	126	126	100
7	72290000TL3S10R1	2015-12-10 12:27	0	139	139	100
8	75010000TL2S01R1	2015-12-03 11:50	0	163	163	100
9	75010000TL2S02R1	2015-12-03 11:50	0	152	152	100
10	75020000TL2S03R1	2015-12-03 10:50	0	212	212	100
11	75030000NTR2S04R1	2015-12-03 01:29	0	174	174	100
12	75030000NTR2S05R1	2015-12-03 01:29	0	302	302	100

Process the selected data by clicking on the 'Process' menu on top, and choose 'Start':

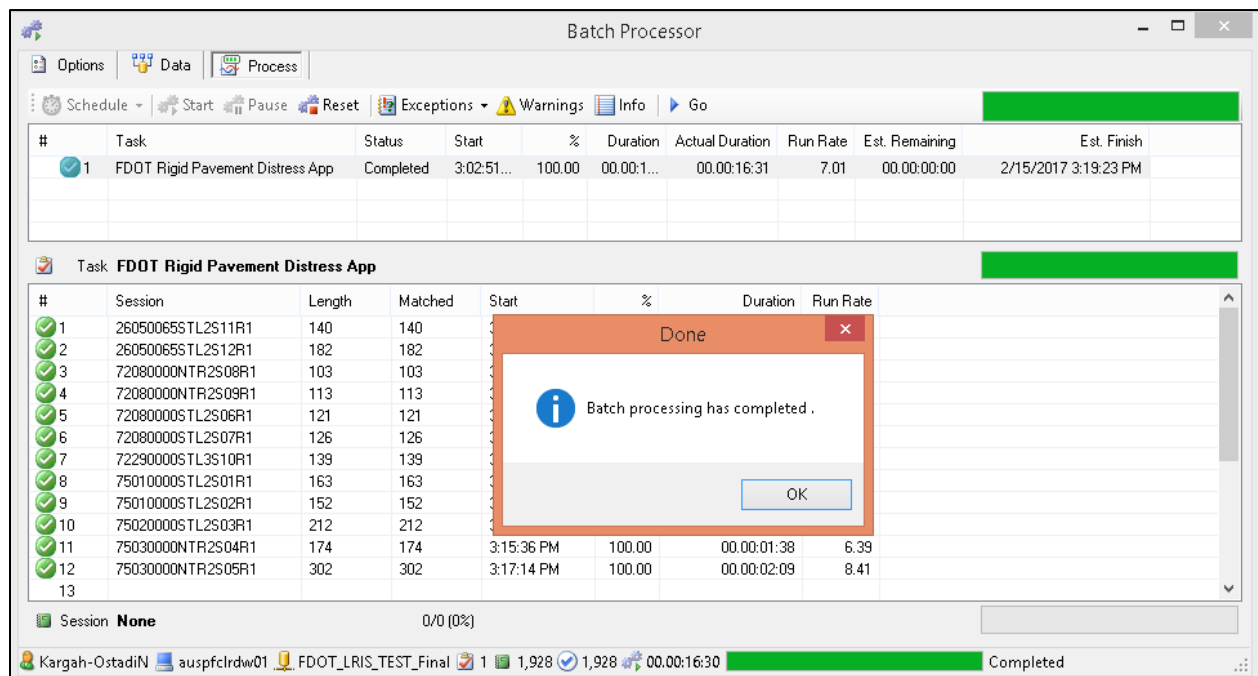


#	Task	Status	Start	%	Duration	Actual Duration
1	FDOT Rigid Pavement Dist...	Busy	11:02:10 AM	0.00	00:00:00:00	00:00:00:00

The 'Process' menu will show you the progress of the processing on each and all of the selected sessions. You can select 'Pause' or 'Stop' at any time during the process:

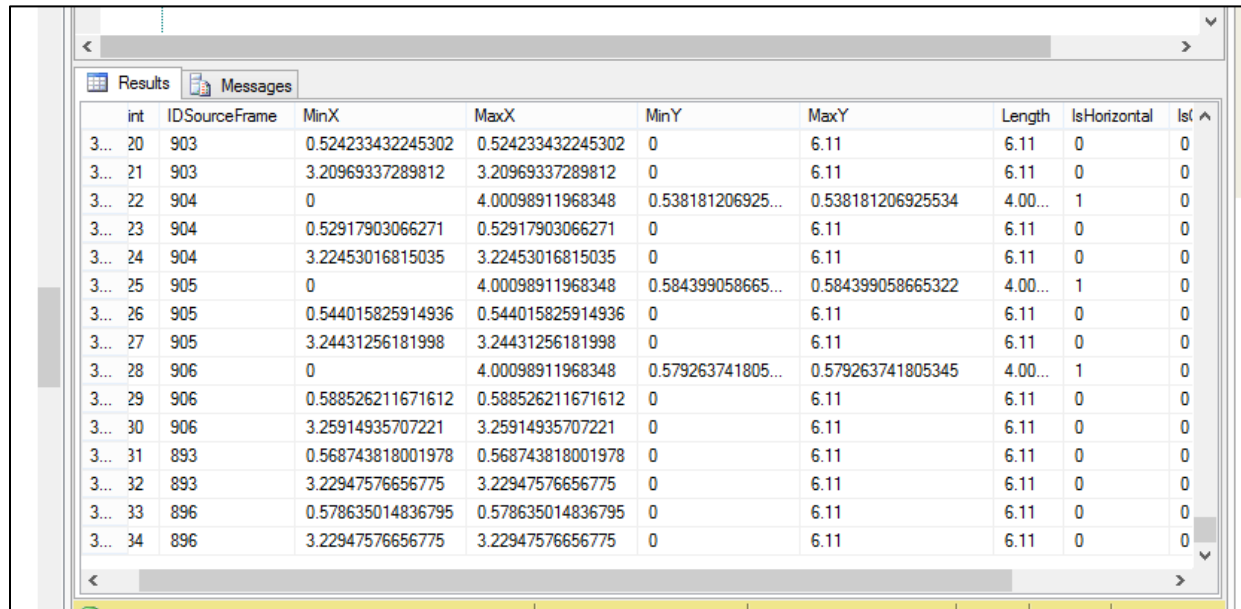


Once the joint detection is complete, you will be notified that 'Batch processing has completed':



You have to click on 'OK' so you can go back to the section to check the detection results. The detected joints have been written to the 'distress.Joints' table in the Vision

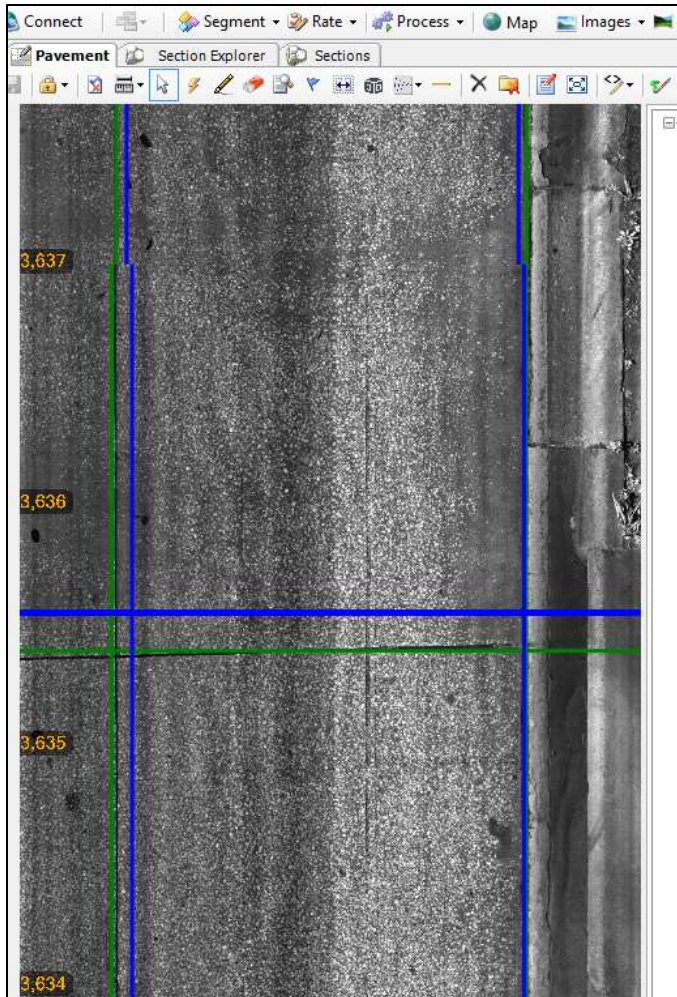
database corresponding to this specific project. The 'distress.Joints' table includes key information for the joints location, length, direction, and the image frame id. The following is a screen capture of the table:



int	IDSourceFrame	MinX	MaxX	MinY	MaxY	Length	IsHorizontal	Is
3... 20	903	0.524233432245302	0.524233432245302	0	6.11	6.11	0	0
3... 21	903	3.20969337289812	3.20969337289812	0	6.11	6.11	0	0
3... 22	904	0	4.00098911968348	0.538181206925...	0.538181206925534	4.00...	1	0
3... 23	904	0.52917903066271	0.52917903066271	0	6.11	6.11	0	0
3... 24	904	3.22453016815035	3.22453016815035	0	6.11	6.11	0	0
3... 25	905	0	4.00098911968348	0.584399058665...	0.584399058665322	4.00...	1	0
3... 26	905	0.544015825914936	0.544015825914936	0	6.11	6.11	0	0
3... 27	905	3.24431256181998	3.24431256181998	0	6.11	6.11	0	0
3... 28	906	0	4.00098911968348	0.579263741805...	0.579263741805345	4.00...	1	0
3... 29	906	0.588526211671612	0.588526211671612	0	6.11	6.11	0	0
3... 30	906	3.25914935707221	3.25914935707221	0	6.11	6.11	0	0
3... 31	893	0.568743818001978	0.568743818001978	0	6.11	6.11	0	0
3... 32	893	3.22947576656775	3.22947576656775	0	6.11	6.11	0	0
3... 33	896	0.578635014836795	0.578635014836795	0	6.11	6.11	0	0
3... 34	896	3.22947576656775	3.22947576656775	0	6.11	6.11	0	0

The detected joints have also been displayed as green solid lines on the pavement images:

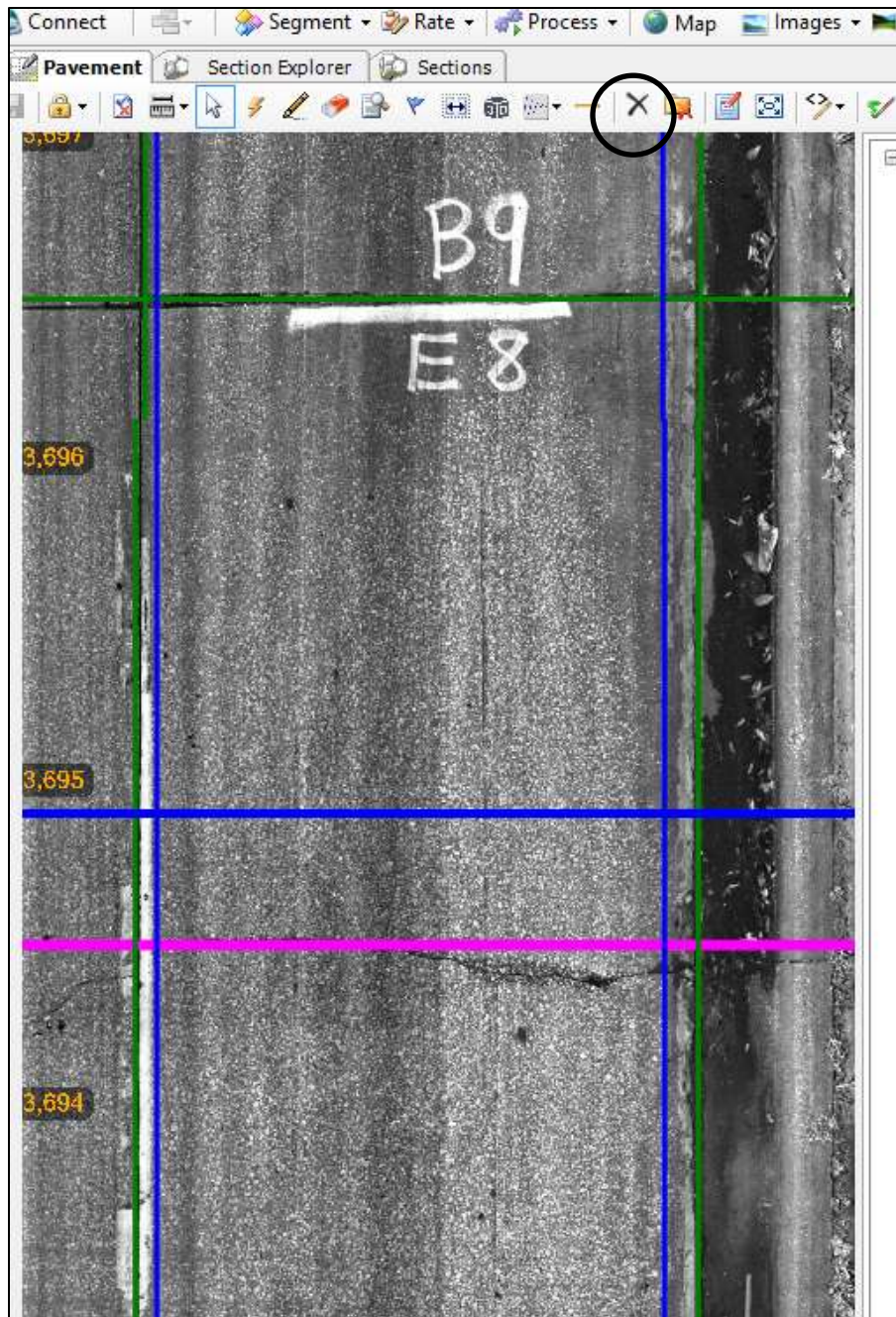




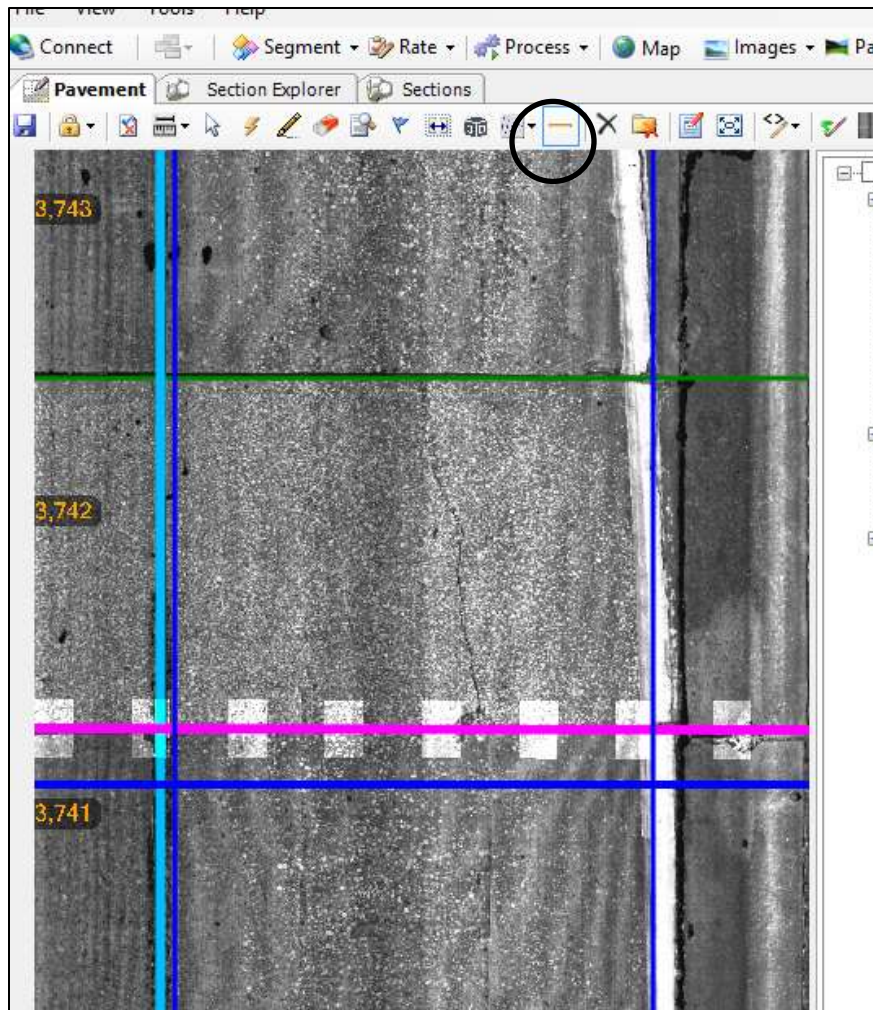
Most of joint detection results are accurate. However, A small number of false detection results and missed joints are unavoidable, specifically when skewed transverse joints or diagonal longitudinal joints are present. The user can go back to the pavement images to control the quality of the results and correct the minor errors.

Select the desired session from the 'Section Explorer' menu. Lock that session under your name to be able to conduct manual changes. To remove the unexpected joint detection results, select the joint using the arrow sign by left-clicking and dragging a window on to the joint. Then, click on the 'Delete' icon:





To insert a missed joint, click on the 'Joints' icon, and draw a joint in the corresponding location manually:



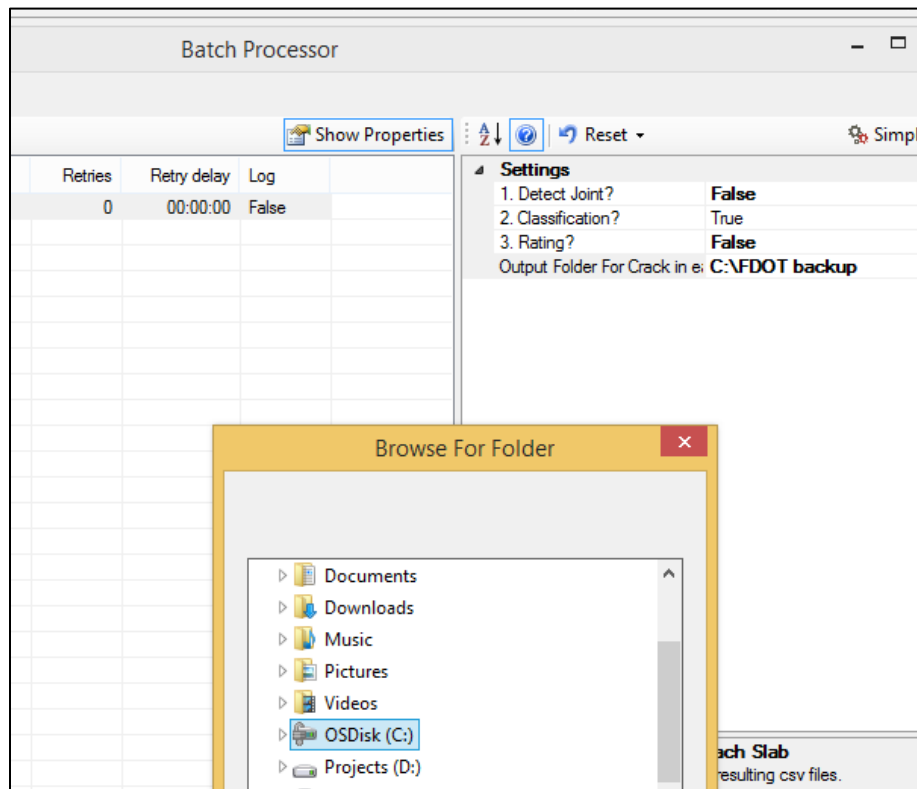
To save the drawn 'Joints', the user must save the results by clicking on the 'save' (floppy disc cartoon) icon. Please remember to unlock the session so that others can also access this session for any required further modification. The database will be automatically updated with these manual interventions. And the classification, and rating would be conducted based on the updated joint data.

#### **G.4.2. Classification, Grouping, Slab Assignment**

Select the batch processor 'FDOT Rigid Pavement Distress App' again. If you only need to classify the lines, set the 'Classification' as True and the 'Detect Joint' and 'Rating' as False. The user can also conduct both the Classification and Rating by setting them both as True. We recommend that the user would perform classification and rating at the same time.

During the classification, the line(s) will be classified as 'transverse' or 'longitudinal' according to their angle, and the slabs would be identified. If you would like to check the

results of identified slabs, you can save the results as a csv file in your chosen output folder:



The classification results would be displayed in the Vision software and written into the distress.CrackSets table in the Vision database.

The screenshot shows the Vision software interface. It features a toolbar with various icons for navigation and analysis. Below the toolbar is a 'Filter' section with a 'Filter crack types' dropdown. The main area displays a table of crack data. The table has columns: Frame, Chainage, Crack..., Sets (...), LaneWid..., Offset..., and U. The data is organized into rows, each representing a different frame and its corresponding crack data.

Frame	Chainage	Crack...	Sets (...)	LaneWid...	Offset...	U
3P000031.jpg	3,692.262	0	0	95.810	-2.567	
3P000032.jpg	3,696.190	1	1	95.504	-1.540	
3P000033.jpg	3,700.118	0	0	95.021	-1.774	
3P000034.jpg	3,704.046	1	1	94.308	-0.705	
3P000035.jpg	3,707.973	1	1	95.131	-0.403	
3P000036.jpg	3,711.901	0	0	96.921	-0.586	
3P000037.jpg	3,715.829	0	0	99.296	-0.111	
3P000038.jpg	3,719.757	1	1	100.009	-0.467	
3P000039.jpg	3,723.685	1	1	97.871	-1.061	
3P000040.jpg	3,727.613	0	0	97.608	-2.143	
3P000041.jpg	3,731.541	0	0	97.659	-2.830	
3P000042.jpg	3,735.469	0	0	97.608	-2.143	
3P000043.jpg	3,739.397	0	0	97.158	-1.655	

Results		Messages			
	IDCrackSet	IDCrackSetType	IsEdited	IDSourceFrame	IDSession
893	200431	2	0	1131	11
894	200432	2	0	1131	11
895	200457	1	0	1131	11
896	200458	2	0	1131	11
897	200459	2	0	1131	11
898	201566	1	0	1131	11
899	201567	2	0	1131	11
900	201568	2	0	1131	11
901	200433	1	0	1132	11
902	200434	2	0	1132	11
903	200435	1	0	1132	11
904	200460	1	0	1132	11
905	200461	2	0	1132	11
906	200462	1	0	1132	11
907	201569	1	0	1132	11

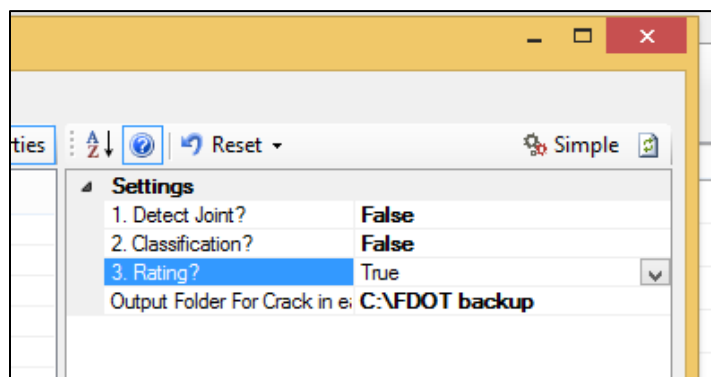
The app would also create a directory named 'Slab Coordinate' in the chosen output folder, the slab coordinates information would be saved in a .csv file with the same name as the session number. This file also includes other slab dimensional information:



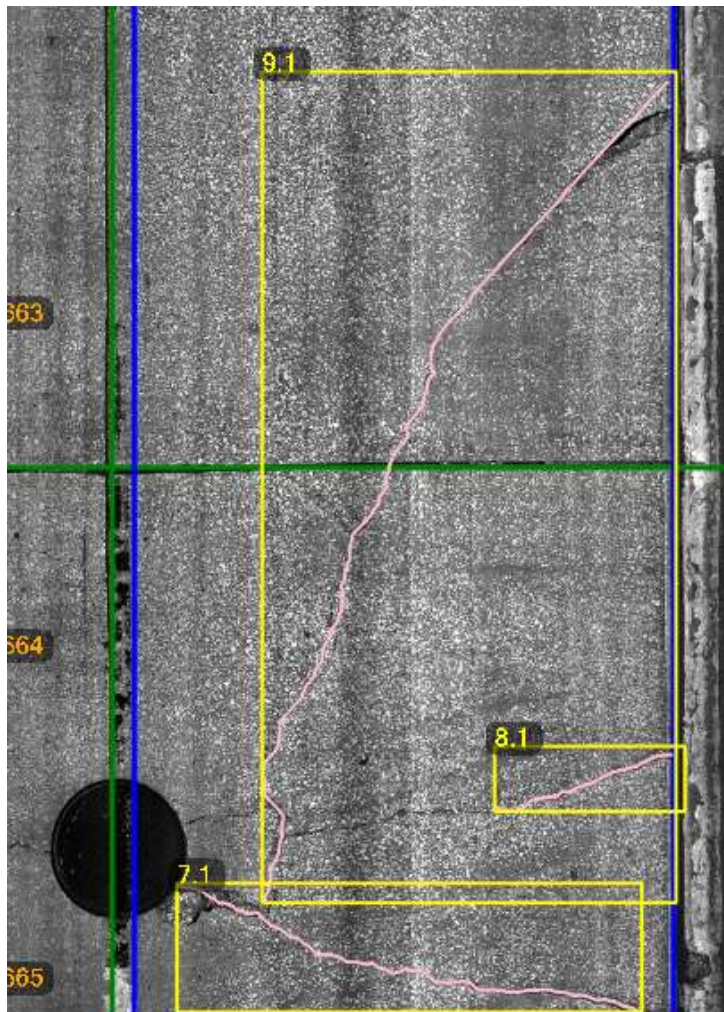
A	B	C	D	E	F	G	H	I	
IdSlab	MinX (m)	MinY (m)	MaxX (m)	MaxY (m)	Width (m)	Height (m)	Area (square meter)		
0	0.718023	190.2684	3.151585	192.7785	2.433562	2.510143	6.108589		
1	0.718023	192.7785	3.151585	198.7858	2.433562	6.007294	14.61912		
2	0.747976	198.7858	3.161713	204.9163	2.413737	6.130541	14.79751		
3	0.748192	204.9163	3.161713	211.0315	2.413521	6.115135	14.75901		
4	0.781593	211.0315	3.179815	215.6728	2.398221	4.641299	11.13086		
5	0.781593	215.6728	3.197916	220.31	2.416323	4.637191	11.20495		
6	0.736124	220.31	3.197916	229.6542	2.461792	9.344223	23.00353		
7	0.718023	229.6542	3.258254	238.8402	2.540231	9.186055	23.3347		
8	0.705955	238.8402	3.185202	248.0972	2.479247	9.256922	22.95019		
9	0.687854	248.0972	3.168393	253.0568	2.48054	4.959689	12.30271		
10	0.687854	253.0568	3.168393	257.3346	2.48054	4.277719	10.61105		
11	0.687854	257.3346	3.168393	266.5497	2.48054	9.21515	22.85855		
12	0.724056	266.5497	3.191882	268.3632	2.467826	1.813456	4.475295		
13	0.796462	268.3632	3.191882	285.0961	2.39542	16.73292	40.08236		
14	0.80853	285.0961	3.270322	286.9448	2.461792	1.848714	4.551149		
15	0.802496	286.9448	1.721068	294.353	0.918572	7.408208	6.804975		
16	1.721068	286.9448	3.270322	294.353	1.549253	7.408208	11.47719		
17	0.802496	294.353	3.306524	303.6623	2.504029	9.309302	23.31076		
18	0.826631	303.6623	1.65183	305.4699	0.825199	1.807632	1.491655		
19	1.65183	303.6623	3.306524	305.4699	1.654695	1.807632	2.991078		

### G.4.3. Distress Rating and QC

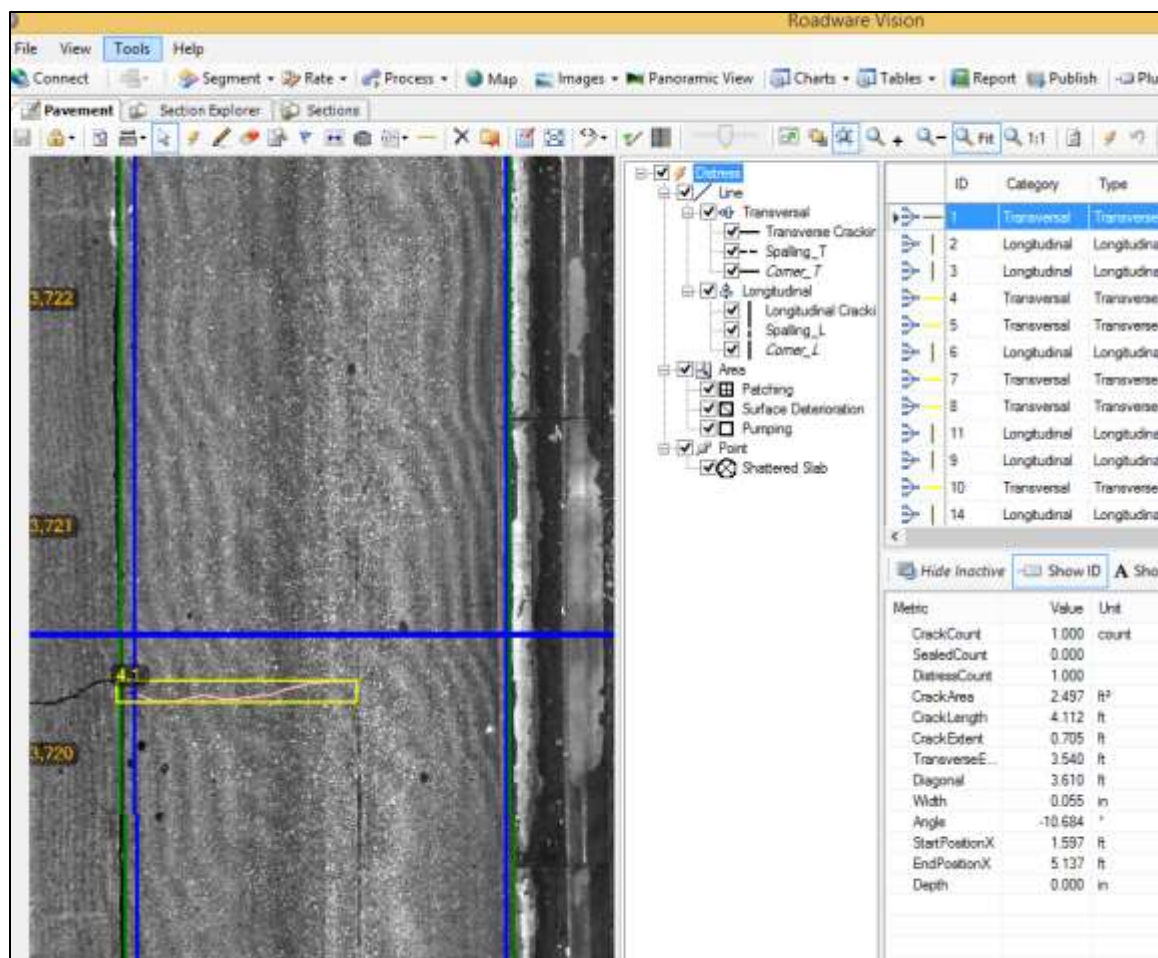
If you already rated the cracks, skip this step. If not, select the batch processor 'FDOT Rigid Pavement Distress App' again, and set the 'Rating' as True, and others as False. Note that you must perform the Classification before Rating.



Here is an example image after processing is complete:



After the distress rating has been completed, the rating results would be displayed on both pavement images in the Vision software and tables in the Vision database.



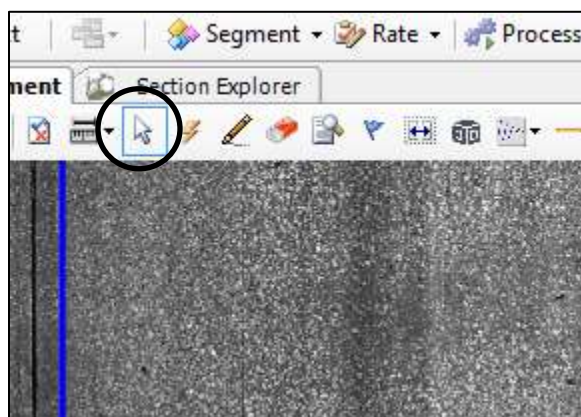
The rating results have been also written to the distress.DistressRecords table in Vision database:

IDDistressRecord	IDDistressType	IDSeverity	IDSession	DistanceStamp	Length	StartX	EndX
100	39071	11	1	11	276.049712187531	3.36260533332825	2.32977247238159
101	39072	11	1	11	286.912961355927	0.558722496032715	2.17144751548767
102	39073	13	1	11	285.090950838806	0.0243072509765625	2.80811095237732
103	39074	11	1	11	284.499362580063	2.31191945075989	2.06923842430115
104	39075	13	2	11	286.871365420105	0.0229377746582031	0
105	39076	13	2	11	288.277488447907	0.467142581939697	1.85459959506989
106	39077	13	1	11	307.125225836517	0.091066837310791	1.72799217700958
107	39078	13	1	11	306.449076468231	0.296393871307373	2.32344222068787
108	39079	11	2	11	314.13219467807	0.576182842254639	1.570392370224
109	39080	13	2	11	312.931215445282	0.0174598693847656	0
110	39081	13	1	11	319.208626772644	0.113661766052246	1.68348181247711
111	39082	13	2	11	328.083823811295	0.330372095108032	3.02670645713806
112	39083	13	2	11	365.867260023834	0.433934211730957	0.0138476770371199
113	38406	11	1	15	141.932027751587	0.880192995071411	2.2729971408844
114	38407	13	1	15	145.866250926636	0.0123248100280762	0.429277986288071
115	38408	13	1	15	145.64000045051	0.217052020552055	2.20200041247650

The app would also create a directory named 'Distress in Slab' in the chosen output folder, the identified distress information would be saved in a .csv file with the same name as the session number.

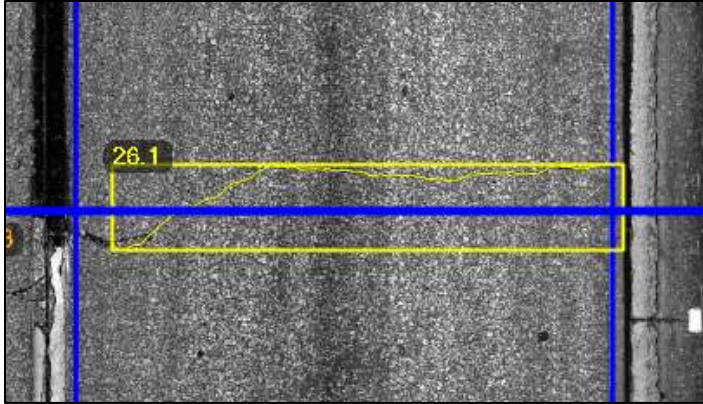
A	B	C	D	E	F	G
IdSlab	IdCrack	Category	Length	Width	Severity	
0	0	Transvers	1.253235	0.001395	Light	
1	1	Longitudi	0.852869	0.001027	Light	
2	1	Longitudi	0.852869	0.001027	Light	
3	2	Longitudi	1.049851	0.001027	Light	
4	3	Transvers	1.711818	0.01431	Moderate	
5	4	Transvers	2.696447	0.014518	Moderate	
6	5	Longitudi	0.592308	0.001027	Light	
7	6	Transvers	3.127531	0.016172	Moderate	
8	7	Transvers	3.657009	0.001027	Light	
9	8	Longitudi	2.835426	0.012069	Moderate	
10	9	Transvers	3.434857	0.002381	Light	
11	10	Longitudi	2.502945	0.001142	Light	
12	10	Longitudi	2.502945	0.001142	Light	
13	11	Longitudi	0.638515	0.002456	Light	
14	12	Transvers	0.609582	0.001027	Light	
15	13	Longitudi	3.602159	0.023969	Moderate	
16	14	Transvers	1.201836	0.003543	Moderate	

The user can go back to the session by double clicking on the session number to check the final distress rating results. The user can select each one of the identified distresses from the list on the right or the images on the left using the cursor button:

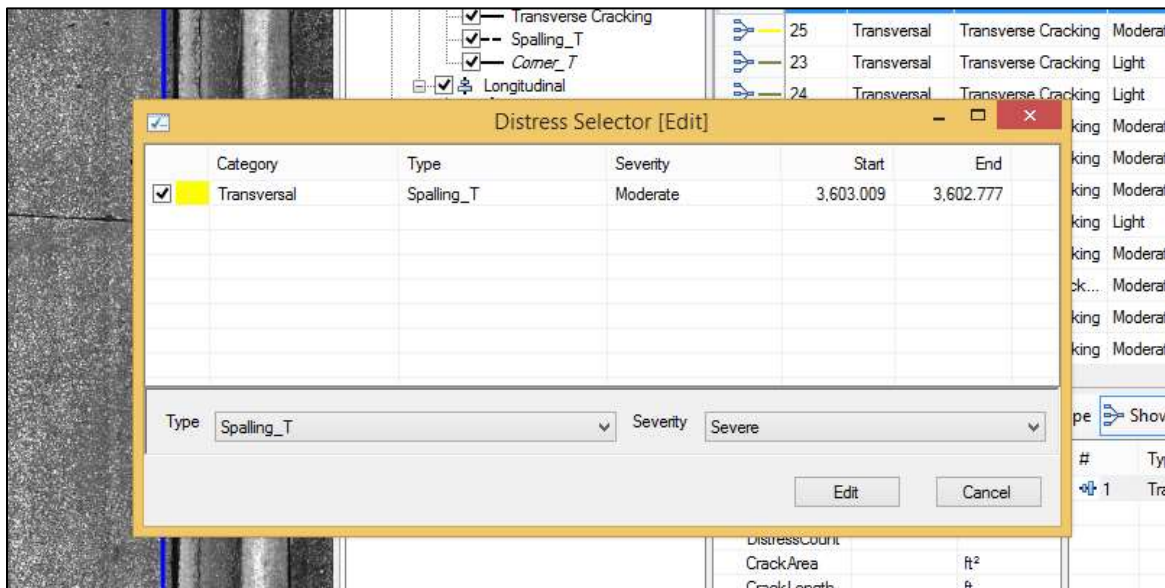


And the blue horizontal line will be centered on the selected distress, which is highlighted in the list of distresses displayed on the right hand side:





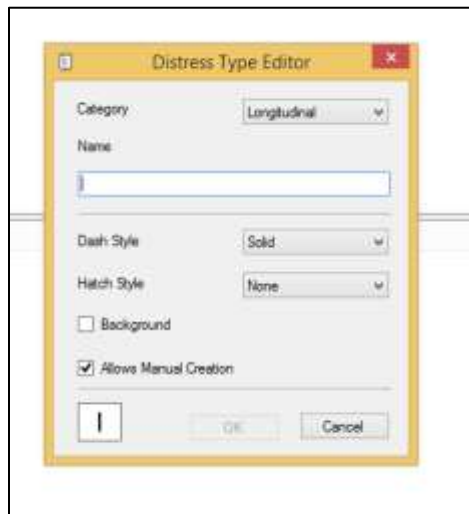
During the QC review of the distress identification results, the user can modify the type and severity of the selected distress by clicking on the modify button, which will open the corresponding edit window:



## G.5. Setting Up a Schema

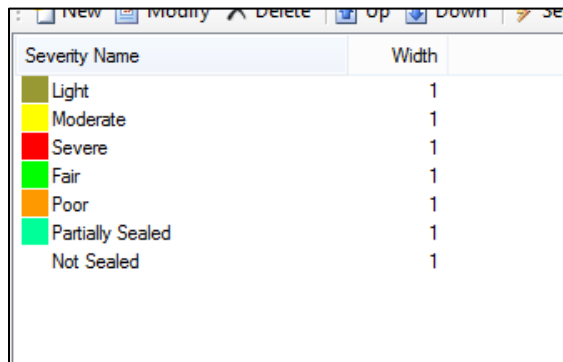
Create Distress Types (Distress Name and category listed as following):

Distress Name	Allows Manual	Category
— Transverse Cracking	Yes	Transversal
Longitudinal Cracking	Yes	Longitudinal
· Spalling_L	Yes	Longitudinal
- Spalling_T	Yes	Transversal
Corner_L	Yes	Longitudinal
- Corner_T	Yes	Transversal
⊗ Shattered Slab	Yes	Point
▣ Patching	Yes	Area
▣ Surface Deterioration	Yes	Area
□ Pumping	Yes	Area



Note: you don't need to set up distress type for 'Joints'. It is an internal distress type in Vision.

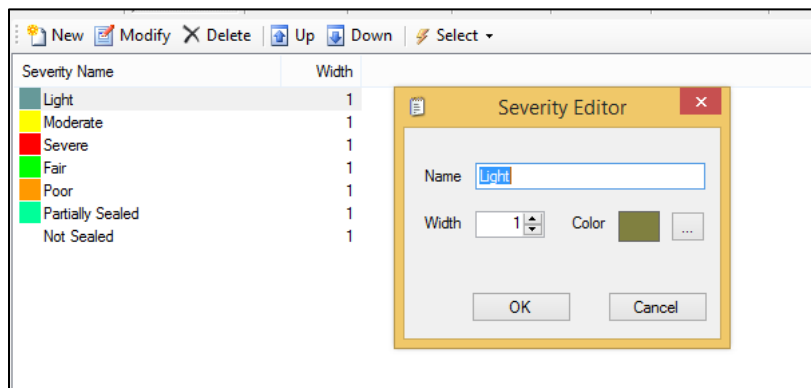
Create severity level list by using severity editor (the rated crack would be displayed according to severity level):



The screenshot shows a window titled 'Severity Editor' with a menu bar containing 'New', 'Modify', 'Delete', 'Up', 'Down', and 'Select'. Below the menu is a table with two columns: 'Severity Name' and 'Width'.

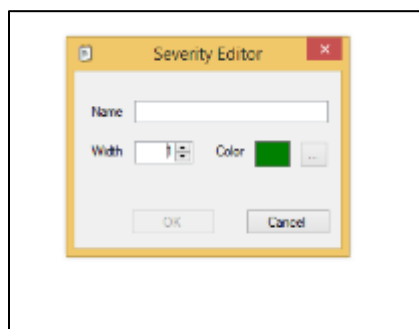
Severity Name	Width
Light	1
Moderate	1
Severe	1
Fair	1
Poor	1
Partially Sealed	1
Not Sealed	1

Modify:



The screenshot shows the 'Severity Editor' window with the 'Light' severity level selected. A dialog box titled 'Severity Editor' is open, showing the 'Name' field with 'Light', the 'Width' field with '1', and the 'Color' field with a brown color swatch. The dialog box has 'OK' and 'Cancel' buttons.

New:



The screenshot shows the 'Severity Editor' dialog box for creating a new severity level. The 'Name' field is empty, the 'Width' field is set to '1', and the 'Color' field has a green color swatch. The dialog box has 'OK' and 'Cancel' buttons.

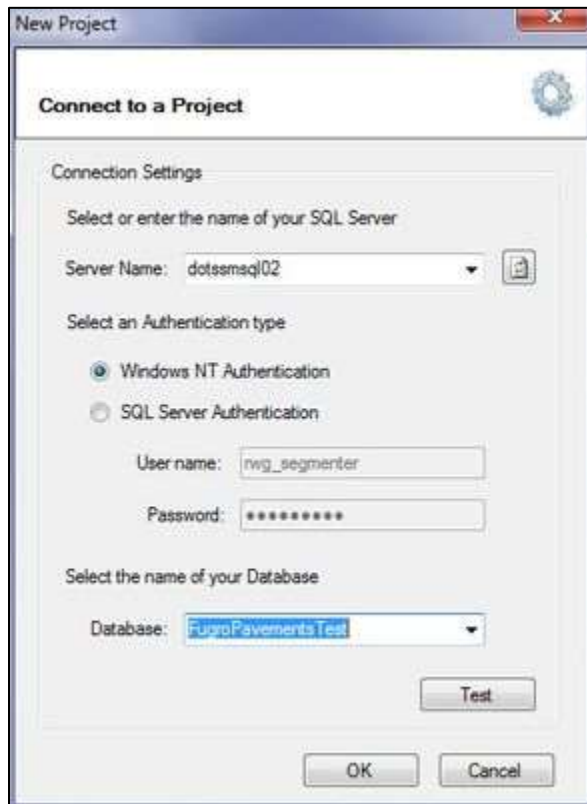
## G.6. Using Basic Vision Functions

The following show some instructions on using basic Vision functions after starting up the software.

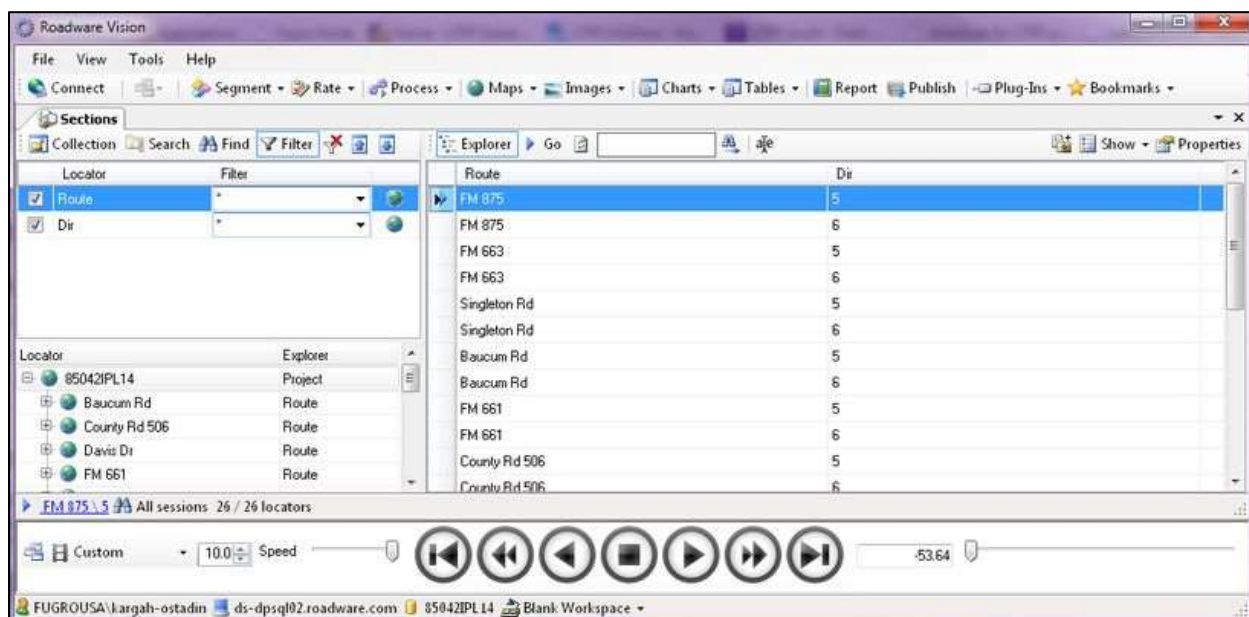
### G.6.1. Connecting to a Project

Click on "Connect" (top left-hand side), and recent databases that you have accessed will be listed. To connect to a new project, click on "New" and a window will allow you to enter the server name where the data is stored, username and password to access the server, and the name of the database which you would like to connect to.

- Database Server Name: **dotssmsql02**
- Database Name: (example) **FugroPavementsTest**
- Select: **Windows NT Authentication**

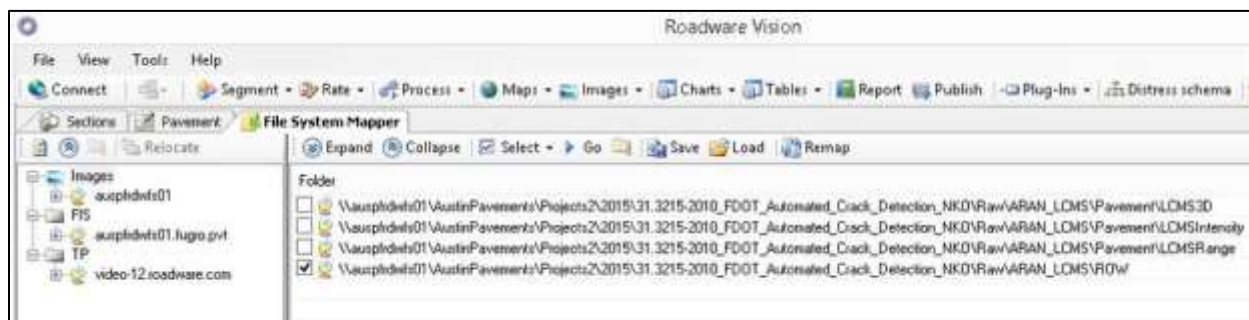


When connected, a list of the sections in the database will appear on the screen. You can click on "Show" to filter out the sections which do not have corresponding data. By double clicking on one of the Routes, you will select that route file and a blue arrow will appear to indicate that selection.

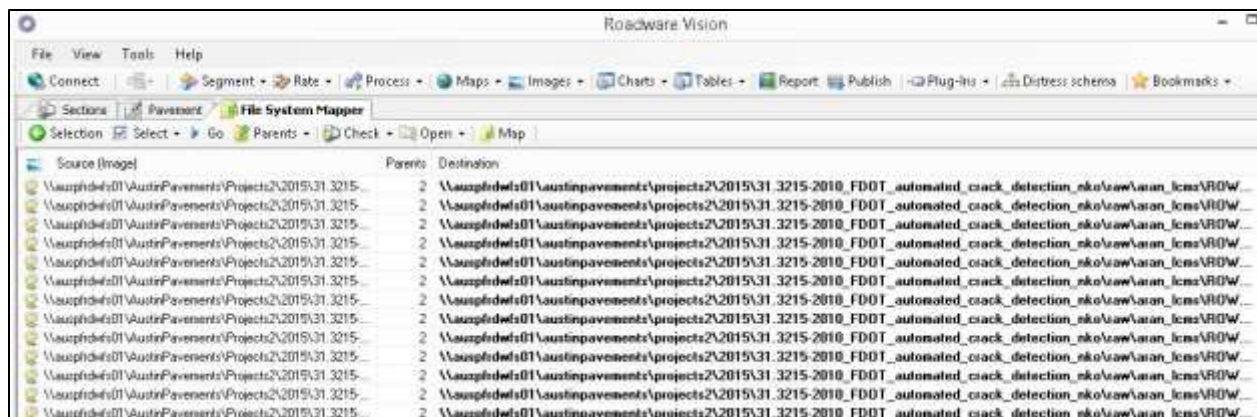


## G.6.2. Connecting to the Images for the Project

If this is the first time you or any of your colleagues are accessing this database, then you need to make sure that the project contains the correct links to the directory where the corresponding images are stored. Go to the File System Mapper under the Tools menu. Select the image type(s) for which you would like to specify a directory and then click on Remap:



Then you will be able to enter a new directory address for those images and click OK. then you will see a list of all the images found. Click on Check >> Destination. If the images exist, the destination addresses will turn bold:



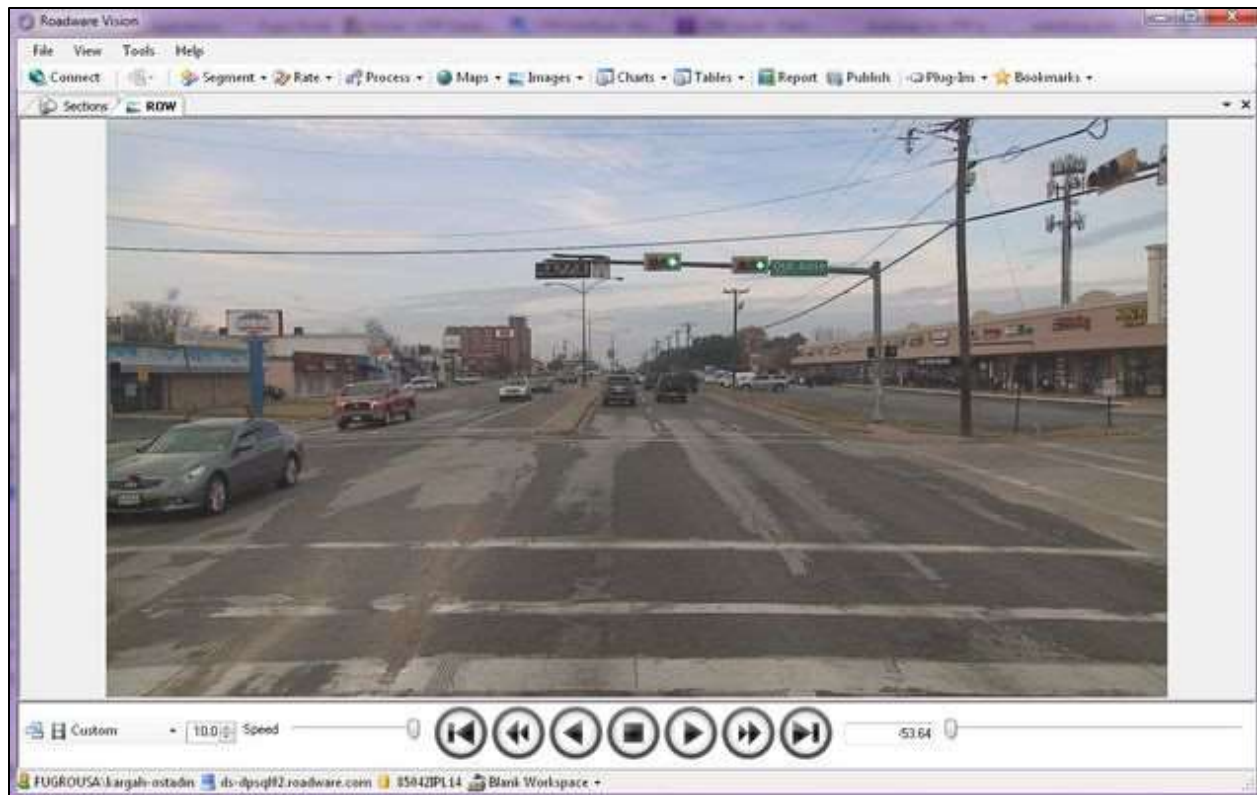
Now you can click on Map and the correct image paths will be restored. Please note that this will update the image paths for this project for all users. Therefore, this needs to be done once, preferably by the administrator of that project and then everyone will be able to see the images. In order for Vision to run faster, it is recommended that the images be stored on the FDOT server.

### G.6.3. Opening ROW and Pavement Images

From the menu bar, select "Images" and then select "ROW" or "Pavement" images.

*Existing database does not yet contain ROW Images.*





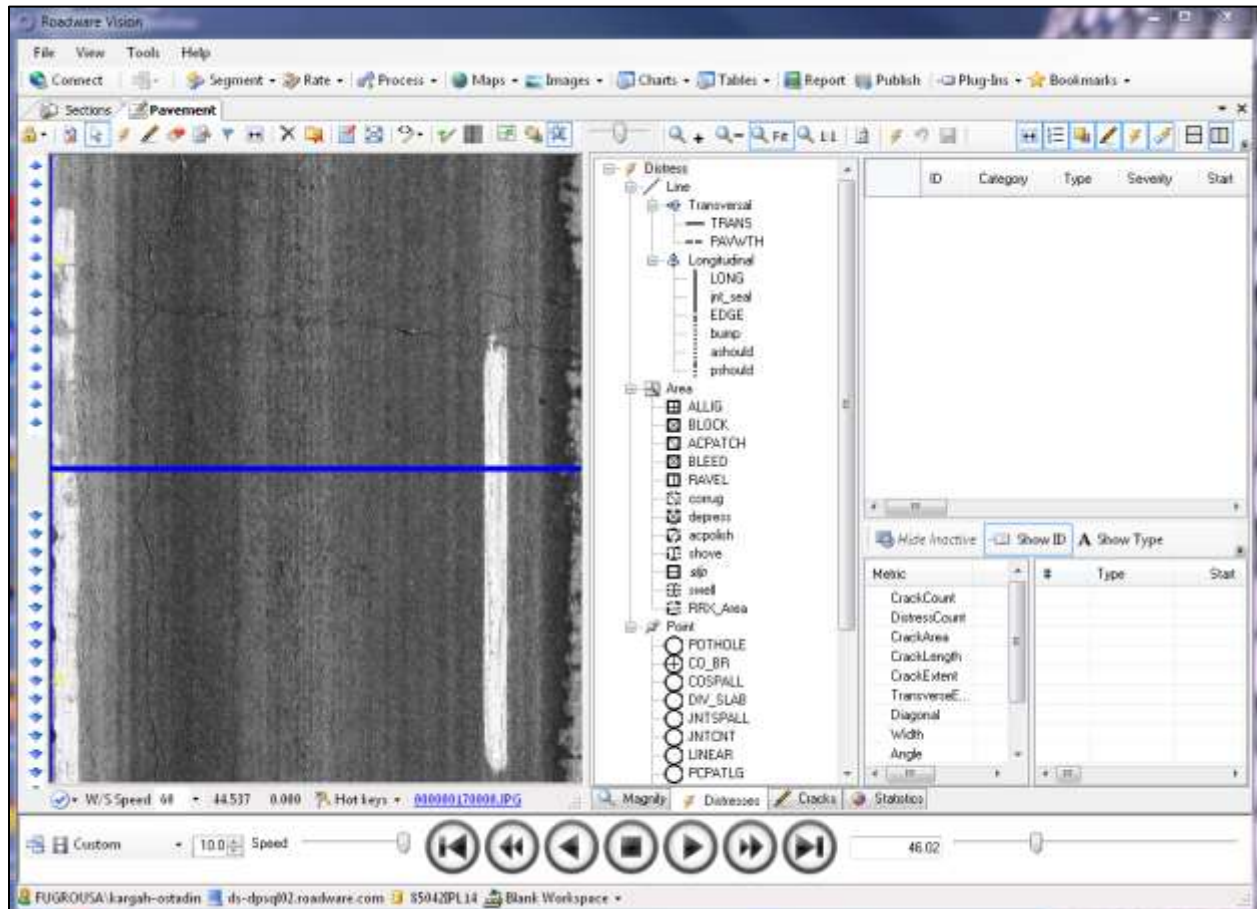
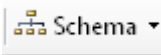
You can move any of the opened tabs ("Sections" and "ROW" in this example) around your screen to arrange the windows according to your preferences. If you have multiple monitors, you can right-click on any tab, select "undock" and then move the new window to another monitor screen.

The play-stop-forward-backward buttons can be used to see images along the length of the roadway. The play speed can be adjusted. The slider bar on the right-hand side shows the location in milli-miles from the beginning of the roadway section.

#### **G.6.4. Pavement Distress Rating**

From the "Rate" menu, select "Pavement Distress" and you will see the module for 1) detecting lines, 2) classifying cracks by type (longitudinal, transverse, etc.), and 3) rating the detected cracks (assigned as specific distresses). The pavement surface distresses can be either rated manually on the collected digital images (a process referred to as semi-automated distress survey) or rated automatically using crack detection software. In the case of automated distress surveys, a post-survey manual QC is required to ensure quality.

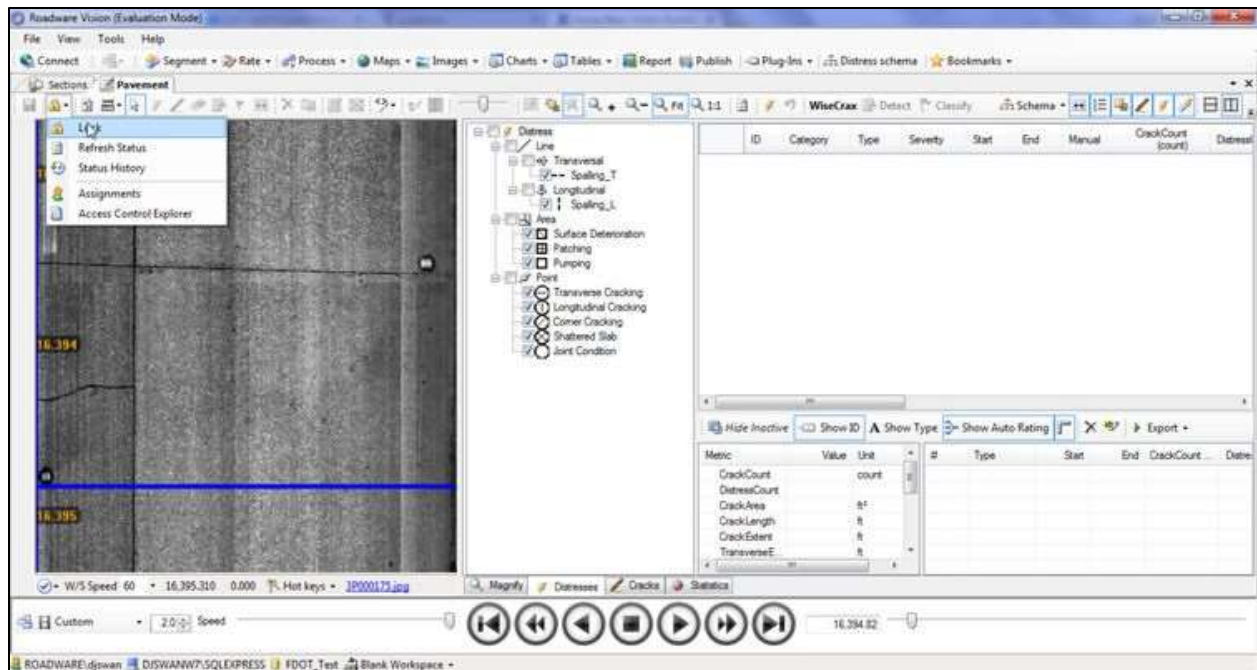
The available distress types and the corresponding severity levels are preset using the distress schema:




You can again use the media buttons at the bottom to see pavement images along the test section. Alternatively, you can use the blue arrows on the left side of the pavement image to move forward or backward in the pavement distress rating module. You can also adjust the speed of scrolling by moving your mouse up and down the arrows. The BLUE horizontal line on the pavement image shows the exact location of the mileage indicated at the bottom of the screen.

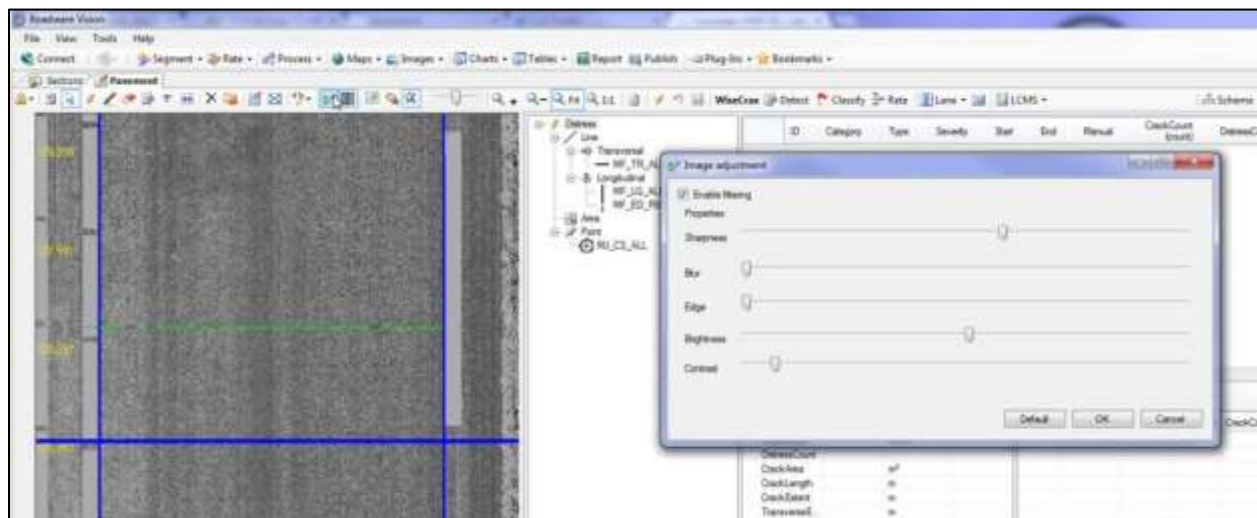
Before one can start a distress survey on any pavement section, that specific section needs to be "locked" under their name. This ensures that only one person at a time can have access to add/edit pavement distresses on that section. Click on the lock icon on the top left side, from the menu select "Assignments" and you can see a list of assignments for each user and the status of the assignments. Here you can select a user and lock or unlock the section. You should lock it under your user name to be able to work on that section.





After you have "locked" a pavement section under your name, you can also edit the appearance of pavement imagery to facilitate manual rating of the pavement images.


Using the  button from the top of the pavement image, you will be provided with an image adjustment window as in the following screen to edit properties such as sharpness, brightness, and contrast. Please note that these modifications will only affect the image appearance for manual rating and will not affect the automated distress identification process.

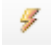


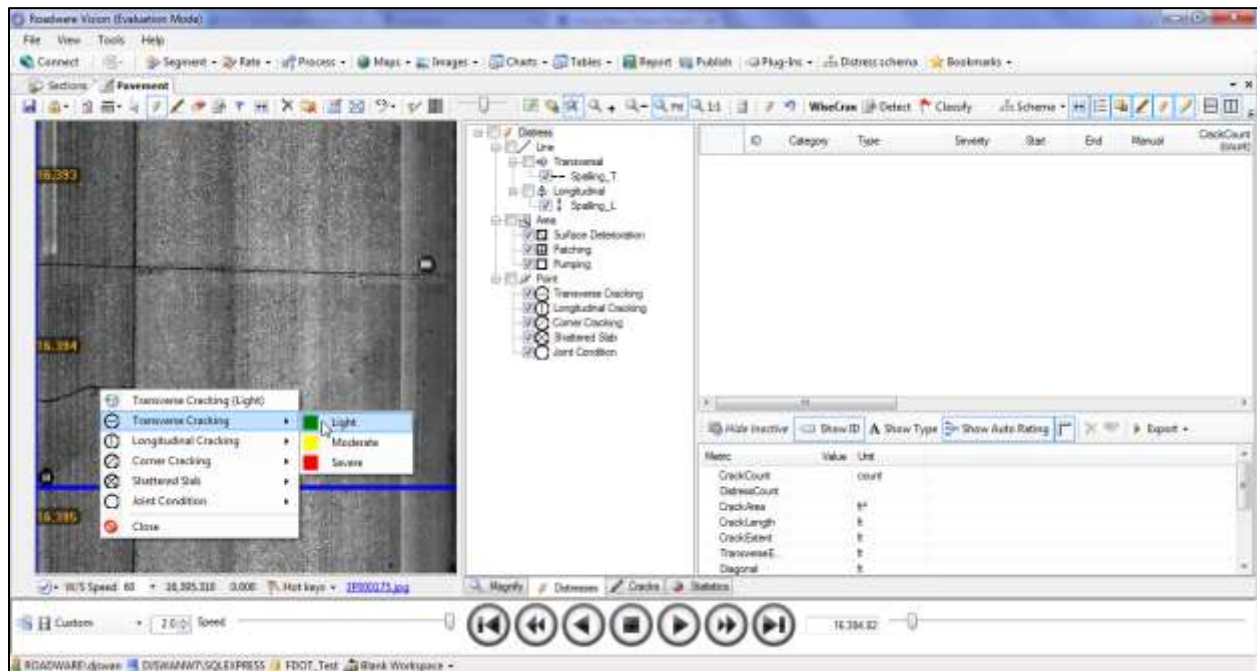
## G.6.5. Manual Distress Rating

There are a variety of tools for drawing cracks and distresses on pavement surface.





At the first step, you will need to identify the edges of the lane that you would like to rate. Using this button  you can drag and adjust the lane edges on the left and right. The lane edge adjustment will need to happen at specified intervals or whenever you deem necessary.


You can use this button  on the top left to draw distresses. If you would like to identify linear distresses such as spalling, you should left-click the beginning and the end points for the crack and depending of the angle of the created line (less than or more than 45 degrees), the software will give you options to select from the available distresses. You can also select from the defined list of severity levels. For example, you can see a longitudinal crack in the following example:




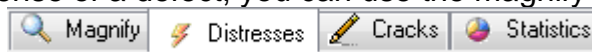
If you would like to identify an area type distress (fatigue cracking, patching, etc.), then you should left-click and drag to draw a box, and the software will give you the available distress options and severity levels for each. If you would like to identify a point type distress (counting the number of joints with defined condition, or number of shattered

slabs), then you should double-click on the pavement image and the software will give you the available distress options and severity levels for each.

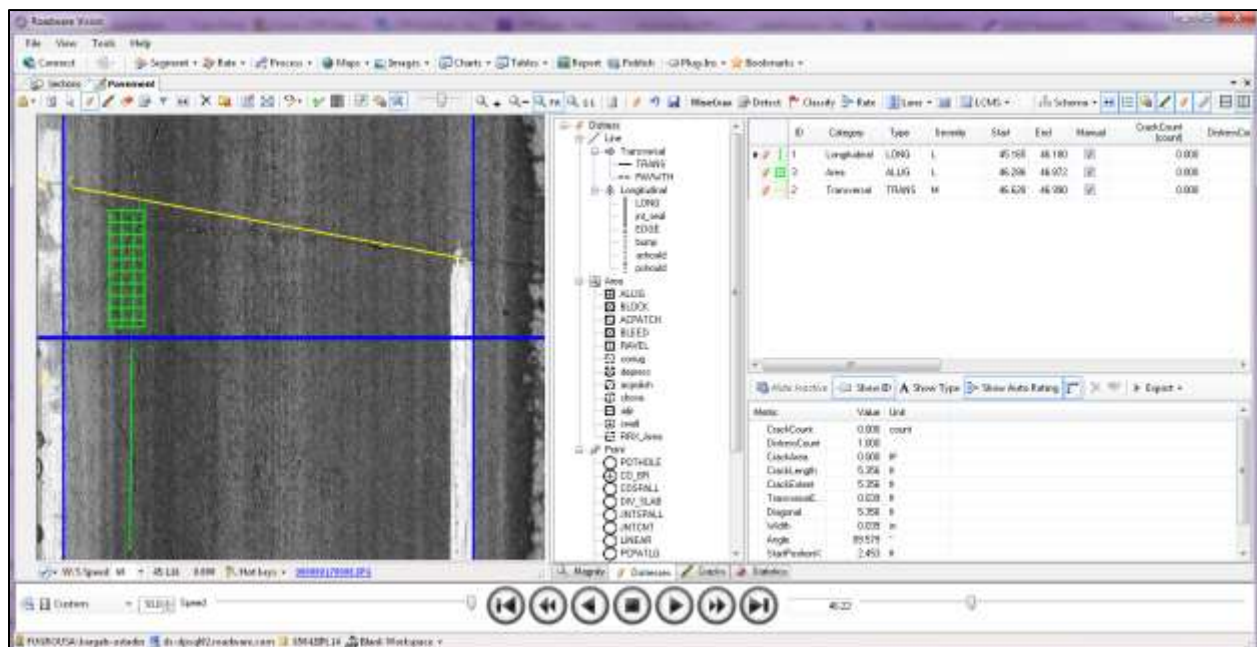
If you would like to erase a distress you can use the erase  button and you can identify the distresses that you would like to erase. An alternative option would be to use the delete  button.



if you would like to modify a distress type or severity, you can use the modify  button.

If you need to measure distress dimensions to assign appropriate severity levels, you can use the measurement  button. Also, if you need to zoom into a specific part on pavement surface to make sense of a defect, you can use the magnify tab at the bottom right of the pavement image:



The following example shows low-severity longitudinal, moderate-severity transverse, and low-severity alligator cracking instances. The identified distresses are listed on the right-hand side according to the mile post.



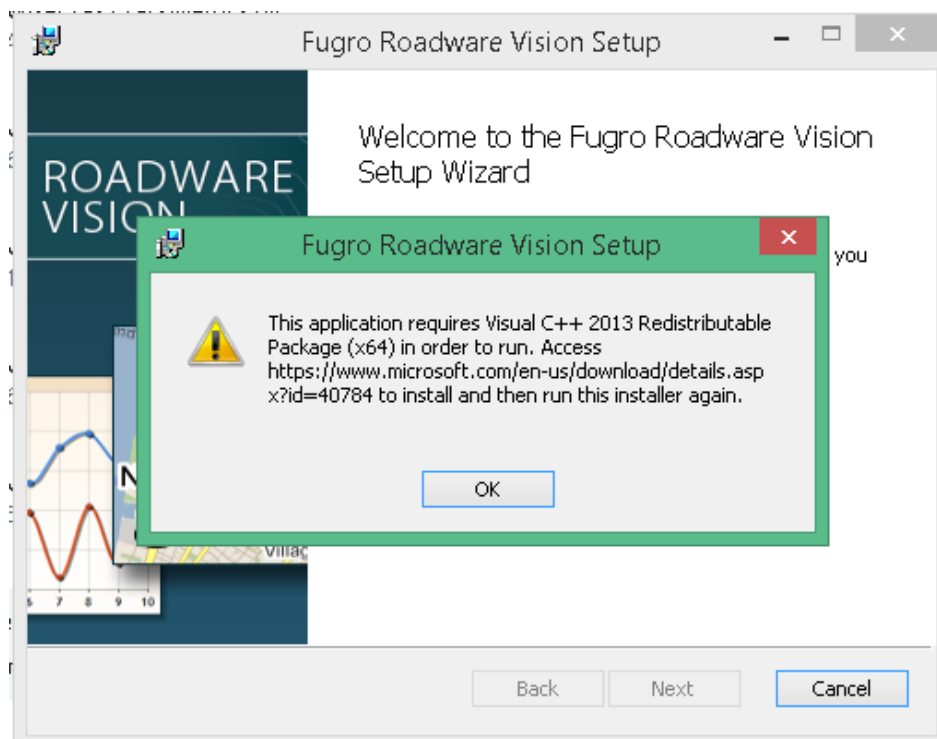
If you would like others to be able to see the results of your distress survey, you should save your work with the save  button. Be CAUTIOUS as the Undo  button will undo all the distresses that you have drawn on the pavement image since the last time that you hit the save button.

## G.7. Installation Instructions for Fugro Vision Platform and the FDOT Rigid Pavement Distress App

0) Uninstall the current Fugro Roadware Vision

1) Install Fugro Roadware Vision 3.1.1 using the provided msi file.

If there is an error regarding C++ (see below), install the vc\_redist\_x64.exe file and then install Vision.



Please note that for the Vision software, you will need to enter the licence key to extend the availability of the software from 30 days to 365 days. Please contact Fugro for a license key if you have not been provided one.

2) Copy the following .dll files into this folder (replace the files in the destination folder):

C:\Program Files\Fugro Roadware\Fugro Roadware  
Vision\LCMS\LcmsAnalyserLib\_4\_13\_0\_0\_64bit\



Roadware.LCMS.Imaging.dll  
17 KB



WiseCrax.Application.dll  
143 KB



WiseCrax.Classify.dll  
84 KB



WiseCrax.Common.dll  
143 KB



WiseCrax.CrackMetrics.dll  
47 KB



WiseCrax.Detect.dll  
644 KB



WiseCrax.Factory.dll  
107 KB



WiseCrax.FisExtract.dll  
64 KB



WiseCrax.Lane.dll  
59 KB

**3) Copy the following .dll file into this folder:**

C:\Program Files\Fugro Roadware\Fugro Roadware Vision\



Roadware.Algorithm.FDOT.JointDetection.dll  
53 KB

**4)** Copy the following .dll file into this folder:

C:\Program Files\Fugro Roadware\Fugro Roadware Vision\Plugin\Processors\Cracks\



Roadware.Processing.FDOT.JointDetection.dll  
61 KB

**5)** Now, run Vision and connect to the following test database to test if everything is working fine:

database name: FDOT\_LRIS\_TEST\_Final

## H. DOCUMENTATION OF 24 SELECTED PROCESSED IMAGES OF RIGID PAVEMENTS

All the processed images can be reviewed through the Fugro Vision platform to observe the performance of the crack detection and classification processes. In this appendix, screen captures of the processed images for 24 selected images (2 images from each of the 12 test sections) have been recorded from Vision.

**Table 108. List of Sample Image Frames Processed for Rigid Pavements**

Image Number	Test Section	Image Frame
1	Section 1	3P000019
2	Section 1	3P000020
3	Section 2	3P000115
4	Section 2	3P000116
5	Section 3	3P000029
6	Section 3	3P000022
7	Section 4	3P000014
8	Section 4	3P000024
9	Section 5	3P000767
10	Section 5	3P000768
11	Section 6	3P000022
12	Section 6	3P000023
13	Section 7	3P000062
14	Section 7	3P000061
15	Section 8	3P000006
16	Section 8	3P000010
17	Section 9	3P000031
18	Section 9	3P000038
19	Section 10	3P000052
20	Section 10	3P000053
21	Section 11	3P000044
22	Section 11	3P000045
23	Section 12	3P000087
24	Section 12	3P000088



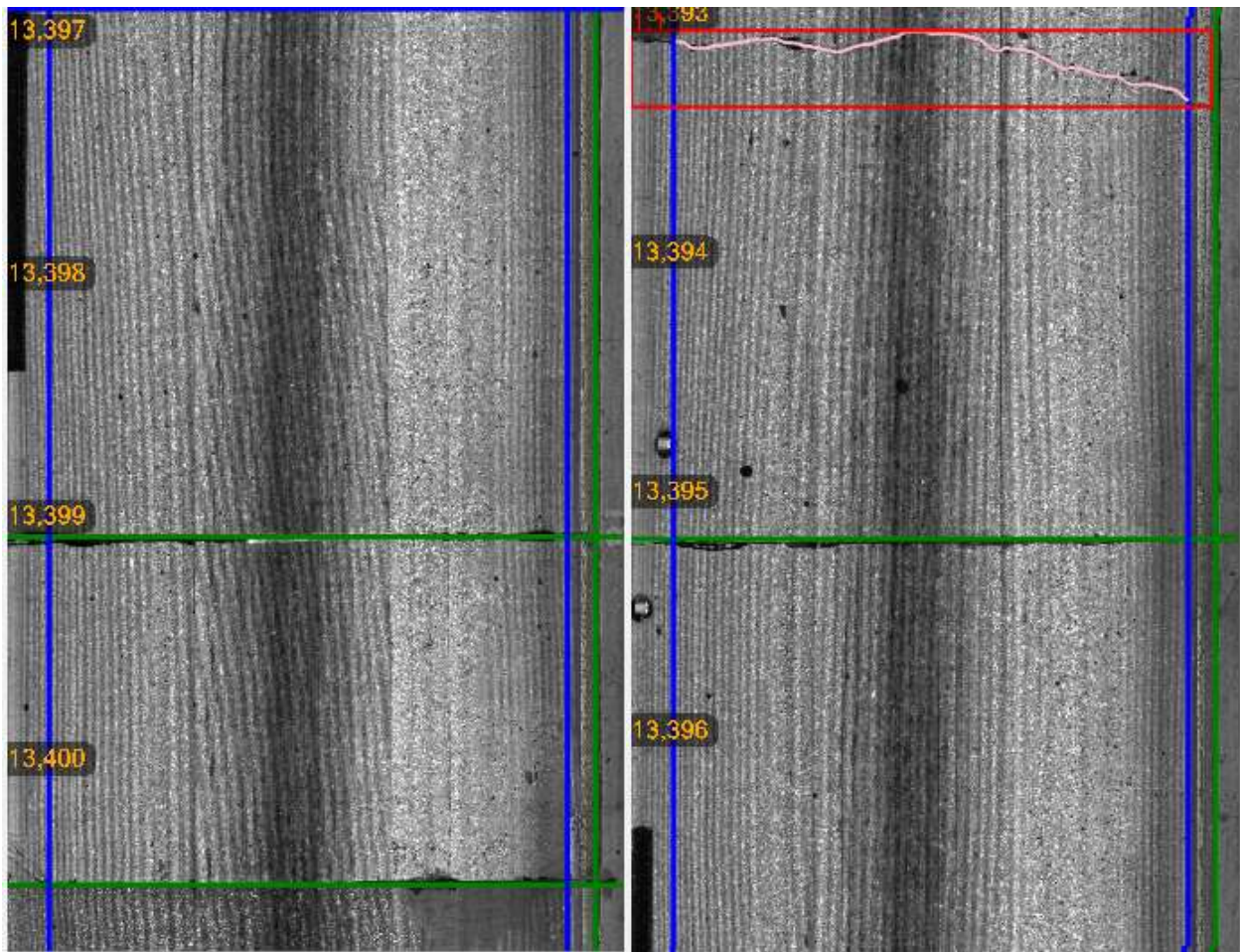
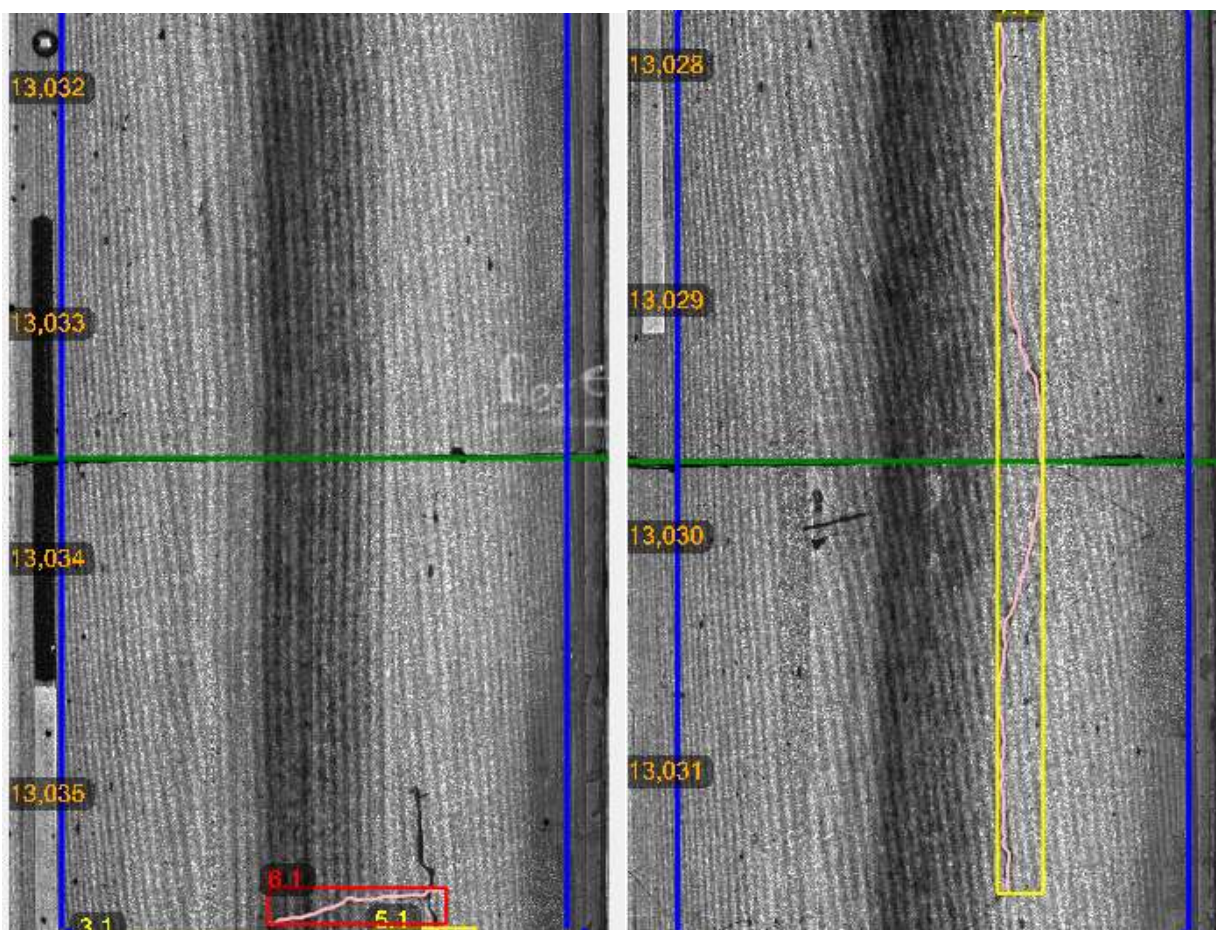


Figure 194. (Left) Image Number 1 (Frame 19); (Right) Image Number 2 (Frame 20) from Section 1





**Figure 195. (Left) Image Number 3 (Frame 115); (Right) Image Number 4 (Frame 116) from Section 2**

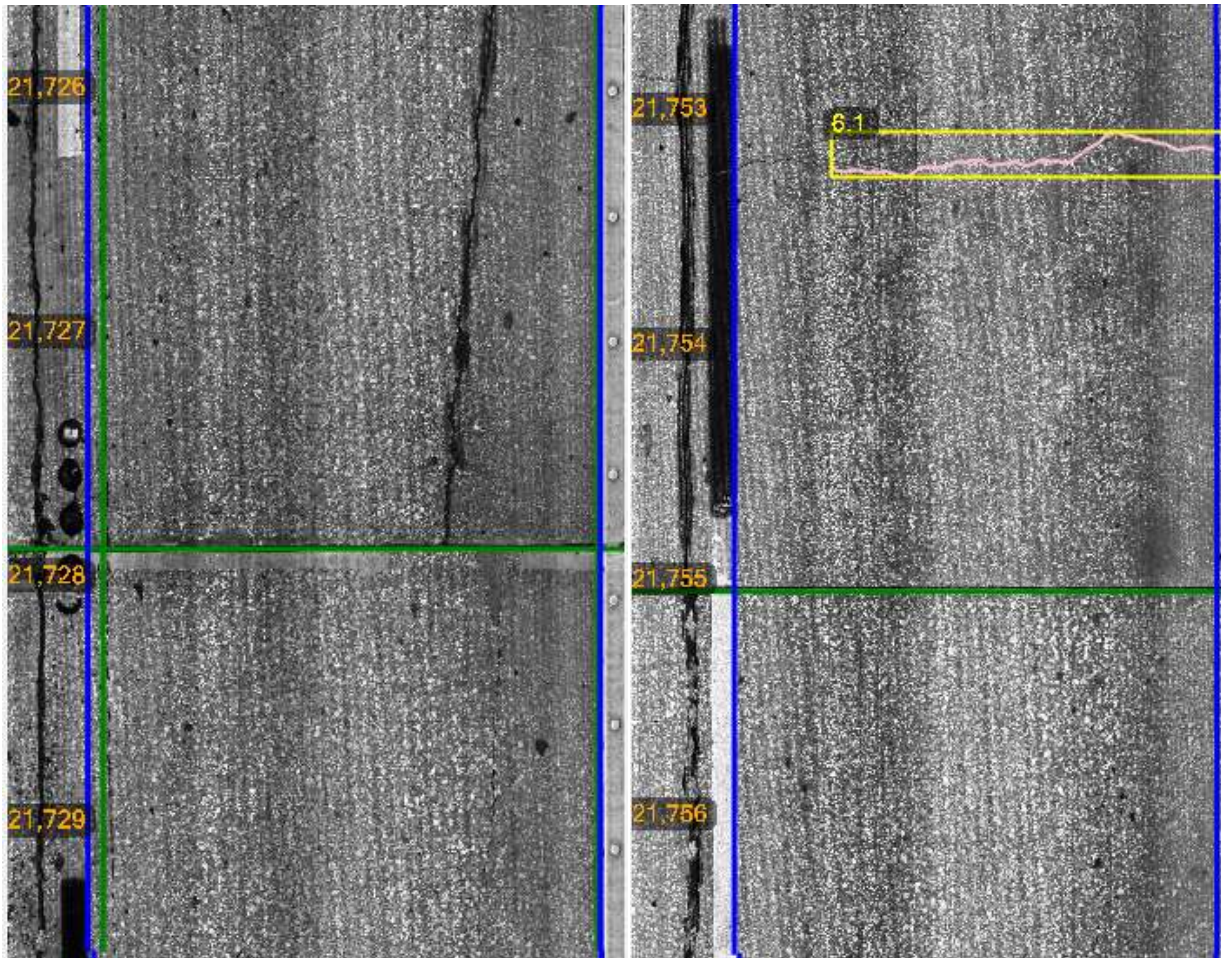


Figure 196. (Left) Image Number 5 (Frame 29); (Right) Image Number 6 (Frame 22) from Section 3



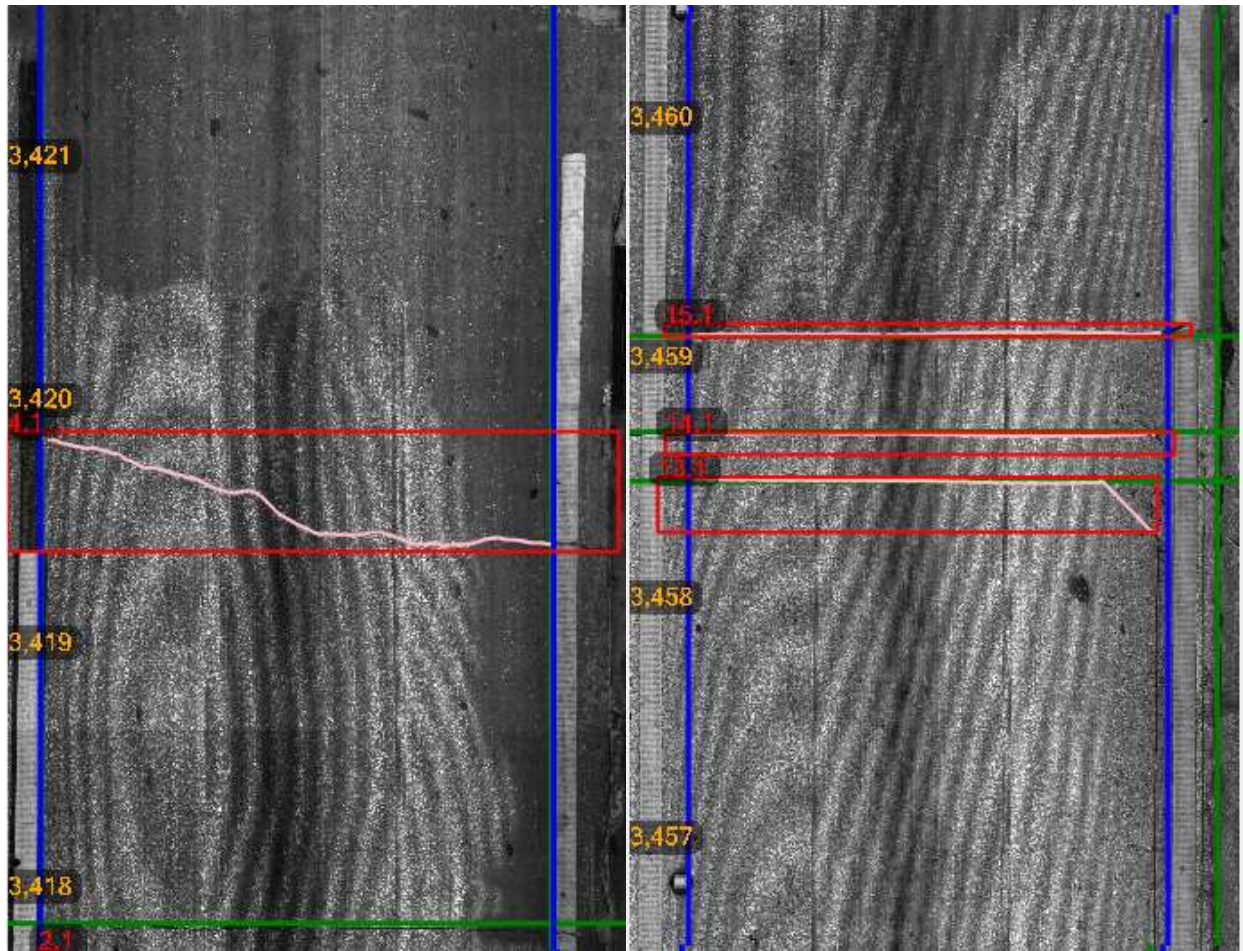


Figure 197. (Left) Image Number 7 (Frame 14); (Right) Image Number 8 (Frame 24) from Section 4

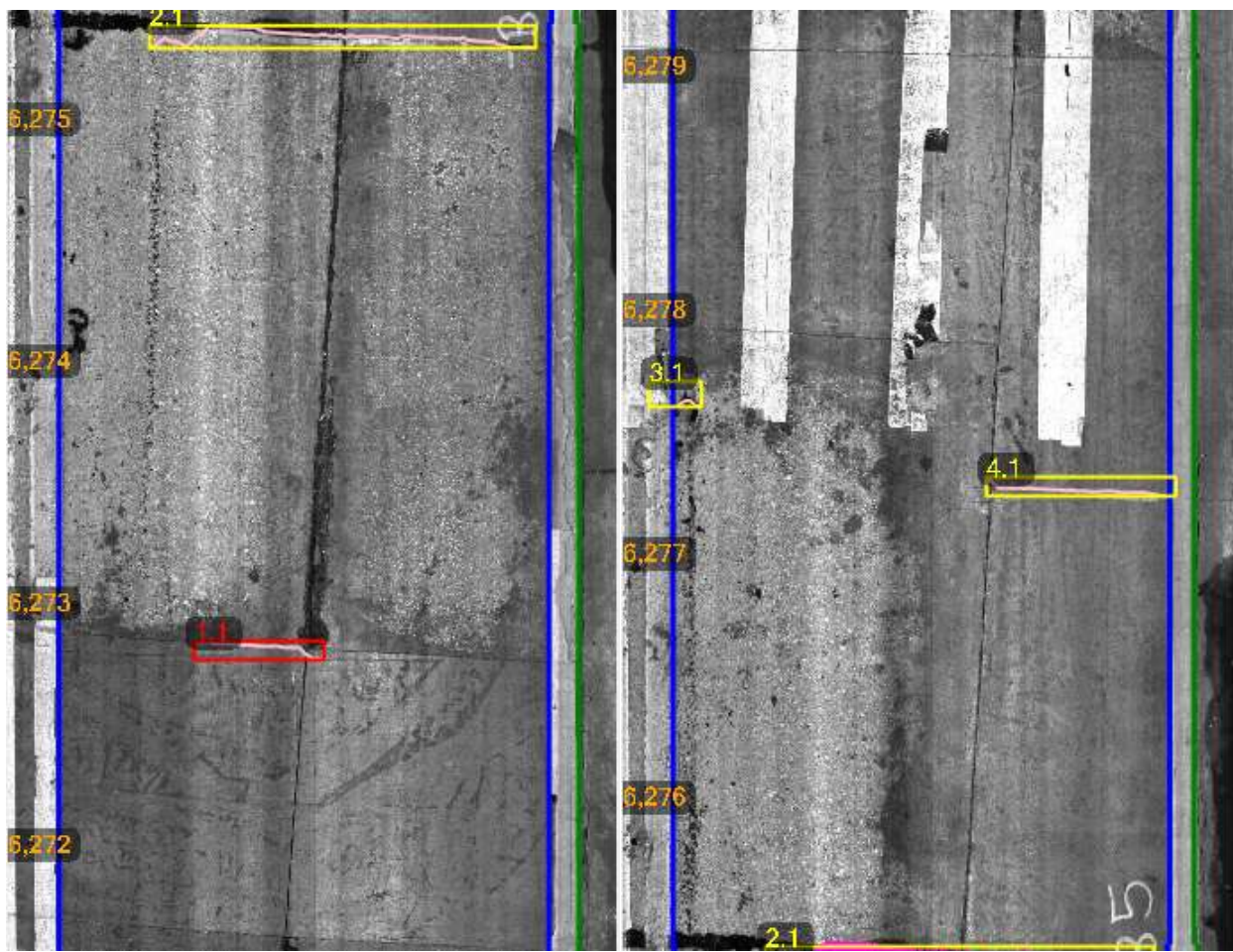


Figure 198. (Left) Image Number 9 (Frame 767); (Right) Image Number 10 (Frame 768) from Section 5



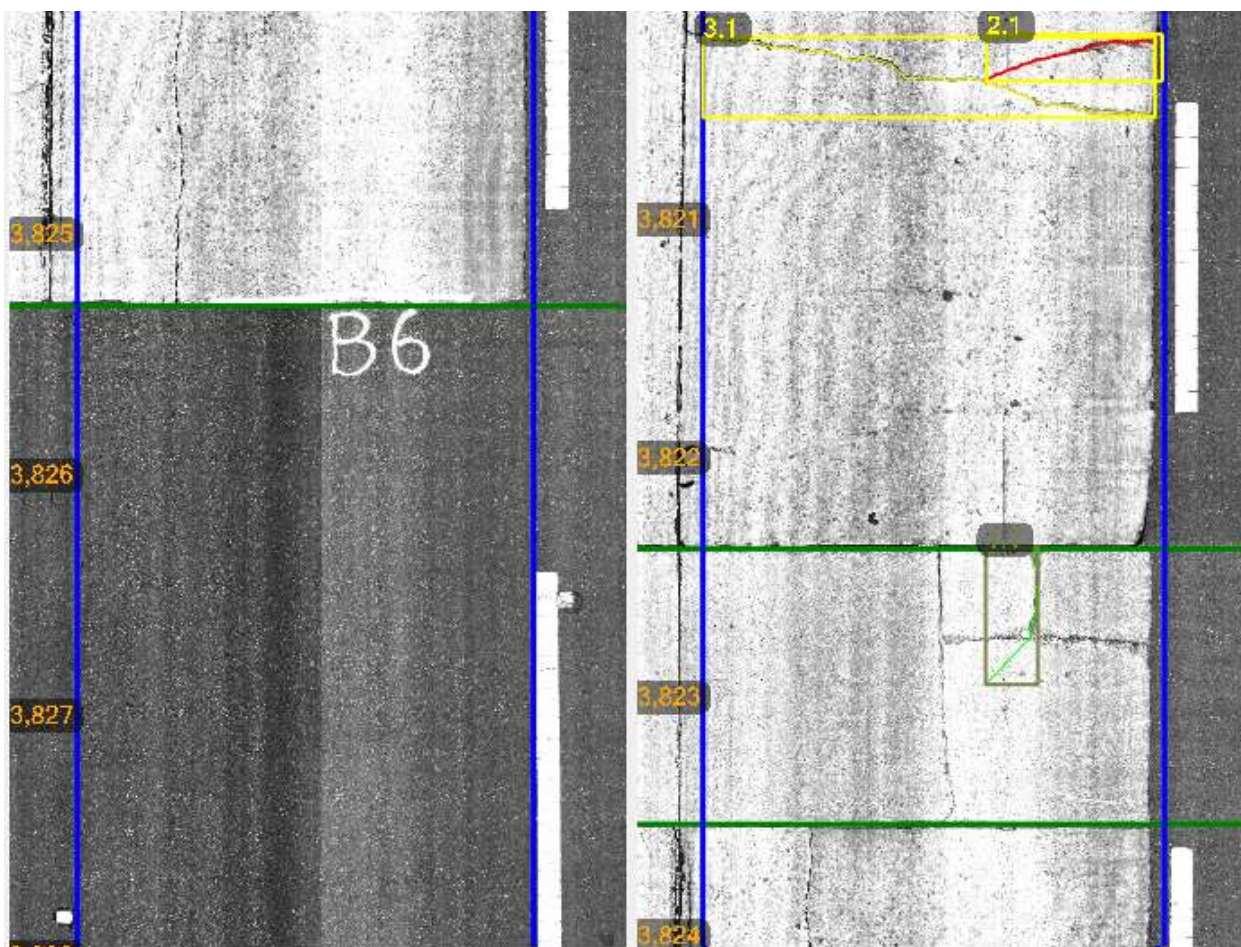


Figure 199. (Left) Image Number 11 (Frame 22); (Right) Image Number 12 (Frame 23) from Section 6

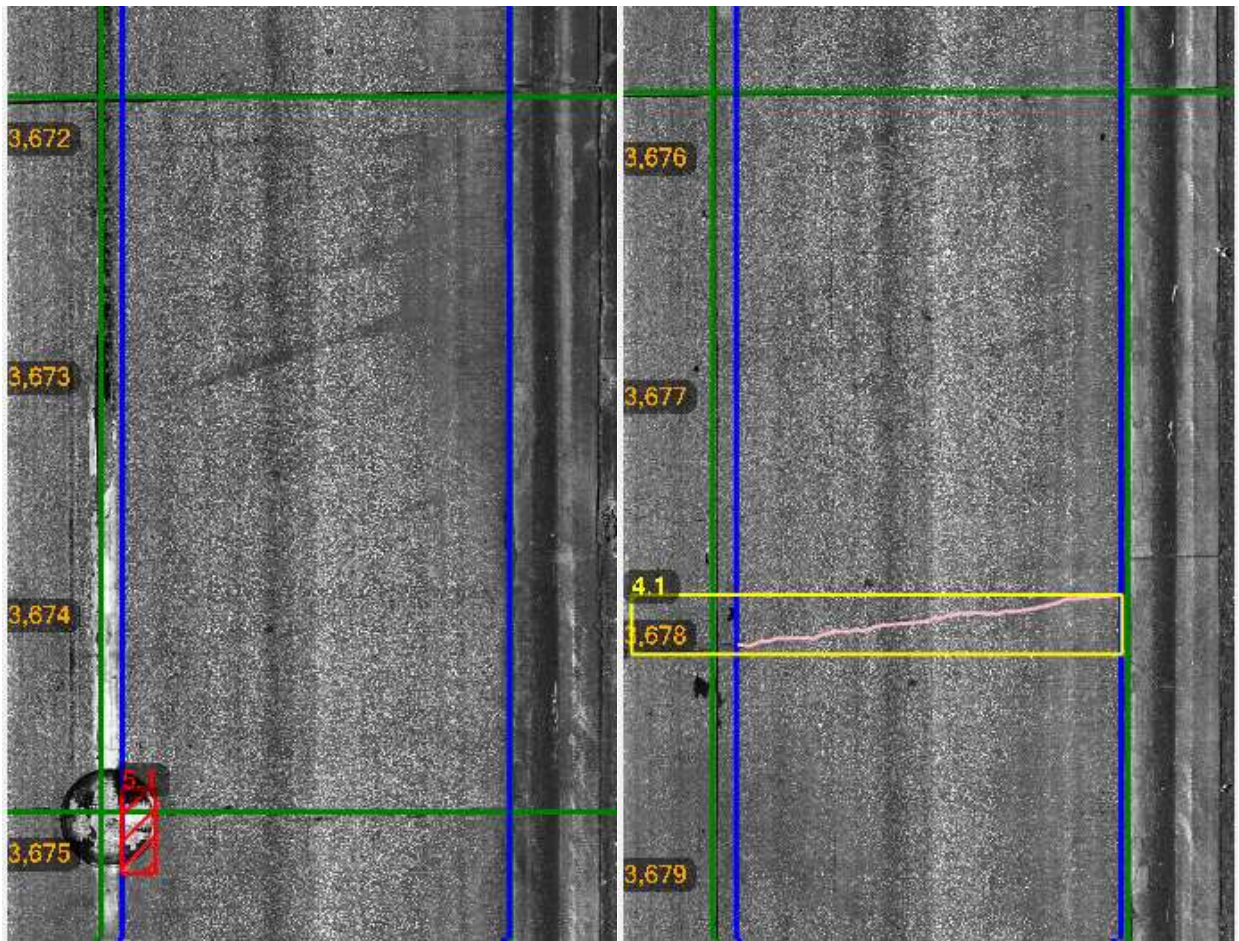


Figure 200. (Left) Image Number 13 (Frame 62); (Right) Image Number 14 (Frame 61) from Section 7



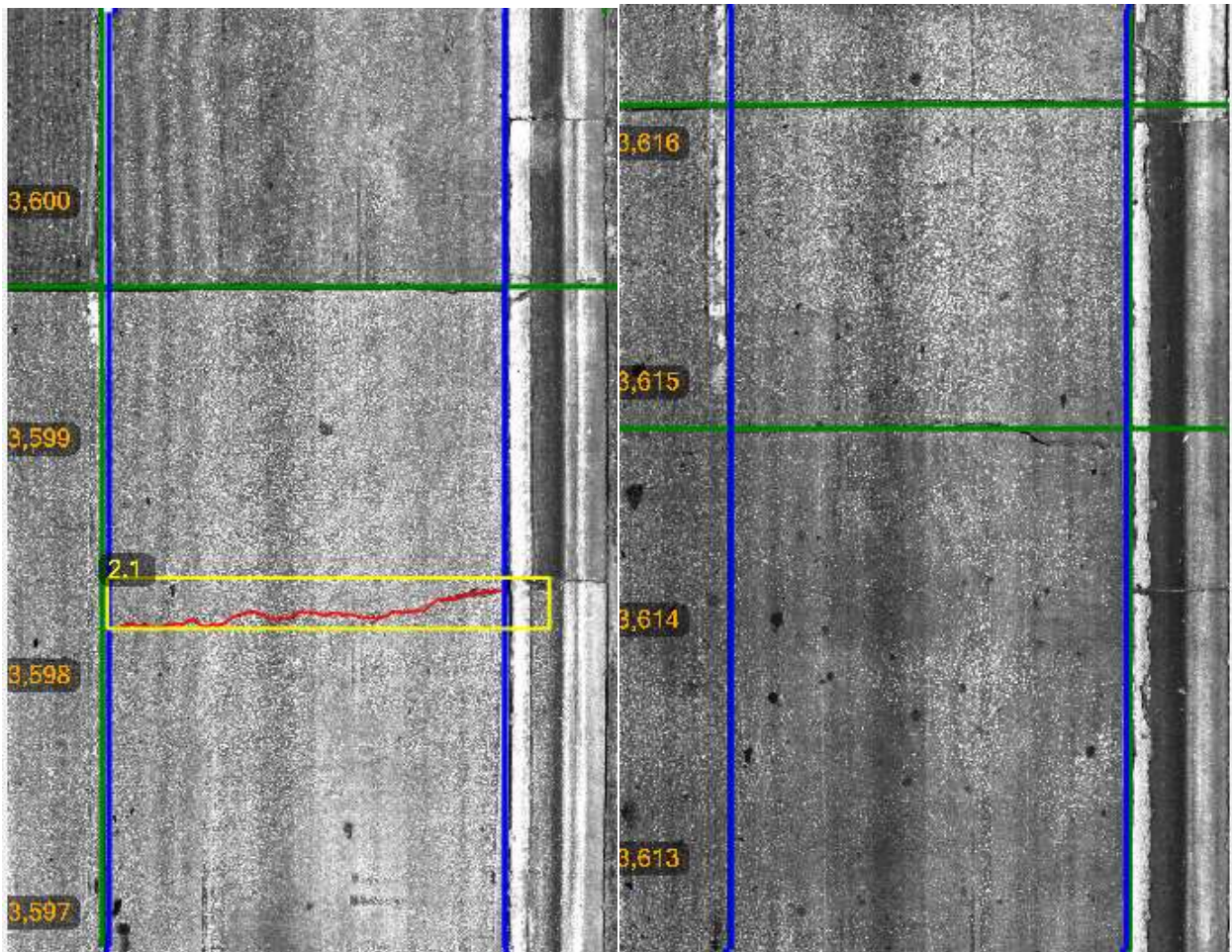


Figure 201. (Left) Image Number 15 (Frame 6); (Right) Image Number 16 (Frame 10) from Section  
8

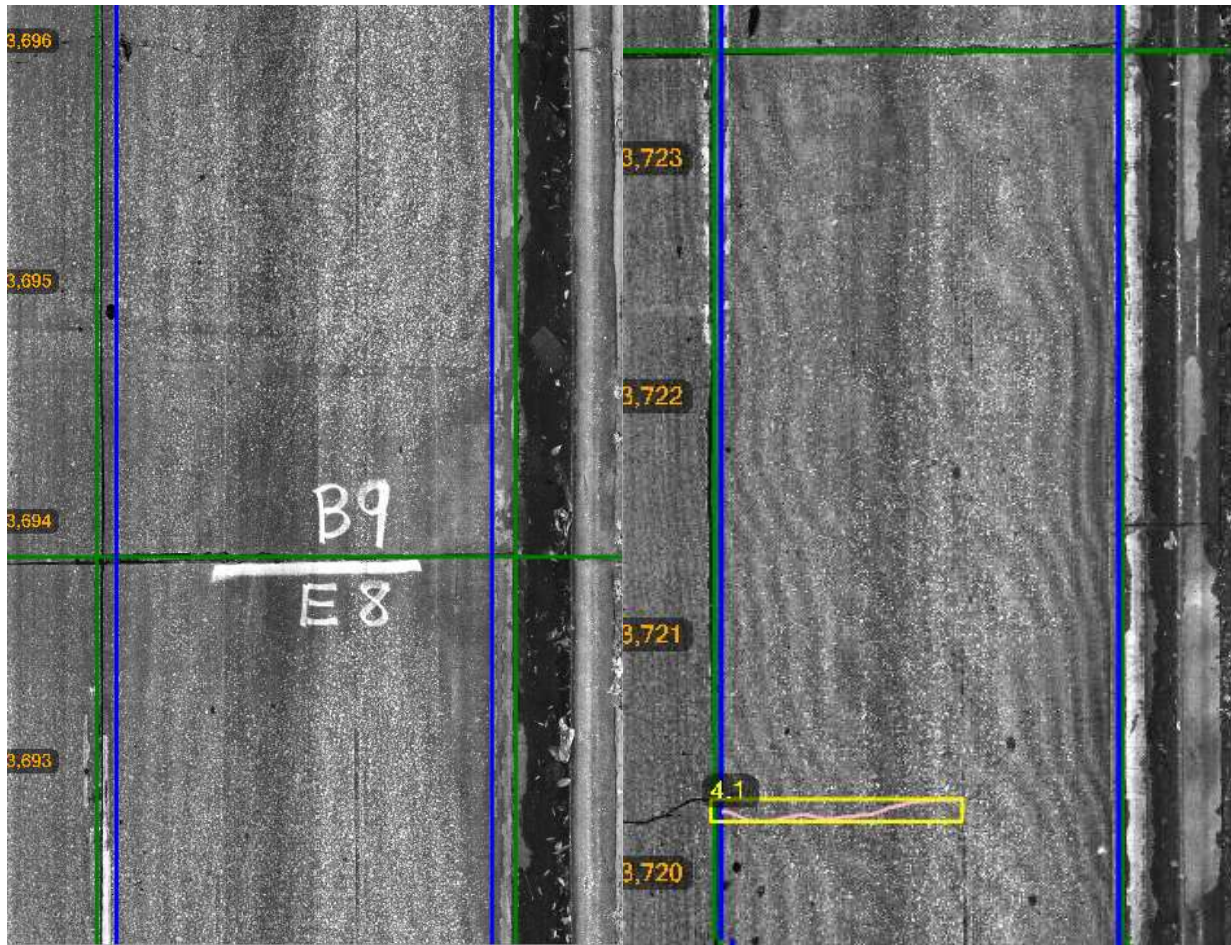


Figure 202. (Left) Image Number 17 (Frame 31); (Right) Image Number 18 (Frame 38) from Section 9



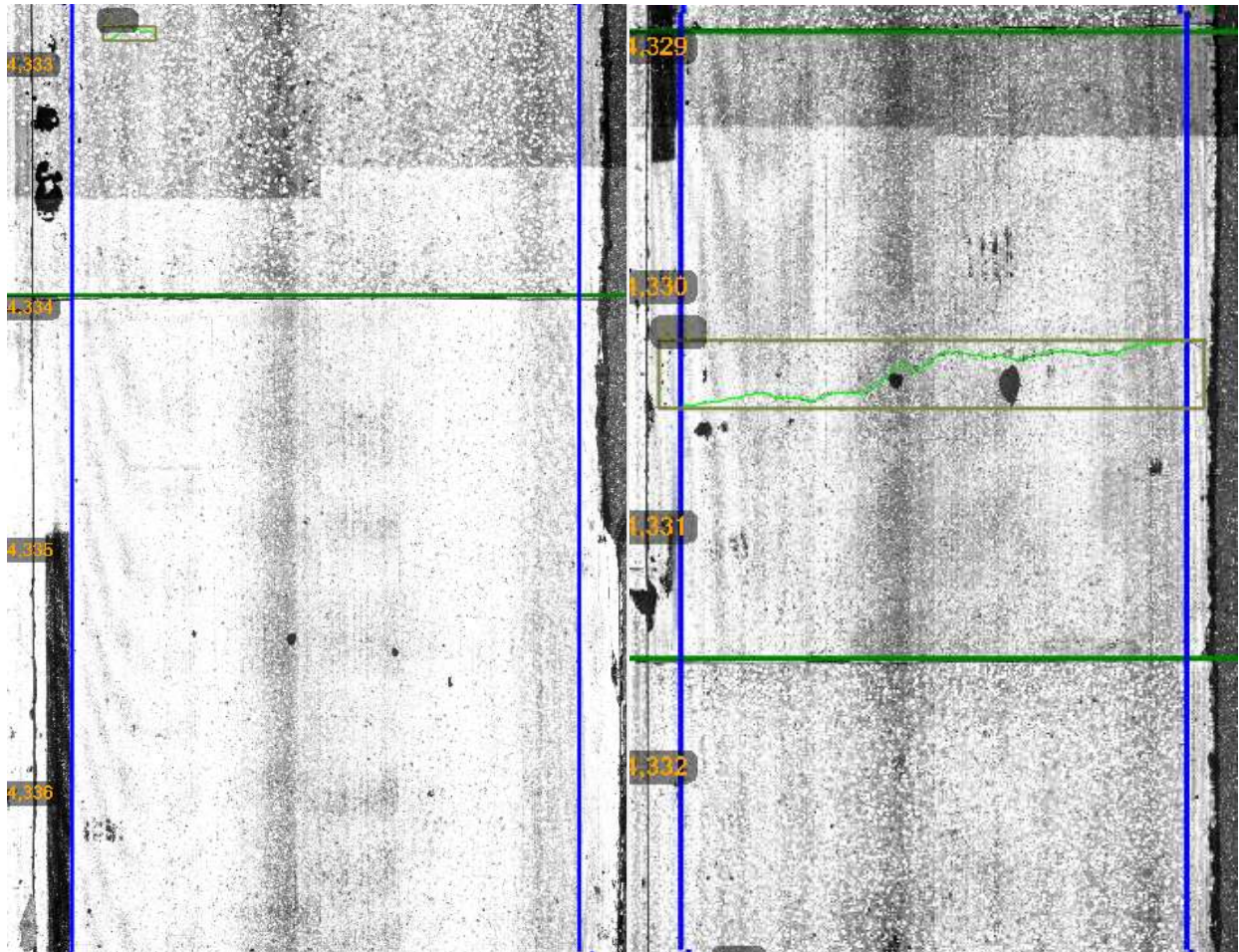
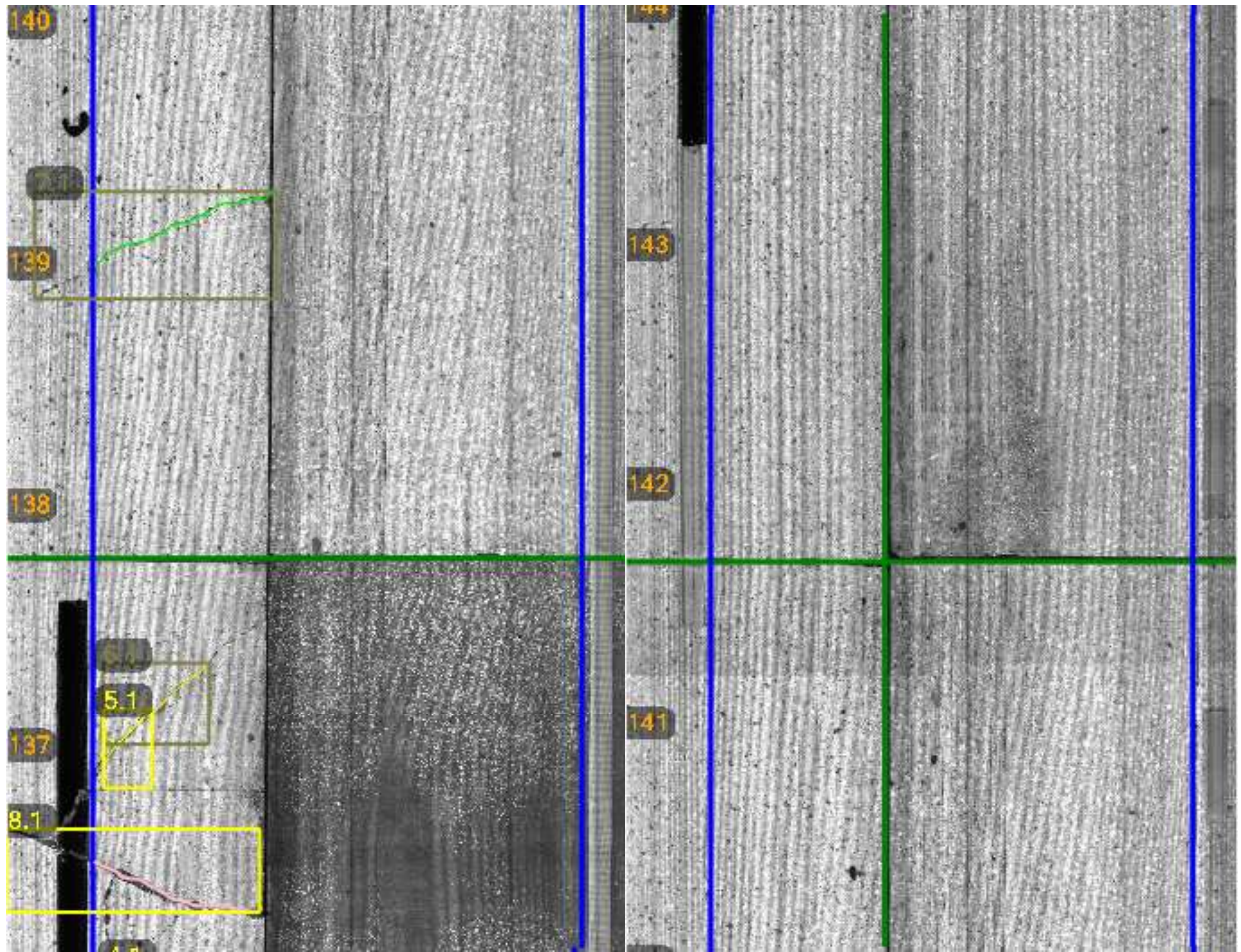


Figure 203. (Left) Image Number 19 (Frame 52); (Right) Image Number 20 (Frame 53) from Section 10



**Figure 204. (Left) Image Number 21 (Frame 44); (Right) Image Number 22 (Frame 45) from Section 11**



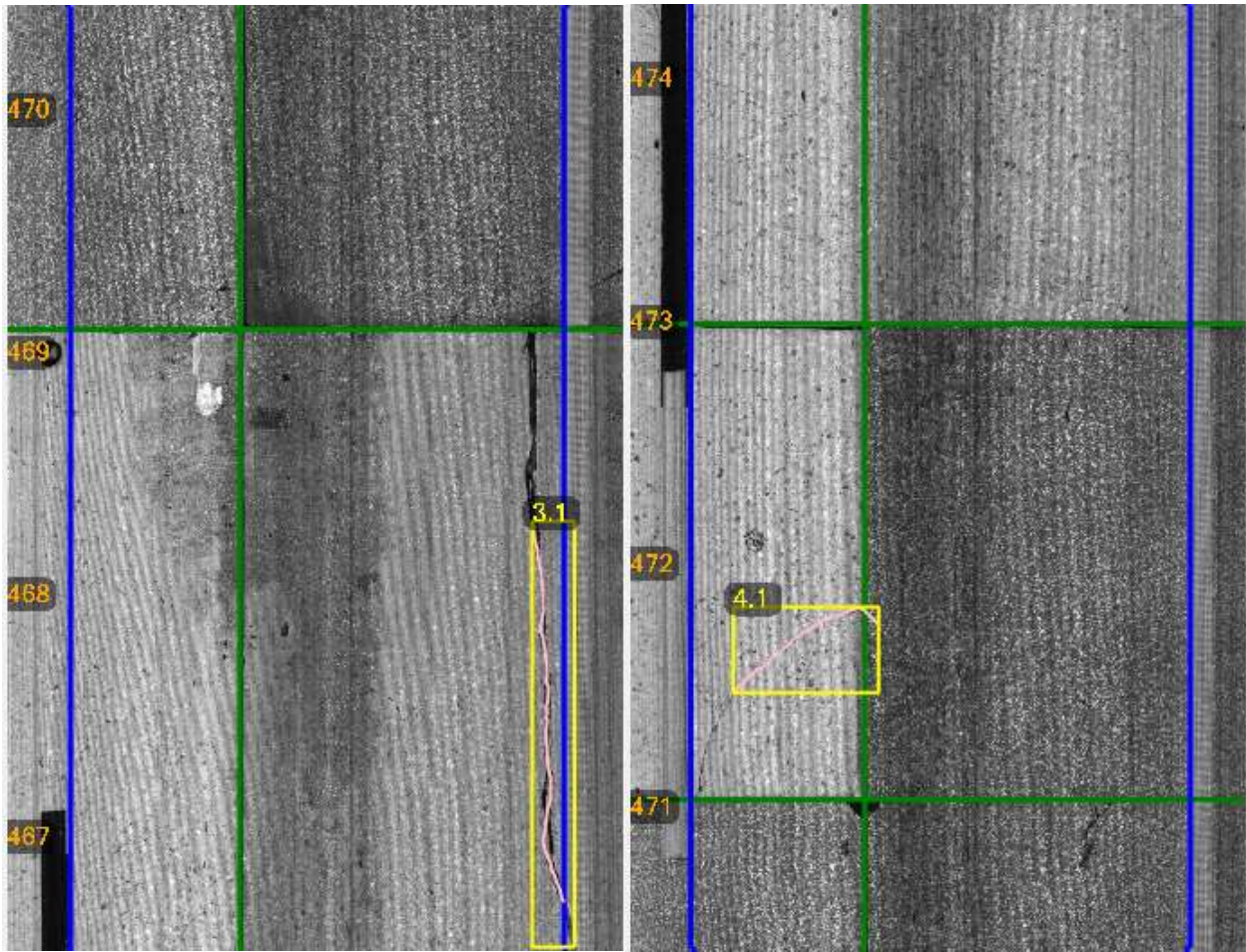


Figure 205. (Left) Image Number 23 (Frame 87); (Right) Image Number 24 (Frame 88) from Section 12

## **I. PURCHASE ORDER NUMBER PR10026557: LCMS FEASIBILITY ON FLEXIBLE PAVEMENTS**

Since the commencement of this research project, new advances in technology have turned three-dimensional (3D) data collection systems into the state of the practice in the industry. These 3D systems provide additional information regarding pavement surface condition that facilitates the reporting of Statewide data in accordance with the federal requirements for the Moving Ahead for Progress in the 21<sup>st</sup> Century (MAP-21) and Fixing of America's Surface Transportation (FAST) acts. As a result, there is a need to investigate feasibility of using 3D data for automated pavement condition surveys. Because Task 4 of Phase II involves a study on the feasibility of the 2D LRIS data for developing an automated crack detection software for flexible pavements, this is the optimum time to conduct the feasibility concurrently based on both 2D and 3D data.

Since Florida Department of Transportation (FDOT) does not own 3D data collection equipment, FDOT staff requested that Fugro provides a scope and estimate of the required level of effort to collect the required 3D images and conduct analysis based on the 3D data. Fugro owns and operates several Automatic Road Analyzer (ARAN) vehicles equipped with 3D Laser Crack Measurement System (LCMS). Therefore, Fugro has the expertise and experience required to conduct the 3D data collection effectively and efficiently. FDOT approved a Purchase Order (Number: PR10026557) for Fugro to conduct the 3D data collection and the corresponding processing and analysis to evaluate feasibility of the 3D technology for this purpose.

Under this purchase order, Fugro analyzed the viability of using 3D LCMS images to detect, quantify and classify cracks in flexible pavements. Fugro collected and processed 3D LCMS images and data to be used in software evaluation. It should be noted that the actual software development effort will be carried out during Task 6 of Phase II of this project, and therefore at this stage of the analysis, the existing Fugro Vision software was used due to its availability with the integrated images and data. Fugro identified the potentials and the limitations of this application with 3D images for flexible pavements and compared it to the results from the 2D LRIS analysis in Task 4 of Phase II. The results from the analysis and recommendations are documented in this Appendix.

The required activities for evaluating the software on 3D images included the following:

- Activity 1: Collect 3D LCMS images and data on the representative flexible pavement test sections identified by FDOT staff.
- Activity 2: Process the collected LCMS data to create a corresponding database for the automated software application.

- Activity 3: Determine proper detection parameter settings for 3D LCMS images
- Activity 4: Conduct classification and rating of detection results
- Activity 5: Summarize the LCMS results and compare it to LRIS results obtained in Task 4 of Phase II; prepare documentation on comparison, potentials, limitations, and recommendations

This Appendix is organized in five sections. Following this introduction, Section I.1 provides a report on the 3D data collection conducted by Fugro staff. Section I.2 explains the data processing details including segmentation, crack detection, and distress identification. Section I.3 provides a comparison of automated crack detection and distress identification results between the 3D analyses conducted under the current Purchase Order and the 2D analyses conducted under Task 4 of Phase II. Section I.4 summarizes the advantages and limitations of the 3D technology for automated crack detection and distress identification. Section I.5 includes conclusions and recommendations.

## **I.1. Data Collection**

Data collection for this FDOT Purchase Order was completed in May 2017. This section describes the data collected, and the equipment used for the collection.

### **I.1.1. Collected Data Elements**

Collection of 3D LCMS images and data was requested by FDOT and conducted by Fugro. All collected data is referenced geographically and linearly to FDOT's inventory based on the provided Location Referencing System (LRS). The collected data include the following:

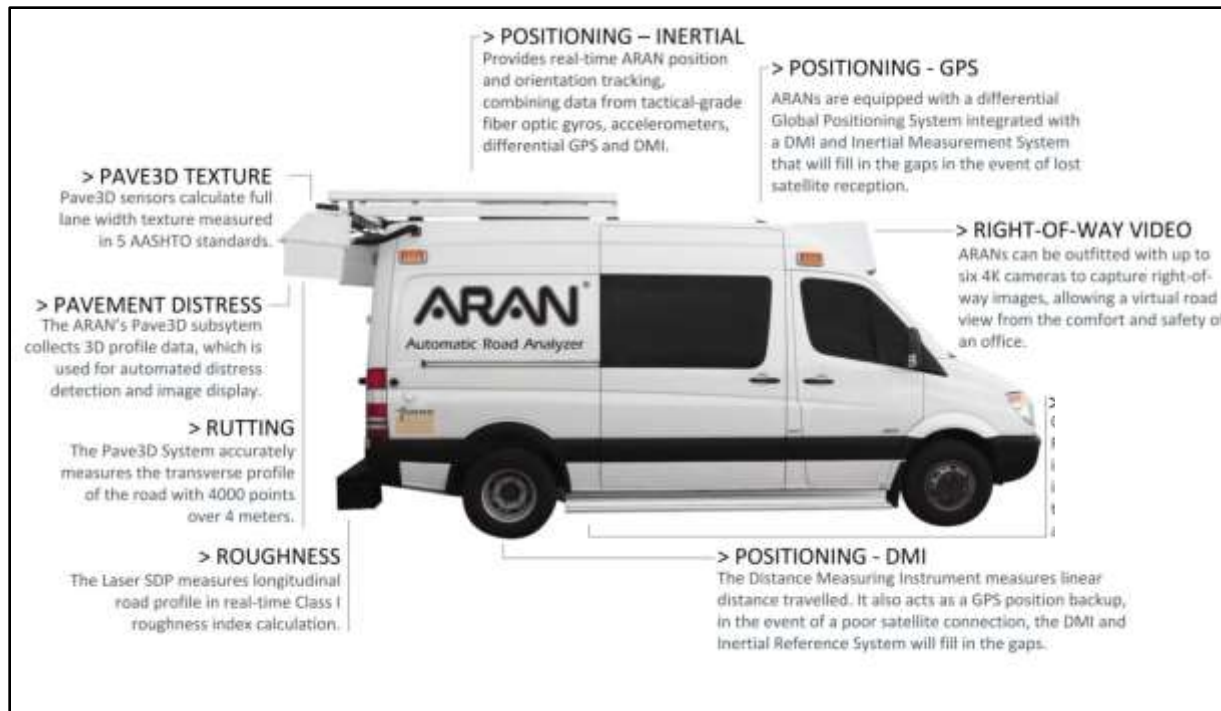
- 3D pavement images used for crack detection and distress identification
- High definition forward viewing right-of-way (ROW) images
- Pavement longitudinal profile using a Laser South Dakota Profiler (SDP)
- Pavement transverse profile using the 3D LCMS data
- Pavement surface texture using the 3D LCMS data

- Differential Global Positioning System (GPS) data
- Distance Measuring Instrument (DMI) data integrated with GPS data
- Inertial position and orientation data from fiber optic gyros and accelerometers, integrated with the GPS and DMI data

### **I.1.2. Data Collection Equipment**

The data was collected using an Automatic Road Analyzers (ARAN), equipped with the Pave3D system, which uses INO/Pavemetrics' Laser Crack Measurement System for collecting 3D images of the pavement surface. Fugro Roadware developed the first ARAN in 1983, one of the very first multi-functional pavement data collection vehicles in the world. Now in its 6th generation, everything learned from then until now has been applied to create a robust, accurate and repeatable integrated pavement data collection system. The ARAN has a modular design which allows it to be configured to meet a large range of agency needs. An overview of the ARAN sensors and capabilities used for the FDOT project is shown in Figure 206 and further described in the section on ARAN Information and Specifications at the end of this Appendix.

The Pave3D system compared to the Pave2D system has the benefits of fewer reruns due to damp collection, less ARAN downtime while waiting for roads to be 95% dry, faster collection due to the fewer down days, lower cost of collection, and faster data turnaround time, operation in all types of lighting conditions both during the day and at night without the need for artificial illumination of pavement, operation under the sun and shadows as well as various types of pavement types ranging from dark asphalt to light colored concrete, measurements at highway survey speeds and on roads reaching 14 feet in width and still achieving a 0.19 inches longitudinal resolution.



**Figure 206. The ARAN Data Collection System Used for the FDOT Project**

### **I.1.3. Testing Locations and Routing**

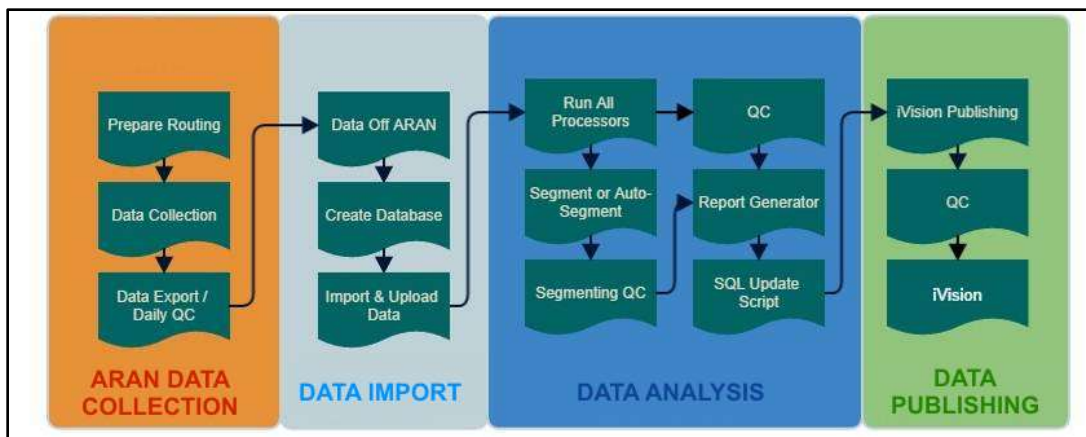
Similar to Phase I of this project, 12 representative flexible pavement test sections (Table 109) were selected by FDOT staff for Phase II evaluations. These representative test sections were selected in a manner that would include the key distress types and severity levels that are frequently encountered on Florida highways. All routes were identified, divided into segments, mapped, and measured for length. This information was assembled into tables and maps (“routing package”) for use on the ARAN. This “routing” process allowed the operators to clearly understand which roads and at which specific locations were to be tested and pick an optimal testing path to reduce testing time.

**Table 109. 12 Representative Flexible Pavement Test Sections**

Index	County ID	Road	City	Lane	Direction	BMP	EMP	Length
1	02050000	SR 44	Crystal River	R2	East	0.000	0.604	0.604
2	02050000	SR 44	Crystal River	L2	West	0.000	0.604	0.604
3	11010000	SR 44	Leesburg	R2	East	0.000	1.592	1.592
4	11100000	SR 19	Umatilla	R2	North	3.816	4.906	1.090
5	11002000	SR 44	Leesburg	R2	East	1.183	2.276	1.093
6	11002000	SR 44	Leesburg	R2	East	3.184	4.514	1.330
7	11080000	SR 19	Howey in the Hills	R1	North	0.000	0.925	0.925
8	18020000	SR 50	Polk City	R1	East	5.356	6.421	1.065
9	26050000	SR 24	Gainesville	L2	South	3.367	6.095	2.728
10	26050000	SR 24	Gainesville	L2	South	6.095	7.670	1.575
11	10190000	SR 400 / I-4	Tampa	R3	East	11.098	12.332	1.234
12	10190000	SR 400 / I-4	Tampa	R3	East	20.407	21.476	1.069

## I.2. Data Processing

Data processing for this FDOT Purchase Order consisted of three major processes: data import and quality control, data analysis, and data publishing. Software packages developed by Fugro are used to help manage the flow of data throughout all stages of a project. Figure 207 provides a high-level overview of the standard operating procedures (SOP) at every step of the data flow process in the Fugro ISO 9001 certified Quality Management System (QMS) for highway data collection.

**Figure 207. Fugro Data Process Flow**

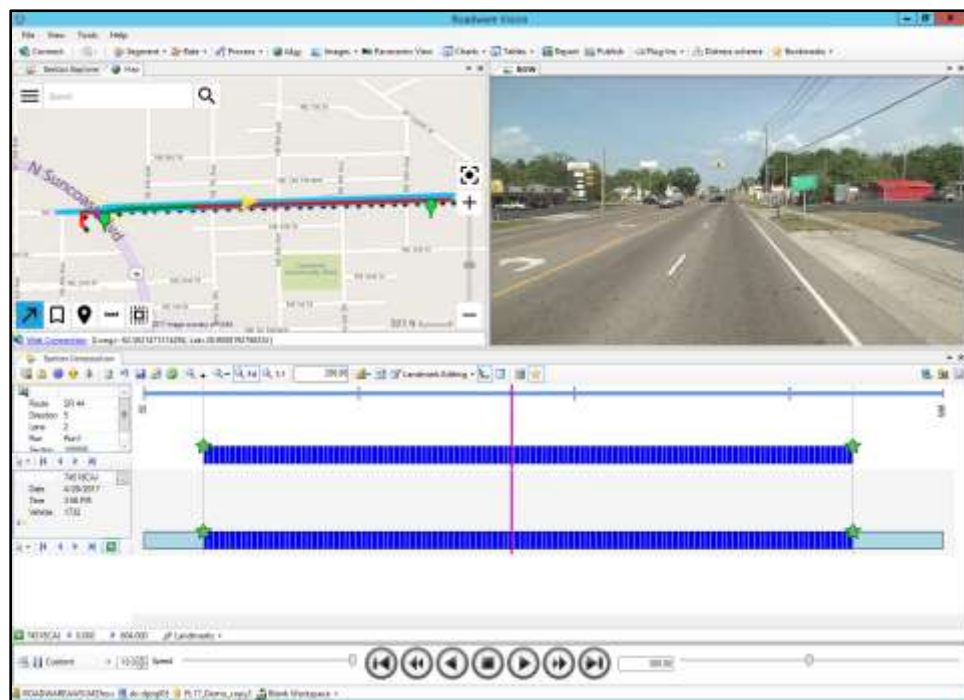


This section provides a brief overview of the methodology behind some of the key processing steps relevant to the topic of this research and any project specifications unique to this project.

### I.2.1. Segmentation

Segmenting is the method of ensuring the data collected by the ARAN matches the geographic and linear references set up by FDOT. The segmenting process is completed to ensure that the true start and stop locations of the road can be best matched to ensure that the data represents the exact location expected by FDOT. The matching of information was completed using Fugro's Vision and utilizes a combination of image streams (ROW and pavement images), electronic field sheets, as well as GIS / web-based maps.

Stationing for all routes was adjusted using a method called “rubber-banding”, to match stationing provided by FDOT. All data collected prior to the start of the route are removed and the chainage of the beginning of the route is set to the FDOT value for that landmark. Chainages for all other landmarks on the route are adjusted to match length and location information provided by FDOT. In the “rubber-banding” process, data between each set landmark may be stretched or compressed accordingly to ensure station chainages match up. The Vision module used to perform segmenting for the 2017 FDOT collection is shown in Figure 208.



**Figure 208. Vision Software for Segmenting**

### **I.2.2. Distress Data Analysis Process**

The actual software development effort for this project will be carried out during Task 6 of Phase II, and therefore at this stage of the analysis, the existing Fugro Vision software was used due to its availability with the integrated images and data. Therefore, the following software descriptions are the Vision software descriptions and not the descriptions for the FDOT customized application at this point of the project. Fugro Vision software includes an automated distress data analysis application, which involves the following main routines:

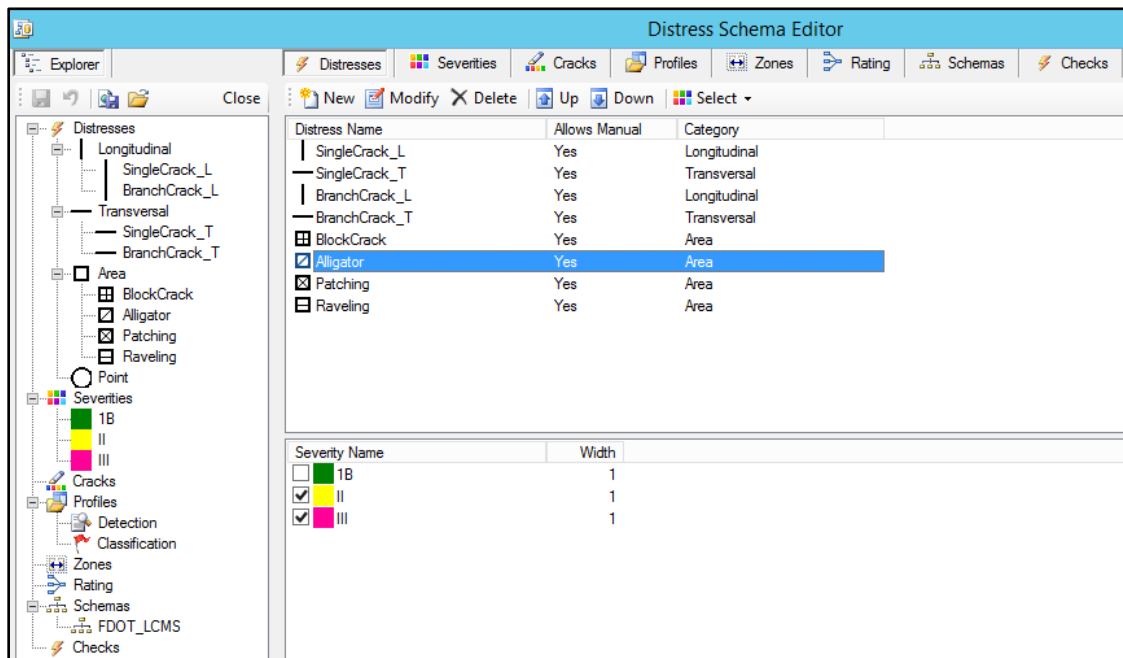
1. Lane Detection: during this step, lane boundaries are automatically detected and marked as blue lines on the pavement images.
2. Defect Detection: also called “Crack Detection,” during which any linear defects on pavement surface is detected and marked with lines.
3. Defect Classification: during this step, all of the detected linear defects are classified into one of the three categories of longitudinal defects, transverse defects, and other (which will eventually be rated as alligator or block cracking) defects according to some criteria for defect angle and density, which can be changed by the user.
4. Distress Rating: during this final step, the software assigns a distress type and severity to each of the classified defects according to a distress schema defined by the user. The user needs to select one or more criteria from a series of criteria such as angle, longitudinal and transverse extent, density, width, and others for each distress type and severity. Once the schema is setup and saved, this schema can be applied for network-level data collection.

### **I.2.3. Distress Schema Specification**

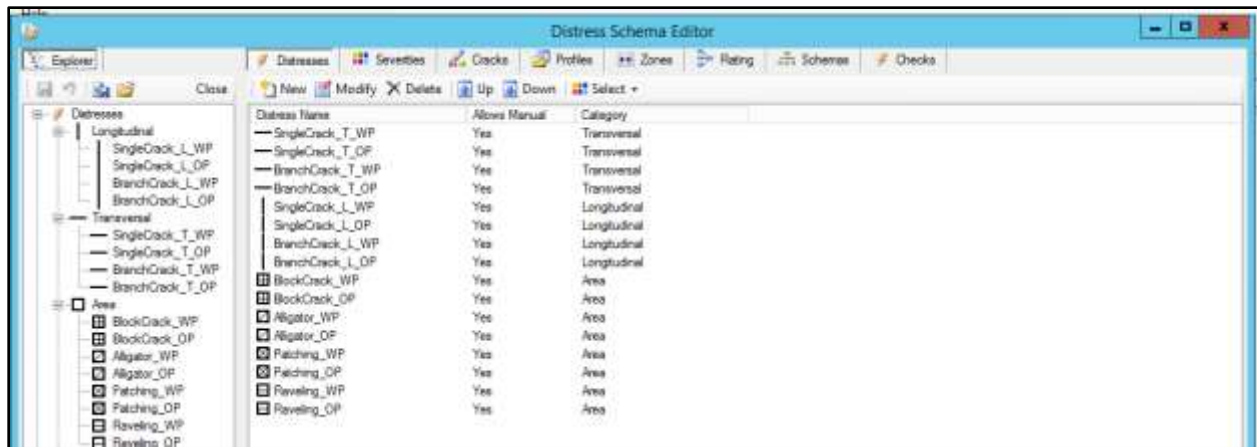
The performance of crack detection, classification and rating is highly dependent on a well-defined distress schema. The setting up of distress schema includes creation of Distress Type, Distress Severities, Crack Ranges, Detection Profile, Classification Profile, Road Zones and Rating Profile (Figure 209). In this project, the distress schema was setup according to the specified criteria for each distress type in the FDOT Flexible Pavement Condition Survey Handbook. Once the schema is setup and saved, this schema can be applied for network-level data collection. The following segments describe how the details of the distress schema are setup.

The Vision software provides two options for distinguishing distresses by zone location:

1. In the distress schema, only one distress type would be setup for both wheel path (WP) and outside wheel path (OP), but then they could be separated using a SQL code on the database based on the location information (Figure 209). This option is more flexible as it does not require reprocessing if it is decided to change the width of wheel path zones in the future. Specifically, if the images are going to be rated manually or if the automated distress needs manual QC and correction, this option is recommended. It is extremely tedious for the manual rater to draw separate distresses for the wheel path and non-wheel path areas (option 2). In this stage of the project, option number 1 was used for establishing the reference survey.
2. In the distress schema, separate distress types could be setup for WP and OP areas (Figure 210). This option is recommended when no manual correction of the automated process is needed. In this stage of the project, option number 2 was used for the automated distress survey.



**Figure 209. Vision Distress Schema Editor Interface with One Distress Type for Both Wheel Path and Outside Wheel Path Zones (Option 1)**



**Figure 210. Vision Distress Schema Editor Interface with Separate Distress Types Defined for Wheel Path and Outside Wheel Path Zones (Option 2)**

### ***Distress Type and Severity***

Distress types are defined under the 'Distresses' tab and the severities under the 'Severities' tab. Then, each distress type is assigned the possible severity options. FDOT's Flexible Pavement Condition Survey Handbook (August 2015) includes the following distress types and severities:

1. Single Cracks (linear length, feet), Class 1B or Class II or Class III
2. Branch Cracks (linear length, feet), Class 1B or Class II or Class III
3. Block Cracks (area, sq. feet), Class 1B or Class II or Class III
4. Alligator or Fatigue Cracks (area, sq. feet), Class II or Class III
5. Patching (area, sq. feet), no severity levels
6. Raveling (area, sq. feet), Light or Moderate or Severe

During the distress rating process, these distress types are identified and quantified individually and then they are added up to generate the total amount of cracking in each one of the Class 1B, Class II, and Class III cracks. All linear distress types are recorded in two groups of longitudinal and transverse to differentiate their orientation and facilitate

quality control, but they are added up for each distress type (for example, branch cracks or single cracks) following the survey.

Following the distress survey, two (2) categories of distress will be recorded for each of these distress types: within the wheel paths (CW), and outside the wheel paths (CO). For automated survey results, this differentiation was made in the schema setup (option 2). For the reference survey, this differentiation was conducted using a SQL code (option 1). This is required for the final calculation of the amount of distress in each class within and outside the wheel paths, because the deduct values are higher for distresses within the wheel paths.

The total area for patching and raveling is added to the total amount of Class III cracks. The details of each distress type and severity are recorded to keep a permanent record that facilitates quality control and quality assurance initiatives. All the summation happens on the recorded data in the SQL database.

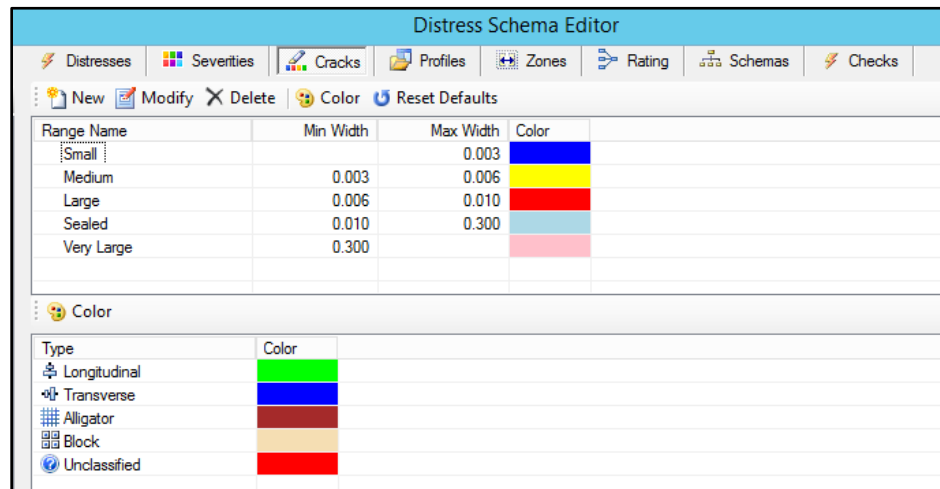
### ***Crack Range***

Under the 'Cracks' tab in the Distress Schema Editor, a coloring scheme is defined for identification of the detected cracks/defects on the pavement image according to crack width (Figure 211). The following crack ranges were determined for this project as they correspond to the severity levels identified in the FDOT manual:

1. Small cracks with crack width less than 3.18 mm are identified with green color lines (later assigned to Class 1B category in distress rating)
2. Medium cracks with crack width equal to or greater than 3.18 and less than 6.35 mm are identified with yellow color lines (later assigned to Class II category in distress rating)
3. Large cracks with crack width equal to or greater than 6.35 mm are identified with a red color lines (later assigned to Class III category in distress rating)

The "Max Width" in Figure 211 means "less than" and the "Min Width" indicates "equal to or greater than". As previously noted, this is NOT the FDOT customized application. At this stage, we are using the existing Vision software to compare 2D versus 3D data. The FDOT customized application will be developed during Task 6 (development). Also patching and raveling are "distresses" and NOT "cracks". This menu is ONLY showing cracks. After the distresses are identified in the "rating" process, patching and raveling can be added.

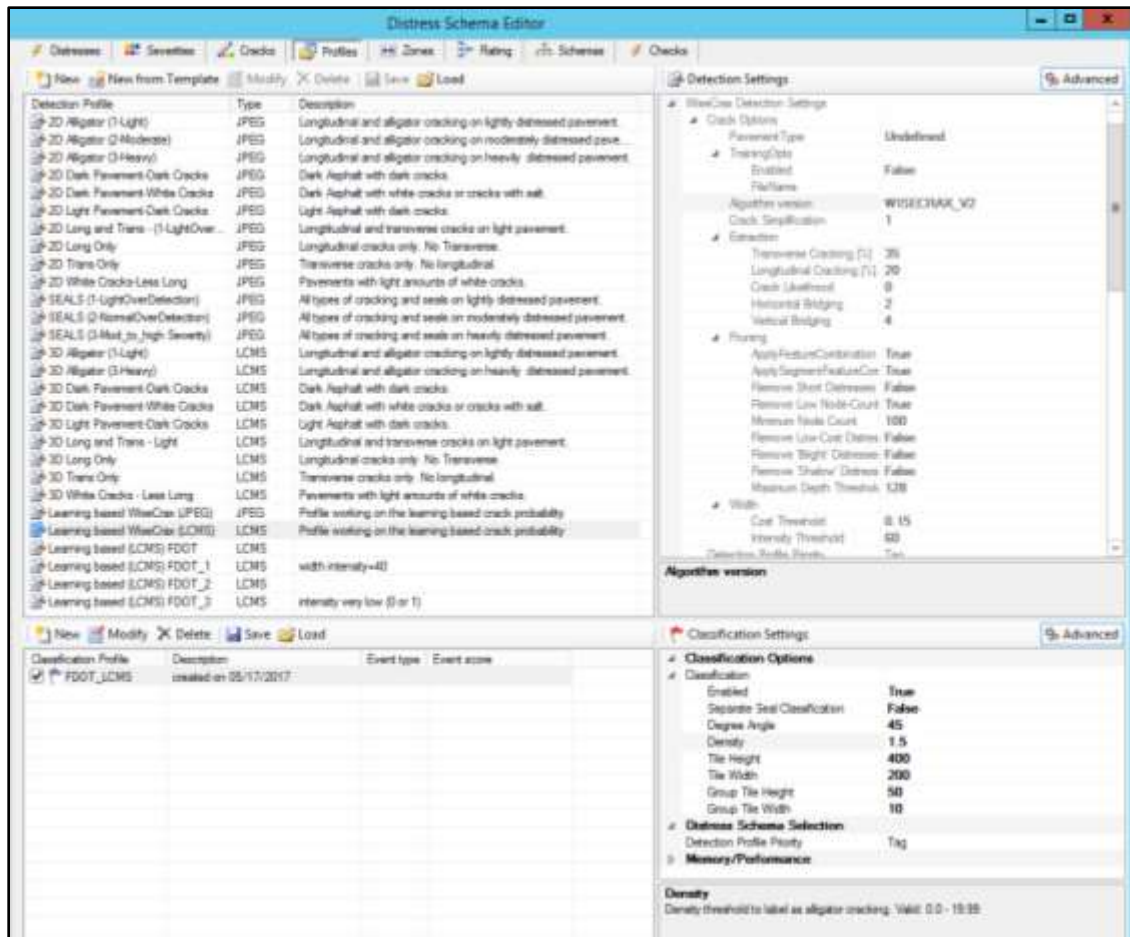
Following the crack detection process, the detected cracks are displayed on top of the pavement images with the colors corresponding to their width. As shown in Figure 211, the Cracks menu also allows selection of specific coloring scheme for the classification categories of Longitudinal, Transverse, Alligator, Block, and Unclassified categories. Following the classification process, each class of cracks are identified on top of pavement images using the corresponding colors. These colors help with quality control of the detection and classification process.



**Figure 211. Cracks Menu in the Distress Schema Editor**

### ***Detection and Classification Profiles***

Under the 'Profiles' tab in the Distress Schema Editor, the control parameters for the crack detection and classification processes are determined. The software typically shows the default values for these control parameters that have been set based on empirical experience. In the Task 2 report for this project, various control parameters for the detection of cracks from 2D images and for the classification of detected cracks into transverse, longitudinal, alligator, and block categories were introduced and the impacts on software performance of changing each control parameter were explained in detail. Figure 212 shows the 'Profiles' tab, which allows for customization of the control parameters for the crack detection and classification processes.



**Figure 212. Detection and Classification Profiles in the Distress Schema Editor**

Vision provides two alternative automated crack detection algorithms to choose from when running this process on 3D images (using both image pixels and depth data):

1. LCMS Global Processor: This automated crack detection algorithm was developed by Pavemetrics Systems, Inc. Pavemetrics is the vendor company for the LCMS devices that have been manufactured by INO.
2. Fugro Machine Learning Crack Detection: This machine learning automated crack detection algorithm was recently developed by Fugro engineers, based on a large database of semi-automated evaluation of 3D images.

Both the Pavemetrics LCMS Global Processor and the Fugro machine learning based 3D crack detection algorithms have been tested on numerous pavement surface images and their corresponding control parameters have been optimized in the latest version of Vision software. As a result, it is recommended that the detection parameters are not

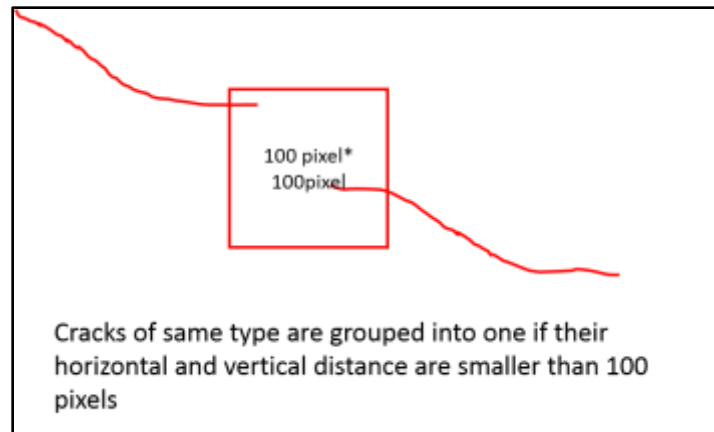
changed. In this project, the Pavemetrics LCMS Global Processor algorithm was used to create crack maps that were manually fixed to establish the reference survey. The Fugro machine learning algorithm was used without manual intervention to evaluate the automated crack detection results on 3D images. There was no specific reason for the selection of one or the other. Either way, one algorithm needed manual correction to establish the reference crack map and a different algorithm was needed to show the automated crack detection results on 3D images.

In the classification step, there are several parameters that can be changed to improve the classification results (Table 110). For this phase of the project, eight classification profiles using eight different control parameter sets were used, and the final classification profile was selected based on the best results among these profiles on the selected representative test sections. It should be noted that the cracking analysis results are very sensitive to these settings and they are not one size fits all.

**Table 110. Classification Parameter Settings**

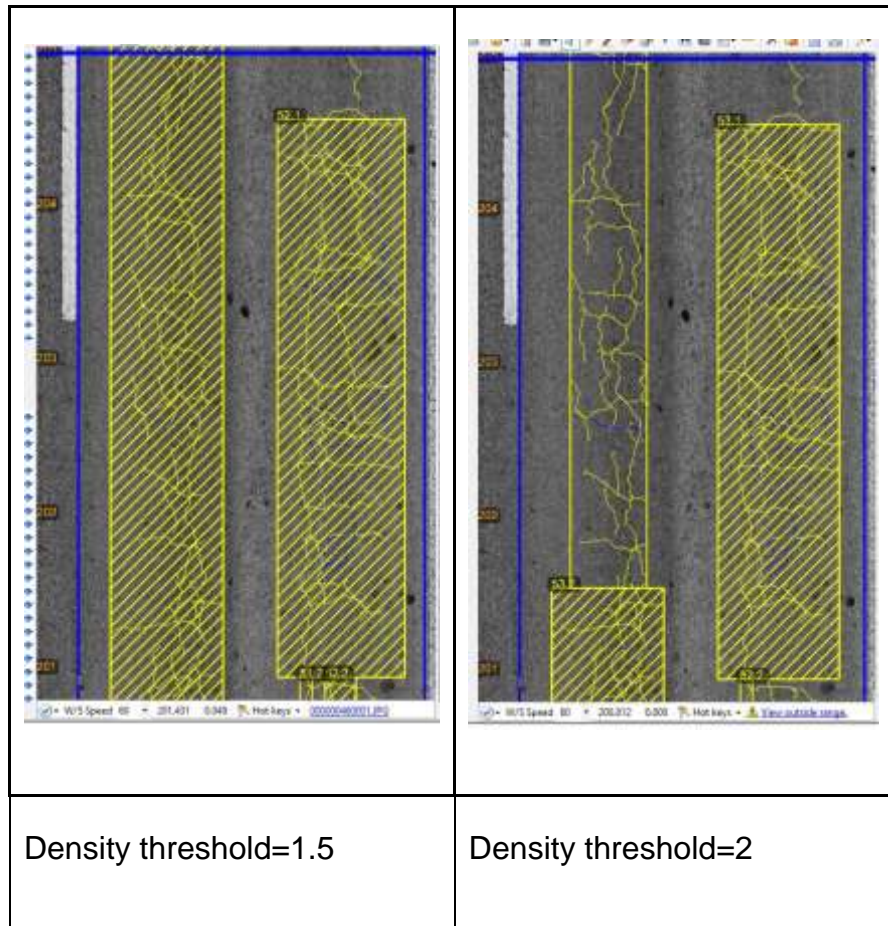
Parameter	Description	Value Used
Classification Enabled	Enables classification	TRUE
Separate Seal Classification	Classifies sealed cracks separately	FALSE
Degree Angle	Angle threshold differentiating between longitudinal and transverse defects, this is the angle for the best fit line across the crack nodes	45
Density	The density threshold beyond which there are enough cracks within a tile to count the tile area as alligator cracking area and not individual cracks.	1.5
Tile Height (pixels)	Tile used for calculating the density of the alligator or block categories	400
Tile Width (pixels)		200
Group Tile Height (pixels)	Tile used for grouping defects together (see Figure 213). Cracks that fall within these grouping tiles and are of the same classification will be grouped together to make one crack set or group of cracks.	50
Group Tile Width (pixels)		10



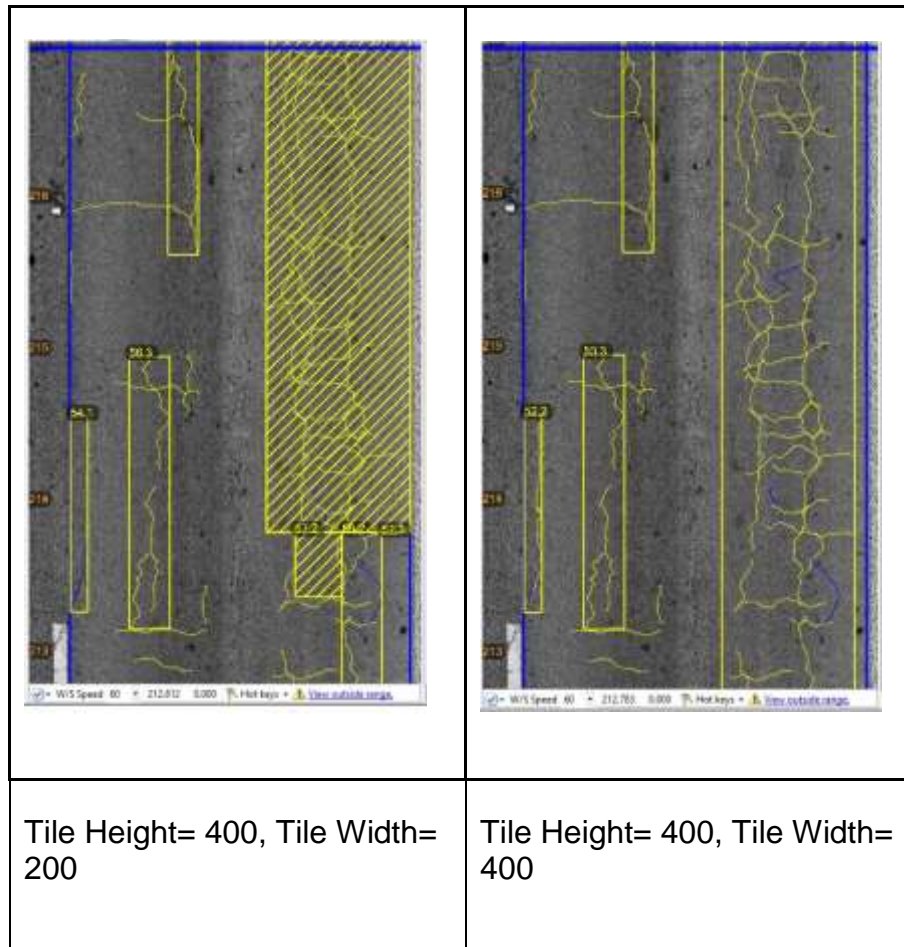


**Figure 213. Group Tile Height and Width**

The tuning of the classification control parameters was conducted by changing the parameters one by one and comparing the one classification result against the other. Figure 214 shows a comparison of the classification results when changing the density threshold that defines when cracks become alligator cracks. To compute crack density, the bounding box of a crack is divided into grids of tiles of user input size. If the density threshold is increased, there will be less distresses classified as alligator cracking. Figure 215 shows a comparison of classification results when changing the dimensions of the Tile used for calculating the density of the alligator or block categories. It is obvious that the larger the tile size, the smaller the density of the cracks. As a result, if the density threshold is fixed but the tile size is increased, there will be less distresses classified into alligator category.

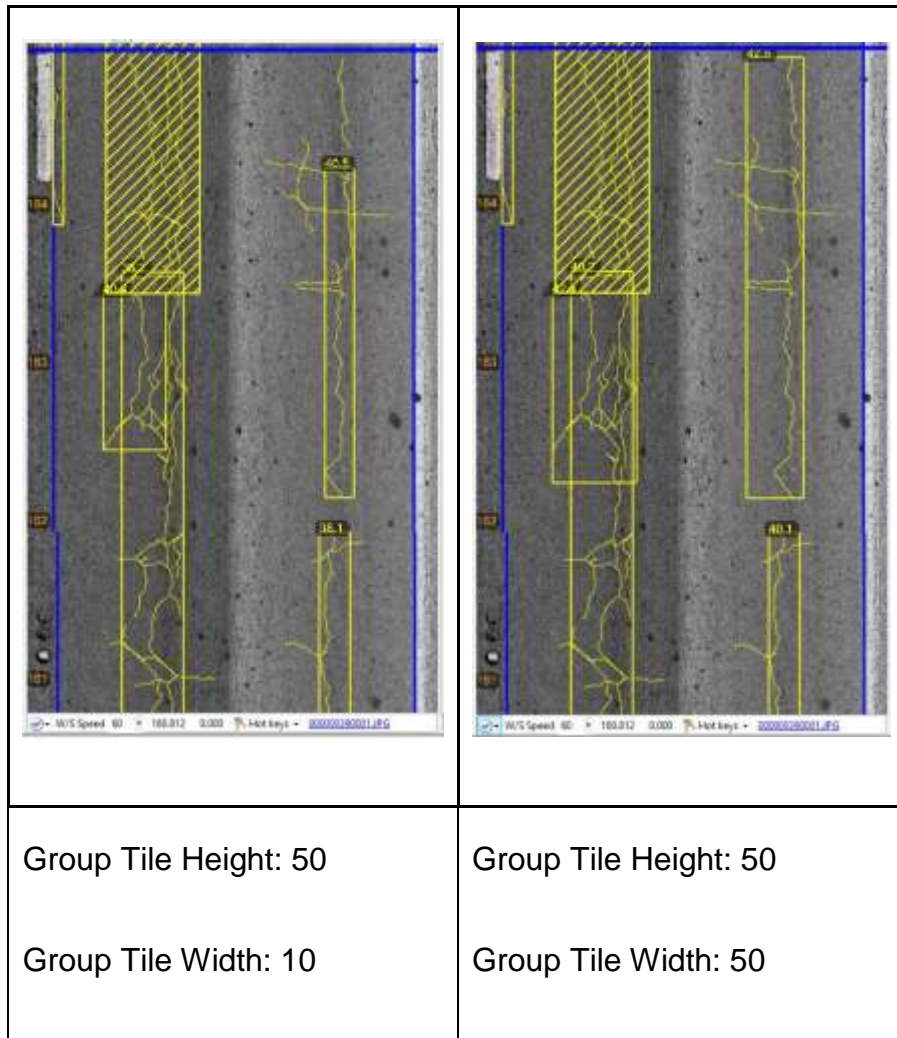


**Figure 214. Comparison of Classification Control Parameter Settings: Density**



**Figure 215. Comparison of Classification Control Parameter Settings: Tile Height and Width**

During the classification, the detected cracks are grouped into crack sets based on their proximity to each other. The distances between each crack bounding box are checked; if the horizontal distance between two adjacent bounding boxes is smaller than the group tile width and the longitudinal distance between the boxes is smaller than group tile height, then the two cracks are merged into one crack set. Each crack set will be rated as one distress. Figure 216 shows a comparison of the classification results when changing the dimensions of the Group Tile used for grouping defects together (see Figure 213).



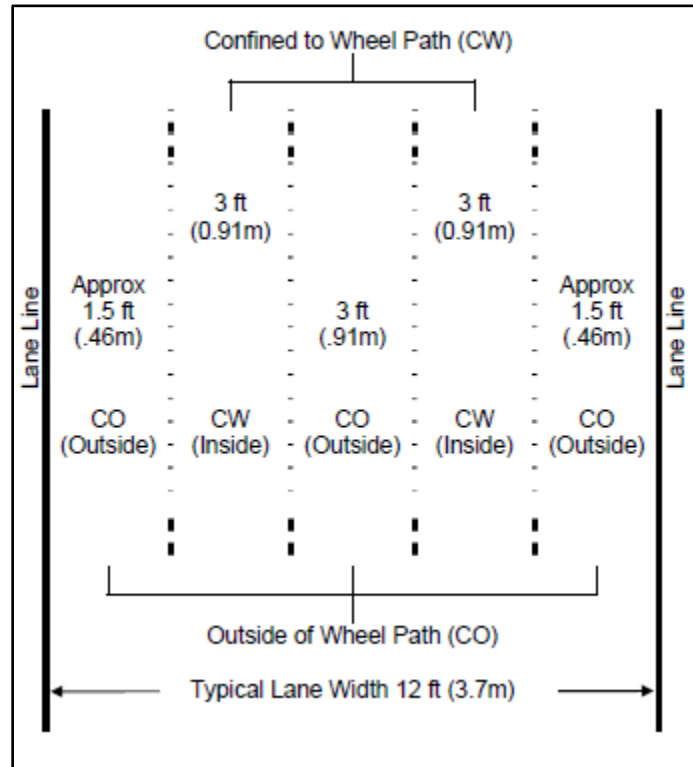
**Figure 216. Comparison of Classification Control Parameter Settings: Group Tile Height and Width**

### ***Road Zone***

Road zone describes the portion of the road that is in the wheel paths and what is outside the wheel paths. The road zones were customized according to the Florida DOT specification of each wheel path being three feet wide (the FHWA HPMS Field Manual of December 2016 specifies 1 meter) and the center zone being three feet (0.91 meters) wide (Figure 217 and Figure 218):

1. Left Exterior: 0 meters offset from the Left Edge to -1.365 meters offset from the Center
2. Left Wheel Path: -1.365 to -0.455 meters offset from the Center

3. Center: -0.455 to 0.455 meters offset from the Center
4. Right Wheel Path: 0.455 to 1.365 meters offset from the Center
5. Right Exterior: 1.365 meters offset from the Center to 0 meters offset from the Right Edge



**Figure 217. Wheel Path Designation in FDOT Flexible Distress Handbook**

New          Modify          Delete						
#	Road Zone	Left Anchor	Offset	Right Anchor	Offset	
1	Left Exterior	LeftEdge	0.000	Centre	-1.365	
2	Left WheelPath	Centre	-1.365	Centre	-0.455	
3	Center	Centre	-0.455	Centre	0.455	
4	Right Wheelpath	Centre	0.455	Centre	1.365	
5	Right Exterior	Centre	1.365	RightEdge	0.000	

**Figure 218. Road Zone Settings**

## Rating Profile

The Rating Profile is used for assigning a distress type and severity to each of the detected and classified surface defects. This profile contains several components including profile name, profile description and rating rules. The rating rules configuration include distress rule set up and severity rule set up. While the Distress Rules specify classification of crack, the road zone, and distress metrics to be calculated, the Severity Rules determine detailed constraints on distresses that will be rated into each severity.

*Distress Rules* are setup based on the following:

1. Crack Classification: following detection and classification, all cracks are classified into Longitudinal, Transverse, Alligator, or Block. As previously noted, there are two options for distinguishing distresses by zone location. Table 111 and Table 112 show the distress types that were considered for this project and their corresponding crack classification for option 1 and option 2, respectively. As it was noted before, these distress types are used for documenting the distresses in a permanent record to facilitate quality control.

**Table 111. Distress Types and Corresponding Crack Classification and Severity Levels (option 1 corresponding to Figure 209 used for the reference survey)**

Distress Name	Crack Classification	Severity Levels
SingleCrack_L	Longitudinal	1B, II, III
SingleCrack_T	Transverse	1B, II, III
BranchCrack_L	Longitudinal	1B, II, III
BranchCrack_T	Transverse	1B, II, III
BlockCrack	Block	1B, II, III
AlligatorCrack	Alligator	II, III
Raveling	NA	III
Patching	NA	III

**Table 112. Distress Types and Corresponding Crack Classification and Severity Levels (option 2 corresponding to Figure 210 used for automated results)**

Distress Name	Crack Classification	Severity Levels
SingleCrack_L_WP	Longitudinal	1B, II, III
SingleCrack_L_OP	Longitudinal	1B, II, III
SingleCrack_T_WP	Transverse	1B, II, III
SingleCrack_T_OP	Transverse	1B, II, III
BranchCrack_L_WP	Longitudinal	1B, II, III
BranchCrack_L_OP	Longitudinal	1B, II, III
BranchCrack_T_WP	Transverse	1B, II, III
BranchCrack_T_OP	Transverse	1B, II, III
BlockCrack_WP	Block	1B, II, III
BlockCrack_OP	Block	1B, II, III

<b>Distress Name</b>	<b>Crack Classification</b>	<b>Severity Levels</b>
AlligatorCrack_WP	Alligator	II, III
AlligatorCrack_OP	Alligator	II, III
Raveling_WP	NA	III
Raveling_OP	NA	III
Patching_WP	NA	III
Patching_OP	NA	III

2. **Lane Type:** Used only with option 2 (Table 112 and Figure 210), this refers to the road zones to be included in the process of identifying a selected Distress Type. For wheel path distresses, the 'Left Wheel Path' and 'Right Wheel Path' zones created in the 'Road Zone' menu of the Schema Editor can be selected. For non-wheel path distresses, the 'Left Exterior', 'Center', and 'Right Exterior' zones created in the 'Road Zone' menu of the Schema Editor are selected. For the reference survey in which manual correction of the automated results was required, this feature was disabled and instead wheel path and non-wheel path distresses were recorded in the same distress type and separated using an SQL code on the database (option 1). In this manner, if the road zone widths change in the future, the data can easily be reprocessed and there would be no need for conducting the manual distress rating again.
  
3. **Metric:** These include metrics to be reported for a selected Distress Type after automated identification and quantification. The following metrics were selected in the created rating rules. They will be calculated and recorded in the Vision Database.
  - a) Crack Count - Number of Cracks that make up a Crack Group
  - b) Crack Area - Area that contains all Cracks (all cracks in Crack Group)
  - c) Crack Length - Actual length along all cracks in a Crack Group
  - d) Crack Extent - Longitudinal length of cracks in a Crack Group (Length in y-axis)
  - e) Transverse Extent - Horizontal length of cracks in a Crack Group (Length in x-axis)
  - f) Width - Width of Crack (Average width of cracks in Crack Group)

- g) Diagonal - Length from bottom left to top right of every distress bounding box

*Severity Rules* are setup based on the following (In current version of Vision software, the unit used in parameter settings is meter):

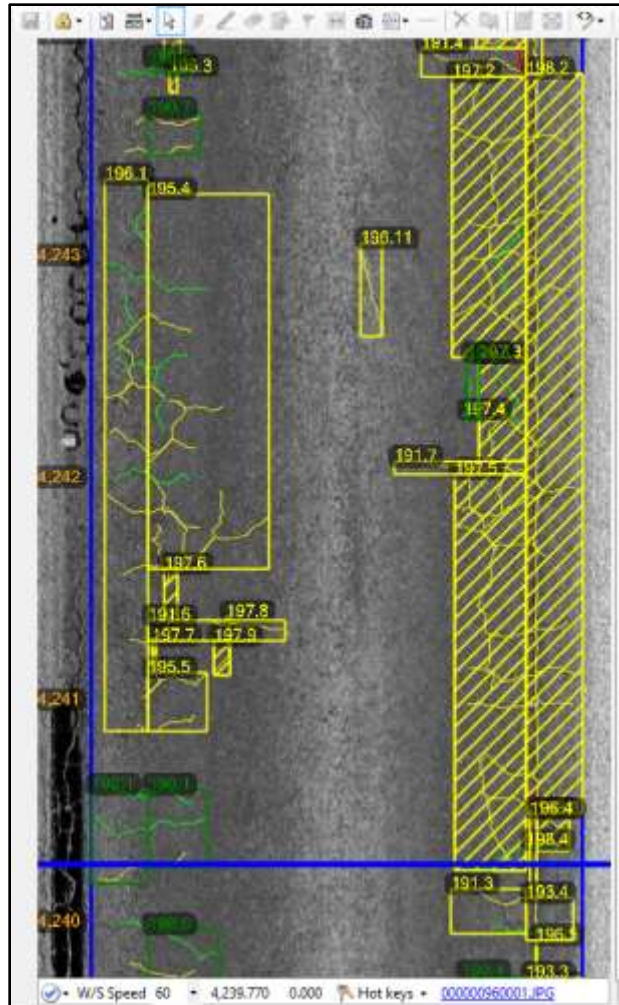
- 4. Crack Width: a crack width range is used as a constraint for selected severity levels in this project as demonstrated in Table 113.

**Table 113. Crack Width Range**

Severity Level	Crack Width Range (meter)
Class 1B	Less than 0.00318
Class II	Greater than or equal to 0.00318 and less than 0.00635
Class III	Greater than or equal to 0.00635 and less than 1

- 5. Crack Length: a minimum extent of 0.3 meter (1.0 ft) is used as a constraint for identifying distresses (this was selected based on past experience):
  - a) Transverse Extent is used for transverse single and branch cracks
  - b) Longitudinal Extent is used for longitudinal single and branch cracks
  - c) No extent limitation was considered for alligator or block cracks
- 6. Road Zone: Used only with option 2 (Table 112 and Figure 210), this refers to the road zones to be included in the process of rating a selected Distress Severity. For wheel path distresses, the 'Left Wheel Path' and 'Right Wheel Path' zones created in the 'Road Zone' menu of the Schema Editor can be selected. For non-wheel path distresses, the 'Left Exterior', 'Center', and 'Right Exterior' zones created in the 'Road Zone' menu of the Schema Editor are selected. This results in only the portion of detected cracks within specified zones to be included in each severity rating. This was only used for the fully automated survey. For example, Figure 219 shows that Distress number 195 shows longitudinal cracking in the wheel path and Distress number 196 shows the adjacent longitudinal cracking outside the wheel path. Similarly, Distress number 197 shows alligator cracking in the wheel path, while Distress number 198 indicates the adjacent alligator cracking outside the wheel path.





**Figure 219. Automatically Separated Wheel Path and Non-Wheel Path Distress Rating**

#### **I.2.4. Automated Pavement Distress Identification**

Fugro Vision software includes batch processors for automated lane detection, crack detection, classification and rating as identified in Table 114. These batch processors can be executed individually or all together. The JPEG Crack Detection Processor is Fugro's solution for detecting surface defects using machine learning algorithms on 2D or 3D pavement images. The LCMS Global Processor is the Pavemetrics solution for detecting surface defects on 3D pavement images. As noted previously, the Pavemetrics algorithm was used to create crack maps that were manually fixed to establish the reference survey. The Fugro machine learning algorithm was used without manual intervention to evaluate the automated crack detection results on both 2D and 3D images. There was no specific reason for the selection of one or the other. Either way, one algorithm needed manual correction to establish the reference crack map and a different algorithm was needed to show the automated crack detection results on 3D images.

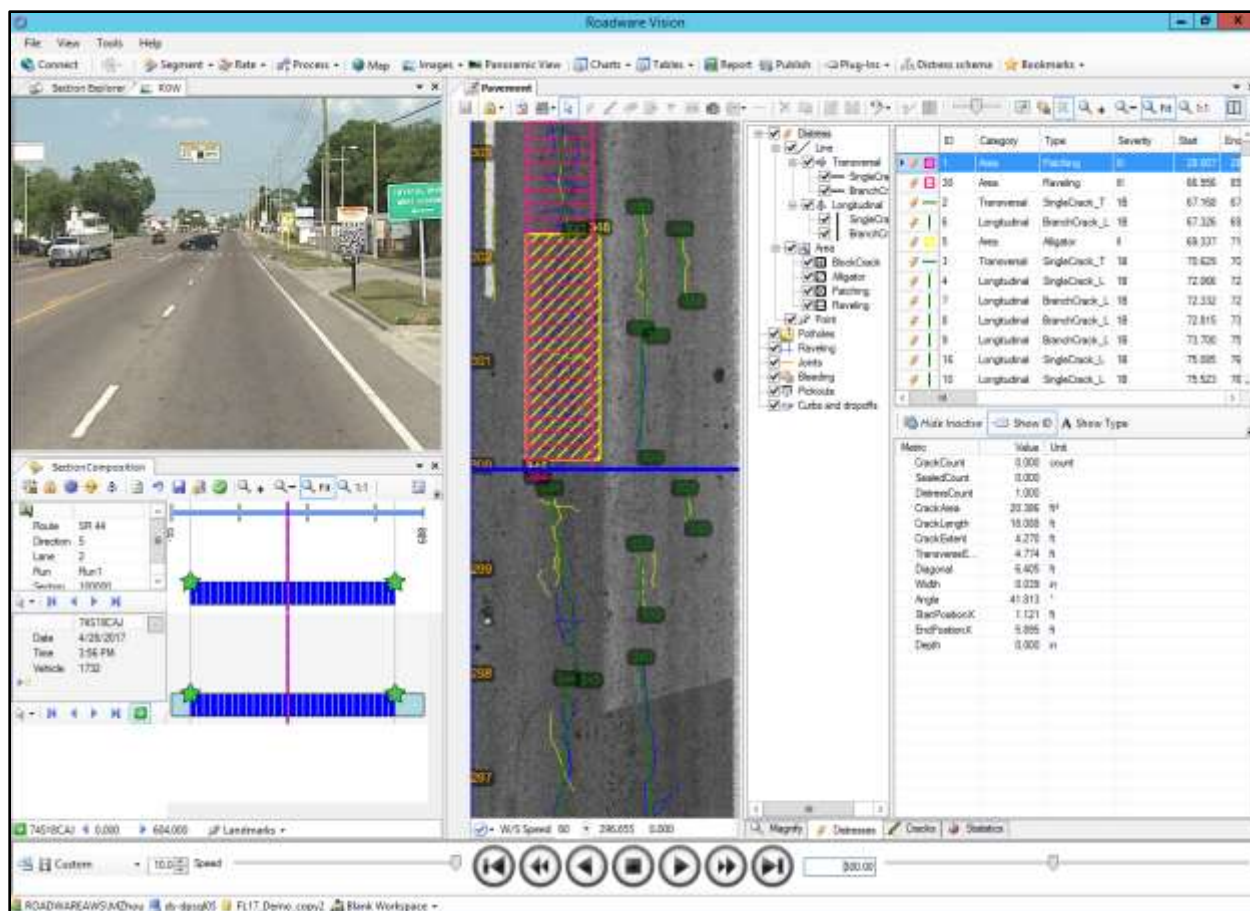
At this stage, the Vision software does NOT have an automated way of identifying patching. There is an automated raveling algorithm developed by Pavemetrics, but it needs to be calibrated according to FDOT raters' subjective identification of the raveling severity levels (This will be done in Task 6).

**Table 114. Vision Automated Batch Processors**

<b>Batch Processor</b>	<b>Function</b>
JPEG Lane Detection Processor	Lane Detection
JPEG Crack Detection Processor	Crack Detection from 2D or 3D Images
LCMS Global Processor	Crack Detection from 3D Images
Classification Processor	Classification
Rating Processor	Rating

#### **I.2.5. Semi-Automated Pavement Distress Identification**

A Fugro rater conducted a manual rating on one run of the images for the 12 test sections using the LCMS images that were imported into the Vision software. Then another Fugro rater reviewed the results of the first rater to reach consensus on the reference survey ("Ground Truth"). During this procedure, linear distresses and area distresses (boxes) are manually drawn on top of the collected pavement images. The results of the crack detection process, including the color-coded cracks were used by raters as guidance to assign severity levels based on crack width. As shown in Figure 220, the Vision Pavement rating module allows the analyst to simultaneously view both the ROW and pavement images while marking and rating pavement distresses.



**Figure 220. Vision Pavement Rating Module for Semi-Automated Distress Survey**

### I.3. Comparison of Automated Distress Survey Results on 2D versus 3D Images

In this chapter of the report, the results of crack detection and distress identification using the 2D and 3D images are contrasted. The 2D data collection was conducted by FDOT using their LRIS equipment and the data were analyzed by Fugro staff during Task 4 of this project. The 3D data collection was conducted by Fugro using the ARAN LCMS equipment and the data were analyzed by Fugro staff as part of the required activities for this Purchase Order. The following will describe the success metrics, the reference values, and the comparison results, which will be analyzed to conclude on feasibility of using 3D LCMS technology and its advantages to the 2D LRIS technology in identification and quantification of flexible pavement distresses.

### I.3.1. Success Metrics

The three principal success metrics of any process are effectiveness, efficiency, and reliability. In the context of automated distress identification, effectiveness can be expressed in terms of accuracy of the crack detection software when compared to a reference baseline. Accuracy is a qualitative term referring to whether there is agreement between a measurement made on an object and its true (target or reference) value. Bias is a quantitative term describing the difference (or error) between the average of measurements made on the same object and its true value.

While systematic errors identified in the bias can be calibrated out, such evaluations must address the random errors as well. The average results may be quite comparable, but individual results can deviate significantly. Efforts must be made to control these deviations to produce results which can ultimately be classified as reliable. Reliability of automated distress surveys is often expressed in terms of precision. Precision is a qualitative term that can describe the degree of repeatability of a measurement value on the same sample, or consistency in accuracy of measurement on different samples. Coefficient of variation of actual measurement values on the same sample is a quantitative estimate of repeatability. Standard deviation of error (standard error) is a quantitative estimate of consistency. Accuracy and precision (or the corresponding quantitative estimates: bias, variance, and standard error) ultimately define how effective and reliable a system is as described in greater detail below. The efficiency of the system is typically measured by the time it takes to conduct these measurements.

With respect to automated condition evaluations, the success metrics could be considered for two aspects of the process, first for the detection of individual surface defects (cracks), and second for the identification and quantification of the distresses in a distinct section.

The following are the success metrics used for evaluating the crack detection results:

- True Positives: length of correctly detected cracking
- False Positives: length of detected cracking that don't exist in the reference survey
- False Negatives: length of missed cracking
- Crack Validity: an indicator to be calculated as the ratio of the correctly detected cracks (true positives) to the total detected cracks (true positives and false positives). This statistic indicates the percentage of the detected cracks that was

actually present in the reference survey, thereby expressing the validity of the cracks detected by algorithms.

$$\text{Validity (\%)} = 100 \times \frac{\text{correctly detected}}{\text{all detected}} = 100 \times \frac{\text{true positives}}{\text{true positives} + \text{false positives}}$$

- Crack Sensitivity (or Recall): a parameter to be calculated as the ratio of the correctly detected cracks to the total actual cracks existing on the pavement surface (true positives and false negatives). This statistic represents the percentage of the cracks in the reference survey that was detected by the automated method, thereby expressing the sensitivity of the algorithms to existing cracks.

$$\text{Sensitivity (\%)} = 100 \times \frac{\text{correctly detected}}{\text{actual cracks}} = 100 \times \frac{\text{true positives}}{\text{true positives} + \text{false negatives}}$$

- Crack Detection Accuracy: based on average normalized error (bias) of automatically detected crack length compared to the reference. Accuracy (%) = 100 – Bias (%)
- Crack Detection Repeatability: based on coefficient of variation (COV) of detected crack length among three runs (independent of the reference and averaged among the sections). Repeatability (%) = 100 – COV (%)
- Crack Detection Consistency: based on coefficient of variation (COV) of crack detection accuracy among 12 test sections. Consistency (%) = 100 – [Standard Deviation of Accuracy (%) / Average Accuracy (%)]
- Crack Detection Efficiency: based on the time required for the automated crack detection. Efficiency (second per foot) = time for cracking detection divided by the total length

Based on the overall cumulative amount of each distress among different test sections and multiple runs, the success metrics used to compare 2D and 3D rating methods are:

1. Distress Identification Accuracy: based on average error (bias) with respect to the reference distress survey values for each distress type. Accuracy (%) = 100 – Bias (%)

2. Distress Identification Repeatability: based on coefficient of variation (COV) of automatically identified distresses among three runs for each distress type (independent of the reference and averaged among the sections). Repeatability (%) =  $100 - \text{COV} (\%)$
3. Distress Identification Consistency: based on coefficient of variation (COV) of distress identification accuracy among 12 sections for each distress type. Consistency (%) =  $100 - [\text{Standard Deviation of Accuracy} (\%) / \text{Average Accuracy} (\%)]$
4. Distress Identification Efficiency: based on the time required for the automated distress survey. Efficiency (second per foot) = time for cracking detection, classification, and rating divided by the total length.

### **I.3.2. Reference Rating or “Ground Truth”**

Two reference ratings were created for this evaluation:

1. Crack Detection Reference: the Pavemetrics LCMS crack detection routine was used to generate a baseline crack map and then a Fugro data technician reviewed all the images in one run of the 12 test sections and modified the crack maps. New cracks were added for missed cracks, false positives were deleted, and some cracks with wrong extent were modified to reflect the actual cracks that can be seen on the 3D intensity and range (depth) images and with assistance from the ROW images.
2. Distress Identification Reference: a reference survey was created by one Fugro engineer and another Fugro technician reviewed the results to reach a consensus for the reference survey. This reference survey was created using the 3D images because they provide both intensity and range (depth) views, along with the ROW images. Therefore, comprehensive sources of data are available in the 3D database for creating this reference survey.

### **I.3.3. Comparison Limitations**

The current comparison was conducted considering the following limitations of this analysis:

1. The 12 test sections were selected as representative of the actual pavement surfaces found across Florida. With such a small sample, it is possible that not all of the actual pavement network is represented in this study. Every effort was made to select a representative sample. However, the budgetary and schedule

limitations of this project would not allow for collection and processing of data across a wider network.

2. The comparison of crack detection is conducted using different automated detection algorithms for 2D versus 3D images. This is because the 3D images provide additional depth information and the corresponding algorithm is inevitably different than the 2D algorithm. As noted previously, both employed algorithms are based on machine learning techniques. The 2D algorithm was trained on a large database of manually rated 2D images; similarly, the 3D algorithm was trained on a large database of manually rated 3D images. The process for generating the corresponding training database and training of the corresponding algorithms were carried out outside this project.
3. The comparison of distress identification was conducted using the same automated distress identification algorithm. This algorithm as it stands does not exactly differentiate between the crack types as defined in the FDOT Flexible Pavement Condition Survey Handbook, because those definitions were originally intended for human raters and not for computers. The automated algorithm used crack angle to differentiate between longitudinal and transverse cracks, and crack density in a given area to differentiate between single linear cracks and an area of alligator cracking. Therefore, the error compared to ground truth is estimated by comparing the total amount of automatically identified longitudinal and transverse cracks to the sum of the single and branch cracks manually identified in the reference survey. Similarly, the total amount of automatically identified alligator cracking is compared to the sum of the alligator and block cracks manually identified in the reference survey. This limitation does not undermine this comparison because the same automated algorithm was used for both 2D and 3D analyses.
4. This study is mainly focused on cracking distresses and patching and raveling were not considered in this comparison. The 3D technology provides pavement surface macro-texture measurements which could potentially be used for identifying raveling. However, these texture measurements need to be calibrated to corresponding areas of raveling identified by experienced raters. This effort is planned to be conducted during Task 6 of this study.
5. The quality assurance practices such as equipment calibration and verification procedures, and the process for certification of the operators could affect the results. The FDOT QA practices for operating their 2D LRIS equipment differ from the Fugro QA practices for operating ARANs with 3D LCMS technology. While proper precautions and coordination were made to limit the impacts of these differences, some impact is inevitable. For example, the vehicle wander could impact the run-to-run repeatability results.

### **I.3.4. Comparison of Automatically Detected Crack Quantities**

False positives are cracks that have been reported by the automated crack detection software, while no crack has been recorded in the Crack Detection Reference (“ground truth”) at the same location. On the other hand, false negatives are existing cracks that have been reported in the “ground truth” but were not detected by the software (i.e. missed cracks). Table 115 and Table 116 show the true positives, false positives, false negatives, validity, and sensitivity of the automated crack detection using Fugro’s machine learning algorithms on 3D and 2D images, respectively. These tables include the crack detection results on run number 1 of the 3 runs. These tables indicate that about 75 percent of the automatically detected cracks from 3D images were actually present on the pavement surface (Validity), compared to only 25 percent of automatically detected cracks from 2D images being true positives. Also, about 89 percent of the cracks in the ground truth were automatically detected from 3D images (Sensitivity), while only about 18 percent of the actual cracks were detected from 2D images. These results demonstrate that the automated crack detection from the 3D images has a significantly superior performance compared to that from the 2D images, in terms of both validity of the detected cracks and sensitivity of the automated algorithm to detecting existing surface cracks.

In Table 115 and Table 116, the yellow highlighted cells indicate significant false positives (more than 50% of the reference) and the orange colored cells indicate significant amounts of false negatives (more than 50% of the reference). It is evident that in Sections number 3, 7, and 9, both the 2D and 3D methods have a significant amount of false positives. This is due to two reasons. First, some patching area boundaries (Figure 221) and Automated Vehicle Counter (AVC) loops and Weigh-In-Motion (WIM) devices (Figure 222) being falsely detected as cracks. Second, the amount of cracking in the semi-automated reference survey for these three sections is lower compared to other sections and as a result, the errors seem higher.

From Table 115, it is also evident that the 3D method does not result in a significant number of missed cracks, as it has detected about 89 percent of the existing cracks. However, Table 116 shows that the 2D method has missed a significant amount of the cracks and only detected about 18 percent of the existing cracks in the reference.

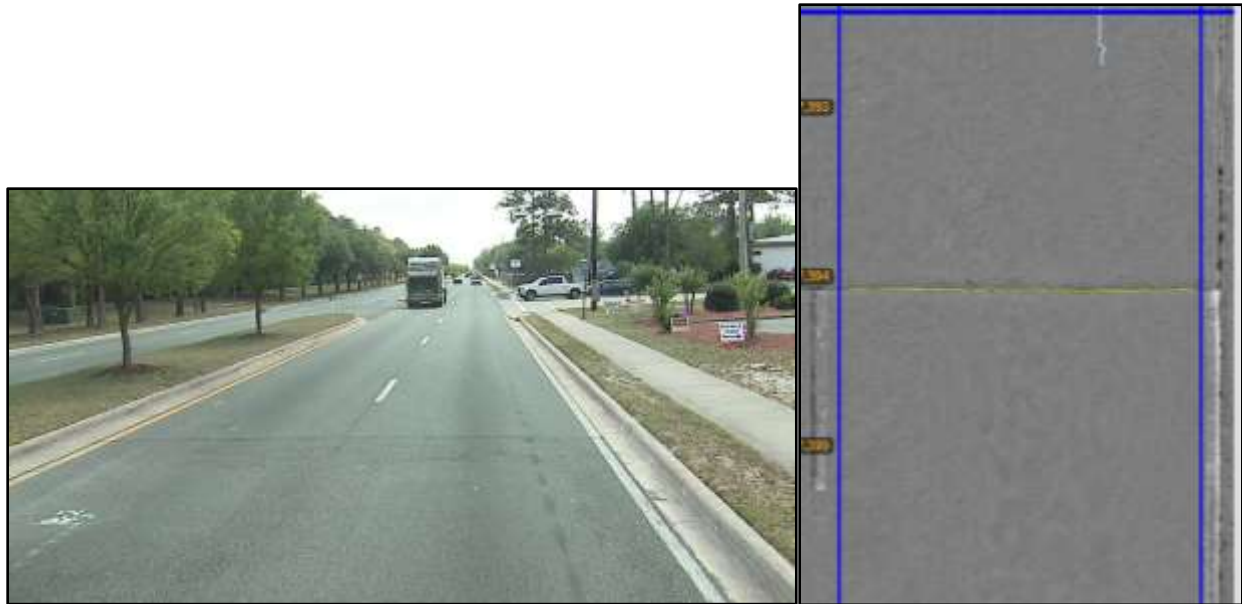


**Table 115. Verification of Crack Detection on 3D images Using Fugro Machine Learning Algorithm**

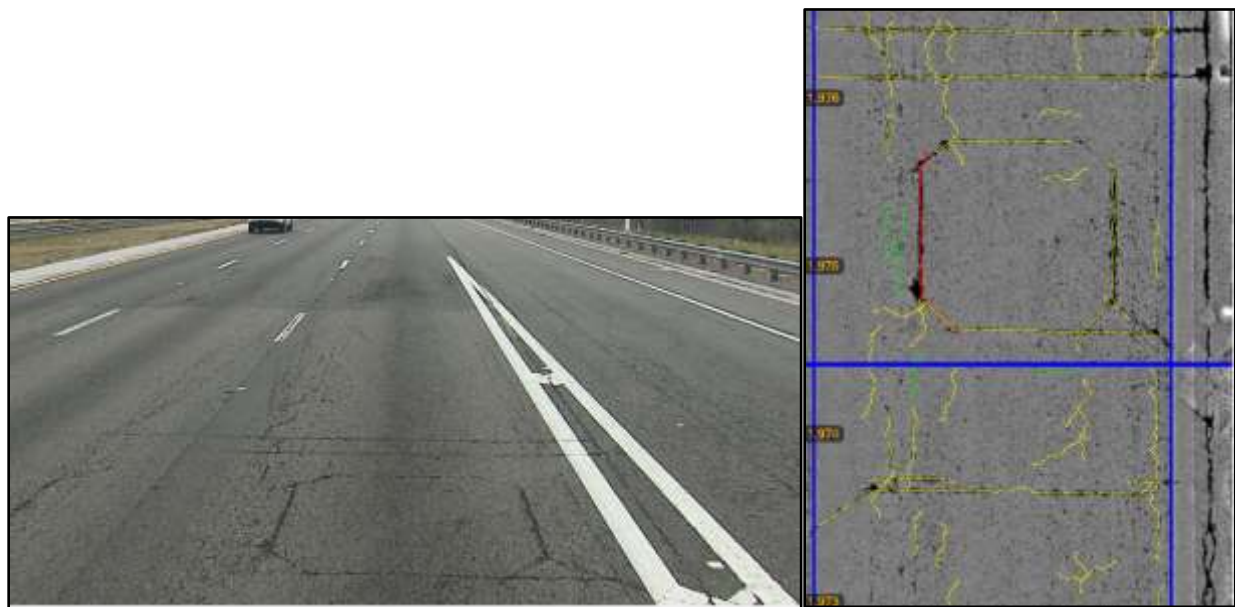
Test Section	Ground Truth (ft)	Crack Detection Results			Crack Validity (%)	Crack Sensitivity (%)
		True Positives (ft)	False Positives (ft)	False Negatives (ft)		
1	22,944.22	18,464.62	2,762.11	4,479.60	86.99	80.48
2	26,741.89	24,873.49	1,217.80	1,868.40	95.33	93.01
3	132.74	126.10	824.84	6.64	13.26	94.99
4	14,823.69	12,015.20	1,429.99	2,808.49	89.36	81.05
5	68,726.86	65,286.40	3,453.19	3,440.46	94.98	94.99
6	112,892.60	102,199.75	11,059.70	10,692.85	90.24	90.53
7	809.34	687.92	1,820.47	121.42	27.42	85.00
8	27,185.46	23,990.87	2,097.65	3,194.59	91.96	88.25
9	3,993.09	2,881.59	6,082.98	1,111.50	32.14	72.16
10	36,631.86	38,825.92	1,803.39	(2,194.06)	95.56	105.99
11	30,517.80	27,386.58	4,025.66	3,131.22	87.18	89.74
12	29,327.95	28,174.06	3,057.05	1,153.89	90.21	96.07
					<b>74.55</b>	<b>89.36</b>

**Table 116. Verification of Crack Detection on 2D images Using Fugro Machine Learning Algorithm**

Test Section	Ground Truth (ft)	Crack Detection Results			Crack Validity (%)	Crack Sensitivity (%)
		True Positives (ft)	False Positives (ft)	False Negatives (ft)		
1	22,944.22	1,162.61	3,337.93	21,781.61	25.83	5.07
2	26,741.89	824.98	3,727.55	25,916.91	18.12	3.08
3	132.74	42.55	16,471.86	90.19	0.26	32.06
4	14,823.69	3,659.58	4,199.93	11,164.11	46.56	24.69
5	68,726.86	6,226.68	10,005.31	62,500.18	38.36	9.06
6	112,892.60	7,139.73	10,005.56	105,752.87	41.64	6.32
7	809.34	523.47	13,969.35	285.87	3.61	64.68
8	27,185.46	5,184.47	13,606.25	22,000.99	27.59	19.07
9	3,993.09	807.72	19,550.12	3,185.37	3.97	20.23
10	36,631.86	1,718.52	12,621.25	34,913.34	11.98	4.69
11	30,517.80	3,507.70	6,274.08	27,010.10	35.86	11.49
12	29,327.95	3,003.47	3,539.88	26,324.48	45.90	10.24
					<b>24.97</b>	<b>17.56</b>



**Figure 221. Patching Area Boundary Falsely Detected as Cracks**



**Figure 222. AVC Loops and WIM Devices Falsely Detected as Cracks**

In addition to the crack detection verification results in Table 115 and Table 116, other crack detection success metrics including normalized error, average error (bias), variation between multiple runs (repeatability), and variation among 12 test sections (consistency) of the automated crack detection algorithms from 3D and 2D images have been listed in Table 117 and Table 118, respectively. The three test sections number 3, 7, and 9 have been highlighted in yellow to indicate the sections that have a significant

amount of false positives in both of the crack detection methods (Figure 221 and Figure 222). The bias has been provided as the average normalized crack detection error both on all the test sections and also excluding the 3 outliers. When excluding the outliers, Table 117 and Table 118 indicate that the accuracy (100 - Bias) of the automated crack detection from 3D images is about 99 percent, which is significantly superior to the accuracy from 2D images (about 31 percent).

**Table 117. Accuracy, Repeatability, and Consistency of Crack Detection based on 3D Images**

Test Section	Ground Truth (ft)	Detected Crack Length			Normalized Error			100 - AVG ABS Error (%)	Repeatability (%)
		Run 1 (ft)	Run 2 (ft)	Run 3 (ft)	Run1 (%)	Run2 (%)	Run3 (%)		
1	22,944.22	21,226.73	20,718.69	20,761.75	-7.49	-9.70	-9.51	91.10	98.65
2	26,741.89	26,091.29	26,564.27	26,905.88	-2.43	-0.66	0.61	99.17	98.46
3	132.74	950.94	658.74	1,020.48	616.39	396.26	668.78	-460.48	78.11
4	14,823.69	13,445.19	12,647.37	13,034.35	-9.30	-14.68	-12.07	87.98	96.94
5	68,726.86	68,739.59	67,648.23	68,637.83	0.02	-1.57	-0.13	99.44	99.12
6	112,892.66	113,259.45	116,185.57	116,723.13	0.32	2.92	3.39	97.79	98.38
7	809.34	2,508.39	2,187.71	2,512.42	209.93	170.31	210.43	-96.89	92.25
8	27,185.46	26,088.52	24,746.74	24,978.47	-4.04	-8.97	-8.12	92.96	97.16
9	3,993.09	8,964.57	9,143.59	8,296.30	124.50	128.99	107.77	-20.42	94.93
10	36,631.86	40,629.31	45,240.06	38,560.87	10.91	23.50	5.27	86.77	91.76
11	30,517.80	31,412.24	29,347.11	30,317.56	2.93	-3.84	-0.66	99.48	96.60
12	29,327.95	31,231.11	30,760.06	29,860.88	6.49	4.88	1.82	95.60	97.73
<b>Bias (%)</b>								<b>72.31</b>	<b>97.20</b>
<b>Bias Excluding Outliers (%)</b>								<b>-1.11</b>	
<b>Accuracy (%) = 100 - Absolute Bias</b>								<b>98.89</b>	
<b>Consistency (%) = 100 - COV(Accuracy)</b>								<b>94.95</b>	

**Table 118. Accuracy, Repeatability, and Consistency of Crack Detection based on 2D Images**

Test Section	Ground Truth (ft)	Detected Crack Length			Normalized Error			100 - AVG ABS Error (%)	Repeatability (%)
		Run 1 (ft)	Run 2 (ft)	Run 3 (ft)	Run1 (%)	Run2 (%)	Run3 (%)		
1	22,944.22	4,500.54	4,564.01	4,090.53	-80.38	-80.11	-82.17	19.11	94.14
2	26,741.89	4,552.53	3,864.70	3,843.54	-82.98	-85.55	-85.63	15.28	90.13
3	132.74	16,514.41	14,055.83	15,632.52	12341.17	10488.99	11676.80	-11402.32	91.91
4	14,823.69	7,859.51	7,699.58	7,906.21	-46.98	-48.06	-46.67	52.77	98.61
5	68,726.86	16,231.99	13,279.23	10,427.46	-76.38	-80.68	-84.83	19.37	78.20
6	112,892.60	17,145.29	18,010.45	17,739.17	-84.81	-84.05	-84.29	15.62	97.49
7	809.34	14,492.82	13,748.75	14,703.70	1690.70	1598.76	1716.75	-1568.74	96.50
8	27,185.46	18,790.72	19,884.37	19,572.17	-30.88	-26.86	-28.01	71.42	97.10
9	3,993.09	20,357.84	19,751.20	20,089.79	409.83	394.63	403.11	-302.53	98.49
10	36,631.86	14,339.77	14,077.36	11,809.28	-60.85	-61.57	-67.76	36.60	89.62
11	30,517.80	9,781.78	9,506.47	9,133.08	-67.95	-68.85	-70.07	31.04	96.56
12	29,327.95	6,543.35	6,448.33	6,702.61	-77.69	-78.01	-77.15	22.38	98.04
<b>Bias (%)</b>								<b>1079.77</b>	<b>93.32</b>
<b>Bias Excluding Outliers (%)</b>								<b>-68.49</b>	
<b>Accuracy (%) = 100 - Absolute Bias</b>								<b>31.51</b>	
<b>Consistency (%) = 100 - COV(Accuracy)</b>								<b>38.84</b>	

The automated detection from 3D and 2D images are comparable in terms of run-to-run repeatability with about 97 and 93 percent agreement among runs for 3D and 2D methods, respectively. The 3D method is showing better performance in terms of consistency of results on different sections as the 3D method has about 95 percent agreement in crack detection accuracy among 12 sections and the 2D method has only about 39 percent.

### I.3.5. Comparison of Automatically Identified Distress Quantities

In this section, the results of automated distress identification from 2D and 3D images are compared to each other. It should be noted that the most significant difference between the results from the two methodologies is caused by the difference in the crack detection performance. As it was demonstrated in the previous section, the crack detection from 2D images is missing a significant amount of cracking and as a result,

there is a significant negative bias in the distress identification results for the 2D methodology.

### ***Comparison of Automatically Identified Longitudinal, Transverse, and Alligator Cracking from 2D Versus 3D Images***

The available Vision software was used for this comparison. In this section, the comparison is conducted based on the amount of automatically identified Longitudinal, Transverse, and Alligator cracking.

It should be noted that the automated algorithm used crack angle to differentiate between longitudinal and transverse cracks, and crack density in a given area to differentiate between single linear cracks and an area of alligator cracking. Therefore, the normalized error compared to ground truth is estimated by comparing the total amount of automatically identified longitudinal and transverse cracks to the sum of single and branch cracks manually identified in the reference survey. Similarly, the total amount of automatically identified alligator cracking is compared to the sum of alligator and block cracks manually identified in the reference survey. This limitation does not undermine this comparison because the same automated algorithm was used for both 2D and 3D analyses. Table 119 and Table 120 show the success metrics for automatically identifying Longitudinal cracks from 3D and 2D images, respectively. Test sections with minimal amount of longitudinal cracking (in the reference survey) have been highlighted in yellow as outliers. Excluding the outliers, the automated longitudinal cracking identification from 3D and 2D images have demonstrated about 93 and 46 percent accuracy, respectively.

The 3D results show a positive bias indicating more automatically identified longitudinal cracks compared to the reference survey. However, the 2D results show a significantly high amount of missed longitudinal cracking compared to the reference survey, reflected in the high negative bias.

On average, there is about 97 percent run-to-run agreement in the length of automatically identified longitudinal cracks from 3D images. This run-to-run repeatability is about 89 percent for the 2D results. There is about 81 percent section-to-section agreement in the accuracy in automatically identifying the length of longitudinal cracks from 3D images. This section-to-section consistency is about 45 percent for 2D results.

**Table 119. Accuracy, Repeatability, and Consistency of Longitudinal Cracks on 3D**

Test Section	Ground Truth (ft)	Automatically Identified Longitudinal Cracks			Normalized Error			100 - AVG ABS Error (%)	Repeatability (%)
		Run 1 (ft)	Run 2 (ft)	Run 3 (ft)	Run1 (%)	Run2 (%)	Run3 (%)		
1	3,596.83	3,657.91	3,722.85	4,231.16	1.70	3.50	17.64	92.39	91.89
2	2,138.43	3,160.27	3,230.07	3,188.40	47.78	51.05	49.10	50.69	98.90
3	9.79	33.61	30.48	91.18	243.31	211.34	831.36	-328.67	33.97
4	2,744.90	2,911.72	2,917.34	2,871.70	6.08	6.28	4.62	94.34	99.14
5	8,468.56	10,649.42	10,563.81	10,635.02	25.75	24.74	25.58	74.64	99.57
6	9,148.41	13,762.54	14,608.56	14,050.04	50.44	59.68	53.58	45.43	96.96
7	481.76	201.21	164.96	188.44	-58.23	-65.76	-60.89	38.37	90.05
8	7,717.18	5,799.07	5,921.45	5,767.01	-24.86	-23.27	-25.27	75.54	98.60
9	807.48	989.11	980.57	1,184.31	22.49	21.44	46.67	69.80	89.04
10	6,599.33	4,630.23	4,755.88	4,113.87	-29.84	-27.93	-37.66	68.19	92.44
11	10,103.90	10,780.99	11,059.53	11,546.60	6.70	9.46	14.28	89.85	96.52
12	19,775.85	13,550.58	13,327.31	13,382.07	-31.48	-32.61	-32.33	67.86	99.13
Bias (%)								38.46	97.02
Bias Excluding Outliers (%)								7.14	
Accuracy (%) = 100 - Absolute Bias								92.86	
Consistency (%) = 100 - COV(Accuracy)								81.23	

**Table 120. Accuracy, Repeatability, and Consistency of Longitudinal Cracks on 2D**

Test Section	Ground Truth (ft)	Automatically Identified Longitudinal Cracks			Normalized Error			100 - AVG ABS Error (%)	Repeatability (%)
		Run 1 (ft)	Run 2 (ft)	Run 3 (ft)	Run1 (%)	Run2 (%)	Run3 (%)		
1	3,596.83	1,310.26	1,260.20	1,126.84	-63.57	-64.96	-68.67	34.26	92.31
2	2,138.43	921.76	794.50	813.26	-56.90	-62.85	-61.97	39.43	91.85
3	9.79	5,845.47	3,380.38	3,255.96	59608.58	34428.91	33158.02	-42298.50	64.90
4	2,744.90	2,492.63	2,629.55	2,541.79	-9.19	-4.20	-7.40	93.07	97.28
5	8,468.56	5,782.13	4,822.60	3,558.99	-31.72	-43.05	-57.97	55.75	76.38
6	9,148.41	4,937.94	5,869.39	5,263.88	-46.02	-35.84	-42.46	58.56	91.18
7	481.76	1,812.05	1,629.81	1,967.13	276.13	238.30	308.32	-174.25	90.64
8	7,717.18	3,996.32	4,238.55	4,446.63	-48.22	-45.08	-42.38	54.78	94.67
9	807.48	1,454.53	1,181.45	1,254.07	80.13	46.31	55.31	39.42	89.09
10	6,599.33	3,914.45	3,497.79	2,383.00	-40.68	-47.00	-63.89	49.48	75.75
11	10,103.90	1,817.90	1,921.66	2,195.46	-82.01	-80.98	-78.27	19.58	90.14
12	19,775.85	1,030.80	979.37	1,151.56	-94.79	-95.05	-94.18	5.33	91.61
Bias (%)								3520.30	89.02
Bias Excluding Outliers (%)								-54.42	
Accuracy (%) = 100 - Absolute Bias								45.58	
Consistency (%) = 100 - COV(Accuracy)								44.67	

Table 121 and Table 122 show the success metrics for automatically identifying Transverse cracks from 3D and 2D images, respectively. Test sections with minimal

amount of transverse cracking have been highlighted as outliers. Excluding the outliers, the automated transverse cracking identification from 3D and 2D images have demonstrated about 90 and 24 percent accuracy, respectively. Both the 3D and 2D results show a negative bias indicating less automatically identified transverse cracks compared to the reference survey. On average, there is about 90 percent run-to-run agreement in the length of automatically identified transverse cracks from 3D images. This run-to-run repeatability is about 91 percent for the 2D results. There is about 74 percent section-to-section agreement in the accuracy in identifying transverse cracking from 3D images. This section-to-section consistency is only about 6 percent for 2D results.

**Table 121. Accuracy, Repeatability, and Consistency of Transverse Cracks based on 3D**

Test Section	Ground Truth (ft)	Automatically Identified Transverse Cracks			Normalized Error			100 - AVG ABS Error (%)	Repeatability (%)
		Run 1 (ft)	Run 2 (ft)	Run 3 (ft)	Run1 (%)	Run2 (%)	Run3 (%)		
1	276.88	99.58	87.88	79.50	-64.03	-68.26	-71.29	32.14	88.67
2	273.01	37.33	46.74	47.47	-86.33	-82.88	-82.61	16.06	87.10
3	10.93	7.84	10.73	9.44	-28.27	-1.83	-13.63	85.42	100.00
4	256.67	452.80	391.54	462.75	76.41	52.55	80.29	30.25	91.15
5	109.35	185.70	174.61	160.16	69.82	59.68	46.47	41.34	92.62
6	157.20	198.29	189.94	187.33	26.14	20.83	19.17	77.96	97.02
7	16.51	15.91	15.14	28.93	-3.63	-8.30	75.23	78.90	61.24
8	965.30	767.31	726.02	834.96	-20.51	-24.79	-13.50	80.40	92.91
9	21.60	126.65	118.27	130.01	486.34	447.55	501.90	-378.60	95.16
10	2,306.42	854.82	836.38	1,009.24	-62.94	-63.74	-56.24	39.03	89.45
11	170.73	292.80	259.16	344.70	71.50	51.80	101.90	24.94	85.58
12	590.56	132.92	102.83	101.02	-77.49	-82.59	-82.89	19.01	84.04
Bias (%)								33.11	89.84
Bias Excluding Outliers (%)								-9.76	
Accuracy (%) = 100 - Absolute Bias								90.24	
Consistency (%) = 100 - COV(Accuracy)								73.80	



**Table 122. Accuracy, Repeatability, and Consistency of Transverse Cracks based on 2D**

Test Section	Ground Truth (ft)	Automatically Identified Transverse Cracks			Normalized Error				Repeatability (%)
		Run 1 (ft)	Run 2 (ft)	Run 3 (ft)	Run1 (%)	Run2 (%)	Run3 (%)	100 - AVG ABS Error (%)	
1	276.88	30.55	29.06	30.52	-88.97	-89.50	-88.98	10.85	97.17
2	273.01	50.95	52.38	55.64	-81.34	-80.81	-79.62	19.41	95.46
3	10.93	0.00	0.00	0.00	-100.00	-100.00	-100.00	0.00	100.00
4	256.67	17.39	18.20	18.56	-93.22	-92.91	-92.77	7.03	96.68
5	109.35	65.53	66.41	63.08	-40.07	-39.27	-42.31	59.45	97.35
6	157.20	68.65	73.08	71.56	-56.33	-53.51	-54.48	45.23	96.83
7	16.51	4.69	1.04	2.29	-71.59	-93.70	-86.13	16.19	30.61
8	965.30	42.60	40.95	39.61	-95.59	-95.76	-95.90	4.25	96.35
9	21.60	115.14	124.41	123.30	433.06	475.97	470.83	-359.95	95.81
10	2,306.42	22.52	18.90	12.81	-99.02	-99.18	-99.44	0.78	72.85
11	170.73	99.33	90.25	93.03	-41.82	-47.14	-45.51	55.18	95.06
12	590.56	101.41	106.83	64.08	-82.83	-81.91	-89.15	15.37	74.36
Bias (%)								<b>-33.86</b>	<b>91.35</b>
Bias Excluding Outliers (%)								<b>-75.83</b>	
Accuracy (%) = 100 - Absolute Bias								<b>24.17</b>	
Consistency (%) = 100 - COV(Accuracy)								<b>5.62</b>	

Table 123 and Table 124 show the success metrics for automatically identifying Alligator cracks from 3D and 2D images, respectively. Test sections free of alligator cracking have been highlighted as outliers. Excluding the outliers, the automated alligator cracking identification from 3D and 2D images have demonstrated about 95 and 0.01 percent accuracy, respectively.



**Table 123. Accuracy, Repeatability, and Consistency of Alligator Cracks based on 3D Images**

Test Section	Ground Truth (Sq Ft)	Automatically Identified Alligator Cracks			Normalized Error			100 - AVG ABS Error (%)	Repeatability (%)
		Run 1 (Sq Ft)	Run 2 (Sq Ft)	Run 3 (Sq Ft)	Run1 (%)	Run2 (%)	Run3 (%)		
1	5,846.75	5,338.05	5,424.37	5,093.62	-8.70	-7.22	-12.88	90.40	96.75
2	9,482.90	8,162.28	8,445.05	8,571.04	-13.93	-10.94	-9.62	88.50	97.51
3	0.00	0.00	0.00	0.00					
4	3,100.22	721.79	549.74	575.11	-76.72	-82.27	-81.45	19.85	84.91
5	18,795.12	16,437.95	17,019.01	16,729.03	-12.54	-9.45	-10.99	89.01	98.26
6	27,372.47	30,219.12	30,618.90	31,145.60	10.40	11.86	13.78	87.99	98.48
7	0.00	0.00	0.00	0.00					
8	4,223.72	1,975.46	1,888.80	1,859.62	-53.23	-55.28	-55.97	45.17	96.84
9	0.00	4.74	4.59	1.28					44.70
10	6,567.40	8,617.27	9,703.71	8,059.52	31.21	47.76	22.72	66.10	90.49
11	1,533.73	1,690.51	1,553.59	1,397.82	10.22	1.29	-8.86	99.11	90.54
12	900.06	1,769.73	1,538.15	1,316.48	96.62	70.89	46.27	28.74	85.30
Bias (%)								-5.45	93.23
Bias Excluding Outliers (%)								-5.45	
Accuracy (%) = 100 - Absolute Bias								94.55	
Consistency (%) = 100 - COV(Accuracy)								68.46	

**Table 124. Accuracy, Repeatability, and Consistency of Alligator Cracks based on 2D Images**

Test Section	Ground Truth (Sq Ft)	Automatically Identified Alligator Cracks			Normalized Error			100 - AVG ABS Error (%)	Repeatability (%)
		Run 1 (Sq Ft)	Run 2 (Sq Ft)	Run 3 (Sq Ft)	Run1 (%)	Run2 (%)	Run3 (%)		
1	5,846.75	0.00	0.00	0.00	-100.00	-100.00	-100.00	0.00	100.00
2	9,482.90	14.21	0.00	0.00	-99.85	-100.00	-100.00	0.05	-73.21
3	0.00	0.00	0.00	0.00					100.00
4	3,100.22	0.18	0.00	0.00	-99.99	-100.00	-100.00	0.00	-73.21
5	18,795.12	0.05	0.00	0.00	-100.00	-100.00	-100.00	0.00	-73.21
6	27,372.47	0.00	0.00	0.00	-100.00	-100.00	-100.00	0.00	100.00
7	0.00	0.00	0.00	0.00					100.00
8	4,223.72	0.00	0.00	0.00	-100.00	-100.00	-100.00	0.00	100.00
9	0.00	0.00	0.00	0.00					100.00
10	6,567.40	0.00	0.01	0.00	-100.00	-100.00	-100.00	0.00	-73.21
11	1,533.73	0.18	0.23	0.04	-99.99	-99.99	-100.00	0.01	34.34
12	900.06	0.00	0.00	0.00	-100.00	-100.00	-100.00	0.00	100.00
Bias (%)								-99.99	15.72
Bias Excluding Outliers (%)								-99.99	
Accuracy (%) = 100 - Absolute Bias								0.01	
Consistency (%) = 100 - COV(Accuracy)								-139.83	

The 3D results show a negative bias indicating less automatically identified alligator cracks compared to the reference survey. The 2D results however show a significant

amount of negative bias, indicating that the 2D distress identification has failed in identifying areas with alligator cracking. This is mainly due to the large amount of missed cracking in 2D crack detection, which in turn results in cracking areas with such low density that cannot be identified by the computer as alligator cracking areas.

On average, there is about 93 percent run-to-run agreement in the automatically identified alligator cracking areas from 3D images. This run-to-run repeatability is about 16 percent for the 2D results. There is about 68 percent section-to-section agreement in the accuracy in automatically identifying the area of alligator cracks from 3D images. This section-to-section consistency is non-existent for 2D results.

The Vision software records the amount of time that each batch processor had spent on each test section to conduct an automated survey. The automated detection, classification, and rating took about 20 seconds per image frame for the 3D images and about 26 seconds per image frame for the 2D images. The main difference in this speed is the crack detection time. The classification and distress identification processes take only about 0.05 seconds per image frame in both technologies.

### ***Comparison of Automatically Identified Wheel Path and Non-Wheel Path Cracking from 2D Versus 3D Images***

In this section, the semi-automated reference rating results were converted to cracking within the wheel path (CW) and outside the wheel path (CO) using a SQL code (see option 1). The automated distress identification results were already available in CW and CO format, because the distress schema was setup accordingly (see option 2). The total amount of cracking within the wheel paths (CW) was calculated by adding the longitudinal, transverse, and alligator cracking areas. The longitudinal and transverse cracking areas were calculated by multiplying their length by 1 foot, as specified in the FDOT Flexible Pavement Condition Survey Handbook.

Table 125 and Table 126 show the automated distress identification results for CO distresses from 3D and 2D images, respectively. The accuracy in determining the CO distresses from 3D and 2D images is about 89 and 33 percent, respectively. The run-to-run repeatability in determining the CO distresses from 3D and 2D images is about 96 and 86 percent, respectively. The section-to-section consistency in determining the CO distresses from 3D and 2D images is about 85 and 34 percent, respectively.

Table 127 and Table 128 show the automated distress identification results for CW distresses from 3D and 2D images, respectively. The accuracy in determining the CW distresses from 3D and 2D images is about 92 and 9 percent, respectively. The run-to-run repeatability in determining the CW distresses from 3D and 2D images is about 97 and 91 percent, respectively. The section-to-section consistency in determining the CW distresses from 3D and 2D images is about 84 and 0.4 percent, respectively.

**Table 125. Accuracy, Repeatability, and Consistency of CO Based on 3D Images**

Test Section	Ground Truth (Sq Ft)	Automatically Identified Cracking			Normalized Error			100 - AVG ABS Error (%)	Repeatability (%)
		Run 1 (Sq Ft)	Run 2 (Sq Ft)	Run 3 (Sq Ft)	Run1 (%)	Run2 (%)	Run3 (%)		
1	2,269.16	2,055.22	2,155.45	2,337.45	-9.43	-5.01	3.01	96.19	93.45
2	2,929.56	2,917.19	2,947.83	3,024.51	-0.42	0.62	3.24	98.85	98.13
3	11.98	37.48	36.06	74.96	212.85	201.00	525.71		55.43
4	3,452.35	2,367.69	2,201.37	2,271.34	-31.42	-36.24	-34.21	66.05	96.34
5	13,550.71	12,028.60	12,097.83	12,358.12	-11.23	-10.72	-8.80	89.75	98.57
6	15,456.96	17,262.52	17,701.37	17,594.28	11.68	14.52	13.83	86.66	98.69
7	296.23	62.06	57.41	84.87	-79.05	-80.62	-71.35		78.42
8	4,232.96	2,679.95	2,452.73	2,549.57	-36.69	-42.06	-39.77	60.50	95.55
9	249.79	345.65	404.21	448.16	38.38	61.82	79.41		87.12
10	6,584.24	5,668.12	5,430.82	4,880.60	-13.91	-17.52	-25.87	80.90	92.42
11	4,653.28	5,627.19	6,086.35	6,154.74	20.93	30.80	32.27	72.00	95.18
12	11,403.25	8,294.84	8,021.22	7,885.04	-27.26	-29.66	-30.85	70.74	97.41
Bias (%)								16.89	96.19
Bias Excluding Outliers (%)								-10.38	
Accuracy (%) = 100 - Absolute Bias								89.62	
Consistency (%) = 100 - COV(Accuracy)								84.81	

**Table 126. Accuracy, Repeatability, and Consistency of CO Based on 2D Images**

Test Section	Ground Truth (Sq Ft)	Automatically Identified Cracking			Normalized Error			100 - AVG ABS Error (%)	Repeatability (%)
		Run 1 (Sq Ft)	Run 2 (Sq Ft)	Run 3 (Sq Ft)	Run1 (%)	Run2 (%)	Run3 (%)		
1	2,269.16	413.16	332.64	276.57	-81.79	-85.34	-87.81	15.02	79.85
2	2,929.56	326.82	267.14	349.21	-88.84	-90.88	-88.08	10.73	86.51
3	11.98	5,845.47	3,380.38	3,255.96	48,693.57	28,116.86	27,078.30	-34529.58	100.00
4	3,452.35	1,675.19	1,837.38	1,755.16	-51.48	-46.78	-49.16	50.86	95.38
5	13,550.71	4,981.47	3,890.31	2,891.53	-63.24	-71.29	-78.66	28.94	73.34
6	15,456.96	3,289.52	3,959.84	3,622.93	-78.72	-74.38	-76.56	23.45	90.75
7	296.23	1,807.72	1,626.94	1,962.51	510.24	449.22	562.50	-407.32	90.66
8	4,232.96	2,919.43	3,178.08	3,411.57	-31.03	-24.92	-19.40	74.88	92.23
9	249.79	1,369.37	1,063.21	1,164.95	448.21	325.64	366.37	-280.07	87.00
10	6,584.24	3,900.46	3,461.47	2,344.54	-40.76	-47.43	-64.39	49.14	75.21
11	4,653.28	1,678.48	1,732.75	2,033.89	-63.93	-62.76	-56.29	39.01	89.45
12	11,403.25	990.18	940.88	1,061.73	-91.32	-91.75	-90.69	8.75	93.91
Bias (%)								2909.81	86.29
Bias Excluding Outliers (%)								-66.58	
Accuracy (%) = 100 - Absolute Bias								33.42	
Consistency (%) = 100 - COV(Accuracy)								34.07	

**Table 127. Accuracy, Repeatability, and Consistency of Cracking within Wheel Paths (CW) Based on 3D Images**

Test Section	Ground Truth (Sq Ft)	Automatically Identified Cracking			Normalized Error			100 - AVG ABS Error (%)	Repeatability (%)
		Run 1 (Sq Ft)	Run 2 (Sq Ft)	Run 3 (Sq Ft)	Run1 (%)	Run2 (%)	Run3 (%)		
1	7,451.30	7,040.32	7,079.65	7,066.83	-5.52	-4.99	-5.16	94.78	99.72
2	8,964.78	8,442.69	8,774.02	8,782.40	-5.82	-2.13	-2.03	96.67	97.76
3	8.74	3.97	5.16	25.66	-54.58	-40.96	193.59		-5.15
4	2,649.44	1,718.61	1,657.26	1,638.22	-35.13	-37.45	-38.17	63.08	97.49
5	13,822.31	15,244.47	15,659.61	15,166.10	10.29	13.29	9.72	88.90	98.27
6	21,221.13	26,917.43	27,716.03	27,788.68	26.84	30.61	30.95	70.53	98.24
7	202.05	155.06	122.70	132.51	-23.26	-39.27	-34.42		87.87
8	8,673.24	5,861.90	6,083.54	5,912.02	-32.41	-29.86	-31.84	68.63	98.05
9	579.29	774.85	699.23	867.43	33.76	20.70	49.74		89.21
10	8,888.91	8,434.21	9,865.16	8,302.03	-5.12	10.98	-6.60	99.76	90.22
11	7,155.08	7,137.11	6,785.94	7,134.38	-0.25	-5.16	-0.29	98.10	97.12
12	9,863.21	7,158.39	6,947.06	6,914.53	-27.42	-29.57	-29.90	71.04	98.11
Bias (%)								-2.69	97.22
Bias Excluding Outliers (%)								-7.49	
Accuracy (%) = 100 - Absolute Bias								92.51	
Consistency (%) = 100 - COV(Accuracy)								83.93	

**Table 128. Accuracy, Repeatability, and Consistency of Cracking within Wheel Paths (CW) Based on 2D Images**

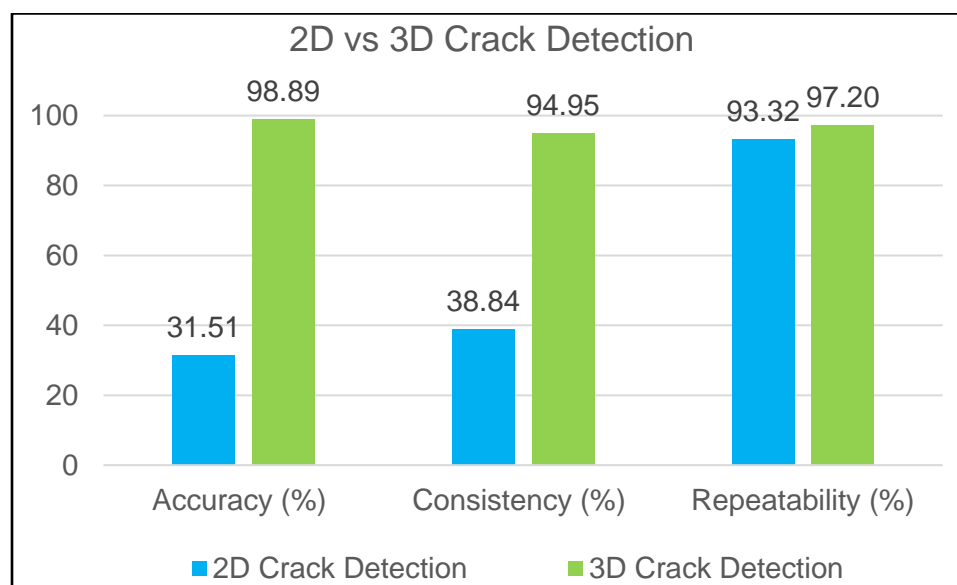
Test Section	Ground Truth (Sq Ft)	Automatically Identified Cracking			Normalized Error			100 - AVG ABS Error (%)	Repeatability (%)
		Run 1 (Sq Ft)	Run 2 (Sq Ft)	Run 3 (Sq Ft)	Run1 (%)	Run2 (%)	Run3 (%)		
1	7,451.30	927.65	956.62	880.79	-87.55	-87.16	-88.18	12.37	95.85
2	8,964.78	660.09	579.74	519.69	-92.64	-93.53	-94.20	6.54	87.99
3	8.74	0.00	0.00	0.00	-100.00	-100.00	-100.00	0.00	100.00
4	2,649.44	835.01	810.36	805.19	-68.48	-69.41	-69.61	30.83	98.05
5	13,822.31	866.24	998.70	730.53	-93.73	-92.77	-94.71	6.26	84.50
6	21,221.13	1,717.08	1,982.63	1,712.50	-91.91	-90.66	-91.93	8.50	91.43
7	202.05	9.02	3.91	6.91	-95.54	-98.06	-96.58	3.27	61.17
8	8,673.24	1,119.50	1,101.42	1,074.67	-87.09	-87.30	-87.61	12.67	97.95
9	579.29	200.31	242.65	212.42	-65.42	-58.11	-63.33	37.71	90.02
10	8,888.91	36.51	55.22	51.26	-99.59	-99.38	-99.42	0.54	79.31
11	7,155.08	238.93	279.39	254.64	-96.66	-96.10	-96.44	3.60	92.08
12	9,863.21	142.03	145.32	153.92	-98.56	-98.53	-98.44	1.49	95.83
Bias (%)								-89.68	91.44
Bias Excluding Outliers (%)								-90.80	
Accuracy (%) = 100 - Absolute Bias								9.20	
Consistency (%) = 100 - COV(Accuracy)								0.38	

## I.4. Advantages of the 3D Technology

Based on the observations outlined in chapter 4, this chapter will describe some of the advantages of the 3D technology over the 2D technology for detection, identification, and quantification of flexible pavement surface distresses.

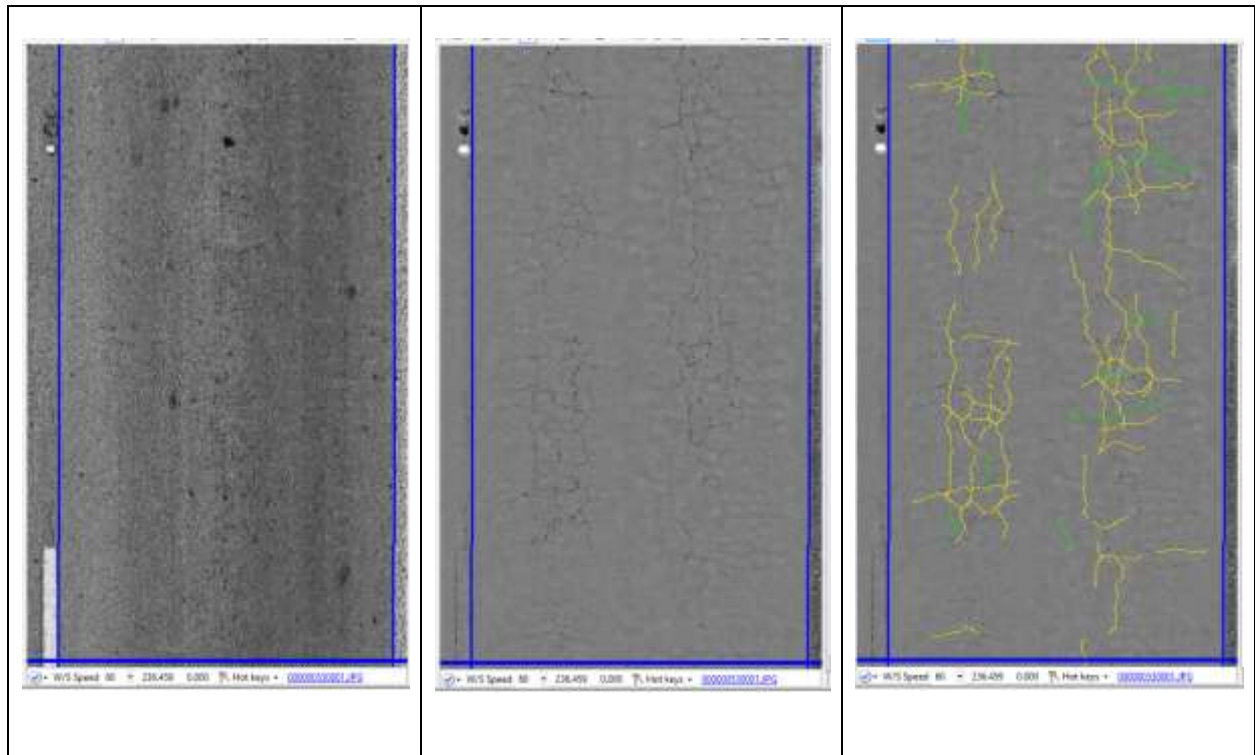
### I.4.1. Improved Crack Detection

As it was clearly demonstrated in crack detection, the 3D technology with the range (depth) data is facilitating detection of significantly more cracking compared to the 2D images. In the 12 representative test sections evaluated for this study, the use of 3D technology resulted in about 67 percent increase in accuracy of crack detection compared to the 2D technology (see Figure 223). This is also evident in the 89 percent of the cracking in the reference survey being detected from the 3D images, compared to only 18 percent from 2D images. This significant amount of missed cracks resulted in a big difference in the performance of automated distress identification as well.



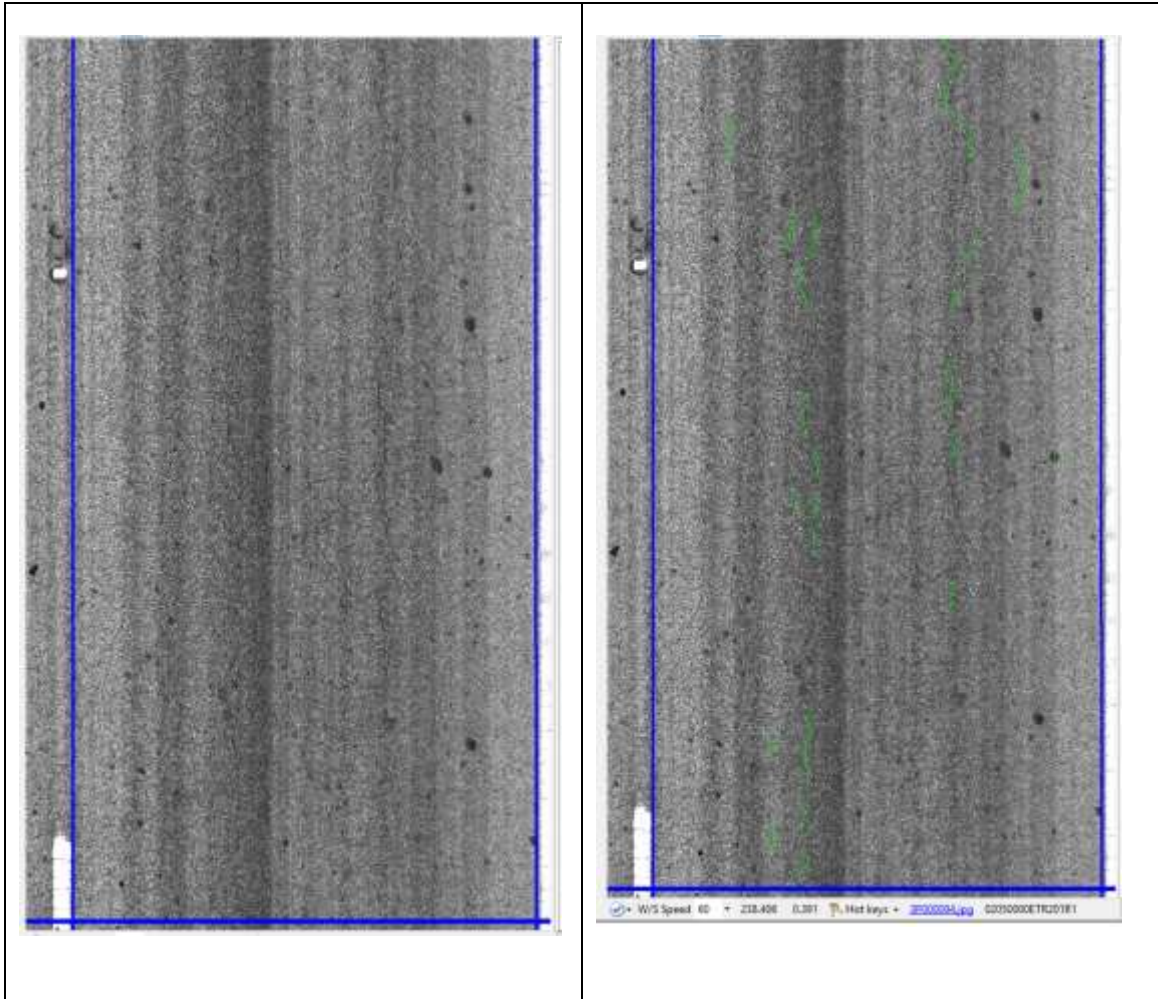
**Figure 223. Comparison of 2D versus 3D Crack Detection Success Metrics**

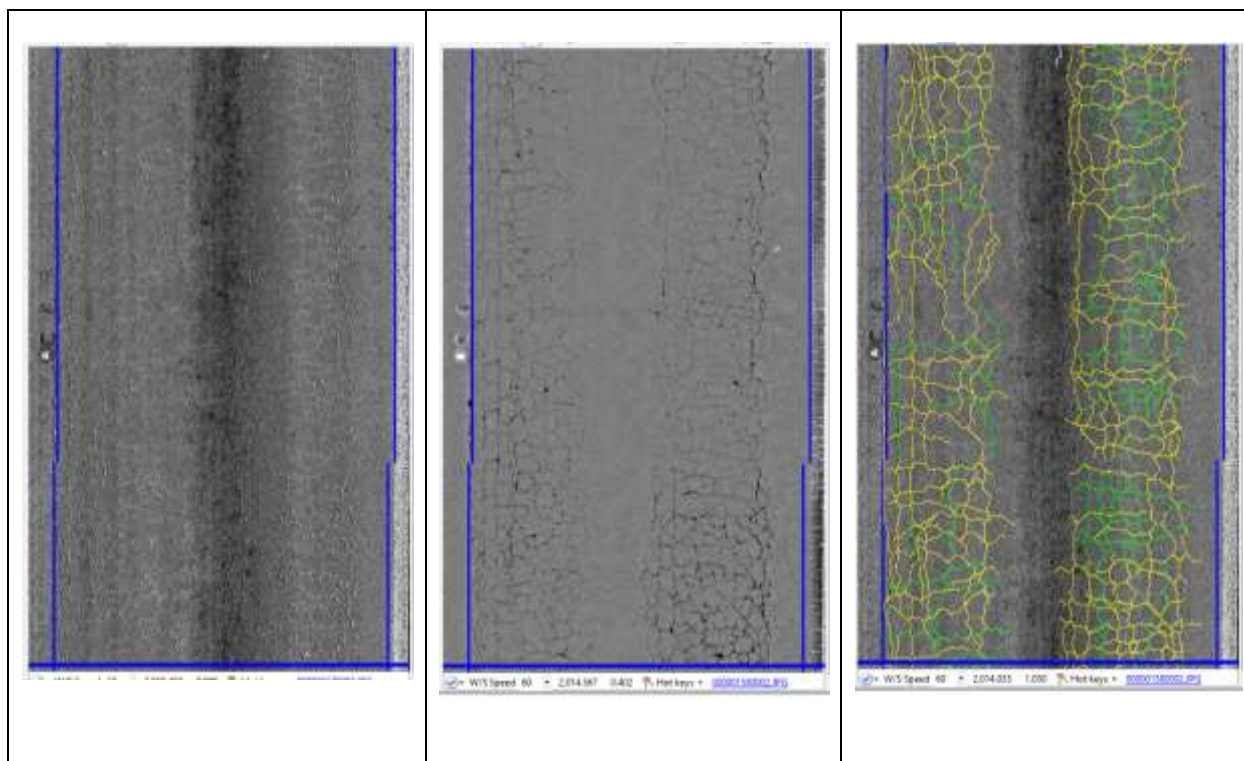
In order to better demonstrate the advantage of 3D technology in detecting surface cracks, two example locations have been selected. Figure 224 and Figure 225 show the 3D and 2D crack detection results for the first example location, respectively. Figure 226 and Figure 227 show the 3D and 2D crack detection results for the second example location, respectively. In both examples, it is evident that the 3D technology significantly improves the chances of detecting surface cracks because of the additional depth information. It can also be seen that due to the enhanced crack detection in the 3D technology, more interconnected cracks are detected and as a result, more networks of alligator cracking can be identified on the pavement surface.



**Figure 224. Example LCMS Intensity (left), Range (center), and Detected Crack Map (right)**

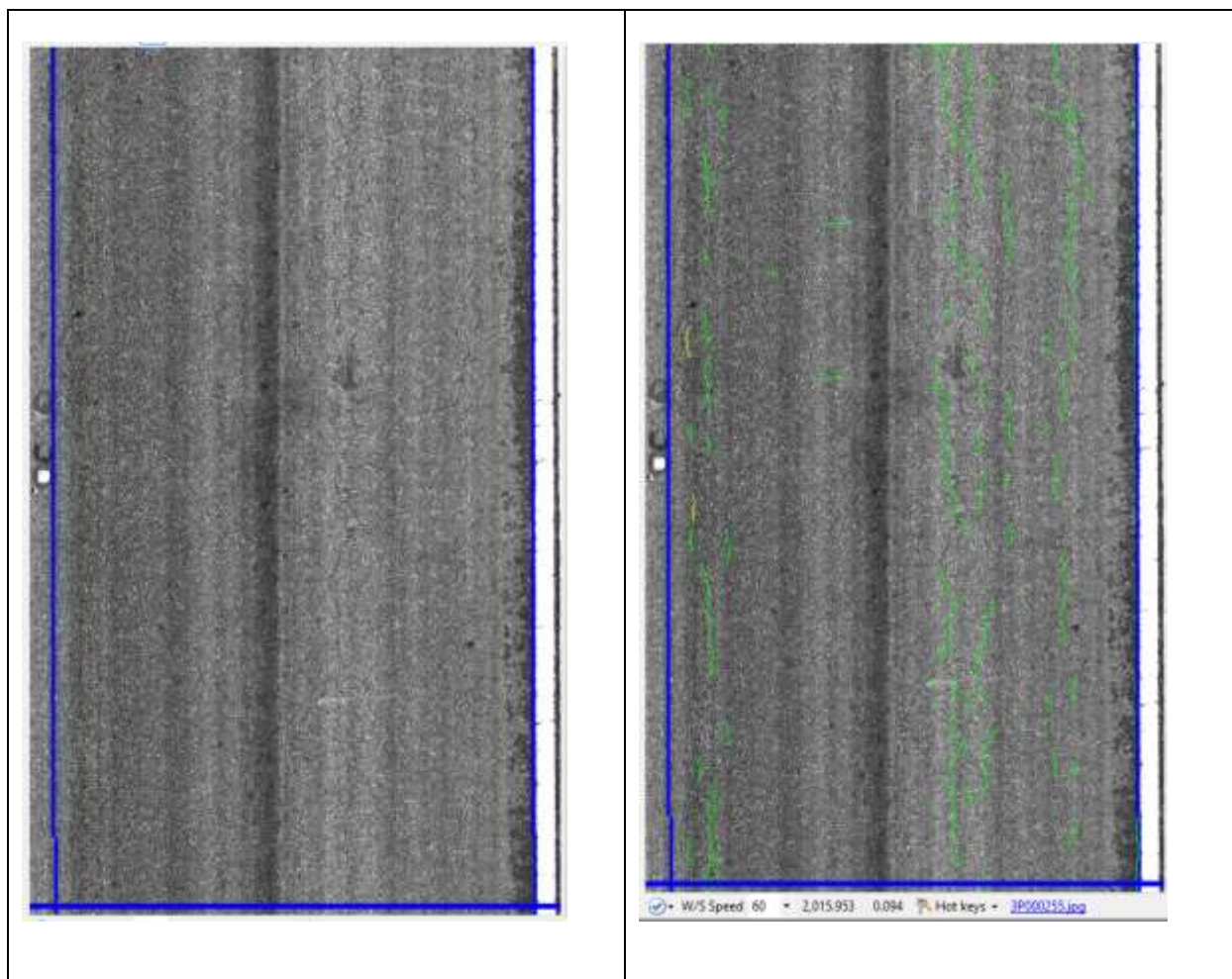






**Figure 226. Example LCMS Intensity (left), Range (center), and Detected Crack Map (right)**





**Figure 227. Example LRIS Image (left) and Detected Crack Map (right) Corresponding to the LCMS Example in Figure 226**

In addition to improved detection of cracking, the 3D technology is also superior to 2D technology in terms of correctly determining crack widths. This is based on work performed outside of this project. When the pavement surface is damp, the area around the crack edges become darker in the 2D images and as a result, the crack detection algorithms result in exaggerated crack width measurements based on pixel intensities. The 3D technology is less prone to these issues because it uses a combination of pixel intensities and crack depth values to determine crack width. As a result, the severity rating is more reliable in the 3D technology. This observation is based on past experience outside this project.

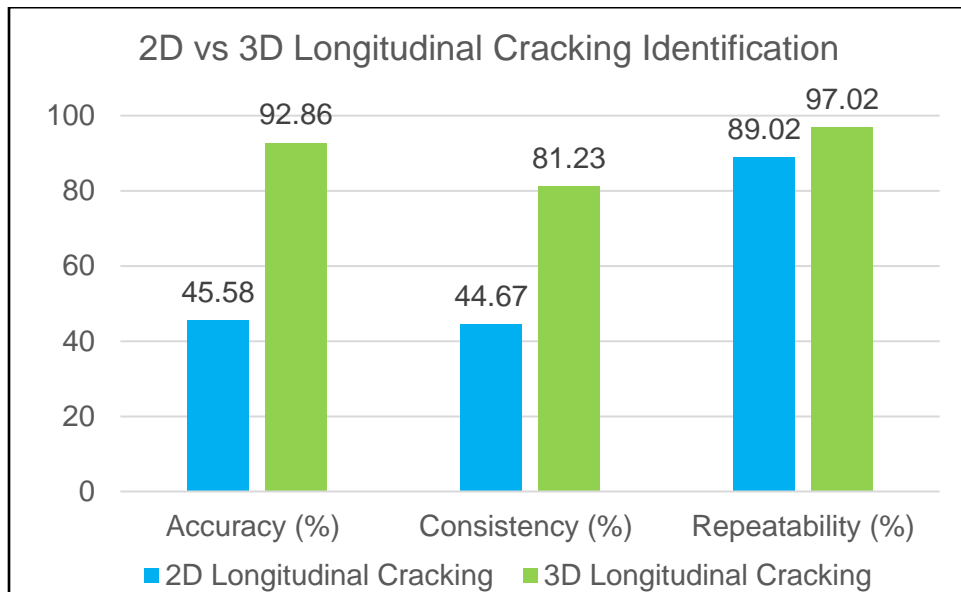
#### **I.4.2. Improved Identification of Cracking Distresses**

Table 129 provides summary statistics for the automated distress identification results based on 2D and 3D images.

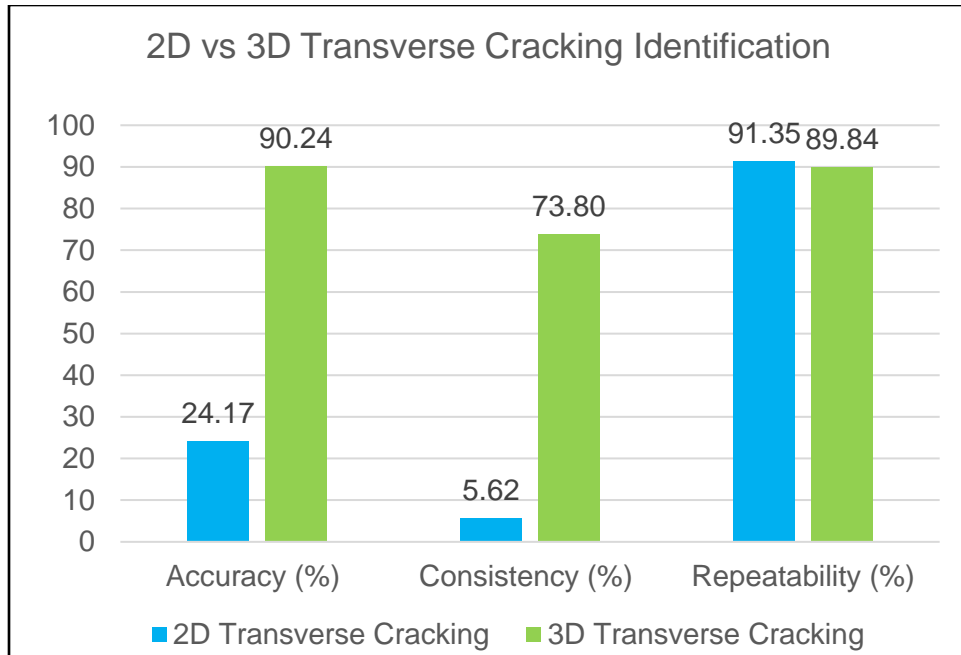
**Table 129. Summary Statistics for Automated Distress Identification Results from 2D and 3D Images**

Distress	Accuracy (%)		Section-To-Section Consistency (%)		Run-To-Run Repeatability (%)	
	2D	3D	2D	3D	2D	3D
<b>Longitudinal Cracking</b>	45.58	92.86	44.67	81.23	89.02	97.02
<b>Transverse Cracking</b>	24.17	90.24	5.62	73.80	91.35	89.84
<b>Alligator Cracking</b>	0.01	94.55	-139.83	68.46	15.72	93.23
<b>CW</b>	9.20	92.51	0.38	83.93	91.44	97.22
<b>CO</b>	33.42	89.62	34.07	84.81	86.29	96.19

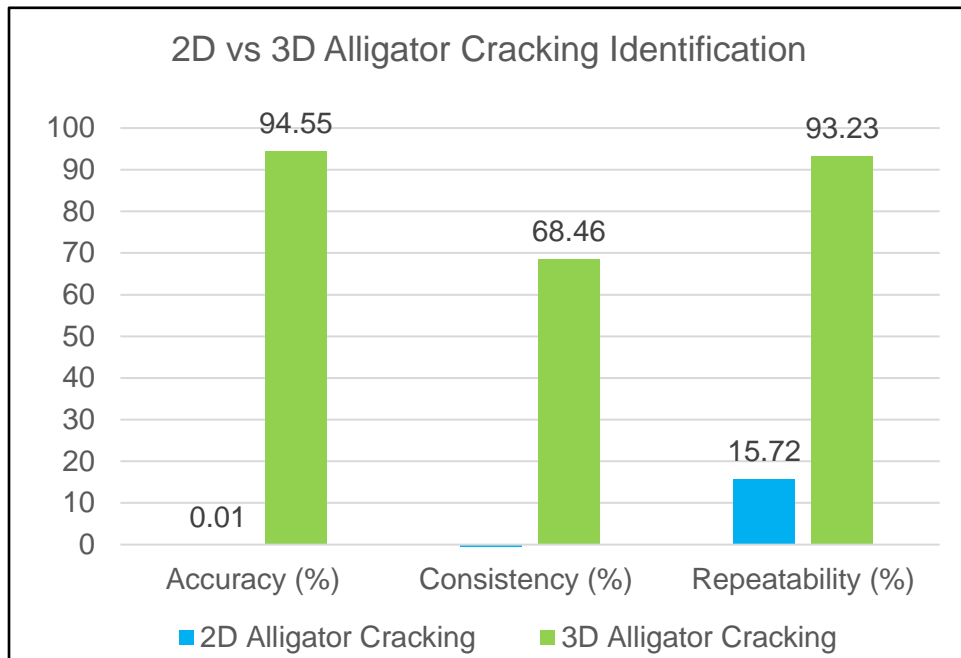
Figure 228, Figure 229, and Figure 230 compare the 2D and 3D distress identification results for longitudinal, transverse, and alligator cracking, respectively. The 3D algorithm has resulted in higher accuracy, section-to-section consistency, and run-to-run repeatability compared to the 2D algorithm in identifying longitudinal, transverse, and alligator cracking.



**Figure 228. Comparison of 2D versus 3D Longitudinal Cracking Success Metrics**



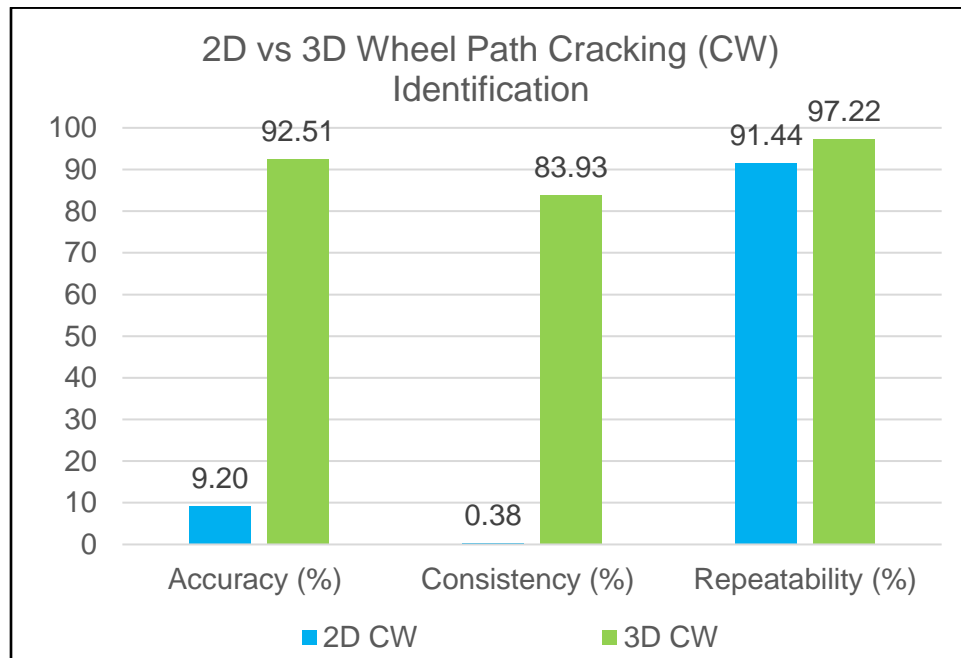
**Figure 229. Comparison of 2D versus 3D Transverse Cracking Success Metrics**



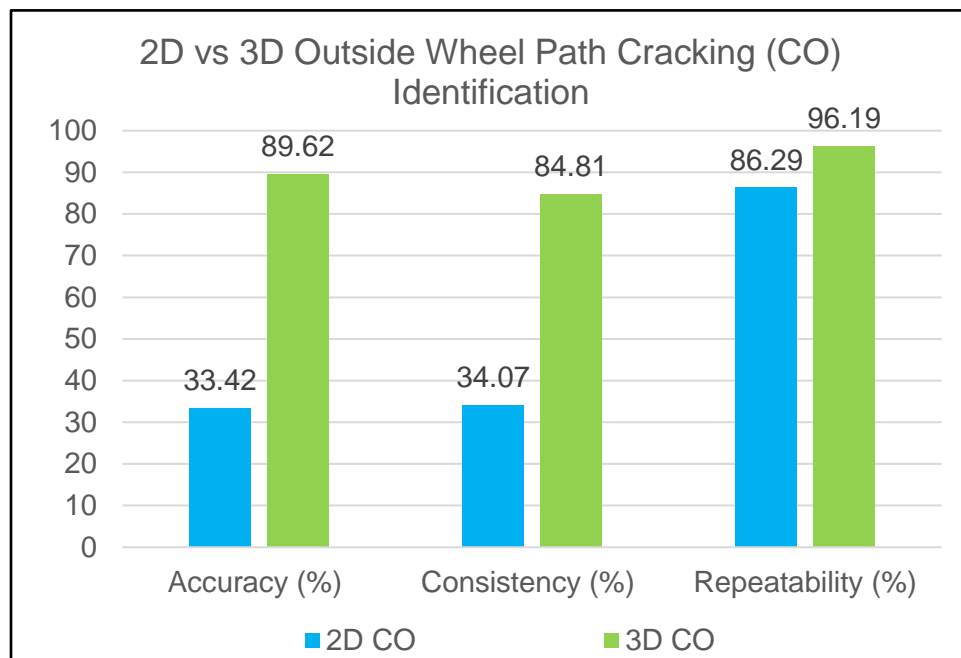
**Figure 230. Comparison of 2D versus 3D Alligator Cracking Success Metrics**

Figure 231 and Figure 232 compare the results of 2D and 3D distress identification according to the FDOT definitions of wheel path cracking (CW) and outside wheel path cracking (CO), respectively. The accuracy, section-to-section consistency, and run-to-

run repeatability of automated CO and CW identification is higher from 3D images compared to 2D images.



**Figure 231. Comparison of 2D versus 3D Wheel Path Cracking (CW) Success Metrics**



**Figure 232. Comparison of 2D versus 3D Outside Wheel Path Cracking (CO) Success Metrics**

#### **I.4.3. Improved Identification of Pavement Texture Distresses**

In addition to the superior performance of the 3D technology in crack detection and the corresponding distress identification that was evaluated in this report, the 3D technology also provides area-based surface macro-texture measurements. Since these measurements are area-based, they have shown a significantly higher run-to-run repeatability compared to the macro-texture measurements with point laser sensors, which are line based and sensitive to vehicle wander. These robust 3D texture measurements can be used to identify change in pavement surface type, areas of weathering and raveling, and quality control of open graded friction courses or chip seal surfaces. The Pavemetrics LCMS processor provides the texture values and a corresponding Raveling Index which is directly proportional to mean texture depth (MPD). However, this Raveling Index has not been calibrated to manual ratings of surface raveling and therefore a high Raveling Index might just be an indicator of open graded friction courses or chip seal surfaces. There is a need to explore the relative values of MPD and root mean square (RMS) of texture between the wheel paths and adjacent areas to see whether that relative difference in texture can be correlated with manual rating of raveling areas.

#### **I.5. Findings and Recommendations**

This report described the effort under Purchase Order Number PR10026557 of this FDOT research project to collect and process 3D LCMS images of 12 representative flexible pavement test sections, and to compare the automated crack detection and distress identification results based on 2D and 3D technologies.

Based on a systematic evaluation framework and pertinent success metrics, it was found that the 3D technology is superior to the 2D technology in the following areas:

6. About 67 percent increase in the crack detection accuracy, which translates into 71 percent more in percentage of detected crack length from the ground truth, and 50 percent more in percentage of the correctly detected cracks.
7. About 47 percent more accuracy in identifying the length of longitudinal cracks, 66 percent more accuracy in identifying the length of transverse cracks, and 95 percent more accuracy in identifying alligator cracking areas. About 83 percent more accuracy in identifying wheel path cracking (CW) and 56 percent more accuracy in identifying outside wheel path cracking (CO).
8. About 8 percent more run-to-run repeatability in identifying the length of longitudinal cracks and 77 percent more repeatability in identifying alligator cracking areas. About 6 percent more run-to-run repeatability in identifying wheel

path cracking (CW) and 10 percent more repeatability in identifying outside wheel path cracking (CO).

9. About 36 percent more section-to-section consistency in identifying the length of longitudinal cracks, 68 percent more consistency in identifying the length of transverse cracks, and 68 percent more consistency in identifying alligator cracking areas. About 83 percent more section-to-section consistency in identifying wheel path cracking (CW) and 51 percent more consistency in identifying outside wheel path cracking (CO).
10. About 6 seconds faster in crack detection per image frame.

Based on past experience with collection of thousands of miles of data with both the 2D LRIS and the 3D LCMS technologies, the following advantages are also known:

3. The 3D technology is less prone to crack width exaggeration on damp pavement surfaces and thereby produces more robust severity rating.
4. The 3D technology provides a more robust surface macro-texture measurement which can potentially be used for identifying raveling and weathering distresses.

Based on this superior accuracy, consistency, repeatability, and efficiency of the 3D technology in detecting pavement surface cracks and identifying the corresponding distress, it is recommended that the 3D technology be considered for automated identification and quantification of flexible pavement distresses.

## **I.6. ARAN Information and Specifications**

### **Right of Way Video**

A single HDTV camera (3CCD broadcast quality) was used for viewing the right of way. The images were recorded every 32 feet and were set up in 2016 to show a 45% to 55% sky-to-pavement ratio. The CCD camera has a rate of 1,000 frames per second and experiences limited to no frame to frame adjustment perceivable to the observer.

## Roughness

Fugro Roadware's South-Dakota Profiler (SDP2) subsystem provides longitudinal profile measurement that will be collected in both wheel paths to calculate the International Roughness Index (IRI) standard. The Laser SDP2 is a non-contact, class 1 (ASTM E950), inertial profiler that uses lasers and accelerometers mounted over each wheelpath to measure the longitudinal profile and calculate IRI in real time.

Some of the technologies, best practices, and limitations of high-speed inertial profilers include:

- *Sensor Technology* – The Laser SDP2 was equipped with LMI RoLine 3.6kHz scanning laser system, providing a full 100mm (4-inch) line of data across the road surface (similar to that of a tire footprint).
- *Flexible Testing Speeds* – The Laser SDP2 is able to collect accurate longitudinal profile and roughness data at testing speeds ranging up to 70 mph while maintaining a bias of 5%.
- *Low Speed Collection Limitation* – Unlike most inertial profilers on the market today, the Laser SDP2 allows for testing at lower speeds and in stop-and-go conditions, for example, in urban environments. This avoids the need to invalidate the IRI for the approximate 300 feet in the vicinity of the low speed zone. Enhanced speed-sensitive filters level the accelerometer influence at low-speed zones and remove parasitic frequencies specific for certain low speed intervals. While reductions to the length of invalidated collection can be greatly shortened using this process, FDOT should be aware of the limitations surrounding the IRI standard for urbanized collection environments, meaning that IRI values collected at speeds lower than 15 mph are typically unreliable.
- *High Accuracy* – Measurements made by a properly calibrated Laser SDP2 are within +/- 5% of the measurements made by manual profiling techniques such as rod and level. Class 1 benchmarking devices that typically used for inertial-profiler conformance testing include the Face Dipstick and the SurPro.
- *High Repeatability* – The Standard deviation for repeat runs for the Laser SDP2 are within +/- 5% of the mean IRI for each run, however summarized IRI results are typically well within this accuracy range. The use of RoLine sensors would further improve on this consistency, regardless of the testing surface type or condition.

- *Real Time* - The ability to calculate IRI in real-time, which facilitates vehicle operators in the identification of non-operational or ill-functioning subsystems (such as the SDP2). This effectively reduces the amount of time to identify problems with the system, limiting the extent of data collection affected.
- *Compliance with Standards* – Inertial profilers, such as the SDP2, should be fully compliant with the range of longitudinal profile collection standards including ASTM E950, AASHTO R 56, and the World Bank Technical Paper #46 protocol. The ARAN conforms to Class I profiling equipment requirements as specified in the most current Highway Performance Monitoring System (HPMS) Field Manual provided by the Federal Office of Highway Policy Information. The ARAN (equipped with a Pave3D system) has passed the Texas Transportation Institute (TTI) inertial profiler certification.
- *Conformance Testing* – To ensure that an inertial profiler system remains accurate, two conformance tests, one static and other dynamic, ensure that the laser and accelerometer components of the system are operating as intended. Without successful completion of these tests to within allowable threshold limits, an ARAN would not be signed off for collection commencement.

### Rut Depth/Transverse Profile

Transverse profile and rutting data were collected by Fugro's Pave3D system utilizing the LCMS sensors. The Pave3D works by laser-illuminating one line of pavement on each half of the driven lane, and then capturing the profile of that laser line with a sensor. Table 130 provides an overview of the Pave3D system rutting capability.

**Table 130. ARAN Rutting Capabilities**

ITEM	Pave3D (LCMS)
1 <i>Num. of laser profilers</i>	2
2 <i>Sampling rate</i>	5600 profiles/s
3 <i>Vehicle speed (max)</i>	(70 mph)
4 <i>Profile spacing</i>	0.2 inches
5 <i>Points per profile</i>	4160 points
6 <i>Transverse field-of-view</i>	13.2 feet
7 <i>Depth range of operation</i>	9.8 inches
8 <i>Z-axis (depth) resolution</i>	0.02 inches
9 <i>X-axis (transverse) resolution</i>	0.04 inches



When the Pave3D's raw transverse data is validated, rutting is calculated in real-time on the ARAN using ASTM E1703 (straight-edge method), AASHTO R48 (wire method), or simulated N-point method (e.g. 7-point).

Some of the technologies, best practices and limitations of pavement transverse profile (TP) and rut depth collection, post processing and reporting include:

- *Advanced Transverse Profile Processor and Rut Depth Settings* – To ensure that the generation of a transverse profile is valid, and that the calculation of rut depths to an overlying straight edge or wire algorithm is measuring the intended pavement performance the following processor settings are used:
  - Validation of transverse profiles, using maximum thresholds for height differentials across the profile length, with a minimum profile length threshold set to ensure only highly valid profiles are incorporated into the rut depth calculation.
  - Ability to define the width of the lane to be incorporated into the transverse profile. This includes options such as using the pavement line marking detection (with or without minimum lane widths) to remove the influence of edge drop-off (unpaved shoulders) and curb-raise on either side of the lane. This will ensure that artificial rut depths due to these phenomena are not created and incorporated into the average for a segment.
  - Where crack detection is not used, an edge detection processor should be used to invalidate changes in height differentials that cannot be characterized by pavement deformation (e.g. edge drop-off or curb-raise).
  - The smoothing of transverse profiles (using either a moving average or wedge) are carried out to remove any ambiguities in the pavement surface that are not attributed to pavement rutting/deformation such as surface texture and cracking.
  - Ability to define the length of a straight-edge (half-lane, full-lane, 6-foot etc.) and its freedom of movement within, or outside of the calculated transverse profile width.
  - The ability to perform rut location optimization, whereby the transverse location of the maximum rut depth between TP intervals (longitudinally) must remain within predefined tolerances. This is very useful where rut

depth data is used primarily for the determination of pavement deformation performance (such as using rut data as part of a structural performance index) within each of the wheel paths.

- Using the inertial component (multi-axis gyroscopes) of the survey vehicles to correct the orientation of the transverse profile (remove the influence of vehicle roll) to determine cross-fall.

## **Positioning**

The Distance Measuring Instrument (DMI) measures ARAN chainage and linear distance travelled. Every ARAN is equipped with a GPS and an Inertial Reference System (POS LV) to fill in satellite gaps. POS LV is a state-of-the art inertial aided navigation system that provides precise roll, pitch, heading, velocity, and position information to other onboard subsystems. The GPS results were post processed as well to increase the level of accuracy of the readings.

## J. MANUAL WINDSHIELD SURVEY RESULTS ON FLEXIBLE PAVEMENTS

CW: Wheel Path Cracking							
Section ID	Statistic	CIB (%)	CII (%)	CIII (%)	CIB + CII + CIII (%)	Raveling (%)	Patching (%)
1	AVG	40	20	0	60	4	0
2	AVG	38	8	0	47	9	0
3	AVG	0	0	0	0	0	0
4	AVG	8	22	2	32	2	0
5	AVG	2	23	12	37	12	0
6	AVG	2	38	8	48	10	2
7	AVG	0	2	0	2	0	0
8	AVG	10	22	0	32	0	0
9	AVG	0	0	0	0	2	13
10	AVG	0	3	0	4	17	0
11	AVG	0	2	12	13	17	5
12	AVG	0	3	22	25	18	3
1	(Min,Max)	(30,50)	(10,25)	(0,0)	(55,65)	(0,10)	(0,0)
2	(Min,Max)	(30,50)	(5,15)	(0,0)	(35,55)	(0,25)	(0,0)
3	(Min,Max)	(0,0)	(0,0)	(0,0)	(0,0)	(0,0)	(0,0)
4	(Min,Max)	(5,15)	(10,35)	(0,5)	(17,45)	(0,5)	(0,0)
5	(Min,Max)	(0,5)	(15,30)	(0,25)	(30,40)	(5,25)	(0,0)
6	(Min,Max)	(0,5)	(35,40)	(0,15)	(35,55)	(1,20)	(1,5)
7	(Min,Max)	(0,1)	(0,5)	(0,0)	(1,5)	(0,0)	(0,0)
8	(Min,Max)	(0,20)	(15,25)	(0,0)	(15,45)	(0,0)	(0,1)
9	(Min,Max)	(0,0)	(0,0)	(0,0)	(0,0)	(0,5)	(5,21)
10	(Min,Max)	(0,0)	(0,10)	(0,1)	(0,10)	(10,25)	(0,0)
11	(Min,Max)	(0,0)	(0,5)	(5,20)	(5,25)	(5,30)	(1,10)
12	(Min,Max)	(0,0)	(0,10)	(15,30)	(15,40)	(5,40)	(2,5)
1	COV	25%	43%	N/A	8%	150%	N/A
2	COV	27%	69%	N/A	22%	163%	N/A
3	COV	N/A	N/A	N/A	N/A	N/A	N/A
4	COV	69%	58%	108%	44%	173%	N/A
5	COV	173%	33%	108%	16%	99%	N/A
6	COV	173%	8%	92%	24%	92%	99%
7	COV	173%	132%	N/A	99%	N/A	N/A
8	COV	100%	27%	N/A	48%	N/A	173%
9	COV	N/A	N/A	N/A	N/A	173%	63%
10	COV	N/A	173%	173%	150%	46%	N/A
11	COV	N/A	173%	65%	78%	75%	85%
12	COV	N/A	173%	35%	53%	103%	46%
OVERALL VARIATION: AVG(COV)		106%	89%	97%	54%	119%	93%
OVERALL PRECISION: 100-AVG(COV)		-6%	11%	3%	46%	-19%	7%

CO: Non-Wheel Path Cracking							
Section ID	Statistic	CIB (%)	CII (%)	CIII (%)	CIB + CII + CIII (%)	Raveling (%)	Patching (%)
1	AVG	17	3	0	20	0	0
2	AVG	16	2	0	18	2	0
3	AVG	0	0	0	0	0	0
4	AVG	10	23	5	38	2	0
5	AVG	2	28	5	35	8	0
6	AVG	2	32	3	37	9	2
7	AVG	0	2	0	2	0	0
8	AVG	8	17	0	25	0	0
9	AVG	0	0	0	0	2	13
10	AVG	0	2	2	3	8	0
11	AVG	0	0	5	5	8	5
12	AVG	0	2	17	18	10	3
1	(Min,Max)	(10,20)	(0,5)	(0,0)	(10,25)	(0,0)	(0,0)
2	(Min,Max)	(8,25)	(0,5)	(0,0)	(0,5)	(0,0)	(0,0)
3	(Min,Max)	(0,0)	(0,0)	(0,0)	(0,0)	(0,0)	(0,0)
4	(Min,Max)	(5,20)	(10,35)	(5,5)	(0,5)	(0,0)	(0,0)
5	(Min,Max)	(0,5)	(20,35)	(0,10)	(5,10)	(0,0)	(0,0)
6	(Min,Max)	(0,5)	(25,40)	(0,5)	(1,15)	(0,5)	(0,5)
7	(Min,Max)	(0,0)	(1,5)	(0,0)	(0,0)	(0,0)	(0,0)
8	(Min,Max)	(0,15)	(5,25)	(0,0)	(0,0)	(0,1)	(0,1)
9	(Min,Max)	(0,0)	(0,0)	(0,0)	(0,5)	(5,21)	(5,21)
10	(Min,Max)	(0,0)	(0,5)	(0,5)	(5,10)	(0,0)	(0,0)
11	(Min,Max)	(0,0)	(0,0)	(1,10)	(5,15)	(1,10)	(1,10)
12	(Min,Max)	(0,0)	(0,5)	(5,35)	(5,15)	(2,5)	(2,5)
1	COV	35%	87%	N/A	43%	N/A	N/A
2	COV	53%	173%	N/A	64%	173%	N/A
3	COV	N/A	N/A	N/A	N/A	N/A	N/A
4	COV	87%	54%	0%	42%	173%	N/A
5	COV	173%	27%	100%	43%	35%	N/A
6	COV	173%	24%	87%	28%	82%	132%
7	COV	N/A	99%	N/A	99%	N/A	N/A
8	COV	92%	62%	N/A	69%	N/A	173%
9	COV	N/A	N/A	N/A	N/A	173%	63%
10	COV	N/A	173%	173%	87%	35%	N/A
11	COV	N/A	N/A	85%	85%	69%	85%
12	COV	N/A	173%	96%	103%	50%	46%
OVERALL VARIATION: AVG(COV)		102%	97%	90%	66%	99%	100%
OVERALL PRECISION: 100-AVG(COV)		-2%	3%	10%	34%	1%	0%

## K. FDOT FLEXIBLE PAVEMENT DISTRESS APPLICATION (FFPDA) TEST RESULTS

**Table 131. Amount of Cracking by Crack Type, Severity, and Road Zone for Each Run**

Run No.	Section No.	By Crack Type (Sq Ft)			By Crack Severity (Sq Ft)			By Road Zone (Sq Ft)	
		Alligator	Branch	Single	1B	II	III	CW	CO
1	1	7,588.11	1,532.92	1,153.56	2,603.20	7,651.61	19.78	9,331.14	943.45
1	2	8,946.50	1,297.20	823.15	2,038.54	8,993.77	34.54	9,936.69	1,130.16
1	3	0.29	5.42	49.53	54.95	0.29	-	15.04	40.20
1	4	1,057.78	1,791.27	1,802.43	1,948.88	2,369.69	332.92	2,403.96	2,247.52
1	5	20,487.05	3,883.75	2,530.17	5,103.22	19,774.07	2,023.68	16,927.41	9,973.56
1	6	33,851.89	4,652.60	2,847.45	6,159.14	31,959.63	3,233.16	28,064.93	13,287.00
1	7	1.52	24.31	194.82	154.58	62.01	4.07	152.72	67.93
1	8	2,306.74	3,066.65	3,991.30	3,225.03	5,328.35	811.31	6,693.50	2,671.19
1	9	51.27	160.59	1,053.97	797.28	444.07	24.48	875.90	389.93
1	10	9,551.10	2,790.71	3,844.70	6,327.73	9,745.01	113.77	10,634.30	5,552.20
1	11	3,632.87	3,429.36	6,902.53	8,771.04	4,672.96	520.77	8,381.75	5,583.02
1	12	4,387.39	5,383.59	6,038.59	10,430.69	5,111.88	267.01	7,692.68	8,116.89
2	1	7,298.45	1,539.14	1,169.93	2,425.28	7,483.51	98.73	9,060.00	947.52
2	2	9,277.17	1,298.56	780.38	1,828.68	9,248.75	278.68	10,179.67	1,176.44
2	3	-	0.97	87.46	88.02	0.41	-	20.39	68.04
2	4	1,041.91	1,763.05	1,756.64	1,694.64	2,417.28	449.67	2,365.40	2,196.19
2	5	20,279.58	3,680.41	2,453.86	4,013.00	18,966.58	3,434.28	16,590.08	9,823.77
2	6	34,857.24	4,658.20	2,792.44	5,354.97	31,739.78	5,213.12	28,904.92	13,402.96
2	7	0.68	2.24	175.97	133.37	44.84	0.68	116.29	62.60
2	8	2,436.32	3,008.02	3,962.41	2,817.46	5,552.25	1,037.04	6,936.54	2,470.20
2	9	32.30	192.02	1,089.31	698.58	600.32	14.74	860.28	453.36
2	10	11,254.60	2,814.09	3,867.42	6,211.84	11,573.18	151.09	12,733.16	5,202.95
2	11	3,494.94	3,358.99	7,381.27	8,356.06	5,214.97	664.18	8,136.94	6,098.27
2	12	4,118.14	4,942.75	6,213.41	9,455.32	5,375.74	443.23	7,278.20	7,996.10
3	1	7,054.82	1,706.58	1,184.66	2,653.30	7,228.25	64.51	8,949.32	996.73
3	2	9,319.85	1,287.12	809.97	2,095.92	9,321.02	-	10,299.48	1,117.46
3	3	0.00	10.47	165.41	166.55	9.33	-	50.01	125.87
3	4	1,108.40	1,844.53	1,667.74	1,685.28	2,478.33	457.07	2,457.78	2,162.89
3	5	20,269.21	3,863.66	2,633.78	4,062.28	19,899.88	2,804.49	16,456.42	10,310.23
3	6	34,595.94	4,856.83	2,659.82	5,346.26	31,532.06	5,234.28	28,717.70	13,394.89
3	7	2.78	7.02	194.25	157.41	43.07	3.56	136.30	67.75
3	8	2,289.16	3,053.49	3,910.31	2,835.68	5,611.77	805.50	6,665.02	2,587.94
3	9	26.29	183.46	1,216.98	852.23	555.05	19.44	967.15	459.58
3	10	9,031.73	2,338.37	3,989.04	5,840.31	9,311.26	207.57	10,649.13	4,710.01

Run No.	Section No.	By Crack Type (Sq Ft)			By Crack Severity (Sq Ft)			By Road Zone (Sq Ft)	
		Alligator	Branch	Single	1B	II	III	CW	CO
3	11	3,351.20	3,520.37	7,449.02	8,104.20	5,452.96	763.43	8,416.94	5,903.65
3	12	3,740.73	5,029.30	6,315.63	9,398.62	5,233.87	453.18	7,176.17	7,909.50

**Table 132. Amount of Cracking by Crack Type and Severity for Each Run**

Run No.	Section No.	Single Cracks (Sq Ft)			Branch Cracks (Sq Ft)			Alligator Cracks (Sq Ft)		
		1B	II	III	1B	II	III	1B	II	III
1	1	1,096.97	50.52	6.08	1,506.23	26.69	-	-	7,574.41	13.70
1	2	775.31	46.35	1.50	1,263.23	33.97	-	-	8,913.45	33.05
1	3	49.53	-	-	5.42	-	-	-	0.29	-
1	4	1,167.93	624.30	10.20	780.95	1,010.32	-	-	735.07	322.72
1	5	2,069.68	434.63	25.86	3,033.54	841.78	8.43	-	18,497.66	1,989.39
1	6	2,378.10	458.89	10.45	3,781.03	871.57	-	-	30,629.17	3,222.71
1	7	144.35	47.35	3.11	10.23	14.08	-	-	0.57	0.96
1	8	2,101.46	1,871.42	18.42	1,123.57	1,943.08	-	-	1,513.85	792.89
1	9	712.91	329.59	11.48	84.38	76.21	-	-	38.26	13.00
1	10	3,615.60	212.26	16.85	2,712.13	78.58	-	-	9,454.18	96.92
1	11	5,988.04	840.90	73.60	2,783.00	645.38	0.99	-	3,186.69	446.19
1	12	5,573.20	390.76	74.64	4,857.49	526.10	-	-	4,195.02	192.37
2	1	1,054.35	112.84	2.73	1,370.93	168.22	-	-	7,202.46	95.99
2	2	641.89	130.76	7.74	1,186.79	111.77	-	-	9,006.22	270.94
2	3	87.46	-	-	0.56	0.41	-	-	-	-
2	4	1,037.14	682.40	37.09	657.50	1,105.54	-	-	629.33	412.58
2	5	1,779.66	659.67	14.53	2,233.34	1,444.74	2.34	-	16,862.17	3,417.41
2	6	2,066.90	707.65	17.89	3,288.07	1,367.77	2.36	-	29,664.37	5,192.87
2	7	132.82	43.15	-	0.55	1.69	-	-	-	0.68
2	8	1,812.32	2,142.38	7.71	1,005.14	2,002.87	-	-	1,407.00	1,029.33
2	9	608.07	478.79	2.45	90.51	101.51	-	-	20.02	12.28
2	10	3,539.88	306.22	21.31	2,671.95	142.14	-	-	11,124.82	129.78
2	11	6,010.16	1,284.36	86.75	2,345.90	1,005.15	7.94	-	2,925.46	569.48
2	12	5,491.30	630.04	92.07	3,964.03	978.72	-	-	3,766.98	351.16
3	1	1,053.90	126.31	4.45	1,599.40	105.46	1.72	-	6,996.48	58.33
3	2	808.81	1.17	-	1,287.12	-	-	-	9,319.85	-
3	3	156.08	9.33	-	10.47	-	-	-	0.00	-
3	4	988.22	658.29	21.23	697.05	1,145.41	2.07	-	674.62	433.77
3	5	1,793.33	822.10	18.34	2,268.94	1,594.71	-	-	17,483.06	2,786.15
3	6	1,999.12	620.71	39.99	3,347.14	1,504.91	4.79	-	29,406.44	5,189.50
3	7	152.10	41.36	0.79	5.31	1.71	-	-	-	2.78
3	8	1,826.15	2,057.67	26.49	1,009.53	2,043.96	-	-	1,510.14	779.01
3	9	749.96	459.14	7.88	102.28	81.18	-	-	14.73	11.56

Run No.	Section No.	Single Cracks (Sq Ft)			Branch Cracks (Sq Ft)			Alligator Cracks (Sq Ft)		
		1B	II	III	1B	II	III	1B	II	III
3	10	3,594.11	367.97	26.97	2,246.20	92.17	-	-	8,851.13	180.60
3	11	5,836.72	1,510.81	101.49	2,267.49	1,250.74	2.14	-	2,691.41	659.80
3	12	5,541.35	737.00	37.28	3,857.27	1,172.04	-	-	3,324.83	415.90

**Table 133. Amount of Cracking by Road Zone and Crack Severity for Each Run**

Run No.	Section No.	Cracking in the Wheel Path (Sq Ft)			Cracking Outside the Wheel Path (Sq Ft)		
		1B	II	III	1B	II	III
1	1	1,731.19	7,581.31	18.63	872.00	70.30	1.15
1	2	1,145.19	8,771.96	19.54	893.35	221.80	15.00
1	3	15.04	-	-	39.91	0.29	-
1	4	551.49	1,583.62	268.85	1,397.39	786.07	64.06
1	5	1,794.49	14,065.63	1,067.28	3,308.72	5,708.44	956.40
1	6	1,716.78	23,980.96	2,367.19	4,442.36	7,978.67	865.97
1	7	96.13	54.13	2.47	58.45	7.88	1.60
1	8	1,617.91	4,376.61	698.98	1,607.12	951.74	112.33
1	9	519.55	342.30	14.05	277.74	101.76	10.43
1	10	3,930.84	6,610.76	92.70	2,396.89	3,134.25	21.07
1	11	4,637.38	3,417.35	327.02	4,133.66	1,255.61	193.75
1	12	4,749.74	2,801.96	140.99	5,680.95	2,309.92	126.02
2	1	1,640.97	7,325.15	93.88	784.31	158.37	4.84
2	2	976.95	8,942.09	260.63	851.73	306.66	18.05
2	3	20.39	-	-	67.63	0.41	-
2	4	507.80	1,520.82	336.78	1,186.84	896.46	112.89
2	5	1,309.94	13,758.09	1,522.04	2,703.05	5,208.49	1,912.23
2	6	1,423.70	23,692.17	3,789.06	3,931.27	8,047.62	1,424.07
2	7	78.76	37.53	-	54.61	7.31	0.68
2	8	1,360.35	4,658.99	917.20	1,457.11	893.26	119.84
2	9	367.05	487.38	5.86	331.54	112.94	8.88
2	10	4,003.24	8,636.34	93.57	2,208.60	2,936.84	57.52
2	11	4,198.92	3,473.57	464.44	4,157.14	1,741.39	199.73
2	12	4,276.52	2,798.85	202.83	5,178.81	2,576.88	240.41
3	1	1,843.67	7,050.35	55.31	809.63	177.90	9.20
3	2	1,241.48	9,058.00	-	854.45	263.01	-
3	3	50.01	-	-	116.55	9.33	-
3	4	507.80	1,593.29	356.69	1,177.48	885.04	100.37
3	5	1,350.45	13,818.04	1,287.93	2,711.82	6,081.84	1,516.56
3	6	1,423.10	23,358.60	3,936.01	3,923.16	8,173.45	1,298.27
3	7	112.57	23.73	-	44.84	19.34	3.56

Run No.	Section No.	Cracking in the Wheel Path (Sq Ft)			Cracking Outside the Wheel Path (Sq Ft)		
		1B	II	III	1B	II	III
3	8	1,307.08	4,703.68	654.26	1,528.60	908.09	151.24
3	9	494.37	456.16	16.62	357.86	98.89	2.82
3	10	3,874.28	6,621.60	153.25	1,966.03	2,689.67	54.32
3	11	4,169.74	3,707.66	539.55	3,934.47	1,745.30	223.88
3	12	4,183.89	2,781.78	210.50	5,214.73	2,452.10	242.68



## L. FDOT FLEXIBLE PAVEMENT DISTRESS APPLICATION (FFPDA) REFERENCE MANUAL

### Document Version Control

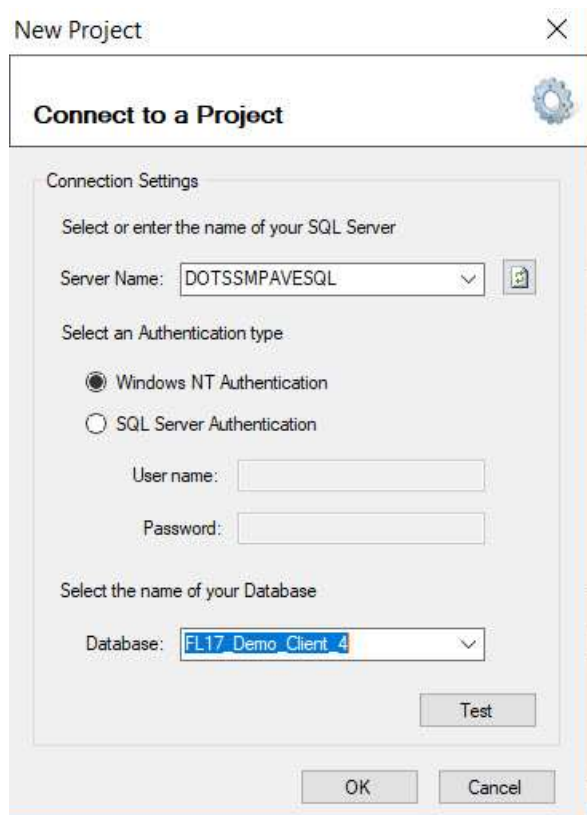
This Reference Manual is intended for Florida DOT staff to use as reference when conducting semi-automated rating of pavement images using Vision software and automated rating using FDOT Flexible Pavement Distress Application (FFPDA). This Reference Manual is updated and improved as needed. The following is the document control for revisions to this document.

Version Number	Date of Issue	Authors	Brief Description of Changes
V.0.5	10/25/2017	Nima Kargah-Ostadi, Mina Zhou	Draft User's Guide for semi-automated rating (manual rating of the images) using Vision 3.1
V 0.8	07/23/2018	Nima Kargah-Ostadi, Thomas Burchett	Draft User's Guide for semi-automated rating using Vision 3.3 and automated rating using FFPDA
V 1.0	10/31/2018	Nima Kargah-Ostadi, Mina Zhou	Changed the name of the document to Reference Manual, made all sentences in active voice, changed the sequence of topics and inserted additional topics
V 1.2	02/25/2019	Nima Kargah-Ostadi, Mina Zhou	Addressed FDOT comments received 12/19/2018; added the Quick Start Guide from 12/06/2018 to this document; updated screen captures according to final software

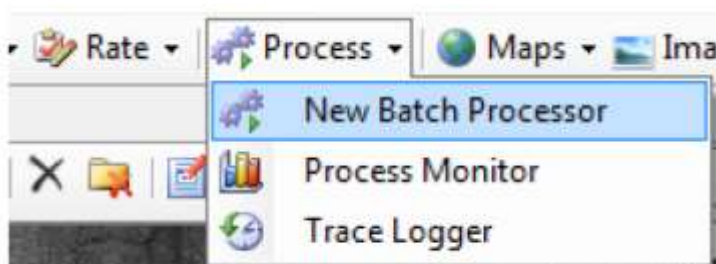
## L.1. Vision Batch Processing Quick Start Guide

This Quick Start Guide was developed with the objective of providing the users with an easy and quick guide to start using the batch processors in the Vision software. For further explanation of the details, please refer to the remainder of the Reference Manual.

After opening Vision, select the Database relevant to your assigned project.



Select <Process> and then <New Batch Processor> from the dropdown menu.



Check the boxes for 'JPEG Lanes Detection Processor', 'JPEG Cracks Detection Processor', 'FDOT Flexible Pavement Distress App', and 'FDOT Flexible Pavement Rating Results Summary'.

<input type="checkbox"/>	Fault Processor	Detect and filter Faults
<input checked="" type="checkbox"/>	FDOT Flexible Pavement Distress App	Flexible pavement classification and rating batch processor customized fo
<input checked="" type="checkbox"/>	FDOT Flexible Pavement Rating Result Summary	Flexible pavement rating result summary processor
<input type="checkbox"/>	Image Copier Processor	Copies original images to a given output folder
<input type="checkbox"/>	Image QC Processor	Measures the brightness of images and compares against acceptable ran
<input type="checkbox"/>	iVision publisher batch processor.	Runs the iVision publisher on the current database.
<input type="checkbox"/>	Joint Detection Processor	Detect joints in a session of images
<input checked="" type="checkbox"/>	JPEG Cracks Detection Processor	Detects cracks from JPEG files.
<input checked="" type="checkbox"/>	JPEG Lanes Detection Processor	Detects lanes from JPEG files.
<input type="checkbox"/>	Ladybug processor	Batch processes Ladybug collected data.

Make sure they are sorted in the correct order:

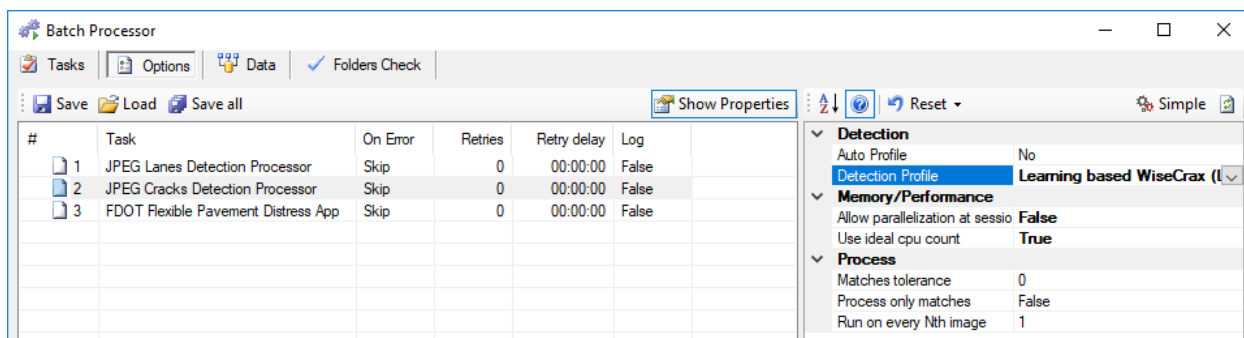
#	Task	Description
<input type="checkbox"/> 1	JPEG Lanes Detection Processor	Detects lanes from JPEG files.
<input type="checkbox"/> 2	JPEG Cracks Detection Processor	Detects cracks from JPEG files.
<input type="checkbox"/> 3	FDOT Flexible Pavement Distress App	Flexible pavement classification and rating batch processor customized
<input type="checkbox"/> 4	FDOT Flexible Pavement Rating Result Summ...	Flexible pavement rating result summary processor

Then Click <Options>

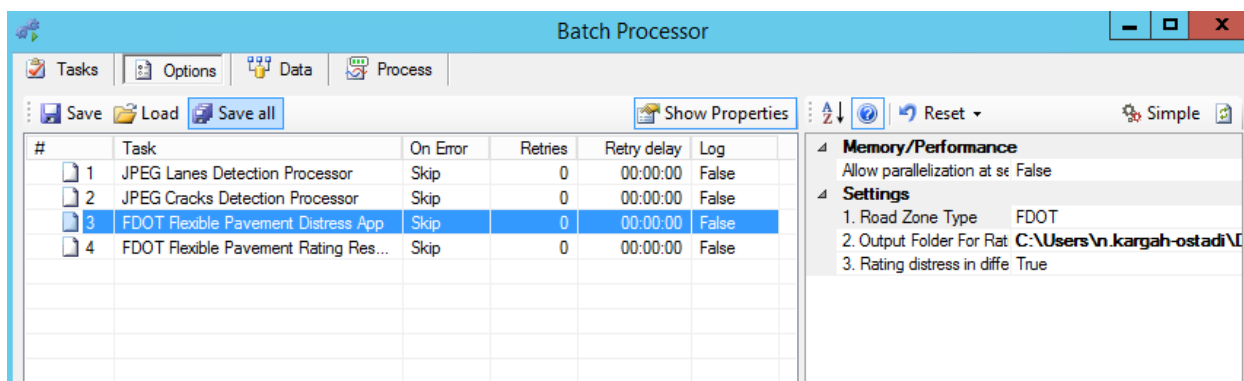
Click on the 'JPEG Lanes Detection Processor' to highlight, then click on the dropdown menu for <Detection> <Algorithm Version> and select "Wisecrax\_V2". Set the <Default lane width> to 3.6 meters and the <Minimum lane width> to 3 meters.

Reset		Simple
<b>Detection</b>		
Algorithm version	Wisecrax_V2	
<b>Lane widths range</b>		
Default lane width	3.6	
Maximum lane width	4.2	
Minimum lane width	3	
<b>Memory/Performance</b>		
Allow parallelization at session level	False	
<b>Process</b>		
Matches tolerance	0	
Process only matches	False	
Run on every Nth image	1	

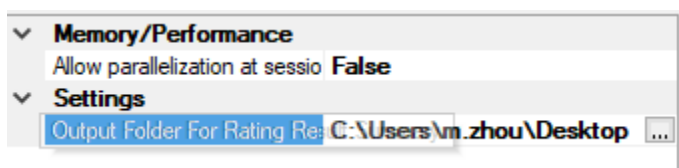
Click on the 'JPEG Cracks Detection Processor' to highlight, then click on the dropdown menu for <Detection> <Detection Profile> and select "Learning based WiseCrax (LCMS)".



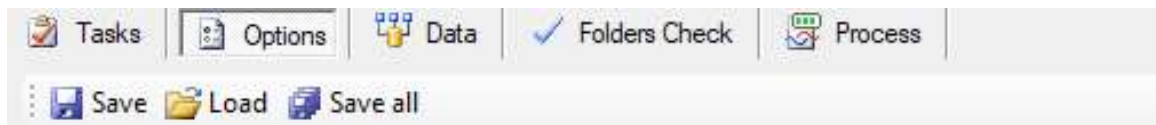
Click on the 'FDOT Pavement Distress App' to highlight, then click on <Settings>, for <Road Zone Type>, select "FDOT" for processing according to the FDOT Flexible Pavement Condition Survey Handbook or "HPMS" for processing according to the HPMS Field Manual. Then, choose an output folder for your report.



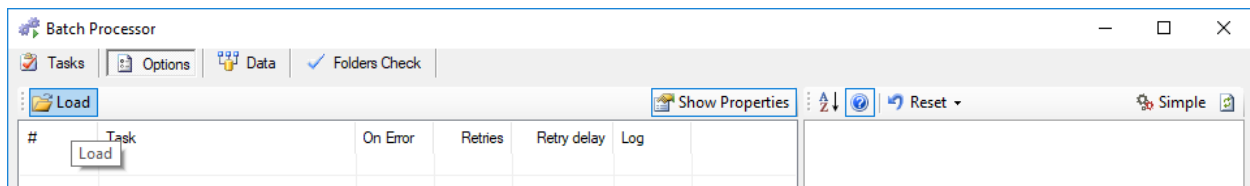
Click on the 'FDOT Flexible Pavement Rating Results Summary' to highlight, then click on <Settings>, choose an output folder for your report.



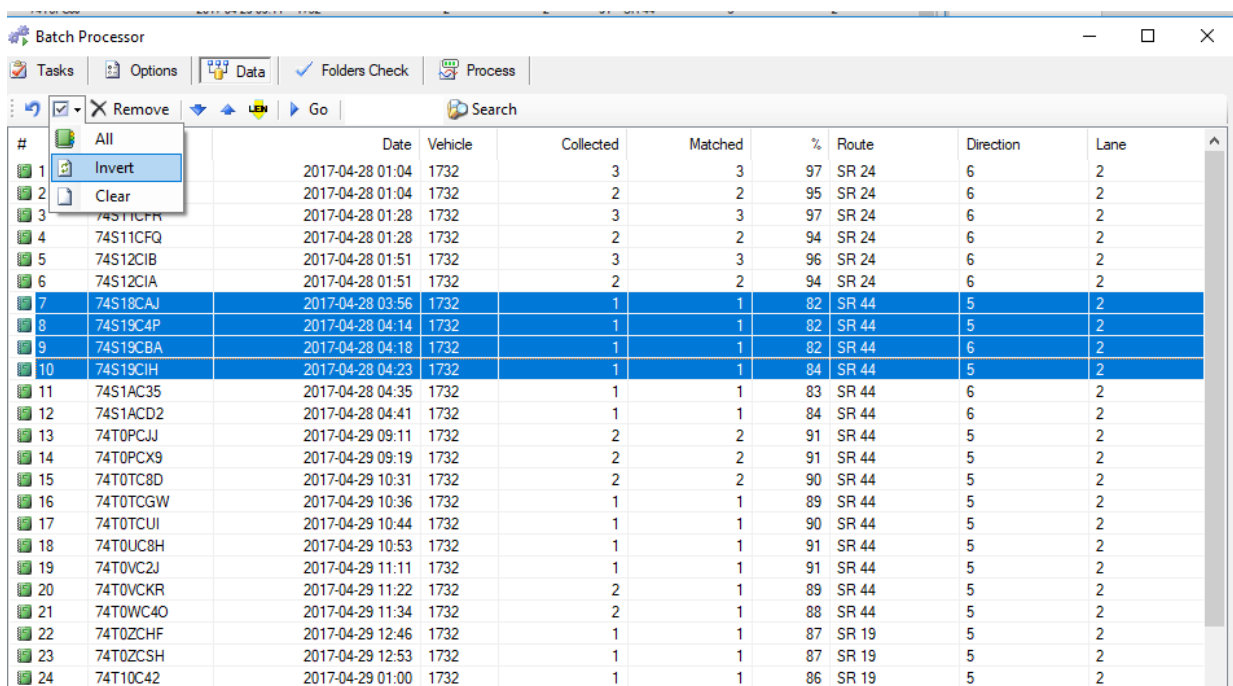
After you have set the above Options up once, choose **Save All** and save that processing setup (the 4 processes, with the settings).



After saving the settings, next time you select <New Batch Processor>, skip the selection, click <Options> <Load> and select that saved process profile.

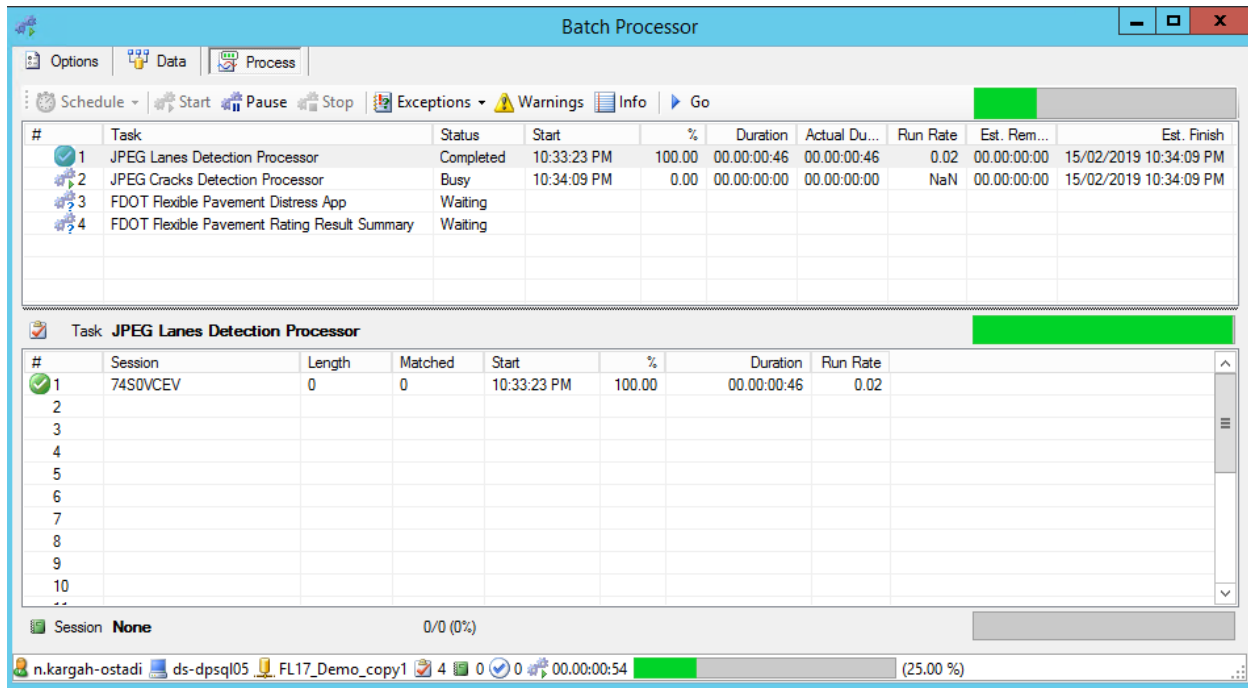


Click <Data>, find your sections, highlight (use Ctrl+[left-click] to select multiple sections), click the dropdown menu next to the little check mark and click <Invert> which selects everything except what you had highlighted, and then click <Remove>.

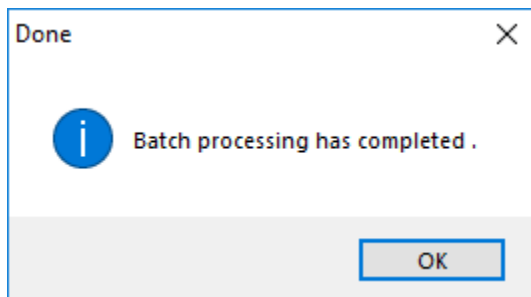




Click <Process>, then <Start>





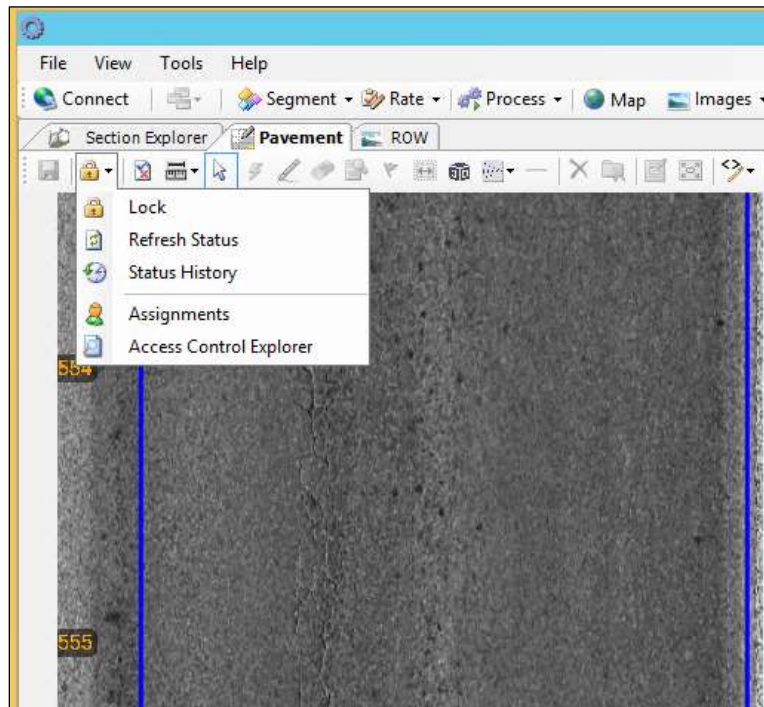
When it is done running, click <OK> to save the processing results.



Select <Rate> and then <Pavement Distress> from the dropdown menu.



Select section by highlighting it in the <Section Explorer> menu. Then, go back to the  module and click on **Lock**  to lock that section under your username.



Use the manual rating options to create manual distress (e.g. raveling, patching, etc.), or modify/delete automated distress results.



Once you're done modifying, click <Save> and <Unlock>

Click <Process> and then <New Batch Processor> from the dropdown menu.

'FDOT Flexible Pavement Rating Results Summary' to highlight, then click on <Settings>, choose an output folder for your report. Click <Data> and reselect the desired sections, <Invert> and <Remove>. Click <Process>, <Start>. When that is done running, Click Ok to confirm the task is completed.

Open the destination folder and rename both output files, move them as needed.

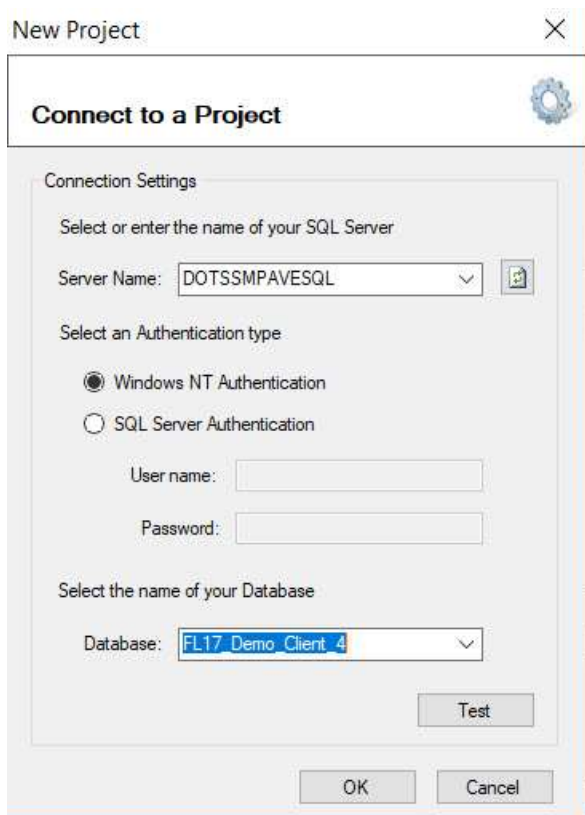


## L.2. Reference Manual

This Reference Manual includes instructions on using basic Vision software functions, and also instructions on using the automated application (batch processors) that was specifically developed during this research project for Florida DOT. The users will need to learn the basic Vision software functions to be able to setup and conduct quality control of the automated application results. Appendices C and D of this Reference Manual have been designated for use by a 'Professional User' (project database owner) because it is recommended that those adjustments be conducted at infrequent intervals by only one user per project.

### Connecting to a Project Database

Vision software works based on SQL databases. Each database is called a project and it may include any number and length of sections. Click on **Connect** (top left-hand side) to display the recent databases that you have accessed. To connect to a new project, click on **New** and a window will allow you to enter the server name where the data is stored, username and password to access the server (or use Windows Authentication), and the name of the database which you would like to connect to. See an example below:



New Project

**Connect to a Project**

Connection Settings

Select or enter the name of your SQL Server

Server Name: DOTSSMPAVESQL

Select an Authentication type

☒ Windows NT Authentication

☐ SQL Server Authentication

User name:

Password:

Select the name of your Database

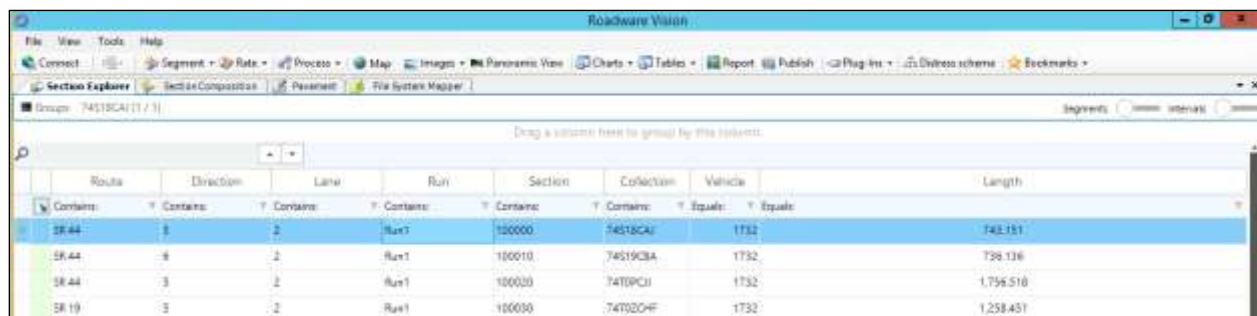
Database: FL17 Demo Client 4

Test

OK Cancel

## Section Explorer

When connected to a specific project (database), a list of sections in the database will appear on the **Section Explorer** screen. These sections are defined during the planning process for data collection. The pavement sections are organized in 'Sessions', where images are stored. Double click on a session in the **Section Explorer** to highlight it. Only one session can be highlighted at a time. A session needs to be highlighted before any manual data processing can be conducted on it (e.g. semi-automated rating of distress). Please refer to the section of this document on Using Batch Processors to select multiple sessions for the automated processing.




The screenshot shows the 'Section Explorer' window in Roadware Vision. The window has a menu bar (File, View, Tools, Help) and a toolbar with icons for Connect, Segment, Rate, Process, Map, Images, Panoramic View, Charts, Tables, Report, Publish, Plug-ins, Distress scheme, and Bookmarks. Below the toolbar is a tabbed interface with 'Section Explorer' selected. The main area displays a table of sections for group '74518CA1 (1 / 3)'. The table has columns: Route, Direction, Lane, Run, Section, Collection, Vehicle, and Length. The first row is highlighted in blue.

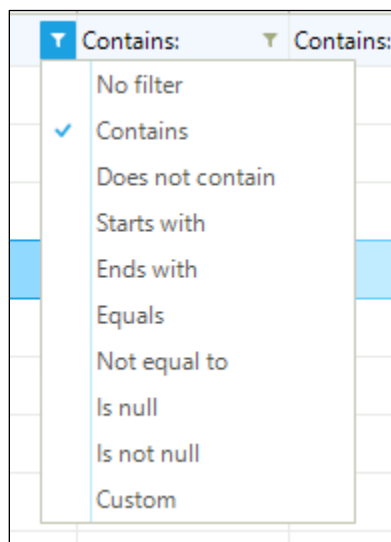
Route	Direction	Lane	Run	Section	Collection	Vehicle	Length
SR 44	3	2	Run1	100000	74518CA1	1T32	743.151
SR 44	3	2	Run1	100010	74519CBA	1T32	736.136
SR 44	3	2	Run1	100020	74T0PCJ1	1T32	1,756.510
SR 19	3	2	Run1	100030	74T0ZCHF	1T32	1,258.451

## Section Filters

You can filter out the sections which do not have the desired data using the section filter, a small drop-down button below the column header.

	Route	Direction	Lane	Run	
	Contains:	Contains:	Contains:	Contains:	Contains:

The default filter is not activated ('No Filter'). To activate the filter function on each column in the **Section Explorer** menu, first select a filter option from the filter drop-down list, input a value, and then click the filter drop-down button again to confirm using the filter. The drop-down list includes ten options, as shown below:



The following explains how each filter option works.

**Contains:** Only test sections in which the column value contains the input characters will be shown on the section list. For example, if you select 'Contains' and use '19' as the input value in the 'Route' column, only sections in which 'Route' value contains 19 will be shown on the section list. This might include 'Route' number 19 or 192 or 219, etc.

	Route	Direction	Lane	Run	Section	Collection	Vehicle	Length
Contains: 19	Contains: 19	Contains: 19	Contains: 19	Contains: 19	Contains: 19	Contains: 19	Equals: 19	Equals: 19
SR 19	3	1	Run1	100060	74113CH5	1732		1,885,160
SR 19	3	1	Run3	103060	74112CKY	1732		1,867,756
SR 19	3	1	Run2	102060	74112CKA	1732		1,855,400
SR 19	3	2	Run3	103030	74110C42	1732		1,283,881
SR 19	3	2	Run2	102030	74102C5H	1732		1,261,048
SR 19	3	2	Run1	100030	74102CHF	1732		1,258,451
Total length: 8,991,488								

**Does not contain:** Only test sections in which the column value does not contain the input characters will be shown on the section list. For example, if you select 'Does not contain' and use '19' as the input value in the 'Route' column, only sections in which 'Route' value doesn't contain 19 will be shown on the section list.

Starts with: Only test sections in which column values start with the given characters will be shown on the section list.

Ends with: Only test sections in which column values end with the given characters will be shown on the section list. The following is an example application of this filter on the Route column:

Route
EndsWith: I-4

EndsWith: I-4	Contains:	Contains:	Contains:	Contains:	Contains:	Equals:	Equals:	
SR 420 - I-4	5	3	Run1	100110	74U0SC0	1732		1,225,000
SR 420 - I-4	5	3	Run3	103110	74U0QCP	1732		1,222,000
SR 420 - I-4	5	3	Run2	102110	74U0PCV	1732		1,228,000
SR 420 - I-4	5	3	Run3	103100	74U0MCRH	1732		1,581,000
SR 420 - I-4	5	3	Run2	102100	74U0MCAX	1732		1,577,000
SR 420 - I-4	5	3	Run1	100100	74U0LGE	1732		1,711,000
Total length: 8,523,000								

Equals: Only test sections in which column values are equal to the given characters will be shown on the section list.

Not equal to: Only test sections in which column values are not equal to the given characters will be shown on the section list. The following shows an example application of this filter on the Direction column:

Direction
NotEquals: 5
6

Route	Direction	Lane	Run	Section	Collection	Vehicle	Length
SR 44	6	2	Run1	103110	7451AC02	1732	728.116
SR 44	6	2	Run2	102010	7451AC35	1732	728.183
SR 44	6	2	Run1	100010	74519CBA	1732	736.136
SR 24	6	2	Run1	109980	74512CB	1732	2,825.667
SR 24	6	2	Run1	100890	74512CA	1732	5,674.890
SR 24	6	2	Run3	103060	74511CR	1732	3,806.559
SR 24	6	2	Run3	103090	74511CRQ	1732	1,672.769
SR 24	6	2	Run2	102060	74510CB5	1732	2,819.396
SR 24	6	2	Run2	102890	74510CB4	1732	1,660.874
Total length: 13,647.729							

Is null: Only test sections in which column values are 'null' will be shown on the section list.

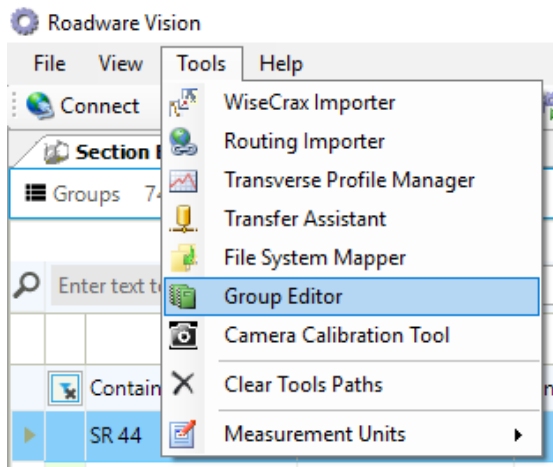
Is not null: Only test sections in which column values are not 'null' will be shown on the section list.

Custom: you can create a more complicated filter by using 'And' and 'Or', for example, 'Ends with I-4' or 'Ends with 24' as shown in the following filter example on the Route column:

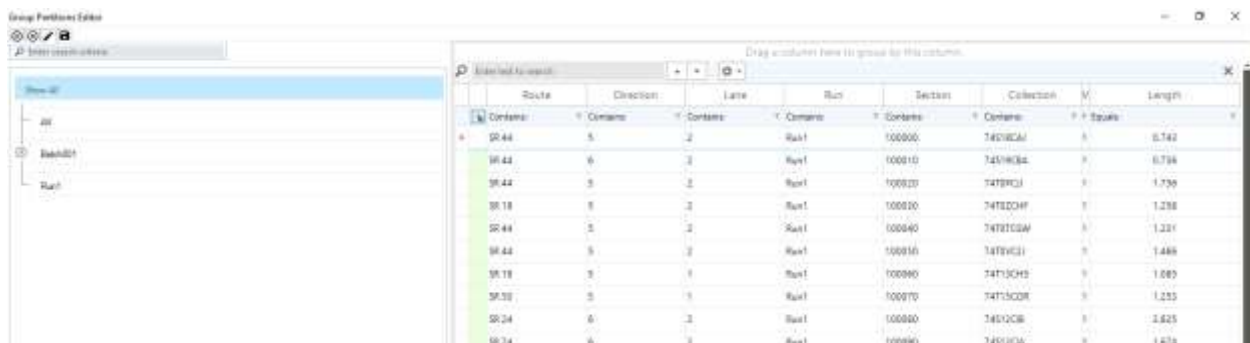
	Route	Direction	Lane	Run	Section	Collection	Vehicle	Length
Custom	Contains	Contains	Contains	Contains	Contains	Equals	Equals	
SR 400 - I-4	S	3	Run1	100110	74U0SC08	1732		1,225,000
SR 400 - I-4	S	3	Run3	103110	74U0OC09	1732		1,222,000
SR 400 - I-4	S	3	Run2	102110	74U0PC0V	1732		1,226,000
SR 400 - I-4	S	3	Run3	103100	74U0MAC0H	1732		1,561,000
SR 400 - I-4	S	3	Run2	102100	74U0MC4X	1732		1,577,000
SR 400 - I-4	S	3	Run1	100100	74U0LC08	1732		1,711,000
SR 24	E	2	Run1	100090	74S12C08	1732		2,825,667
SR 24	E	2	Run1	100090	74S12C0A	1732		1,674,930
SR 24	E	2	Run3	103080	74S11C0H	1732		2,808,558
SR 24	E	2	Run3	103090	74S11C0Q	1732		1,672,769
SR 24	E	2	Run2	102080	74S10C0S	1732		2,818,106
SR 24	E	2	Run2	102090	74S10C04	1732		1,692,974
Total length: 21,882,395								

## Group Editor

This function will allow you to save all the filters for Section Explorer. From the **Tools** drop-down menu, select **Group Editor**:



The **Section Explorer** will appear within the **Group Editor** window:



Apply the filtering criteria as described previously. Then, select all the filtered sections to be highlighted:

Group Partitions Editor

Enter search criteria:

Enter text to search

Drag a column here to group by this column.


Route	Direction	Lane	Run	Section	Collection
Contains: SR 44	Contains: 5	Contains: 2	Contains: Run2	Contains: 102000	Contains: 74S19C4P
SR 44	5	2	Run2	102010	74S1AC35
SR 44	5	2	Run2	102020	74T0PCX9
SR 19	5	2	Run2	102030	74T0ZCSH
SR 44	5	2	Run2	102040	74T0TCUI
SR 44	5	2	Run2	102050	74T0VCKR
SR 19	5	1	Run2	102060	74T12CKA
SR 30	5	1	Run2	102070	74T15CVY
SR 24	5	2	Run2	102080	74S10CB5
SR 24	6	2	Run2	102090	74S10CB4
SR 400 - 3-4	5	3	Run2	102100	74U0MC4X
SR 400 - 3-4	5	3	Run2	102110	74U0PCVW

Right click on the selected sections, and click on **Create Group**:

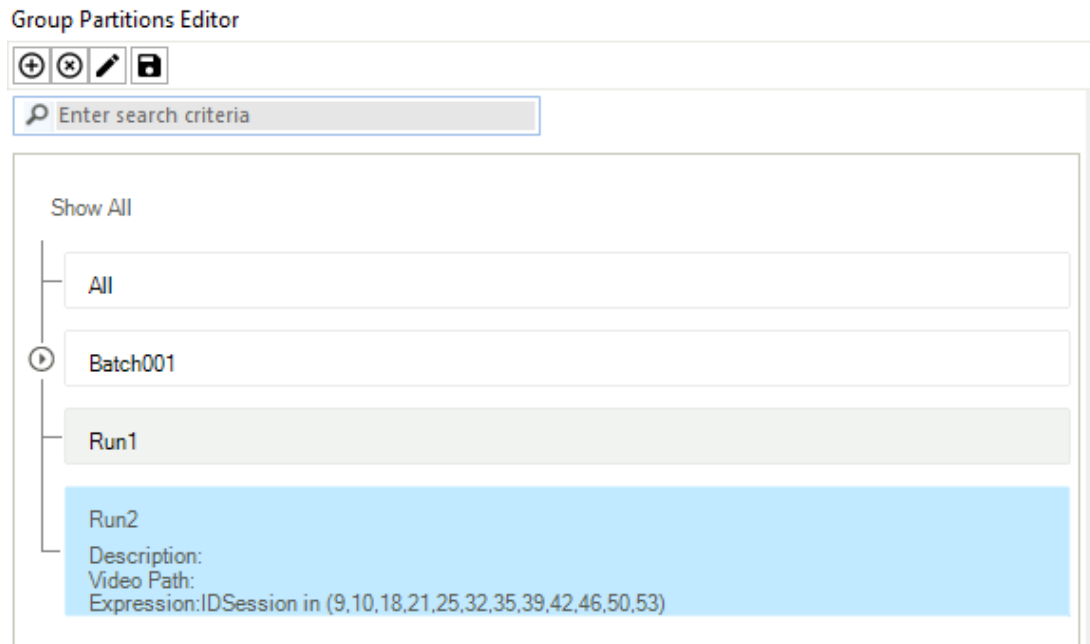
Run	Section	Collection	V	Length
Contains: Run2	Contains:	Contains:	Equals:	
Run2	102000	74S19C4P	1	0.738
Run2	102010	74S1AC35	1	0.728
Run2	102020	74T0PCX9	1	1.756
Run2	102030	74T0ZCSH	1	1.261
Run2	102040	74T0TCUI	1	1.218
Run2	102050	74T0VCKR	1	1.502
Run2	102060	74T12CKA	1	1.055
Run2	102070	74T15CVY	1	1.250
Run2	102080	74S10CB5	1	2.819
Run2	102090	74S10CB4	1	1.660
Run2	102100	74U0MC4X	1	1.577
Run2	102110	74U0PCVW	1	1.226
				Total length: 16.790

The **Group Editor** window appears (see below). The IDSession values for the selected sections will appear in this window and can be modified if needed (see the last white box in the following screen capture). Input a Name and a Description for your group:

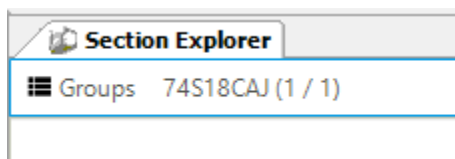
The screenshot shows a 'New' window titled 'New' with standard window controls. Inside, there's a 'Group' section with a folder icon. Below it are three input fields: 'Name' (containing 'Run2'), 'Description' (empty), and 'Image Path' (empty). Below these is a 'Root group' section with a toolbar containing icons for filter, list, table, formula, and other functions. Below the toolbar is a text box containing 'IDSession in (9,10,18,21,25,32,35,39,42,46,50,53)'. At the bottom are 'OK' and 'Cancel' buttons.

Click **OK** to confirm the creation of the group. The following conformation window will appear. Click the **Save** button (  ) to save the group:

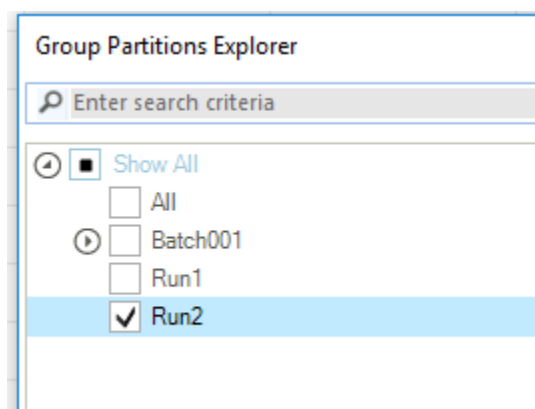




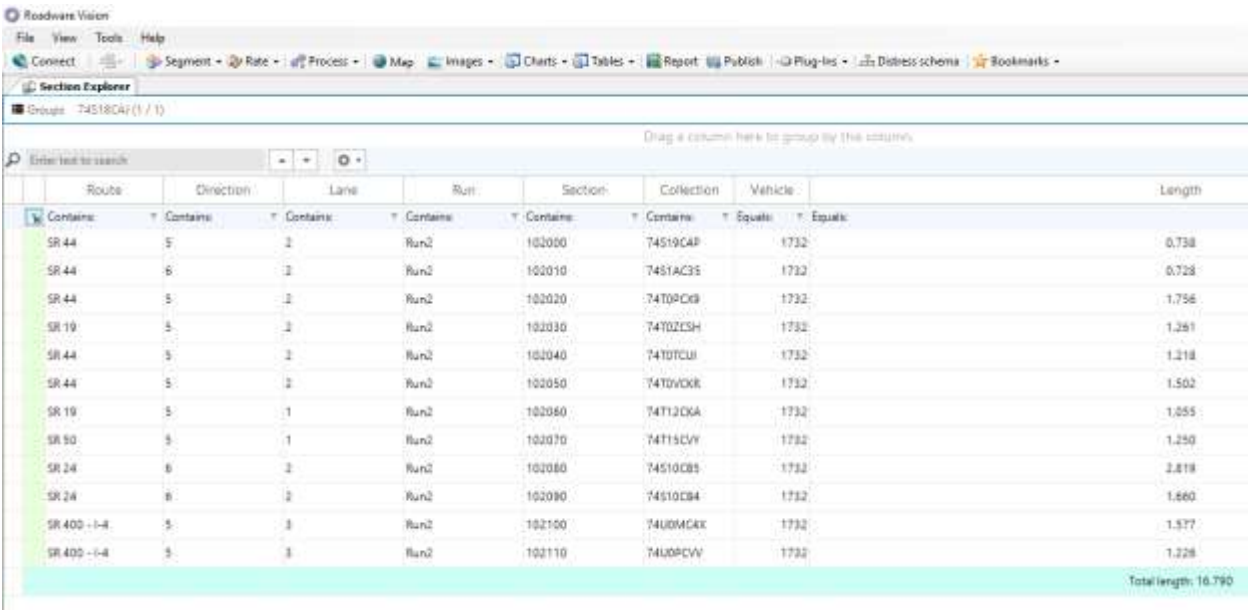
The next time you open Vision, click **Groups** in **Section Explorer** to view the saved group:



The **Group Partitions Explorer** appears. Click on the desired saved group (e.g. 'Run2'), and you will see the group you had created:



The **Section Explorer** will only display the filtered sections in the created group:



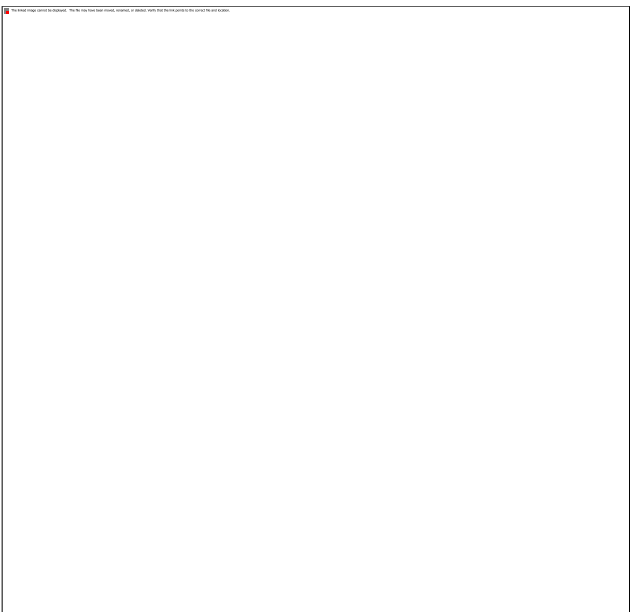
The screenshot shows the 'Section Explorer' window in the Roadware Vision application. The window title is 'Roadware Vision' and the menu bar includes 'File', 'View', 'Tools', and 'Help'. Below the menu bar is a toolbar with icons for 'Connect', 'Segment', 'Rate', 'Process', 'Map', 'Images', 'Charts', 'Tables', 'Report', 'Public', 'Plug-ins', 'Distress schema', and 'Bookmarks'. The main area of the window displays a table of road sections. The table has columns for 'Route', 'Direction', 'Lane', 'Run', 'Section', 'Collection', 'Vehicle', and 'Length'. The 'Route' column is highlighted with a green background. The table contains 15 rows of data, each representing a different road section. The 'Length' column shows values ranging from 0.738 to 1.328. A 'Total length: 16.790' is displayed at the bottom right of the table.

Route	Direction	Lane	Run	Section	Collection	Vehicle	Length
SR 44	5	2	Run2	102000	74519CAP	1732	0.738
SR 44	6	2	Run2	102010	7451AC35	1732	0.728
SR 44	5	2	Run2	102020	74T0PCK9	1732	1.756
SR 19	5	2	Run2	102030	74T0ZC5H	1732	1.261
SR 44	5	2	Run2	102040	74T0TCU1	1732	1.218
SR 44	5	2	Run2	102050	74T0VCKR	1732	1.502
SR 19	5	1	Run2	102060	74T12CKA	1732	1.055
SR 50	5	1	Run2	102070	74T15CVY	1732	1.250
SR 24	6	2	Run2	102080	74510CB5	1732	2.818
SR 24	6	2	Run2	102090	74510CB4	1732	1.660
SR 400 - I-4	5	3	Run2	102100	74U0MCAK	1732	1.577
SR 400 - I-4	5	3	Run2	102110	74U0PCVY	1732	1.228

Total length: 16.790

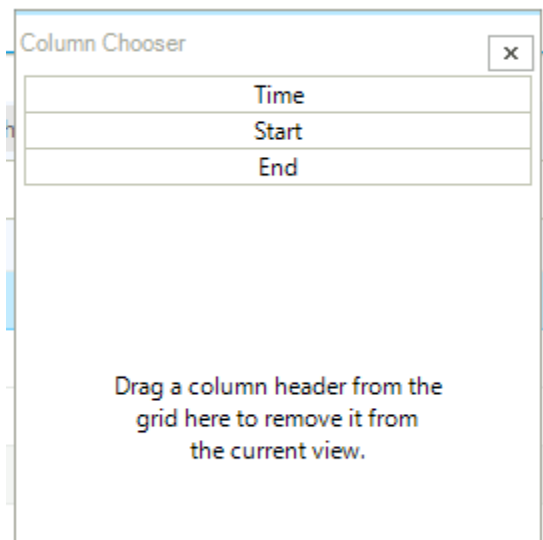
### Column Chooser

You can add/remove more column(s) to/from the table in **Section Explorer** by using **Column Chooser**. Move the mouse over one of the header columns, and right click the header, a drop-down menu appears as shown below:



Click the **Column Chooser** in the menu, and the **Column Chooser** menu appears.

Add column: Drag the desired field from the list to the table header to add it to the current view as an additional column:

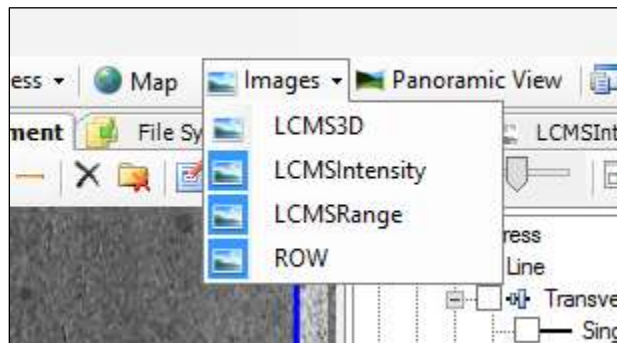


Remove Column: Drag a column header from the table to the list to remove it from the current view.

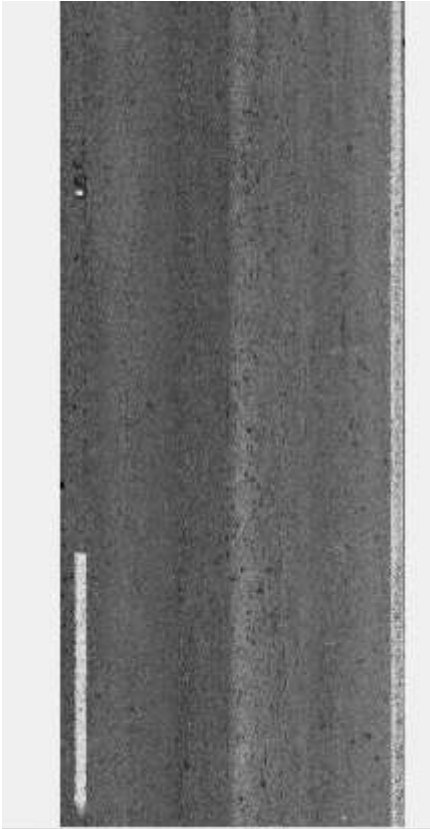
NOTE: Time is when the data was collected. Start is the start milepost in the actual collection. End is the end milepost in the actual collection. These start and end points might not necessarily be the boundaries within which the data is processed. Those boundaries can be adjusted through the Segmentation process, which is explained in the section on Segmentation at the end of this Appendix.

### Opening Pavement and ROW Images

From the menu bar, select **Images** and then select **LCMS3D**, **LCMSIntensity**, **LCMSRange**, or **ROW** images:



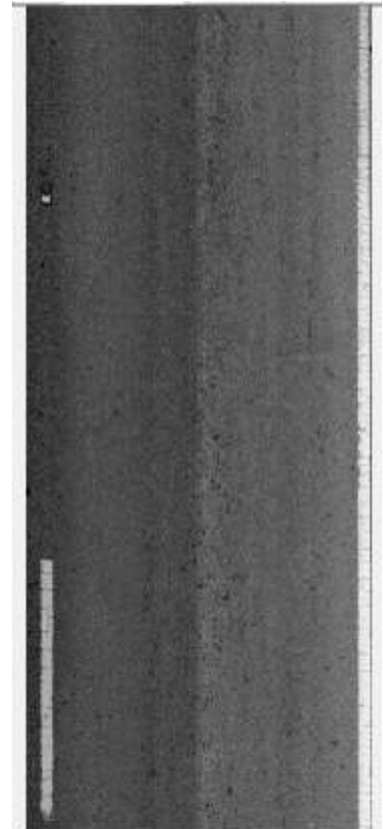
While the LRIS system only collects intensity images, the LCMS 3D image system is able to acquire both intensity images and range images, which includes depth information of pavement surface. The LCMS3D image is the combination of intensity image (LCMSIntensity) and range image (LCMSRange). All of these images are displayed if a path is provided to the location where the images are stored. Please refer to the section on Advanced Project Settings in this Appendix for instructions on providing the image path.



LCMS 3D Image



LCMS Range Image



LCMS Intensity Image

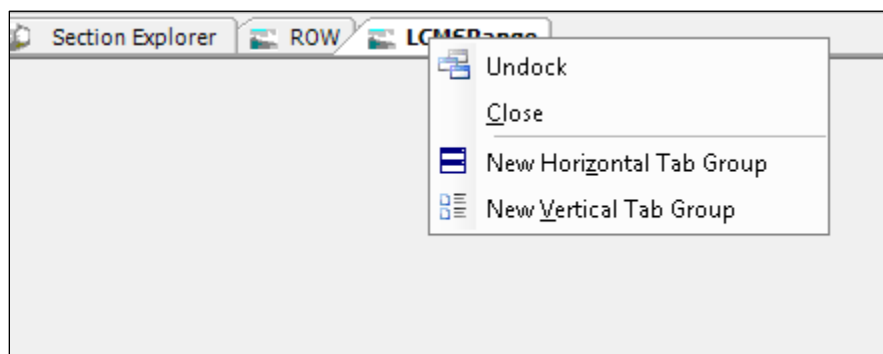
ROW image shows the forward-facing Right-of-Way image. If more than one image is provided, the software is capable of displaying more forward or rear facing images.



The play-stop-forward-backward buttons can be used to see images along the length of the roadway. The play speed can be adjusted. The slider bar on the right-hand side shows the location in 0.001-miles from the beginning of the roadway section.

## Customizing the Work Space

You can move any of the opened tabs ('Section Explorer', 'LCMS3D' and 'ROW' in this example) around one or multiple monitor screens to arrange the windows according to your preferences. If you have multiple monitors, you can right-click on any tab, select **Undock** and then move the new window to another monitor screen:



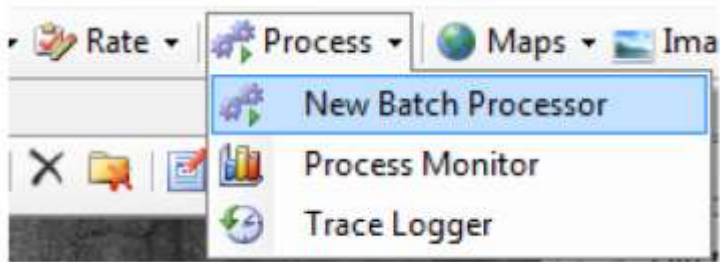
## Using Batch Processors

Batch processors are used for any automated data processing in Vision. The use of batch processor(s) includes the following five steps:

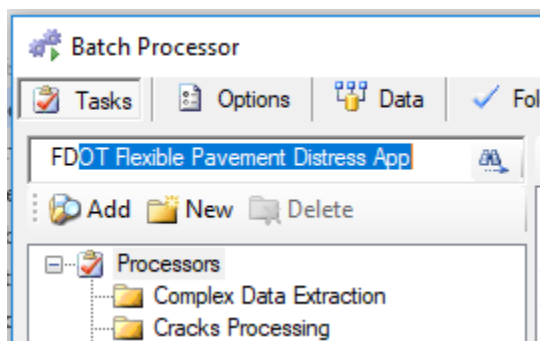
1. Select Batch Processor
2. Set Parameters and Options
3. Select Data
4. Run Batch Processor(s)
5. Save Batch Processor Settings (optional but recommended)

### ***Step1. Select Batch Processor***

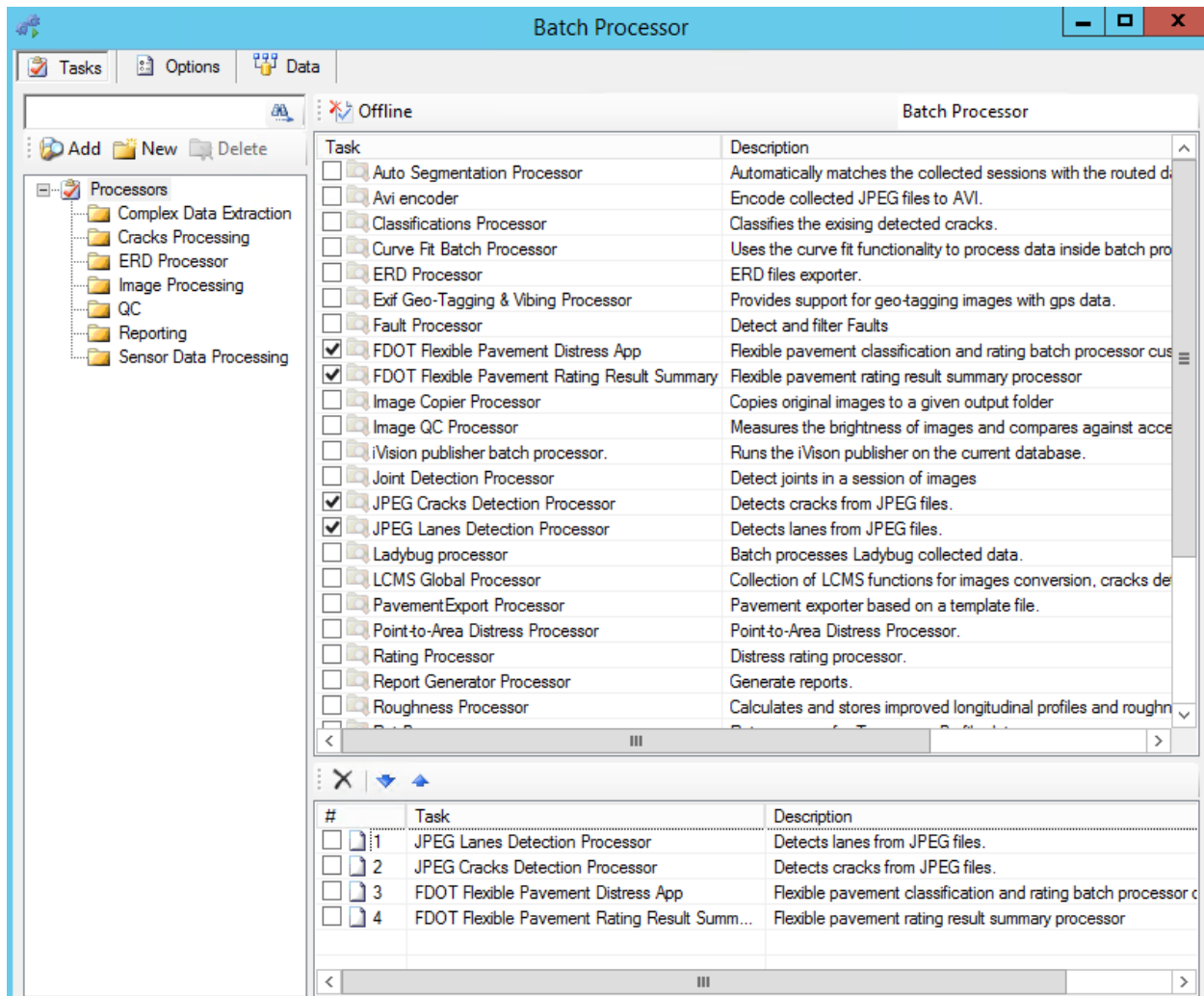
To launch the batch processor, click on the **Process** icon located on the upper toolbar (as shown in the following figure). Select **New Batch Processor** from the drop-down menu.



To select a batch processor, locate the processor from the list, or type in the name of the processor into the search bar and click on the search icon.



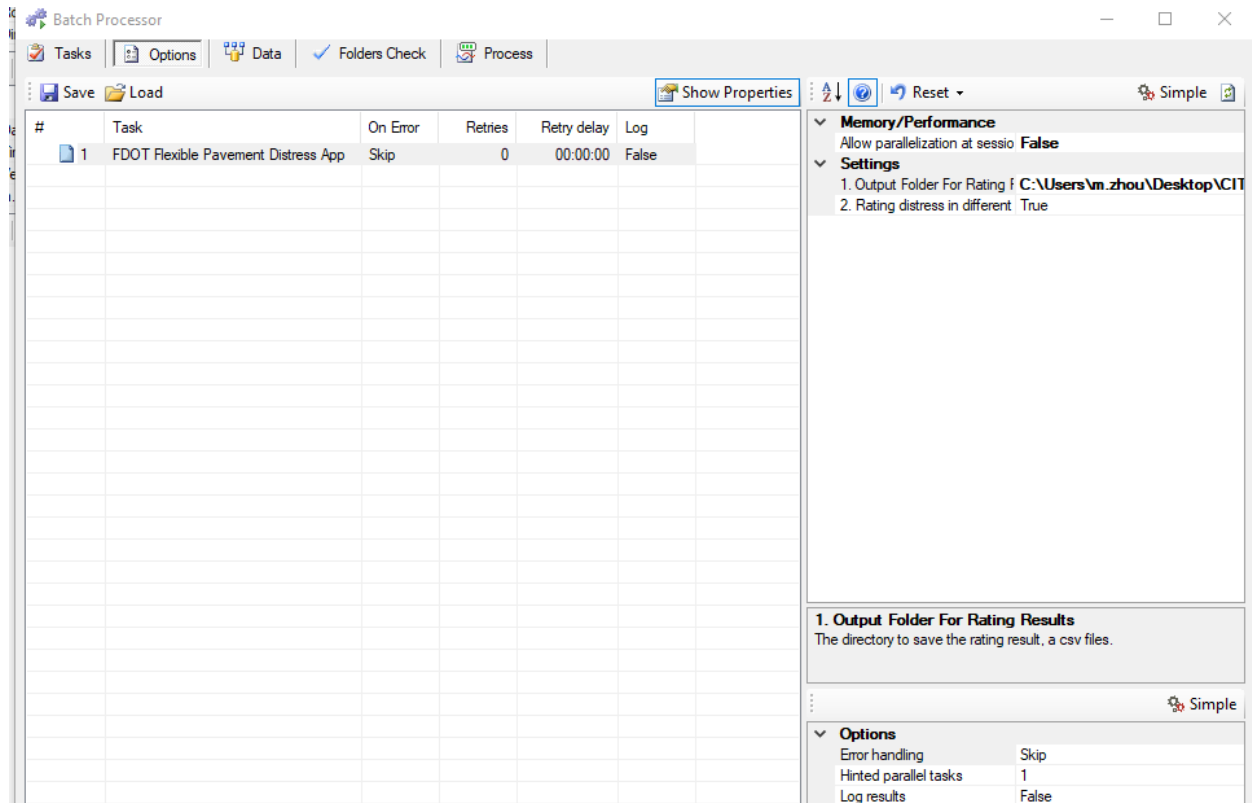
Click on the checkbox to select the batch processor. The selected batch processor will be displayed in the table at the bottom of the window:



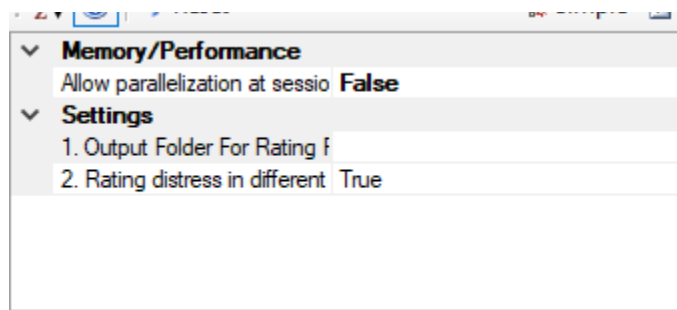


## Step2. Set Parameters and Options

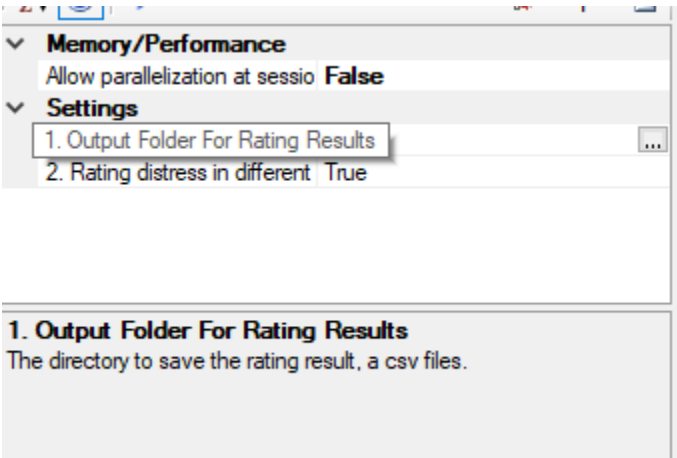
Once you have selected the processor(s), the next step is to set the parameters and other options for the processing. Click on the **Options** tab and options of the batch processor will be displayed:



Select the parameters for each processor from the table on the right:



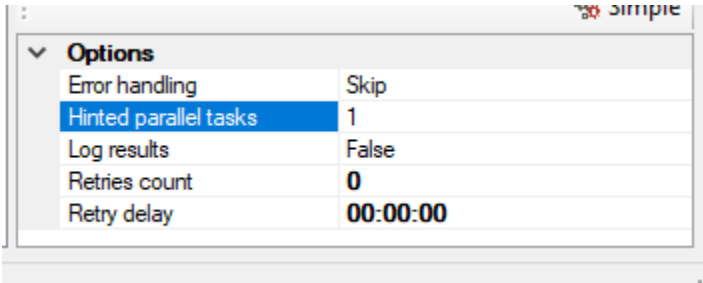
A description of each selected parameter is also provided in the table below it:



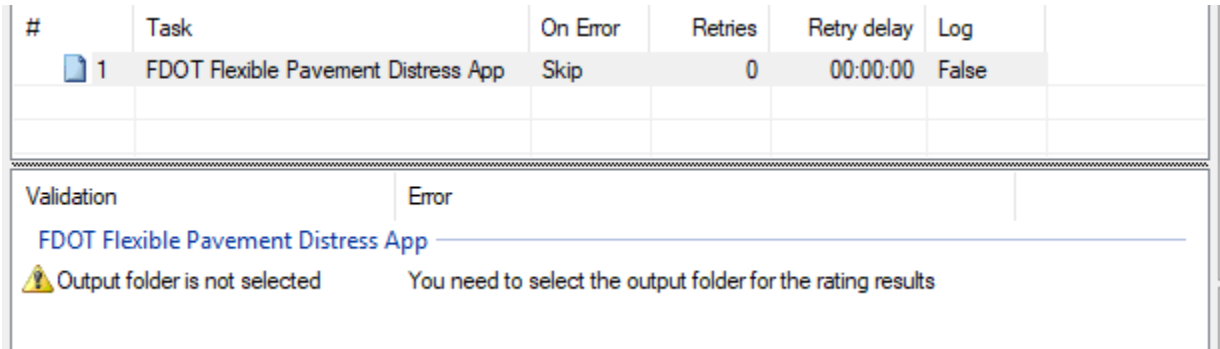
To reset any of the changes in the parameters or the options, click on the **Reset** button:



Select the options from the **Options** table:

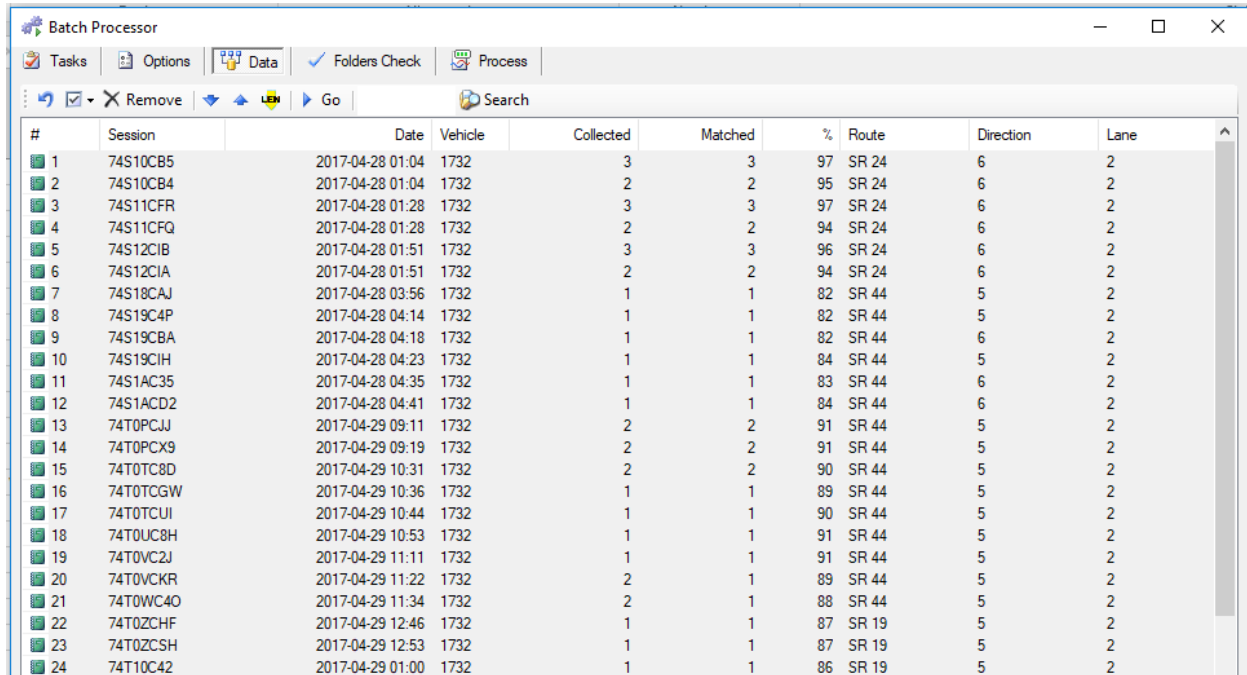


Any errors or missing values for parameters are displayed at the bottom of the window:



### Step3. Select Data

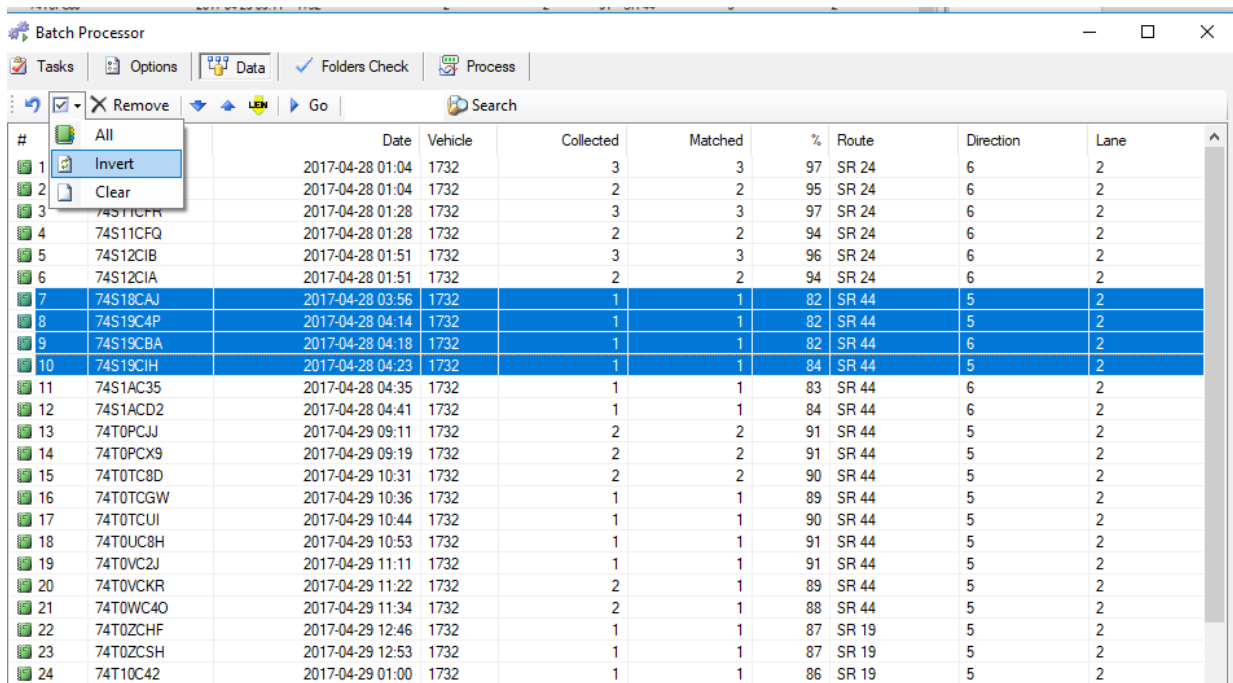
The next step is to select the data on which the batch processors will run. Click on the **Data** tab. All sessions (sections) have been selected by default and you need to remove the sessions that you are not interested in:



The screenshot shows the 'Batch Processor' application window with the 'Data' tab selected. The window has a menu bar with 'Tasks', 'Options', 'Data', 'Folders Check', and 'Process'. Below the menu bar is a toolbar with icons for 'Remove', 'Go', and 'Search'. The main area displays a table with the following columns: #, Session, Date, Vehicle, Collected, Matched, %, Route, Direction, and Lane. The table contains 24 rows of data, each representing a session. The sessions are listed in descending order of their 'Collected' value, with session 1 having the highest value (3) and session 24 having the lowest (1).

#	Session	Date	Vehicle	Collected	Matched	%	Route	Direction	Lane
1	74S10CB5	2017-04-28 01:04	1732	3	3	97	SR 24	6	2
2	74S10CB4	2017-04-28 01:04	1732	2	2	95	SR 24	6	2
3	74S11CFR	2017-04-28 01:28	1732	3	3	97	SR 24	6	2
4	74S11CFQ	2017-04-28 01:28	1732	2	2	94	SR 24	6	2
5	74S12CIB	2017-04-28 01:51	1732	3	3	96	SR 24	6	2
6	74S12CIA	2017-04-28 01:51	1732	2	2	94	SR 24	6	2
7	74S18CAJ	2017-04-28 03:56	1732	1	1	82	SR 44	5	2
8	74S19C4P	2017-04-28 04:14	1732	1	1	82	SR 44	5	2
9	74S19CBA	2017-04-28 04:18	1732	1	1	82	SR 44	6	2
10	74S19CIH	2017-04-28 04:23	1732	1	1	84	SR 44	5	2
11	74S1AC35	2017-04-28 04:35	1732	1	1	83	SR 44	6	2
12	74S1ACD2	2017-04-28 04:41	1732	1	1	84	SR 44	6	2
13	74T0PCJJ	2017-04-29 09:11	1732	2	2	91	SR 44	5	2
14	74T0PCX9	2017-04-29 09:19	1732	2	2	91	SR 44	5	2
15	74T0TC8D	2017-04-29 10:31	1732	2	2	90	SR 44	5	2
16	74T0TCGW	2017-04-29 10:36	1732	1	1	89	SR 44	5	2
17	74T0TCUI	2017-04-29 10:44	1732	1	1	90	SR 44	5	2
18	74T0UC8H	2017-04-29 10:53	1732	1	1	91	SR 44	5	2
19	74T0VC2J	2017-04-29 11:11	1732	1	1	91	SR 44	5	2
20	74T0VCKR	2017-04-29 11:22	1732	2	1	89	SR 44	5	2
21	74T0WC4O	2017-04-29 11:34	1732	2	1	88	SR 44	5	2
22	74T0ZCHF	2017-04-29 12:46	1732	1	1	87	SR 19	5	2
23	74T0ZCSH	2017-04-29 12:53	1732	1	1	87	SR 19	5	2
24	74T10C42	2017-04-29 01:00	1732	1	1	86	SR 19	5	2

To select specific sessions (sections) only, click on those sessions in the list and they will be highlighted in blue:



Batch Processor

Tasks Options Data Folders Check Process

Remove Go Search

#		Date	Vehicle	Collected	Matched	%	Route	Direction	Lane
1		2017-04-28 01:04	1732	3	3	97	SR 24	6	2
2		2017-04-28 01:04	1732	2	2	95	SR 24	6	2
3	74S11CFR	2017-04-28 01:28	1732	3	3	97	SR 24	6	2
4	74S11CFQ	2017-04-28 01:28	1732	2	2	94	SR 24	6	2
5	74S12CIB	2017-04-28 01:51	1732	3	3	96	SR 24	6	2
6	74S12CIA	2017-04-28 01:51	1732	2	2	94	SR 24	6	2
7	74S18CAJ	2017-04-28 03:56	1732	1	1	82	SR 44	5	2
8	74S19C4P	2017-04-28 04:14	1732	1	1	82	SR 44	5	2
9	74S19CBA	2017-04-28 04:18	1732	1	1	82	SR 44	6	2
10	74S19CIH	2017-04-28 04:23	1732	1	1	84	SR 44	5	2
11	74S1AC35	2017-04-28 04:35	1732	1	1	83	SR 44	6	2
12	74S1ACD2	2017-04-28 04:41	1732	1	1	84	SR 44	6	2
13	74T0PCJJ	2017-04-29 09:11	1732	2	2	91	SR 44	5	2
14	74T0PCX9	2017-04-29 09:19	1732	2	2	91	SR 44	5	2
15	74T0TC8D	2017-04-29 10:31	1732	2	2	90	SR 44	5	2
16	74T0TCGW	2017-04-29 10:36	1732	1	1	89	SR 44	5	2
17	74T0TCUI	2017-04-29 10:44	1732	1	1	90	SR 44	5	2
18	74T0UC8H	2017-04-29 10:53	1732	1	1	91	SR 44	5	2
19	74T0VC2J	2017-04-29 11:11	1732	1	1	91	SR 44	5	2
20	74T0VCKR	2017-04-29 11:22	1732	2	1	89	SR 44	5	2
21	74T0WC4O	2017-04-29 11:34	1732	2	1	88	SR 44	5	2
22	74T0ZCHF	2017-04-29 12:46	1732	1	1	87	SR 19	5	2
23	74T0ZCSH	2017-04-29 12:53	1732	1	1	87	SR 19	5	2
24	74T10C42	2017-04-29 01:00	1732	1	1	86	SR 19	5	2

Batch Processor

Tasks Options Data Process

Remove Go Search

#	Session	Date	Vehicle	Collected	Matched	% Route	Direction	Lane
1	74S10CB5	2017-04-28 01:04	1732	3	3	97 SR 24	6	2
2	74S10CB4	2017-04-28 01:04	1732	2	2	95 SR 24	6	2
3	74S11CFF8	2017-04-28 01:28	1732	3	3	97 SR 24	6	2
4	74S11CFQ	2017-04-28 01:28	1732	2	2	94 SR 24	6	2
5	74S12CB8	2017-04-28 01:51	1732	3	3	96 SR 24	6	2
6	74S12CBA	2017-04-28 01:51	1732	2	2	94 SR 24	6	2
7	74S18CAJ	2017-04-28 03:56	1732	1	1	82 SR 44	5	2
8	74S19C4P	2017-04-28 04:14	1732	1	1	82 SR 44	5	2
9	74S19CBA	2017-04-28 04:18	1732	1	1	82 SR 44	6	2
10	74S19CH	2017-04-28 04:23	1732	1	1	84 SR 44	5	2
11	74S1AC35	2017-04-28 04:35	1732	1	1	83 SR 44	6	2
12	74S1ACD2	2017-04-28 04:41	1732	1	1	84 SR 44	6	2
13	74T8PCAJ	2017-04-29 09:11	1732	2	2	91 SR 44	5	2
14	74T8PCX9	2017-04-29 09:16	1732	2	2	91 SR 44	5	2
15	74T9TC8D	2017-04-29 10:31	1732	2	2	90 SR 44	5	2
16	74T9TCGW	2017-04-29 10:36	1732	1	1	89 SR 44	5	2
17	74T9TCUJ	2017-04-29 10:44	1732	1	1	90 SR 44	5	2
18	74T8UCB4	2017-04-29 10:53	1732	1	1	91 SR 44	5	2
19	74T9VCJ3	2017-04-29 11:11	1732	1	1	91 SR 44	5	2
20	74T9VCKR	2017-04-29 11:22	1732	2	1	89 SR 44	5	2
21	74T9WC4O	2017-04-29 11:34	1732	2	1	88 SR 44	5	2
22	74T9ZCHP	2017-04-29 12:46	1732	1	1	87 SR 19	5	2
23	74T9ZC5H	2017-04-29 12:53	1732	1	1	87 SR 19	5	2
24	74T10C42	2017-04-29 01:00	1732	1	1	86 SR 19	5	2

Batch Processor

Tasks Options Data Folders Check Process

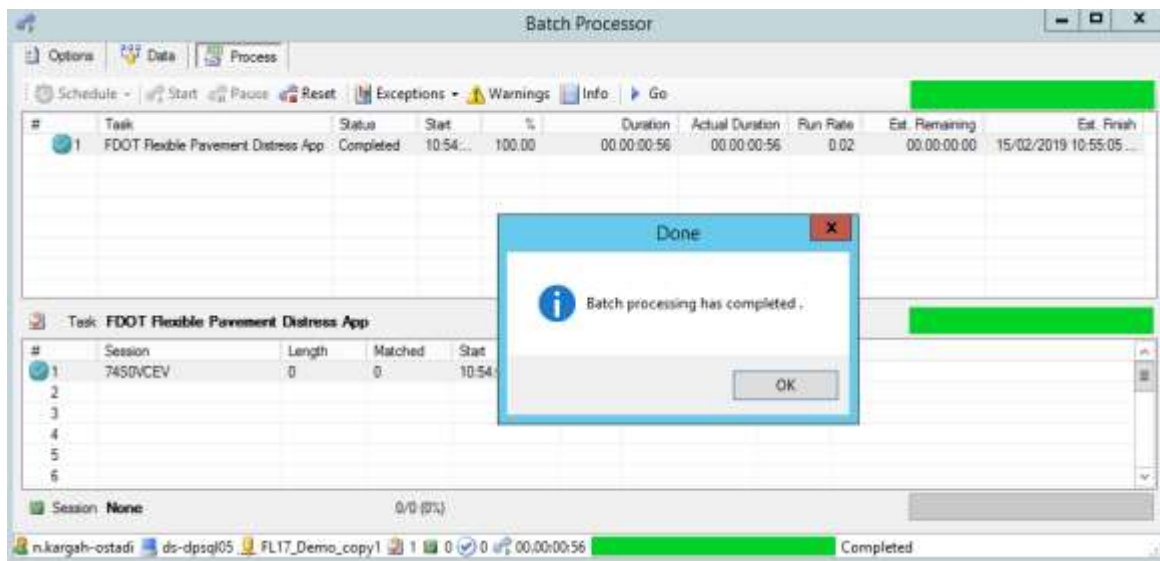
Remove Go Search

#	Session	Date	Vehicle	Collected	Matched	%	Route	Direction	Lane
1	74S18CAJ	2017-04-28 03:56	1732	1	1	82	SR 44	5	2
2	74S19C4P	2017-04-28 04:14	1732	1	1	82	SR 44	5	2
3	74S19CBA	2017-04-28 04:18	1732	1	1	82	SR 44	6	2
4	74S19CIH	2017-04-28 04:23	1732	1	1	84	SR 44	5	2

#### Step4. Run Batch Processor

After selecting the processor, its options, and the data, the last step is to run the batch processing. Click on the **Process** tab, which will appear after all the parameters have been set correctly.

1. To schedule a batch process, click on **Schedule** and select **Immediate** to process immediately or click on **Delayed** and select the date and time when it should be processed.
2. Click on **Start** to begin processing immediately. If you have selected **Delayed** in the first step, you do NOT need to click on **Start**.
3. The progress for each batch processor and the overall progress will be displayed at the bottom of the window.
4. Once the processing is complete, a pop-up window will be displayed, which will report whether the process was completed without errors. After clicking on the **OK** button on that pop-up window, the **Tasks** tab is no longer available. To carry out another batch process, close the window and reopen the **Batch Processor**.



#### Running Multiple Batch Processors

Vision allows you to select multiple processors and process the data with each processor one after another:

1. Select the desired processors from the **Task** tab:

<input type="checkbox"/>	Fault Processor	Detect and filter Faults
<input checked="" type="checkbox"/>	FDOT Flexible Pavement Distress App	Flexible pavement classification and rating batch processor customized fo
<input checked="" type="checkbox"/>	FDOT Flexible Pavement Rating Result Summary	Flexible pavement rating result summary processor
<input type="checkbox"/>	Image Copier Processor	Copies original images to a given output folder
<input type="checkbox"/>	Image QC Processor	Measures the brightness of images and compares against acceptable ran
<input type="checkbox"/>	iVision publisher batch processor.	Runs the iVision publisher on the current database.
<input type="checkbox"/>	Joint Detection Processor	Detect joints in a session of images
<input checked="" type="checkbox"/>	JPEG Cracks Detection Processor	Detects cracks from JPEG files.
<input checked="" type="checkbox"/>	JPEG Lanes Detection Processor	Detects lanes from JPEG files.
<input type="checkbox"/>	Ladybug processor	Batch processes Ladybug collected data.

2. Make sure the desired processors are selected in the correct order by checking the table in the bottom of the window:

#	Task	Description
<input type="checkbox"/> 1	JPEG Lanes Detection Processor	Detects lanes from JPEG files.
<input type="checkbox"/> 2	JPEG Cracks Detection Processor	Detects cracks from JPEG files.
<input checked="" type="checkbox"/> 3	FDOT Flexible Pavement Distress App	Flexible pavement classification and rating batch processor customized
<input type="checkbox"/> 4	FDOT Flexible Pavement Rating Result Summ...	Flexible pavement rating result summary processor

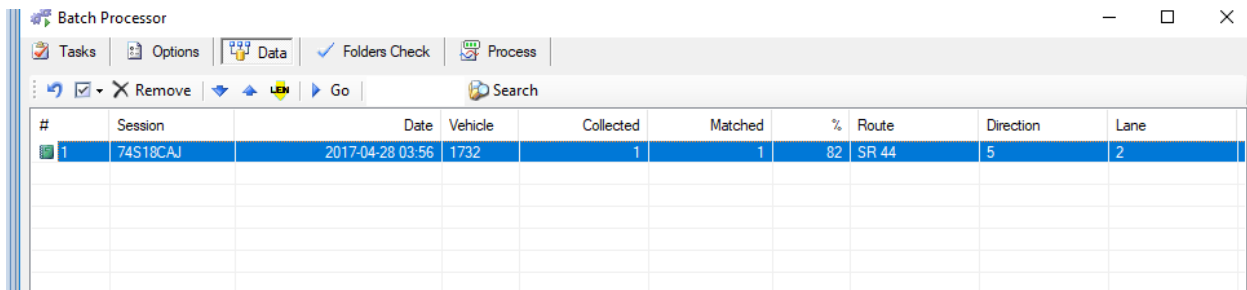
3. Set **Options** for each batch processor:

Batch Processor						
Tasks Options Data Process						
#	Task	On Error	Retries	Retry delay	Log	
1	JPEG Lanes Detection Processor	Skip	0	00:00:00	False	
2	JPEG Cracks Detection Processor	Skip	0	00:00:00	False	
3	FDOT Flexible Pavement Distress App	Skip	0	00:00:00	False	
4	FDOT Flexible Pavement Rating Res...	Skip	0	00:00:00	False	

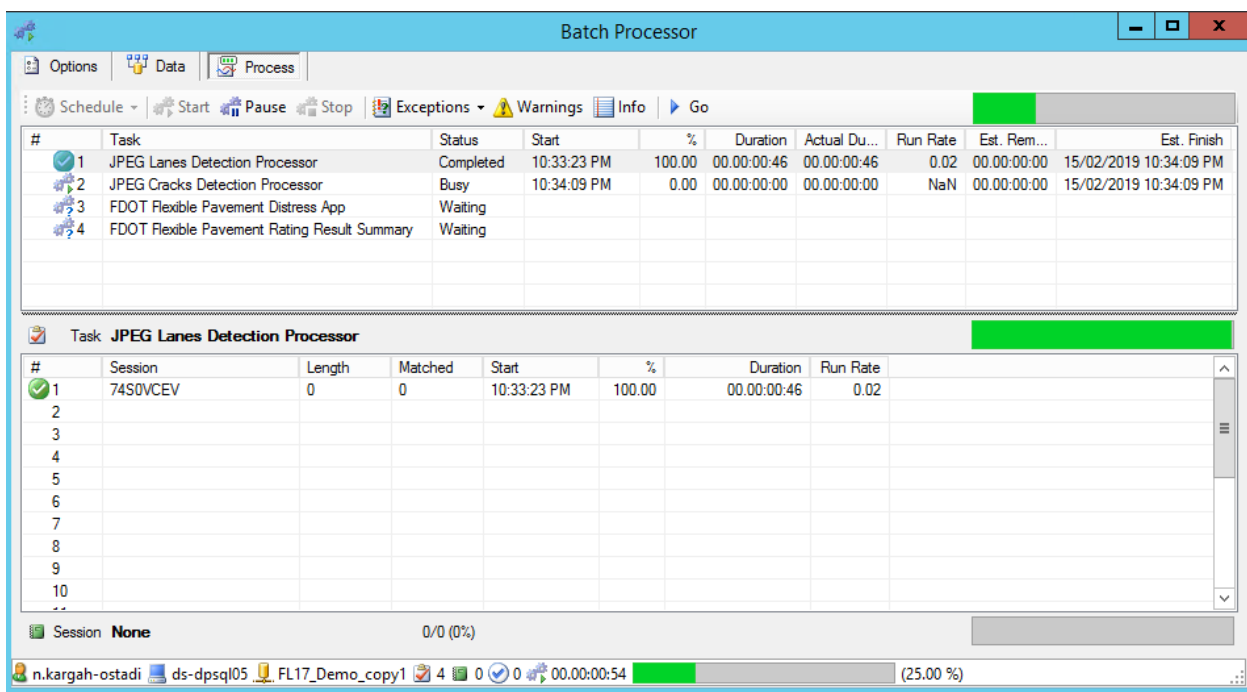
  

<b>Memory/Performance</b>	Allow parallelization at se	False
<b>Settings</b>	1. Road Zone Type	FDOT
	2. Output Folder For Rat	C:\Users\vn.kargah-ostadi\N
	3. Rating distress in diffe	True

4. Click on the **Data** tab and select section(s) that you want to process. Note that by default, all sections in a project are selected and the desired section(s) are chosen by selecting and removing the undesired section(s).

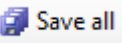


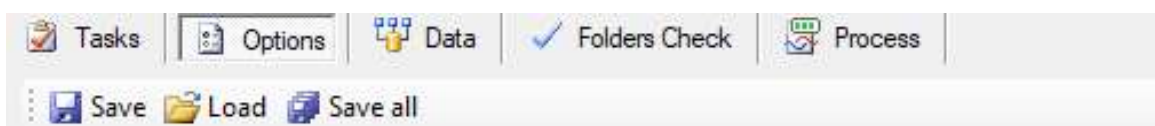
- Click on the **Process** tab and click on the **Start** button to process the selected section(s):



### Step5. Save Batch Processor Settings

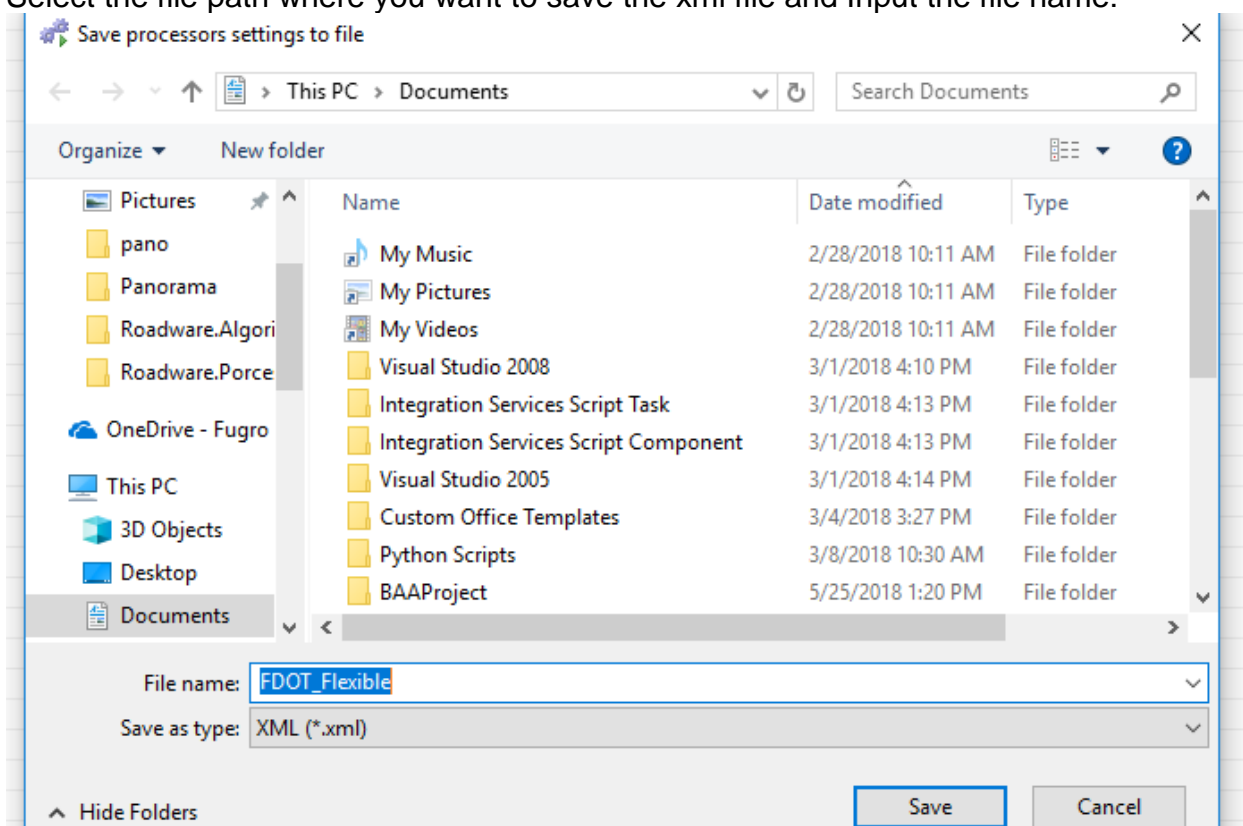
You can save all the settings for the batch processors so that the same settings can be applied the next time you open Vision software.

Click on the **Save all** button (  ) to save all options for all selected processors:

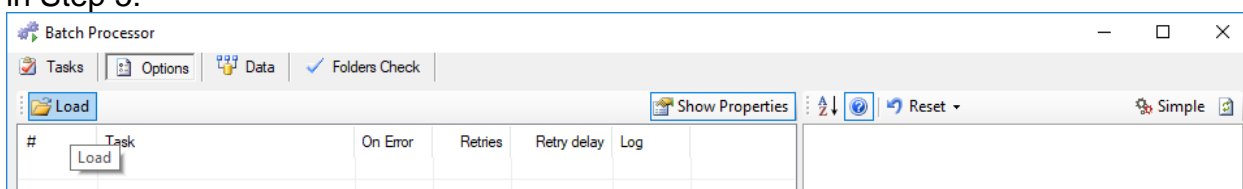


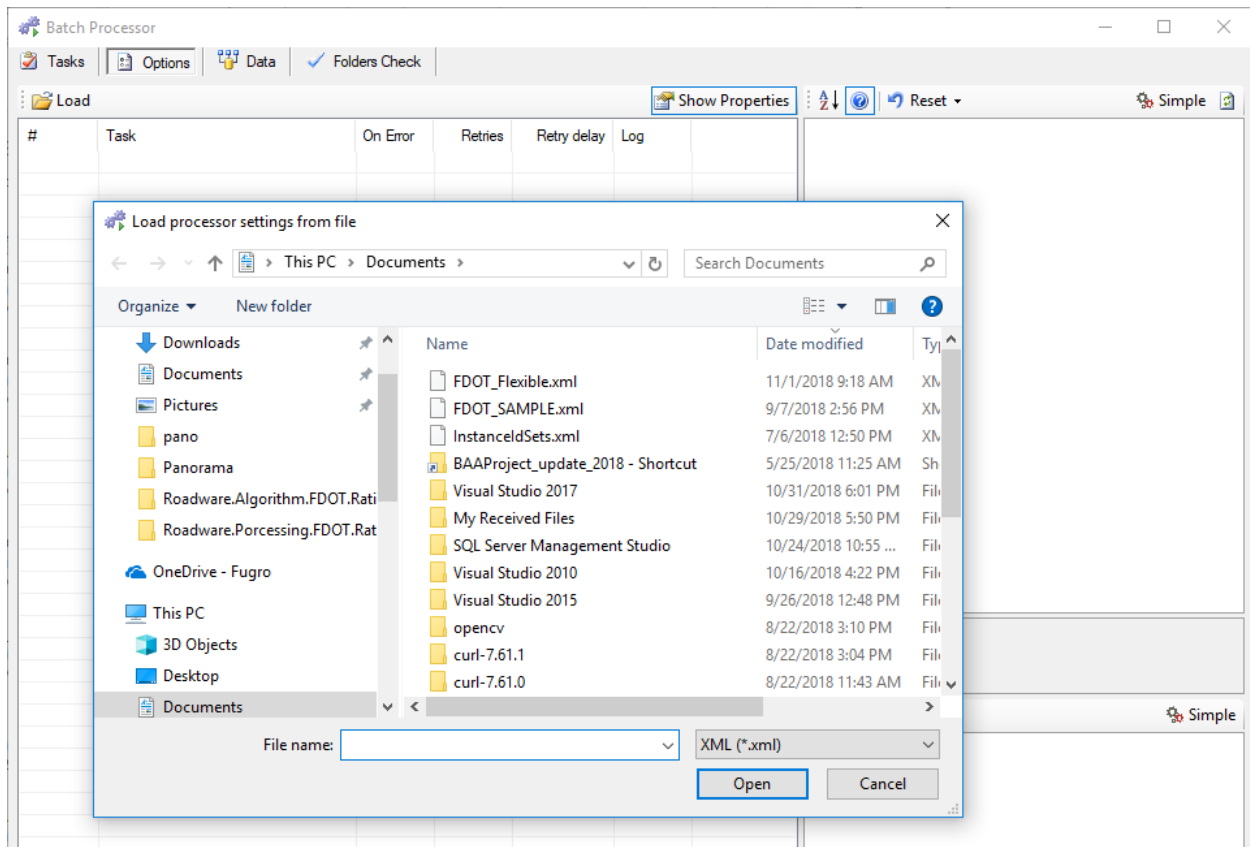


Select the file path where you want to save the xml file and Input the file name:

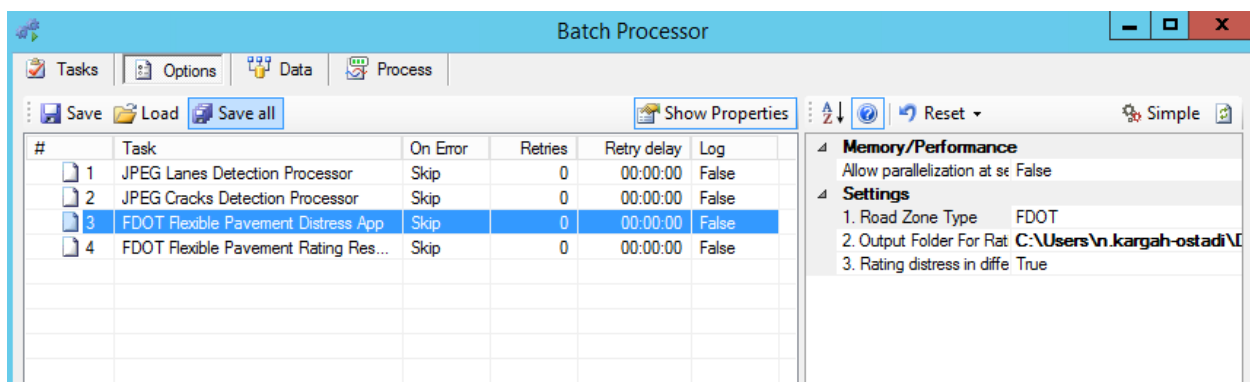


The next time you run multiple batch processors, you can skip the steps of selecting **Tasks** and go directly to **Options**. Click the **Load** button to load the settings file saved in Step 5:





Four processors are selected in this example, and the previous settings are loaded for all four processors:



Next, you need to select the desired sections and run the processors. By using this save and load operation, the same batch processors with the same settings can be used on multiple databases and multiple sections.

## Automated Distress Rating

There are five steps for automated pavement distress rating:

1. Vision Lane Detection: the 'JPEG Lanes Detection Processor'
2. Vision Crack Detection: the 'JPEG Cracks Detection Processor'
3. 'FDOT Flexible Pavement Distress Application (FFPDA)'
4. Quality Control of Automated Distress Rating Results using Manual Rating (this is a non-mandatory manual process)
5. 'FDOT Flexible Pavement Rating Results Summary'

It is recommended to utilize the first three batch processors simultaneously to automatically detect the lanes, detect cracks from pavement images, and classify and rate the detected cracks to be assigned as distresses according to the FDOT protocol. After automated rating has been completed, you can perform an optional quality control check to investigate whether the automated rating was completed successfully and use the manual rating tools to make adjustments where necessary (semi-automated rating). Running the final summary batch processor will summarize both the automated and semi-automated rating results and export them in a comma-separated value (csv) file.

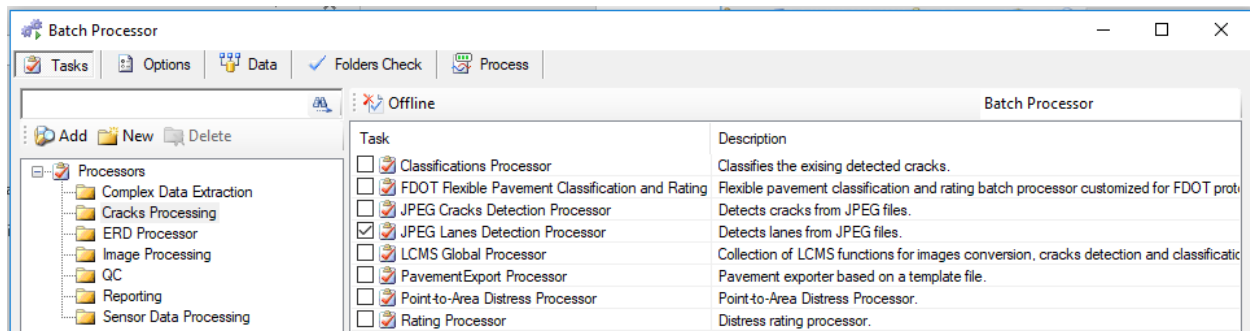
If you want to skip the quality control step, you may select the 'FDOT Flexible Pavement Rating Results Summary' processor together with the initial three batch processors for automated distress rating in the following order:

#	Task	Description
<input type="checkbox"/> 1	JPEG Lanes Detection Processor	Detects lanes from JPEG files.
<input type="checkbox"/> 2	JPEG Cracks Detection Processor	Detects cracks from JPEG files.
<input type="checkbox"/> 3	FDOT Flexible Pavement Distress App	Flexible pavement classification and rating batch processor customized for ...
<input type="checkbox"/> 4	FDOT Flexible Pavement Rating Res...	Flexible pavement rating result summary processor

This way, the selected section(s) will be processed using all four processors one after the other. To ensure the data quality, it is recommended to NOT skip the manual quality control step.

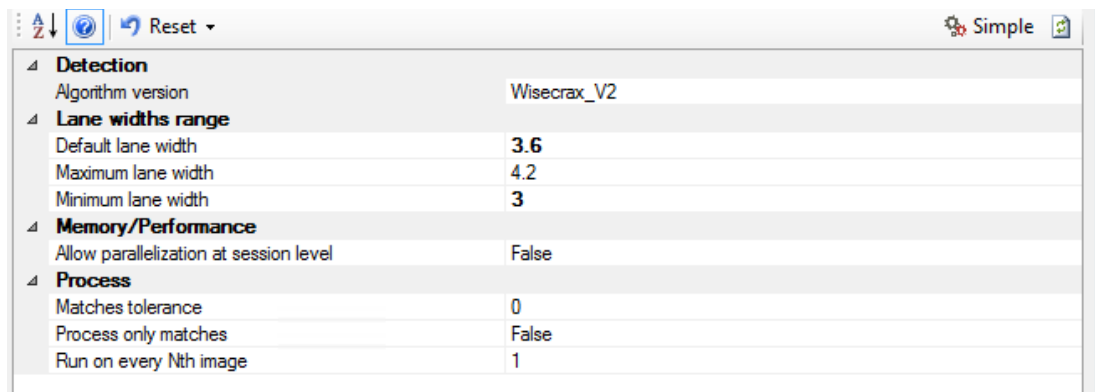
## Lane Detection Processor

Automated lane boundary detection can be completed on pavement images using the 'JPEG Lanes Detection Processor'.



## Lane Detection Options

There are four groups of options for 'JPEG Lanes Detection Processor'.



- Detection

**Algorithm Version:** Select algorithm version used for the lane detection. It is recommended to use the latest version.

- Lane Width Range

**Default lane width:** The default lane width to be stored when no lanes are detected. When lane stripes are detected, and the detected lane width is not within the range

identified by the minimum and maximum, this number will be stored. Please set this according to project specifics, e.g. 3.6 meters.

**Maximum lane width:** Only lanes smaller than this value will be stored to the database. When the detected lane width is more than this threshold, the default lane width will be stored.

**Minimum lane width:** Only lanes greater than this value will be stored to the database. When the detected lane width is smaller than this threshold, the default lane width will be stored. Please set this according to project specifics, e.g. 3.0 meters.

- Memory/Performance

**Allow parallelization at session level:** If set to true, whole sessions are processed in parallel while keeping all images of each session together. If set to False, images from multiple sessions can be processed simultaneously if the computer has adequate number of cores available for such an operation. This is set to false by default for improved speed.

**Use ideal CPU count:** If parallelization at session level is set to True, this option will be available. If this is set to True, the number of CPU cores to use is determined automatically based on the hardware available and the amount of memory the processor uses. If this is set to False, the user should enter the number of CPU cores to use.

- Process

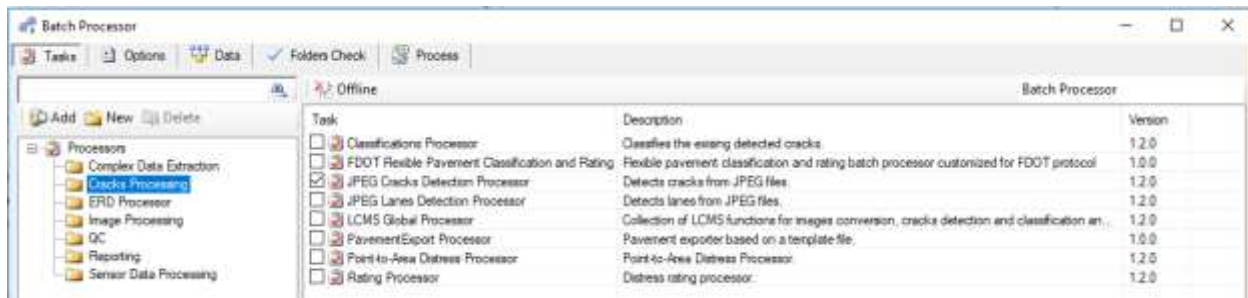
**Matches tolerance:** Tolerance threshold, which will extend the matches if the next option is set to True.

**Process only matches:** If set to true, only the images contained in matches (parts of the sessions where collected data matches routed data) will be processed. It is recommended to keep this option at False to process all images in each session.

**Run on every Nth image:** Run on every Nth image, after 1 frame is added to the output. For example, if set to '2', it only processes every other image.

## Cracks Detection Processor

Automated crack detection can be completed on pavement images using the 'JPEG Cracks Detection Processor'.



## Crack Detection Options

There are three groups of options for 'JPEG Cracks Detection Processor'.

- Detection

**Detection Profile:** Select the profile used for crack detection, as defined in the schema editor. It is recommended to select the 'Learning based WiseCrax (LCMS)' as detection profile if the LCMS range images are available. This profile was developed by training a machine learning algorithm on LCMS range (depth) images. The 'Learning based WiseCrax (JPEG)' option was developed by training a machine learning algorithm on intensity images. The other options on this list were developed for specific past projects and are not recommended to be used on new projects.

- Memory/Performance

**Allow parallelization at session level:** If set to true, whole sessions are processed in parallel while keeping all images of each session together. If set to False, images from multiple sessions can be processed simultaneously if the computer has adequate number of cores available for such an operation. This is set to false by default for improved speed.

**Use ideal CPU count:** If parallelization at session level is set to True, this option will be available. If this is set to True, the number of CPU cores to use is determined automatically based on the hardware available and the amount of memory the

processor uses. If this is set to False, the user should enter the number of CPU cores to use.

- Process

**Matches tolerance:** Tolerance threshold, which will extend the matches if the next option is set to True.

**Process only matches:** If set to true, only the images contained in matches (parts of the sessions where collected data matches routed data) will be processed. It is recommended to keep this option at False to process all images in each session.

**Run on every Nth image:** Run on every Nth image, after 1 frame is added to the output. For example, if set to '2', it only processes every other image.

The screenshot shows a settings window with a 'Reset' button and a 'Simple' icon. The settings are organized into three expandable sections:

- Detection**
  - Auto Profile: No
  - Detection Profile: Learning based WiseCrax (LCMS)
- Memory/Performance**
  - Allow parallelization at session level: False
  - Use ideal cpu count: True
- Process**
  - Matches tolerance: 0
  - Process only matches: False
  - Run on every Nth image: 1

### ***FDOT Flexible Pavement Distress Application (FFPDA)***

The 'FDOT Flexible Pavement Distress Application' is a crack classification and rating tool customized for FDOT according to classification and rating protocols defined in the FDOT Flexible Pavement Condition Survey Handbook.

<input type="checkbox"/>	Fault Processor	Detect and filter Faults
<input checked="" type="checkbox"/>	FDOT Flexible Pavement Distress App	Flexible pavement classification and rating batch processor customized for FDOT pr
<input type="checkbox"/>	FDOT Flexible Pavement Rating Result Summary	Flexible pavement rating result summary processor
<input type="checkbox"/>	Image Center Processor	Center of image processor to align output folder

### **FFPDA Options**

There are four options that you need to select in the FFPDA batch processor.

- Memory/Performance

**Allow parallelization at session level:** If set to true, whole sessions are processed in parallel while keeping all images of each session together. If set to False, images from multiple sessions can be processed simultaneously if the computer has adequate number of cores available for such an operation. This is set to false by default for improved speed.

**Use ideal CPU count:** If parallelization at session level is set to True, this option will be available. If this is set to True, the number of CPU cores to use is determined automatically based on the hardware available and the amount of memory the processor uses. If this is set to False, the user should enter the number of CPU cores to use.

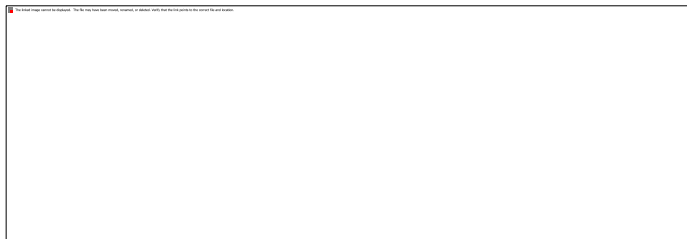
- Settings

**Output Folder for Rating Results:** This is the file location to save the rating results, a csv file.

**Rating Distress in Different Road Zone? (True or False):** The batch processor provides two ways to rate the distress. It is recommended to use the default value, which is True.

1. False: First classify and rate the distresses, then divide the rated distresses into different road zones.
2. True: First divide the cracks into the different road zones, and then classify and rate them.

**RoadZone Type:** use FDOT for the FDOT defined wheel paths and use HPMS for FHWA defined wheel paths for calculating Percent Cracking.





## FFPDA Results

The Rating Results are saved as a 'distressRecord.csv' file in the output folder that you had chosen in the settings. If FFPDA is executed multiple times with the same folder selected for output, then the csv file created in the initial run will be amended with results from the following runs. The table in the csv file includes the following fields:

- DistressID: ID of the specific distress within the entire section.
- SectionID: ID of the specific section.
- RunID: ID of Run on the specific section. In the sample data, each section has been collected for three times. The RunID ranges from 1 to 3 in that example.
- Type: Type of distress, alligator, branch or single cracking.
- SeverityID: severity level of distress, value can be 1B, II or III.
- IsWheelPath: a Boolean value, true means the distress is within wheel path road zones (CW), 'False' means the distress is outside wheel path road zones (CO).
- TransExtent: transverse extent (in feet) of the distress bounding box.
- LongiExtent: longitudinal extent (in feet) of the distress bounding box.
- Area: distress area (in square feet). For alligator cracking the area is the TransExtent multiplied by LongiExtent. For single cracking and branch cracking, the area is distress length (the diagonal length of the distress bounding box) multiplied by 1ft.
- ImageName: the corresponding range (depth) image file path (including the file name), which contains the distress.

- DistanceStamp: distance of distress from the beginning of the session (in feet).

The following is an example screen shot of the output file format:

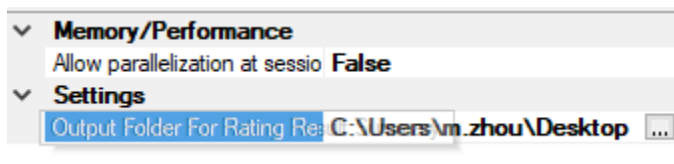
	A	B	C	D	E	F	G	H	I	J	K
1	DistressID	SectionID	RunID	Type	SeverityID	IsWheelPath	TransExtent	LongiExtent	Area	ImageName	DistanceStamp
2	1	103010	Run3	Alligator	2	TRUE	3.031499957	32.7953214	99.41901539	Q:\Road Survey I	282.8884651
3	2	103010	Run3	Alligator	2	TRUE	2.926513061	6.351714419	18.58837521	Q:\Road Survey I	283.9908287
4	3	103010	Run3	Single Crack	1	FALSE	0.035542399	1.706039866	1.706410058	Q:\Road Survey I	298.1771993
5	4	103010	Run3	Branch Crack	1	TRUE	2.270344121	2.195979111	3.15860518	Q:\Road Survey I	305.7712599
6	5	103010	Run3	Single Crack	1	TRUE	0.247156691	1.286090713	1.309624279	Q:\Road Survey I	290.6312581
7	6	103010	Run3	Single Crack	1	TRUE	1.377954618	0.371829743	1.427240795	Q:\Road Survey I	304.1702087
8	7	103010	Run3	Single Crack	1	TRUE	1.824149368	0.086616033	1.826204603	Q:\Road Survey I	311.549921
9	8	103010	Run3	Single Crack	1	TRUE	1.522311281	0.524933899	1.610275515	Q:\Road Survey I	313.183783
10	9	103010	Run3	Single Crack	1	FALSE	0.403543796	1.872268387	1.915264083	Q:\Road Survey I	288.6277554
11	10	103010	Run3	Single Crack	1	FALSE	0.044994468	0.656168939	0.657709798	Q:\Road Survey I	300.0144726
12	11	103010	Run3	Alligator	2	FALSE	0.761155836	3.018376179	2.297454644	Q:\Road Survey I	342.6916957
13	12	103010	Run3	Alligator	2	TRUE	3.044623735	32.7953214	99.8494139	Q:\Road Survey I	315.6969077
14	13	103010	Run3	Alligator	2	TRUE	2.992129797	12.83466388	38.40298022	Q:\Road Survey I	335.6575652
15	14	103010	Run3	Single Crack	1	FALSE	0.37007915	1.253282344	1.306780476	Q:\Road Survey I	338.3806653
16	15	103010	Run3	Single Crack	1	FALSE	0.866142342	0.328082123	0.926196759	Q:\Road Survey I	344.2533782
17	16	103010	Run3	Branch Crack	1	TRUE	1.75853263	2.034124336	2.688884309	Q:\Road Survey I	327.7704148
18	17	103010	Run3	Branch Crack	1	TRUE	2.047246744	3.123363272	3.734517018	Q:\Road Survey I	332.4160909
19	18	103010	Run3	Single Crack	1	TRUE	0.242782556	1.023623408	1.052021032	Q:\Road Survey I	315.7494012

### ***Automated Rating Results Summary***

The 'FDOT Flexible Pavement Rating Results Summary' processor has been designed to summarize all the rating results either directly following the FFPDA automated rating or after conducting a manual QC of the FFPDA results. This batch processor exports the summarized results into a csv file.

### **Summary Options**

There are two options that you need to select in the 'FDOT Flexible Pavement Rating Results Summary'.



- Memory/Performance

**Allow parallelization at session level:** If set to true, whole sessions are processed in parallel while keeping all images of each session together. If set to False, images from multiple sessions can be processed simultaneously if the computer has adequate number of cores available for such an operation. This is set to false by default for improved speed.

**Use ideal CPU count:** If parallelization at session level is set to True, this option will be available. If this is set to True, the number of CPU cores to use is determined automatically based on the hardware available and the amount of memory the processor uses. If this is set to False, the user should enter the number of CPU cores to use.

## 1. Settings

**Output Folder for Rating Results Summary:** This is the file location to save the rating results, a csv file.

## Summary Results

The rating results are saved as 'distressResultSummary.csv' in the output folder that you had chosen in the settings. The table in the csv file includes the following fields:

- SectionID: ID of the specific section.
- RunID: ID of Run on the specific section. In the sample data, each section has been collected for three times. The RunID ranges from 1 to 3 in that example.
- Section Length (ft):
- Avg Section Width (ft):
- Section Area (sq ft):
- CW (%): Percentage area of section wheel paths with distress.
- CO (%): Percentage area of section non-wheel path zones with distress.

- SeverityID\_WP: predominant severity level of distress in the wheel paths, value can be 1B, II or III.
- SeverityID\_NWP: predominant severity level of distress in the non-wheel path zones, value can be 1B, II or III.
- Code\_WP: assigned according to the FDOT Flexible Pavement Condition Survey Handbook.
- Code\_NWP: assigned according to the FDOT Flexible Pavement Condition Survey Handbook.
- SectionScore: calculated according to the FDOT Flexible Pavement Condition Survey Handbook.

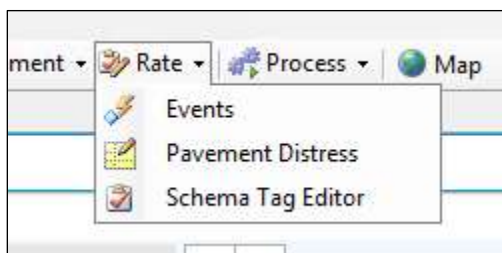
	A	B	C	D	E	F	G	H	I	J	K	L
1	SectionID	RunID	Section_Length (ft)	Avg_Section_Width (ft)	Section_Area (sq ft)	CW (%)	CO (%)	SeverityID_WP	SeverityID_NWP	Code_WP	Code_NWP	SectionScore
2	102080	Run2	14403.84	10.95	157681.48	1	0.64	II	1B	E	A	9.5
3	102090	Run2	8316	11.04	91782.71	25.52	12.42	II	II	F	F	7
4	102000	Run2	3189.12	10.21	32557.13	47.35	7.06	II	1B	G	B	6.5
5	102010	Run2	3189.12	10.21	32566.65	53.2	8.76	II	1B	H	B	4.5
6	102020	Run2	8405.76	10.63	89372.76	0.04	0.17	1B	1B	A	A	10
7	102040	Run2	5771.04	11.06	63815.48	47.91	33.66	II	II	G	G	5.5
8	102050	Run2	7022.4	10.5	73737.18	68.6	42.41	II	II	H	G	3.5
9	102030	Run2	5755.2	10.19	58665.54	6.85	9.1	II	1B	F	B	7.5
10	102060	Run2	4884	9.84	48054.95	0.4	0.33	1B	1B	A	A	10
11	102070	Run2	5623.2	9.62	54117.38	20.56	12.12	II	1B	F	B	7.5
12	102100	Run2	6515.52	9.26	60319.38	20.81	28.73	1B	1B	B	C	8
13	102110	Run2	5644.32	10.39	58645.62	21.49	32.27	1B	1B	B	C	8
14	103080	Run3	14403.84	11.03	158843.69	1.12	0.63	1B	1B	A	A	10
15	103090	Run3	8316	10.96	91138.54	21.34	11.42	II	II	F	F	7
16	103000	Run3	3189.12	10.39	33142.83	46.77	7.12	II	1B	G	B	6.5
17	103010	Run3	3189.12	10.28	32769.35	53.83	8.2	II	1B	H	B	4.5
18	103020	Run3	8405.76	10.66	89610.39	0.1	0.32	1B	1B	A	A	10
19	103040	Run3	5771.04	11.16	64389.7	47.53	34.64	II	II	G	G	5.5
20	103050	Run3	7022.4	10.38	72880.96	68.16	43.57	II	II	H	G	3.5
21	103030	Run3	5755.2	10.25	58971.72	7.12	8.85	II	1B	F	B	7.5
22	103060	Run3	4884	9.81	47902.64	0.47	0.36	1B	1B	A	A	10
23	103070	Run3	5623.2	9.71	54580.43	19.75	12.42	II	1B	F	B	7.5

## Quality Control of Automated Distress Rating Results

In this optional step, you can modify or delete the automatically identified distresses, or add a new distress that was not detected by the automated process. For example, you might want to increase the severity level of a distress or identify an area of patching or raveling that cannot be automatically identified.

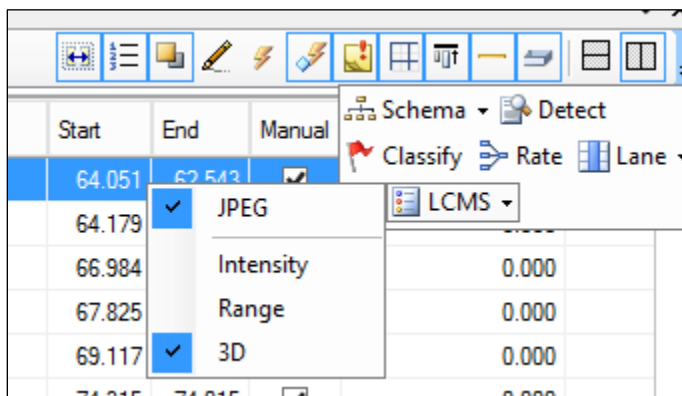
### *Setup for Distress Rating*

Select the **Pavement Distress** module from the **Rate** menu located along the Vision toolbar to rate pavement distress:



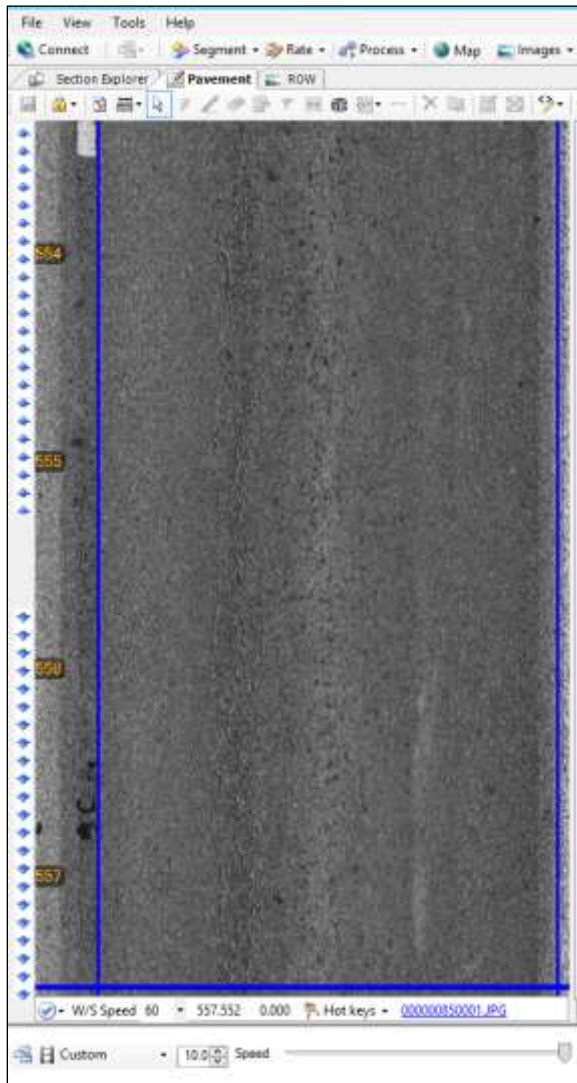
### *Switching Image Type*

The default image displayed is LCMS 3D image, which is the combination of both intensity image and depth image. You can change the displayed image to Range image, and Intensity image using the **LCMS** button.



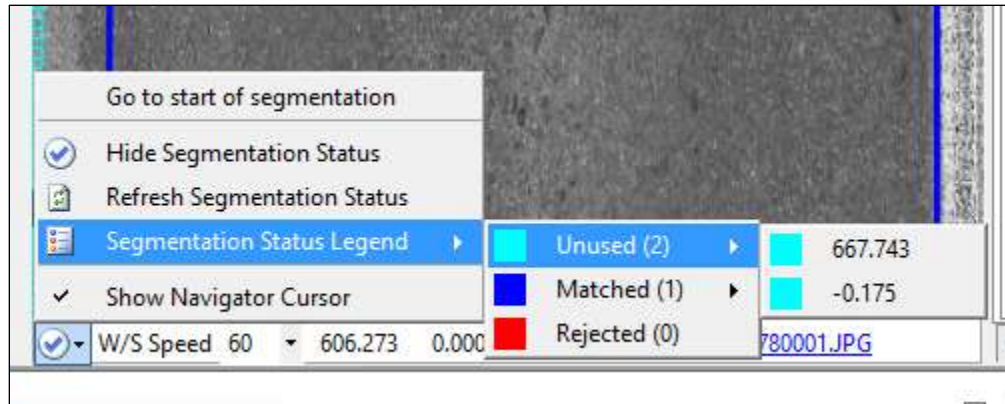
## ***Pavement Image Control***

To scroll image forward or backward, place cursor on the left edge to see the blue arrows. The scroll speed is controlled by placement of the cursor along the left edge. Speed increases as cursor position is further away from the middle zone along the left edge and speed decreases as cursor position is closer to the middle. Placing the cursor in the middle zone or moving it away from the left edge will stop the scrolling.

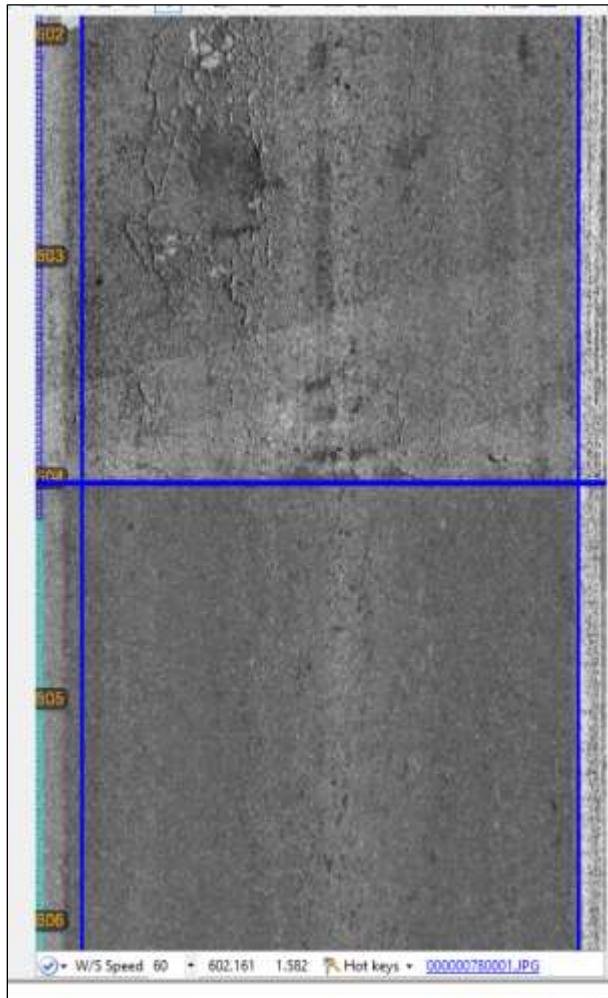


### ***Segmentation Status Check***

Click on the check-mark icon at the bottom left side of the pavement image. From the menu, click on the **Segmentation Status Legend**, which will appear on the left edge of the screen when turned on to indicate whether the current pavement image is segmented:




It will show a navy-blue line for segmented, light blue line for non-segmented, and red for rejected, along the left edge of the pavement image:



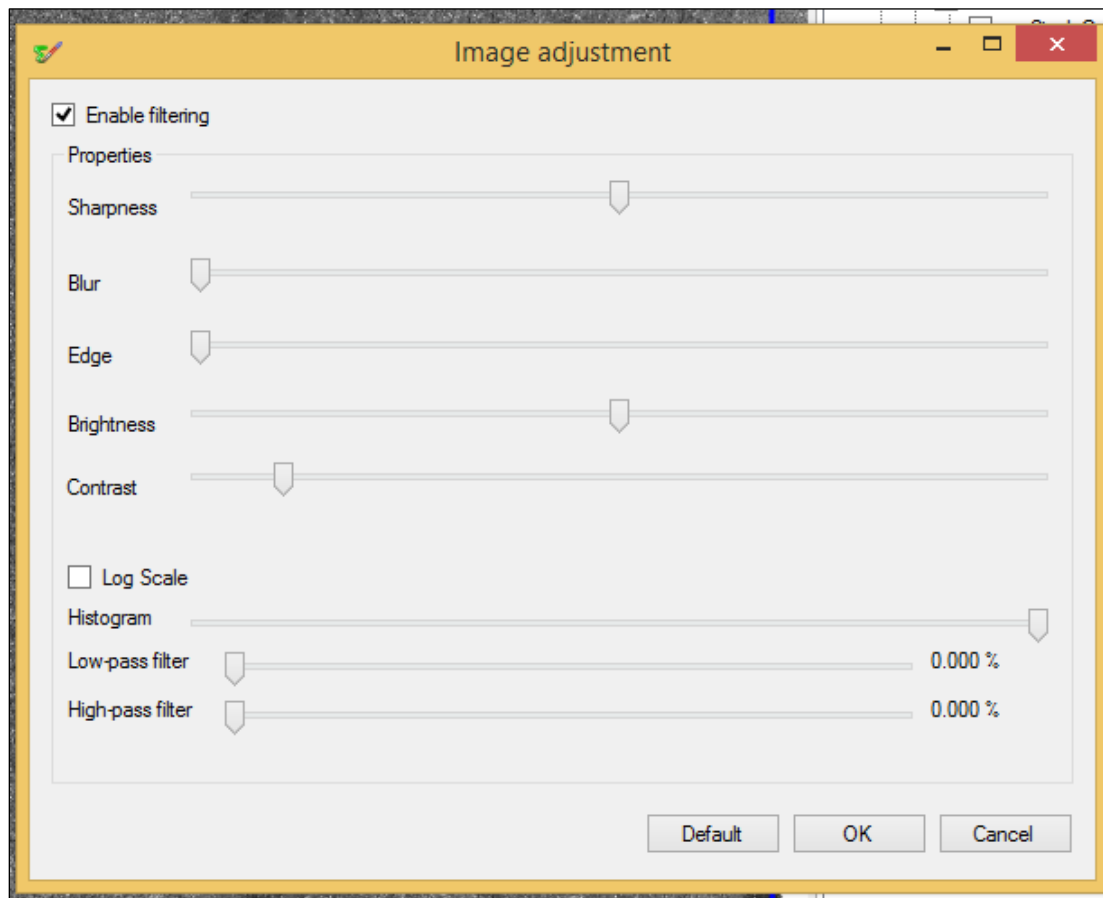
This allows you to differentiate between the different sections, i.e. segmented, non-segmented or rejected. If any part of the image is not segmented, the data processing cannot be saved. Please refer to the section on Segmentation at the end of this Appendix for segmentation instructions.

### ***Pavement Image Adjustment***

You can edit the appearance of pavement imagery to facilitate manual rating of the pavement images. The  button from the top of the pavement image provides an **Image Adjustment** window as in the following screen to edit properties such as sharpness, brightness, and contrast. These modifications will only affect the image



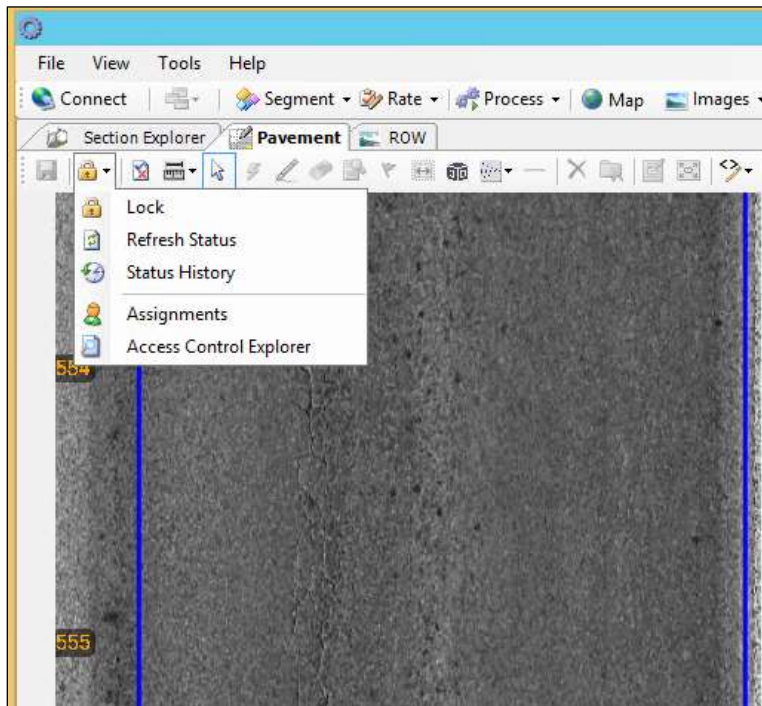
appearance for manual rating, and will not affect the automated distress identification process.



### ***'Lock' Sessions***

Before you can start a manual distress survey on any pavement section, that specific session/section needs to be "locked" under your name. This ensures that only one person at a time can have access to add/edit pavement distresses on that section. As a general rule, automated processes can be executed without locking sessions, but any manual adjustments would require you to lock the session.

Click on the lock icon on the top left side and select **Lock** from the menu to lock that section under your user name.



Select **Assignments** from the menu and you can see a list of assignments for each user and the status of the assignments. If you are the administrator, you can select a user, **Assign** them an activity, **Lock** or **Unlock** the section under their user name, and mark that assignment as **Complete**.

User	Session	Start	End	%	Route	Direction	Lane	Run	Section
mzhou	74101CGW	1.1	2.4	100	SR 44	5	2	Run1	5_1
mzhou	74T0VC2J	3.1	4.7	100	SR 44	5	2	Run1	6_1
mzhou	74T13CH5	-0.1	1.0	101	SR 19	5	1	Run1	7_1
mzhou	74S0VCEV	6.0	5.7	102	SR 24	6	2	Run1	10_1
mzhou	74S19CBA	0.6	-0.2	100	SR 44	6	2	Run1	2_1
mzhou	74T0TCGW	1.1	2.4	100	SR 44	5	2	Run1	5_1
mzhou	74T0VC2J	3.1	4.7	100	SR 44	5	2	Run1	6_1
mzhou	74T13CH5	-0.1	1.0	101	SR 19	5	1	Run1	7_1
mzhou	74S0VCEV	6.0	5.7	102	SR 24	6	2	Run1	10_1
mzhou	74S19CBA	0.6	-0.2	100	SR 44	6	2	Run1	2_1
mzhou	74T0TCGW	1.1	2.4	100	SR 44	5	2	Run1	5_1
mzhou	74T0VC2J	3.1	4.7	100	SR 44	5	2	Run1	6_1
mzhou	74T13CH5	-0.1	1.0	101	SR 19	5	1	Run1	7_1
n.kargah-osta	74T0OCJI	-0.1	0.3	101	SR 44	5	2	Run1	3_1


User	Start	Workstation	Comment
n.kargah-osta	21/02/2019 5:21:16 PM	FRDW-AUS-05	
n.kargah-osta	21/02/2019 5:17:55 PM	FRDW-AUS-05	Please manually rate the distresses for this s
n.kargah-osta	21/02/2019 5:17:07 PM	FRDW-AUS-05	
n.kargah-osta	21/02/2019 5:16:47 PM	FRDW-AUS-05	
n.kargah-osta	21/02/2019 5:16:15 PM	FRDW-AUS-05	cleared lane edges
n.kargah-osta	21/02/2019 5:12:57 PM	FRDW-AUS-05	

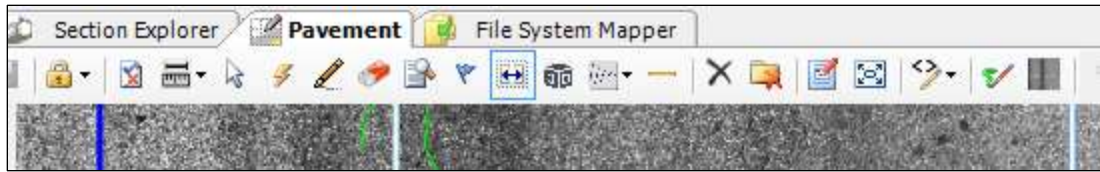
## Manual Rating of Pavement Distress (Semi-Automated Survey)

The available distress types and the corresponding severity levels are preset using the **Distress Schema**. Please refer to the section on Advanced Project Settings in this Appendix for setting up the **Distress Schema** for each **Project**. There are a variety of tools for drawing cracks and distresses on pavement surface.

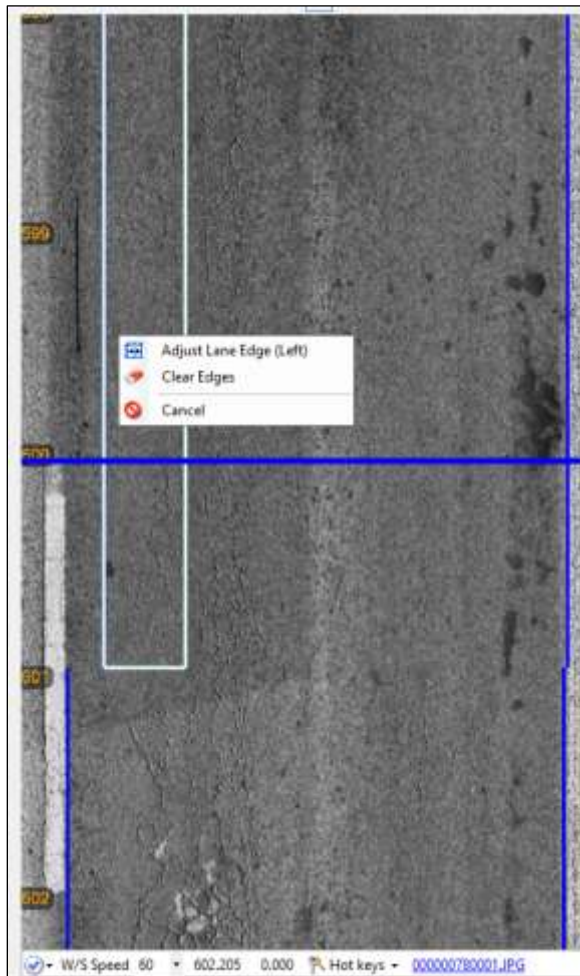
### Adjust Lane Edge

At the first step, you will need to identify the edges of the lane that you would like to


rate. Using this button  you can drag and adjust the lane edges on the left and right. The lane edge adjustment will need to happen at specified intervals or wherever you deem necessary.



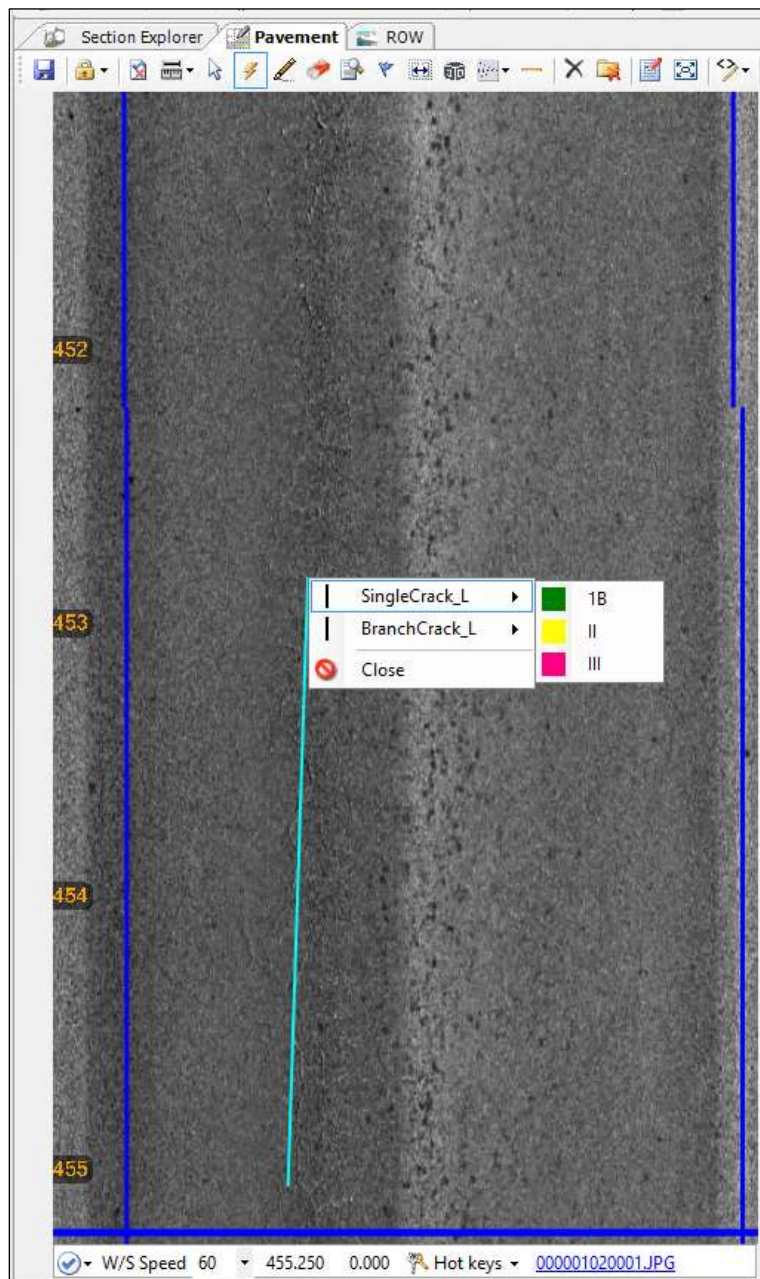
Click on left/right half of the image, left click your mouse and select **Adjust Lane Edge (left/right)**:



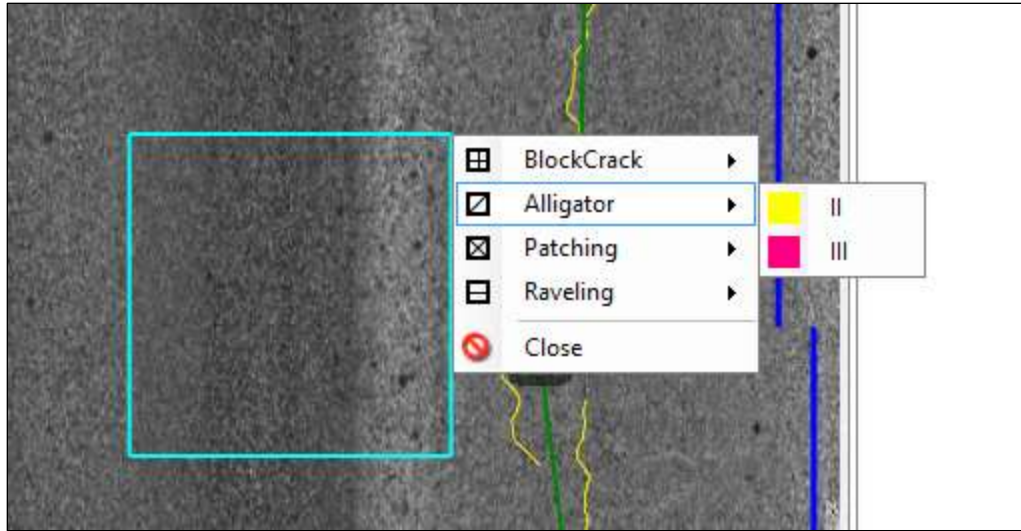
### ***Draw Distresses***

You can use the **Distress** button  on the top to draw distresses. If you would like to identify linear distresses such as spalling, you should left-click the beginning and the end points for the crack, and depending on the angle of the created line (less than or more than 45 degrees), the software will give you options to select from the available distresses. You should also select from the defined list of severity levels. For example,

you can see a longitudinal crack in the following example, which can be a Single or Branch crack:





If you would like to identify an area type distress (fatigue cracking, patching, etc.), then you should left-click and drag to draw a box, and the software will give you the available distress options and severity levels for each. For example, you can see an area distress in the following example, which can be Block Cracking, Alligator Cracking, Patching, or Raveling:

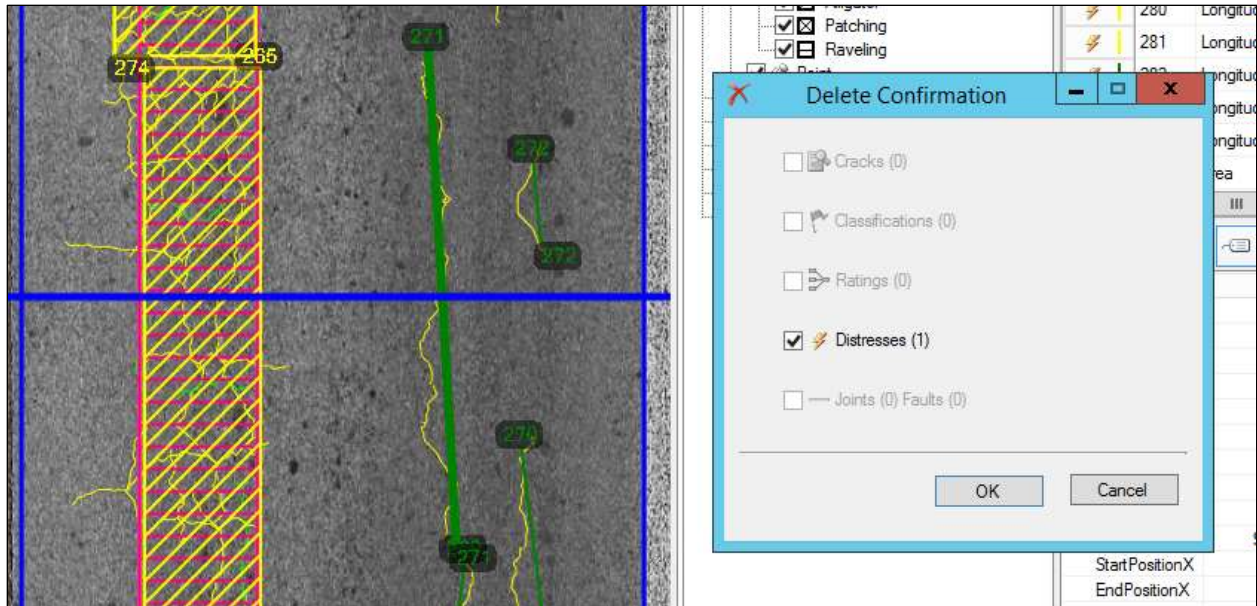


If you would like to identify a point type distress (counting the number of joints with defined condition, or number of shattered slabs), then you should double-click on the pavement image and the software will give you the available distress options and severity levels for each distress type.

### ***Erase Distresses***

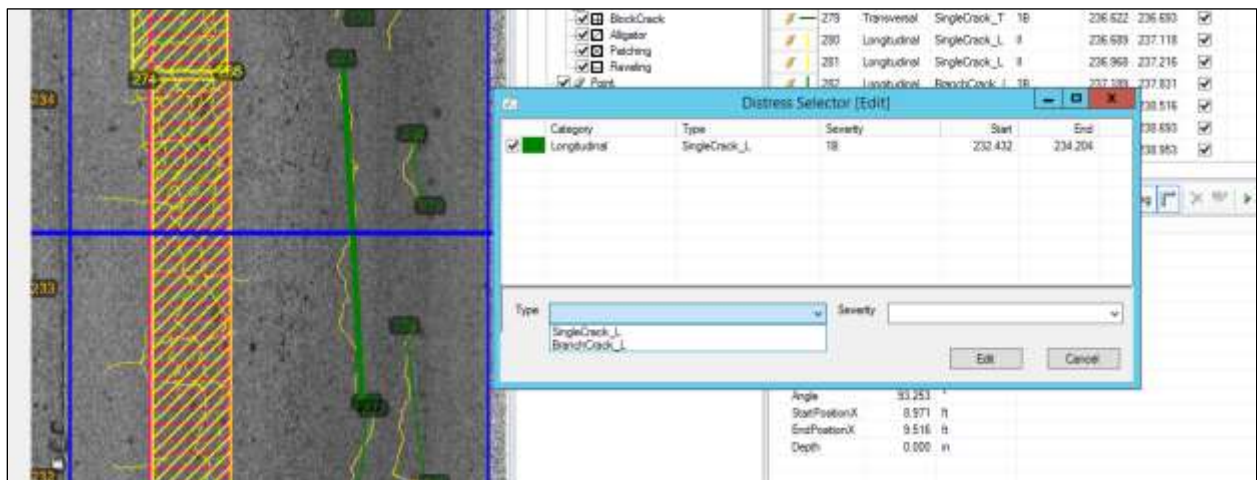
If you would like to erase a distress you can use the **Eraser**  button and you can identify the distresses that you would like to erase. An alternative option would be to use the **Delete**  button for which, the distress needs to be selected before using this button.







### ***Modify Distress Type and Severity Level***

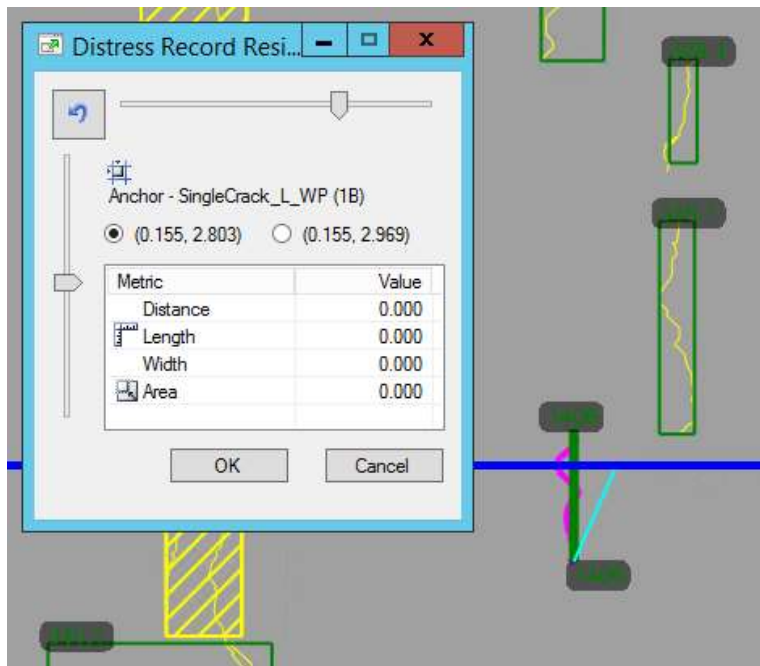
To modify a distress type or severity, you can use the **Modify Distress** button:




### ***Modify Distress Size***

To modify the size of a manually drawn distress, first use the **Select** () button to select the distress and then click the **Resize Distress** button:  In the following example, distress record 1406 is being modified. The coordinates of the bottom of the distress have been selected as the anchor for this resizing. The horizontal and vertical scroll bars help change the length and angle of the selected linear distress. If this was



an area distress, the horizontal and vertical scroll bars would change the dimensions of the selected distress. You cannot modify the size of an automatically identified distress.



### ***Manual Measurements***

If you need to measure distress dimensions to assign appropriate severity levels, you can use the **Measure**  button.

### ***Finish Manual Changes***

If you would like others to be able to see the results of your distress survey, you should save your work with the **Save**  button. Be CAUTIOUS as the **Reload**  button will undo all of the distresses that you have drawn on the pavement image since the last time that you hit the save button. Make sure you **Unlock** the section after you have completed any manual changes.



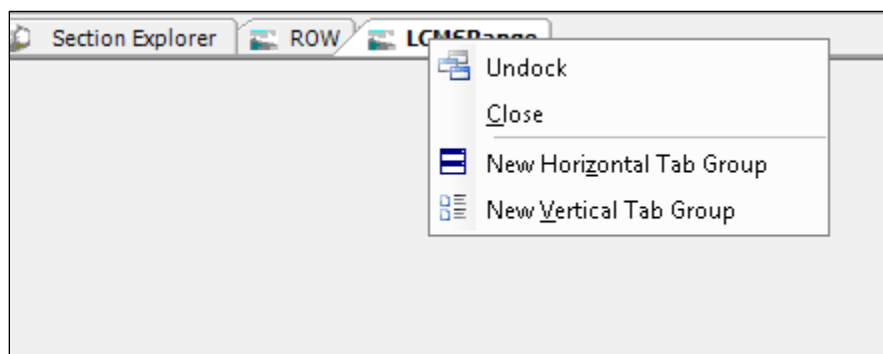
## Recommendations

The following are recommendations for FDOT staff to consider while using the software.

### ***Build Workspace***

It is recommended to build your own work space by using **Dock**, **Undock**, **New Horizontal Tab Group** and **New Vertical Tab Group**. Vision provides you with flexibility when building your workspace. If you are using dual monitors, you may wish to undock your video or your map views and move them to a second monitor.

Undock a Window: To undock a window from its tabbed location, right click on the tab of the window and select **Undock**.

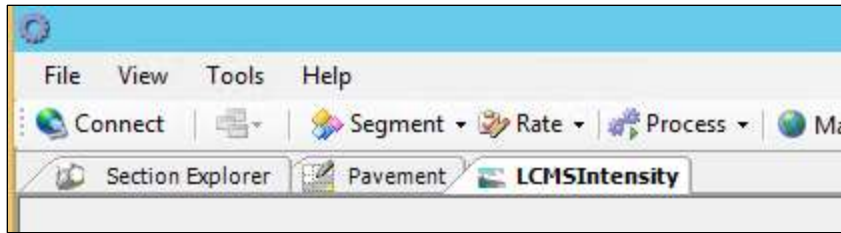


### Dock a Window:

1. To dock a floating window into a tabbed location, click on the **Dock** window icon on the toolbar.

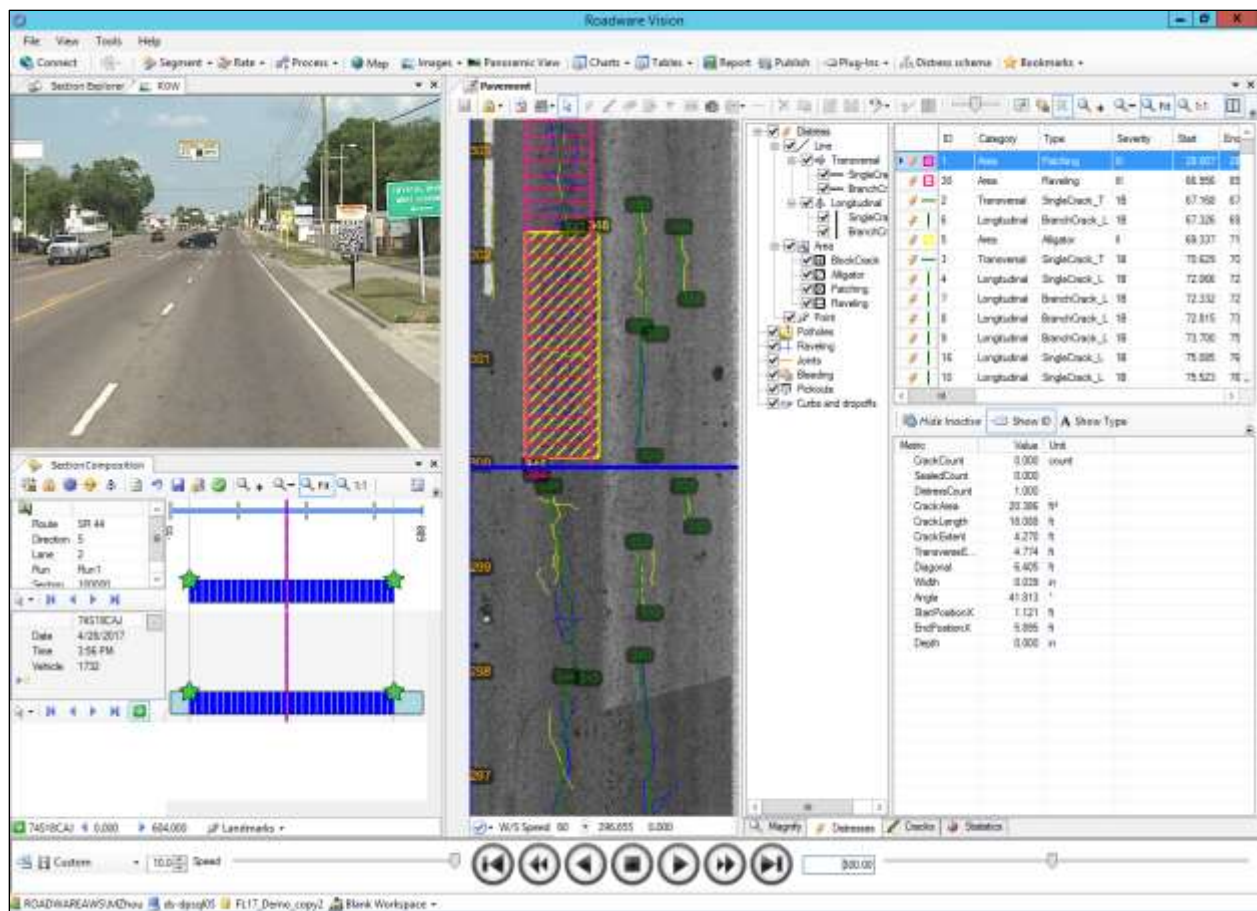


2. From the dropdown list, select the view you wish to dock as a tab in the Vision window.
3. The floating window now becomes a tab in the main Vision window.



Create Split Window: Split Windows provide you with the capability to split your workspace views into frames; providing the advantage of having all of your views in one workspace.

1. Right click on the tab you wish to move into the split window.
2. Select between **New Horizontal Tab Group** or **New Vertical Tab Group**, and the active tab now appears in a split window below or to the right, respectively.
3. Continue to split tabs using either horizontal or vertical splits until you have achieved the views that work for you. Then go to the **File** menu and select **Save Workspace** to save these settings. Next time you open Vision, you can go to the **File** menu and **Select Workspace** to reload the same settings.



### ***Check Segmentation status***

You should check the segmentation status (page 559) frequently to make sure the manual rating is only conducted on pavement images in the segmented sections, which are within the provided mileage range.

### ***Use LCMS Range Image and ROW Image***

It is recommended to use both LCMS range image and ROW image as references for manual quality control of the automated results.

### ***Wheel Path Crack and Non-Wheel Path Crack***

You don't need to differentiate between wheel path crack and non-wheel path crack when conducting the manual rating. The developed SQL code in the 'FDOT Flexible Pavement Rating Results Summary' processor will separate them based on their x coordinates. These x coordinates are affected by the adjusted lane lines and vehicle wander. If lanes are adjusted after distress identification, the summary processor will use the adjusted lanes to identify the wheel path zones. Vehicle wander is always an

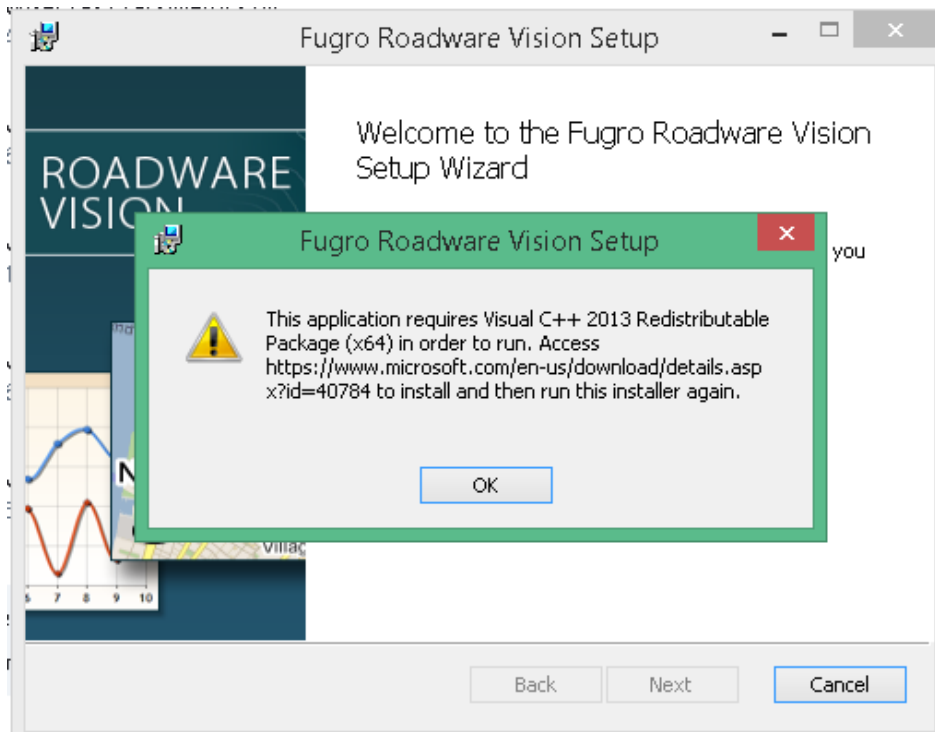
issue and drivers need to do their best to drive in the middle of the lane. However, if there are clear lane markings on the pavement, vehicle wander will not impact the lane detection significantly and thereby the location of the wheel paths would not be impacted either.

### L.3. Installation Instructions for Vision Platform and the FFPDA

0) Uninstall the current Fugro Roadware Vision

1) Install Fugro Roadware Vision 3.1.1 using the provided msi file.

If there is an error regarding C++ (see below), install the vc\_redist\_x64.exe file and then install Vision.



Please note that for the Vision software, you will need to enter the licence key to extend the availability of the software from 30 days to 365 days. Please contact Fugro for a license key if you have not been provided one.

3) Copy the following Roadware.Algorithm.FDOT.Rating.dll file into this folder:

C:\Program Files\Fugro Roadware\Fugro Roadware Vision\



4) Copy the Roadware.Processing.FDOT.FlexibleCrackRating.dll file into this folder:

C:\Program Files\Fugro Roadware\Fugro Roadware Vision\Plugin\Processors\Cracks\

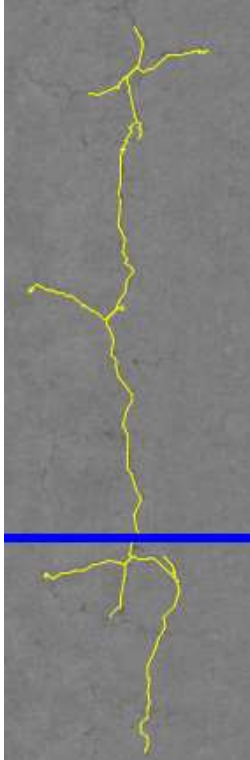
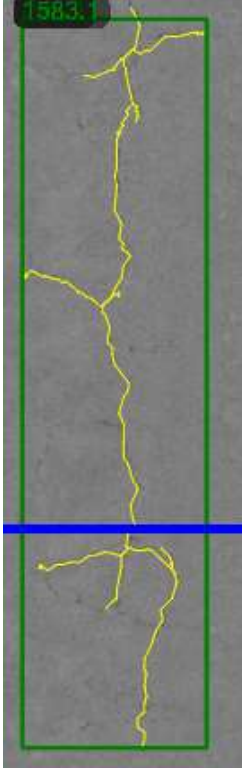
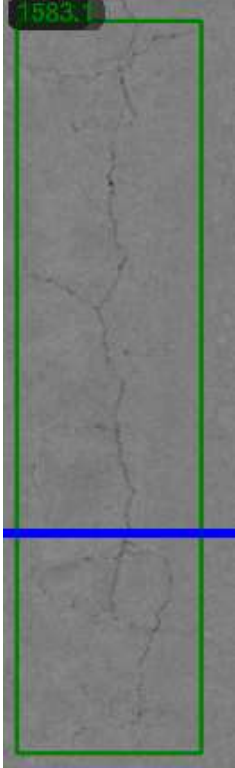


5) Now, run Vision and connect to the following test database to test if everything is working fine:

database name: FDOT\_LRIS\_TEST\_Final

## L.4. The Difference Between Crack and Distress

The following provides a clarification on the Crack and Distress nomenclature in Vision software. Cracks are linear features detected from pavement surface images.

		
Crack	Cracks Rated as Distress	Distress

After classification and rating, type and severity are assigned to cracks. Then the cracks become distresses.

The length of crack is the actual length of the crack lines.

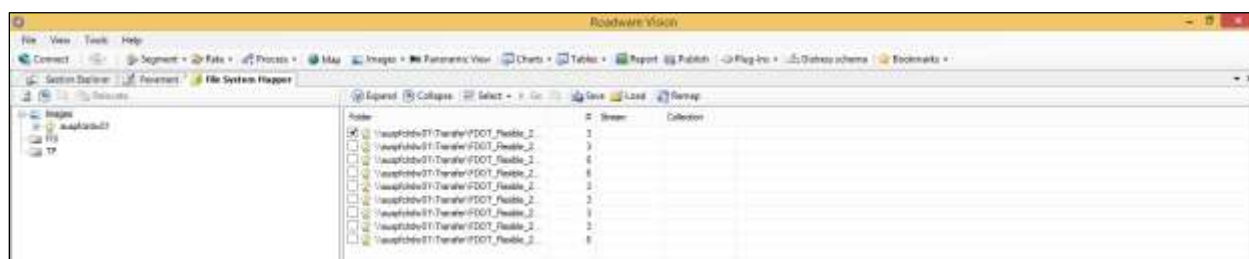
We use diagonal lengths of distress bounding boxes in order to match the semi-automated result and what raters do in reality.

## L.5. Project Advanced Settings

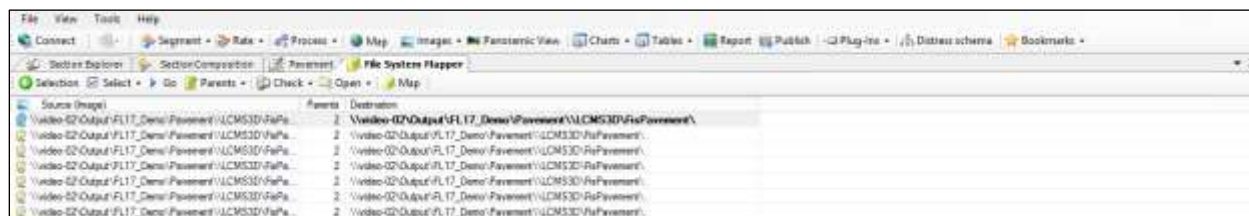
It is recommended that only a professional user (project database owner) would setup these advanced settings on each project. After the professional user conducts these preliminary settings, the parameters will be saved against the corresponding project SQL database. Therefore, any other user who accesses the project will not need to modify these settings.

### Connecting to the Images for the Project (Professional User)

If this is the first time you or any of your colleagues are accessing this database, then you need to make sure that the project contains the correct links to the directory where the corresponding images are stored. This setting would also be required if the project images have been moved to a new location on the server. Go to the File System Mapper under the Tools menu. Select the image type(s) for which you would like to specify a directory and then click on Remap:



Then you will be able to enter a new directory address for those images and click OK. then you will see a list of all the images found. Click on Check >> Destination. If the images exist, the destination addresses will turn bold:

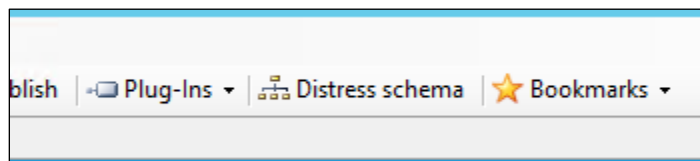


Now you can click on Map and the correct image paths will be restored. Please note that this will update the image paths for this project for all users. Therefore, this needs to be done once, preferably by the administrator of that project and then everyone will be able to see the images. In order for Vision to run faster, it is recommended that the images be stored on the FDOT server.

## Preliminary Adjustments (Professional User)

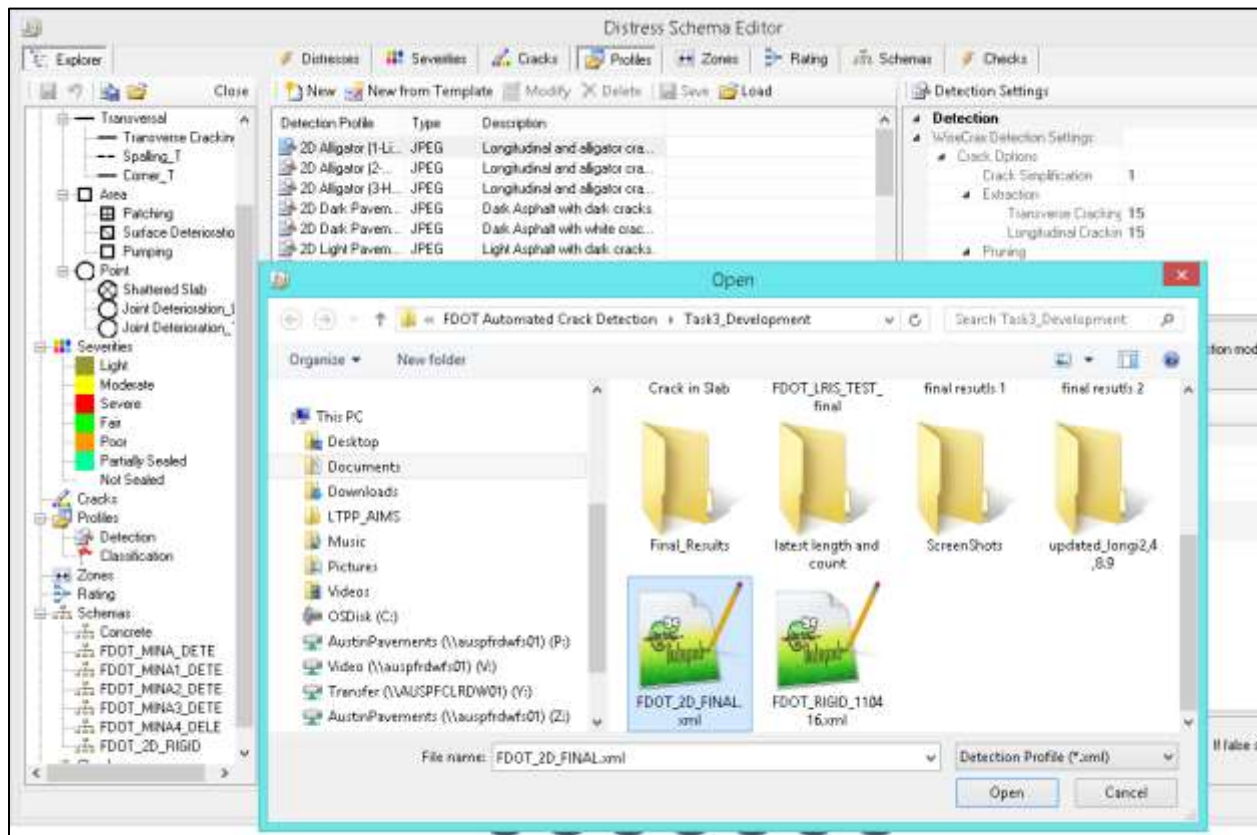
The correct 'Distress Schema' needs to be loaded before running the application. The schema specifies the included distress types and their severities. Fugro engineers create project specific schema that can be saved, emailed, and loaded. If you do not have a distress schema, or if you would like to create one for a specific different project, then you need to use the process for 'Setting Up a Schema,' which is explained at the end of this Appendix. It is recommended that the new users would refrain from creating or modifying distress schema, unless approved by a more professional user. Different profiles will impact the detection results a lot, because each profile contains different parameter settings for the detection process. It is very important that you use the detection profile specifically created for you by a professional user. Once a schema is loaded for a project, other users can access it. Therefore, it is recommended that a professional user loads the schema.

The following screen captures show where the professional user can load a previously saved schema. Click the 'Schema' button to go to the 'Distress Schema Editor'.





Then go to the 'Profiles' tab, and load the schema file from the saved location on your hard drive or server.

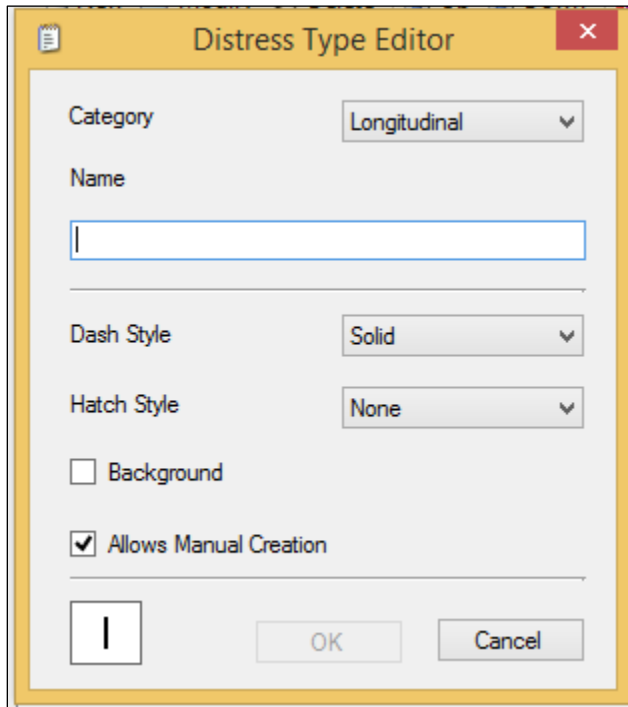


### Distress Schema Setup (Professional User)

Click on the **New** button in the 'Distress Schema Editor' window. Create Distress Types (Distress Name and category listed as follows):

Distress Name	Allows Manual	Category
SingleCrack_L	Yes	Longitudinal
— SingleCrack_T	Yes	Transversal
BranchCrack_L	Yes	Longitudinal
— BranchCrack_T	Yes	Transversal
▣ BlockCrack	Yes	Area
☑ Alligator	Yes	Area
☒ Patching	Yes	Area
▣ Raveling	Yes	Area

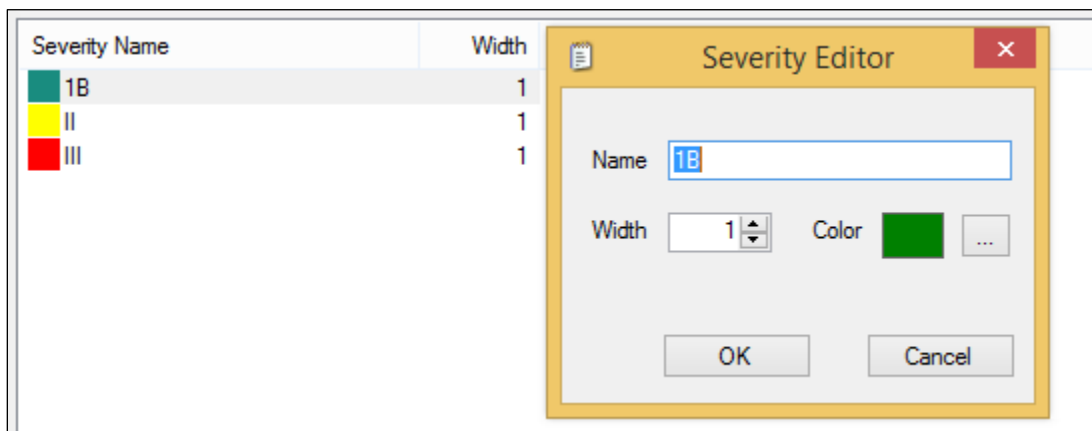
Create distress type by using the Distress Type Editor:



The Distress Type Editor dialog box is shown. It has a title bar with a document icon and a close button. The main area contains the following fields and controls:

- Category: A dropdown menu set to "Longitudinal".
- Name: A text input field containing a single vertical bar character "|".
- Dash Style: A dropdown menu set to "Solid".
- Hatch Style: A dropdown menu set to "None".
- Background: An unchecked checkbox.
- Allows Manual Creation: A checked checkbox.
- Preview: A small square box showing the character "|".
- Buttons: "OK" and "Cancel" buttons at the bottom right.

You can create and/or modify severity levels by using the Severity Editor. The rated crack would be displayed according to severity level.



The Severity Editor dialog box is shown, overlaid on a table of severity levels. The table has two columns: "Severity Name" and "Width".

Severity Name	Width
1B	1
II	1
III	1

The Severity Editor dialog box contains the following fields and controls:

- Name: A text input field containing "1B".
- Width: A spinner box set to "1".
- Color: A color selection area showing a green swatch and a button with three dots.
- Buttons: "OK" and "Cancel" buttons at the bottom.

## **L.6. Segmentation**

Vision software relies on location referencing data provided by roadway owners, also known as Routing data to collect inventory and condition data. Routing data is the list of all the roads to be collected, defined using locators, GPS markers, associated chainages etc. and Routing is the process that prepares that data for collection.

The Routing data is imported twice during the span of data collection to processing, using the 'Routing Importer' tool. First, the Routing data is imported into the ARAN Collection Software (ACS) to inform the truck-operators which roads they need to collect. Second, the Routing data is imported into the processing database for all sorts of data handling using Vision software, including especially the Segmentation process. Vision software accepts a certain format of Routing data to be imported for these purposes.

Segmentation is a combination of multiple processes (match, transfer, order, reject, etc.), which evaluate the Routing expected data, that is linear references, GPS positions, landmarks, etc. and compare them against the collected data.

This assessment can be performed using two concepts: 'rubber-banding' and 're-chaining'. For example, if the Routing data (before collection) suggest that a piece of road is 100 feet and the collected data suggest it is 110 feet, but the owner desires the data to be tagged according to their own system as 100 feet, you can rubber-band the data. On the other hand, if the owner desires to correct their system according to the collected data, then you can re-chain the data. In other words, rubber-banding is used when there is more confidence in the Routing package and re-chaining is used when there is more confidence in the actual collected data than the pre-collection Routing information.

The Section Composition module in addition to a few other modules allow you to perform all of these complex tasks through a simple user interface.

### **Segmentation Workflow**

The steps below are simplified instructions for the segmentation process:

1. Connect to the project database.
2. Review the project-specific location referencing data to get familiar with the sections and their boundaries.

3. Perform auto-matching (See instructions in the remainder of this Appendix for more details) if a standard Routing package is available. NOTE: The Java code developed for this research project for transferring data into a Vision database is already conducting the automated matching and there is no need for a Routing package if this Java code is executed.
4. Manual matching can be used to QC the results of the automated matching. In the 'Section Composition' module, go to each 'session' (section), QC the matching results and if any corrections are needed, perform the manual matching steps explained below.
5. 'Save', 'Check-In', and 'Complete' to submit your segmentation work.

The following will focus on details in steps 4 and 5 of the above workflow.

## Manual Matching

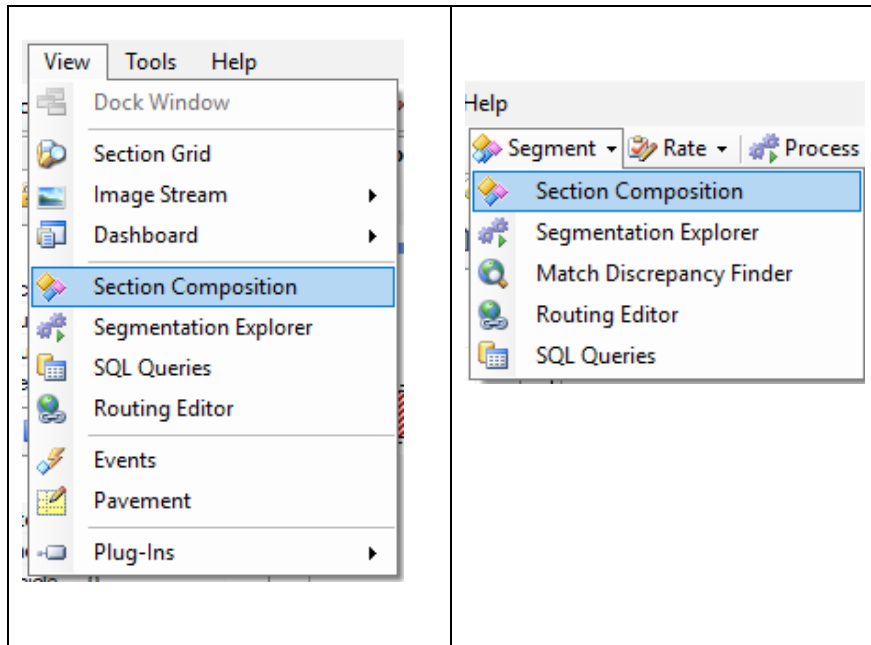
The following will start with the introduction of the Section Composition View to help you get familiar with this interface. Then the procedure of performing manual matching in Section Composition is explained.

## Section Composition View

The Section Composition View presents a linear representation of all the sections that have been collected, and allows you to match the collected data with the routed data through automatic or manual matching. To perform matching, the Section Composition view is used along with the Map View, Image Stream and the Web Map.

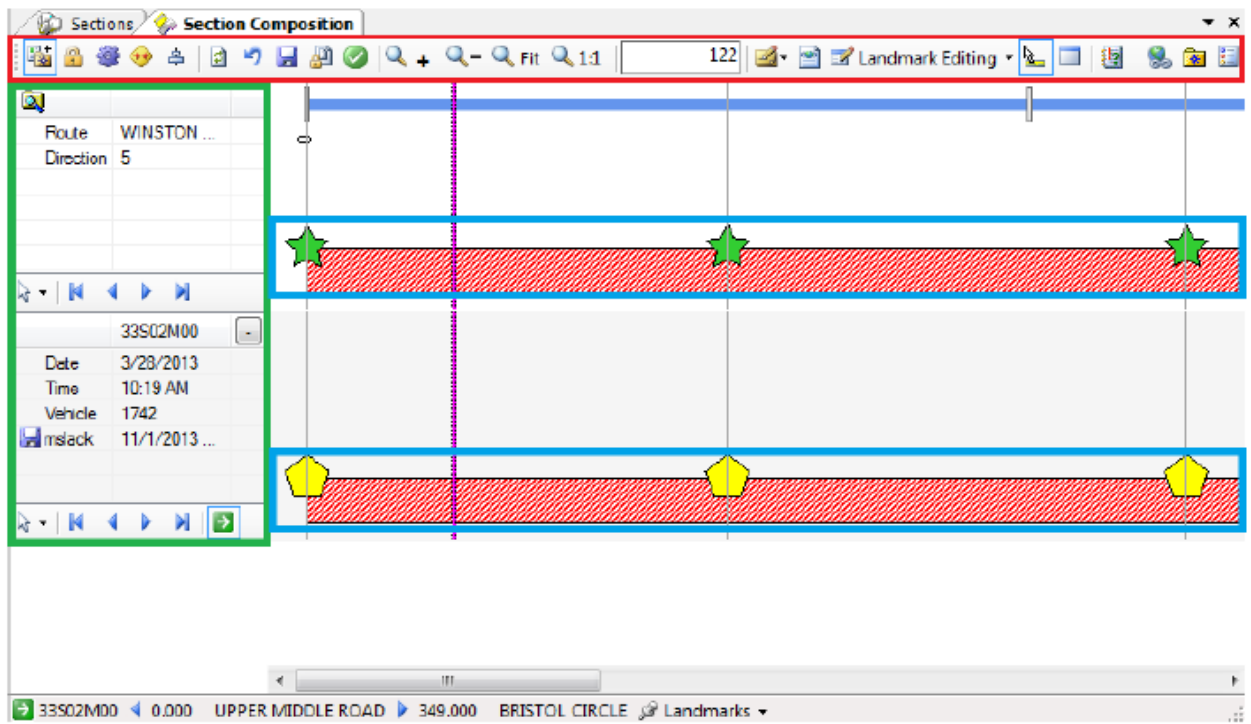
To launch the Section Composition View, click on View drop down menu and select Section Composition or select it from the Segment drop down menu.

Section Composition in View Menu	Section Composition in the Segment drop down menu.
----------------------------------	----------------------------------------------------



There are three main components in the Section Composition as shown in the figure below: two bars (highlighted in blue), a tool bar on the top (highlighted in red) and two tables on the left hand side (highlighted in green).

The tool bar on top provides general tools that will be discussed in this Appendix and it also shows the length of the matched section in the white box. Of the two bars highlighted in blue in the following picture, the top bar shows the routed section and the bottom bar shows the collected section.




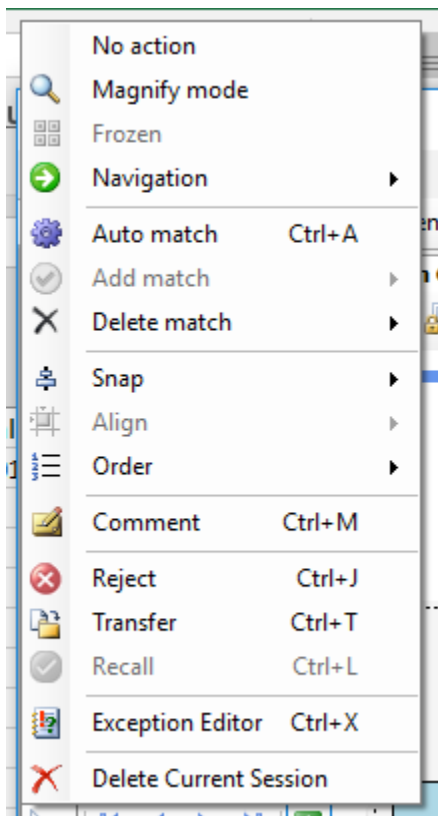
Located at the top left, the Section table provides locator information and the associated values. Located below the Section table, the Session table provides information about the session, such as Time, Date, Collection Vehicle, and current user.


Section table	Session table

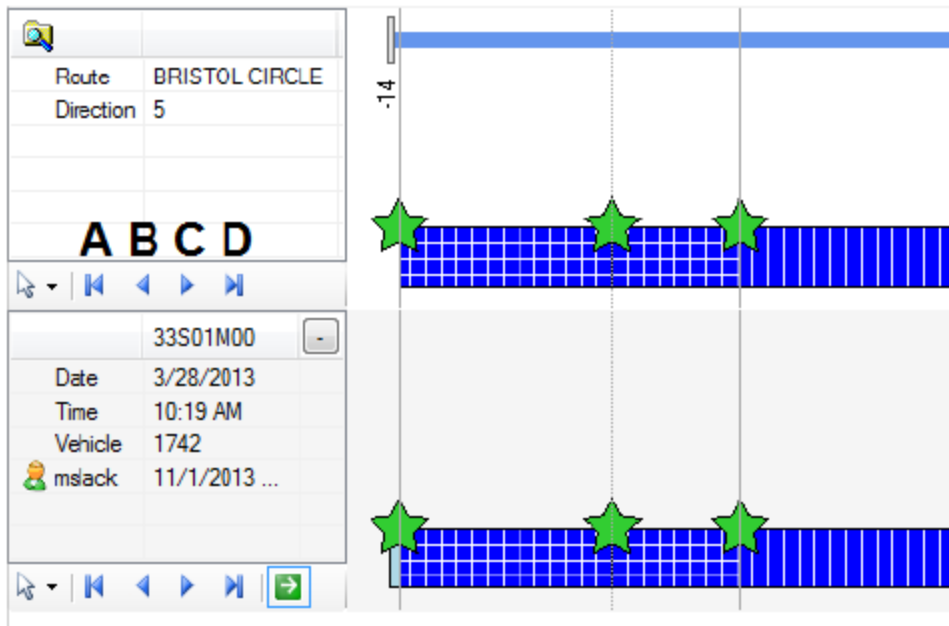
Navigation Tool bar: Below the Section and Session tables is a Navigation Tool bar.



Action drop down list: The cursor icon in Navigation Tool bar (see  above) opens the actions drop down list. For instructions on how to use these actions, see the remainder of this Appendix.




Following the first cursor icon (  ), there are four pointers, A, B, C and D.



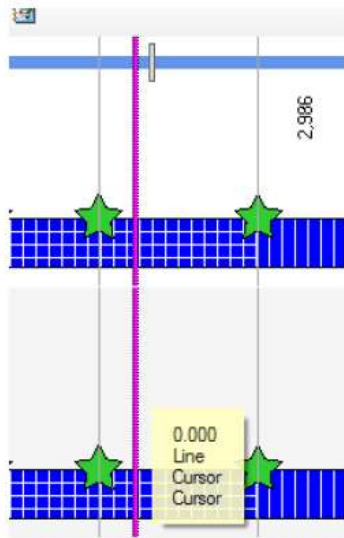
The table below explains functions of these four pointers.

Icon	Description
First pointer (A)	Jump to the beginning chainage
Previous pointer (B)	Navigate to previous landmark
Next pointer (C)	Navigate to next landmark
Last pointer (D)	Jump to the end chainage

Go: If there are multiple collected segments in one session (typically this happens because collection was started ahead of the intended section and/or ended after the end of the intended section), this button () selects one of the segments in the Section Composition view.

Cursor: Use the pink cursor shown below to navigate to different positions along the Section Composition View. The cursor is useful as a visual aid to help line up the nodes when performing manual matches or making adjustments.





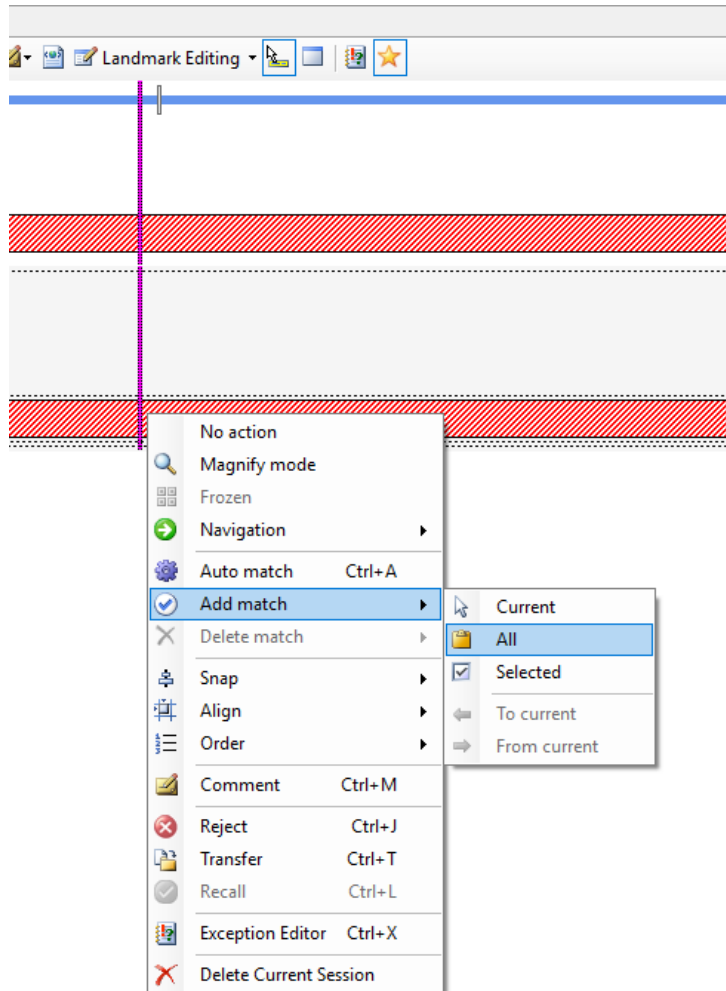
Click and drag the cursor to the desired location. All views, including the Map View, Image Stream and the Web Map will reflect the new location.

### **Perform Manual Matching**

Performing manual matching in the Section Composition includes two steps:

1. Open the Section Composition view.
2. Right click on the collected session (the bottom bar), click 'Add Match' and select the 'All' option.

The option to Add Match will be available if the segment is not already matched. If the segment has already been matched, the option for Add Match will be greyed out and the option to Delete Match will be available.



The Match Editor will open (as shown below).

**Match Editor**

**Match coverage**

☒ Complete ☐ Partial

**Chainage adjustment**

☒ Rubber-band ☐ Re-chain

**Direction**

☒ Forward ☐ Backward

☒ Propagate re-chaining

☐ Split landmarks with same chainage

**Anchor**

☒ Begin ☐ End

**Comments**

☐ Other

**Summary**

← Begin	12,899	Matched to routed data	
→ End	12,819	Matched to routed data	
Routed len...	79	Given by the routed length	
Actual len...	79	Given by the collected length	
<input checked="" type="checkbox"/> Length %	100	Exact match	
Difference	0	Expected length achieved	

**Range visualizer**

☐ Begin  End ☐

OK Cancel

3. Select how to adjust the chainage, i.e rubber-band or re-chain, depending on the project protocol.

Note: Rubber-band will match the beginning and end chainages of the collected data to the routed data, while re-chain will modify the routed landmark's start or end chainage based on the collected data, depending on the direction of propagation.

4. Insert a comment into the Comments box.
5. Click on OK to add match.

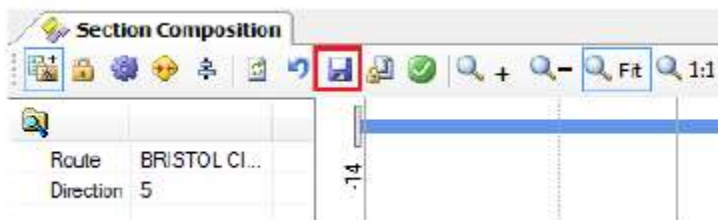
### **Save, Check-In and Complete**

After segmenting is complete, it needs to be saved and marked completed.

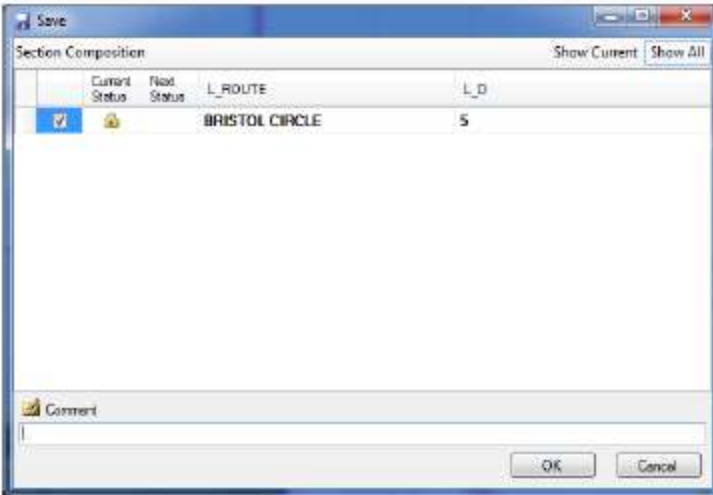
#### ***'Save' Segmentation Work***

Saving is required to protect what you have accomplished thus far for a particular section from getting lost. Saving will still leave a section checked out to the initial user that checked out the file or had it assigned to them initially.

1. Click on the 'Save' icon from the upper tool-bar in Section Composition view:



The following window appears:



2. Insert a Comment into the comment box (OPTIONAL).
3. Click on OK.

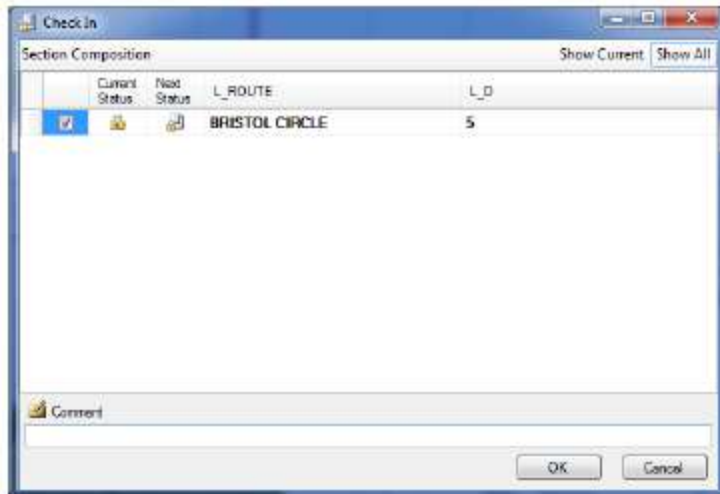
### ***'Check-In'***

Once a section is partially or fully segmented, you can 'Check-In' the file. This task unlocks the file so that other users may 'Check-out' the section and perform more segmenting adjustments on that particular file. The process of checking in a file also saves a file, and unlocks it for other users to access. The process of checking files in and out is implemented so that there is no conflict if two users try to access the same file at the same time.

1. Click on the 'Check-In' icon from the upper tool-bar in Section Composition view:



The following window appears:



2. Insert a Comment into the comment box (OPTIONAL).
3. Click on OK.

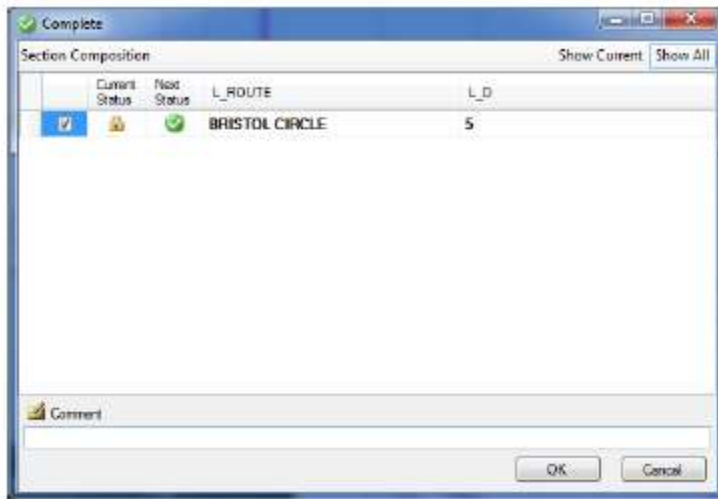
### ***'Complete'***

The last option is to 'Complete' a file. Marking a file as complete, checks-in and saves and also marks the file with a green check mark. This is beneficial to users when they are trying to figure out when a file has been fully segmented to the point of completion.

1. Click on the 'Complete' icon from the upper tool-bar in Section Composition view:



The following window appears:



2. Insert a Comment into the comment box (OPTIONAL).
3. Click on OK.

### **Automatic Matching (PROFESSIONAL USER)**

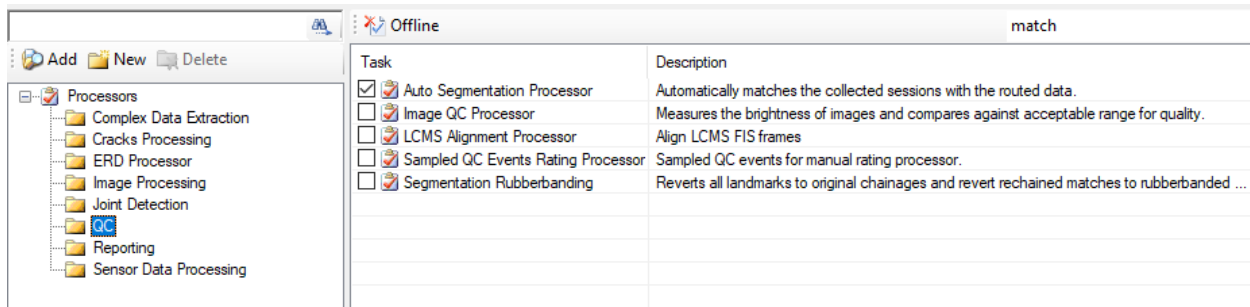
The Java code developed for this research project for transferring data into a Vision database is already conducting the automated matching. If there is a Routing package developed for a project in the Vision format, then the instructions in this Appendix can be used to conduct auto-matching of collected data to the Routing package.

With Fugro Vision 3.1.1, you have the option to perform auto-matching via either one of the following methods:

1. Perform auto matching on several sessions at once using a Batch Processor called 'Auto Segmentation Processor'.
2. Perform auto matching on each session/section using the Section Composition

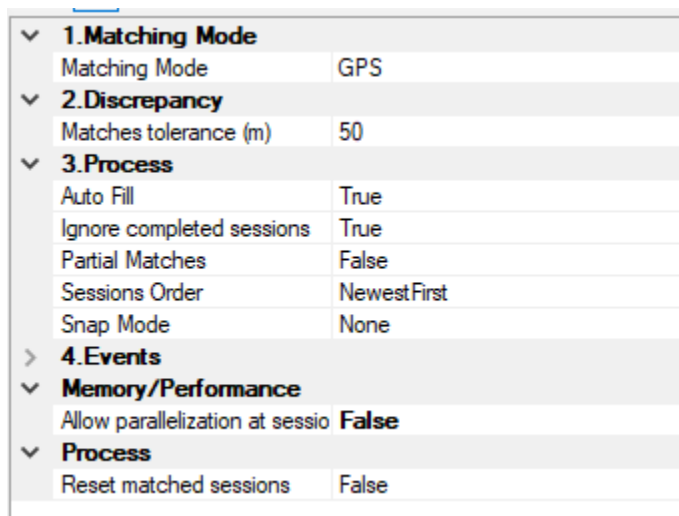
#### ***Perform Auto Matching in the Batch Processor***

Automated Matching can be completed using 'Auto Segmentation Processor'.



## Options

There are six groups of options for Auto Segmentation Processor.



### 1. Matching Mode:

Auto-matching mode based on GPS or on Events

### 2. Discrepancy

Matches tolerance (m): Tolerance threshold which will be used to discard matches that are further away from the landmarks than the specified value

### 3. Process



- a) Auto Fill: If set to true, the unmatched fragments between matches within the same collection/session will be distributed evenly to fill the gaps
  - b) Ignore completed sessions: If set to true, the sections that belong to sessions marked as Complete will be ignored.
  - c) Partial Matches: If set to true, partial matches will be created. Otherwise only full segment matches will be created and if a segment cannot be filled, it will be left unmatched.
  - d) Sessions Order: Select the order in which the available fragments from sessions will be processed.
  - e) Snap mode: designated how nodes are matched. Snap matches begin and ends to the closest position within the data stream (images, station data) that was selected, if one was selected. Otherwise, it will just snap the match based on GPS.
4. Events: This option has been disabled since Vision 3.1.1 to avoid confusion. Please ignore.

## 5. Memory/Performance

If set to true, whole sessions are processed in parallel. If false, some processors split each session and process parts of it in parallel.

## 6. Process

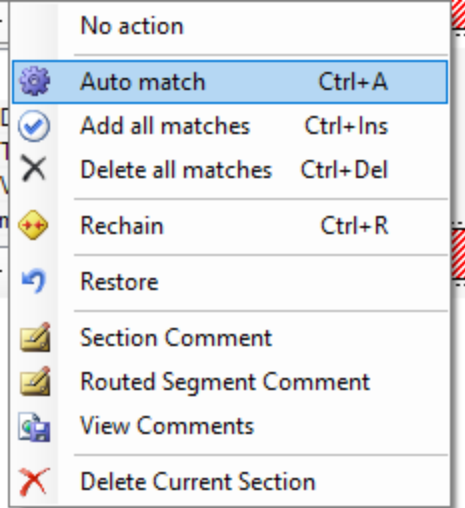
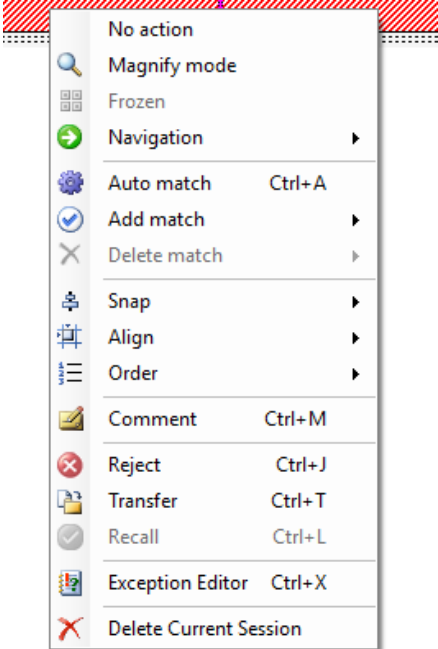
If set to true, matches for the sessions will be deleted before doing auto segmenting.

### ***Perform Auto Matching in the Section Composition***

Automatic matching within the Composition can be done on a section by section basis or on a per session basis.

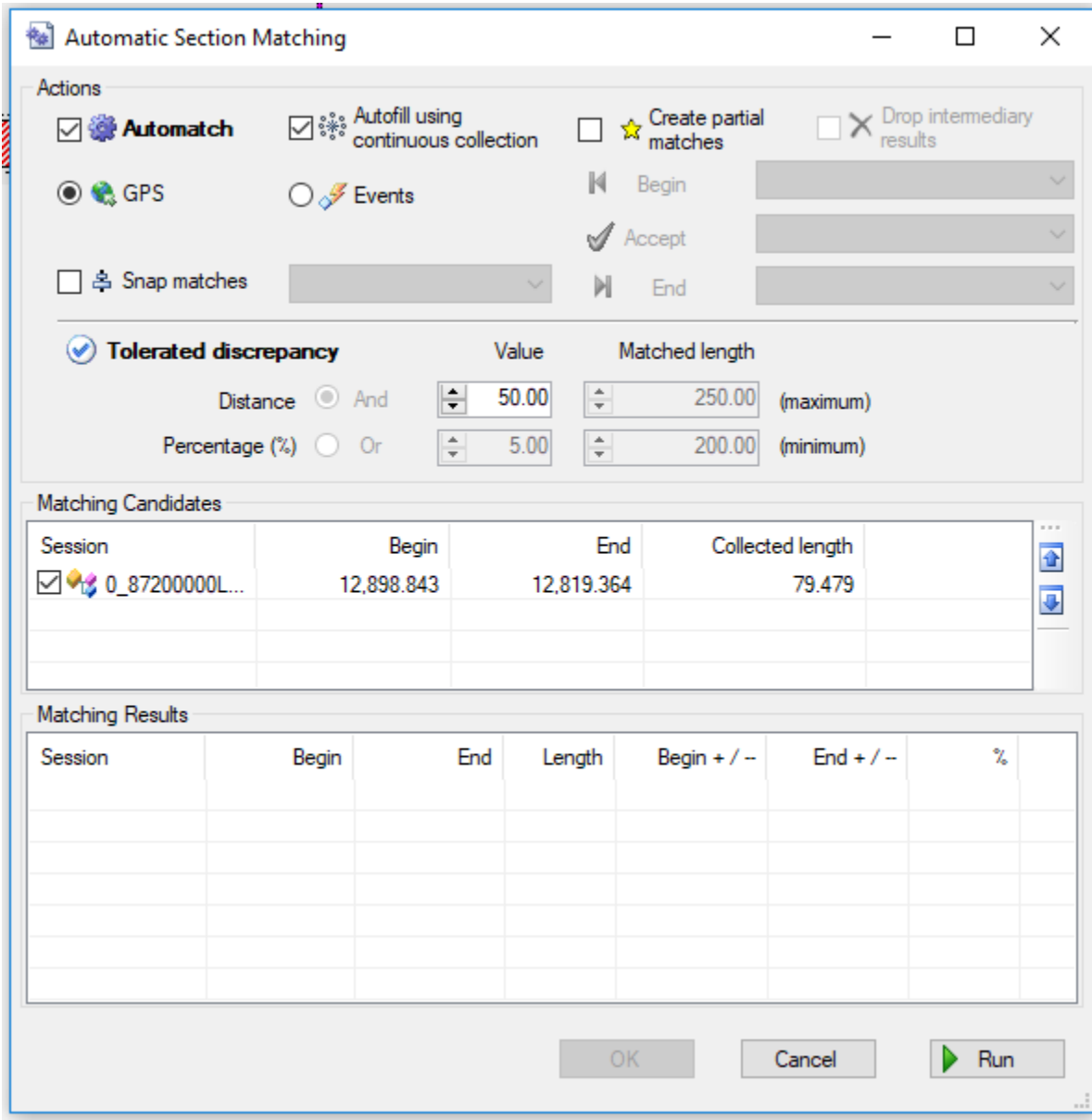
1. Check out the section you wish to segment by clicking the lock icon on the Section Composition toolbar.

2. The two different methods to perform Auto matching as mentioned, include performing the task on a section level or on a session by session basis as shown in the table below. If performing on a section level, right click on the top routing bar and select Auto match. If performing on a per session level, right click on the bar corresponding to the session you want to match, and the menu will display.

Section Action Menu	Session Action Menu
	

3. The Automatic Section Matching dialog box appears.

NOTE: If you have not checked out the file; the section composition checkout dialog box appears. You can then check the file out and right click on the file again and select auto match.



The dialog box is titled "Automatic Section Matching". It contains several sections for configuring the matching process.

**Actions**

- ☒ **Automatch**
- ☒ Autofill using continuous collection
- ☐ Create partial matches
- ☐ Drop intermediary results
- ☒ GPS
- ☐ Events
- ☐ Snap matches
- Buttons: Begin, Accept, End

**Tolerated discrepancy**

Distance ☒ And Value: 50.00 Matched length: 250.00 (maximum)

Percentage (%) ☐ Or Value: 5.00 Matched length: 200.00 (minimum)

**Matching Candidates**

Session	Begin	End	Collected length
<input checked="" type="checkbox"/> 0_87200000L...	12,898.843	12,819.364	79.479

**Matching Results**

Session	Begin	End	Length	Begin + / -	End + / -	%

Buttons: OK, Cancel, Run

4. Make your desired selections within this dialog box and click Run.

### ***Auto Matching Parameter Descriptions***

The table below provides descriptions for the parameters in the Automatic Section Matching dialog box.

Parameter	Description
Auto matching using GPS	Match customer data to collected data based on GPS location
Auto matching using Events	Match customer data to collected data based on ARAN Events set.
Autofill Using Continuous Collection	Assumes ARAN travels from point A to point B and if GPS or Event matches cannot be made, length of data will be resolved equally across segments unable to be matched.
Tolerated discrepancy Data	Data will be matched using the nearest GPS points within the tolerance set by this parameter.
Matching Candidates	A list of sessions that can be selected to match using the parameters that were selected.

### ***Unmatch the Automatic Matching for the Entire Section***

1. Select the section you wish to Unmatch
2. From the section tool menu, select the X icon (Delete All Matches).
3. The section will revert back to being completely unmatched.

### **Other Segmentation Tasks (PROFESSIONAL USER)**

Besides matching, segmenting involves other functionalities such as the following:

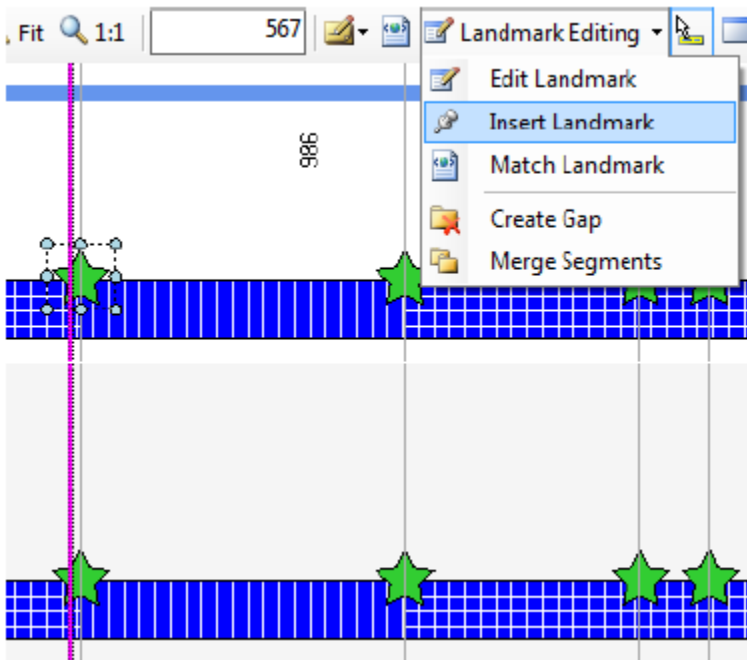
#### ***Landmark Editing***

In certain scenarios, landmarks need to be edited to meet customer requirements or to provide feedback to customers.

Insert Landmark: Inserts a new landmark into a selected section.

1. Click on the exact chainage where the landmark needs to be inserted,

2. Click on Landmark Editing > Insert Landmark.



The following window appears. If the pink bar is at the beginning of the section and you want to Insert Landmark, then automatically the Extend option is selected. If the pink bar is at the middle of the matched section, then automatically, the Split option is selected.

**Insert Landmark**

☒ Split ☐ Fill ☐ Extend ☐ Back ☐ Forward

Chainage  366.000 -> 586.000

Event type

Description

Node

☒ None

☐ Vehicle position at original chainage (567.000)

☐ Position of selected bookmark:

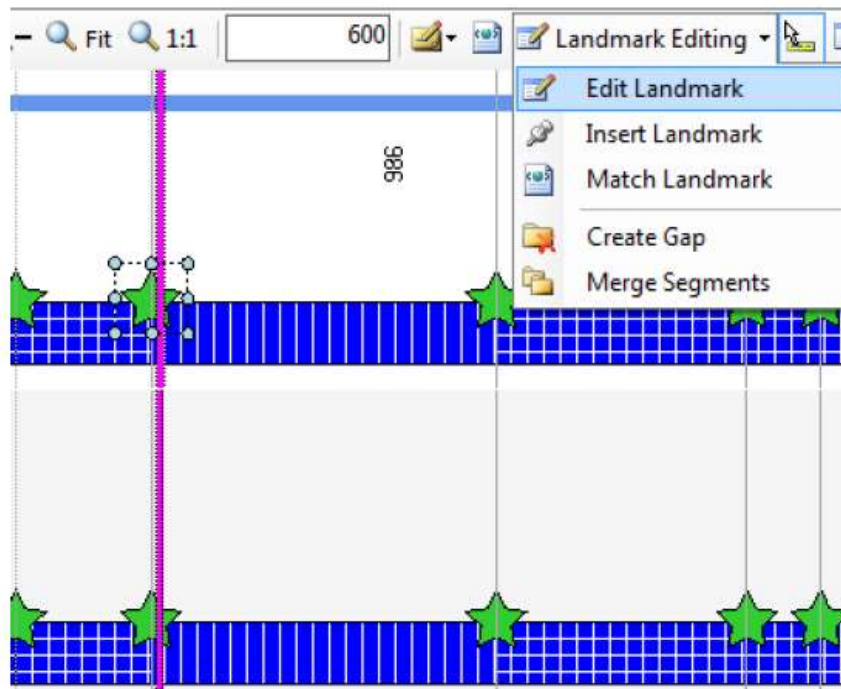
#		

OK Cancel

- Verify the chainage or enter a new value (highlighted in red)
- Enter an Event type and Description (highlighted in blue)
- Click on OK

Edit Landmark: Changes the position, event type, description etc. of current landmarks.

Select the landmark to be edited and click on Landmark Editing >Edit Landmark from the upper tool-bar in Section Composition.



The following window appears:

Original Current

Chainage 586.000 586.000

Event type

Description LONDON LANE

Rechaining effect within current section

☐ None (rechain only current landmark)

☒ Propagate forward (rechain next landmarks within section)

☐ Propagate backward (rechain previous landmarks within section)

☐ Propagate forward and backward (rechain whole section)

OK Cancel

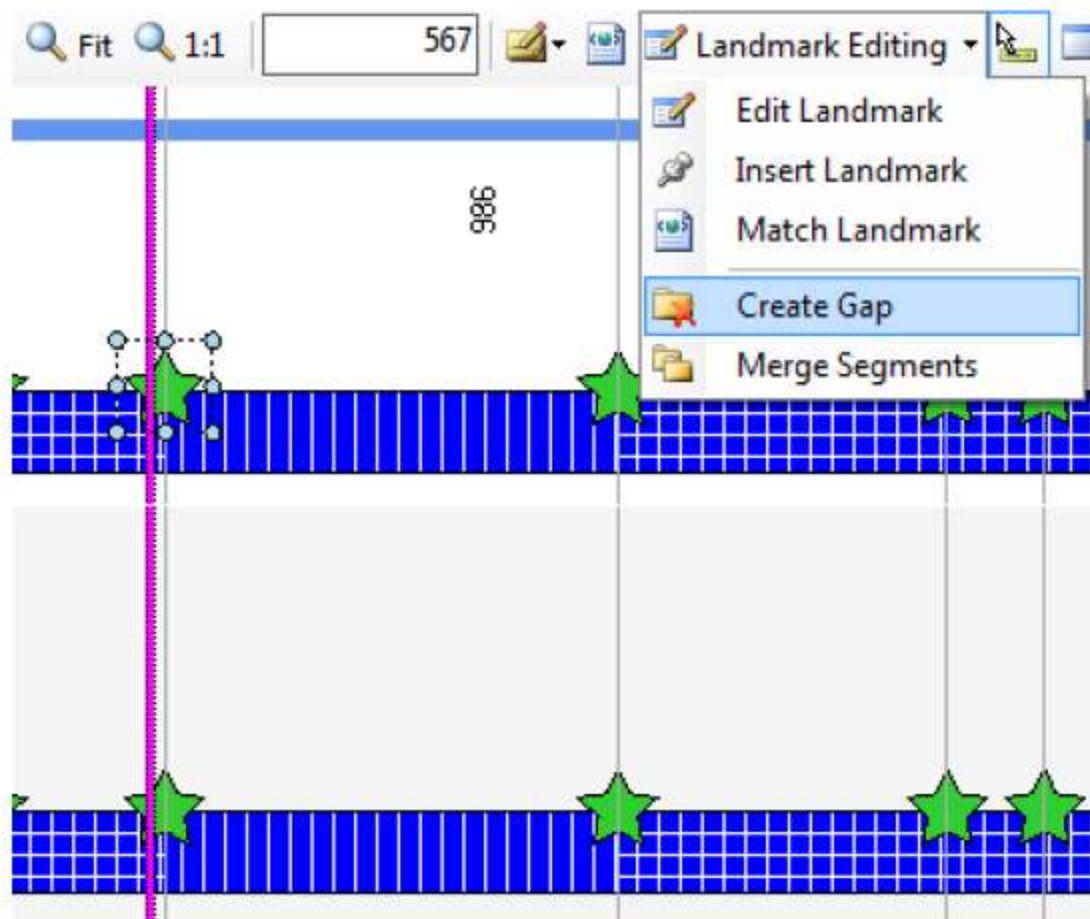
- Select the chainage to where the landmark needs to be moved (highlighted in red)
- Change the Event type and Description (highlighted in blue) if necessary
- Select the rechaining effect (highlighted in green), i.e either to propagate forward or backward etc.
- Click on OK

### **Create Gap**

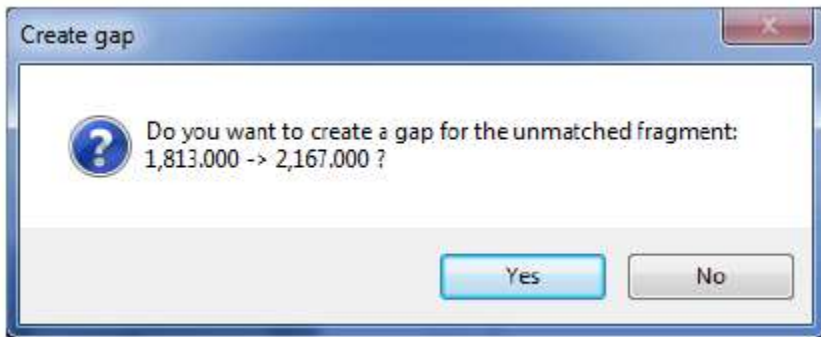
Creates gaps between landmarks.

Click the area between which two landmarks the gap needs to be created, and then click on Landmark Editing >Create gaps





The following window will appear:

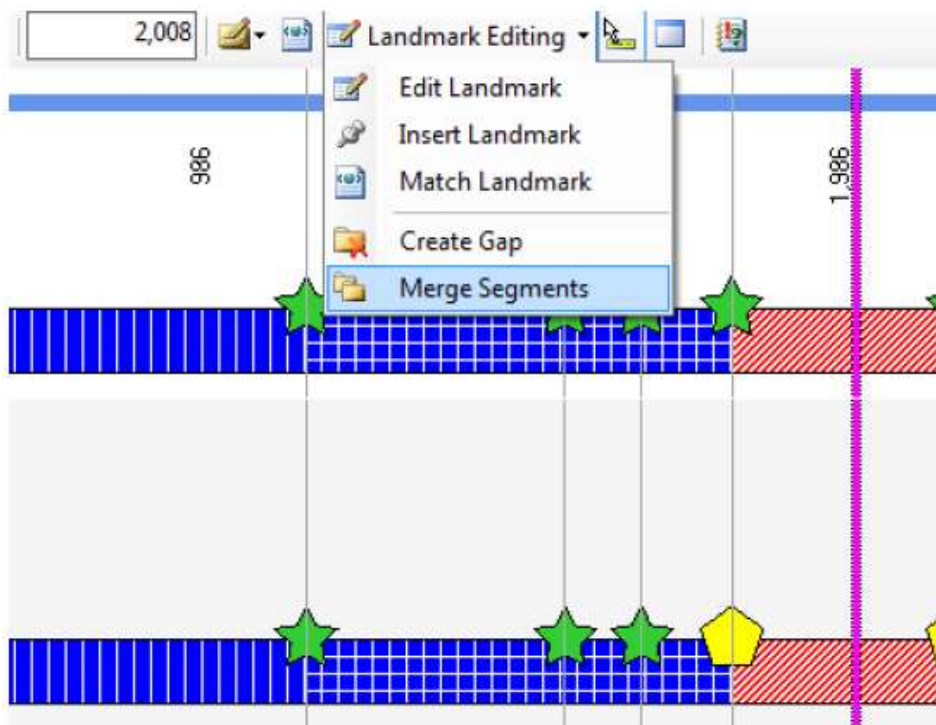


- Verify the chainage lengths and click on Yes.

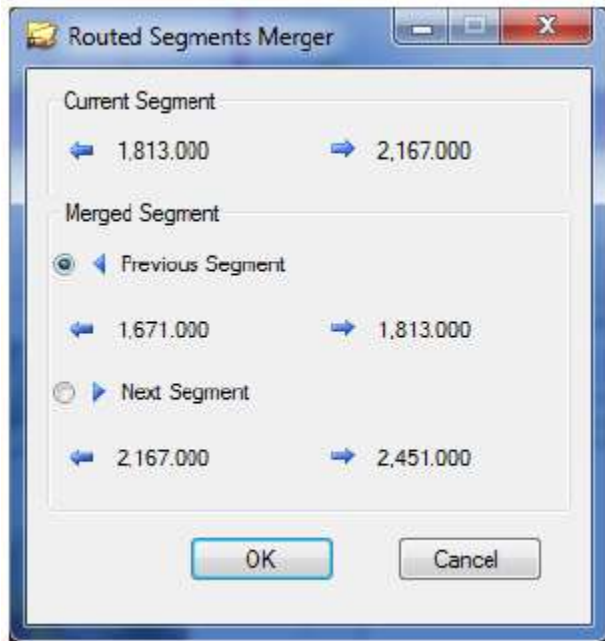
### ***Merge Segments***

Merges two segments by removing the landmarks between them.

Select the segment which needs to be merged and click on Landmark Editing > Merge Segments



The following window will appear:

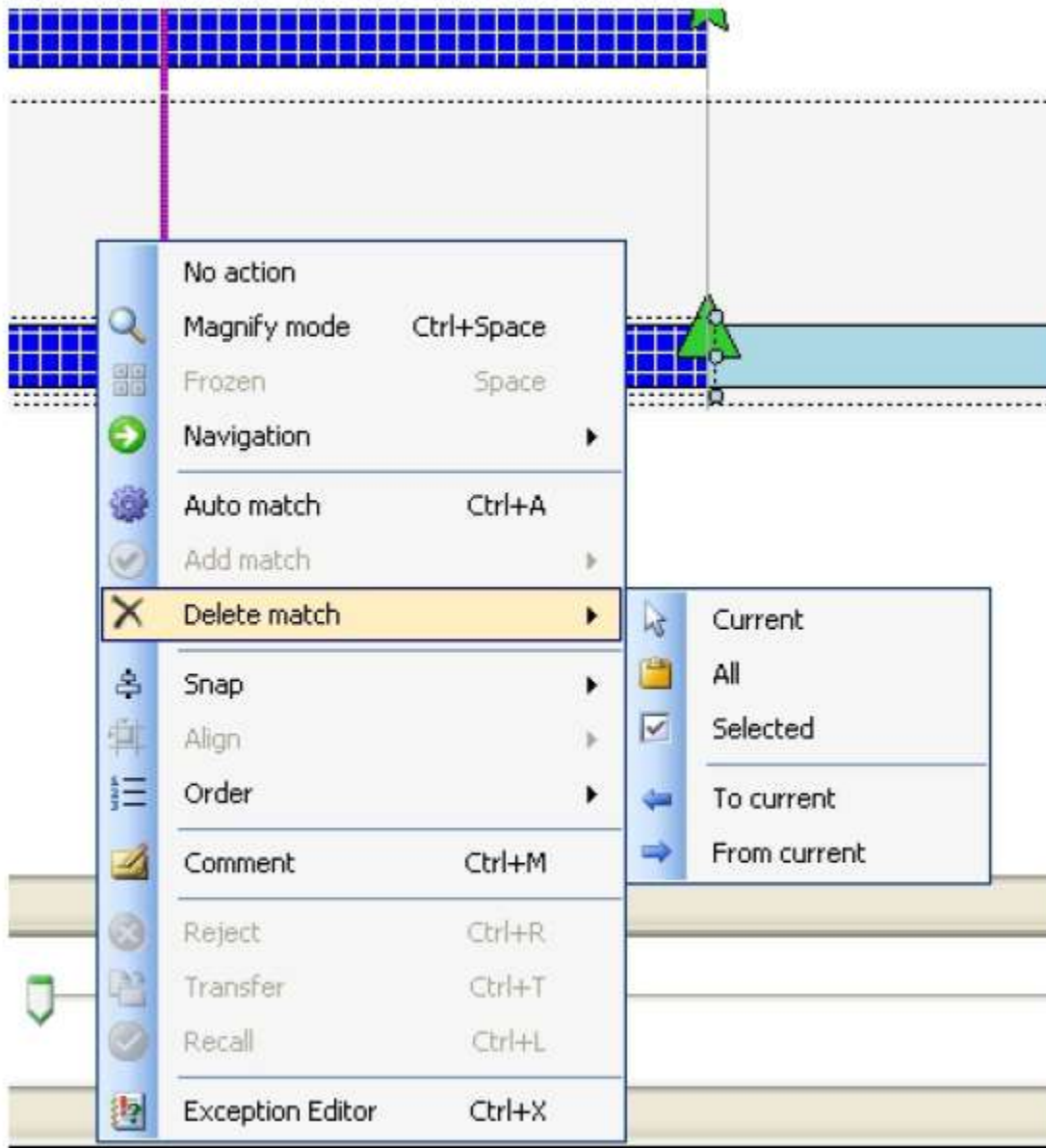


Choose the segment to merge (highlighted in red) and click on OK.

### ***Delete match***

Auto-matching is not always accurate and to perform certain tasks such as align, transfer and reject, the match needs to be deleted and then re-matched.

1. To delete a match, right-click on the matched, collected section



2. To delete all matches, click Delete Match >All.
3. To delete the current match from the section, i.e the portion between the two landmarks,

click Delete Match >Current

4. To delete a selected matched portion from the section, select a portion of the section and

click Delete Match >Selected.

### ***Align***

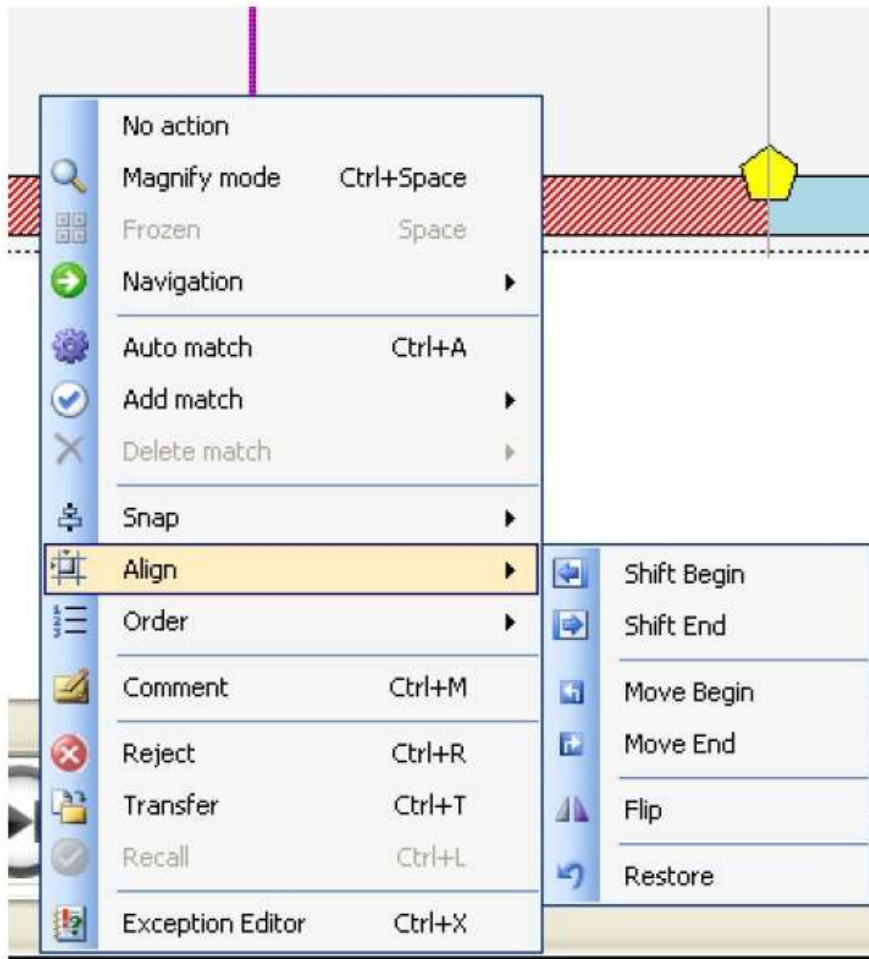
During certain occasions, landmarks need to be moved / shifted / flipped depending on collection or network data. This is also used when one section has multiple segments which need to be aligned. Note: Aligning cannot be done after the sections are matched, hence the match needs to be deleted or aligning needs to be performed before matching.

1. Shifting: Shifts the begin/end landmarks of the collected section to a new position, keeping the collected length the same.
2. Moving: Moves the begin/end landmarks of the collected section to a new position by stretching/compressing the collected length.
3. Flipping: Flips the whole section (this needs to be done when the collected section in the Section

Composition is opposite to all other views, for example moving forward in the Section Composition

takes the ROW images backward.)

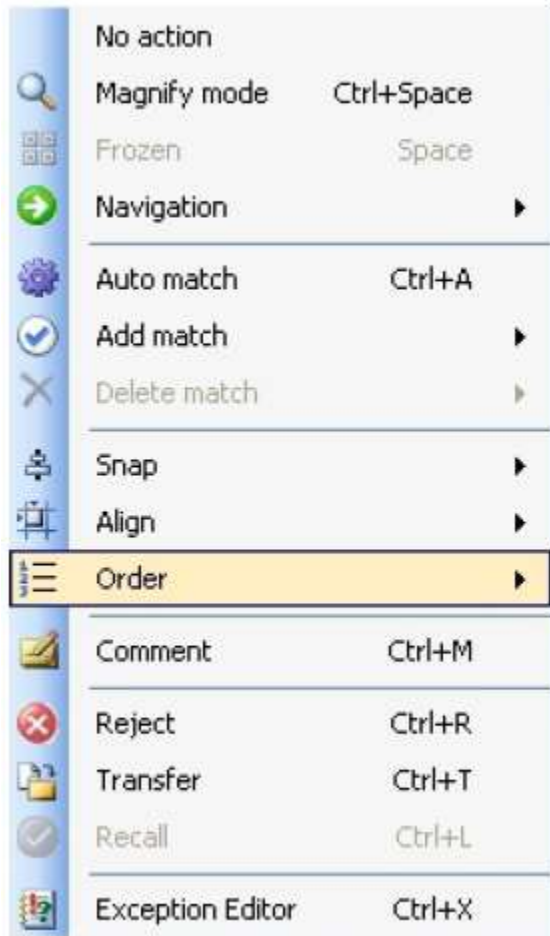
- Right-click on the collected section and select Align



- Select Shift Begin to shift the beginning landmark
- Select Shift End to shift the end landmark.
- Select Move Begin to move the beginning landmark
- Select Move End to move the end landmark
- Select Flip to flip the whole section
- Select Reload to undo any changes

## ***Order***

When one section has multiple segments, the segments are not always correctly ordered.



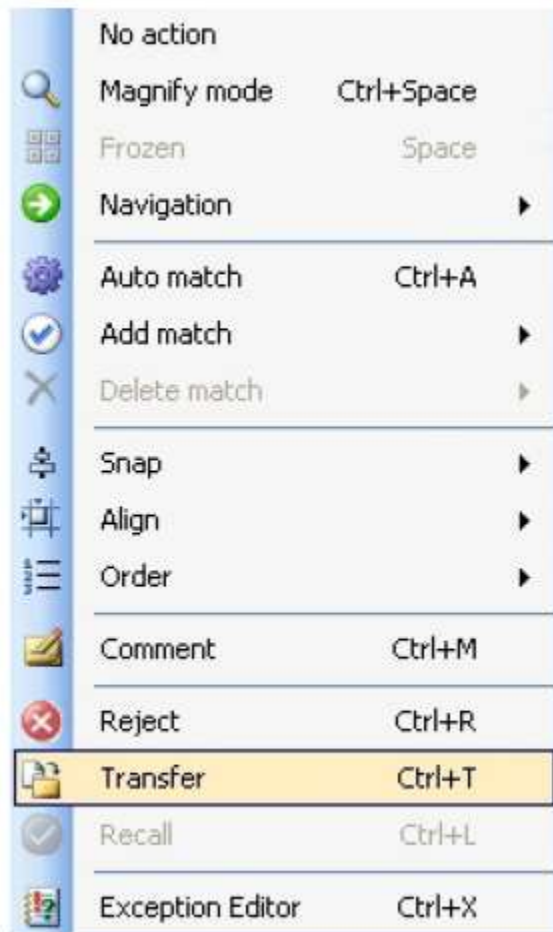
1. To order segments, right-click on the segment to be moved up/down.
2. Select Order >Move Up to move the selected segment up.
3. Select Order >Move Down to move the selected segment down.

## ***Transfer***

When a fragment of a section/segment belongs to the wrong collection, then that fragment needs to be transferred to the correct section.

Note: Transferring cannot be done after the sections are matched, hence the match needs to be deleted or transferring needs to be performed before matching.

1. Right-click on the section to be transferred and select Transfer





2. The following window appears:

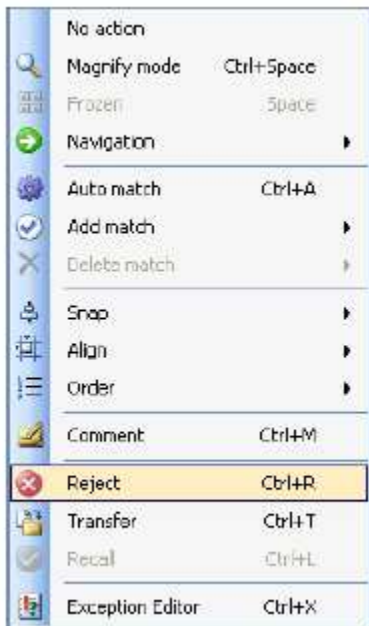


- Select the fragment to be transferred (highlighted in red)
- Click on Select (highlighted in blue) to select the transfer location, i.e the section to which the fragment will be transferred.
- Insert a comment into the Comment box (highlighted in green)
- Click on OK.

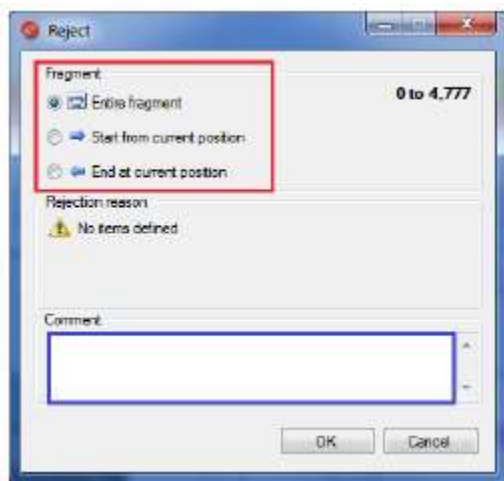
### ***Reject***

During certain collections, certain sections might contain fragments with wrong/missing/not needed data, therefore the fragment is rejected. Note: Rejecting cannot be done after the sections are matched, hence the match needs to be deleted or rejecting needs to be performed before matching.

1. Right-click on the section to be rejected and select Reject.



2. The following window will appear:



- Select the fragment (highlighted in red) to be rejected
- Insert a comment into the comment-box (highlighted in blue)
- Click on OK.

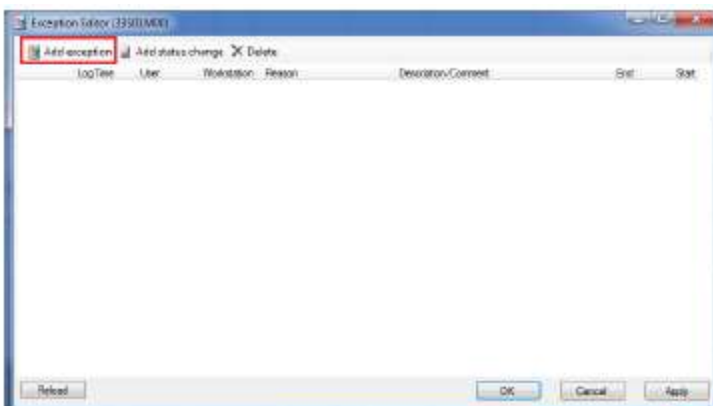
## Exceptions

Certain collections might contain missing/poor images and/or GPS etc. which can be categorized and marked as errors, warnings or just information using the Exception Editor in Section Composition.

1. Identify the exception using the appropriate view, such as too dark images using the Image Stream, and select the appropriate section.
2. Right-click on the section and click on Exception Editor.



3. The following window appears:



4. Click on Add Exception (highlighted in red) and the following window appears:



- Select the fragment where the exception exists (highlighted in red)
- Click on Select (highlighted in blue) to select the reason/category for the exception
- Select the status (error/warning/info) of the exception (highlighted in green)
- Insert a comment into the comment-box (highlighted in purple)
- Click on OK

## M. WORKFLOW FOR TRANSFER OF FDOT MPSV DATA TO VISION SOFTWARE

Here are instructions that were developed as a customized means for transforming LRIS data from FDOT MPSV (provided at a specific folder structure and format) into a Vision database.

### M.1. Folder Instructions

The folder structure should be the same as that finalized with FDOT and shown in Figure 233.



Road Survey Data > PCS Network > Duvall&Hills-Vision > 2017-2018 > By County > 10 Hillsborough > Rigid > 10190000L1_01			
Name	Date modified	Type	Size
Images	5/30/2018 4:35 PM	File folder	
0_10190000L1_01.G01	11/27/2017 5:06 PM	G01 File	891 KB
0_10190000L1_01_img_3.csv	11/27/2017 5:08 PM	Microsoft Excel C...	155 KB
1_10190000L1_01.G01	11/27/2017 5:07 PM	G01 File	1,232 KB
1_10190000L1_01_img_3.csv	11/27/2017 5:08 PM	Microsoft Excel C...	416 KB
10190000L1_01.001	11/27/2017 4:42 PM	001 File	12 KB
10190000L1_01.3.10.6Log.txt	11/27/2017 11:28 ...	Text Document	10 KB
10190000L1_01.301	11/27/2017 4:42 PM	301 File	352 KB
10190000L1_01.601	11/20/2017 4:48 PM	601 File	4 KB
10190000L1_01.csv	11/27/2017 4:42 PM	Microsoft Excel C...	0 KB
10190000L1_01.E01	11/20/2017 4:47 PM	E01 File	11 KB
10190000L1_01.H01	11/27/2017 4:42 PM	H01 File	8 KB
10190000L1_01.I01	11/27/2017 4:42 PM	I01 File	16 KB
10190000L1_01.N01	11/20/2017 4:47 PM	N01 File	3,552 KB
10190000L1_01.P01	11/20/2017 4:47 PM	P01 File	7,291 KB
10190000L1_01.V01	11/20/2017 4:47 PM	V01 File	10 KB
10190000L1_01.Z01	11/20/2017 4:49 PM	Z01 File	6 KB
10190000L1_01_ImageEvents.Z01	11/20/2017 4:49 PM	Z01 File	368 KB
10190000L1_01_six.601	11/27/2017 11:29 ...	601 File	4 KB
10190000L1_01_six_01.csv	11/27/2017 11:29 ...	Microsoft Excel C...	2 KB
orig.G01	11/27/2017 4:42 PM	G01 File	2,499 KB
orig_img_3.csv	11/27/2017 4:42 PM	Microsoft Excel C...	593 KB
WINRP 2.3.10.6Log.txt	11/27/2017 4:42 PM	Text Document	2 KB

**Figure 233. Folder Structure for FDOT MPSV Data**

The encapsulating box in Figure 233 shows 6 folder names:

1. **Duval&Hills-Vision:** This is an example folder, and the name of this folder is not linked with the underlying code. Therefore, the name of this folder should provide a general description of what the folder contains, which in this case is data for Duval and Hillsborough counties.
2. **2017-2018:** This folder represents the year.
3. **By County:** This folder name indicates that the next child folder would have data broken down by counties; e.g. 10 Hillsborough and/or 72 Duval.
4. **10 Hillsborough:** At this level, the data should be broken down by counties as explained in point 3.
5. **Rigid:** At this level of the folder structure, the type of data is outlined; i.e. Rigid or Flexible.
6. **10190000L1\_01:** At this level, the folder name displays as Roadway ID\_Run Number
7. **Images:** This level of the folder structure can be seen inside the 10190000L1\_01 folder. All the images for this county should be stored here

The Roadway ID\_Run Number folder (i.e. 10190000L1\_01 in the example above) should contain four files starting with the Roadway ID\_Run Number and ending with .G01, .N01, \_Img\_3.csv, and \_six\_01.csv. In this example, the four files would be named 10190000L1\_01.G01, 10190000L1\_01.N01, 10190000L1\_01\_Img\_3.csv, and 10190000L1\_01\_six\_01.csv.

## M.2. Steps to Converting the Data Format

The detailed queries for converting the data into a format compatible with Vision database are listed below. For this purpose, a Java code was developed. The zipped Java App (file name: ListFolder.zip) has been provided to FDOT. This Java code conducts the following steps:

1. Lists full path of files except for the image files
2. Renames the xxxx\_img\_3.csv file, xxxx.N01 files and xxxx.G01 files.

3. Changes the image path and Filename in xxxx\_Img\_3.csv and xxxx.N01 files to make Vision work. At the same time, the xxxx\_Img\_3.csv and xxxx.G01 files are split into separate img\_3.csv and .G01 files for each segment. The new created \_Img3.csv files are named in this format:  
(Segment#)\_[(Section)(SubSection)(Lane+Lane#)]\_(Run#), for example, 0\_50010000L1\_01\_Img\_3.csv is the \_Img\_3.csv file for the first segment (segment index starts from 0).

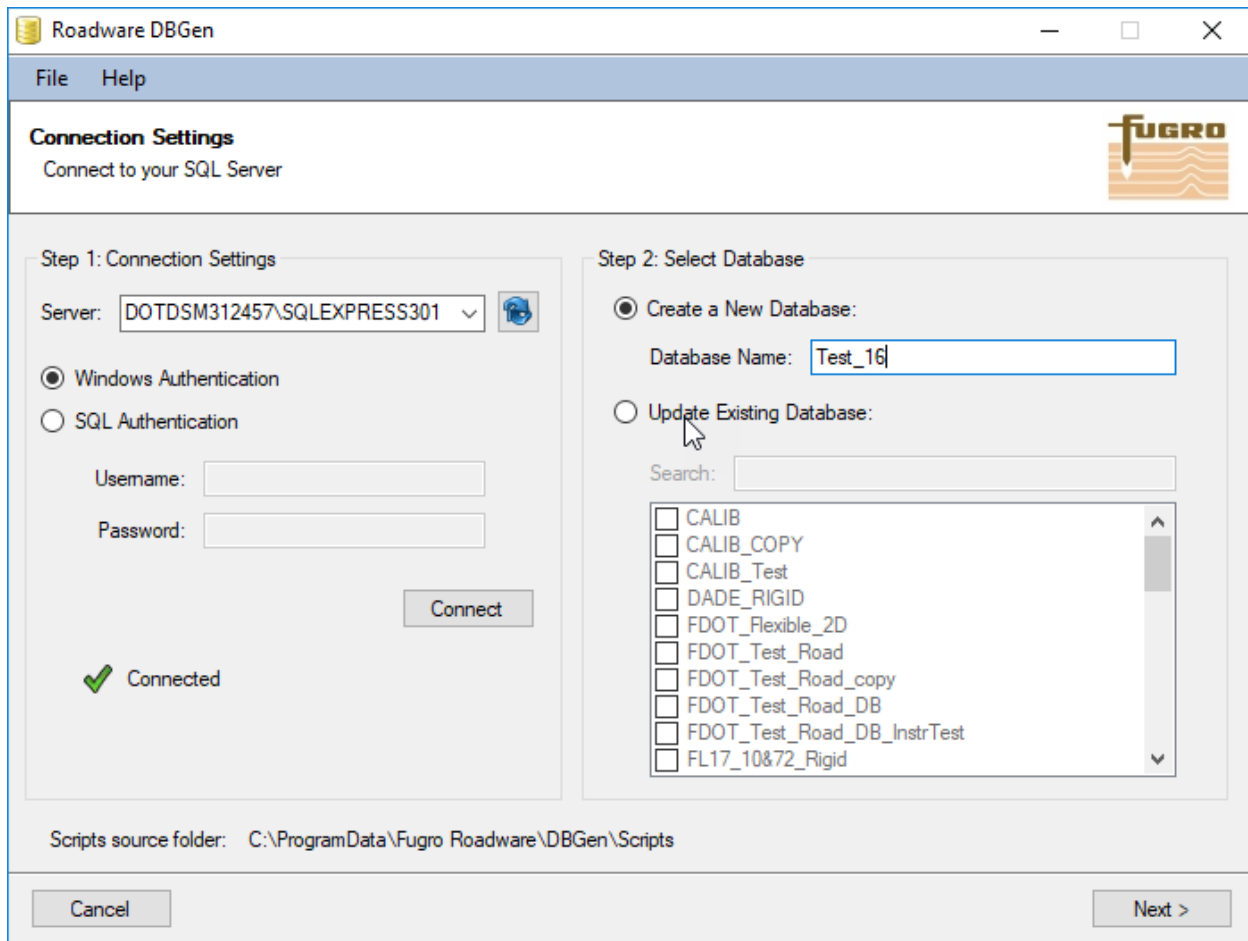
The following steps need to be executed in the following sequence to run this Java code. If your machine was already installed with Java, please skip steps 1 and 2, and jump to step 3.

1. Download the latest version of Java. Go to this web page, and follow the instructions  
[https://www.java.com/en/download/help/windows\\_offline\\_download.xml](https://www.java.com/en/download/help/windows_offline_download.xml)
2. Set Up the Java Path for Windows. Assuming you have installed Java in C:\Program Files\java\jdk directory, right-click on 'My Computer' and select 'Properties'. Click the 'Environment variables' button under the 'Advanced' tab. Alter the 'Path' variable so that it also contains the path to the Java executable. For example, if the path is currently set to 'C:\WINDOWS\SYSTEM32', then change your path to read 'C:\Program Files\java\jdk\bin'.
3. Run the ListFolder.Segment java apps. Open the command prompt window by typing cmd in the Windows search bar. Change the current directory to the directory where you put the java code (e.g. C:\JavaDir) by typing this command in the command prompt: cd /d C:\JavaDir. Type this command in the cmd window: java ListFolder.Segment. Follows instructions in the cmd window; it will ask for the full file path (including folder name) of the root folder. Copy and paste the root folder name in the cmd window.

### M.3. Steps to Transfer the Converted Data into a Vision Database

The following are the steps to transfer the converted data into a Vision database:

1. **STEP1:** Use Roadware DBGen software (see Figure 234) to create a blank Vision database by selecting the Server under 'Step 1: Connection Settings' and selecting the 'Create a New Database' option under 'Step 2: Select Database' and give the database a name (e.g. call it Test\_16).



**Figure 234. Screen Capture of Roadware DBGen**

2. **STEP2:** Execute the first SQL code that will conduct the following:
  - 2-1: Add extra tables and functions to the Vision database
  - 2-2: Grab the paired \_Img\_3.csv and .G01 file names into the T\_G01 and Timg3 tables, suggest using the following commands to check whether the files are paired:  

```
select * from T_G01
select * from Timg3
```
  - 2-3: Importing all the data
  - 2-4: Populate the locator, 'uniquerun' info and the GPS data,



- 2-5: Populate the images info. Note: the physical dimension info can't be found from the pavement JPG provided so the size is evaluated e.g assuming the width is 4 meters and the length of the pavement is evaluated by the average value of the station interval in each 'uniquerun'.
- 2-6: Populate routing (predefined segments) info and assigned the matched segments info.
- 2-7: Clean the extra records in the image tables.

The first SQL code for step 2 is as following according to the steps described above:

### **STEP 2-1:**

```

use "DBName"
GO
create table T (txt varchar(max))
BULK INSERT T FROM 'fullPath\files_f.csv'
WITH ( FIRSTROW = 1,
FIELDTERMINATOR = ',',
ROWTERMINATOR = '\n' )

SET ANSI_NULLS ON
GO
SET QUOTED_IDENTIFIER ON
GO
create function [dbo].[fn_GetGPStimefromUTCtime] (
@UTCtime datetime
)
returns float
AS
BEGIN
return (DATEPART ( WEEKDAY, @UTCtime)-1)*86400 ---day
+DATEPART ( HOUR, @UTCtime)*3600 ---hour
+DATEPART ( MINUTE, @UTCtime)*60 ----minutes
+DATEPART ( SECOND, @UTCtime) ---second
+(DATEPART ( MILLISECOND, @UTCtime))*0.001 ---ms
+(DATEPART ( MICROSECOND, @UTCtime))*0.000001 ---us
+16 ----leap seconds
end;

GO

```

```

create FUNCTION [dbo].[udf_Split]( @Text NVARCHAR(2000),@Splitor CHAR(1) )
RETURNS @Result TABLE ( id int identity, value NVARCHAR(50))
AS
BEGIN
DECLARE @PathInd INT
Set @Text+=@Splitor
WHILE LEN(@Text) > 0
BEGIN
SET @PathInd=PATINDEX('%'+@Splitor+'%',@Text)
INSERT INTO @Result VALUES(SUBSTRING(@Text, 0, @PathInd))
SET @Text= SUBSTRING(@Text, @PathInd+1, LEN(@Text))
END
RETURN
END
GO

```

```

create FUNCTION [dbo].[udf_lastpos_Split]( @Text NVARCHAR(2000),@Splitor
CHAR(1) )
RETURNS int
AS
BEGIN
DECLARE @PathInd INT
DECLARE @returnPathInd INT =0
Set @Text+=@Splitor
WHILE LEN(@Text) > 0
BEGIN
SET @PathInd=PATINDEX('%'+@Splitor+'%',@Text)
SET @Text= SUBSTRING(@Text, @PathInd+1, LEN(@Text))
set @returnPathInd=@returnPathInd+@PathInd
END
RETURN @returnPathInd-@PathInd
END
GO

```

```

-----
create table TImgpath(IDsession int, filename varchar(30), imgpath varchar(300))
create table Img_3_staging(
Num int ,
ImageNum varchar(10),
AdjDmi int ,
FromDist float,
ToDist float,
Latitude varchar(20),
LatDir varchar(10),
Longitude varchar(20),
LongDir varchar(10),

```

```

Q int,
Sat int,
HDOP float,
Height float,
HeightU varchar(10),
GeoSep varchar(8),
GeoSepU varchar(8),
AgeDif varchar(8),
Track varchar(8),
TrackU varchar(8),
GpsSpeed float,
SpeedU varchar(10),
UTCTime varchar(20),
DeltaUTCTime float,
AccumDist float,
GPSDist float,
DeltaAccumDist float,
DeltaGPSDist varchar(20) ,
Time float,
DiffDist float,
DBF int ,
Filename varchar(30),
FromCounty varchar(10) ,
ToCounty varchar(10) ,
FromRoute varchar(255),
ToRoute varchar(255),
FromSect varchar(12),
FromAdjRP float,
ToSect varchar(12),
ToAdjRP float,
DateCollected varchar(20),
TimeCollected varchar(20),
ImagePath varchar(255))

```

-----

```

create table G01_staging(DBF int ,
Filename varchar(30),
FromCounty int ,
ToCounty int ,
FromRoute varchar(255),
ToRoute varchar(255),
FromSect varchar(12),
FromAdjRP float,
ToSect varchar(12),
ToAdjRP float,
DateCollected Datetime,
TimeCollected Datetime,

```

```

ImageNum varchar(8),
Dontknow1 varchar(8),
Dontknow2 int ,
AdjDmi int ,
SpeedU varchar(10),
FromDist float,
Latitude float,
LatDir varchar(10),
Longitude float,
LongDir varchar(10),
Q int,
Sat int,
HDOP float,
Height float,
HeightU varchar(10),
GeoSep varchar(8),
GeoSepU varchar(8),
AgeDif varchar(8),
Track varchar(8),
TrackU varchar(8),
GpsSpeed float,
Dontknow3 varchar(10),
UTCTime varchar(12),
Dontknow4 int,
Dontknow5 int,
AdjDmi2 int, ----- pre sign as GPSDist
GPSDist float, -----pre sign as DeltaAccumDist
GPSDist2 float, -----pre sign as DeltaGPSDist
Dontknow6 varchar(8))

```

### **STEP 2-2:**

```

Select * into T_G01 from T where txt like '%.G01' AND txt not like '%orig%'
Select REPLACE(txt, '.G01', '_Img_3.csv') as txt into Timg3 from T_G01
GO

```

### **STEP 2-3:**

```

declare @query varchar(1000)
DECLARE @table_name varchar(1000);
DECLARE table_cursor CURSOR FOR
select txt from T_G01;
OPEN table_cursor;
FETCH NEXT FROM table_cursor INTO @table_name;

```

```

WHILE @@FETCH_STATUS = 0 BEGIN
--SELECT @query = 'BULK INSERT G01_staging FROM
'+QUOTENAME(@table_name,'')+ ' WITH ( FIRSTROW = 1,
SELECT @query = 'BULK INSERT G01_staging FROM '''+@table_name+''' WITH (
FIRSTROW = 1,
FIELDTERMINATOR = ";",
ROWTERMINATOR = "\n" )';
print @query
EXEC (@query );
FETCH NEXT FROM table_cursor INTO @table_name;
END
CLOSE table_cursor;
DEALLOCATE table_cursor;
-----
DECLARE table_cursor CURSOR FOR
select txt from TImg3;
OPEN table_cursor;
FETCH NEXT FROM table_cursor INTO @table_name;
WHILE @@FETCH_STATUS = 0 BEGIN
--SELECT @query = 'BULK INSERT Img_3_staging FROM
'+QUOTENAME(@table_name,'')+ ' WITH ( FIRSTROW = 1,
SELECT @query = 'BULK INSERT Img_3_staging FROM '''+@table_name+''' WITH (
FIRSTROW = 1,
FIELDTERMINATOR = ";",
ROWTERMINATOR = "\n" )';
print @query
EXEC (@query );
FETCH NEXT FROM table_cursor INTO @table_name;
END
CLOSE table_cursor;
DEALLOCATE table_cursor;
-----
update Img_3_staging
set Latitude=replace(Latitude,'',''),
LatDir=replace(LatDir,'',''),
Longitude=replace(Longitude,'',''),
UTCTime=replace(UTCTime,'',''),
FromCounty=replace(FromCounty,'',''),
ToCounty=replace(ToCounty,'',''),
FromRoute=replace(FromRoute,'',''),
ToRoute=replace(ToRoute,'',''),
DateCollected=replace(DateCollected,'',''),
TimeCollected=replace(TimeCollected,'',''),
ImagePath=replace(ImagePath,'',''),
LongDir=replace(LongDir,'',''),
Filename=replace(Filename,'',''),

```

```

HeightU=replace(HeightU,'',''),
GeoSepU=replace(GeoSepU,'',''),
TrackU=replace(TrackU,'',''),
SpeedU=replace(SpeedU,'','')
GO

```

#### **STEP 2-4:**

```

alter table Locators add Section varchar(15),
County varchar(3),RouteName varchar(50),
Direction varchar(2),
Lane varchar(2), TestSection varchar(2),RunNumber varchar(2)
GO

```

```

select distinct identity(int,1,1) as IDLocator,filename, fromcounty, fromroute
into Tlocator
from Img_3_staging order by filename

```

```

set identity_insert Locators on
insert into Locators(IDLocator,
Section,County,RouteName,Lane,TestSection,RunNumber)
select IDLocator, LEFT(filename,11), FromCounty, fromroute,
SUBSTRING(filename,12,2),
IDlocator, SUBSTRING(filename,16,1)
from Tlocator
set identity_insert Locators off

```

```

update Locators
set Direction=(CASE WHEN Lane LIKE 'L%' THEN '-' WHEN Lane LIKE 'R%' THEN '+'
ELSE NULL END)

```

-----AccumDist (ft) convert to meter as DS, from/toDist (Mile) convert to mmile as  
distancestamp-----

```

set identity_insert DCSessions on
Insert into DCsessions(IDSession, IDLocator, UniqueRun,
StartDistanceStamp, EndDistanceStamp,StartChainage,
EndChainage,DCSTimeStamp)
select b.IDlocator, b.IDLocator,left(a.filename,16),
MIN(AccumDist*0.3048), MAX(AccumDist*0.3048),
(select distinct FromDist from Img_3_staging where Filename=a.filename and
AdjDmi=MIN(a.adjDmi))*1000,
(select distinct ToDist from Img_3_staging where Filename=a.filename and
AdjDmi=Max(a.adjDmi))*1000,
cast (replace(DateCollected,'/','-')+ ' ' + min(TimeCollected) as datetime)
from Img_3_staging a inner join Tlocator b on a.Filename=b.filename

```

```

where a.AccumDist is not null group by a.filename, a.DateCollected, b.IDLocator
set identity_insert DCSessions off
--- make chainage = distancestamp *0.6213712, ~ 4-8 mmile difference
update DCSessions set Endchainage = case when StartChainage<EndChainage then
round(startchainage+(EndDistanceStamp-StartDistanceStamp)*0.6213712,0)
else round(startchainage-(EndDistanceStamp-StartDistanceStamp)*0.6213712,0) end

--- elapsedtime may not correct-----
set identity_insert stationdata on
Insert into stationdata(IDStation,
IDSession, DistanceStamp, Chainage, ElapsedTime, Speed,
StationTime,
PositionStatus, Interpolated, Latitude, Longitude, Elevation)
select ROW_NUMBER() over (order by b.IDLocator, a.AdjDmi),
b.IDLocator, AccumDist*0.3048, FromDist*1000,time,GpsSpeed*0.44704,
[dbo].[fn_GetGPStimefromUTCtime](cast (replace(DateCollected,',' '-')+' '+ a.UTCTime
as datetime)),
'CADifferential','GPSReceiverOutput', Latitude*PI()/180, Longitude*PI()/180,
Height*0.3048
from Img_3_staging a inner join Tlocator b on a.FileName=b.filename
order by b.IDLocator, a.AdjDmi
set identity_insert stationdata off
-----the GPSDist/AccumDist has offset b/w G01_staging and Img_3_staging----
(GPSDist-offsetdist) to approxiamly equal to AccumDist in img_3--
set identity_insert VehiclePositions on
insert into VehiclePositions (IDVehiclePosition, Status, Interpolated, Satellites, HDOP,
IDSession, GPSTime, Latitude,
Longitude, Elevation, DistanceStamp)
select ROW_NUMBER() over (order by y.IDLocator, x.DateCollected+x.UTCTime),
'CADifferential', 'GPSReceiverOutput',x.Sat,
x.HDOP,y.IDLocator,[dbo].[fn_GetGPStimefromUTCtime](x.DateCollected+x.UTCTime),
x.latitude*PI()/180,x.longitude*PI()/180,x.height*0.3048, (x.GPSDist-z.offsetdist)*0.3048
from
(select a.DateCollected,a.UTCTime,a.Sat, a.HDOP,a.latitude,a.longitude,a.height,
a.GPSDist, a.filename, a.adjdmi
from G01_staging a inner join (
select DateCollected,min(UTCTime) as UTCTime, filename, AdjDmi from G01_staging
group by DateCollected, filename, AdjDmi) b
on a.filename=b.filename and a.UTCTime=b.UTCTime) x inner join
(select a.FileName,b.IDLocator,MIN(AccumDist) as mindist, MAX(AccumDist) as
maxdist,
MIN(cast (replace(DateCollected,',' '-')+' '+ a.UTCTime as datetime)) as minUTC,
MAX(cast (replace(DateCollected,',' '-')+' '+ a.UTCTime as datetime)) as maxUTC
from Img_3_staging a inner join Tlocator b on a.FileName=b.filename group by
a.filename, a.DateCollected, b.IDLocator) y
on x.FileName=y.FileName and

```

```

x.DateCollected+x.UTCtime between y.minUTC and y.maxUTC
inner join (
select filename, AVG(offset) as offsetdist from (
select a.AccumDist, b.GPSDist, (b.GPSDist- a.AccumDist) as offset, a.filename
from Img_3_staging a inner join G01_staging b
on a.FileName=b.FileName and a.AdjDmi=b.AdjDmi) results group by filename) z
on x.FileName=z.FileName
order by y.IDlocator, x.DateCollected+x.UTCtime
set identity_insert VehiclePositions off

```

GO

## **STEP 2-5:**

```

---images---
delete from TImgpath
insert into TImgpath(imgpath,filename)
select distinct LEFT(txt,[dbo].[udf_lastpos_Split](txt,'\')),right(txt,len(txt)-
([dbo].[udf_lastpos_Split](txt,'\'))) from T where txt like '%_Img_3.csv%' AND txt not
like '%orig%'
update TImgpath set imgpath=imgpath+'Images\' , filename=replace(filename,
'_Img_3.csv', '.N01')
update a set IDsession=b.IDsession from TImgpath a inner join DCsessions b on
left(a.filename, len(a.filename)-4)=b.uniquerun
-----CCDWidth/Height=ourvalue in DB * FDOTpixel/ourpixel
set identity_insert ImageStreams on
Insert into ImageStreams(IDImageStream,
IDSession, CameraID, Name, ImagePath,ImageCompression, CCDWidth, CCDHeight)
select ROW_NUMBER() over (order by IDLocator),
IDlocator, '4','Pavement',LEFT(b.imgPath,[dbo].[udf_lastpos_Split](b.imgPath,'Images\'-
1),
3, round(1392*1.618895116,0), round(1040*1.497734139,0)
from Tlocator a inner join Timgpath b on a.filename=b.filename order by IDLocator
set identity_insert ImageStreams off

select a.*,
substring(b.txt, len(a.imgpath)+1,100) as Imgname,cast(right(substring(b.txt,
len(a.imgpath)+1,100),12) as varchar(12)) as jpgname
into Tjpg
from Timgpath a inner join
(select REPLACE(txt, 'JPG', 'jpg') as txt from T where UPPER(right(txt,3))='JPG') b
on a.imgpath=left(b.txt, len(a.imgpath))
go
create index ixT1 on Tjpg(IDSession, jpgname)
go

```



-----imagename includes subfolder to make Vision work-----

```
set identity_insert ImageFrames on
Insert into ImageFrames(IDImageFrame, IDImageStream, ImageName,
DistanceStamp)
select ROW_NUMBER() over (order by b.IDLocator, a.AdjDmi),
b.IDLocator, right(c.imgpath,len(c.imgpath)-
[dbo].[udf_lastpos_Split](c.imgpath,'Flexible\')-
8)+ltrim(a.ImageNum+'.jpg'),AccumDist*0.3048
from Img_3_staging a inner join Tlocator b on a.FileName=b.filename
inner join Tjpg c on a.filename=c.filename and
ltrim(a.ImageNum+'.jpg')=ltrim(c.jpgname)
where a.AccumDist is not null
order by b.IDLocator, a.AdjDmi
set identity_insert ImageFrames off
update ImageFrames
set ImageName=right(ImageName,len(ImageName)-
[dbo].[udf_lastpos_Split](ImageName,'Images\')+1)
```

-----sourceframes table has more records than Images-----

```
set identity_insert distress.SourceFrames on
Insert into distress.SourceFrames(IDSourceFrame, SourceFrameType, IDSession,
DistanceStamp, LeftLaneOffset, RightLaneOffset)
select ROW_NUMBER() over (order by IDLocator, DS),'JPEG',IDLocator,DS,0,0 from
(select distinct b.IDLocator, AccumDist*0.3048 as DS
from Img_3_staging a inner join Tlocator b on a.FileName=b.filename
where a.AccumDist is not null) x
order by IDLocator, DS
```

```
set identity_insert distress.SourceFrames off
```

----- Imageheight in meter may be an issue b/c the variable station length-----

```
set identity_insert distress.SourceFramesDimensions on
Insert into distress.SourceFramesDimensions(IDSourceFramesDimensions, IDSession,
ImageWidthInPixels, ImageHeightInPixels,
ImageWidthInMeters, ImageHeightInMeters)
select a.IDLocator, a.IDLocator, 4044, 5949, 4, b.avgdeltadist
from Tlocator a inner join (
select AVG(DeltaAccumDist)*0.3048 as avgdeltadist, Filename from Img_3_staging
group by Filename) b
on a.filename=b.FileName
order by a.IDLocator
set identity_insert distress.SourceFramesDimensions off
```

-----clean extra data and GPS

```
delete x from stationdata x left join (select distinct a.*, b.IDsession, c.uniquerun+'.N01'
as filename, c.IDLocator from (
select min(distancestamp) minDS, max(distancestamp) maxDS, IDImagestream from
imageframes group by IDImagestream) a
inner join ImageStreams b on a.IDImageStream=b.IDImageStream
```

```

inner join DCSessions c on b.IDSession=c.IDsession) y
on x.IDsession=y.IDsession and x.Distancestamp between y.minDS-0.5 and
y.maxDS+0.5
where y.IDsession is null
delete x from vehiclepositions x left join (select distinct a.*, b.IDsession,
c.uniquerun+'.N01' as filename, c.IDLocator from (
select min(distancestamp) minDS, max(distancestamp) maxDS, IDImagestream from
imageframes group by IDImagestream) a
inner join ImageStreams b on a.IDImageStream=b.IDImageStream
inner join DCSessions c on b.IDSession=c.IDsession) y
on x.IDsession=y.IDsession and x.Distancestamp between y.minDS-0.5 and
y.maxDS+0.5
where y.IDsession is null

```

```

set identity_insert VehicleOrientations on
insert into VehicleOrientations(IDVehicleOrientation,GPSTime,IDSession,
DistanceStamp)
select IDVehiclePosition,GPSTime,IDSession, DistanceStamp
from VehiclePositions order by IDVehiclePosition
set identity_insert VehicleOrientations off

```

## **STEP 2-6:**

```

-----routing info,
set identity_insert Sections on
insert into sections(IDSection,IsRouted,IDLocator)
select IDLocator,1,IDLocator from Tlocator
set identity_insert Sections off
-----use the data with the physical JPG parts as the mathed segment and use it clean
the extra data from the stationdata and GPS
select ROW_NUMBER() over (order by y.IDlocator, y.IDsession, y.minDS) as
IDsegment,y.IDLocator,y Filename,
y.minDS as begDS,y.maxDS as endDS,
(select distinct FromAdjRP from Img_3_staging where Filename=y.filename and
AccumDist*0.3048=y.minDS)*1000 as Begchg,
(select distinct ToAdjRP from Img_3_staging where Filename=y.filename and
AccumDist*0.3048=y.maxDS)*1000 as endchg,
(select distinct Latitude from Img_3_staging where Filename=y.filename and
AccumDist*0.3048=y.minDS)*PI()/180 as BegLat,
(select distinct Latitude from Img_3_staging where Filename=y.filename and
AccumDist*0.3048=y.maxDS)*PI()/180 as EndLat,
(select distinct Longitude from Img_3_staging where Filename=y.filename and
AccumDist*0.3048=y.minDS)*PI()/180 as BegLong,
(select distinct Longitude from Img_3_staging where Filename=y.filename and
AccumDist*0.3048=y.maxDS)*PI()/180 as Endlong

```

```

into Tsegments
from (
select distinct a.*, b.IDsession, c.uniquerun+'.N01' as filename, c.IDLocator from (
select min(distancestamp) minDS, max(distancestamp) maxDS, IDImagestream from
imageframes group by IDImagestream) a
inner join ImageStreams b on a.IDImageStream=b.IDImageStream
inner join DCSessions c on b.IDSession=c.IDsession) y
set identity_insert Nodes on
Insert into Nodes(IDNode, Latitude, Longitude)
select ROW_NUMBER() over (order by IDsegment, DS),lat,long from (
select IDsegment, IDLocator, begDS as DS, Begchg as chainage, BegLat as lat,
BegLong as long
from Tsegments
union
select IDsegment, IDLocator, EndDS as DS, Endchg as chainage, EndLat as lat,
EndLong as long
from Tsegments) a
order by IDsegment, DS
set identity_insert Nodes off
---
set identity_insert Landmarks on
Insert into Landmarks(IDLandmark, Chainage, IsAnchor,IsRouted,IDSection,IDNode)
select ROW_NUMBER() over (order by IDsegment, DS),Chainage,1,1,IDLocator,
ROW_NUMBER() over (order by IDsegment, DS)
from (
select IDsegment, IDLocator, begDS as DS, Begchg as chainage, BegLat as lat,
BegLong as long
from Tsegments
union
select IDsegment, IDLocator, EndDS as DS, Endchg as chainage, EndLat as lat,
EndLong as long
from Tsegments) a
order by IDsegment, DS
set identity_insert Landmarks off
set identity_insert routedsegments on
insert into routedsegments(
IDRoutedSegment, Direction, Lane, SegmentRoutingId, SegmentLength,
IDBeginLandmark, IDEndLandmark, IDSection, SequenceIndex)
select IDsegment,case when Begchg>endchg then '5' else '6'
end,1,IDsegment,abs(Begchg-endchg),
IDsegment*2-1, IDsegment*2, IDLocator,1 from Tsegments
set identity_insert routedsegments off
update a
set endDS=b.begDS
from Tsegments a

```

```
inner join Tsegments b on a.IDLocator=b.IDLocator and a.IDSegment=b.IDsegment-1
where abs(a.endDS-b.begDS)<3.5
```

```
insert into matches(IDSegment, BeginChainage,EndChainage, BeginDistanceStamp,
EndDistanceStamp,
Mode, Status, IDSession)
select IDsegment,Begchg, endchg,begds,endds,'Manual','Good',IDLocator from
Tsegments
order by IDsegment
```

### **STEP 2-7:**

```
update m
set ImageHeightInMeters=n.deltaheight
from distress.SourceFramesDimensions m inner join (
select IDImagestream, avg(deltaDS) as deltaheight from (
select a.IDImagestream, (b.Distancestamp-a.Distancestamp) as deltaDS from
imageframes a inner join
imageframes b on a.IDImagestream=b.IDImagestream and
a.IDImageframe=b.IDImageframe-1) x group by IDImagestream) n
on m.IDsession=n.IDImagestream
```

```
update a
set StartChainage=b.begchg, EndChainage=b.endchg, StartDistanceStamp=b.begDS,
EndDistanceStamp=b.endDS
from dcsessions a inner join Tsegments b on a.IDLocator=b.IDLocator
```

3. **STEP 3:** Add necessary SQL permission to the database, and then open it in Vision software, and run the "Vehicle Positions Processor" from the batch processor menu once.
4. **STEP 4:** remove gaps and overlaps between consecutive images using the following SQL code:

use FDOT\_LRIS\_TEST -----if DB name is changed, please use the actual name instead.

```
go
alter table distress.SourceFrames add odistancestamp float
alter table ImageFrames add odistancestamp float
alter table distress.SourceFramesDimensions add olmageHeightInMeters float
go
update distress.SourceFramesDimensions set
olmageHeightInMeters=ImageHeightInMeters
```

```

update distress.SourceFrames set odistancestamp = DistanceStamp
update ImageFrames set odistancestamp = DistanceStamp
delete a
from distress.SourceFrames a left join ImageFrames b
on a.IDSession=b.IDImageStream and a.DistanceStamp=b.DistanceStamp
where b.DistanceStamp is null
select MIN(IDImageframe) as minID,IDImagestream into #t1 from ImageFrames group
by IDImagestream
update a
set DistanceStamp=(a.IDImageFrame-b.minID)*6.11
+(select top 1 odistancestamp from ImageFrames where
IDImageStream=a.IDImageStream and IDImageFrame=b.minID)
from ImageFrames a inner join #t1 b on a.IDImageStream=b.IDImageStream
update a
set distancestamp=b.distancestamp
from distress.SourceFrames a inner join ImageFrames b on
a.IDSession=b.IDImageStream and a.oDistanceStamp=b.oDistanceStamp
update distress.SourceFramesDimensions set ImageHeightInMeters=6.11

--change the unit from millimile to mile
UPDATE DCSessions
set StartChainage=StartChainage/1000
UPDATE DCSessions
set EndChainage=EndChainage/1000

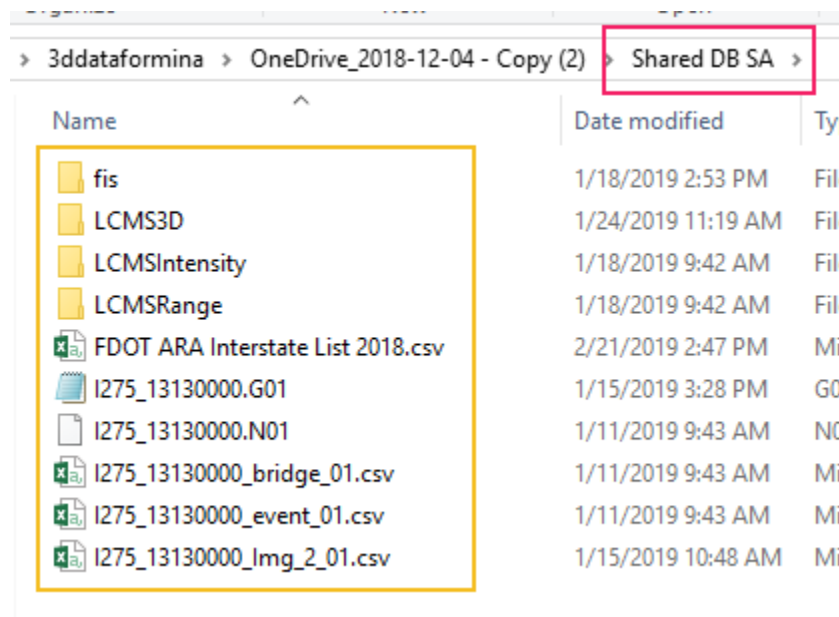
```

## N. WORKFLOW FOR TRANSFER OF FDOT CONTRACTOR DATA TO VISION SOFTWARE

Here are instructions that were developed as a customized means for transforming LCMS data (provided at a specific folder structure and format) into a Vision database. These instructions were tested successfully on the data collected by an FDOT contractor on Florida Interstate Highways.

### N.1. Folder Instructions

The folder structure should be the same as that finalized with FDOT and shown in Figure 235.



Name	Date modified	Type
fis	1/18/2019 2:53 PM	Folder
LCMS3D	1/24/2019 11:19 AM	Folder
LCMSIntensity	1/18/2019 9:42 AM	Folder
LCMSRange	1/18/2019 9:42 AM	Folder
FDOT ARA Interstate List 2018.csv	2/21/2019 2:47 PM	CSV file
I275_13130000.G01	1/15/2019 3:28 PM	Image
I275_13130000.N01	1/11/2019 9:43 AM	Image
I275_13130000_bridge_01.csv	1/11/2019 9:43 AM	CSV file
I275_13130000_event_01.csv	1/11/2019 9:43 AM	CSV file
I275_13130000_img_2_01.csv	1/15/2019 10:48 AM	CSV file

**Figure 235. Folder Structure for FDOT Data**

In Figure 235, the "Shared DB SA" is the parent folder in this example and has no significance. There are no restrictions on folder name, it could be anything that explains the data collected.

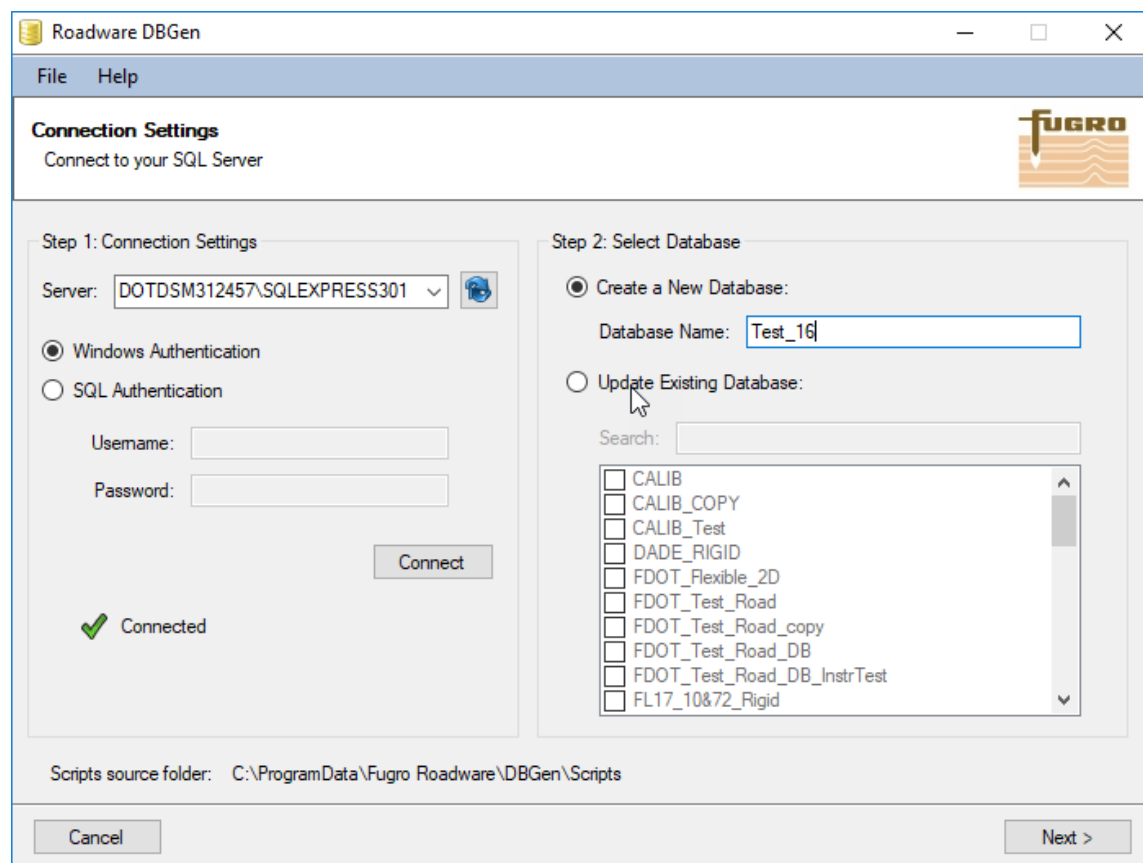
The folders inside "Shared DB SA" are required to be as identified, that is: "fis" folder should contain all the fis files, "LCMS3D" folder should contain all the 3D images, "LCMSIntensity" folder should contain all the Intensity images, and "LCMSRange" folder should contain all the Range images.

There are three required files in this folder:

1. FDOT ARA Interstate List 2018.csv contains a list of all PCS sections and the relevant attributes of each section
2. I275\_13130000\_bridge\_01.csv contains a division of all tenth mile sections and an indication of bridges that needs to be excluded from the data
3. I275\_13130000\_Img\_2\_01.csv contains the Image names and the relevant attributes (This file is generated through the Fugro INI for WinPro)

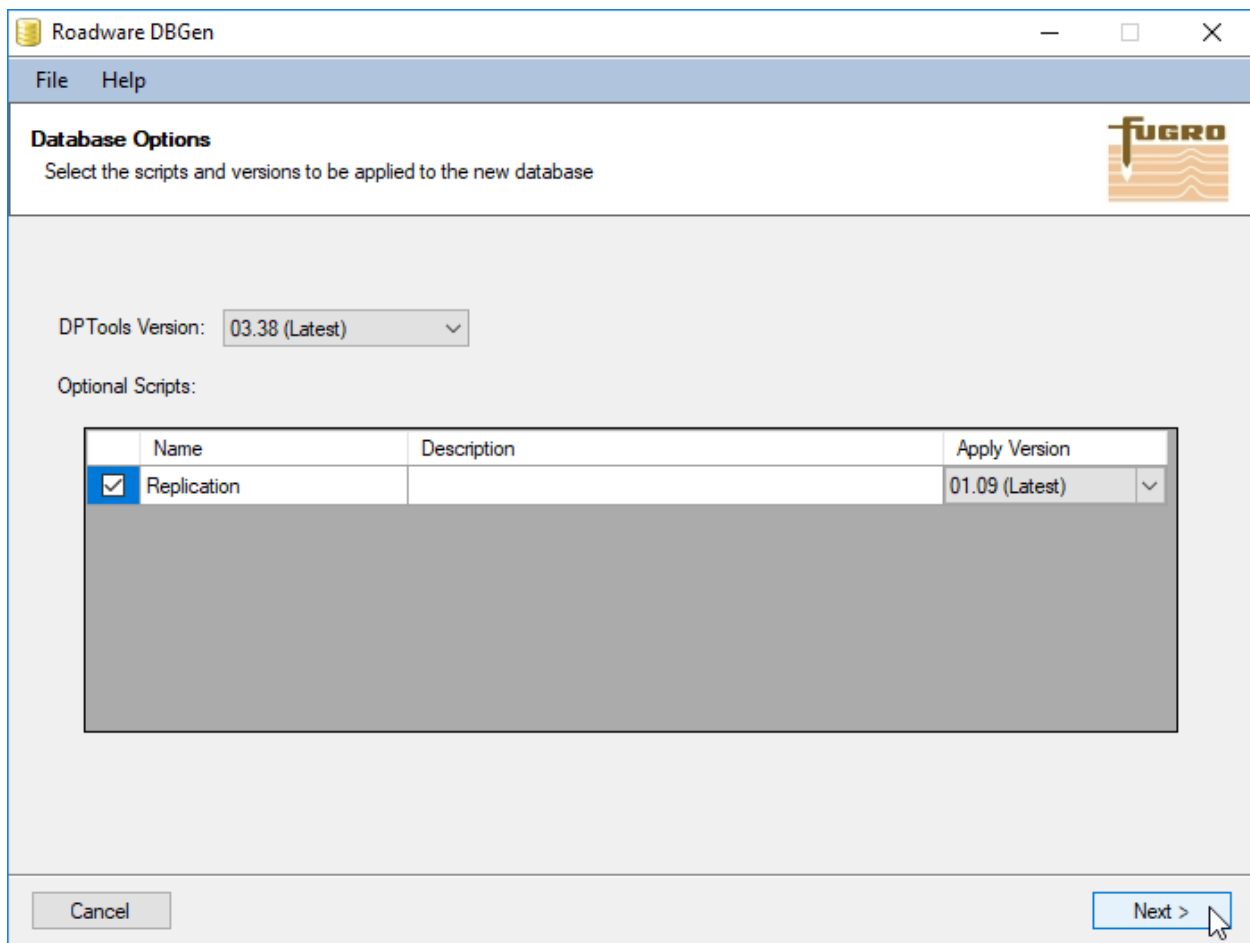
## N.2. Transferring the Data into a Vision Database

Open the Roadware DBGen software and create a new database by selecting the Server under 'Step 1: Connection Settings' and selecting the 'Create a New Database' option under 'Step 2: Select Database' and give the database a name (see Figure 236).



**Figure 236. Roadware DBGen Software Screen Capture**

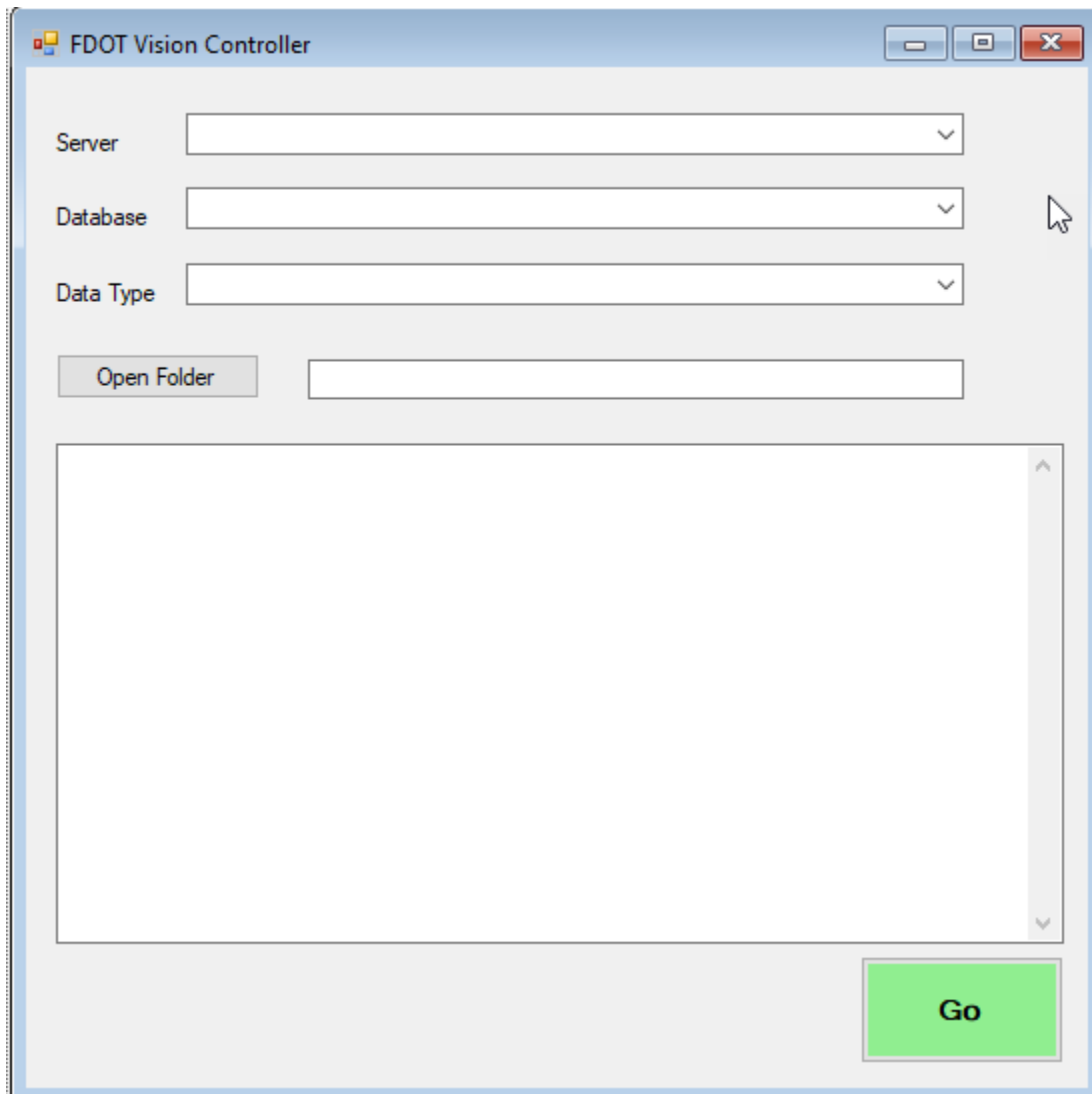
Click 'Next' to get to database options and choose the latest version (see for example Figure 237).



**Figure 237. Database Settings in Roadware DBGen software**



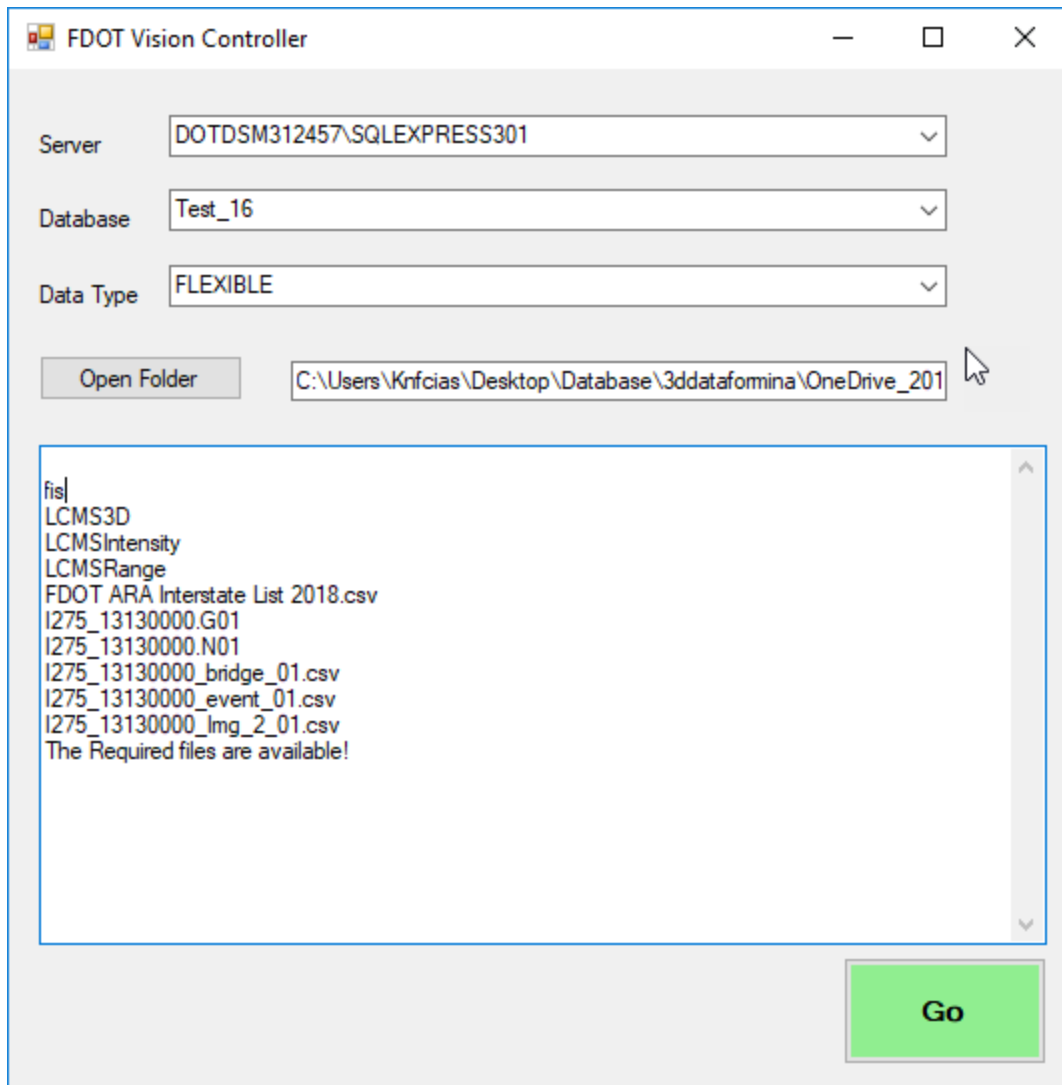
After creating a new Vision database, Open the 'FDOT Vision Controller' interface (see Figure 238). This interface can be used to run the SQL code that is included at the end of this Appendix.



**Figure 238. FDOT Vision Controller Blank Interface**

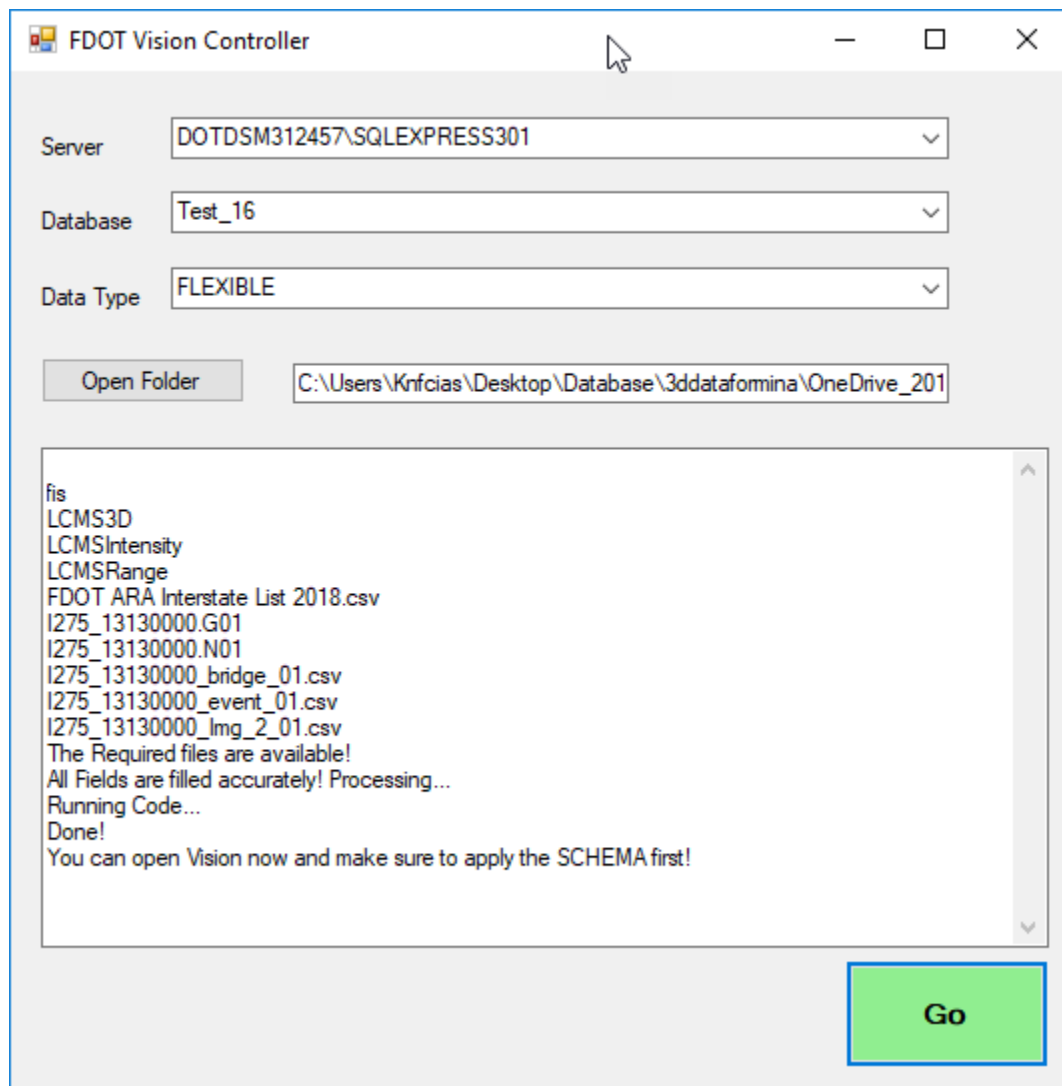
Figure 239 is a filled-out image of the interface. Follow these steps:

1. Select the server by opening the Server drop-down.
2. Select the Database that you just created using Roadware DBGen.
3. Select the type of data that you want to process i.e. Flexible or Rigid.
4. Click the Open Folder button to select the folder that contains the data as mentioned in the Folder Instructions portion of this appendix.
5. The panel in the interface will indicate if all the required files are available, if not it would give a warning.



**Figure 239. FDOT Vision Controller Interface with Options Selected**

Click the Go button to process the files. Once done, the panel will say "Done!" as shown in Figure 240.



**Figure 240. FDOT Vision Controller Interface After Running the SQL Code**

If the folder structure and file formats are followed, the SQL code can transfer the data into a Vision database. The SQL code that is executed using the 'FDOT Vision Controller' interface is as follows:

```
SET ANSI_NULLS ON
GO
SET QUOTED_IDENTIFIER ON
GO
```

```

create function [dbo].[fn_GetGPStimefromUTCtime] (
@UTCtime datetime
)
returns float
AS
BEGIN
return (DATEPART ( WEEKDAY, @UTCtime)-1)*86400
+DATEPART ( HOUR, @UTCtime)*3600
+DATEPART ( MINUTE, @UTCtime)*60
+DATEPART ( SECOND, @UTCtime)
+(DATEPART ( MILLISECOND, @UTCtime))*0.001
+(DATEPART ( MICROSECOND, @UTCtime))*0.000001
+16
end
GO

```

```

create FUNCTION [dbo].[udf_Split]( @Text NVARCHAR(2000),@Splitor CHAR(1) )
RETURNS @Result TABLE ( id int identity, value NVARCHAR(50))
AS
BEGIN
DECLARE @PathInd INT
Set @Text+=@Splitor
WHILE LEN(@Text) > 0
BEGIN
SET @PathInd=PATINDEX('%'+@Splitor+'%',@Text)
INSERT INTO @Result VALUES(SUBSTRING(@Text, 0, @PathInd))
SET @Text= SUBSTRING(@Text, @PathInd+1, LEN(@Text))
END
RETURN
END
go

```

```

create FUNCTION [dbo].[udf_lastpos_Split]( @Text NVARCHAR(2000),@Splitor
CHAR(1) )
RETURNS int
AS
BEGIN
DECLARE @PathInd INT
DECLARE @returnPathInd INT =0
Set @Text+=@Splitor
WHILE LEN(@Text) > 0
BEGIN
SET @PathInd=PATINDEX('%'+@Splitor+'%',@Text)
SET @Text= SUBSTRING(@Text, @PathInd+1, LEN(@Text))
set @returnPathInd=@returnPathInd+@PathInd
END

```

```
RETURN @returnPathInd-@PathInd
END
GO
```

```
create table TImgpath
(
  IDsession int,
  filename varchar(30),
  imgpath varchar(300)
);
create table Img_3_staging
(
  Num varchar(15) ,
  ImageNum varchar(10),
  AdjDmi varchar(15) ,
  FromDist varchar(15),
  ToDist varchar(15),
  Latitude varchar(20),
  LatDir varchar(10),
  Longitude varchar(20),
  LongDir varchar(10),
  Q varchar(15) ,
  Sat int,
  HDOP float,
  Height varchar(15),
  HeightU varchar(10),
  GeoSep varchar(8),
  GeoSepU varchar(8),
  AgeDif varchar(8),
  Track varchar(8),
  TrackU varchar(8),
  GpsSpeed varchar(15),
  SpeedU varchar(10),
  UTCTime varchar(20),
  GPSDistance varchar(15),
  DeltaUTCTime varchar(15),
  AccumDist varchar(15),
  GPSDist varchar(15),
  DeltaAccumDist varchar(15),
  DeltaGPSDist varchar(20) ,
  Time varchar(15),
  DiffDist varchar(15),
  DBF varchar(15) ,
  Filename varchar(30),
  FromCounty varchar(10),
  ToCounty varchar(10) ,
```

```

FromRoute varchar(255),
ToRoute varchar(255),
FromSect varchar(12),
FromAdjRP varchar(15),
ToSect varchar(12),
ToAdjRP varchar(15),
DateCollected varchar(20),
TimeCollected varchar(20),
ImagePath varchar(255)
);

```

```

create table bridge_staging
(
Filename varchar(30),
DateCollected varchar(30) ,
TimeCollected varchar(30) ,
Operator varchar(255),
Route varchar(255),
HdrLane varchar(12),
Direction varchar(30) ,
BeginningRef varchar(30) ,
DCF varchar(30) ,
Vehicle varchar(30) ,
SampleDistance varchar(30) ,
SensorCalDate varchar(30) ,
AvgSpeed varchar(30) ,
Frm varchar(30) ,
RRCode varchar(30) ,
T varchar(30) ,
RghDist varchar(30) ,
Rut1 varchar(30) ,
Rut1Std varchar(30) ,
Rut2 varchar(30) ,
Rut2Std varchar(30) ,
AvgRut varchar(30) ,
STD varchar(30) ,
IRI1 varchar(30) ,
IRI2 varchar(30) ,
AvgIRI varchar(30) ,
Latitude varchar(30) ,
LatDir varchar(30) ,
Longitude varchar(30) ,
LongDir varchar(30) ,
Height varchar(30) ,
HeightU varchar(30) ,
Q varchar(30) ,

```

```
Sat varchar(30) ,
Msg varchar(30)
);
```

```
create table ARA_staging-->>2/21
(
District varchar(15),
RoadwayID varchar(30),
SR varchar(30) ,
US varchar(30) ,
System varchar(255),
Roadway varchar(255),
Type varchar(12),
BMP varchar(12),
EMP varchar(12),
Lanes varchar(15),
R_LN varchar(15),
Length varchar(12),
Surface varchar(50)
);
```

```
select * into Timg3 from T1 where txt like '%_Img_%'
select * into Tbrdg from T1 where txt like '%_bridge_%'
select * into TARA from T1 where txt like '%ARA%'
declare @query varchar(1000)
DECLARE @table_name varchar(1000);
```

```
DECLARE table_cursor CURSOR FOR
select Concat(fullpath,'\',txt) from Timg3;
OPEN table_cursor;
FETCH NEXT FROM table_cursor INTO @table_name;
WHILE @@FETCH_STATUS = 0 BEGIN
```

```
SELECT @query = 'BULK INSERT Img_3_staging FROM "'+@table_name+'"' WITH (
FIRSTROW = 2,
FIELDTERMINATOR = ",",
ROWTERMINATOR = "\n" );
print @query
EXEC (@query );
FETCH NEXT FROM table_cursor INTO @table_name;
END
CLOSE table_cursor;
DEALLOCATE table_cursor;
DECLARE table_cursor CURSOR FOR
select Concat(fullpath,'\',txt) from Tbrdg;
OPEN table_cursor;
```



```

FETCH NEXT FROM table_cursor INTO @table_name;
WHILE @@FETCH_STATUS = 0 BEGIN

SELECT @query = 'BULK INSERT bridge_staging FROM "'+@table_name+'" WITH (
FIRSTROW = 2,
FIELDTERMINATOR = ",",
ROWTERMINATOR = "\n" )';
print @query
EXEC (@query );
FETCH NEXT FROM table_cursor INTO @table_name;
END
CLOSE table_cursor;
DEALLOCATE table_cursor;
DECLARE table_cursor CURSOR FOR
select Concat(fullpath,'\','txt) from TARA;
OPEN table_cursor;
FETCH NEXT FROM table_cursor INTO @table_name;
WHILE @@FETCH_STATUS = 0 BEGIN

SELECT @query = 'BULK INSERT ARA_staging FROM "'+@table_name+'" WITH (
FIRSTROW = 2,
FIELDTERMINATOR = ",",
ROWTERMINATOR = "\n" )';
print @query
EXEC (@query );
FETCH NEXT FROM table_cursor INTO @table_name;
END
CLOSE table_cursor;
DEALLOCATE table_cursor;

delete from Img_3_staging where Num='Num'
delete from bridge_staging where FileName='FileName'
delete from ARA_staging where RoadwayID='RDWYID'
update Img_3_staging
set Latitude=replace(Latitude,'"',"),
AccumDist=Replace(AccumDist,'*',"),
LatDir=replace(LatDir,'"',"),
Longitude=replace(Longitude,'"',"),
UTCTime=replace(UTCTime,'"',"),
FromCounty=replace(FromCounty,'"',"),
ToCounty=replace(ToCounty,'"',"),
FromRoute=replace(FromRoute,'"',"),
ToRoute=replace(ToRoute,'"',"),
DateCollected=replace(DateCollected,'"',"),
TimeCollected=replace(TimeCollected,'"',"),
ImagePath=replace(ImagePath,'"',"),

```

```

LongDir=replace(LongDir,'"',''),
Filename=replace(Filename,'"',''),
HeightU=replace(HeightU,'"',''),

TrackU=replace(TrackU,'"',''),
SpeedU=replace(SpeedU,'"','');
Alter table Img_3_staging
Alter column Num int;
Alter table Img_3_staging
Alter column AdjDmi int;
Alter table Img_3_staging
Alter column FromDist float;
Alter table Img_3_staging
Alter column ToDist float;
Alter table Img_3_staging
Alter column Q int;
Alter table Img_3_staging
Alter column Height float;
Alter table Img_3_staging
Alter column GPSSpeed float;
Alter table Img_3_staging
Alter column DeltaUTCTime float;
Alter table Img_3_staging
Alter column AccumDist float;
Alter table Img_3_staging
Alter column GPSDist float;
Alter table Img_3_staging
Alter column DeltaAccumDist float;
Alter table Img_3_staging
Alter column Time float;
Alter table Img_3_staging
Alter column DiffDist float;
Alter table Img_3_staging
Alter column DBF int;
Alter table Img_3_staging
Alter column FromAdjRP float;
Alter table Img_3_staging
Alter column ToAdjRP float;
Alter table bridge_staging
Alter column Frm float;
Alter table bridge_staging
Alter column T float;
Go
SELECT distinct identity(int,1,1) id,*
into ogX

```

```

FROM [bridge_staging]
order by Frm;

;with cte as
(
select top 1 *
from ogX tab
order by tab.id
union all
select tab.id,tab.[Filename],tab.[DateCollected] ,tab.[TimeCollected]
,tab.[Operator],tab.[Route],tab.[HdrLane],tab.[Direction] ,tab.[BeginningRef] ,tab.[DCF]
,tab.[Vehicle] ,tab.[SampleDistance],tab.[SensorCalDate]
,tab.[AvgSpeed],tab.[Frm] ,tab.[RRCode],tab.[T] ,tab.[RghDist] ,tab.[Rut1],tab.[Rut1Std]
,tab.[Rut2],tab.[Rut2Std],tab.[AvgRut],tab.[STD],tab.[IRI1],tab.[IRI2],tab.[AvgIRI],tab.[Lat
itude],tab.[LatDir],tab.[Longitude]
,tab.[LongDir],tab.[Height],tab.[HeightU],tab.[Q],tab.[Sat], case when tab.msg = " and
cte.msg = ' (S)BB ' then cte.msg else tab.msg end
from ogX tab
inner join cte cte on cte.id + 1 = tab.id
)
select *
into bridge_staging_final
from cte
option (maxrecursion 0);
drop table ogX
Update bridge_staging_final
set msg=" where msg=' (R)(S) ' or msg like '%PLAZA';
delete from bridge_staging_final where msg=' (S)BB ';
delete from ARA_staging where Surface like 'EXCLUSION%' or Surface like
'BRIDGE%' or Surface like ',,,%';-->>2/21

Alter table bridge_staging_final
Add Section varchar(30);
Alter table ARA_staging
Alter column BMP float;
Alter table ARA_staging
Alter column EMP float;
Update bridge_staging_final
Set
Section=Concat(id,'_',Format(Convert(numeric,parsename(REPLACE(SUBSTRING(File
Name, CHARINDEX('_', FileName), LEN(FileName)), '_', ''),2)), '00000000'));

Alter table Img_3_staging
Alter column ToAdjRP float;

```

```

Declare @DType varchar(30)
Set @DType='FLEXIBLE'
Select distinct a.*,Left(a.RoadwayID,2) County, CASE WHEN Right(Direction,3) like
'+%' THEN 'R' ELSE 'L' END Dir,b.*
into bridge_staging_final2
from
bridge_staging_final b
left join
(
select distinct * from ARA_staging Where Surface Like 'FLEXIBLE%'--<<This is updated
to RIGID% of RIGID data
) a
on
a.roadwayid=Format(Convert(numeric,parsename(REPLACE(SUBSTRING(FileName,
CHARINDEX('_', FileName), LEN(FileName)), '_', ''),2)), '00000000') and (b.Frm + b.T) /
2 >= a.BMP AND (b.Frm + b.T) / 2 < a.EMP;

```

```

alter table Locators
add Section varchar(30),
County varchar(15),
RoadwayID varchar(50),
Direction varchar(2),
Lane varchar(2),
TestSection varchar(15),
RunNumber varchar(15),
L_Section varchar(30),
L_Run varchar(15),
-->>2/21
District varchar(15),
SR varchar(15),
US varchar(15),
System varchar(15),
Type varchar(15),
Lanes varchar(15),
R_LN varchar(15),
Surface varchar(15)
GO

```

```

Declare @pth varchar(225);
select distinct @pth=fullpath from T1 where txt='LCMS3D';--This would need to be
changed to fis if thats all that the user is required to provide
Update Img_3_staging
Set ImagePath=CONCAT(@pth,'\');
GO
select distinct
a.[RoadwayID]

```

-->>2/21  
,a.District  
,a.SR  
,a.us  
,a.system  
,a.type  
,a.lanes  
,a.r\_In  
,a.[County]  
,a.[Dir]  
,a.[id]  
,a.[Filename] fn  
,a.[DateCollected] dc  
,a.[TimeCollected] tc  
,a.[Operator]  
,a.[Route]  
,a.[HdrLane]  
,a.[Direction]  
,a.[BeginningRef]  
,a.[DCF]  
,a.[Vehicle]  
,a.[SampleDistance]  
,a.[SensorCalDate]  
,a.[AvgSpeed]  
,a.[Frm]  
,a.[RRCode]  
,a.[T]  
,a.[RghDist]  
,a.[Rut1]  
,a.[Rut1Std]  
,a.[Rut2]  
,a.[Rut2Std]  
,a.[AvgRut]  
,a.[STD]  
,a.[IRI1]  
,a.[IRI2]  
,a.[AvgIRI]  
,a.[Latitude] lat  
,a.[LatDir] ld  
,a.[Longitude] long  
,a.[LongDir] lod  
,a.[Height] hght  
,a.[HeightU] hghtU  
,a.[Q] qq  
,a.[Sat] saat

```

,a.[Msg] mssg
,a.[Section]
,b.[Num]
,b.[ImageNum]
,b.[AdjDmi]
,b.[FromDist]
,b.[ToDist]
,b.[Latitude]
,b.[LatDir]
,b.[Longitude]
,b.[LongDir]
,b.[Q]
,b.[Sat]
,b.[HDOP]
,b.[Height]
,b.[HeightU]
,b.[GeoSep]
,b.[GeoSepU]
,b.[AgeDif]
,b.[Track]
,b.[TrackU]
,b.[GpsSpeed]
,b.[SpeedU]
,b.[UTCTime]
,b.[GPSDistance]
,b.[DeltaUTCTime]
,b.[AccumDist]
,b.[GPSDist]
,b.[DeltaAccumDist]
,b.[DeltaGPSDist]
,b.[Time]
,b.[DiffDist]
,b.[DBF]
,b.[Filename]
,b.[FromCounty]
,b.[ToCounty]
,b.[FromRoute]
,b.[ToRoute]
,b.[FromSect]
,b.[FromAdjRP]
,b.[ToSect]
,b.[ToAdjRP]
,b.[DateCollected]
,b.[TimeCollected]
,b.[ImagePath] into bridge_img3_staging from bridge_staging_final2 a left join
Img_3_Staging b on

```

```

Format(Convert(numeric,parsename(REPLACE(SUBSTRING(a.FileName,
CHARINDEX('_', a.FileName), LEN(a.FileName)), '_',
'),2)), '00000000')=Format(Convert(numeric,parsename(REPLACE(SUBSTRING(b.File
Name, CHARINDEX('_', b.FileName), LEN(b.FileName)), '_', '),2)), '00000000') and
(b.FromDist + b.ToDist) / 2 >= a.Frm AND (b.FromDist + b.ToDist) / 2 < a.T;
alter table bridge_img3_staging
add reallmg varchar(100);

update bridge_img3_staging
set bridge_img3_staging.reallmg=parsename(Right(b.txt,Len(b.txt)+1-
patindex('%0%',b.txt)),2)
from
bridge_img3_staging a inner join T1 b on
Right(a.imagenum,6)=parsename(Right(b.txt,Len(b.txt)+1-patindex('%0%',b.txt)),2);
delete from bridge_img3_staging where reallmg is NULL or reallmg="";
select distinct
identity(int,1,1) as IDLocator,
y.section filename, y.county, y.roadwayid ,dir
,Convert(int,LEFT(section, CHARINDEX('_', section) - 1)) tis
-->>2/21
,y.district,y.sr,y.us,y.system,y.type,y.lanes,y.r_ln
into TLocator
from bridge_img3_staging y where (y.county is not null or y.roadwayid is not null)
order by tis;

set identity_insert Locators on
insert into Locators(IDLocator,
Section,County,RoadwayID,Direction,TestSection,RunNumber
-->>2/21
,District,sr,us,System,Type,lanes,R_LN)
select IDlocator, filename, County, roadwayid, dir,tis,1
-->>2/21
,district,sr,us,system,type,lanes,r_ln
from Tlocator
set identity_insert Locators off
Go
set identity_insert DCSessions on
Insert into DCsessions(IDSession, IDLocator, UniqueRun,
StartDistanceStamp, EndDistanceStamp,StartChainage,
EndChainage,DCSTimeStamp)
select b.IDlocator, b.IDLocator,a.Section,
MIN(AccumDist*0.3048), MAX(AccumDist*0.3048),
(select distinct FromDist from bridge_img3_staging where section=a.section and
AdjDmi=MIN(a.adjDmi))*1000,
(select distinct ToDist from bridge_img3_staging where section=a.section and
AdjDmi=Max(a.adjDmi))*1000,

```

```

cast (replace(DateCollected, '/', '-')+' '+ min(TimeCollected) as datetime)
from bridge_img3_staging a inner join Tlocator b on a.Section=b.filename
where a.AccumDist is not null group by a.section, a.DateCollected, b.IDLocator
order by b.IDLocator
set identity_insert DCSessions off

```

```

update DCSessions set Endchainage = case when StartChainage<EndChainage then
round(startchainage+(EndDistanceStamp-StartDistanceStamp)*0.6213712,0)
else round(startchainage-(EndDistanceStamp-StartDistanceStamp)*0.6213712,0) end;

```

```

set identity_insert stationdata on
Insert into stationdata(IDStation,
IDSession, DistanceStamp, Chainage, ElapsedTime, Speed,
StationTime,
PositionStatus, Interpolated, Latitude, Longitude, Elevation)
select ROW_NUMBER() over (order by b.IDLocator, a.AdjDmi),
b.IDLocator, AccumDist*0.3048, FromDist*1000,time,GpsSpeed*0.44704,
[dbo].[fn_GetGPStimefromUTCtime](cast (replace(DateCollected, '/', '-')+' '+ a.UTCtime
as datetime)),
'CADifferential','GPSReceiverOutput', Latitude*PI()/180, Longitude*PI()/180,
Height*0.3048
from bridge_img3_staging a inner join Tlocator b on a.Section=b.filename
order by b.IDLocator, a.AdjDmi
set identity_insert stationdata off

```

```

set identity_insert VehiclePositions on
insert into VehiclePositions (IDVehiclePosition, Status, Interpolated, Satellites, HDOP,
IDSession, GPSTime, Latitude,
Longitude, Elevation, DistanceStamp)
select
ROW_NUMBER() over (order by y.IDLocator, x.DateCollected+x.UTCtime),
'CADifferential',
'GPSReceiverOutput',
x.Sat,
x.HDOP,
y.IDLocator,
[dbo].[fn_GetGPStimefromUTCtime](x.DateCollected+x.UTCtime),
x.latitude*PI()/180,
x.longitude*PI()/180,
x.height*0.3048,
(x.GPSDist-z.offsetdist)*0.3048
from
(
select
a.DateCollected,
a.UTCtime,

```



```

a.Sat,
a.HDOP,
a.latitude,
a.longitude,
a.height,
a.GPSDist,
a.section,
a.adjdm
from bridge_img3_staging a
inner join
(
select
DateCollected,
min(UTCtime) as UTCtime,
section,
AdjDmi
from bridge_img3_staging
group by DateCollected, section, AdjDmi
) b
on a.section=b.section and a.UTCtime=b.UTCtime) x
inner join
(
select
a.Section,
b.IDLocator,
MIN(AccumDist) as mindist,
MAX(AccumDist) as maxdist,
MIN(cast (replace(DateCollected,'/','-')+ ' ' + a.UTCtime as datetime)) as minUTC,
MAX(cast (replace(DateCollected,'/','-')+ ' ' + a.UTCtime as datetime)) as maxUTC
from bridge_img3_staging a
inner join
Tlocator b on a.section=b.filename group by a.section, a.DateCollected, b.IDLocator
) y
on x.Section=y.section and x.DateCollected+x.UTCtime between y.minUTC and
y.maxUTC
inner join
(
select
section,
AVG(offset) as offsetdist
from
(
select
AccumDist,
GPSDist,
(GPSDist- AccumDist) as offset,

```

```

section
from bridge_img3_staging
) results
group by section
) z
on x.section=z.section
order by y.IDlocator, x.DateCollected+x.UTCtime

set identity_insert VehiclePositions off
go
select distinct b.fullpath,section filename,Convert(int,LEFT(section, CHARINDEX('_',
section) - 1)) tis
into timg
from bridge_img3_staging a left join T1 b on parsename(a.Filename,2)=left(b.txt,12)
order by tis--since we dont need .n01 files anymore, the on condition tricks in getting
just the right combination
delete from Timgpath
insert into Timgpath(imgpath,filename)
select distinct fullpath,filename from timg
update a set IDsession=b.IDsession from Timgpath a inner join DCsessions b on
a.filename=b.uniquerun

set identity_insert ImageStreams on
Insert into ImageStreams(IDImageStream,
IDSession, CameraID, Name, ImagePath,ImageCompression, CCDWidth, CCDHeight)
select ROW_NUMBER() over (order by IDLocator,Nam),x.* from
(
select
IDlocator, '9' Cam,'LCMSIntensity' Nam,Concat(b.imgPath,'\LCMSIntensity\') Imag,
3 Comp, round(1392*1.618895116,0) CCDW, round(1040*1.497734139,0) CCDH
from Tlocator a inner join Timgpath b on a.filename=b.filename
Union all
select
IDlocator, '10' Cam,'LCMSRange' Nam,Concat(b.imgPath,'\LCMSRange\') Imag,
3 Comp, round(1392*1.618895116,0) CCDW, round(1040*1.497734139,0) CCDH
from Tlocator a inner join Timgpath b on a.filename=b.filename
Union all
select
IDlocator, '11' Cam,'LCMS3D' Nam,Concat(b.imgPath,'\LCMS3D\') Imag,
3 Comp, round(1392*1.618895116,0) CCDW, round(1040*1.497734139,0) CCDH
from Tlocator a inner join Timgpath b on a.filename=b.filename
) x order by IDLocator
set identity_insert ImageStreams off

select distinct a.IDsession,a.filename,b.fullpath as imgpath,
b.txt as Imgname,b.txt as jpgname

```

```

into Tjpg
from Timgpath a inner join
(select REPLACE(txt, 'JPG', 'jpg') as txt,fullpath from T1 where
UPPER(right(txt,3))='JPG') b
on a.imgpath=left(b.fullpath, len(a.imgpath))
go
create index ixT1 on Tjpg(IDSession, jpgname);
go
set identity_insert ImageFrames on
Insert into ImageFrames(IDImageFrame, IDImageStream, ImageName,
DistanceStamp)
Select Row_number() over(order by y.idimagestream)
idimageframe,y.idimagestream,x.Imgname,AdjDmi
from
(
select ROW_NUMBER() over (order by b.IDLocator, a.AdjDmi) idimageframe,
b.IDLocator idimagestream,c.Imgname,AccumDist*0.3048 AdjDmi,a.Section,CASE
WHEN Imgname like '%Int%' then 'LCMSIntensity' WHEN Imgname like '%3D%' then
'LCMS3D' WHEN Imgname like '%Rng%' then 'LCMSRange' Else NULL End name,b.tis
from bridge_img3_staging a
inner join Tlocator b on a.section=b.filename
inner join Tjpg c on a.Section=c.filename
and Right(a.ImageNum,6)=parsename(Right(Imgname,Len(Imgname)+1-
patindex('%0%',Imgname)),2)
where a.AccumDist is not null
) x
join
dbo.imagestreams y on x.idimagestream=y.idsession and x.name=y.name
order by tis,x.name, AdjDmi;

set identity_insert ImageFrames off
go
set identity_insert distress.SourceFrames on
Insert into distress.SourceFrames(IDSourceFrame, SourceFrameType, IDSession,
DistanceStamp, LeftLaneOffset, RightLaneOffset)
select ROW_NUMBER() over (order by IDLocator, DS),'LCMS',IDlocator,DS,0,0 from
(select distinct b.IDlocator, AccumDist*0.3048 as DS
from bridge_img3_staging a inner join Tlocator b on a.section=b.filename
where a.AccumDist is not null) x
order by IDLocator, DS
set identity_insert distress.SourceFrames off
go
set identity_insert distress.SourceFramesDimensions on
Insert into distress.SourceFramesDimensions(IDSourceFramesDimensions, IDSession,
ImageWidthInPixels, ImageHeightInPixels,
ImageWidthInMeters, ImageHeightInMeters)

```

```

select a.IDLocator, a.IDlocator, 2067, 3048, 4, b.avgdeltadist
from Tlocator a inner join (
select AVG(DeltaAccumDist)*0.3048 as avgdeltadist, section from bridge_img3_staging
group by section) b
on a.filename=b.section
order by a.IDLocator
set identity_insert distress.SourceFramesDimensions off

```

```

delete x from stationdata x left join (select distinct a.*, b.IDsession, c.uniquerun as
filename, c.IDLocator from (
select min(distancestamp) minDS, max(distancestamp) maxDS, IDImagestream from
imageframes group by IDImagestream) a
inner join ImageStreams b on a.IDImageStream=b.IDImageStream
inner join DCSessions c on b.IDSession=c.IDsession) y
on x.IDsession=y.IDsession and x.Distancestamp between y.minDS-0.5 and
y.maxDS+0.5
where y.IDsession is null;
delete x from vehiclepositions x left join (select distinct a.*, b.IDsession, c.uniquerun as
filename, c.IDLocator from (
select min(distancestamp) minDS, max(distancestamp) maxDS, IDImagestream from
imageframes group by IDImagestream) a
inner join ImageStreams b on a.IDImageStream=b.IDImageStream
inner join DCSessions c on b.IDSession=c.IDsession) y
on x.IDsession=y.IDsession and x.Distancestamp between y.minDS-0.5 and
y.maxDS+0.5
where y.IDsession is null;
set identity_insert VehicleOrientations on
insert into VehicleOrientations(IDVehicleOrientation,GPSTime,IDSession,
DistanceStamp)
select IDVehiclePosition,GPSTime,IDSession, DistanceStamp
from VehiclePositions order by IDVehiclePosition
set identity_insert VehicleOrientations off

```

```

set identity_insert Sections on
insert into sections(IDSection,IsRouted,IDLocator)
select IDLocator,1,IDLocator from Tlocator
set identity_insert Sections off

```

```

select ROW_NUMBER() over (order by y.IDlocator, y.IDsession, y.minDS) as
IDsegment,y.IDLocator,y.FileName,
y.minDS as begDS,y.maxDS as endDS,
(select distinct FromAdjRP from bridge_img3_staging where section=y.filename and
AccumDist*0.3048=y.minDS)*1000 as Begchg,
(select distinct ToAdjRP from bridge_img3_staging where section=y.filename and
AccumDist*0.3048=y.maxDS)*1000 as endchg,
(select distinct Latitude from bridge_img3_staging where section=y.filename and

```

```

AccumDist*0.3048=y.minDS)*PI()/180 as BegLat,
(select distinct Latitude from bridge_img3_staging where section=y.filename and
AccumDist*0.3048=y.maxDS)*PI()/180 as EndLat,
(select distinct Longitude from bridge_img3_staging where section=y.filename and
AccumDist*0.3048=y.minDS)*PI()/180 as BegLong,
(select distinct Longitude from bridge_img3_staging where section=y.filename and
AccumDist*0.3048=y.maxDS)*PI()/180 as Endlong
into Tsegments
from (
select distinct
a.*,
b.IDsession,
c.uniquerun as filename,
c.IDLocator
from (
select
min(distancestamp) minDS,
max(distancestamp) maxDS,
IDImagestream
from imageframes
group by IDImagestream
) a
left join ImageStreams b on a.IDImageStream=b.IDImageStream
left join DCSessions c on b.IDSession=c.IDsession
) y;
set identity_insert Nodes on
Insert into Nodes(IDNode, Latitude, Longitude)
select ROW_NUMBER() over (order by IDsegment, DS),lat,long from (
select IDsegment, IDLocator, begDS as DS, Begchg as chainage, BegLat as lat,
BegLong as long
from Tsegments
union
select IDsegment, IDLocator, EndDS as DS, Endchg as chainage, EndLat as lat,
EndLong as long
from Tsegments) a
order by IDsegment, DS
set identity_insert Nodes off

set identity_insert Landmarks on
Insert into Landmarks(IDLandmark, Chainage, IsAnchor,IsRouted,IDSection,IDNode)
select ROW_NUMBER() over (order by IDsegment, DS),Chainage,1,1,IDLocator,
ROW_NUMBER() over (order by IDsegment, DS)
from (
select IDsegment, IDLocator, begDS as DS, Begchg as chainage, BegLat as lat,
BegLong as long
from Tsegments

```

```

union
select IDsegment, IDLocator, EndDS as DS, Endchg as chainage, EndLat as lat,
EndLong as long
from Tsegments) a
order by IDsegment, DS
set identity_insert Landmarks off

set identity_insert routedsegments on
insert into routedsegments(
IDRoutedSegment, Direction, Lane, SegmentRoutingId, SegmentLength,
IDBeginLandmark, IDEndLandmark, IDSection, SequenceIndex)
select IDsegment,case when Begchg>endchg then '5' else '6'
end,1,IDsegment,abs(Begchg-endchg),
IDsegment*2-1, IDsegment*2, IDLocator,1 from Tsegments
set identity_insert routedsegments off
update a
set endDS=b.begDS
from Tsegments a
inner join Tsegments b on a.IDLocator=b.IDlocator and a.IDSegment=b.IDsegment-1
where abs(a.endDS-b.begDS)<3.5;

insert into matches(IDSegment, BeginChainage,EndChainage, BeginDistanceStamp,
EndDistanceStamp,
Mode, Status, IDSession)
select IDsegment,Begchg, endchg,begds,endds,'Manual','Good',IDLocator from
Tsegments
order by IDsegment;

update m
set ImageHeightInMeters=n.deltaheight
from distress.SourceFramesDimensions m inner join (
select IDImagestream, avg(deltaDS) as deltaheight from (
select a.IDImagestream, (b.Distancestamp-a.Distancestamp) as deltaDS from
imageframes a inner join
imageframes b on a.IDImagestream=b.IDImagestream and
a.IDImageframe=b.IDImageframe-1) x group by IDImagestream) n
on m.IDsession=n.IDImagestream;

update a
set StartChainage=b.begchg, EndChainage=b.endchg, StartDistanceStamp=b.begDS,
EndDistanceStamp=b.endDS
from dcsessions a inner join Tsegments b on a.IDLocator=b.IDlocator;

alter table distress.SourceFrames add odistancestamp float;
alter table ImageFrames add odistancestamp float;
alter table distress.SourceFramesDimensions add olmageHeightInMeters float;

```

```

go
update distress.SourceFramesDimensions set
oImageHeightInMeters=ImageHeightInMeters;
update distress.SourceFrames set oDistanceStamp = DistanceStamp;
update ImageFrames set oDistanceStamp = DistanceStamp;
delete a
from distress.SourceFrames a left join ImageFrames b
on a.IDSession=b.IDImageStream and a.DistanceStamp=b.DistanceStamp
where b.DistanceStamp is null;
select MIN(IDImageFrame) as minID,IDImageStream into t2 from ImageFrames group by
IDImageStream;
update a
set DistanceStamp=(a.IDImageFrame-b.minID)*6.11
+(select top 1 oDistanceStamp from ImageFrames where
IDImageStream=a.IDImageStream and IDImageFrame=b.minID)
from ImageFrames a inner join t2 b on a.IDImageStream=b.IDImageStream;
drop table t2;
update a
set distanceStamp=b.distanceStamp
from distress.SourceFrames a inner join ImageFrames b on
a.IDSession=b.IDImageStream and a.oDistanceStamp=b.oDistanceStamp;
update distress.SourceFramesDimensions set ImageHeightInMeters=6.809232;
update distress.SourceFramesDimensions set ImageWidthInPixels=2067;
update distress.SourceFramesDimensions set ImageHeightInPixels=3048;

```

```

UPDATE DCSessions
set StartChainage=StartChainage/1000;
UPDATE DCSessions
set EndChainage=EndChainage/1000;

```

```

set identity_insert LCMSFisFrames on
Insert into LCMSFisFrames(IDLCMSFisFrames, IDSession, Filename,
FrameNumber, DistanceStamp,DistanceStampOrig)
select
ROW_NUMBER() over (order by substring(parsename(Right(a.txt,Len(a.txt)+1-
patindex('%0%',a.txt)),2), patindex('%[^0]%',parsename(Right(a.txt,Len(a.txt)+1-
patindex('%0%',a.txt)),2)), 10)) idfr
,Dense_rank() over (order by c.id) den
,Concat(a.fullpath,'\',txt) filename
, substring(parsename(Right(a.txt,Len(a.txt)+1-patindex('%0%',a.txt)),2),
patindex('%[^0]%',parsename(Right(a.txt,Len(a.txt)+1-patindex('%0%',a.txt)),2)), 10)
framenumber
,b.distanceStamp
,b.distanceStamp
from
T1 a

```

```

inner join
(select distinct substring(parsename(Right(Right(Imagename,LEN(Imagename))-
charindex('_',Imagename)),LEN(Right(Imagename,LEN(Imagename))-
charindex('_',Imagename))) - charindex('_',Right(Imagename,LEN(Imagename))-
charindex('_',Imagename))))),2),
patindex('%[^0]%',parsename(Right(Right(Imagename,LEN(Imagename))-
charindex('_',Imagename)),LEN(Right(Imagename,LEN(Imagename))-
charindex('_',Imagename))) - charindex('_',Right(Imagename,LEN(Imagename))-
charindex('_',Imagename))))),2)), 10)name,distancestamp from Imageframes) b on
substring(parsename(Right(a.txt,Len(a.txt)+1-patindex('%0%',a.txt)),2),
patindex('%[^0]%',parsename(Right(a.txt,Len(a.txt)+1-patindex('%0%',a.txt)),2)),
10)=b.name
inner join
bridge_img3_staging c on substring(parsename(Right(a.txt,Len(a.txt)+1-
patindex('%0%',a.txt)),2), patindex('%[^0]%',parsename(Right(a.txt,Len(a.txt)+1-
patindex('%0%',a.txt)),2)), 10)=c.num
where a.txt like '%.fis'
order by c.id,framenummer
set identity_insert LCMSFisFrames off

update Locators
set L_Section=TestSection,
L_Run=RunNumber

```